Respiratory Medicine
Series Editor: Sharon I.S. Rounds

Matthew Jankowich
Eric Gartman *Editors*

Ultrasound in the Intensive Care Unit

AMERICAN THORACIC SOCIETY 1905 ATS
We help the world breathe®
PULMONARY • CRITICAL CARE • SLEEP

Humana Press

Respiratory Medicine

Series Editor:
Sharon I.S. Rounds

More information about this series at http://www.springer.com/series/7665

Matthew Jankowich • Eric Gartman
Editors

Ultrasound in the Intensive Care Unit

Humana Press

We help the world breathe®
PULMONARY • CRITICAL CARE • SLEEP

Editors
Matthew Jankowich, MD
The Warren Alpert Medical School
Brown University
Providence VA Medical Center
Providence, RI, USA

Eric Gartman, MD
The Warren Alpert Medical School of
Brown University
Memorial Hospital of Rhode Island
Pawtucket, RI, USA

Videos to this book can be accessed at
http://www.springerimages.com/videos/978-1-4939-1722-8

ISSN 2197-7372 ISSN 2197-7380 (electronic)
ISBN 978-1-4939-1722-8 ISBN 978-1-4939-1723-5 (eBook)
DOI 10.1007/978-1-4939-1723-5
Springer New York Heidelberg Dordrecht London

Library of Congress Control Number: 2014950429

Printed on acid-free paper

Humana Press is a brand of Springer
Springer is part of Springer Science+Business Media (www.springer.com)

Preface

Physicians have long attempted to gain knowledge of a patient's inner conditions by interpreting sounds, impulses, and vibrations. For many centuries, they have placed an ear to a patient's chest, palpated a pulse, or percussed the body with fingers and assessed the resulting waves. Innovations in technology eventually led to the modern stethoscope, a tool for intensifying certain sounds generated within the body while at the same time damping other frequencies, allowing for better auscultation. A new sound-based tool for examining the body, ultrasound, emerged in the last century, using sophisticated technology to generate high frequency sound waves and receive the reflected waves from within the body and project them onto a display. Ultrasound began to be implemented widely, though not universally, within the field of medicine. Limiting factors included physician knowledge and expertise and the cumbersome nature and expense of early ultrasound machines. However, the technology provided information far beyond what could be gleaned by physical examination or stethoscope, and allowed actual internal imaging of many organs and body parts as well as measurements of blood flow allowing a number of hemodynamic inferences.

With advances in miniaturization and decreases in costs, modern ultrasound machines have assumed a size and weight not much beyond that of the traditional stethoscope. This has allowed the bedside clinical application of ultrasound to an expanded number of clinical fields. Perhaps the most rapidly growing use of ultrasound today is within critical care medicine, where the benefits of ultrasound in guiding difficult bedside procedures such as thoracentesis and central line placement led to a growing familiarity with this technology amongst practitioners. Not surprisingly, critical care physicians, led by a few pioneers, began to apply ultrasound technology to other non-procedural clinical problems in the ICU, such as the emergency diagnosis of pericardial tamponade and pneumothorax. This textbook illustrates the many innovative uses of ultrasound currently taking place in intensive care units; some, like echocardiography, have been adapted from other clinical settings, while others are novel to critical care medicine.

We believe that ultrasound has great potential within the intensive care unit, and that further innovations will take place as more physicians are exposed early in their training to ultrasound technology, leading to a ubiquitous application within critical care. On a cautionary note, the rise and fall of pulmonary artery catheter use within the intensive care unit should be pointed out. Similar to ultrasound, this technology became widely available over the course of a few years, and provided much desired information on the hemodynamics of critically ill patients. It was heralded as an essential tool to guide resuscitation and to assess therapeutic manipulations. However, its application outstripped the evidence base supporting its use, and only over the course of many years did increasing amounts of research indicate that this tool was being misapplied. The reasons for this were multiple, and included errors in the acquisition of the data, the incorrect interpretation of the data, and, likely, that our ability to use the data from these catheters to generate meaningful changes in outcomes was lacking. We hope that this is not the case with critical care ultrasound, and we emphasize in each clinical chapter a structured approach to the application of ultrasound and the current evidence base in the field. In many areas, such as the use of ultrasound to guide volume resuscitation, more supporting data is clearly needed.

As such, this text provides current snapshots of the field—on many more topics than would have existed just a few years ago. We suspect textbooks on this topic in the coming years will detail applications of ultrasound as yet unimagined. We hope this text will inspire further investigation and innovation, will serve as an up-to-date document of the current state of knowledge in this field, and, as important, will expose gaps in knowledge that need to be filled while encouraging responsible clinical implementation of a powerful technology.

Providence, RI, USA

Matthew Jankowich
Eric Gartman

Acknowledgements

We wish to acknowledge the accomplishments and teachings of the many pioneers in ultrasound who have influenced the field of ultrasound imaging and its application to pulmonary and critical care medicine.

Contents

1 Principles of Ultrasound for the Intensivist 1
Jigme M. Sethi and Karin Halvorson

2 Critical Care Ultrasound Education 19
Andrew T. Levinson and Otto Liebmann

3 Ultrasound for Vascular Access 35
Abdullah Sulieman Terkawi, Ariel L. Shiloh, Mahmoud Elbarbary, and Dimitrios Karakitsos

4 Ultrasound Evaluation of Shock and Volume Status in the Intensive Care Unit 65
Keith Corl, Sameer Shah, and Eric Gartman

5 Critical Care Echocardiography: Acute Left Ventricular and Valvular Dysfunction 77
Girish B. Nair, Pierre Kory, and Joseph P. Mathew

6 Critical Care Echocardiography: Right Ventricular Dysfunction 123
Johannes Steiner and Gaurav Choudhary

7 Critical Care Echocardiography: Pericardial Disease, Tamponade, and Other Topics 147
Girish B. Nair and Joseph P. Mathew

8 Ultrasound and Airway Management 175
Alan Šustić and Alen Protić

9 Lung Ultrasound in Respiratory Failure and Pneumonia 191
Keith P. Guevarra

10 Pleural Ultrasound 207
Samuel K. Evans and Matthew Jankowich

11 Diaphragm Ultrasound in the Intensive Care Unit 235
F. Dennis McCool and Taro Minami

12 Abdominal Ultrasound and Genitourinary Ultrasound in the Intensive Care Unit 249
Taro Minami

13 Intensive Care Unit Ultrasound for Venous Thromboembolism 273
Genese Lamare and Chee M. Chan

14 Ultrasound in Trauma Critical Care 295
Amie Hall Woods

15 Ultrasound in the Neurointensive Care Unit 323
Venkatakrishna Rajajee

16 Ultrasound in the Neonatal Intensive Care Unit 355
Hussnain S. Mirza, Gregory Logsdon, and James Padbury

Index 379

Contributors

Chee M. Chan Department of Pulmonary & Critical Care Medicine, Washington Hospital Center, Washington, DC, USA

Gaurav Choudhary Department of Medicine, Division of Cardiology, The Warren Alpert Medical School of Brown University/Providence VA Medical Center, Providence, RI, USA

Keith Corl Division of Pulmonary, Critical Care and Sleep Medicine, Rhode Island Hospital, Providence, RI, USA

Mahmoud Elbarbary Pediatric Cardiac ICU, King Abdulaziz Cardiac Center, King Saud Bin Abdulaziz University for Health Sciences, Riyadh, Saudi Arabia

Samuel K. Evans Division of Pulmonary, Critical Care and Sleep Medicine, Providence VA Medical Center, Providence, RI, USA

Eric Gartman The Warren Alpert Medical School of Brown University, Providence, RI, USA

Division of Pulmonary, Critical Care, and Sleep Medicine, Memorial Hospital of Rhode Island, Pawtucket, RI, USA

Keith P. Guevarra Division of Pulmonary & Critical Care Medicine, New Jersey Medical School-Rutgers, The State University of New Jersey, Newark, NJ, USA

Karin Halvorson Division of Pulmonary, Critical Care and Sleep Medicine, The Warren Alpert Medical School of Brown University/Rhode Island Hospital, Providence, RI, USA

Matthew Jankowich Division of Pulmonary, Critical Care and Sleep Medicine, The Warren Alpert Medical School of Brown University, Providence VA Medical Center, Providence, RI, USA

Dimitrios Karakitsos Department of Internal Medicine, University of South Carolina, School of Medicine, Columbia, SC, USA

Pierre Kory Division of Pulmonary, Critical Care & Sleep Medicine, Beth Israel Medical Center, New York, NY, USA

Genese Lamare Department of Pulmonary & Critical Care Medicine, MedStar Washington Hospital Center, Washington, DC, USA

Andrew T. Levinson Division of Pulmonary, Critical Care and Sleep Medicine, The Warren Alpert Medical School of Brown University, Miriam Hospital and Rhode Island Hospital, Providence, RI, USA

Otto Liebmann Department of Emergency Medicine, The Warren Alpert Medical School of Brown University, Miriam Hospital and Rhode Island Hospital, Providence, RI, USA

Gregory Logsdon Department of Pediatric Radiology, Florida Hospital for Children, Orlando, FL, USA

Joseph P. Mathew Department of Medicine, Division of Pulmonary & Critical Care Medicine, Winthrop-University Hospital, Mineola, NY, USA

F. Dennis McCool Division of Pulmonary, Critical Care and Sleep Medicine, Memorial Hospital of Rhode Island, Pawtucket, RI, USA

Taro Minami Division of Pulmonary, Critical Care and Sleep Medicine, Memorial Hospital of Rhode Island, Pawtucket, RI, USA

Hussnain S. Mirza Center for Neonatal Care/Florida Hospital for Children, UCF College of Medicine, Orlando, FL, USA

Girish B. Nair Division Pulmonary and Critical Care Medicine, Winthrop-University Hospital, Mineola, NY, USA

James Padbury Department of Neonatal-Perinatal Medicine, Women & Infants Hospital, Providence, RI, USA

Alen Protić Department of Anesthesiology and Intensive Care Unit, University Hospital Rijeka, Rijeka, Croatia

Venkatakrishna Rajajee Departments of Neurosurgery & Neurology, University of Michigan Health System, Ann Arbor, MI, USA

Jigme M. Sethi Division of Pulmonary, Critical Care and Sleep Medicine, Memorial Hospital of Rhode Island, Pawtucket, RI, USA

Sameer Shah Division of Pulmonary, Critical Care and Sleep Medicine, Rhode Island Hospital, Providence, RI, USA

Ariel L. Shiloh Jay B. Langner Critical Care Service, Montefiore Medical Center/ Albert Einstein College of Medicine, Bronx, NY, USA

Johannes Steiner Division of Cardiology, The Warren Alpert Medical School of Brown University/Rhode Island Hospital, Providence, RI, USA

Alan Šustić Department of Anesthesiology and Intensive Care Unit, University Hospital Rijeka, Rijeka, Croatia

Abdullah Sulieman Terkawi Department of Anesthesiology, University of Virginia Health System, Charlottesville, VA, USA

Department of Anesthesiology, King Fahad Medical City, Riyadh, Saudi Arabia

Amie Hall Woods Department of Emergency Medicine, Inova Fairfax Hospital, Falls Church, VA, USA

Chapter 1
Principles of Ultrasound for the Intensivist

Jigme M. Sethi and Karin Halvorson

Why Study the Basic Physics?

Ultrasound imaging uses high frequency sonic waves that are produced at a transmitter using the piezoelectric phenomenon and transmitted through the body tissue, the reflections of which are then captured and used to generate an image of the underlying organ structure. Each of these processes of beam generation, transmission, reflection, and capture has limitations that affect the quality and nature of the image produced, and therefore an understanding of the physics involved is crucial to the correct interpretation and use of ultrasound in clinical medicine. For example, the brightness (whiteness) of the image on computed tomography (CT) scans is proportional to the density of an organ, but this does not work for ultrasound images, where the brightness of the structure corresponds to the *difference in reflectivity* at the interface of tissues differing in density, not the tissue density per se. For example, air bubbles in the body can resonate and generate ultrasonic waves that make them appear just as brightly white, or reflective, as bone. The liver distal to the gallbladder in the path of the ultrasound beam can appear brighter than surrounding liver tissue but this represents an artifact, not increased density of the tissue. The lung cannot be "imaged" in the conventional sense using ultrasound since it is full of air; instead, knowledge of the artifacts that result from sound beams interacting with the lung is relied upon to

J.M. Sethi, M.B.B.S., M.D., FCCP (✉)
Division of Pulmonary, Critical Care and Sleep Medicine,
Memorial Hospital of Rhode Island,
111 Brewster Street, Pawtucket, RI 02860, USA
e-mail: jigme_sethi@brown.edu

K. Halvorson, M.D.
Division of Pulmonary, Critical Care and Sleep Medicine, Alpert Medical School of Brown University/Rhode Island Hospital, 593 Eddy Street, Providence, RI 02903, USA
e-mail: karinhalvorson@gmail.com

M. Jankowich, E. Gartman (eds.), *Ultrasound in the Intensive Care Unit*,
Respiratory Medicine, DOI 10.1007/978-1-4939-1723-5_1

recognize the underlying pathology. Many of the adjustments made to improve image quality are best explained in terms of the physical properties of ultrasound in tissue. For all these reasons, a sound understanding of the physics as discussed in this chapter will facilitate accurate generation and interpretation of ultrasound images.

A Brief History of Ultrasound Imaging

Echolocation using sound waves is a natural phenomenon first identified by Lazzaro Spallanzani, an Italian physicist, who noticed that bats use it to navigate. Pierre and Jacques Curie (French physicists) discovered the piezoelectric effect, when they found that quartz crystals vibrate at a precise frequency when exposed to a constant electric field, and conversely become electrically polarized when deformed by vibration. The first application of ultrasound was in World War I when a physicist from France, Paul Langevin, developed a hydrophone to detect icebergs and submarines underwater. A physician from Vienna, Dr. Karl Dussik, used ultrasound to identify brain tumors—possibly the first medical application of the technology. Ultrasound began to really make its mark in medical care when Dr. Ian Donald applied ultrasound to the field of obstetrics and gynecology in the late 1950s.

Generation of Ultrasonic Waves

The production of ultrasonic waves invokes the principle of piezoelectricity, commonly used in cigarette lighters and stovetop gas burners to generate sparks and trigger gas ignition. Currently used piezoelectric materials are ceramics, not quartz, which have the unique property of being able to generate electric charges if mechanically deformed and conversely to undergo deformation when exposed to an alternating current. Thus, the piezoelectric effect is harnessed both to generate an ultrasound beam by causing the crystals to vibrate in response to an alternating current and to capture returning echoes which deform the crystals and create electric currents that are proportional to the mechanical energy, i.e., the amplitude, of the echo. These currents are then converted to images. The frequency of a probe depends on the thinness of the piezoelectric elements present in its tip, and the beam width depends on the number of these intricately positioned elements. The probe sends out intermittent pulses of ultrasonic energy lasting about 1–5 microseconds and no more than a few wavelengths in length, then spends >99 % of the time before the next pulse listening for the returning echoes. The deeper the structure being imaged, the more time is needed for the echo to return, i.e., "*time of flight,*" and the longer the time spent listening, which reduces the *pulse repetition frequency*, or PRF. A shorter emitted pulse and lower PRF improve the resolution of structures along the length of the beam, or *axial resolution*. This is because the shorter emitted pulses and the longer time to "listen" allow for increased separation between the echoes from two adjacent structures along the length of the beam.

As it traverses through a medium, a beam of ultrasonic waves will start off as a cylinder with parallel sides in the "near," or Fresnel, field but as it penetrates deeper it will begin to diverge in the "far," or Fraunhofer, field. The length of the near field is given by

$$L = r^2 f$$

where r is the radius of aperture of the probe and f is the frequency of the beam, i.e., the wider the aperture and the higher the frequency, the longer the near field (within limits as described later).

This is important because the *lateral resolution*, or the ability to distinguish as separate two objects lying side by side perpendicular to the incident beam, depends on the thickness of the beam. Higher frequency beams are *thinner*; therefore, the image sharpness and resolution improves with higher frequency beams and in the *near field* rather than the far field. The divergence in the beam with increased depth causes the increased blurring of deeper structures, as two point structures appear to meld together rather than appearing distinct.

Ultrasound beams can also be focused to direct the maximum energy of the beam to the focal zone of the beam either by using an acoustic lens or by electronically shaping the beam as described below.

Types of Ultrasound Beams and Probes

A single beam of ultrasound can only image a very thin cylinder of tissue (1-D mode). If a larger rectangular section of tissue (2-D mode) is to be imaged, then multiple ultrasound beams originating sequentially from side-by-side piezoelectric elements in a *linear* transducer will create a parallel array of beams in a single plane. This type of transducer is typically used in vascular imaging. The width of the section imaged using a linear transducer is limited by the width or "footprint" of the linear array transducer. A *curvilinear array* has a curved surface with beams sent out in a diverging array allowing imaging of a larger "sector" of tissue than the linear probe, but with attendant image distortion and loss of lateral resolution for the reasons described above.

However, the need to image large sections of the thorax while retaining a footprint small enough to fit between the ribs requires a narrow array of beams originating from the center of a tiny probe being swept electronically from side to side as in conventional radar (*phased array scanning*). In this method, the sequential firing of the individual piezoelectric elements is infinitesimally separated in time so that Huygens' wave interference between these individual beams deflects the entire wave front. Varying the firing sequence of these piezoelectric elements accomplishes steering of the beam from side-to-side across a sector. These are the typical probes used in thoracic and cardiac imaging. Examples of these probes are shown in Fig. 1.1.

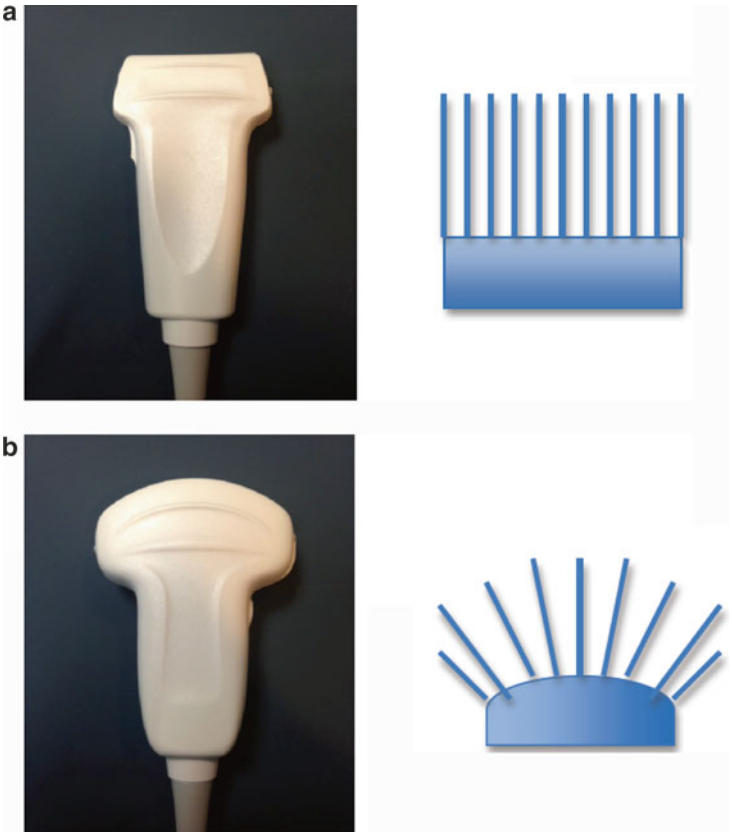

Fig. 1.1 (**a**) Linear probe: typically used for imaging vascular structures. (**b**) Curvilinear or convex probe: this is the standard abdominal probe and scans a wide sector allowing imaging of abdominal viscera including the uterus

Electronic focusing of a beam uses the same principle by triggering outer beams before more central beams thus creating a concave, focused ultrasound front.

Ultrasound probes may be (a) *moved* to a different position on the surface of the body; (b) *rotated* along the long axis in the same position, in a clockwise or anticlockwise direction; (c) *angled* from side to side to obtain images in the same plane on either side; or (d) *tilted* back and forth to point towards or away from a deeper structure. By convention, the transducer position is on the top of the screen so that structures closer to the skin are on the top of the screen and those further from the transducer are positioned lower on the screen. Also, left-right orientation is ensured by confirming that the location of the physical ridge or button on the side of the probe corresponds to the green dot at the top of the sector scan on the image screen.

Tissue Transmission of Ultrasound Waves

Sound is a vibration propagating through a medium in longitudinal waves of compression and rarefaction. Audible sound waves in air have a frequency ranging from 20 to 20,000 cycles per second, or Hertz (Hz), whereas ultrasound waves used in clinical devices have an "ultra" high frequency of 1–10 million, or mega, Hz (MHz). Unlike lower frequency audible sounds that can be heard around corners, for example, these ultrasonic waves travel through tissue in straight lines.

Sound waves are defined by frequency (f), wavelength (λ), and velocity (v) of travel in a medium, such that $v = f\lambda$.

Thus, frequency and wavelength are inversely related to each other. The amplitude of a wave is an expression of its energy, and together with frequency, wavelength, and velocity, these four characteristics define the most important properties of sound waves.

The velocity, v, of sound in a medium is given by the equation: $v = (B/D)^{1/2}$, where B is the modulus of elasticity of the medium and D is the density. Therefore, sound generally travels *faster* through *stiffer* materials, such as bone, compared with muscle. The *average* velocity of sound in body tissue is 1,540 m/s, which is approximately equal to the velocity of sound in saline, or seawater. On the other hand, the resistance a material offers to the passage of sound waves through it is called its acoustic impedance, Z, and is the product of the material density and the sound velocity. Again, bone will resist the passage of ultrasound much more than soft tissue or muscle. Table 1.1 shows comparative propagation velocities of sound waves through media of different densities.

When traversing tissue, sound waves can be affected in the following ways:

1. Absorption: This is the deposition of sound energy within tissue, where it is converted to heat, diminishing any return signal back to the transducer to generate an image. Absorption is proportional to the distance of travel (path of the interrogating beam + the return path of the echo) so that deeper tissues are more difficult to image. Absorption also varies with the square of the wave frequency. This explains why low frequency waves penetrate deeper into tissue (e.g., you

Table 1.1 Propagation velocities of sound waves in material of different densities

Medium	Velocity (m/s)
Air	330
Water	1,500
Fat	1,440
Soft tissue	1,540
Muscle	1,565
Blood	1,570
Bone	4,080
Metal	5,090

can "feel" the deep vibrations of a bass drum in your "bones"), but high frequency waves are only available to image superficial tissues. However, the longer the wavelength (i.e., the lower the frequency), the less *spatial resolution* that can be provided in a resulting image, which explains why intracellular structural detail is resolved by electron microscopes which use electron beams with an effective wavelength in the order of nanometers. Herein lies the trade-off in the use of US to interrogate biological structures—higher frequencies provide better resolution of smaller structures but can only do so relatively close to the surface of tissue, but imaging of deeper structures requires a penetrating lower frequency with resultant loss of spatial resolution and more scatter and poorer image quality (see below). Generally, frequencies of 5–10 MHz are used in clinical applications such as catheter placement in vascular structures close to the skin, whereas frequencies of 1–4 Mz are better suited to display images of heart, liver, kidneys, and other deeper structures.

Absorption is dependent too on the *density* of the tissue, with denser tissues absorbing more energy, and this is expressed in terms of the attenuation coefficient (in decibels/cm) of the tissue. In general [1], cortical bone (attenuation coefficient 13–26 dB/cm) absorbs more energy than muscle(attenuation coefficient 2.5 dB/cm) which in turn absorbs more energy than fat (attenuation coefficient 0.5–1.8 dB/cm), and water absorbs the least energy of the preceding structures (attenuation coefficient 0.002 dB/cm). Air has an absorption coefficient 100× that of tissue so it does not allow any transfer of energy (e.g., lung has an attenuation coefficient of 40 dB/cm). Application of a transducer over bone will prevent any sound energy reaching underlying structures, as will any air that comes between the surface of the probe and the skin. Liberal application of gel on the skin reduces reflection of sound energy at the air-tissue interface and enhances transmission of sound into the body for the imaging of viscera.

2. Refraction: Bending of sound waves when obliquely crossing an interface of two media differing only slightly in acoustic impedance. Image brightness suffers when sound waves are bent away from the transducer, and this can also create artifacts.
3. Diffraction: Interference patterns produced by sound waves when they encounter an obstacle.
4. Reflection: This occurs at a boundary between structures with very different acoustic impedances, such as the interface between myocardium and blood in the heart or the interface between soft tissue and bone or between solid liver tissue and bile in the gallbladder. *This property of reflection is the basis for the generation of all ultrasound images.*

   Several factors affect how sound is *reflected:*

   (a) The fraction of energy reflected is proportional to the *square* of the difference in impedance, and is called the reflection coefficient; the remaining fraction is transmitted or absorbed. The greater the difference in the impedance between tissues, the more incident sound energy is reflected back to the transducer for image production. The acoustic impedance of various body tissues is listed Table 1.2 [2].

Table 1.2 Acoustic impedance values of different body tissues

Tissue	Acoustic impedance (10^6 rayls)
Air	0.0004
Fat	1.35
Blood	1.7
Muscle	1.75
Bone	7.8

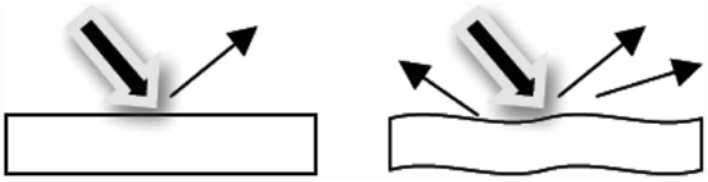

Fig. 1.2 Specular reflection and scatter

(b) The amount of energy reflected back to the transducer also depends on the angle of incidence of the sound beam at the tissue boundary. Structures that lie perpendicular to the ultrasound beam will reflect the most energy back to the transducer—the greater the inclination of the beam away from the perpendicular, the more the echo will be reflected away from the transducer. This explains *drop-out artifacts* when imaging moving structures, e.g., cardiac valves, and also why a valve leaflet may appear bright white when it moves into view at right angles to the interrogating beam. *This must not be confused with calcification of the leaflet*!

(c) Size and surface properties of the boundary: reflection from a smooth or specular interface sends most echoes back to the transducer giving a bright image, whereas scattering from rough surfaces sends echoes in all directions, reducing the energy returning to the probe for image acquisition (Fig. 1.2). Specular reflections arise from objects much larger than the wavelength of the incident beam, and are useful in delineating tissue boundaries such as the surface of the gallbladder or the outline of cardiac chambers. Objects that are smaller than the wavelength of the interrogating beam produce scattered waves (particularly prominent with low frequency probes) that are subsequently reflected by surrounding tissue back to the probe and provide the granular "background noise" or "speckles" on the image. Scatter provides information about the structure of the tissue rather than the interface or boundary and so this property of "speckling" is harnessed in tissue harmonic imaging of the myocardial tissue.

5. Transmission: Energy that escapes reflection or absorption is transmitted through the material or through the interface between materials of different acoustic impedances. This transmitted energy is available to be reflected by, and therefore image, deeper structures.

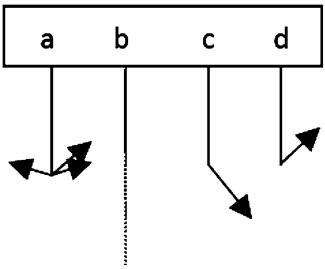

Fig. 1.3 Mechanisms of loss of ultrasound beam energy: (**a**) scatter, (**b**) absorption, (**c**) refraction, and (**d**) reflection

Table 1.3 Typical ultrasound appearance of common body structures

Tissue	Image
Air bubbles	Hyperechoic
Fat	Hypoechoic
Muscles	Hyperechoic lines within hypoechoic tissue
Bone	Extremely hyperechoic (with shadowing)
Pleura	Hyperechoic line
Arteries	Echogenic to hyperechoic wall with anechoic/hypoechoic lumen (and pulsatile)
Veins	Thinner echogenic wall with anechoic/hypoechoic lumen (easy to compress, non-pulsatile)

Attenuation refers to the loss of signal energy by absorption, refraction, or scatter (Fig. 1.3). Since the largest component of energy loss is due to absorption, the terms attenuation and absorption are sometimes used interchangeably. To summarize, returning sound energy and hence brightness of the image depends upon incident energy/strength, direction of reflection, and depth of structures. Contrast, on the other hand, depends on the reflectivity of a structure compared with the reflectivity of surrounding tissue at the same depth and the direction of reflection from the structure compared to surrounding tissues.

Body tissues have a characteristic brightness signal ranging from very bright (hyperechoic) to dark (anechoic) derived from the ability to reflect or transmit ultrasonic waves as discussed above. Table 1.3 describes where different tissues lie on this "white-gray-black" continuum.

Image Generation

The information from ultrasonic echoes or reflected waves is displayed on the image in terms of two characteristics: first, *depth*, d, which is interpreted as a function of the time, t, of travel ($t = 2d/v$), and second, *amplitude*, or the energy retained after passage and reflection and converted using the piezoelectric effect into electrical signals. This amplitude can be displayed as an amplitude signal (A mode) or a brightness signal on the image (B mode). This brightness signal uses a black-gray-white tonal scale, with anechoic regions appearing black, areas with strongest signal

amplitude appearing white (hyperechoic), and other reflections of intermediate intensity appearing gray (hypoechoic). Thus the typical image would have a signal (A or B) plotted against depth calculated from "t." If the echo is derived from a moving target, such as a heart valve, then the same information can be plotted against time, showing brightness, depth, and motion over time, which is the M (motion) mode of the typical ultrasound image.

Modulation of Images: Basic Ultrasound Machine Controls

There are several mechanisms to modulate the images generated by an ultrasound machine and these will be described below.

1. Depth control: Increasing the depth control allows imaging of deeper structures by reducing the pulse repetition frequency of the probe allowing for the increased time of flight of echoes returning from deeper tissues. Deeper tissues thus imaged may be more blurred (with reduced lateral resolution) if they lie in the Fraunhofer zone of the incident beam and will be more attenuated necessitating manipulation of gain (see below). Depth of the tissues being imaged is, as explained earlier, limited by the frequency spectrum of the probes being used. Using an unnecessarily deeper setting will reduce the image size of pertinent structures and contract the field of view into the upper part of the image screen, as shown in Fig. 1.4.

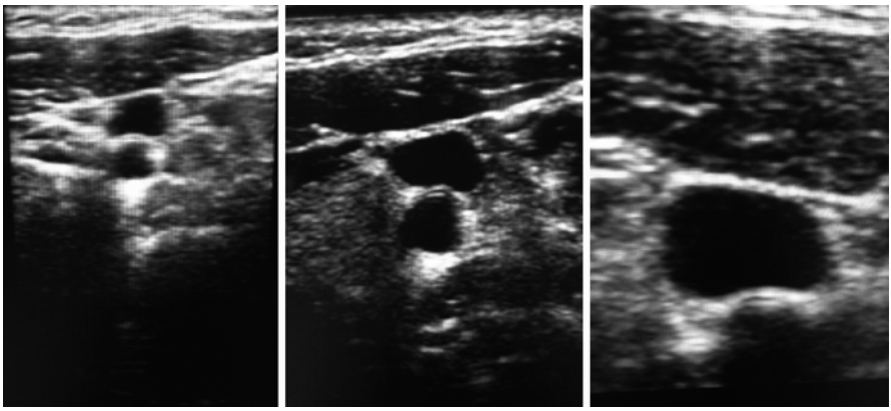

Fig. 1.4 Ultrasound images of a vein and underlying artery, viewed at three different depth settings, from *left* to *right*: (**a**) too deep, (**b**) correct depth, and (**c**) too shallow. Note the change in perspective: the near field region of the image is sharply reduced in size compared to the far field in (**a**) while in (**c**) the near field of the image is so magnified as to nearly lose the view of the artery. Also note the enhanced "whiteness" of the tissue immediately deep to the artery in images (**a**) and (**b**). This does not represent calcification or thickening of the tissue but is an example of posterior enhancement artifact, as shown more clearly in Fig. 1.6

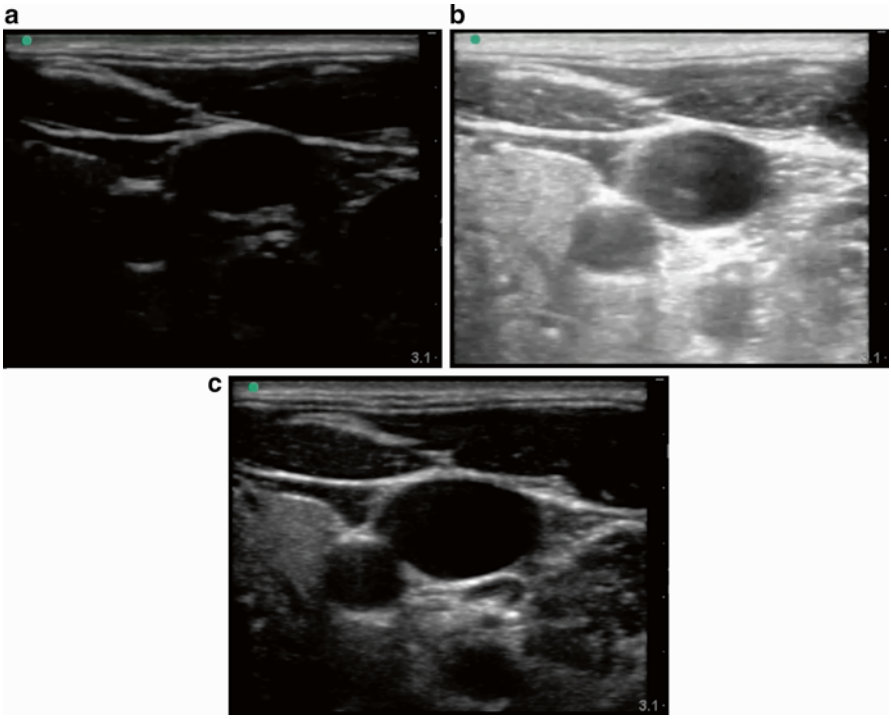

Fig. 1.5 Ultrasound images of a jugular vein and adjacent carotid artery manipulated by using too little (**a**), too much (**b**), or optimal gain (**c**) (Images by Dr. Taro Minami)

2. Gain: Gain is a mechanism to amplify the brightness of the ultrasound image, similar to volume controls on an audio system. Both the echoes from the desired object, i.e., the signals, and the unwanted background scatter, i.e., the noise, will be equally increased. Too much gain reduces contrast and obscures detail, while too little gain also reduces detail and darkens the image (Fig. 1.5).
3. Timed gain control: Since attenuation increases with depth, signals from deeper tissues will be less prominent than those from structures closer to the surface. Timed gain control (TGC) consists of a stack of slider bars, each corresponding to a particular depth, allowing for the progressive amplification of signals from deeper tissues, i.e., selective gain with depth. Most modern ultrasound machines employ *automatic* TGC, whereby delayed signals are automatically amplified in proportion to the delay. While desired signals from deeper structures are increased as a result, any scatter originating from the same depth will also be amplified.

Imaging Artifacts

The way sound waves interact with tissues and the processing algorithms employed by the image processor to generate images can result in certain characteristic and common artifacts that must be immediately recognized as such by the ultrasonographer and the interpreting clinician. Recognition of the artifact at the time of image acquisition may facilitate repositioning of the probe or use of alternative windows to ensure anatomically correct images are recorded and to reduce the possibility that artifacts may be misinterpreted to represent pathology. This is of even greater importance for the proceduralist using ultrasound guidance.

Shadowing

Calcified structures such as bone and gallstones reflect and attenuate incident sound energy so completely as to cast an *acoustic shadow*, whereby the areas deeper to such structures will appear black and anechoic (Fig. 1.6).

Such shadows are readily appreciated, but subtler shadowing originating closer to the skin surface is often missed by beginner ultrasonographers and drastically reduces image quality. For example, a probe placed with its extreme edge abutting a rib may result in a band-like sector of reduced brightness, i.e., a shadow, on the image. Alternatively, the rib edge *effectively reduces the probe aperture*, simply reducing lateral resolution and resulting in slightly blurred images without a clearly discernible shadow. This is illustrated in Fig. 1.7.

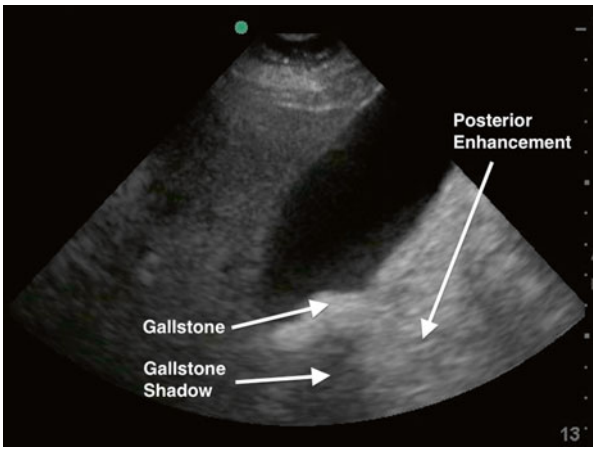

Fig. 1.6 Ultrasound image of a gallbladder and surrounding liver tissue. Note the acoustic shadow cast by a calcific gallstone. Also note the apparent increased reflectivity (*brightness*) of the liver tissue imaged through the gallbladder, compared with surrounding liver tissue. This is an example of enhancement (Image by Dr. Taro Minami)

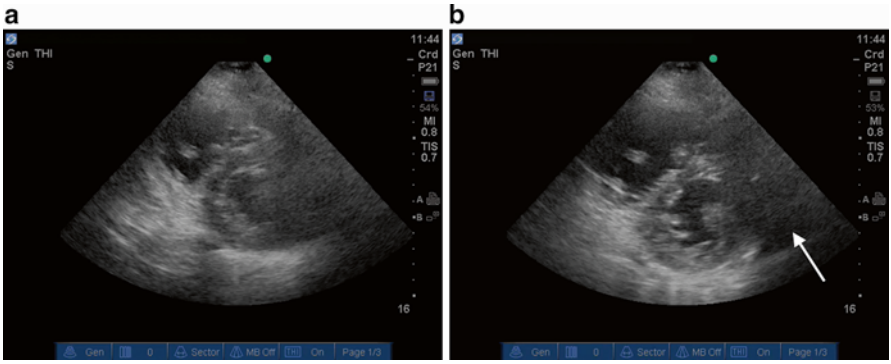

Fig. 1.7 Short axis view of the left ventricular at the level of the papillary muscles. In (**a**), the entire image appears blurred and grainy, particularly on the *right side* of the image where all detail is lost. No rib shadow is visible. This is because placement of the probe over a rib has effectively reduced the probe aperture. Slight adjustment of the probe position in (**b**) results in a much better definition of the endocardium, myocardium, and papillary muscles, although a rib shadow is now seen on the *right* (*arrow*) (Images by Dr. Philip Lamberty, MD, Assistant Professor of Medicine, University of Pittsburgh School of Medicine, Pittsburgh, PA)

Enhancement

This is the opposite of the shadowing artifact. Liquid-filled structures attenuate sound energy less than surrounding tissue allowing more energy to illuminate deeper tissues that then appear abnormally bright. This artifact is commonly seen when imaging the liver through the bile-filled gallbladder—liver tissue in the "shadow" of the gallbladder appears brighter than surrounding liver. An example of posterior enhancement is shown in Fig. 1.6.

This artifact can also be seen deep to a larger blood-filled vessel, such as the femoral artery and is often deliberately used to better image the uterus through a full urinary bladder.

Reverberations

The algorithm employed by the ultrasound processor determines the depth of the reflecting source from the time of flight of returning echoes, presuming a straight-line return to the transducer and using the standard velocity of ultrasonic waves in tissue of 1,540 m/s. The processor then displays the calculated source on the processed image accordingly. If an echo is reflected multiple times from a source to a more superficial tissue reflector, or even the probe, and back again, each of the subsequent or higher order reflections is presumed to originate from a deeper source and is displayed as a series of equally spaced bands along a ray extending deeper

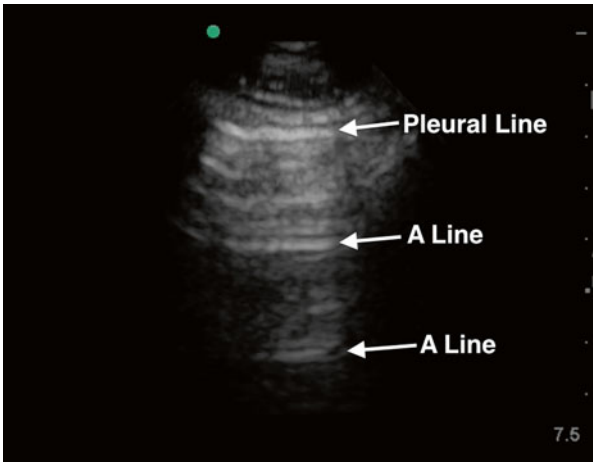

Fig. 1.8 A-lines in the lung as examples of a reverberation artifact. See text for details (Image by Dr. Philip Lamberty)

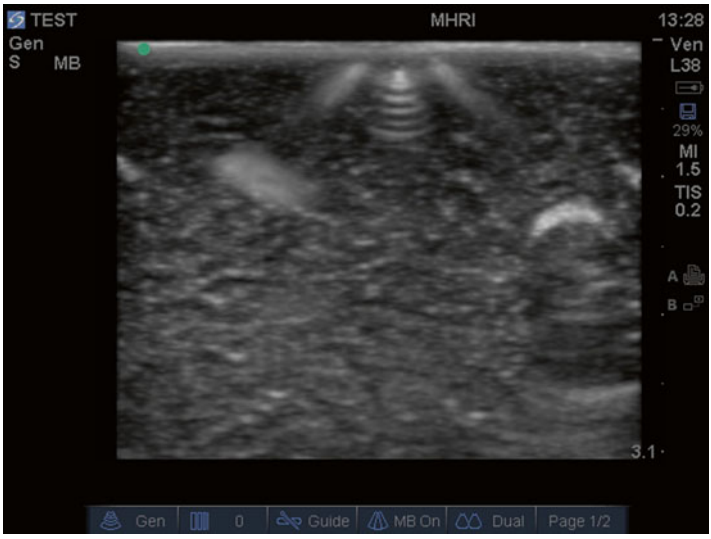

Fig. 1.9 Ultrasound image of a needle piercing the synthetic tissue simulation material of a Blue Phantom™ (CAE Healthcare, Sarasota, FL). The *bright dot* at the *top* of the image is the needle in cross section. The successive bright arcs represent reverberation images. See text for explanation (Image by Dr. Taro Minami)

into the tissue from the primary reflecting position. The A line or pleural artifact of the lung is an example of this phenomenon. Why Study The Basic Physics Of Ultrasound and forth between the transducer and the brightly echogenic pleura, and the later reverberations appear as progressively less bright lines spaced at equal distances as the transducer-pleural distance (Fig. 1.8). Figure 1.9 shows an ultrasound image of a catheter introducer needle inserted into the synthetic tissue

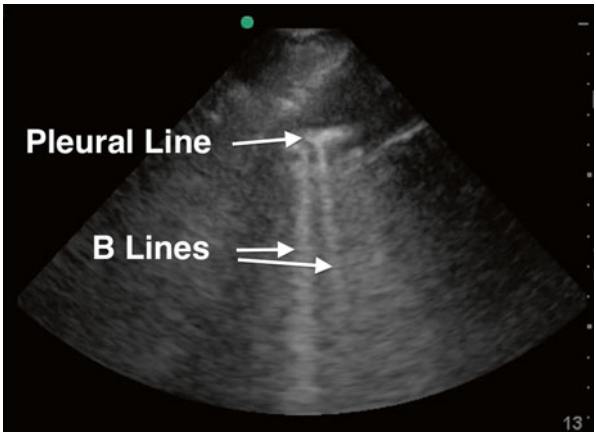

Fig. 1.10 Ultrasound image of lung B lines, also called "comet-tails" (Image by Dr. Philip Lamberty)

simulation material of a Blue Phantom™ (CAE Healthcare, Sarasota, FL). The bright white dot in the upper center is the actual needle, imaged in cross section. The ultrasound beam reflects back and forth between the luminal surfaces of the needle and using the time of flight algorithm, the processor generates a series of equally spaced arcs deep to the needle. In this image, the depth control has been set too shallow to enhance visualization of this reverberation artifact. Not uncommonly, while imaging a needle during placement of a central line the reverberation caused by multiple reflections of the ultrasound beam from the luminal surface of the needle gives the appearance of a bright, thin, hyperechoic ray extending into the tissue (rather than a series of arcs) and is *mistaken by the inexperienced ultrasonographer as depicting the actual needle*. In reality, the needle itself is simply the bright white dot at the source of the ray. Another artifact that has a similar origin is the B line, or "comet tail" of alveolar-interstitial syndrome (Fig. 1.10). In this case the sources of the reverberations are the highly reflective, edematous, and thickened alveolar septae lying just under the pleura and creating multiple back and forth reflections of the ultrasound beam. As in the example shown in Fig. 1.9, this generates a series of small arcs separated by less than a millimeter, i.e., just under the limit of resolution of the ultrasound beam, giving the appearance of a hyperechoic ray extending into the deeper lung tissue. If the lung were to be totally fluid-filled and airless, i.e., consolidated, this comet-tail appearance would be lost.

One other kind of reverberation artifact—the "near-field reverberation artifact"—is caused by multiple reflections between surface tissues and a reflective cystic interface, such as the wall of the gallbladder or a cyst. The delayed reverberating echoes of the superficial soft tissue reflected from the cyst wall are erroneously placed *within* the lumen attached to the near-field wall of the (in reality, anechoic) cystic structure. This must not be confused with solid tissue in the cyst and should be recognized for the artifact that it is.

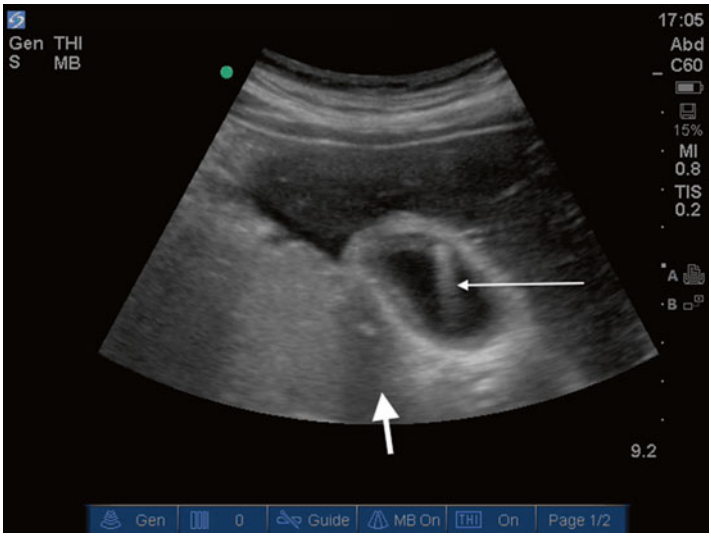

Fig. 1.11 Ring-down artifact. A hyperechoic line is produced by resonant vibrations of a cholesterol crystal in the wall of the gallbladder (*thin arrow*). Note also the edge artifact labeled with the *thick arrow* (Image by Dr. Philip Lamberty)

Ring-Down

Ring-down artifact is produced by air bubbles or crystals that utilize the incident ultrasonic energy to resonate at the ultrasound frequency, producing high amplitude sound waves. Since the resonation persists after the transducer has already received the initial reflection, the subsequent echoes are interpreted as originating from progressively deeper tissues and appear as a hyperechoic ray extending deeper from the original source. This is basically a version of reverberation artifact, except that the reverberations are continuous. Ring-down artifact generated from vibrations of a cholesterol crystal in the wall of the gallbladder in the condition known as adenomyomatosis of the gallbladder is shown in Fig. 1.11.

Reflection Artifact

This is another example of erroneous time of flight assumptions by the image processor. In this artifact, sound waves are obliquely reflected back and forth from the back to the sides of a fluid-filled cavity with a highly reflective wall such as the bladder, a large vessel, or the renal pelvis and then back to the probe. The delayed reflections are interpreted to result from deeper structures giving the image of a second, or multiple, fluid-filled cavity/cavities lying at a deeper position than the original structure.

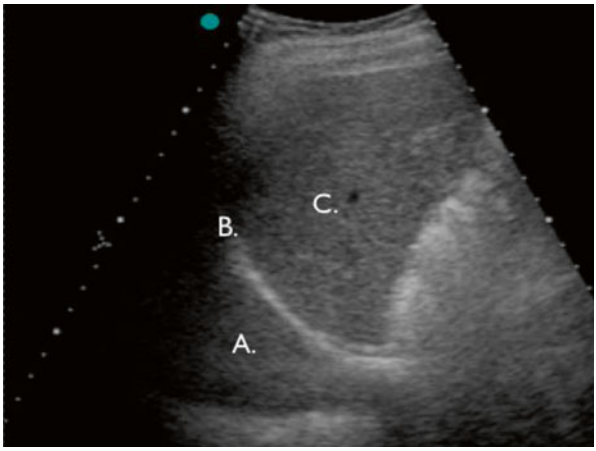

Fig. 1.12 Mirror-image artifact. Note the apparent appearance (A=artifact) of liver (C) above the diaphragm (B) (Image by Dr. Amie Hall Woods)

Mirror Image Artifact

Similar to the above artifact, tissue echoes from a structure may be reflected off the surface of a highly reflective specular interface such as the diaphragm, resulting in two mirror images positioned equidistant on either side of the diaphragm. This is seen with images of the liver, or rarely the kidney, duplicated both superficial and deep to the diaphragm, as shown in Fig. 1.12.

Refraction Artifacts

Sound waves traveling through materials of differing density are refracted, or bent, away from the original line-of-sight, resulting in several different types of possible artifacts.

Edge Shadow: This is seen with sound waves directed to the edges of a curved surface of different density such as a cyst being bent away from the original direction. Little energy is therefore directed to the deeper tissues directly beyond the curved surface along the initial direction of the wave, causing an acoustic shadowing of the tissues just deeper to the *edge* of the curved cystic structure (Figs. 1.11 and 1.13).

Split Image Artifact: Abdominal structures may be falsely duplicated on ultrasound images, caused by the ultrasound beam being partially refracted at the curved interface of the rectus abdominii muscles and the underlying pre-peritoneal fat. The two beams then each produce side-by-side images of central structures such as the aorta or sometimes falsely implicate two gestational sacs in a gravid uterus.

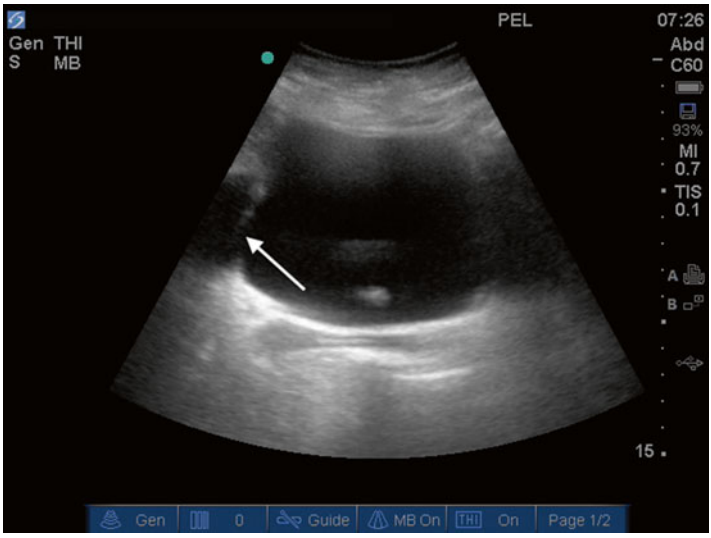

Fig. 1.13 Edge artifact. Note the anechoic region at the edge of the fluid-filled urinary bladder, giving the impression of discontinuity of the lateral bladder wall (*arrow*) (Image by Dr. Philip Lamberty)

This artifact can be recognized by slowly moving the probe to the lateral aspect of the abdomen away from the rectus sheath, keeping the organ in view until the two images merge, thus demonstrating the presence of just a single organ.

Bayonet Artifact

This artifact is typically seen when imaging a metallic needle, e.g., during a nerve block. In this artifact, the tip of the needle may appear separated and offset from the main body of the needle. As the needle tip penetrates tissues with a different sound propagation velocity from those containing the main body of the needle, the image processor, assuming a standard velocity, interprets the echoes from the needle tip as coming from a deeper or more shallow position (Fig. 1.14).

Diaphragm Discontinuity Artifact: The diaphragm is usually imaged as a bright hyperechoic line, but at times, if ascites is present, may appear to be falsely discontinuous with two discontinuous but overlapping segments created by refraction of the ultrasound beam as it traverses from ascitic fluid or fat into liver. This is similar to the bayonet artifact in its origin.

There are numerous other categories of artifacts that commonly complicate ultrasound imaging, including volume-averaging artifact, side-lobe and grating artifact, beam-width artifact, anisotropy, and others that are beyond the scope of this chapter.

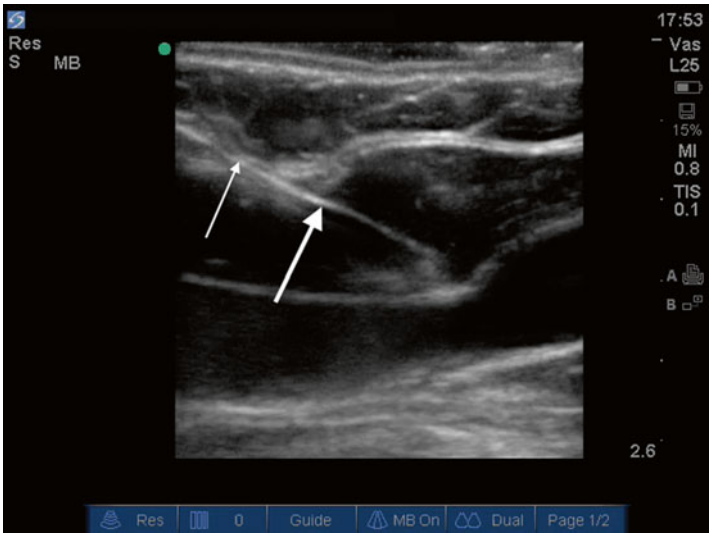

Fig. 1.14 A subtle example of the bayonet artifact. The distal part of a needle, beginning at the position indicated by the *thick arrow*, appears offset from the proximal body of the needle marked by the *thin arrow*. The site of displacement corresponds to passage through tissue of differing density (Images by Dr. Philip Lamberty, MD, Assistant Professor of Medicine, University of Pittsburgh School of Medicine, Pittsburgh, PA)

Conclusion

As should be apparent, the physical properties of ultrasonic waves in tissue influence every aspect of the daily clinical use of this technology, from selection of the appropriate transducer, fine-tuning the depth selection, knowing how to maximize gain, recognizing artifacts, and distinguishing real characteristics of tissue structures from those falsely suggested by echo reflections. Perhaps the most important realization for the clinical ultrasonographer is that the representation on the screen is a series of reflections and not a real image per se, as we usually understand an image from other modalities such as x-rays and CT scans.

References

1. Bushberg JT, Seibert JA, Leidholdt EM, Boone JM. Interaction of ultrasound with matter. In: Bushberg JT, Seibert JA, Leidholdt EM, Boone JM, editors. The essential physics of medical imaging. 3rd ed. Philadelphia: Wolters Kluwer; 2012.
2. Arbona FL, Khabiri B, Norton JA. Introduction to ultrasound. In: Arbona FL, Khabiri B, Norton JA, editors. Ultrasound-guided regional anesthesia: a practical approach to peripheral nerve blocks and perineural catheters. New York: Cambridge University Press; 2010.

Chapter 2
Critical Care Ultrasound Education

Andrew T. Levinson and Otto Liebmann

Introduction

Goal-directed ultrasound offers a powerful diagnostic tool to assist providers caring for critically ill patients. The primary objective of critical care ultrasound education, training, and certification, as with any endeavor in medical education, is to ensure safety and clinical competency. Issues of education and certification remain poorly defined and are continuing to evolve.

While point-of-care ultrasound was initially used by physicians practicing critical care to aid in bedside procedures, its application to cardiac, thoracic, and vascular diagnosis and monitoring is now becoming widespread. As portable ultrasound machines become ubiquitous in intensive care units (ICUs), a growing challenge is ensuring—through a well-designed educational program with a robust quality assurance component—that users are qualified to perform and interpret goal-directed ultrasounds and that the information obtained safely supports the care of patients.

The goal of ultrasound education for critical care providers is to develop and maintain competence in bedside ultrasound in the areas of image acquisition and interpretation. A major challenge in educating intensivists in critical care ultrasound is to develop both breadth and depth of knowledge and technical skill. Education

A.T. Levinson, M.D., MPH (✉)
Division of Pulmonary, Critical Care and Sleep Medicine, Warren Alpert Medical School of Brown University, Miriam Hospital and Rhode Island Hospital,
164 Summit Avenue, Ste 227, Providence, RI 02906, USA
e-mail: andrew_levinson@brown.edu

O. Liebmann, M.D., FACEP
Department of Emergency Medicine, Warren Alpert Medical School of Brown University, Miriam Hospital and Rhode Island Hospital,
593 Eddy Street, Davol 141, Providence, RI 02903, USA
e-mail: otto@brown.edu

M. Jankowich, E. Gartman (eds.), *Ultrasound in the Intensive Care Unit*,
Respiratory Medicine, DOI 10.1007/978-1-4939-1723-5_2

and training should emphasize goal-directed and easily reproducible techniques. Advanced levels of expertise should be developed in a sequential manner. It is essential to remember that the goals of basic critical care ultrasound studies are often much more limited than comprehensive advanced studies interpreted by radiologists, cardiologists, and intensivists with very advanced training, especially when developing core competencies. However, educational efforts must also emphasize that a major strength of critical care ultrasound is that intensivists are at the bedside and can repeat studies and reevaluate patients as clinical conditions change.

The levels of competency in point-of-care ultrasound and the extent of its utilization are highly variable—both broadly in terms of geography and between providers within the same institution. Given this diversity, the need for the continued development of standardized training pathways and certification in order to improve provider knowledge and patient care is crucial [1].

An essential role of critical care ultrasonography education and certification is to ensure that the clinicians utilizing the technology have the required skills, knowledge base, and technical expertise and are able to recognize the potential pitfalls and limitations of point-of-care ultrasound. To be successful, intensivists must be trained not to overstep their scope of practice and need to recognize when comprehensive formal studies are indicated. As such, it is necessary to develop a collaborative environment with the divisions of cardiology and radiology in order to develop proper supports for a critical care ultrasound program [2].

Certification and Accreditation of Individual Intensivists

General Principles of Certification

The primary goal of training programs and curricula is to develop clinical competency. Certification and accreditation are a means of assessing if a provider is well trained and competent. *Certification* is a statement that an individual completed a specified training curriculum. *Accreditation*, in contrast, is more rigorous and includes quantitative and qualitative demonstrations of competency. Accreditation is an official recognition that an individual has undergone a rigorous program of training and assessment and can perform at a high standard [3].

At present there is no clear consensus of how to achieve adequate training and how to assess clinician competence in critical care ultrasound [3]. How often a clinician who achieves accreditation should undergo a process of reaccreditation remains controversial [3, 4]. There are currently efforts in several countries and at the international level to develop standardized curricula and to better elucidate key components of critical care ultrasound training [3, 5]. Experts in critical care ultrasound have proposed that intensivists currently in training who receive appropriate training in the use of basic critical care ultrasound and achieve clinical competency do not need formal accreditation to so [3]. They advocate that accreditation be reserved

for intensivists currently in practice who did not receive formal fellowship training and/or intensivists who want advanced training to perform comprehensive rather than only goal-directed ultrasonography (e.g., complete transthoracic echocardiography (TTE) and transesophageal echocardiography (TEE)) [3]. The ultimate goal is a unified training pathway leading to certification and accreditation in critical care ultrasound [3].

General Certification in Critical Care Ultrasound

As critical care ultrasound education for intensivists becomes more widespread, there is growing support for developing varying levels of competency and certification [6]. Specifically with regard to critical care echocardiography, some propose a tiered system of demonstrated competency and accreditation [7]. Recent international guidelines propose that all intensivists receive training in basic-level critical care echocardiography and general critical care ultrasound. The international guidelines further propose that advanced-level education and training in critical care echocardiography should be optional in the training of all critical care physicians [8].

The specific components of tiered levels of competency have been identified in detail by international experts in critical care ultrasound [8, 9]. A joint consensus statement from the American College of Chest Physicians/La Société de Réanimation de Langue Française recommends that critical care ultrasound and echocardiography competence be delineated into basic and advanced levels. Skills required to identify important clinical findings and answer basic clinical questions comprise the basic level of competence. The authors recommend that all intensivists be trained in general critical care ultrasound and basic critical care echocardiography. The consensus statement also proposes that general critical care ultrasound competencies and basic critical care transthoracic echocardiography training be required components in the training programs of all intensivists [9]. Those that desire further competence are encouraged to pursue additional training in advanced critical care echocardiography, including TEE, emphasizing comprehensive evaluation of cardiac anatomy and function [8].

Certification in Critical Care Echocardiography

A comprehensive three-tiered system of critical care echocardiography practice, training, and accreditation has been proposed by the World Interactive Network Focused on Critical Ultrasound (WINFOCUS). The authors delineate four proposed levels of competency for the use of echocardiography by intensivists (Fig. 2.1). The levels of competency range from acquiring standard transthoracic views in a

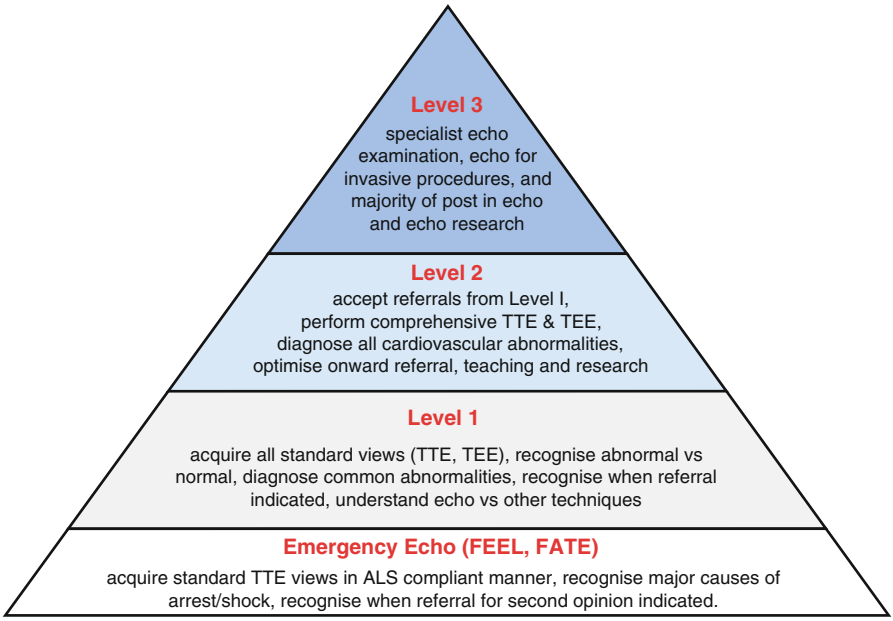

Fig. 2.1 Proposed levels of competence of echocardiography in ICU. *TTE* transthoracic echocardiography, *TEE* transesophageal echocardiography, *ALS* advanced life support, *FEEL* focused echocardiographic evaluation in life support, *FATE* focused assessment with transthoracic echocardiography (Reprinted from Price S, Via G, Sloth E, Guarracino F, Breitkreutz R, Catena E, et al. Echocardiography practice, training and accreditation in the intensive care: document for the World Interactive Network Focused on Critical Ultrasound. Cardiovasc Ultrasound. 2008;6:49)

hemodynamically unstable patient (emergency echo) up to performing specialized comprehensive echocardiography exams (level 3) [7].

Need for Universal Pathway for Certification and Accreditation

All proponents of critical care ultrasound agree that there should exist a clearly defined universal pathway for training and accreditation [2, 10]. Currently, there is no internationally recognized accreditation in general critical care ultrasound specifically for intensivists. Experts recommend that programs should be tailored specifically to intensivists, not merely replicated from the curricula for sonographers and cardiologists [6].

There are currently efforts to develop standard curriculum and program requirements, especially in the area of echocardiography [5, 11, 12]. Recently developed expert guidelines on training standards for critical care ultrasonography recommend that basic echocardiography and general critical care ultrasound be a required component of all critical care training programs. It is recommended that trainees receive

a combination of didactic, computer-based, and hands-on training as part of their educational curriculum and that a logbook be kept to document competence in image acquisition and interpretation [8]. The guidelines recommend that basic training be part of regular critical care education and that physicians who desire advanced skills complete formal advanced certification programs.

Training Requirements

Basic critical care ultrasound education must balance developing an adequate knowledge of image acquisition and interpretation across a variety of organ systems, emphasizing both normal and clinically important pathology. Various educational and certification entities have begun to recognize the importance of incorporating the development of key competencies in goal-directed ultrasound for trainee physicians in emergency and critical care. In the USA, the Accreditation Council for Graduate Medical Education (ACGME) requires that all critical care medicine physicians-in-training receive education in the use of ultrasound. The 2012 guidelines require that all graduating critical care medicine fellows demonstrate competency in the use of ultrasound to place intravascular access, to perform thoracentesis, and to place intra-cavitary tubes and catheters. Graduating critical care fellows are also required to demonstrate knowledge of ultrasound in the evaluation of critically ill patients [13]. For emergency medicine residents, the ACGME requires that residents must be trained in "the use of ultrasound for the bedside diagnostic evaluation of emergency medical conditions and diagnoses, resuscitation of the acutely ill or injured patient, and procedural guidance" [14, 15]. In other countries, there is also a trend towards developing competency in critical care ultrasound as part of the educational curricula for emergency medicine, anesthesia, and critical care [3]. A major challenge is that current training requirements provide few details about how to develop competence and what specific skills are necessary.

Key Components of an Educational Program

Key components of critical care ultrasound education and training include didactic training in ultrasound physics, image acquisition and image interpretation, hands-on training, and the critical review of images and their resulting interpretation by a clinician experienced in critical care ultrasound [8].

Learning Curve

Educational efforts must recognize that there is a learning curve to developing competency in critical care ultrasound that is highly variable, and that is dependent on the specific competency that is being taught [16]. For example, a study of emergency medicine physicians found that with respect to right-upper quadrant ultrasound, image quality and clinical interpretation were significantly increased after performing seven ultrasounds, and that after 25 studies clinicians-in-training had obtained diagnostic accuracy equal to that of highly experienced providers [17]. Some skills have been shown to require little training and time to develop a high level of competency and diagnostic accuracy. In one study, critical care fellows received 4 h of didactic and hands-on training in compression ultrasonography to evaluate critically ill patients for deep venous thrombosis (DVT). The trainees then conducted 128 subsequent compression studies as part of their critical care duties and were found to have a very high level of diagnostic accuracy in diagnosing DVT compared to subsequent formal comprehensive radiology DVT studies [18]. A similar study of physicians-in-training in an academic emergency department found equally high levels of diagnostic accuracy with only a focused 10-min training session [19]. However, the development of many advanced skills, such as the ability to accurately assess subtle cardiac valvular abnormalities, requires very intensive training for an extended period of time [7].

The clinical confidence in interpreting acquired images also increases with time. A study of emergency medicine physicians who obtained certification in ultrasound found that there was a significant association between provider confidence in their image quality and interpretation in the accuracy of their diagnosis [20].

Web-Based/Computer

The use of web-based learning programs to augment hands-on and live didactic teaching in critical care ultrasound is quickly gaining popularity. Web-based education has proven to be particularly useful in helping intensivists to increase accuracy in image interpretation. A strength of web-based curricula is that they offer participants the flexibility to develop skills in image interpretation at their own pace and on their own time. In one recent study, intensivists who had completed a traditional didactic and hands-on course in critical care ultrasound were subsequently given access to a web-based learning program [21]. Completion of the web-based curriculum resulted in significant improvements in diagnostic accuracy. Clinicians also reported a significant increase in their confidence in their diagnoses after completing the web-based curriculum.

Simulation

Simulation-based medical education has the potential to greatly improve clinical knowledge and technical skills related to the use of critical care ultrasound. In one study, first-year anesthesia residents learning basic transesophageal echocardiography were randomized to traditional didactic teaching alone or to a 90-min simulator-based transesophageal echocardiography teaching session with a virtual 3-D model of a heart incorporated into a mannequin. Both groups were given pre- and post-training video-based questions pertaining to image interpretation and probe position and manipulation. While both groups showed an improvement on their post-training test scores, those that received simulation training scored significantly higher than the group that received traditional didactic training [22]. Another recent study found that the use of medical simulation with an ultrasound-compatible mannequin to train internal medicine residents in ultrasound-guided central venous catheter (CVC) placement resulted in significantly reduced rates of CVC complications and much greater reliance on ultrasonography for CVC placement compared to before the development of the medical simulation curriculum [23].

The use of medical simulation to facilitate the learning of critical care echocardiography image acquisition skills has become increasingly sophisticated in recent years. A variety of echocardiography simulators are currently available. One simulator utilizes real echocardiography data combined with a probe tip and an electromagnetic field in a mannequin (EchoCom, Leipzig, Germany) and can be used for TTE and TEE. Another medical simulator uses a digital model incorporated into a mannequin (CAE Healthcare Inc., Montreal, Canada) and can be used with TTE, TEE, and abdominal ultrasound probes. Many other simulators are available or are currently in development with varying levels of fidelity and capabilities [24].

Longitudinal Curriculum and Other Key Components

Longitudinal curricula (ongoing ultrasound education) during medical training have been shown to significantly increase both the quality of image acquisition and interpretation skills, compared to short intensive 1–3-day courses. One study of emergency medicine residents found that there was a significant increase in diagnostic accuracy after an intensive 1-month dedicated ultrasound rotation [25].

Other key components of critical care ultrasound curricula that have been identified in the literature include combining didactic teaching with equal amounts of hands-on time learning image acquisition; ongoing assessment and evaluation; and individualized review of student images by a clinician experienced in critical care ultrasound [8, 12, 26].

Incorporating Ultrasound Into an Educational Curriculum: Our Experience

Over the past several years we have developed a comprehensive ultrasound program for pulmonary and critical care fellows. First-year fellows attend a critical care ultrasound course taught by pulmonary and critical care faculty. A monthly 1-h ultrasound conference includes time for review of relevant critical care journal articles as well as image review and interpretation. Ongoing assessment of the developing skills of all fellows is conducted on an annual basis.

At our institution we also have a collegial relationship with our emergency medicine colleagues which offers further focused educational opportunities. Critical care fellows have a dedicated rotation with the emergency medicine ultrasound team. The program includes daily bedside ultrasound scanning rounds under the supervision of an experienced sonographer for instruction in hands-on skills (image acquisition) as well as recognition of normal anatomy and pathology (image recognition). In conjunction with weekly video review (open to residents, fellows, and attending physicians) there is a weekly ultrasound literature journal club to keep up-to-date with current literature as well as to review seminal articles. The video review allows junior sonographers to interpret and discuss a wide variety of normal and abnormal images with immediate feedback from advanced sonographers.

Based on our own experiences and on a review of the literature, we recommend a comprehensive approach to incorporate ultrasound into an educational training program. Key components include the following:

Introductory Didactic Course: Prior to a 2–3-day introductory course for intensivists, all participants should be given pre-course articles and course materials. Key curriculum components of an introductory critical care course include vascular access, DVT studies, pleural and lung, abdomen, and basic echocardiography. Strong consideration should be made to organizing a regional course with other programs so that resources such as faculty and ultrasound machines and standardized patients/models can be shared. Ideally, hands-on training should utilize a ratio of no greater than four learners to one instructor. Collaborating with other departments in your own institution that have a strong interest in critical care ultrasound (emergency medicine, surgery, pulmonary, anesthesia) can greatly enhance the quality of training and augment the resources available for an introductory course.

Ongoing Assessment: Ongoing assessment and training is essential. This can be initiated at the conclusion of the introductory course but should continue throughout clinical training. To assess basic technical skills at the conclusion of an introductory course, a hands-on assessment utilizing a checklist can be used to assess a trainee's competence. To evaluate clinical knowledge, a multiple choice test requiring interpretation of ultrasound films can be used. Keep in mind that skills that are used regularly, such as vascular access, will be maintained while skills that are less frequently practiced, such as DVT studies, will be quickly forgotten

by most trainees. For continued assessment of trainees throughout their clinical training we recommend assessment of both technical and clinical competence at the bedside. In addition, archiving software such as Q-path™ (Telexy HealthCare, Everett, Washington, USA) can facilitate retrospective review of a trainee's images offsite and allow ongoing feedback. In addition, establishing a regularly scheduled ultrasound case conference for image review and interpretation of saved films can be very useful for education, ongoing assessment, and quality control.

Faculty Development: There is currently a paucity of clinical faculty in many critical care programs adept at teaching ultrasound [27]. In many programs there may be only one or two intensivists, if any, who utilize critical care ultrasound as a regular part of their clinical practice. Training programs must make a conscious effort to develop the ultrasound skills and competencies of their own faculty. Expert faculty need to focus their educational efforts not only on their trainees but also on their colleagues. Divisional "train-the-trainer" programs and ongoing quality assessment of all images acquired in ICUs can be very helpful in this regard. Most importantly, faculty need to be supported and encouraged to obtain training and utilize critical care ultrasound on a regular basis in their own clinical practice.

Core Competencies

Multiple studies have shown that time-limited and focused ultrasound education in specific targeted areas can result in the attainment of competency. It is recommended that all intensivists develop specific basic competencies in vascular, thoracic, abdominal, and cardiac ultrasound [9].

Vascular (Chap. 3)

The ability to obtain ultrasound-guided vascular access is now an essential skill for all intensivists and should be considered standard of care [9]. Critical care physicians should be educated and trained in evidence-based best practices for ultrasound guided vascular access [28]. Intensivists should also be trained to develop competency in diagnosing DVT and in visualizing the aorta and inferior vena cava (IVC) [8].

Thoracic (Chaps. 9 and 10)

The ability to use ultrasound to diagnose pleuro-pulmonary disease, including pleural effusions, pulmonary edema, and pneumothorax, should be taught to all intensivists [9]. Utilizing ultrasound to safely perform thoracentesis and chest tube placement is an important skill that should be taught to all intensivists. There is growing evidence that basic lung ultrasound can easily and accurately be adopted by providers with limited prior experience. A study of 27 French physicians found that they could accurately diagnose pulmonary edema and pneumothorax with ultrasound after completing a brief training module [29].

Abdomen (Chap. 12)

Key components of abdominal ultrasound that intensivists should be trained in include identifying free fluid and assessing the kidneys and bladder. Procedural ultrasound to reduce complications from paracentesis is also a key competency [9].

Basic Echocardiography (Chaps. 5, 6, and 7)

Education of intensivists in basic echocardiography should focus on the development of competency in basic image acquisition and image interpretation that focuses on a qualitative and target-oriented approach. The curriculum should focus on developing the ability to answer focused and specific clinical questions. Education should emphasize the development of fundamental qualitative image interpretation skills utilizing standardized views of the left ventricle (LV) and right ventricle (RV). Training should focus on recognizing clear and unequivocal findings while emphasizing consulting expert echocardiographers for more subtle and equivocal findings [9]. Cognitive training should emphasize recognition of important clinical findings relevant to the intensivists such as hypovolemia (Chap. 4), LV failure, RV failure, and tamponade. In basic critical care echocardiography education and practice, the emphasis should at all times be on reviewing and confirming any abnormal findings with expert experienced echocardiographers. Education in basic critical care echocardiography should stress that any unusual findings have to be confirmed by expert consultation before they are deemed clinically relevant.

Cardiac Function

In the area of critical care echocardiography, several studies have shown that experienced intensivists can be trained to accurately assess cardiac function qualitatively. In one study in a medical ICU, attending intensivists with minimal ultrasound training

received 2 h of didactic training and 4 h of hands-on training in how to acquire basic cardiac images and qualitatively assess LV function. They were subsequently asked to assess LV function as normal, mildly to moderately decreased, or severely decreased. Their results were compared to the results obtained within 2 h of the initial study by certified sonographers and read by experienced echocardiographers. The intensivists correctly identified normal LV function 92 % of the time. The authors also found excellent concordance in the classification of decreased LV function between the goal-directed cardiac ultrasound and the results of the formal echocardiogram [30].

Other studies have looked at educating physicians-in-training. In one study, medical and anesthesia residents with minimal prior ultrasound experience were given 3 h of didactic training in goal-oriented echocardiography followed by 5 h of hands-on training in obtaining standard views of the heart. Trainees were then asked to assess LV systolic function and RV function as normal or abnormal in their ICU patients. Results were compared to studies obtained at the same time by intensivists with advanced (level III) echocardiography training. The study found excellent concordance in assessment for RV dilation and LV systolic dysfunction [31]. Subsequent studies of medical and anesthesia residents who received a more extensive 12-h curriculum also found a high level of concordance with the interpretations of skilled echocardiographers when assessing the cardiac function of ICU patients [32]. Similar results have also been found when emergency medicine residents were trained for 6 h in basic goal-directed echocardiography [33].

Advanced Transthoracic Echocardiography and Transesophageal Echocardiography (Chaps. 5 and 6)

Assessment of Valvular Function

The development of the skills and knowledge base for intensivists to accurately assess major abnormalities in valvular function by TTE requires additional time and effort. In one study, 100 intensivists, emergency medicine physicians, and anesthesiologists were given 16 h of training in both 2-D and Doppler goal-directed echocardiography. In addition to training in the assessment of ventricular function, didactic and hands-on training was provided in the assessment of valvular function. Participants were then asked to evaluate cases presented in video format. Their answers were compared to that of expert echocardiographers. In cases of moderate to severe valvular abnormalities, agreement between study participants and expert echocardiographers ranged from 90 % to 98 %. However, there was significantly less diagnostic accuracy among participants when it came to identifying mild valvular abnormalities [34]. A potential limitation of this study was that 10 % of study participants were anesthesiologists with significant experience in TEE.

TEE

While most basic educational programs emphasize TTE, the use of transesophageal echocardiography (TEE) for emergent assessment of unstable patients is becoming more commonplace. Recently, especially among academic anesthesiologists, there have been efforts to formally teach the use of focused TEE to rapidly assess critically ill surgical patients [35]. TEE has also been proposed as an advanced-level skill in the ICU for intensivists who desire more than basic training in critical care ultrasound [7].

Barriers to Training in Critical Care Ultrasound

A major barrier to implementing an ICU ultrasound program is the lack of qualified faculty. In a survey of critical care program directors, 41 % of respondents noted that they did not have proficient faculty members capable of training their fellows in critical care ultrasound. The survey also identified fellow turnover, financial constraints, and mistaken beliefs about the need to be a certified ultrasound technician to perform scans as barriers to ultrasound training and education in critical care fellowship programs. The study also found that while almost all programs teach trainees in the uses of ultrasound for vascular access and thoracentesis, only 55 % of programs instruct trainees in basic echocardiography and only 33 % instruct trainees in vascular diagnostic ultrasound [27]. As the use of critical care ultrasound becomes more widespread, more clinician-educators hopefully will develop the clinical competence to teach the next generation of intensivists [36, 37]. Developing the skills of additional critical care faculty beyond one or two people is essential to a sustained ICU ultrasound program.

Another barrier to implementing an ICU ultrasound program is potential resistance from other departments. Variable acceptance from other departments (e.g., cardiology, radiology) of new point-of-care ultrasound programs should be expected and anticipated. This resistance often stems from a misunderstanding about the nature and function of point-of-care ultrasound. Specifically, it is different from radiology comprehensive exams in terms of time to result (seconds/minutes vs. minutes/hours), scope (limited, focused exam vs. comprehensive examination), sonographer (clinician-performed/clinician interpreted vs. technician-performed/radiologist interpreted), and cost/billing codes (limited/clinician-performed vs. comprehensive exam). American Medical Association House of Delegates resolution 802 (AMA resolution HR 802) supports hospital credentialing committees to grant point-of-care ultrasound privileging based on specialty-specific guidelines without the need to seek approval from other departments [38]. Resistance from other departments, however, can be a potential obstacle to implementing a comprehensive ICU ultrasound program. Developing strong quality control, ICU credentialing, and ongoing educational efforts can help obviate these concerns.

Potential Pitfalls

Potential diagnostic and technical pitfalls that must be emphasized in any ultrasound education training program include incomplete image acquisition, improper image acquisition, and incorrect image interpretation (i.e., diagnosing cardiac tamponade when there is only a pleural and not a pericardial effusion) [1]. Like clinical training in any modality, education programs must emphasize strategies for avoiding misdiagnoses that carry significant clinical and legal consequences and recognizing the potential limitations of the technology used [2].

A major pitfall to implementing an ICU ultrasound program is starting a program too quickly without quality assessment and educational programs in place from the outset. Such programs are usually of poor quality and may quickly fail. It is essential to institute an ongoing hospital-approved quality review process with image and video review, as well as to provide feedback to trainees and clinicians. If there are no strict quality assurance measures in place, the utilization of ultrasound in the ICU occurs haphazardly and can be a detriment rather than an asset to patient care, and the program will not be sustainable.

It is essential to provide continuous feedback, assessment, and correlation with intra-departmental video review interpretations as well as with any formal radiology and echocardiographic exams. Cases that require review, including those that involve errors in point-of-care ultrasound, should be discussed at standard departmental morbidity and mortality conferences. Finally, there should be departmental policies established to prepare for incidental findings or discrepancies that may arise.

Conclusions

In conclusion, as the use of goal-directed ultrasound becomes widespread in the care of critically ill patients, formally educating providers is crucial to ensuring quality care. The continued development of effective standardized program requirements and curricula is very important, as is further developing and defining issues of certification and accreditation. All educational efforts should incorporate a variety of different modalities, including web-based curriculums, didactic training, the use of medical simulation, and image review by teachers experienced in critical care ultrasound. Ongoing review processes should be in place to ensure continued quality and safety.

References

1. Huang SJ, McLean AS. Do we need a critical care ultrasound certification program? Implications from an Australian medical-legal perspective. Crit Care. 2010;14(3):313.

2. Lau G, Swanevelder J. Echocardiography in intensive care–where we are heading? Anaesthesia. 2011;66(8):649–52.
3. Bennett S. Training guidelines for ultrasound: worldwide trends. Best Pract Res Clin Anaesthesiol. 2009;23(3):363–73.
4. Marik PE, Mayo P. Certification and training in critical care ultrasound. Intensive Care Med. 2008;34(2):215–7.
5. Beaulieu Y. Specific skill set and goals of focused echocardiography for critical care clinicians. Crit Care Med. 2007;35(5 Suppl):S144–9.
6. Vieillard-Baron A, Slama M, Cholley B, Janvier G, Vignon P. Echocardiography in the intensive care unit: from evolution to revolution? Intensive Care Med. 2008;34(2):243–9.
7. Price S, Via G, Sloth E, Guarracino F, Breitkreutz R, Catena E, et al. Echocardiography practice, training and accreditation in the intensive care: document for the World Interactive Network Focused on Critical Ultrasound (WINFOCUS). Cardiovasc Ultrasound. 2008;6:49.
8. International expert statement on training standards for critical care ultrasonography. Intensive Care Med. 2011;37(7):1077–83
9. Mayo PH, Beaulieu Y, Doelken P, Feller-Kopman D, Harrod C, Kaplan A, et al. American College of Chest Physicians/La Societe de Reanimation de Langue Francaise statement on competence in critical care ultrasonography. Chest. 2009;135(4):1050–60.
10. McLean A, Yastrebov K. Echocardiography training for the intensivist. Crit Care Resusc. 2007;9(4):319–22.
11. WINFOCUS. USCMC Certification. 2014. Available from: http://www.winfocus.org/uscme/uscmc/certification. Accessed 18 Feb 2014.
12. Neri L, Storti E, Lichtenstein D. Toward an ultrasound curriculum for critical care medicine. Crit Care Med. 2007;35(5 Suppl):S290–304.
13. Accreditation Council for Graduate Medical Education A. ACGME Program Requirements for Graduate Medical Education in Critical Care Medicine. 2012. Available from: http://www.acgme.org/acgmeweb/Portals/0/PFAssets/ProgramRequirements/142_critical_care_int_med_07012012.pdf Accessed 9 Apr 2014.
14. American College of Graduate Medical Education A. ACGME Program Requirements for Graduate Medical Education in Emergency Medicine. 2013. Available at: http://www.acgme.org/acgmeweb/Portals/0/PFAssets/2013-PR-FAQ-PIF/110_emergency_medicine_07012013.pdf. Accessed 13 May 2014.
15. Akhtar S, Theodoro D, Gaspari R, Tayal V, Sierzenski P, Lamantia J, et al. Resident training in emergency ultrasound: consensus recommendations from the 2008 Council of Emergency Medicine Residency Directors Conference. Acad Emerg Med. 2009;16 Suppl 2:S32–6.
16. Jang TB, Ruggeri W, Dyne P, Kaji AH. Learning curve of emergency physicians using emergency bedside sonography for symptomatic first-trimester pregnancy. J Ultrasound Med. 2010;29(10):1423–8.
17. Gaspari RJ, Dickman E, Blehar D. Learning curve of bedside ultrasound of the gallbladder. J Emerg Med. 2009;37(1):51–6.
18. Kory PD, Pellecchia CM, Shiloh AL, Mayo PH, DiBello C, Koenig S. Accuracy of ultrasonography performed by critical care physicians for the diagnosis of DVT. Chest. 2011;139(3):538–42.
19. Crisp JG, Lovato LM, Jang TB. Compression ultrasonography of the lower extremity with portable vascular ultrasonography can accurately detect deep venous thrombosis in the emergency department. Ann Emerg Med. 2010;56(6):601–10.
20. Davis DP, Campbell CJ, Poste JC, Ma G. The association between operator confidence and accuracy of ultrasonography performed by novice emergency physicians. J Emerg Med. 2005;29(3):259–64.
21. Sekiguchi H, Bhagra A, Gajic O, Kashani KB. A general critical care ultrasonography workshop: results of a novel web-based learning program combined with simulation-based hands-on training. J Crit Care. 2013;28(2):217.e7–12.

22. Bose RR, Matyal R, Warraich HJ, Summers J, Subramaniam B, Mitchell J, et al. Utility of a transesophageal echocardiographic simulator as a teaching tool. J Cardiothorac Vasc Anesth. 2011;25(2):212–5.
23. Sekiguchi H, Tokita JE, Minami T, Eisen LA, Mayo PH, Narasimhan M. A prerotational, simulation-based workshop improves the safety of central venous catheter insertion: results of a successful internal medicine house staff training program. Chest. 2011;140(3):652–8.
24. Shakil O, Mahmood F, Matyal R. Simulation in echocardiography: an ever-expanding frontier. J Cardiothorac Vasc Anesth. 2012;26(3):476–85.
25. Mahler SA, Swoboda TK, Wang H, Arnold TC. Dedicated emergency department ultrasound rotation improves residents' ultrasound knowledge and interpretation skills. J Emerg Med. 2012;43(1):129–33.
26. Mazraeshahi RM, Farmer JC, Porembka DT. A suggested curriculum in echocardiography for critical care physicians. Crit Care Med. 2007;35(8 Suppl):S431–3.
27. Eisen LA, Leung S, Gallagher AE, Kvetan V. Barriers to ultrasound training in critical care medicine fellowships: a survey of program directors. Crit Care Med. 2010;38(10):1978–83.
28. Lamperti M, Bodenham AR, Pittiruti M, Blaivas M, Augoustides JG, Elbarbary M, et al. International evidence-based recommendations on ultrasound-guided vascular access. Intensive Care Med. 2012;38(7):1105–17.
29. Noble VE, Lamhaut L, Capp R, Bosson N, Liteplo A, Marx JS, et al. Evaluation of a thoracic ultrasound training module for the detection of pneumothorax and pulmonary edema by prehospital physician care providers. BMC Med Educ. 2009;9:3.
30. Melamed R, Sprenkle MD, Ulstad VK, Herzog CA, Leatherman JW. Assessment of left ventricular function by intensivists using hand-held echocardiography. Chest. 2009;135(6):1416–20.
31. Vignon P, Dugard A, Abraham J, Belcour D, Gondran G, Pepino F, et al. Focused training for goal-oriented hand-held echocardiography performed by noncardiologist residents in the intensive care unit. Intensive Care Med. 2007;33(10):1795–9.
32. Vignon P, Mucke F, Bellec F, Marin B, Croce J, Brouqui T, et al. Basic critical care echocardiography: validation of a curriculum dedicated to noncardiologist residents. Crit Care Med. 2011;39(4):636–42.
33. Jones AE, Tayal VS, Kline JA. Focused training of emergency medicine residents in goal-directed echocardiography: a prospective study. Acad Emerg Med. 2003;10(10):1054–8.
34. Royse CF, Haji DL, Faris JG, Veltman MG, Kumar A, Royse AG. Evaluation of the interpretative skills of participants of a limited transthoracic echocardiography training course (H.A.R.T.scan course). Anaesth Intensive Care. 2012;40(3):498–504.
35. Peng YG, Janelle GM. Emergent limited perioperative transesophageal echocardiography: should new guidelines exist for limited echocardiography training for anesthesiologists? Front Med. 2012;6(3):332–7.
36. Poelaert J, Mayo P. Education and evaluation of knowledge and skills in echocardiography: how should we organize? Intensive Care Med. 2007;33(10):1684–6.
37. Kaplan A, Mayo PH. Echocardiography performed by the pulmonary/critical care medicine physician. Chest. 2009;135(2):529–35.
38. Moore CL, Gregg S, Lambert M. Performance, training, quality assurance, and reimbursement of emergency physician-performed ultrasonography at academic medical centers. J Ultrasound Med. 2004;23(4):459–66.

Chapter 3
Ultrasound for Vascular Access

Abdullah Sulieman Terkawi, Ariel L. Shiloh, Mahmoud Elbarbary, and Dimitrios Karakitsos

Introduction

Central venous access is an invasive procedure that carries its own inherent life-threatening risks and complications (Table 3.1) [1–4]. Precision and protocol are required for implementation of a proper ultrasound technique. In the intensive care unit (ICU), central venous access is required for fluid management in shock patients, delivery of inotropes and vasopressors, measurements and monitoring of central venous pressure, total parenteral nutrition, hemodialysis, plasmapheresis, transvenous pacemakers, and facilitation of vascular and cardiac procedures.

Electronic supplementary material Supplementary material is available in the online version of this chapter at 10.1007/978-1-4939-1723-5_3. Videos can also be accessed at http://www.springerimages.com/videos/978-1-4939-1722-8.

A.S. Terkawi, M.D. (✉)
Department of Anesthesiology, University of Virginia, P.O. Box 800710, Charlottesville, VA 22903, USA
e-mail: asterkawi@gmail.com

A.L. Shiloh, M.D.
Jay B. Langner Critical Care Service, Montefiore Medical Center/Albert Einstein College of Medicine, 111 E. 210th St, Bronx, NY 10467, USA
e-mail: ashiloh@montefiore.org

M. Elbarbary
Pediatric Cardiac ICU, King Abdulaziz Cardiac Center, King Saud Bin Abdulaziz University for Health Sciences, Riyadh, Saudi Arabia
e-mail: elbarbary.mahmoud@yahoo.com

D. Karakitsos, M.D., Ph.D., D.Sc.
Department of Internal Medicine, University of South Carolina, School of Medicine, Building 3, DVAMC Campus, 216-3301, Columbia, SC 29208, USA
e-mail: karakitsosdimitrios@gmail.com

M. Jankowich, E. Gartman (eds.), *Ultrasound in the Intensive Care Unit*, Respiratory Medicine, DOI 10.1007/978-1-4939-1723-5_3

Table 3.1 Complications of central venous access

Regional
Immediate
• Inadvertent arterial puncture
• Hematoma
• Pneumothorax
• Hemothorax
• Catheter malposition
• Air embolism
• Arrhythmias
• Thoracic duct injury (left neck)
• Brachial plexus nerve injury
Late
• Lumen occlusion
• Venous thrombosis
• Arteriovenous fistula
• Exit-site infection
Systemic
• Catheter-related bloodstream infection (CRBSI)

Table 3.2 Advantages of ultrasound-guided central venous access

• Increased cannulation success rate
• Increased first-attempt success
• Decreased complication rate
• Detection of anatomical variation
• Detection of thrombosis
• Optimal vessel selection (e.g., internal jugular, subclavian, femoral vein)
• Confirmation of catheter site
• Rule out complications (e.g., pneumothorax)

Insertion is contraindicated at sites of infection or thrombosis. Relative contraindications include severe coagulopathy and bleeding disorders, systemic infection, presence of a right ventricular assist device, or pacing wires at the insertion site [5]. Advantages of ultrasound-guided vascular access (UGVA) are summarized in Table 3.2 and further analyzed in this chapter.

Traditional sites for central venous access are the internal jugular, subclavian, and femoral veins. Additionally, over the past decade, peripherally inserted central catheters (PICC) have gained popularity and have been increasingly used in patients needing prolonged central venous access. Ultrasound guidance has been used to augment successful placement of peripheral intravenous lines and arterial catheters – especially in patients with difficult anatomic landmarks or in the very young.

Technical and Patient Considerations

Vein Selection

A pre-procedural scan is strongly recommended to guide the selection of an optimal target vessel [6]. Criteria that favor the selection of a vein are:

1. Vessel patency (venous collapse during breathing or compression without signs of thrombosis)
2. Easy accessibility (measure the distance between the skin surface and the vessel wall)
3. Diameter (vessel size less than three times the caliber of catheter may carry a greater risk for thrombosis) [7].
4. Anatomical variation
5. Intended purpose (i.e., neck surgery often requires infra-clavicular vascular access)
6. Intended duration for catheter placement

Complication rates after the implementation of landmark techniques differ between sites. The internal jugular vein carries the highest risk of accidental arterial puncture and hematoma, the subclavian carries the highest risk for pneumothorax, hemothorax, and catheter malposition, while the femoral vein carries the highest risk for thrombosis and infection (Table 3.3) [1, 5, 8]. The 2011 Guidelines for the Prevention of Intravascular Catheter-Related Infections recommends the use of the subclavian vein site (rather than internal jugular or femoral veins) in adult patients to minimize the risk of infection. However, the aforementioned guidelines were based on data obtained prior to the introduction of standardized insertion bundles and modern anti-infective techniques such as the use of chlorhexidine gluconate (CHG) dressing devices. Recent studies show that CHG-impregnated sponge dressing when used with the standard care decreases the incidence of major catheter-related infections from 1.4 to 0.6 per 1,000 catheter-days [9].

Table 3.3 Complication rates in different central veins[a]

Complication	Internal jugular [1]	Subclavian [8]	Femoral [5]
Arterial puncture %	10.6	5.4	6.25
Hematoma %	8.4	5.4	–
Pneumothorax %	2.4	4.9	–
Hemothorax %	1.7	4.4	–
Malposition %	–	11	–
Infection (rate per 1,000 catheter-days) [5]	8.6	4	15.3
Thrombosis (rate per 1,000 catheter-days) [5]	1.2–3	0–13	8–34

[a]Results associated with the landmark/blind method

Pre-procedural Preparations

- Selection of probe: a high-frequency (10–15 MHz) linear probe (Fig. 3.1) is commonly used for UGVA, while low frequency curved-array probes (Fig. 3.2) are reserved for vessels that might be located deeper than expected for various reasons (i.e., obese patients, subcutaneous edema, anatomical anomalies, etc.). Hockey-stick probes bearing smaller footprints are oftentimes used in pediatric patients and in neonates (Fig. 3.3).
- Sterile techniques should be followed in all cases: hand washing, full sterile barrier protection, sterile probe cover and gel (Figs. 3.4) [6].
- The ultrasound machine should be positioned opposite to the operator to facilitate direct and straightforward visualization of the screen (Fig. 3.5).

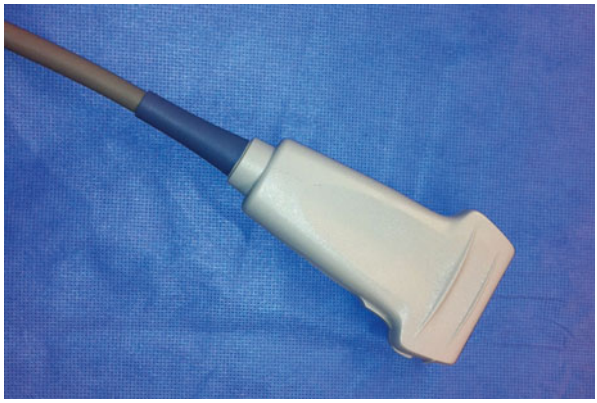

Fig. 3.1 A high-frequency linear probe is commonly used for vascular scanning

Fig. 3.2 A low-frequency convex probe can be used to scan vessels located at greater depth from the skin surface as low-frequency enhances the deeper penetration of the ultrasound beam

Fig. 3.3 A hockey-stick probe combines high-frequency scanning with a smaller footprint and is commonly used in pediatric patients

Fig. 3.4 A standard central venous access kit and ultrasound probe with a sterile cover

Tips to Differentiate Veins from Arteries

- Shape: arteries tend to be circular and veins elliptical.
- Size: the vein is usually larger than the adjacent artery and increases in size with Trendelenburg positioning.
- Compressibility: veins are easily compressible.
- Color flow fills venous lumen completely (color mode).
- Normal central venous flow on Doppler mode demonstrates spontaneity, phasicity, and augmentation.

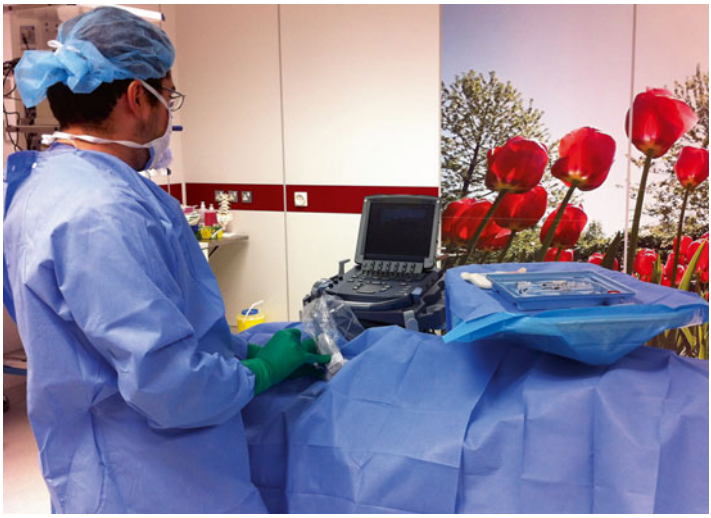

Fig. 3.5 The ultrasound machine is positioned opposite to the operator to facilitate direct and straightforward visualization of the screen in this supraclavicular cannulation of the right subclavian vein

Procedure Checklist and Bundle

The American Society of Anesthesiologists Task Force on Central Venous Access recommends the use of a central line insertion work and safety checklist and bundling of required equipment to minimize errors, risk of infection, and complications [10]. These simple measures (Pronovost's checklist) have shown tremendous reduction (up to 66 %) in central line-associated bloodstream infections (CLABSIs) [11].

Image Acquisition and Interpretation

A few practical tips when performing an ultrasound-guided central venous cannulation for the first time include:

- Always adhere to a strict sterilization process by implementing a sterile probe cover and sterile gel as previously mentioned.
- Initially, avoid pressing too hard with the probe on the cannulation site as normal veins are collapsible vessels (Fig. 3.6).

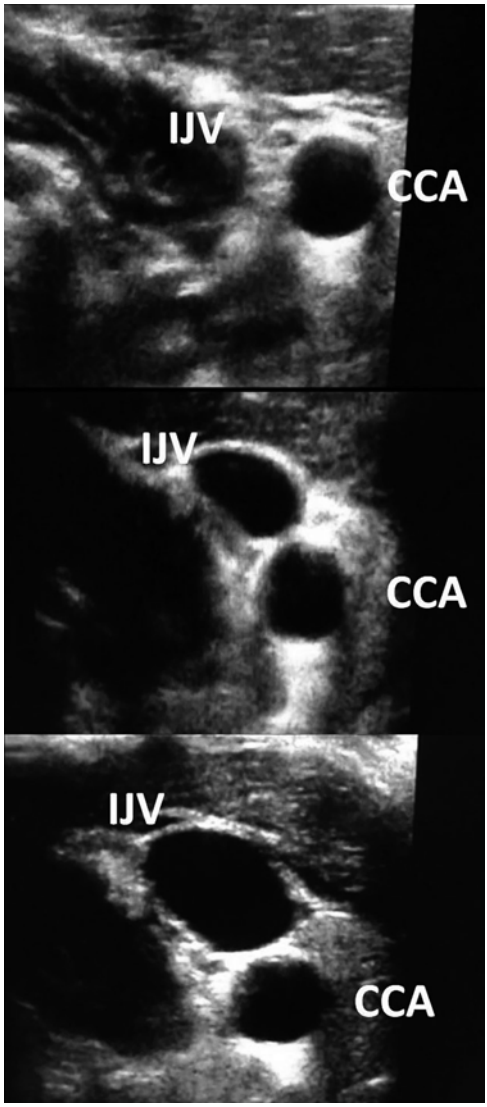

Fig. 3.6 Applying full probe pressure this patent internal jugular vein (IJV) which accompanies the common carotid artery (CCA) in the left lateral neck fully collapses and vanishes (*top*) while using less (*middle*) and light (*bottom*) probe pressure the vein gradually reappears until it reaches its full size (*bottom*)

- Optimize the two-dimensional image: center the image on the screen and adjust depth, gain, and focus, while obtaining the proper orientation of anatomy with standardization of the dot on the left.
- Once the two-dimensional image of the vein is obtained, check its patency by applying probe pressure to exclude thrombosis (Video 3.1).

Two-dimensional ultrasound can demonstrate either a short-axis view (a transverse view of the vessels) or a long-axis view (a longitudinal view of the vessels). The

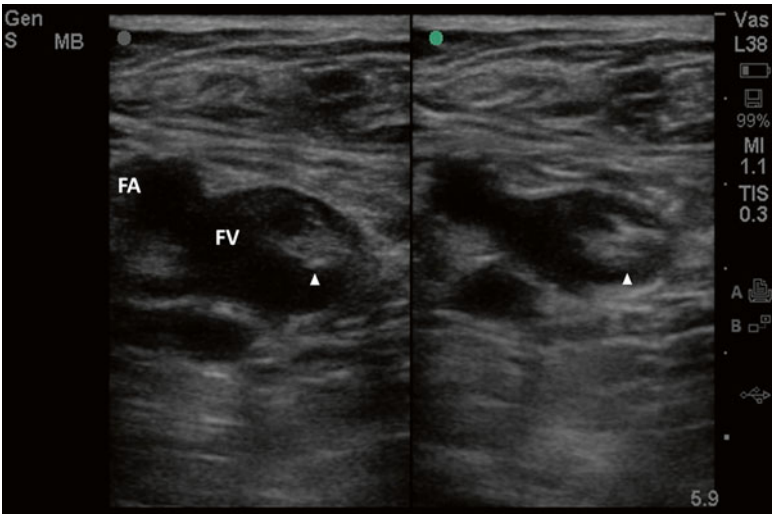

Fig. 3.7 Femoral vein thrombosis: Compression with the probe fails to collapse the vessel. *FA* femoral artery, *FV* femoral vein, *Arrow head* denotes thrombus

longitudinal axis view allows for continuous visualization of the needle trajectory and reduces the risk of posterior wall puncture. However, it requires advanced procedural skill and experience to synchronize the needle trajectory within the real-time ultrasound image. When using color-Doppler mode, operators should interpret the generated color (blue or red) dependent on probe orientation. Flow directed towards the probe will generate a red shift and flow directed away from the probe will generate a blue shift. Thus, red and blue shades in color flow do not necessarily represent the respective artery and vein but the direction of flow towards or away from the probe.

Pre-procedural scanning: detection of vessel size and patency and exclusion of possible thrombosis (Fig. 3.7). Notably, pre-procedural lung ultrasound should also be performed to exclude pneumothorax (Fig. 3.8) and thus confirm the presence of a normal aeration pattern.

For obvious reasons, catheter insertion should not be attempted when a preexisting clot exists in the target vessel. It is essential to scan the latter prior to catheterization to exclude thrombosis, especially in ICU patients. Notably, 90 % of potential thrombi originate from the femoral-popliteal system; however, upper extremity deep venous thrombosis may also occur in ICU patients. In a cohort of critical care patients, Blaivas et al. reported an incidence of upper extremity deep vein thrombosis around 11.25 % [12]. Risk factors included central venous catheter-associated

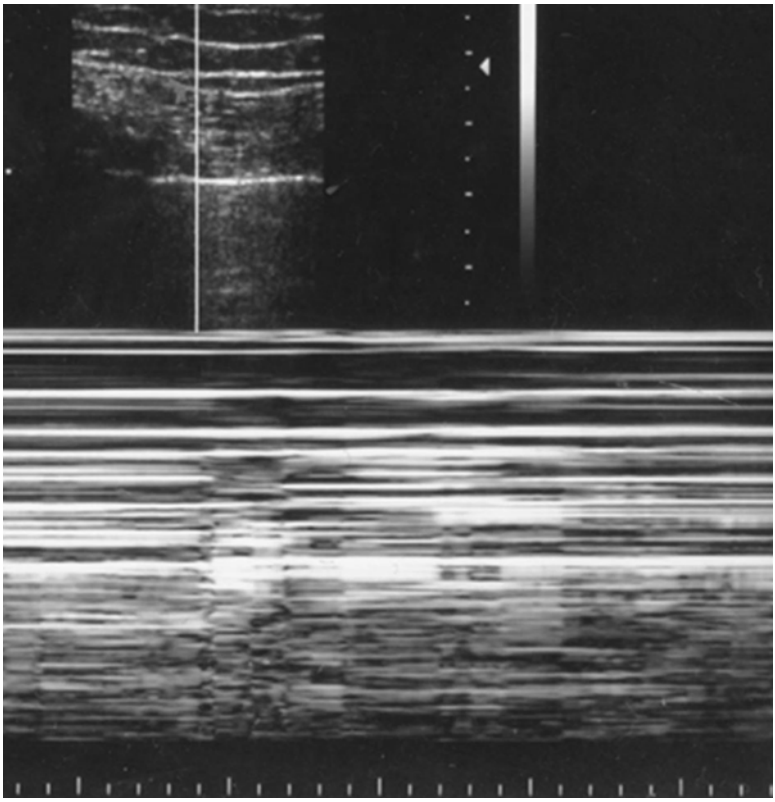

Fig. 3.8 Depiction of the barcode sign (indicative of pneumothorax) on M-mode in a patient's left anterior chest (mid-clavicular line) prior to cannulation

thrombosis, malignancy, total parenteral nutrition, hypercoagulable states, and obesity (body mass index or BMI $\geq$35 kg/m^2).

Ultrasound signs of venous thrombosis include lack of complete vein compression, presence of intraluminal echoes (although acute thrombus can be echolucent), decrease or absence of color flow. Also, venous Doppler demonstrates decreased or absent spontaneity, phasicity or augmentation and either dilated or contracted veins (Fig. 3.9). The sonographic detection of thrombosis aids in the diagnosis of catheter-related infections [13].

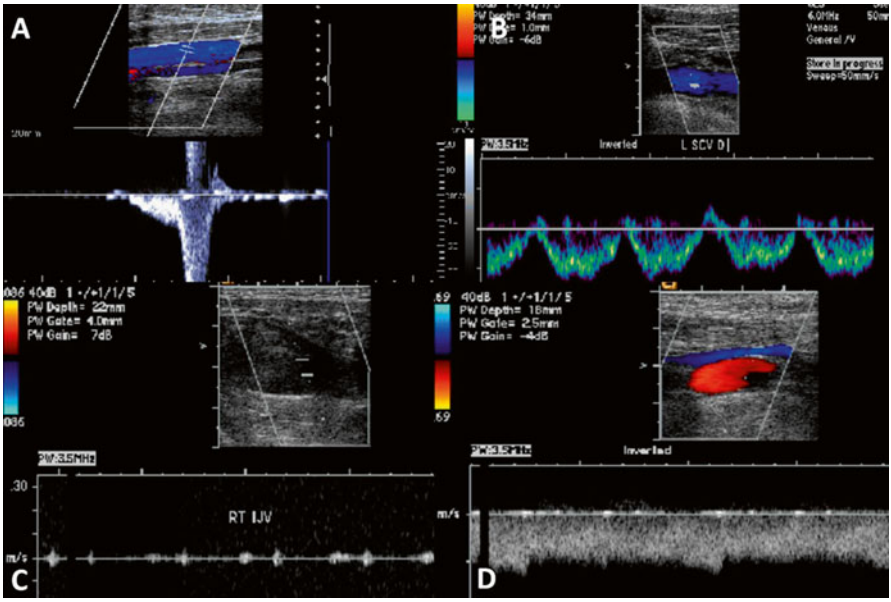

Fig. 3.9 Normal venous flow is spontaneous (automatically heard with Doppler), phasic (flow increases and decreased with respiration), and augmented (increased with distal compression). Although normal Doppler signs may be present with partially occlusive thrombosis, the usual Doppler findings include: absence of spontaneity (no venous flow) indicating venous obstruction, continuous flow indicating proximal obstruction or extrinsic compression, while distal compression does not produce augmentation. Note the flow augmentation in a normal brachial vein that has been compressed distally (**a**) and the spontaneous, phasic flow occurring in a normal subclavian vein (**b**). Observe the absence of flow in a totally thrombosed internal jugular vein (**c**) and continuous flow in an extrinsically compressed internal jugular vein (**d**)

Basic Competencies

Operators who perform ultrasound-guided placement of central venous catheters should be familiar with the sonoanatomy of the cannulation site and possess basic ultrasound skills such as the ability to differentiate between arteries and veins, detect venous thrombosis, and select the optimal vessel for cannulation. We recommend using real-time techniques where the operator moves the probe and needle slowly, in a simultaneous fashion, to ensure that the needle tip is visualized continuously [6]. This technique can be performed by a freehand approach or by the implementation of needle guides which keep the needle attached to the plane of the probe at all times. The former approach is technically demanding as it depends largely on the fine coordination of probe positioning and needle movement; however, it allows a great degree of freedom in maneuvers and adjustments of the penetrating needle trajectory (Figs. 3.10 and 3.11).

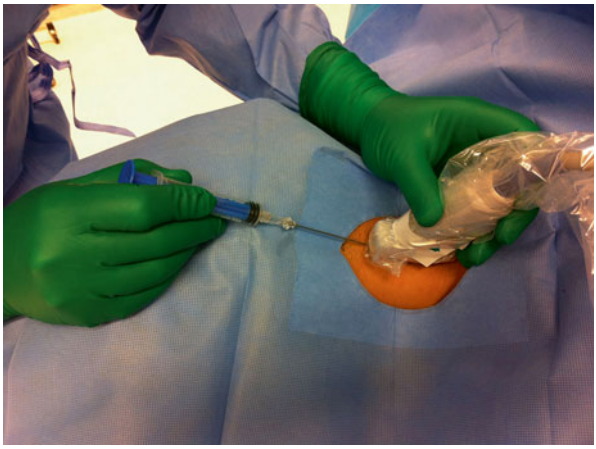

Fig. 3.10 Freehand access cannulation of the internal jugular vein on the long axis requires fine coordination of movements (note that the plane and trajectory of the needle follows the plane of the probe)

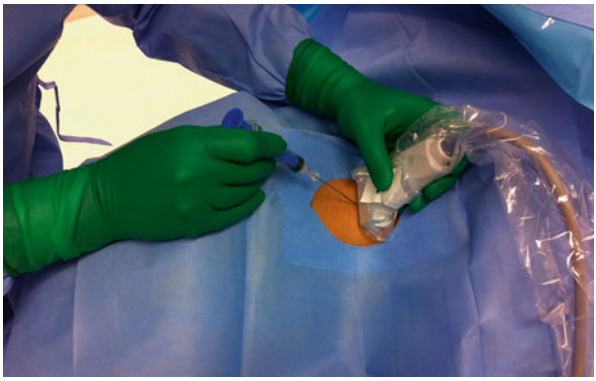

Fig. 3.11 Freehand access cannulation of the internal jugular vein on the short axis is relatively easier compared to the long-axis approach. However, needle visualization on the short-axis approach is more problematic (note that the angle of the penetrating needle is around 40–45°)

Internal Jugular Vein Cannulation

Anatomy

The internal jugular vein drains blood from the brain, face, and neck. It begins at the jugular foramen in the skull, merges through the carotid sheath (along with the common carotid artery medially and vagus nerve posteriorly), and joins the subclavian vein behind the medial end of the clavicle to form the brachiocephalic vein. Rotating the head will lead to overlapping of internal jugular vein with the common carotid artery. The thoracic duct ascends on the left side of the neck along the left margin of the esophagus until C-7, where it bends laterally behind the carotid sheath and then turns down again to drain into the left brachiocephalic vein [14].

Procedure

A high-frequency linear transducer is placed over the groove between the sternal and clavicular head of the sternocleidomastoid muscle at the lateral side of the neck (Figs. 3.10 and 3.11). Pre-procedural scanning is performed to identify the adjacent structures and evaluate the vein's depth, caliber, and patency (Figs. 3.12, 3.13, and 3.14). Electrocardiogram monitoring is necessary to evaluate the occurrence of possible dysrhythmias during guide wire insertion. Strict sterility is achieved by means

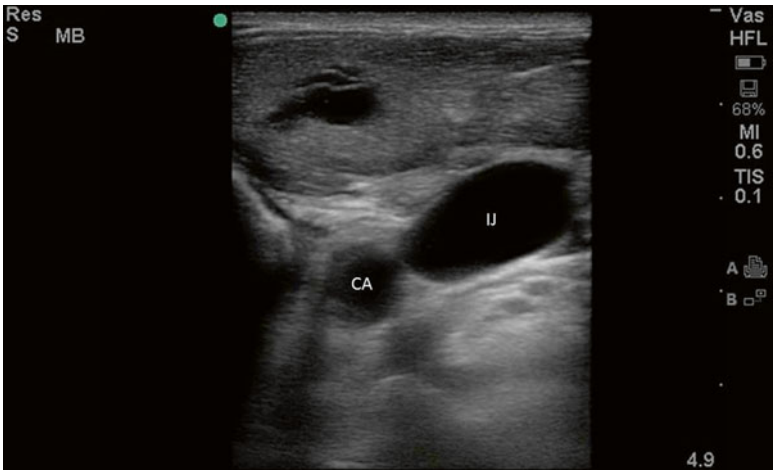

Fig. 3.12 Transverse view of the internal jugular vein and carotid artery. *CA* carotid artery, *IJ* internal jugular vein

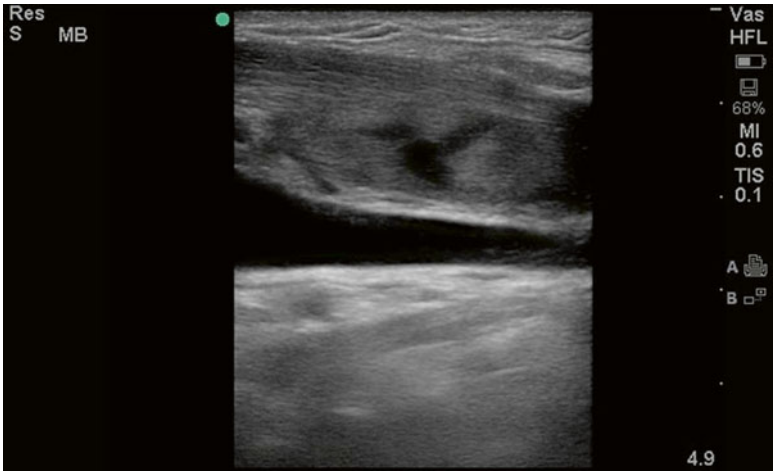

Fig. 3.13 Longitudinal view of the internal jugular vein

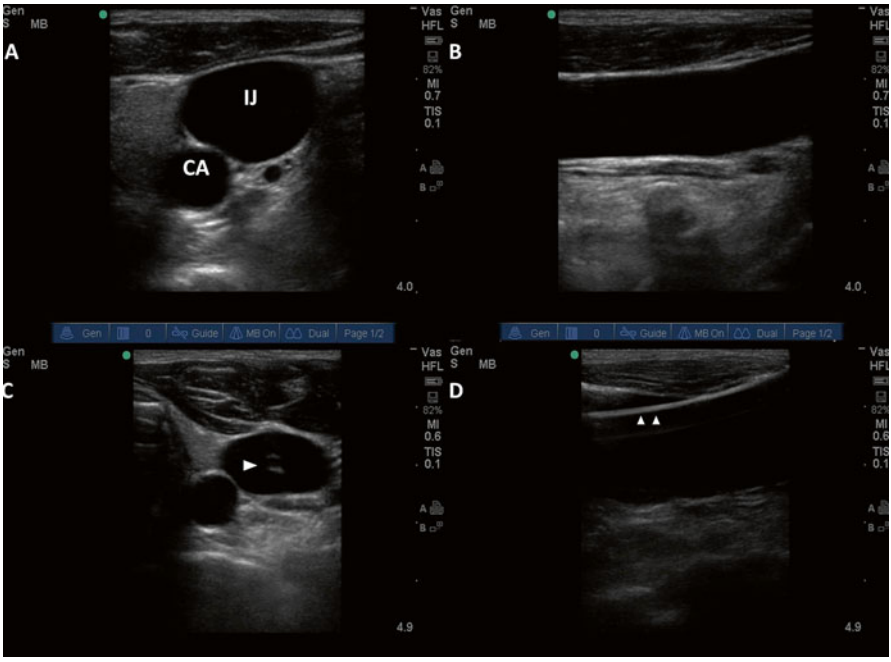

Fig. 3.14 Internal jugular vein cannulation (short-axis technique): (**a**) transverse view *IJ* internal jugular vein, *CA* carotid artery; (**b**) longitudinal view of the internal jugular vein; (**c**) needle tip in the vessel lumen denoted by *arrow head*; (**d**) guide wire confirmation in longitudinal view denoted by *arrow heads*

of a sterile probe cover and sterile single-use gel as previously described. The internal jugular vein can be cannulated using either the long-axis or short-axis techniques. When using the short-axis technique the penetration angle of the needle is usually around 45 ° to the skin (Fig. 3.11).

Subclavian Vein Cannulation

Anatomy

The axillary vein is the continuation of the brachial vein into the chest wall and becomes the subclavian vein as it passes medially under the first rib. The subclavian vein joins the internal jugular vein at the medial border of scalenus anterior, where it gives rise to the brachiocephalic vein (also known as the innominate vein). Notably, the dome of the pleura is adjacent to the subclavian vein. In the blind landmark technique, the deltopectoral groove formed at the inferior junction of the middle and medial third of the clavicle is the most common needle insertion site [14].

Procedure

The patient is placed in a supine position with a slight retraction of the shoulder to best expose the vein. The needle bevel should be directed anteriorly during insertion and then be turned caudally upon venipuncture to direct the guide wire toward the right atrium. Electrocardiographic monitoring and sterile techniques should be applied as previously described. Ultrasound-guided cannulation of the subclavian vein can be achieved using either a supraclavicular or an infraclavicular approach (Figs. 3.15, 3.16, 3.17, 3.18, 3.19, and 3.20).

- *Supraclavicular approach*

  Key points of this approach include:

  – Scan the neck and localize the internal jugular vein. Follow the vein caudally to the junction of the subclavian vein, orient the probe in the longitudinal axis in the supraclavicular fossa, and angulate it anteriorly. The subclavian vein is usually seen (within 1–2 cm) at the level where it joins the brachiocephalic vein medially.
  – Identify the adjacent structures (e.g., artery and pleura).

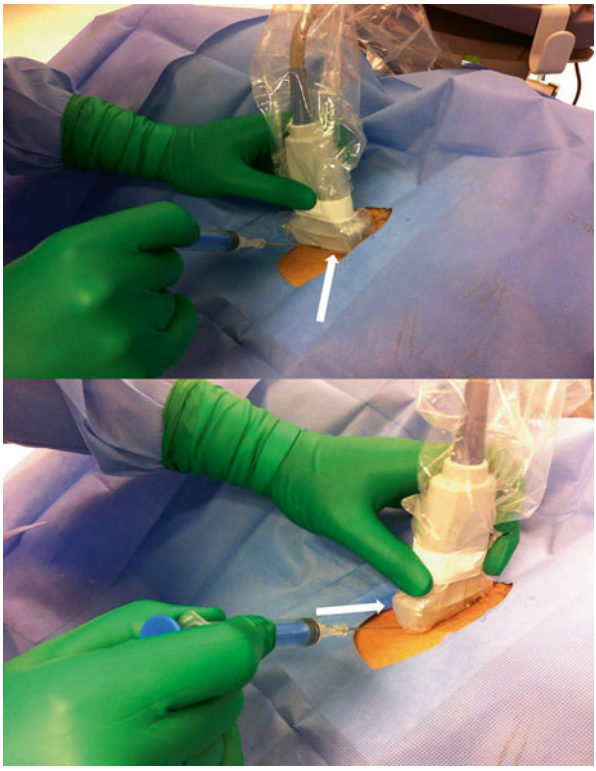

Fig. 3.15 Supraclavicular short-axis approach (*top*) and infraclavicular long-axis approach (*bottom*) in the cannulation of the subclavian vein (the *arrow* is showing the position of the clavicle)

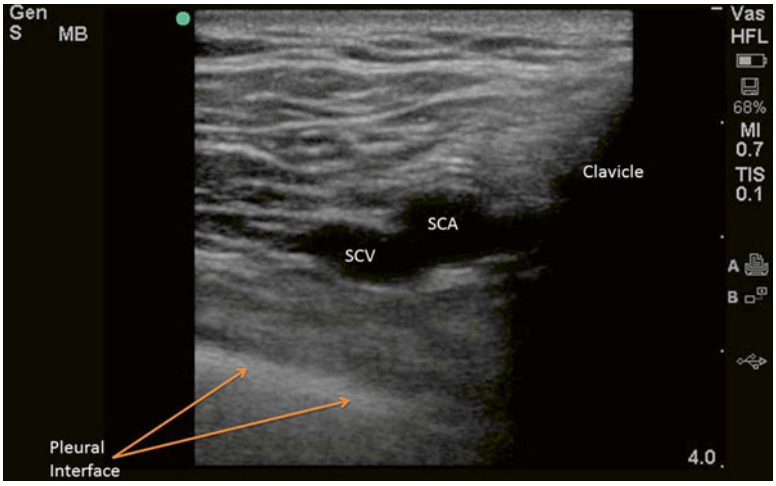

Fig. 3.16 Transverse view of the infraclavicular subclavian vasculature demonstrating the relationship of the vessels to the pleural interface and clavicle. *SCA* subclavian artery, *SCV* subclavian vein

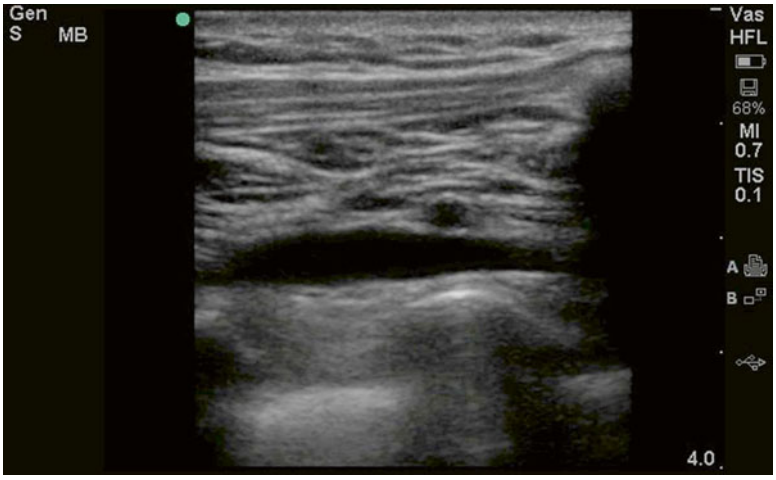

Fig. 3.17 Longitudinal view of the infraclavicular subclavian vein

- At the back of the clavicle insert the needle just lateral to the probe (long-axis), while directing the needle tip slowly towards the sternal notch.
- Under ultrasound guidance the guide wire is introduced; then, the ipsilateral internal jugular vein is scanned before catheter insertion to rule out malpositioning of the guide wire.

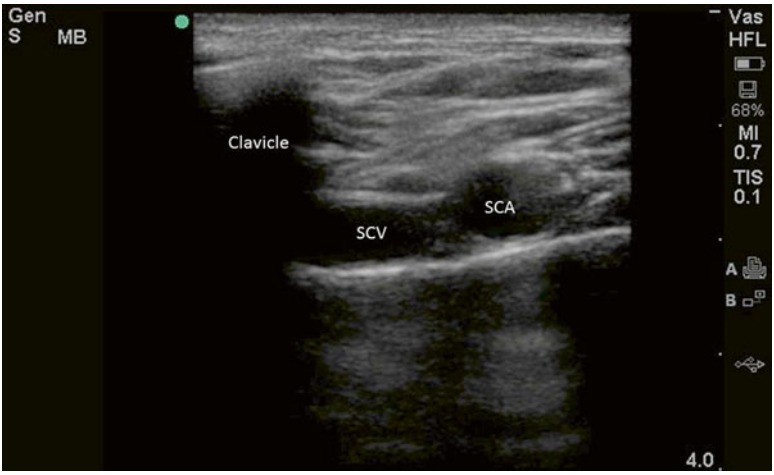

Fig. 3.18 Transverse view of the supraclavicular subclavian vasculature demonstrating the relationship of the vessels to clavicle. *SCA* subclavian artery, *SCV* subclavian vein

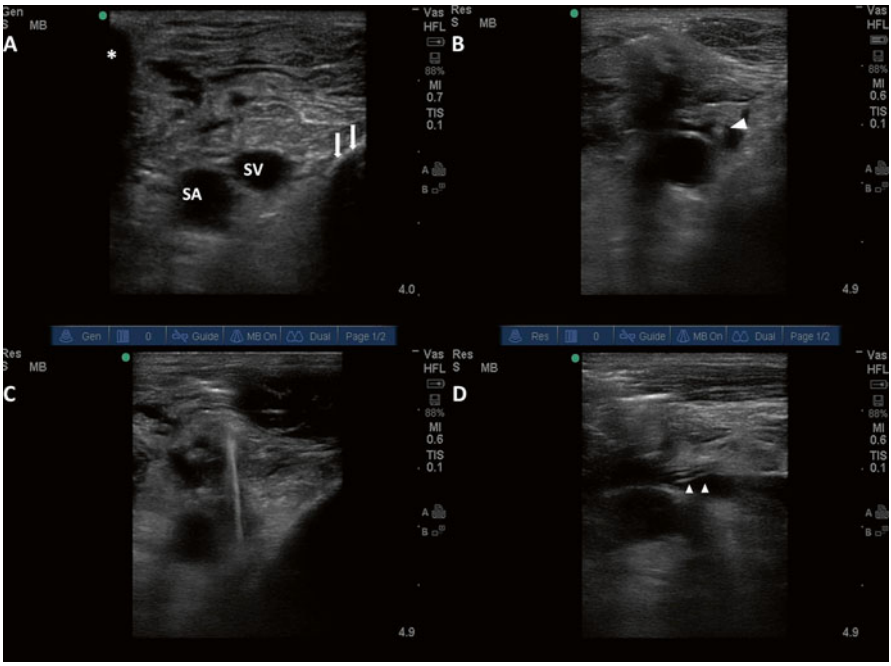

Fig. 3.19 Subclavian vein cannulation (short-axis technique): (**a**) transverse view *SA* subclavian artery, *SV* subclavian vein, *Arrows* pleural line, * clavicle; (**b**) needle tip in the vessel lumen denoted by *arrow head*; (**c**) guide wire insertion in the subclavian vein; (**d**) longitudinal view and catheter confirmation in the subclavian vein denoted by *arrow heads*

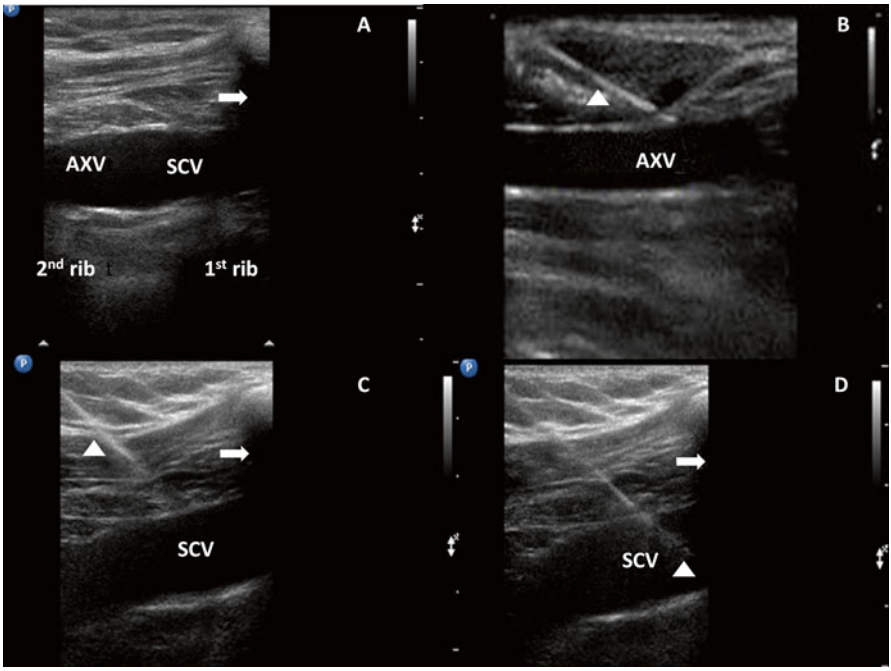

Fig. 3.20 Cannulation of the subclavian vein (*SCV*) on the longitudinal axis (infraclavicular approach): (**a**) transition of the axillary vein (*AXV*) to SCV at the level of the first rib (*arrow* sternum shadow); (**b**) echogenic needle (*arrowhead*) advancing towards the AXV; (**c**) echogenic needle (*arrowhead*) advancing towards the SCV (*arrow* sternum shadow); (**d**) echogenic needle (*arrowhead*) in the SCV lumen (*arrow* sternum shadow)

- *Infra-clavicular and axillary approaches*:
  - Place the probe on the lateral chest wall just below the clavicle. The subclavian vein can be visualized and cannulated using either a long-axis technique (the probe marker is oriented laterally) or a short-axis technique. The penetration point of the needle can be located either medially/towards the sternum (in this case the subclavian vein itself is usually cannulated) or laterally/towards the axilla (in this case the axillary vein is usually cannulated) [8, 15].
  - Using a smaller gauge needle might be safer when puncturing deeper vessels (e.g., axillary) when compared with the traditional central venous line introducer needle [16].

Tips to differentiate between the subclavian vein and artery include:

1. Although the vein is not pulsatile, it is important to distinguish transferred pulsatility and respiratory variation of the vein from arterial pulsation.
2. The vein is usually anterior to the artery.
3. Pulsed-wave Doppler demonstrates the characteristic pulsation of the artery and respiratory hum of the vein.

Factors that are associated with difficult subclavian vein cannulation and high rates of complications include obesity (BMI >30 kg/m^2), history of previous

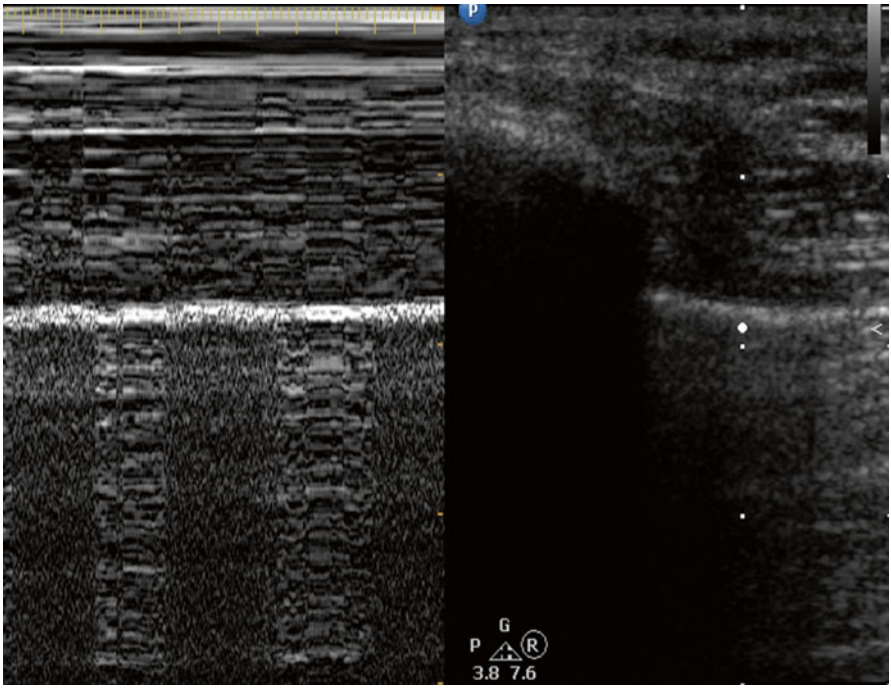

Fig. 3.21 Depiction of the lung point sign (indicative of pneumothorax) on M-mode in a patient following the placement of a subclavian vein catheter

catheterization, and prior radiotherapy or regional surgery. The current evidence recommends the use of ultrasound for high-risk patients [4].

Post-procedural evaluation to rule out pneumothorax (Fig. 3.21) by lung ultrasound (i.e., absence of lung sliding, barcode sign on M-mode, absent B-lines, lung-point sign are all suggestive of pneumothorax) should be performed after the cannulation of the internal jugular and subclavian veins due to their close proximity to the pleura.

Femoral Vein Cannulation

Anatomy

The common femoral vein is formed by the superficial (continuation of the popliteal vein) and deep femoral veins; it lies to the medial side of the common femoral artery (inside the femoral sheath) and passes behind the inguinal ligament to form the external iliac vein. The greater saphenous vein empties into the common femoral vein about 4 cm below the inguinal ligament. The femoral triangle, which is formed superiorly by the inguinal ligament, medially by the adductor longus muscle, and

laterally by the sartorius muscle, includes the neurovascular bundle (femoral vein, artery, and nerve). Due to its proximity to the perineum, infection is a major complication for femoral vein catheters [14].

Procedure

The femoral vein is visualized at the inguinal crease (Figs. 3.22 and 3.23). Sweeping the probe caudally aids in identifying its tributaries and its relationship to the adjacent artery (i.e., possible overlapping), as well as in detecting any other venous

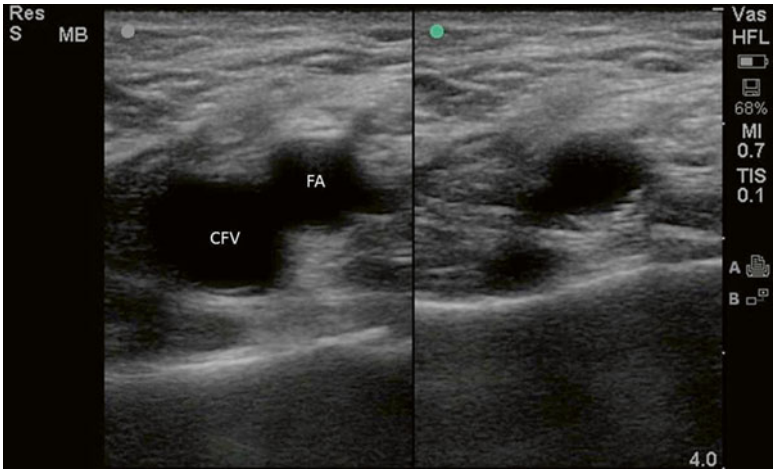

Fig. 3.22 Transverse view of the femoral vasculature demonstrating compression of the common femoral vein. *CFV* common femoral vein, *FA* femoral artery

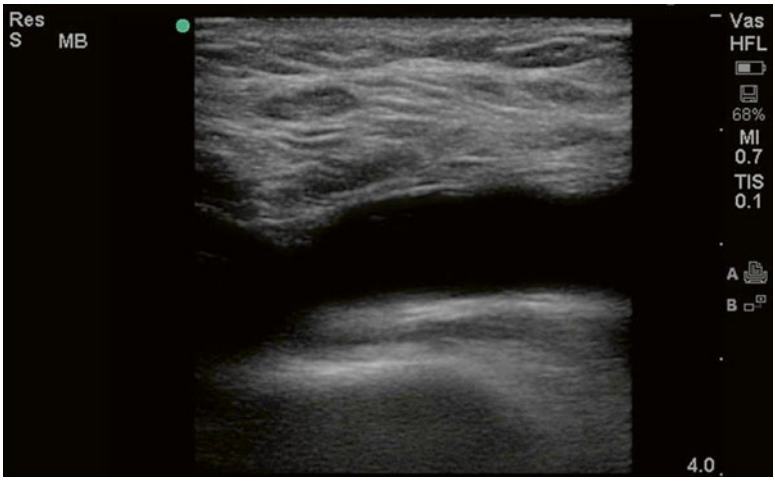

Fig. 3.23 Longitudinal view of the common femoral vein

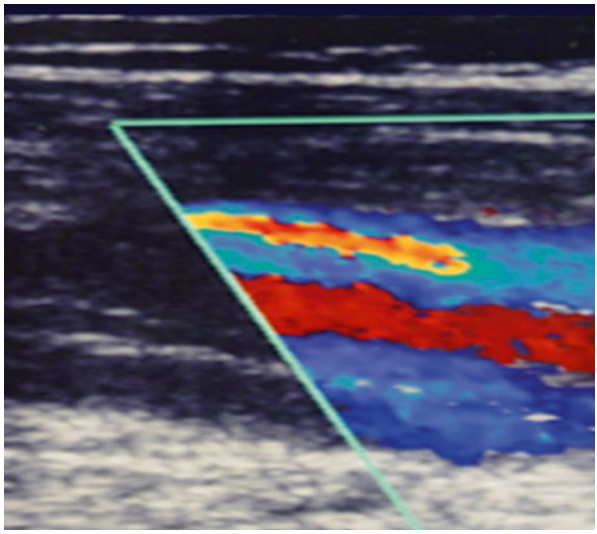

Fig. 3.24 The femoral artery (*red color*) is accompanied by a double system of femoral veins (*blue color*)

anomalies such as thrombosis or a double femoral venous system (Figs. 3.7 and 3.24). The best entry point is devoid of branching veins. Current evidence recommends the use of ultrasound to identify overlapping vessels and patency [4].

Tips for facilitating access of the femoral vein:

1. Slightly abduct the hip with external rotation.
2. Reverse Trendelenburg position can increase the common femoral vein cross-sectional area by more than 50 % [4].

Advanced Competencies

Experienced operators usually cannulate a central vein using a real-time longitudinal axis approach, which allows better control of the needle trajectory and avoidance of posterior wall puncture (Fig. 3.20). However, complications may occur even under ultrasound-guidance. Advanced competencies regarding ultrasound-guided vascular access also include the ability of the physician to diagnose abnormal vascular anatomy, such as the presence of pseudoaneurysms, fistulas, and non-thrombotic vessel obstructions (Fig. 3.25).

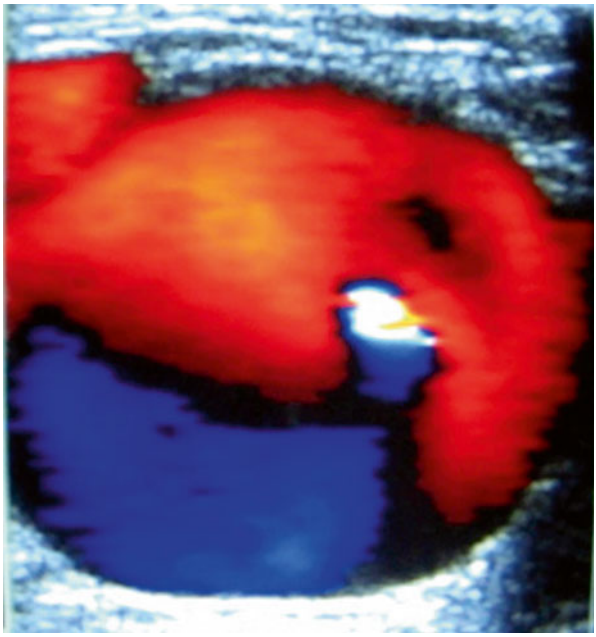

Fig. 3.25 Color mode depicting a traumatic pseudoaneurysm of the femoral artery after a blind femoral vein cannulation (observe the typical "yin–yang" sign on color mode)

Ultrasound-Guided Arterial Cannulation

The procedure for arterial cannulation is the same as for venous cannulation. Real-time guided cannulation is preferred over the skin-marking static-imaging technique (Fig. 3.26) [4]. Ultrasound-guided arterial cannulation is helpful in many scenarios commonly encountered in ICU practice such as obese patients, abnormal anatomy, hypoperfusion, non-pulsatile artery, and previously unsuccessful cannulation attempt [17]. A meta-analysis has demonstrated that ultrasound-guided radial artery cannulation improves first pass success [18].

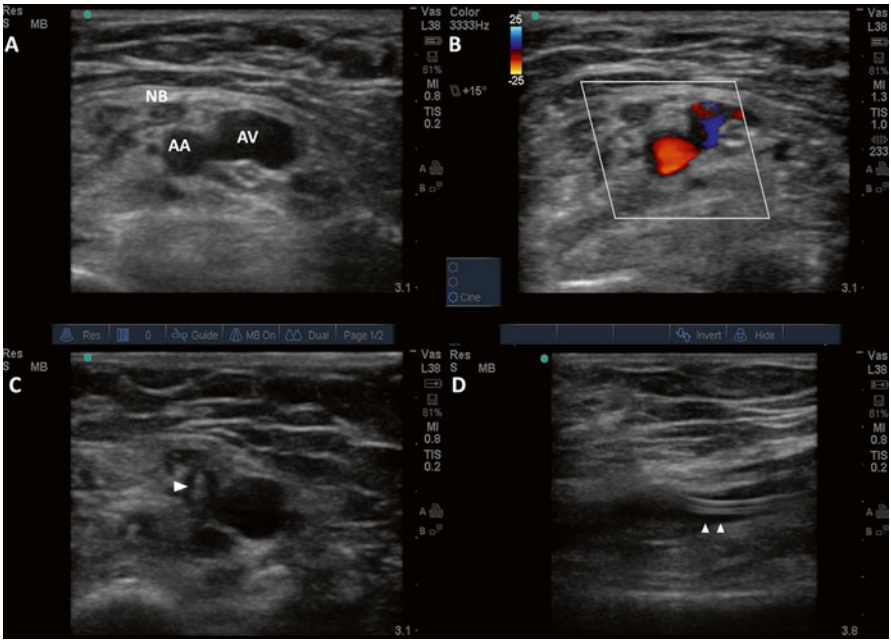

Fig. 3.26 Axillary artery cannulation: (**a**) transverse view *AA* axillary artery, *AV* axillary vein, *NB* nerve bundle; (**b**) Color-Doppler confirmation of the artery and vein; (**c**) needle tip in the vessel lumen denoted by *arrow head*; (**d**) longitudinal view and catheter confirmation in the axillary artery (*arrow heads*)

Ultrasound-Guided Venous Access Considerations in Pediatric Patients and Neonates

The current recommendations support the use of real-time ultrasound during internal jugular and femoral vein cannulation to improve success and to reduce the incidence of complications in pediatric patients [4].

Internal Jugular Vein Cannulation

The neck should be scanned along the course of the vein to identify the best access point for cannulation. Trendelenburg positioning and liver compression techniques are used for increasing the vein size [4]. After the guide wire insertion, another scan should be performed to confirm its presence within the vein before dilatation and catheter insertion.

Subclavian Vein Cannulation

A hockey-stick probe, as previously mentioned, at the supraclavicular level assists in obtaining a longitudinal view. Needle insertion is performed via infraclavicular route under direct ultrasonic guidance [19].

Femoral Vein Cannulation

Femoral vein access in pediatrics is a challenging procedure due to the high prevalence of anatomic variations. Hopkins et al. [20] demonstrated an overlap between the femoral artery and vein in 36 % of patients placed in straight leg position and in 45 % of patients placed in frog leg position. Moreover, the overlap increased distal to the inguinal ligament (75 % in straight leg position and 88 % in frog leg position 1 cm below the inguinal ligament on the left ($p=0.02$) versus 93 % in straight leg position and 88 % in frog leg position at this level on the right). Vein diameter was significantly greater in the frog leg position versus straight leg position on the left, but not on the right, and diameter change with the frog leg position varied by age. Thus, the authors suggested considering placing the patient ≥2 years of age in a frog leg position (60° leg abduction and external hip rotation) to increase the diameter of the femoral vein and to cannulate the vessel by means of sonography. Cannulation should be done at the level of the inguinal crease where less overlap occurs. Additional tips to improve venous visualization in small children include putting a small towel under the child's buttock, reverse Trendelenburg positioning, and gentle abdominal compression [4].

Peripheral Vascular Access in Pediatrics

Peripheral venous access can be a challenge, especially in small, obese, or dehydrated children, and in cases of previously failed venipuncture. Ultrasound-guided peripheral vascular access may improve the success rate in difficult cases when performed by trained physicians [21]. Recently, the High-frequency Ultrasound in Kids Study (HUSKY) group [22] demonstrated that high-frequency (50 MHz) micro-ultrasound (HFMU) facilitated better visualization in sub-10-mm spaces when compared to conventional ultrasound. HFMU may be a valuable tool for accessing peripheral vasculature in pediatrics.

Peripherally Inserted Central Lines

PICCs are inserted via a peripheral vein in the arm with a tip that terminates centrally, at the junction of the right atrium and superior vena cava. It can remain in position for prolonged periods of time and carries less incidence of infection than

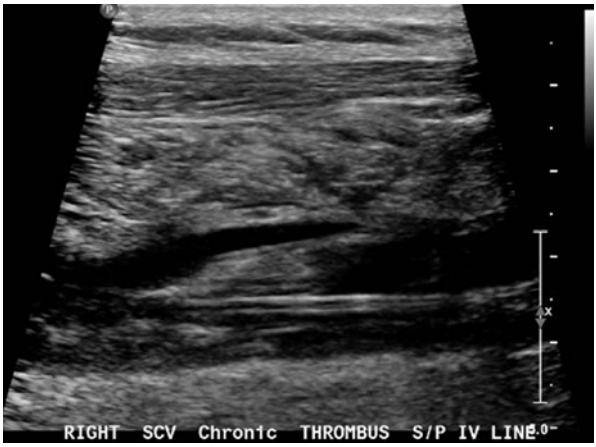

Fig. 3.27 Surveillance scanning after the placement of a subclavian vein catheter in a cancer patient has depicted a catheter-associated chronic thrombosis. However, this is not by itself an indication for removing the catheter. Absolute indications include: catheter malfunction and documented catheter-associated bloodstream infection

traditional central venous catheters [6], and it is a preferable choice in patients who need prolonged central access. Ultrasound can be used to optimize the selection of an upper extremity vein for insertion of the PICC line and facilitate catheter surveillance (Fig. 3.27).

Special Challenges

Challenging cannulation scenarios commonly occur in the ICU (e.g., previous cannulation attempts, prohibitive bracing, tubing, or dressings at access sites, significant anatomic anomalies, presence of subcutaneous air and/or edema, etc.). The advent of ultrasound guidance has afforded the opportunity to adapt insertion procedures to establish venous access. Sofi and Arab reported successful ultrasound-guided cannulation of the internal jugular vein in a prone-positioned patient during a surgery complicated by unpredicted massive blood loss [23]. Castillo et al. reported a patient with kyphosis and a fixed chin-on-chest deformity in whom successful cannulation was performed by ultrasound-guided catheterization of the left axillary vein using a micropuncture technique [16].

Evidence Review and Evidence-Based Use

The US Agency for Healthcare Research and Quality (AHRQ) lists ultrasound-guided vascular access as one of the top 11 evidence-based practices, while several other evidence-based guidelines support the use of the ultrasound method over the landmark technique [4, 24, 25]. Virtually all medical societies related to the care of

critically ill patients advocate for the use of ultrasound for obtaining vascular access [4, 6, 10]. Current recommendations of the American Society of Cardiovascular Anesthesiologists include [4]:

- *Internal jugular vein*: Trained clinicians should use real-time ultrasound whenever possible to improve cannulation success and to reduce the incidence of complications (Category A, Level 1 evidence).
- *Subclavian vein*: High-risk patients may benefit from ultrasound screening before cannulation to identify vessel location, patency, and thrombus (Category A, Level 3 evidence).
- *Femoral vein*: Ultrasound should be used for examining the femoral vein for identification of vessel overlap and examining patency (Category C, Level 2 evidence).
- *Pediatric patients*: Trained clinicians should use real-time ultrasound during internal jugular cannulation whenever possible to improve cannulation success and reduce the incidence of complications (Category A, Level 1 evidence; Category C, Level 2 evidence for femoral vein cannulation).
- *Arterial lines*: Although the council does not recommend routine real-time ultrasound use for arterial cannulation in general, in the case of radial artery, supporting evidence does exist as previously mentioned (Category A, Level 1 evidence).
- *Peripheral venous access*: The council does not recommend routine use of real-time ultrasound use. However, there is supporting evidence advocating the use of ultrasound for PICC insertion (Category B, Level 2 evidence).

Pitfalls and Precautions

Complications may occur even under ultrasound guidance. Oftentimes these complications are due to lack of experience. One of the major complications, especially when using a short-axis approach, is puncture of the posterior vessel wall. The incidence has been reported to be as high as 64 % in a resident-based study [26]. Additional training with simulation models and optimization of the ultrasound technique (i.e., less probe pressure over the vein, use of an in-plane technique) could minimize the incidence of the aforementioned complication. French et al. suggested the use of four-dimensional imaging (real-time three-dimensional imaging) to reduce the errors in identifying vessels and complications during ultrasound-guided central venous cannulation; however, this method is not yet widely available [27].

Hereby, we wish to underline once again the advantages of the three-step real time ultrasound technique. The ultrasound method facilitates the identification of the vein prior to the needle insertion and confirms the proper placement of the guide wire prior to dilation, thus avoiding the pitfall of dilating an artery (Fig. 3.28). The

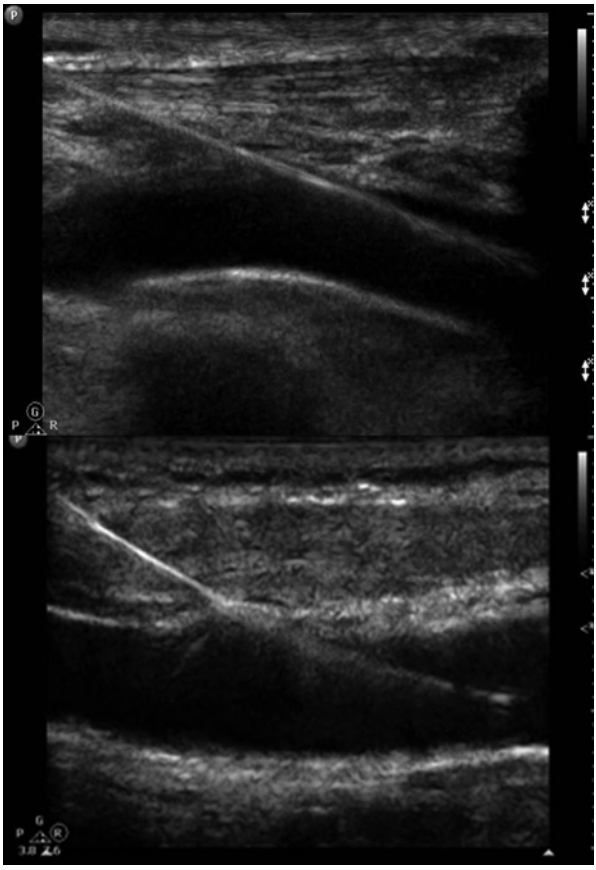

Fig. 3.28 Sonographic identification of the guide wire prior to dilation in the subclavian (*top*) and the internal jugular (*bottom*) veins, respectively

latter may occur in critical care patients who have coded and have severe hypotension. Finally, post-procedural scanning enables the prompt identification of various complications (i.e., catheter malpositioning, hematoma, pneumothorax, etc.)

Notably, recent randomized case–control studies have demonstrated that echogenic technology significantly improved cannula visibility, decreased access time and mechanical complications during the real-time ultrasound-guided internal jugular vein cannulation via a transverse approach and subclavian vein cannulation via a longitudinal approach (Fig. 3.20) [28]. Apart from the aforementioned technological developments, the implementation of a real-time ultrasound technique is essential in both training and routine practice. We strongly advocate using a three-step approach for the optimization of the ultrasound method in the ICU (Fig. 3.29).

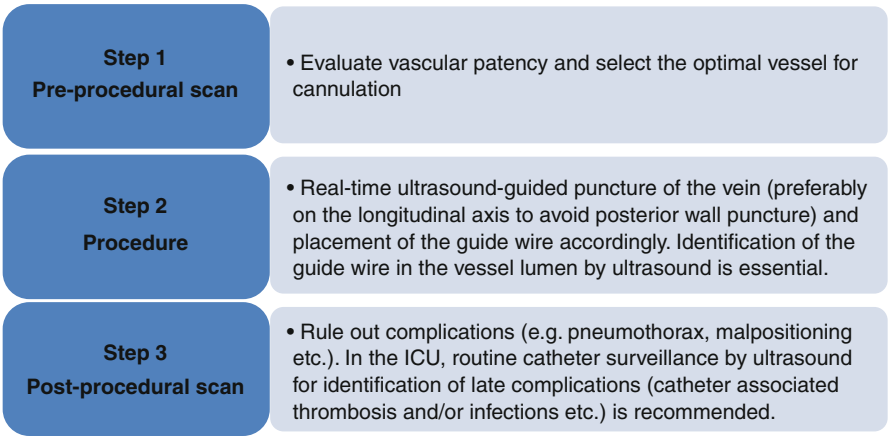

Fig. 3.29 A three-step approach for the optimization of ultrasound-guided central venous access in the ICU

Training Requirements

Further discussion regarding this topic is available in its own chapter, but in general here is what is recommended. Recommended training and curriculum for ultrasound-guided central venous access includes knowledge of [4, 29] principles of ultrasound physics and knobology/equipment operation; infection control standards; basic sonoanatomy: differentiation between arteries/veins, image optimization; ultrasound guided cannulation procedural steps and indications; complication prevention; and catheter surveillance.

Summary

Real-time ultrasound-guided catheterization of the vein is a skill that requires proper training and considerable experience. The implementation of a simple three-step approach (pre-procedural scanning, real-time technique, post-procedural scanning including catheter surveillance) may optimize ultrasound-guided central venous access in the ICU (Fig. 3.29). Ultrasound guided vascular access is one of the top 11 evidence based practices, while its implementation in routine practice increases the safety of the procedure and the satisfaction of patients, thus improving the standard of care.

Acknowledgment We are thankful to Dr. Rayan S. Terkawi and Dr. Khaled S. Doais, for their help in preparing the pictures in this chapter.)

References

1. Karakitsos D, Labropoulos N, De Groot E, Patrianakos AP, Kouraklis G, Poularas J, Samonis G, Tsoutsos DA, Konstadoulakis MM, Karabinis A. Real-time ultrasound-guided catheterisation of the internal jugular vein: a prospective comparison with the landmark technique in critical care patients. Crit Care. 2006;10:R162.
2. Millet JD, Gunabushanam G, Ojili V, Rubens DJ, Scoutt LM. Complications following vascular procedures in the upper extremities: a sonographic pictorial review. Ultrasound Q. 2013;29:33–45.
3. McGee DC, Gould MK. Preventing complications of central venous catheterization. N Engl J Med. 2003;348:1123–33.
4. Troianos CA, Hartman GS, Glas KE, Skubas NJ, Eberhardt RT, Walker JD, Reeves ST. Special articles: guidelines for performing ultrasound guided vascular cannulation: recommendations of the American Society of Echocardiography and the Society of Cardiovascular Anesthesiologists. Anesth Analg. 2012;114:46–72.
5. Graham AS, Ozment C, Tegtmeyer K, Lai S, Braner DA. Videos in clinical medicine. Central venous catheterization. N Engl J Med. 2007;356:e21.
6. Lamperti M, Bodenham AR, Pittiruti M, Blaivas M, Augoustides JG, Elbarbary M, Pirotte T, Karakitsos D, Ledonne J, Doniger S, Scoppettuolo G, Feller-Kopman D, Schummer W, Biffi R, Desruennes E, Melniker LA, Verghese ST. International evidence-based recommendations on ultrasound-guided vascular access. Intensive Care Med. 2012;38:1105–17.
7. Pittiruti M, Malerba M, Carriero C, Tazza L, Gui D. Which is the easiest and safest technique for central venous access? A retrospective survey of more than 5,400 cases. J Vasc Access. 2000;1:100–7.
8. Fragou M, Gravvanis A, Dimitriou V, Papalois A, Kouraklis G, Karabinis A, Saranteas T, Poularas J, Papanikolaou J, Davlouros P, Labropoulos N, Karakitsos D. Real-time ultrasound-guided subclavian vein cannulation versus the landmark method in critical care patients: a prospective randomized study. Crit Care Med. 2011;39:1607–12.
9. Timsit JF, Schwebel C, Bouadma L, Geffroy A, Garrouste-Orgeas M, Pease S, Herault MC, Haouache H, Calvino-Gunther S, Gestin B, Armand-Lefevre L, Leflon V, Chaplain C, Benali A, Francais A, Adrie C, Zahar JR, Thuong M, Arrault X, Croize J, Lucet JC. Chlorhexidine-impregnated sponges and less frequent dressing changes for prevention of catheter-related infections in critically ill adults: a randomized controlled trial. JAMA. 2009;301:1231–41.
10. Rupp SM, Apfelbaum JL, Blitt C, Caplan RA, Connis RT, Domino KB, Fleisher LA, Grant S, Mark JB, Morray JP, Nickinovich DG, Tung A. Practice guidelines for central venous access: a report by the American Society of Anesthesiologists Task Force on Central Venous Access. Anesthesiology. 2012;116:539–73.
11. Pronovost P, Needham D, Berenholtz S, Sinopoli D, Chu H, Cosgrove S, Sexton B, Hyzy R, Welsh R, Roth G, Bander J, Kepros J, Goeschel C. An intervention to decrease catheter-related bloodstream infections in the ICU. N Engl J Med. 2006;355:2725–32.
12. Blaivas M, Stefanidis K, Nanas S, Poularas J, Wachtel M, Cohen R, Karakitsos D. Sonographic and clinical features of upper extremity deep venous thrombosis in critical care patients. Crit Care Res Pract. 2012;2012:489135.
13. Lordick F, Hentrich M, Decker T, Hennig M, Pohlmann H, Hartenstein R, Peschel C. Ultrasound screening for internal jugular vein thrombosis aids the detection of central venous catheter-related infections in patients with haemato-oncological diseases: a prospective observational study. Br J Haematol. 2003;120:1073–8.
14. Snell RS. Clinical anatomy for medical students. Philadelphia: Lippincott Williams & Wilkins; 2000.
15. O'Leary R, Ahmed SM, McLure H, Oram J, Mallick A, Bhambra B, Bodenham AR. Ultrasound-guided infraclavicular axillary vein cannulation: a useful alternative to the internal jugular vein. Br J Anaesth. 2012;109:762–8.

16. Castillo D, McEwen DS, Young L, Kirkpatrick J. Micropuncture needles combined with ultrasound guidance for unusual central venous cannulation: desperate times call for desperate measures–a new trick for old anesthesiologists. Anesth Analg. 2012;114:634–7.
17. Sandhu NS, Patel B. Use of ultrasonography as a rescue technique for failed radial artery cannulation. J Clin Anesth. 2006;18:138–41.
18. Shiloh AL, Savel RH, Paulin LM, Eisen LA. Ultrasound-guided catheterization of the radial artery: a systematic review and meta-analysis of randomized controlled trials. Chest. 2011;139:524–9.
19. Pirotte T, Veyckemans F. Ultrasound-guided subclavian vein cannulation in infants and children: a novel approach. Br J Anaesth. 2007;98:509–14.
20. Hopkins JW, Warkentine F, Gracely E, Kim IK. The anatomic relationship between the common femoral artery and common femoral vein in frog leg position versus straight leg position in pediatric patients. Acad Emerg Med. 2009;16:579–84.
21. Oakley E, Wong AM. Ultrasound-assisted peripheral vascular access in a paediatric ED. Emerg Med Australas. 2010;22:166–70.
22. Latham GJ, Veneracion ML, Joffe DC, Bosenberg AT, Flack SH, Low DK. High-frequency micro-ultrasound for vascular access in young children – a feasibility study by the High-frequency UltraSound in Kids studY (HUSKY) group. Paediatr Anaesth. 2013;23(6):529–35.
23. Sofi K, Arab S. Ultrasound-guided central venous catheterization in prone position. Saudi J Anaesth. 2010;4:28–30.
24. Hind D, Calvert N, McWilliams R, Davidson A, Paisley S, Beverley C, Thomas S. Ultrasonic locating devices for central venous cannulation: meta-analysis. BMJ. 2003;327:361.
25. Milling Jr TJ, Rose J, Briggs WM, Birkhahn R, Gaeta TJ, Bove JJ, Melniker LA. Randomized, controlled clinical trial of point-of-care limited ultrasonography assistance of central venous cannulation: the Third Sonography Outcomes Assessment Program (SOAP-3) Trial. Crit Care Med. 2005;33:1764–9.
26. Blaivas M, Adhikari S. An unseen danger: frequency of posterior vessel wall penetration by needles during attempts to place internal jugular vein central catheters using ultrasound guidance. Crit Care Med. 2009;37:2345–9. quiz 59.
27. French JL, Raine-Fenning NJ, Hardman JG, Bedforth NM. Pitfalls of ultrasound guided vascular access: the use of three/four-dimensional ultrasound. Anaesthesia. 2008;63:806–13.
28. Stefanidis K, Fragou M, Pentilas N, Kouraklis G, Nanas S, Savel RH, Shiloh AL, Slama M, Karakitsos D. Optimization of cannula visibility during ultrasound-guided subclavian vein catheterization, via a longitudinal approach, by implementing echogenic technology. Crit Care Res Pract. 2012;2012:617149.
29. Moureau N, Lamperti M, Kelly LJ, Dawson R, Elbarbary M, van Boxtel AJ, Pittiruti M. Evidence-based consensus on the insertion of central venous access devices: definition of minimal requirements for training. Br J Anaesth. 2013;110:347–56.

Chapter 4
Ultrasound Evaluation of Shock and Volume Status in the Intensive Care Unit

Keith Corl, Sameer Shah, and Eric Gartman

Introduction

Point-of-care ultrasound is particularly well suited for the urgent evaluation of shock in the critically ill patient. In order to maximize the potential of this technology, one must possess the ability to employ several of the basic imaging techniques discussed throughout this text. This chapter will first present a proposed algorithm for approaching a critically ill patient in shock, and how to systematically conduct a goal-directed ultrasound examination. Subsequently, we will discuss the role of ultrasound in the assessment of volume status and fluid responsiveness.

K. Corl, M.D.
Division of Pulmonary, Critical Care and Sleep Medicine, Rhode Island Hospital, 593 Eddy Street, Providence, RI 02903, USA
e-mail: keithcorlmd@gmail.com

S. Shah, M.D.
Division of Pulmonary, Critical Care and Sleep Medicine, Rhode Island Hospital, 593 Eddy St, Providence, RI 02903, USA
e-mail: sshah4@lifespan.org

E. Gartman, M.D. (✉)
Warren Alpert Medical School of Brown University, Providence, RI, USA

Division of Pulmonary, Critical Care, and Sleep Medicine, Memorial Hospital of Rhode Island, 111 Brewster Street, Pawtucket, RI 02860, USA
e-mail: eric_gartman@brown.edu

M. Jankowich, E. Gartman (eds.), *Ultrasound in the Intensive Care Unit*, Respiratory Medicine, DOI 10.1007/978-1-4939-1723-5_4

Undifferentiated Shock

Shock is a complicated pathophysiologic process that can manifest as hypotension, oliguria, neurologic derangement, or other evidence of poor systemic perfusion. Shock is typically classified into one of four categories: cardiogenic, hypovolemic, distributive, or obstructive; although clinically, a combination of the types may be present. Ultrasound offers the potential for the critical care physician to accurately identify the etiology of shock in a timely fashion, and subsequently use ongoing ultrasound imaging to assess changes in a patient's physiology to direct management.

Systematic Approach to the Patient in Shock

The sonographic evaluation of a patient in shock should be tailored to the clinical picture. For example, if a patient's blood pressure abruptly drops following the placement of a subclavian central line, ultrasounding the lung pleura to detect the presence of a pneumothorax is clinically warranted and one's ultrasound investigation should be directed accordingly. However, more frequently the etiology of shock is not clear and a systematic sonographic approach is required. A variety of algorithms have been proposed for the bedside ultrasound evaluation of undifferentiated shock. In an effort to maximize efficiency while ensuring a thorough ultrasound exam is performed, we suggest the following algorithm for nontraumatic shock, which is modified from the Rapid Ultrasound for Shock and Hypotension (RUSH) protocol (Fig. 4.1) [1]. An alternative algorithm, the ACES protocol (Abdominal and Cardiac Evaluation with Sonography in Shock), has the clinical advantage of taking less time to complete, however it omits key components such as assessing lung sliding to rule out a pneumothorax [2].

Following the initial echocardiogram, the clinician should prioritize the following studies based upon clinical suspicion. If the clinical picture is unclear, we suggest cardiac echo, followed by IVC ultrasound, then abdominal, including the aorta, followed by lung pleura, and finally a lower extremity venous study. This approach allows the clinician to minimize probe and location changes.

Goal-Directed Echocardiography

A rapid four-view echocardiogram utilizing parasternal long and short axis views, an apical four-chamber view, and a subcostal view should be performed. This will give an assessment of overall left ventricle (LV) function, size and function of the right ventricle (RV), and the presence of pericardial effusion and possible tamponade. See Chaps. 5, 6, and 7 on critical care echocardiography for complete details.

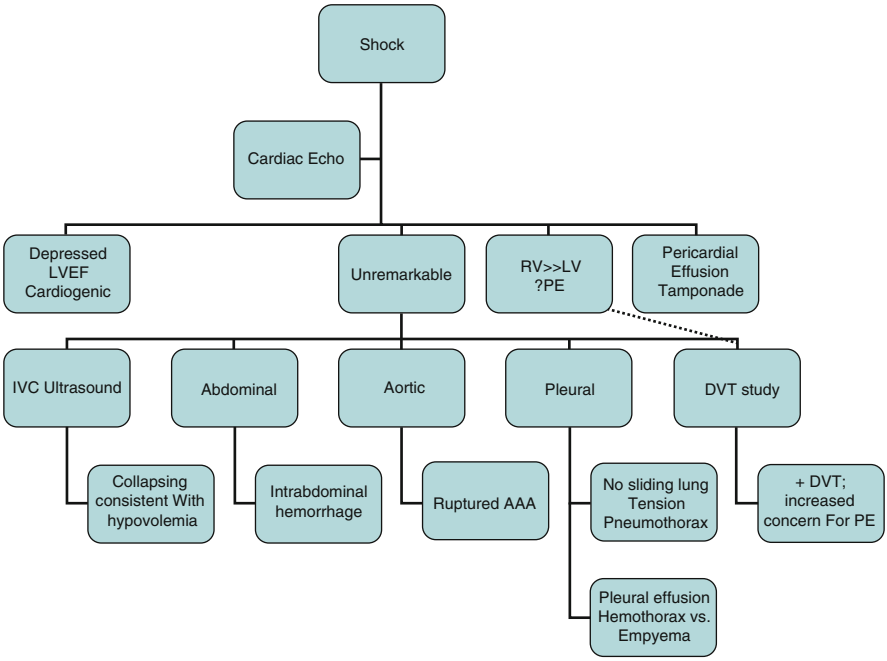

Fig. 4.1 Algorithm for ultrasound assessment of undifferentiated shock, modified from the RUSH protocol. The algorithm begins with critical care echocardiography, with subsequent focused exams as described in the chapter text

IVC Ultrasound

From the subxiphoid position used for echocardiography slide the probe to 1–2 cm to the patient's right, the inferior vena cava (IVC) is examined by fanning and sliding the probe to assess the vessel's diameter and collapsibility. See below for discussion of volume assessment.

Abdominal Exam

The four views of the FAST exam should be obtained: right upper quadrant (RUQ), subcostal, left upper quadrant (LUQ), and suprapubic to rapidly assess the presence of free fluid in the peritoneal cavity. Please refer to Chap. 12 for full details.

Aorta

In brief, the probe is placed in the midline, the aorta identified, and then tracked from a cephalad position in the abdomen to its bifurcation into the iliac arteries. Both transverse and longitudinal views of the aorta are obtained to assess for aneurysm. See Chap. 12 for the details of this exam.

Pleural Ultrasound

Three to four sites are examined on each hemithorax to confirm presence or absence of lung sliding as well as identifying any clinically significant pleural effusion. Lack of lung sliding may indicate pneumothorax, while a large pleural effusion may represent empyema or hemothorax. Additional images and details on pleural ultrasound can be found in Chap. 10.

Assessment of Venous Thrombosis

Switching to a high frequency probe, identify the femoral vein and track the deep veins distally to the level of the popliteal vein. Assess for echogenic material within the vessel, lack of compressibility, or abnormal Doppler flow to diagnose deep vein thrombosis (DVT). Lack of vessel compressibility is the most significant finding suggestive of deep venous thrombosis. Full details and images of venous ultrasound can be found in Chap. 13.

Evidence-Based Review

Rapid diagnostic assessment and implementation of appropriate treatment in a critically ill patient can be lifesaving. In the emergency room setting, the early use of bedside ultrasound has been shown to be superior to delayed use of ultrasound in formulating a clinically meaningful differential diagnoses. In patients with undifferentiated, nontraumatic, shock, Jones et al. compared the ability to correctly diagnose shock between those who were immediately evaluated with bedside ultrasound versus implementation of 15–30 min of standard care followed by a delayed ultrasound. Physicians in the early ultrasound group had a more focused differential diagnosis and were able to correctly identify shock etiology in 80 % of cases 15 min into the resuscitation, while the traditional management algorithm correctly identified shock etiology only 50 % of the time [3]. Despite this supportive data, and the intuitive benefit of the use of bedside ultrasound in the assessment of undifferentiated shock, there is limited prospective data validating the use of ultrasound-based algorithms to diagnose and manage shock.

Ultrasound offers the advantages of rapid, noninvasive, point of care use, which produces data that is often superior to the traditional physical exam. Brennan et al. substantiated this assertion in a study that showed medical students with limited didactic and ultrasound training were more accurately able to estimate right atrium (RA) pressures with ultrasound than with traditional jugular venous pressure measurements (90 vs. 63 %) [4]. The superiority of ultrasound over the physical exam was further demonstrated by Kobal et al. who compared medical students using handheld ultrasound with the physical exams of board certified cardiologists in diagnosing common cardiac conditions. Following 18 h of ultrasound training, the

medical students significantly outperformed the cardiologists in all measured categories [5]. Clearly, the use of ultrasound by physicians to diagnose and direct management patient care at the bedside is rapidly expanding. Further elaboration on ultrasound training programs and standards can be found in Chap. 2.

Volume Status and Fluid Responsiveness

Introduction

Physicians frequently face the clinical challenge of accurately assessing a critically ill patient's volume status; moreover, predicting which patients will be responsive to fluids is an elusive task. Clinical parameters such as vital signs and the physical exam have been shown to be imprecise, are variably interpreted amongst providers, and are therefore unable to accurately predict the hemodynamic status of critically ill patients [6, 7]. The traditional gold standard of hemodynamic monitoring, pulmonary artery catheterization, is invasive, labor-intensive, and of questionable benefit when used routinely in intensive care unit (ICU) patients [8]. With pulmonary artery catheterization now performed infrequently during the management of the critically ill, clinicians are in need of a dependable, noninvasive modality to estimate volume status and fluid responsiveness.

Central venous pressure (CVP) is the most commonly used static measure of preload and is currently recommended by internationally endorsed guidelines for treating patients with septic shock [9]. While IVC collapsibility has been shown to correlate with low CVP [10], static measures such as CVP are poor surrogates for cardiac preload and are unable to predict which patients will respond to fluid loading [11]. A meta-analysis by Marik and Cavallazzi illustrated that CVP is unable to predict fluid responsiveness (FR) and concluded that "there are no data to support the widespread practice of using CVP to guide fluid therapy" [12]. Furthermore, the results of the Protocolized Care for Early Septic Shock (ProCESS) trial question the utility of routinely placing central lines in patients with septic shock who do not require vasopressors [13]. These findings have led a number of physicians to look for alternatives to CVP, and instead use dynamic and noninvasive modalities to direct fluid resuscitation. Ultrasound measurement of the IVC diameter and caval index (the relative change in diameter observed during respiration) has been proposed as a noninvasive means of determining volume status and identifying those patients whose cardiac output may be improved by further volume administration.

Technical and Patient Considerations

In general, when assessing volume status and responsiveness the best images are acquired with the patient in the supine position. However, there are a number of clinical circumstances where laying a patient flat will not be possible; for example,

a patient with severe orthopnea is unlikely to tolerate supine positioning. In these circumstances, keeping the patient semi-recumbent at a 30–45° angle is appropriate. Be aware that semi-recumbent positioning will modify the IVC diameter; however, the magnitude of its effect is not clearly established. Obese patients and abdominal bowel gas pose challenges to image acquisition. Properly adjusting depth and gain can help to maximize image quality. Applying gentle pressure with the probe to the abdomen, while resting the hand holding the probe on the abdominal wall, will help clear bowel gas from the study image. Constant contact with the probe hand is important, since proprioception will provide feedback and prevent the application of undue pressure to the patient's abdomen.

Image Acquisition and Interpretation

For proper IVC image acquisition select the low frequency (1–5 MHz) phased array probe, as this will provide optimal abdominal penetration and visualization of deep structures. With the patient in the supine position, rest the hand holding the probe on the patient's epigastric area (subxiphoid view) with the probe marker directed cranially and the probe angled about 45° off the skin (Fig. 4.2). Apply gradual pressure with the lateral aspect of the smallest finger in direct contact with the patient's abdomen, then slide the probe a few centimeters to the patient's right. As the probe moves off the midline, the long-axis IVC will come into view. The IVC can be identified as it transverses the liver, where the hepatic veins feed into it, and it can be followed cranially to where it terminates in the right atrium. Some general characteristics of the IVC can be observed that may immediately suggest a given physiologic state. For example, if the clinician observes an IVC that completely collapses during respiration, this strongly suggests volume depletion and does not necessarily require direct measurement [14]. A more formal approach to quantifying the collapsibility of the IVC, known as the caval index, will be outlined below.

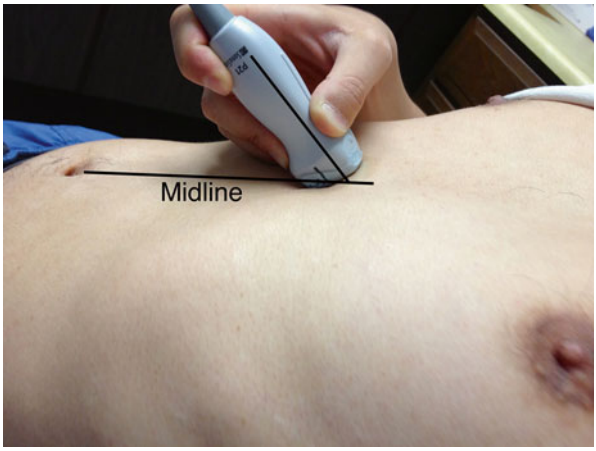

Fig. 4.2 Transducer placement to examine the inferior vena cava (IVC). Note the transducer is slightly shifted to patient's right from midline. Also note it is tilted almost 45° to cephalad (Image by Dr. Taro Minami)

Occasionally the patient's body habitus or abdominal gas may make it impossible to adequately visualize the IVC from the subxiphoid approach. In this case, the examiner should scan from the lateral chest/abdominal wall, using the same technique as in the FAST exam or when performing an ultrasound of the right hemidiaphragm. This alternative approach will often provide a non-obscured view of IVC (see Chap. 12 for further imaging details).

Basic Competencies

To obtain IVC measurements ensure that the center of the IVC is being imaged in the long-axis view. It is important to obtain images of the IVC in the center of its lumen as lateral displacement of the probe in either direction will affect the measurement of the vessel's diameter. Obtain IVC diameter measurements at maximal inspiration and maximal expiration 3 cm caudal from the right atrial boarder or just proximal to the junction of the hepatic veins and the IVC. Both locations reliably produce consistent measurements (Fig. 4.3). Optimal measurements are obtained by recording a video clip of the IVC in B-mode and performing frame-by-frame analysis with calipers to record maximal and minimal caval diameters. Alternatively using M-mode to obtain a time-motion record of the IVC diameter is also an effective strategy (Fig. 4.4).

The caval index quantifies the vessel's distensibility in ventilated patients, and collapsibility in spontaneously breathing patients. It is important to remember

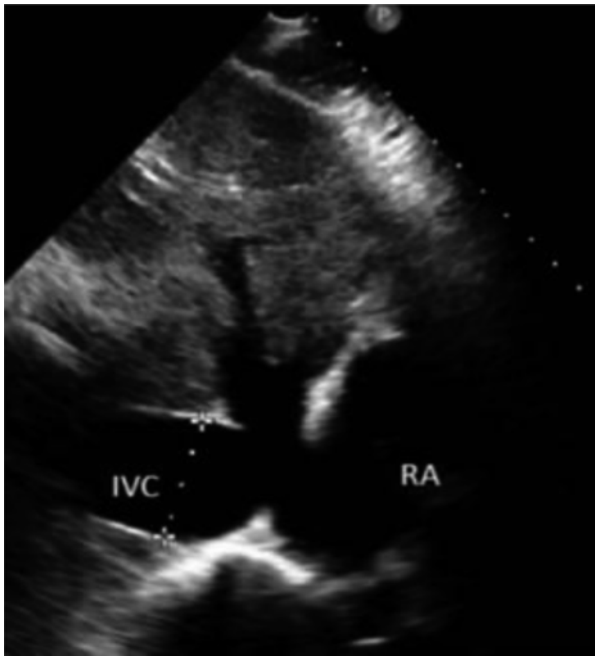

Fig. 4.3 Demonstration of inferior vena cava (IVC) diameter measurement. IVC diameter is measured just proximal to the entrance of the hepatic veins or about 3 cm from the right atrium. Measurements are taken at the same position in inspiration and expiration to assess for respirophasic changes in diameter. *RA* right atrium (Image by Drs. Johannes Steiner and Gaurav Choudhary)

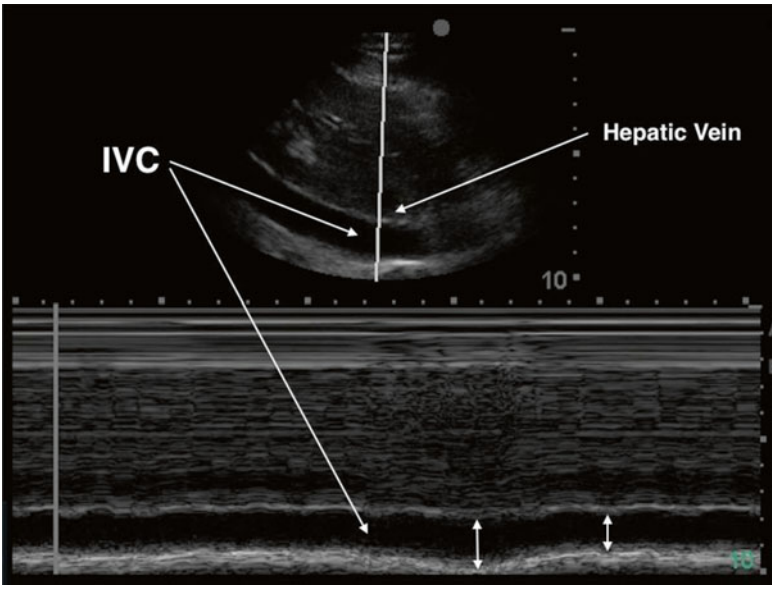

Fig. 4.4 Use of M-mode for determination of inferior vena cava (IVC) diameter measurement. Placing the sampling line through the point in the IVC designated for measurement allows for assessment of respirophasic changes. In the M-mode image at the bottom, the *arrows* measuring the two diameters of the IVC are shown and whether they represent inspiration or expiration diameters depends on whether the patient is breathing spontaneously or is on mechanical ventilation (see text) (Image by Dr. Taro Minami)

that in ventilated patients the inspiratory diameter will be the Dmax, while in spontaneously breathing patients the expiratory diameter will be Dmax. Therefore in ventilated patients the caval index = (IVC inspiration – IVC expiration)/IVC expiration × 100; while in spontaneous breathing patients the caval index = (IVC expiration – IVC inspiration)/IVC expiration × 100. For ventilated patients it is advised to standardize ventilator conditions prior to measuring the IVC. Conventionally the patient is temporarily placed on tidal volumes of 10 cc/kg ideal body weight, and sedated so that they are not triggering the ventilator.

Advanced Competencies

Measurement of Stroke Volume and Cardiac Output

Using bedside sonography to visualize the left ventricular outflow tract (LVOT) and calculate velocity-time integrals (VTI) has been proposed as a way to noninvasively assess stroke volume and calculate cardiac output – and this technique can be particularly useful before and after an intervention is applied (e.g., intravenous fluids). This technique is discussed in detail in Chap. 5.

Evidence Review and Evidence-Based Use

Several studies have examined the ability of the IVC caval index to predict fluid responsiveness (FR) in mechanically ventilated and spontaneously breathing patients. Conceptually, separating these two groups of patients is vital since their physiology is markedly different. In the ventilated patient, intrathoracic pressure increases above abdominal pressure during inspiration, resulting in a dilation of the IVC. The degree of IVC dilation (dIVC) is dependent upon vessel compliance and the ability of the vessel to receive a volume load. Theoretically, the greater the dIVC, the more likely the patient will respond to a fluid challenge. The physiology in a spontaneously breathing patient is quite different. A spontaneous inspiration produces a negative intrathoracic pressure, causing an increase in venous return to the right side of the heart, and a relative collapse in the IVC. Under this set of physiologic parameters the hypothesis is that the greater collapsibility of the IVC (cIVC), the more hypovolemic the patient is and the more likely that the patient will be a fluid responder [15]. Both dIVC and cIVC are synonymous when calculating the caval index, given that they both represent a percentage change in the IVC diameter. Conventionally, FR is defined as an increase in cardiac index, stroke volume, or cardiac output by 10–15 %, indicating that the patient is on the upward slope of the Frank-Starling curve [16].

In mechanically ventilated patients several authors have shown a correlation between caval index and FR. In 20 ICU patients being treated for septic shock, Barbier et al. found that an IVC distensibility of >18 % was able to distinguish fluid responders from nonresponders [17]. Another ICU-based study that included 39 patients in undifferentiated shock found that a dIVC >12 % predicted FR [18]. These findings were subsequently replicated in later studies [19]. While these studies are small and the literature lacks a single, large, definitive study, the results between the trials are consistent in supporting the use of dIVC to predict FR among ventilated patients.

In spontaneously breathing patients the evidence supporting the use of IVC measurements in the prediction of FR is substantially weaker. A 2012 meta-analysis involving a total of 86 patients showed a correlation between hypovolemia and a diminished IVC diameter; however, the included studies did not address fluid responsiveness [20]. The most robust study to address FR enrolled 40 hemodynamically unstable ICU patients and used receiver operating curve analysis to determine the optimal IVC variation that predicted FR. The data suggested that while patients with an IVC caval index >40 % were more likely to respond to fluids the results did not reach statistical significance. Conversely, there were several patients who were fluid responsive with an IVC caval index <40 %. These results suggest that IVC caval index cannot reliably predict FR in patients who are observed to have IVC collapse nor does a plethoric IVC indicate adequate fluid resuscitation [21]. These results were corroborated in other small studies, which showed limited utility of cIVC in predicting fluid responsiveness [22, 23].

Given the paucity of large, high quality studies investigating the validity of the IVC caval index's ability to predict FR, no definite conclusion can be drawn regarding

its incorporation into current clinical practice. At a minimum, it is generally accepted that practitioners may use ultrasound of the IVC to guide resuscitation with the aim of achieving "fluid tolerance" [24]. The concept is that while a collapsing IVC may or may not correlate with FR, giving fluid until the IVC is full will allow the clinician to continue resuscitation without inadvertently exposing patients to volume overload.

Pitfalls and Precautions

As with any clinical tool, the limitations and potential opportunities for the introduction of errors need to be recognized.

- A common error made in early learners arises from the misconception that the IVC is located in the midline. The IVC is located slightly right of the midline.
- Shifting the angle of transducer to the left may inadvertently image the aorta, not the IVC, and the two vessels may then be confused. Discrimination of IVC from the aorta can be made by observation of wall thickness, pulsatility, vessel course, relationship to other vessels, and by following the IVC into the right atrium.
- A patient's clinical status, such as respiratory compromise, may prohibit the practitioner from laying the patient supine to measure the IVC. Semi-recumbent imaging of the IVC will likely change the observed caval index; however, the degree of this effect has not been clearly established.
- Body habitus and bowel gas occasionally limit the ability of the clinician to obtain quality standard images. The use of the alternative imaging site in the right lower thorax/right upper quadrant described above and in Chap. 12 may prove helpful, however is not validated in the literature.
- The IVC is compliant and does not collapse uniformly. This has been demonstrated by comparing several measurements of the IVC at various points along the cranial/caudal axis [25]. Furthermore, the IVC is most plethoric when a patient is in the right lateral decubitus position, intermediate when supine, and smallest when in left lateral decubitus position; thus, patient position must be kept in mind while measuring the IVC [26]. For this reason, standardization of IVC measurements is of great importance.

References

1. Perera P, Mailhot T, Riley D, et al. The RUSH exam: rapid ultrasound in SHock in the evaluation of the critically Ill. Emerg Med Clin North Am. 2010;28(1):29–56.
2. Atkinson PR, McAuley DJ, Kendall RJ, et al. Abdominal and cardiac evaluation with sonography in shock (ACES): an approach by emergency physicians for the use of ultrasound in patients with undifferentiated hypotension. Emerg Med J. 2009;26:87–91.

3. Jones AE, Tayal VS, Sullivan DM, Sullivan VS, Kline JA. Randomized, controlled trial of immediate versus delayed goal-directed ultrasound to identify the cause of nontraumatic hypotension in emergency department patients. Crit Care Med. 2004;32(8):1703–8.
4. Brennan JM, Blair JE, Goonewardena S, et al. A comparison by medicine residents of physical examination versus hand-carried ultrasound for estimation of right atrial pressure. Am J Cardiol. 2007;99:1614–6.
5. Kobal SL, et al. Comparison of effectiveness of hand-carried ultrasound to bedside cardiovascular physical examination. Am J Cardiol. 2005;96(7):1002–6.
6. Eisenberg PE, Jaffe AS, Schuster DS. Clinical evaluation compared to pulmonary artery catheterization in the hemodynamic assessment of critically ill patients. Crit Care Med. 1984; 12(7):549–53.
7. Wo CC, Shoemaker WC, Appel PL, et al. Unreliability of blood pressure and heart rate to evaluate cardiac output in emergency resuscitation and critical illness. Crit Care Med. 1993; 21(2):218–23.
8. Harvey S, Harrison DA, Singer M. Assessment of the clinical effectiveness of pulmonary artery catheters in management of patients in intensive care (PAC-Man): a randomized controlled trial. Lancet. 2005;366(9484):472–7.
9. Dellinger RP, Levy MM, Rhodes A, et al. Surviving sepsis campaign: international guidelines for management of severe sepsis and septic shock, 2012. Intensive Care Med. 2013;39(2): 165–228.
10. Nagdev AD, Merchant RC, Tirado-Gonzalez A, et al. Emergency department bedside ultrasonographic measurement of the caval index for noninvasive determination of low central venous pressure. Ann Emerg Med. 2010;55(3):290–5.
11. Kumar A, Anel R, Bunnell E, et al. Pulmonary artery occlusion pressure and central venous pressure fail to predict ventricular filling volume, cardiac performance, or the response to volume infusion in normal subjects. Crit Care Med. 2004;32(3):691–9.
12. Marik PE, Cavallazzi R. Does the central venous pressure predict fluid responsiveness? An updated meta-analysis and a plea for some common sense. Crit Care Med. 2013;41(7): 1774–81.
13. The ProCESS Investigators, Yealy DM, Kellum JA, Huang DT, et al. A randomized trial of protocol-based care for early septic shock. N Engl J Med. 2014;370(18):1683–93. Epub 2014 Mar 18.
14. Weekes AJ, Tassone HM, Babcock A, et al. Comparison of serial qualitative and quantitative assessments of caval index and left ventricular systolic function during early fluid resuscitation of hypotensive emergency department patients. Acad Emerg Med. 2011;18(9):912–21.
15. Bodson L, Vieillard-Baron A. Respiratory variation in inferior vena cava diameter: surrogate of central venous pressure or parameter of fluid responsiveness? Let the physiology reply. Crit Care. 2012;16(6):181.
16. Bendjelid K, Romand JA. Fluid responsiveness in mechanically ventilated patients: a review of indices used in intensive care. Intensive Care Med. 2003;29(3):352–60.
17. Barbier C, Loubieres Y, Schmit C, et al. Respiratory changes in inferior vena cava diameter are helpful in predicting fluid responsiveness in ventilated septic patients. Intensive Care Med. 2004;30(9):1740–6.
18. Feissel M, Michard F, Faller JP, et al. The respiratory variation in inferior vena cava diameter as a guide to fluid therapy. Intensive Care Med. 2004;30(9):1834–7.
19. Machare-Delgado E, Decaro M, Marik PE. Inferior vena cava variation compared to pulse contour analysis as predictors of fluid responsiveness: a prospective cohort study. Intensive Care Med. 2011;26(2):116–24.
20. Dipti A, Soucy Z, Surana A, Chandra S. Role of inferior vena cava diameter in assessment of volume status: a meta-analysis. Am J Emerg Med. 2012;30(8):1414–9.
21. Muller L, Bobbia X, Toumi M, et al. Respiratory variations of inferior vena cava diameter to predict fluid responsiveness in spontaneously breathing patients with acute circulatory failure: need for a cautious use. Crit Care. 2012;16(5):R188.

22. Lanspa MJ, Grissom CK, Hirshberg EL. Applying dynamic parameters to predict hemodynamic response to volume expansion in spontaneously breathing patients with septic shock. Shock. 2013;39(2):155–60.
23. Corl K, Napoli AM, Gardiner F. Bedside sonographic measurement of the inferior vena cava caval index is a poor predictor of fluid responsiveness in emergency department patients. Emerg Med Australas. 2012;24(5):534–9.
24. Weingart S. Podcast 86 – IVC ultrasound for fluid tolerance in spontaneously breathing patients. EMCrit Blog. 2012. Available from: http://emcrit.org/podcasts/ivc-ultrasound-for-fluid-tolerance-in-spontaneously-breathing-patients/. Accessed 5 May 2014.
25. Wallace DJ, Allison M, Stone MB. Inferior vena cava percentage collapse during respiration is affected by the sampling location: an ultrasound study in healthy volunteers. Acad Emerg Med. 2010;17(1):96–9.
26. Nakao S, Come PC, McKay RG, Ransil BJ. Effects of positional changes on inferior vena caval size and dynamics and correlations with right-sided cardiac pressure. Am J Cardiol. 1987;59:125–32.

Chapter 5
Critical Care Echocardiography: Acute Left Ventricular and Valvular Dysfunction

Girish B. Nair, Pierre Kory, and Joseph P. Mathew

Introduction

Bedside applications of echocardiography in the critical care and emergency department have undergone rapid advancements over the last decade. A rapid bedside critical care echocardiography (CCE) exam performed by an intensivist can provide an accurate dynamic assessment of left ventricular and valvular function and accordingly help direct resuscitative efforts. Traditional technician performed transthoracic echocardiography studies in Intensive Care Unit (ICU) patients are often suboptimal in that decisions based on the study have an inherent delay based on the time factors of when the study is actually performed, when it is read by a cardiologist, and when the results are communicated to the managing clinician. However, advances in ultrasound technology, including harmonic imaging and digital acquisition of images, combined with the availability of portable ultrasound devices, have made bedside CCE performed by critical care physicians a reality. With proper training, CCE can be practical, accurate, and easy to perform, providing real-time answers to clinically meaningful questions in critically ill patients [1].

G.B. Nair, M.D., FCCP
Division of Pulmonary and Critical Care Medicine, Winthrop-University Hospital, 222 Station Plaza, Suite 400, Mineola, NY 11501, USA
e-mail: gbnair@winthrop.org

P. Kory, M.D., MPA, FCCP
Division of Pulmonary, Critical Care and Sleep Medicine, Mount Sinai Beth Israel Medical Center, First Avenue & 16th Street, Dazian Building, 7th floor, New York, NY 10004, USA
e-mail: pkory@chpnet.org

J.P. Mathew, M.D., FCCP (✉)
Department of Medicine, Division of Pulmonary and Critical Care Medicine, Winthrop-University Hospital, 222 Station Plaza North, Suite 400, Mineola, NY 11501, USA
e-mail: jpmathew@winthrop.org

M. Jankowich, E. Gartman (eds.), *Ultrasound in the Intensive Care Unit*, Respiratory Medicine, DOI 10.1007/978-1-4939-1723-5_5

The competence statement by the American College of Chest Physicians (ACCP) and La Societe de Reanimation de Langue Francaise in critical care ultrasonography categorizes the skill set and the training required into basic and advanced competencies [2]. With basic competence in CCE, the intensivist is able to identify specific findings and able to answer straightforward clinical questions based on their proficiency in image interpretation. With advanced competence, the intensivist undergoes progressive training to achieve skill sets for comprehensive evaluation of cardiac anatomy and hemodynamic function, and is able to integrate the results into an effective management strategy [3]. Thus, critical care physicians with more advanced training may use more complex, quantitative measures to assess left ventricular function and determine the need for specific therapies, assess contributions of valve pathology, and categorize deterioration from various disease processes.

In this chapter, we will provide an overview of the major echocardiographic measures to assess acute left ventricular dysfunction and valvular integrity and function. The discussion is highlighted for practice in the critical care setting.

Technical and Patient Considerations

Ultrasound Principles

The piezoelectric crystals in the transducer work on the pulse echo principle. The ultrasound waves generated by the piezoelectric crystals propagate in a medium at a predetermined velocity and are reflected from tissue interfaces. The returning echoes are received by the same transducer and are converted to electrical impulses. The transducers can switch alternatively from generation to listening mode. The percentage of time spent producing ultrasound pulse is termed the duty factor. Transducers can generate sound intermittently as in pulsed-wave Doppler (low duty factor) or continuously as in continuous wave Doppler (duty factor of 100 %). The speed of sound in a medium is a constant and the wavelength of sound waves is inversely proportional to frequency. Commonly used probes for CCE are lower-frequency (1–5 MHz) 'microconvex' or phased array probes (Fig. 5.1).

The heart can be visualized in various modes depending on the point of interest. In B-mode or brightness mode, the structures are displayed in 2-dimensional (2D) images. This mode is better for anatomical evaluation and helps intensivists to have a visual assessment of the global ventricular function and valve integrity in the acute setting. The 'M-mode' or motion mode displays images over a time on a single plane when a scan line is placed over the structures of interest. This mode is better for assessing the movements and excursion of structures such as the free ventricular wall or valve leaflets.

Doppler techniques are useful in assessing valve integrity and also for calculation of velocity-time integral (VTI) and cardiac output measurements. Doppler ultrasound measures the frequency of returning echoes that are reflected from a moving object. The Doppler effect is the increase in sound frequency as a sound source moves toward the observer and the decrease in sound frequency as the source

Fig. 5.1 Phased array or microconvex transducer, a low frequency (1–5 MHz) probe with small footprint. These transducers tend to be more compact allowing easier imaging and maneuverability within the intercostal space

Box 5.1. Doppler Velocity

$$V = \frac{c\,(F_S - F_T)}{2F_T(\cos\Theta)}$$

$$\textit{Reflector velocity} = \frac{(\textit{Doppler shift} \times \textit{propagation speed})}{2x\ (\textit{incident}\ f\ \times\ \textit{cosine of incidence angle})}$$

In the above equation, V is the blood flow velocity, c is the speed of sound in blood (1,540 m/s), 2 is a correctional factor for transit time of the ultrasound wave, and Θ is the angle of intercept of the ultrasound beam. F_T is the ultrasound frequency that the transmitter emits and F_S is the backscattered frequency that returns to the transducer. Note that the cosine of 90° is 0; hence, no Doppler shift would occur if the ultrasound beam is perpendicular to flow. Any angle higher than 20° would lead to underestimation of velocities and inaccurate calculation of hemodynamic parameters.

moves away (similar to sirens from an ambulance). For cardiac imaging, the red blood cell is the target [4]. Doppler shift is the change in frequency between the sound transmitted from the transducer and the sound reflected back from the moving objects (static objects do not cause frequency shifts). Once the frequency of the reflected wave is identified, the known frequency of the transmitted wave can be used to calculate the velocity of the moving object (Box 5.1). When using Doppler, it is important to emphasize that the ultrasound beam of interrogation should be as close to parallel (cosine 0 = 1) or within 20° to the direction of red blood cell flow in order to obtain accurate velocities. As the angle Θ increases, the corresponding cosine becomes progressively less than one, resulting in underestimation of the Doppler shift. Note that the cosine of 90° is zero; hence, no Doppler shift would occur if interrogating at an angle that is perpendicular to flow.

With pulsed-wave Doppler (PWD), flow velocities are measured in one specific location or a small sample volume. The transducer sends out a pulsed signal to a depth chosen by the operator and listens for the reflected frequency shift from that depth, allowing the computer to calculate the velocity. A single crystal sends and receives ultrasound beams. The ultrasound is reflected from moving red blood cells and is received by the same crystal. The pulse repetition frequency (PRF) is the frequency at which the crystal emits a short burst of sound waves. Since the same crystal receives the ultrasound wave, the maximal frequency shift that can be determined by PWD is one-half the PRF, or the Nyquist limit. PWD measures flow velocities at a specific location, within a sample volume. A limitation of PWD is that velocities higher than the Nyquist limit cannot be measured due to aliasing. Aliasing in a phenomenon that results in red blood cells (RBCs) appearing to be moving in a direction opposite to their actual direction. In other words, if the RBCs within a sample volume are moving at a velocity that is greater than half the PRF, aliasing will occur, where flow will appear to be going in the opposite direction and Doppler signals are recorded on opposite sides of the baseline. Continuous wave Doppler (CWD), on the other hand, allows the measurement of velocities along an entire line of interrogation. The transducer uses two crystals in this modality; one continuously transmits pulses at a very high frequency, while a separate crystal continuously is able to receive returning echoes. Although CWD is not able to identify the exact site of highest frequency shift or velocity along its line of interrogations, it is not limited in its ability to measure high velocity RBCs like when using PWD.

Color flow Doppler (CFD) is frequently utilized in the ICU to evaluate for major valvular failure. Color Doppler is a form of PWD but with multiple sample volumes over an area. CFD samples multiple sites using multiple ultrasound beams (multigated) and displays intracardiac blood flow direction and velocity using colors. CFD converts the frequency shift at each sampled site to a preset color scheme and superimposes these colors onto 2D imaging. The higher the velocity, the brighter the color, and the direction of flow is set by the operator, traditionally set as red (flow toward transducer), blue (away from transducer), and green (mix of directions or turbulent flow). The width and size of abnormal intracavitary flows are used to quantify degree of valvular regurgitation [4].

Basic Anatomy

It is important to have an understanding of the orientation of the various cardiac chambers in relation to one other and to know the direction of blood flow, especially when using Doppler measurements. The atria act as receiving chambers and a conduit to the ventricles, which pump blood to the pulmonary and systemic circulation. The left atrium (LA) is the posterior-most cardiac chamber and has thicker walls compared to the right atrium (RA). The left ventricle (LV) is situated posterior to right ventricle (RV) and has thicker walls compared to the RV. The two ventricles

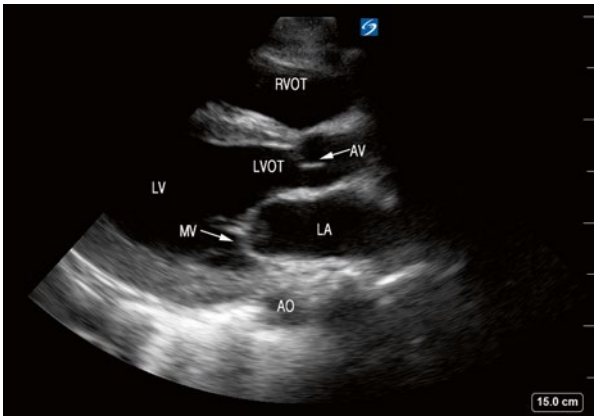

Fig. 5.2 Structures seen via the parasternal long-axis view (*PLAX*). The LVOT consists of the anterior mitral valve leaflet and the LV free wall up to the AV. *LA* left atrium, *MV* mitral valve, *LV* left ventricle, *LVOT* left ventricular outflow tract, *RVOT* right ventricular outflow tract, *AO* aorta, *AV* aortic valve

are separated by the interventricular septum. The LV outflow tract (LVOT) consists of the anterior mitral valve leaflet and the LV free wall up to the aortic valve (AV) (Fig. 5.2). The LVOT directs blood from the LV toward the AV superiorly and rightward.

The atrioventricular valves are located between atrium and ventricle and consist of the annulus fibrosis, valvular leaflets, chordae tendineae, and papillary muscles. The valves are surrounded by dense fibrous tissue forming a partial or complete ring or annulus, which helps anchor and support the valve. In general, the function of the valves will be affected by impairment of any of the components of the valvular apparatus or the ventricular wall. The mitral valve (MV) resides in the left atrioventricular groove and has two leaflets: anterior leaflet, which is located closest from the aorta, and posterior leaflet, which is contiguous with the posterolateral LV wall (Fig. 5.3). The anterior and posterior leaflets connect at the anterolateral and the posteromedial commissures (Fig. 5.4). There are two distinct papillary muscles that are attached to the LV: anterolateral and posteromedial (Fig. 5.5). The chordae tendineae connect the papillary muscle to the mitral annulus and leaflet. The anterolateral papillary muscle has dual blood supply from the left anterior descending artery, whereas the posteromedial papillary muscle has single blood supply by the posterior descending branch of the right coronary artery and is more prone to infarction during myocardial ischemia, leading to severe valvular failure. The tricuspid valve (TV) is located between the RA and RV and has three leaflets: anterior, posterior, and septal. On the ventricular side of the tricuspid valve leaflets, the chordae tendineae are connected to three papillary muscles in the right ventricle.

The aortic and pulmonic valves or the semilunar valves are smaller in size compared to the atrioventricular valves. Named semilunar valves after their three crescent-shaped cusps, they are situated between the ventricle and great vessels and

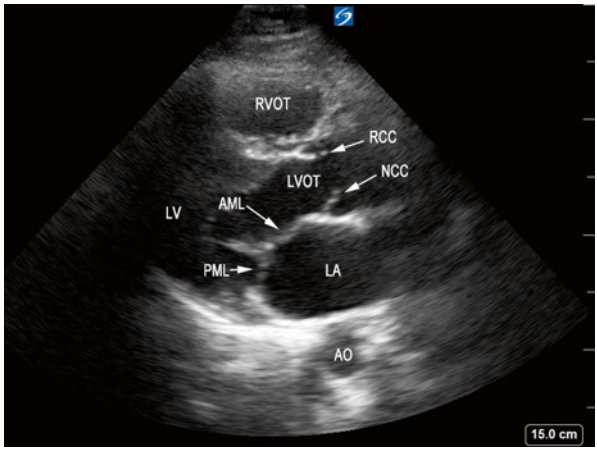

Fig. 5.3 Parasternal long-axis view showing mitral valve leaflets. *AML* anterior mitral leaflet, *PML* posterior mitral leaflet, *LA* left atrium, *LV* left ventricle, *LVOT* left ventricular outflow tract, *RVOT* right ventricular outflow tract, *AO* aorta, *RCC* right coronary cusp, *NCC* noncoronary cusp

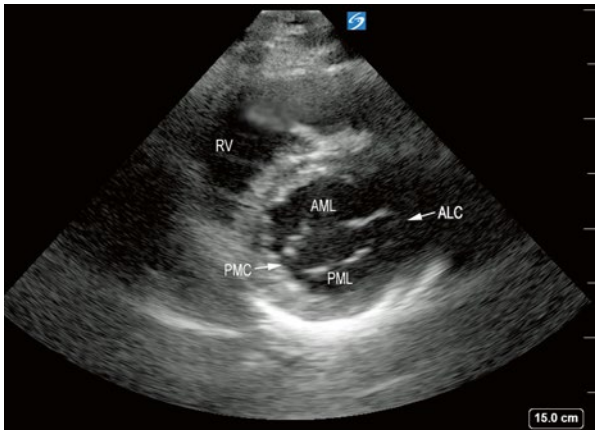

Fig. 5.4 Parasternal short axis view demonstrating anterior and posterior mitral leaflets joining at the anterolateral and the posteromedial commissures. *AML* anterior mitral leaflet, *PML* posterior mitral leaflet, anterolateral and posteromedial commissures (*ALC* and *PMC*, respectively), *RV* right ventricle

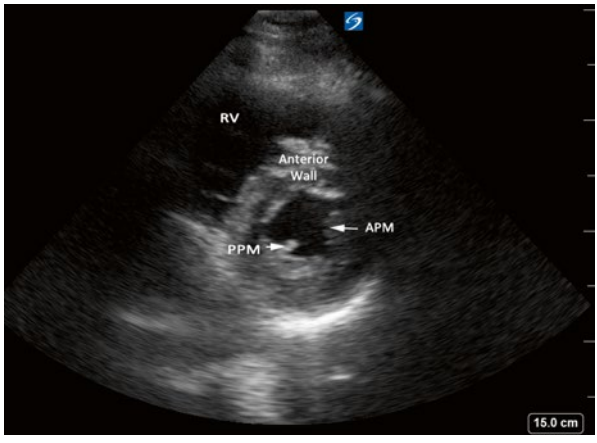

Fig. 5.5 Parasternal short axis – midpapillary view showing anterolateral and posteromedial papillary muscles. *APM* anterolateral papillary muscle, *PPM* posteromedial papillary muscles, *RV* right ventricle

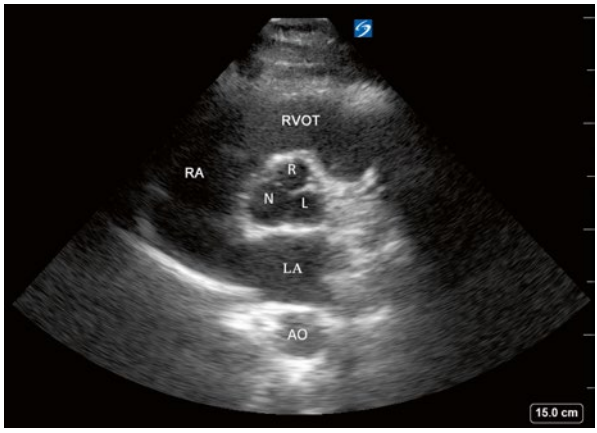

Fig. 5.6 Parasternal short axis view of the aortic valve showing aortic leaflets or cusps (right (*R*), left (*L*), and noncoronary (*N*)). *RVOT* right ventricular outflow tract, *RA* right atrium, *LA* left atrium, *AO* aorta

consist of three leaflets supported by an annulus. The AV separates the LVOT from the ascending aorta and has three leaflets or cusps: the left coronary cusp, the right coronary cusp (named after the respective sinuses of Valsalva which give rise to the main coronary arteries), and the posterior or noncoronary cusp (Fig. 5.6). They are composed of collagenous fibers that anchor into the media of the aorta and provide structural support of valvular structures, transmitting stress on the valve cusps on to the aortic wall. The AV commissures are the small spaces between each cusp's attachment-point. The sinotubular junction is at the level of attachment of the cusps to the wall of the aorta. The pulmonic valve divides the right ventricular outflow tract (RVOT) from the pulmonary artery and is located anterior, superior, and to the left of the aortic valve. It has three cusps, which are defined by their relationship to the AV and are thus termed anterior or nonseptal, right, and left cusps. In contrast to the AV valve, the cusps of the pulmonic valve are supported by freestanding musculature with no direct relationship with the muscular septum; its cusps are much thinner and lack a fibrous continuity with the anterior leaflet of the tricuspid valve.

Cardiac Physiologic Concepts

Systole is the segment of the cardiac cycle from the closure of the MV to AV closure, and the onset of systole is coincident with the onset of the QRS complex or ventricular depolarization on electrocardiogram (EKG). It ends with ventricular repolarization, which occurs at the end of the T wave. During systole the myocardial fibers contract circumferentially and longitudinally, causing inward motion of the endocardium and myocardial wall thickening resulting in ejection of blood to the aorta and pulmonary artery. The "true" measure of LV function is best defined by contractility, or the ability of the heart to perform work under different loading conditions. This ability to eject blood to deliver sufficient oxygen to tissues is the

Box 5.2. Definitions

Cardiac output (CO): volume of blood pumped by left ventricle in one minute. Average in males 5.6 L/min, female 4.9 L/min

Stroke volume (SV): amount of blood pumped by the left ventricle with one cardiac cycle

$$\text{SV} = \text{end diastolic volume (EDV)} - \text{end systolic volume (ESV)}$$

Ejection fraction (EF): fraction of blood ejected by the left ventricle (LV) during the ejection phase of the cardiac cycle or systole; expressed in percentage

$$\text{EF} = (\text{SV/EDV}) \times 100$$

$$\text{CO} = \text{stroke volume (SV)} \times \text{heart rate (HR)}$$

$$\text{Cardiac index (CI)} = \text{CO/body surface area (BSA)}$$

essential function of the heart (Box 5.2). Ventricular systolic function depends on contractility, preload (initial ventricular pressure), afterload (resistance offered by great vessels and end systolic wall stress), and ventricular geometry [5].

Unfortunately, contractility cannot be assessed at a single point in time because it would require the plotting of measured blood volumes ejected at a range of filling pressures (i.e., various loading conditions or volume states), an impractical feat outside of experimental conditions. This is often forgotten in clinical practice, where we instead are forced to measure and record LV systolic performance under a specific set of loading conditions at a single point in time during a specific stage in critical illness or recovery. In a dynamic setting, such as in the ICU or emergency department, the "contractile function," most often denoted by "ejection fraction" (EF) may change (i.e., after volume resuscitation, initiation of medications that can reduce the afterload, use of balloon pumps or ventricular assist devices). Thus, interplay of multiple factors influences the measured EF by affecting both preload and afterload conditions. These include use of vasopressors, coexistent valve dysfunction, volume status, and presence of myocardial insults such as sepsis, ischemia, stress, and inflammation. Such changes in function can occur within hours or days in the ICU, a fact increasingly recognized by intensivists and often underappreciated in the traditional echocardiography lab, where exams are infrequently repeated and often done under a similar set of stable, resting, and loading conditions.

Image Acquisition and Interpretation

With adequate training in CCE, intensivists can assess global and regional ventricular function, as well as qualitative and quantitative valvular function. In a recent statement, the American Society of Echocardiography (ASE) identified the role of a focused cardiovascular examination to be based on a predefined image acquisition

Box 5.3. Terminologies related to transducer handling

Move: Transducer is shifted across the thoracic wall to a different position.
Tilt: Transducer is gently pointed along the same tomographic plane with a rocking motion.
Angle: Transducer is angulated to obtain a different tomographic plane
Rotate: The tip is rotated at the same position to obtain an intersecting tomographic plane.

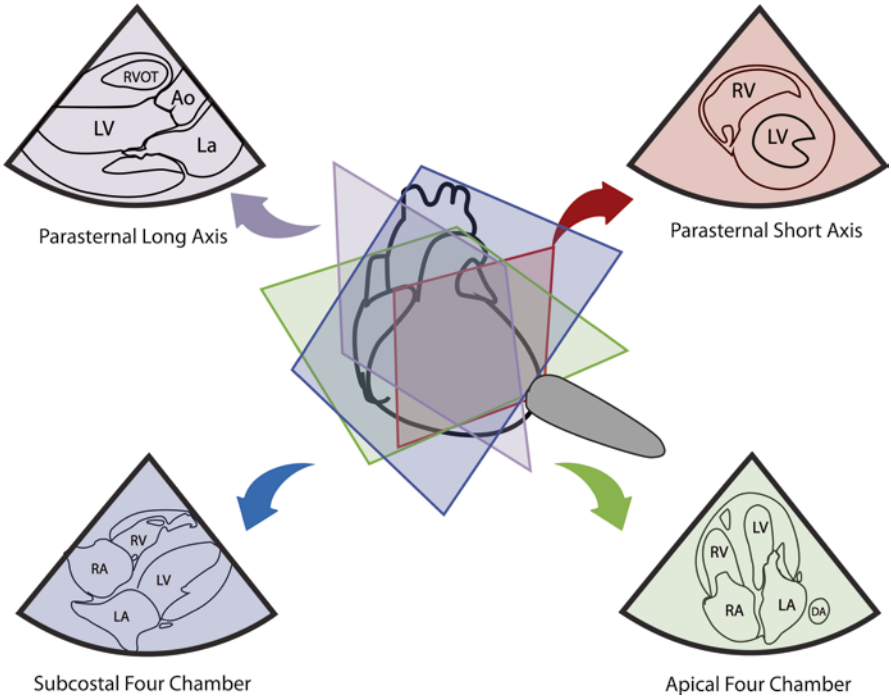

Fig. 5.7 Basic echocardiographic views and corresponding planes. Image courtesy of Guy Aristide, MD

and interpretation protocol to facilitate initial management in critically ill patients [6]. Acquisition of optimal images requires a good understanding of the options available on the ultrasound machine (gain, depth, zoom, etc.) and subtle transducer manipulations (Box 5.3). A constant orientation to the various planes in which the sound waves traverse and dissect the cardiac structures is important (Fig. 5.7). In general, a systematic approach should be taken with regard to the echocardiographic exam. Once the patient position is optimized and the best ultrasonographic window found, the gain and depth should always be optimized. Always keep the structure of interest in the center of the screen. Subsequently, images should be

acquired in a goal-directed, systematic fashion each time, with evaluation of each view to look for ventricular dysfunction and valvular abnormalities.

Images should be acquired using a phased array probe. A "cardiac" exam preset should be selected if using a portable ultrasound machine rather than a dedicated echocardiography machine. This ensures that the machine uses a high frame rate since the heart is a rapidly moving organ. By convention, the screen marker is at the upper right-hand corner of the screen. The ASE recommends that the probe marker should in general point in the direction of either the patients' head or left side [7]. An electrocardiogram (EKG) should be placed on the patient, if specific portions of the cardiac cycle are being interrogated (i.e., systole vs. diastole), however this is not an essential requirement for goal-directed echocardiography. On the monitor, structures closest to the transducer appear on the top or near field and deep structures appear on the bottom of the screen or far field. When color Doppler is used, the color gain should be increased to the point that it just begins to create background noise and then decreased to the level that optimizes color flow imaging of blood flow. The size of the color flow sector should be optimized as well because the frame rate for color flow imaging is inversely proportional to the area of imaging [4].

Patient Positioning and Standard Views

Positioning is often limited in the ICU patient due to the myriad of equipment such as drips, monitors, EKG leads, indwelling catheters, and devices, leading to suboptimal imaging. Critically ill patients may also not always have good acoustic windows, especially those who are mechanically ventilated, have advanced chronic obstructive pulmonary disease (COPD), chest trauma, or are severely obese. Hence whenever possible, positioning of the patient in the bed should be optimized in order to maximize the chances of the best image quality. A good working knowledge of the positioning and orientation of the transducer for each view is also of paramount importance. The transducer should be held like a pencil and stabilized by placing the ultrasonographer's hypothenar eminence on the patient, so as to obtain a steady image of the structure of interest (Fig. 5.8). Adequate pressure should be applied to the transducer and lubricant gel should be used to obtain good images.

Critically ill patients are generally examined in the supine position. Since a portion of the heart is located behind the sternum, patients can be turned to the left lateral position, with the left arm abducted in order to widen the intercostal space and move the heart away from the sternum. This is particularly useful for obtaining good parasternal and apical views. Since critically ill patients often cannot move on their own, using pillows or soft wedges to obtain a lateral decubitus position helps optimize the desired view. For the subcostal view, the patient should be supine; bending the legs at the knees helps decrease abdominal wall tension and improves visualization.

Fig. 5.8 Transducer holding technique. Note the transducer probe is stabilized by placing the ultrasonographer's hypothenar eminence on the patient

With basic CCE, there are five different views that are commonly used: parasternal long axis, parasternal short axis, apical four chamber, apical five chamber, and subcostal (Fig. 5.7). The long axis plane is parallel to the long axis of the LV (line drawn from the apex to the base of the heart) and short axis is perpendicular to the long axis [7]. The four-chamber plane is marked by a plane through LV apex and intersects LV, RV, and atria (perpendicular to both long and short axes). Note that each patient is different, hence exact positioning and orientation of the transducer on the chest wall will vary from patient to patient, depending on the anatomical position and orientation of the heart. If good acoustic images cannot be obtained on one tomographic plane, gentle tilting, rotating or angling of the footprint, or repositioning the patient in a lateral decubitus position should be attempted to obtain the desired image.

Parasternal Long-Axis (PLAX) View

In this view, the transducer is placed on the third or fourth rib space along the left parasternal region with the marker on the probe pointing facing the right shoulder (Fig. 5.9). The ideal image includes the LV cavity in the long axis (elongated horizontally, not oblong) with the MV and AV in a single plane. In the PLAX view, the right ventricular outflow tract (RVOT) is in the upper portion of the image, as it is the closest to the transducer (Fig. 5.10). The interventricular septum (IVS) divides the RVOT from the LV. The posterior wall of the LV is imaged in this view but the LV apex may be missed. The LA can be seen in the lower right-hand portion of the screen. The AV is visualized as thin linear echogenic structures separating the LV from the aortic root. The upper aortic cusp corresponds to the right coronary cusp and the lower aortic cusp to the noncoronary cusp (Fig. 5.3). The MV is located furthest from the transducer, below the aortic root. The posterior leaflet is attached to the posterior LV wall and the anterior leaflet is closest to the aorta, in close

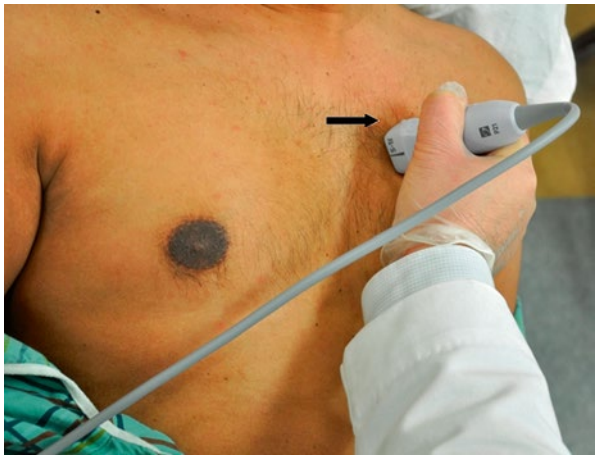

Fig. 5.9 Transducer orientation in parasternal long axis. Note the marker on the probe (*thick arrow*) pointing toward the *right* shoulder

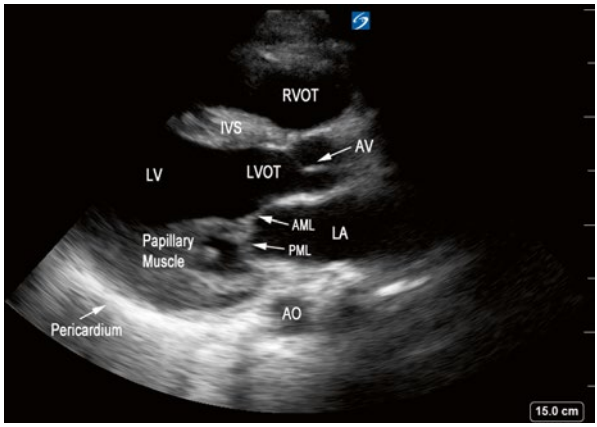

Fig. 5.10 Parasternal long-axis view with left ventricular outflow tract and mitral valve in the same plane. Interventricular septum (*IVS*) divides the right ventricular outflow tract (*RVOT*) from left ventricle (*LV*). *LA* left atrium, *LV* left ventricle, *LVOT* left ventricular outflow tract, *RVOT* right ventricular outflow tract, *AO* aorta, *AV* aortic valve, *AML* anterior mitral leaflet, *PML* posterior mitral leaflet

proximity to the noncoronary AV cusp. The papillary muscles can be visualized well in this view, attaching to the mitral leaflets by the chordae tendineae (Fig. 5.10).

The PLAX view is useful for assessment of LV chamber size and contractility, segmental wall function, wall thickness, and the interventricular septum. Color Doppler can be utilized to evaluate for aortic or mitral valvulopathies. This is the best view to visualize the coaptation of the mitral leaflets and visualize the dynamics of the annulus, chordae, and papillary muscle to determine the cause of pathology. PLAX was the preferred window of examination for estimation of LV function

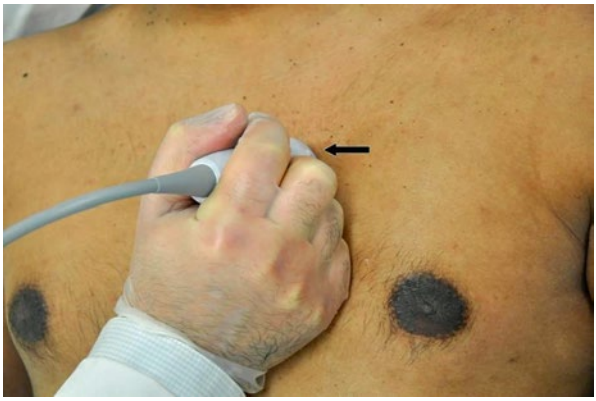

Fig. 5.11 Transducer orientation in parasternal short axis view. Note the marker on the probe (*thick arrow*) pointing toward the left shoulder

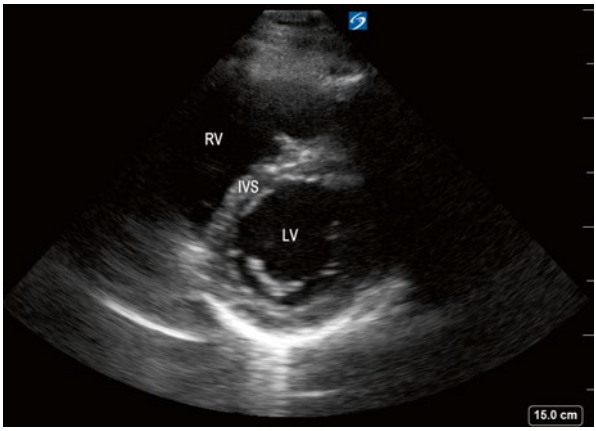

Fig. 5.12 Parasternal short axis view with left ventricular chamber appearing as a *circle*, along with right ventricular cavity that appears as a semicircle. *LV* left ventricle, *RV* right ventricle, *IVS* interventricular septum

in a prospective study of emergency medicine physicians performing focused bedside CCE [8]. However, caution should be exercised in assessment of LV size as off-axis views can lead to erroneous assessment of LV size and function.

Parasternal Short Axis (PSAX) View

From the PLAX view, with steady hands the transducer is turned 90° clockwise, so that the pointer is oriented toward the left shoulder to achieve PSAX view (Fig. 5.11). Optimal image would include a concentric view of the walls of the left ventricular chamber that appear as a circle, along with right ventricular cavity that appears as a semicircle (Fig. 5.12). By angling the transducer superiorly toward the base of the heart, the AV level is obtained with all three leaflets: right, left, and noncoronary cusps in view (Fig. 5.6). The AV lies posterior to the RVOT and anterior to the LA. The pulmonic valve can also be seen in long axis in this plane with RV outflow

tract by gently angling superiorly. Angling the transducer inferiorly will bring the mitral valve into view. The anterior leaflet is on top, closer to the RV, and the posterior mitral leaflets can be seen at the bottom of the screen, further away from the transducer (Fig. 5.4). Angling further down, a view with anterolateral and posteromedial papillary muscles is seen (Fig. 5.5). The mid-ventricular or papillary muscle level is where assessment of LV function should be performed. This mid-ventricular level allows assessment of segmental endocardial motion, wall thickening, and septal kinetics. Angling the transducer superiorly to inferiorly, from the base to the apex, can give the intensivist a general idea of the global systolic function of the LV.

Apical Four-Chamber (A4C) View

In the "apical four-chamber" (A4C) view, the transducer is placed near the apex of the heart or point of maximum impulse (inferolateral to the left nipple) with the transducer pointing to the right shoulder. The transducer may have to be moved slightly medially until the heart falls into view. The probe marker should be facing a 2–3 o' clock position (Fig. 5.13). With the ideal image, the LV appears elliptical and tapered with a rounded apex and all four cardiac chambers and the atrioventricular valves are visualized (Fig. 5.14). If the image is off-axis, the LV appears foreshortened and can lead to incorrect conclusions with assessment of relative wall thickness and EF. The A4C view is good for measurement of EF, stroke volume, wall thickness, and segmental wall function. It is also used to assess the MV and TV anatomy and color Doppler analysis can be utilized for assessment of regurgitation and stenosis. In the A4C view, the anterior mitral leaflet can be seen adjacent to the aorta and the posterior mitral leaflet on the lateral wall. The chordae

Fig. 5.13 Transducer orientation in apical four-chamber view. The marker on the probe is facing 3 o'clock position. For better visualization the patient is positioned in left lateral decubitus position

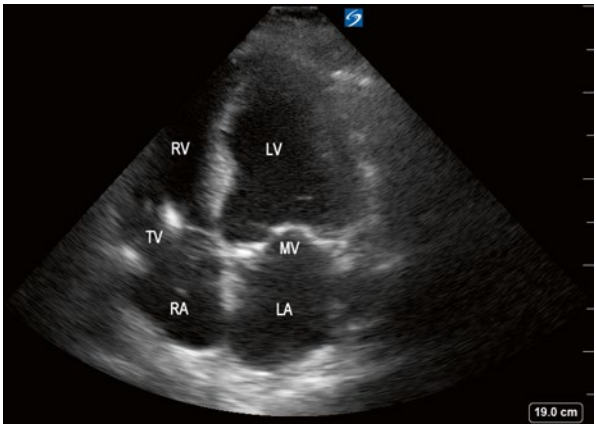

Fig. 5.14 Apical four-chamber view showing left atrium (*LA*), mitral valve (*MV*), left ventricle (*LV*), right atrium (*RA*), tricuspid valve (*TV*), and right ventricle (*RV*)

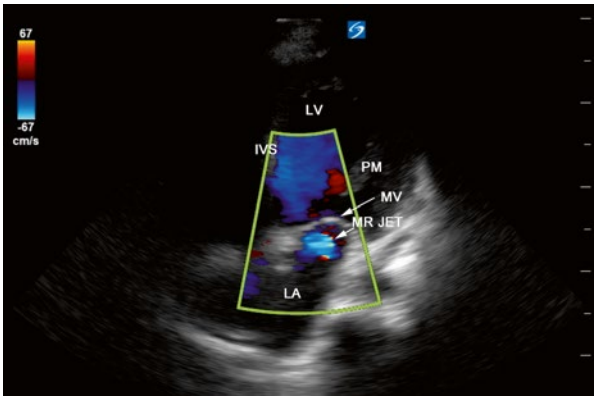

Fig. 5.15 Color Doppler flow mapping showing mitral regurgitant flow back into the left atrium. *LA* left atrium, *MV* mitral valve, *MR jet* mitral regurgitant jet, *IVS* interventricular septum, *LV* left ventricle, *PM* papillary muscle

tendineae can be seen attaching the leaflet to the papillary muscle. Color Doppler can be used in this view to assess for mitral regurgitant flow back into the LA (Fig. 5.15). The A4C is one of the most difficult views to obtain in critically ill patients for basic CCE and repetitive practice is needed to achieve proficiency [6, 9].

Apical Two-Chamber (A2C) View

From the A4C view, the transducer is rotated counterclockwise by about 60° in order to obtain this view. This view is useful to evaluate LV function and regional wall motion abnormalities (Fig. 5.16). LV EF can be quantified from this view using the biplane method of discs (Simpson's method).

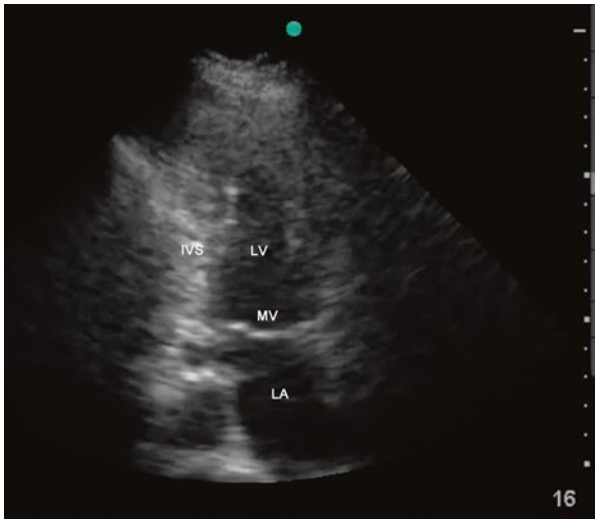

Fig. 5.16 Apical two-chamber view showing left atrium (*LA*), mitral valve (*MV*), and left ventricle (*LV*). *IVS* interventricular septum

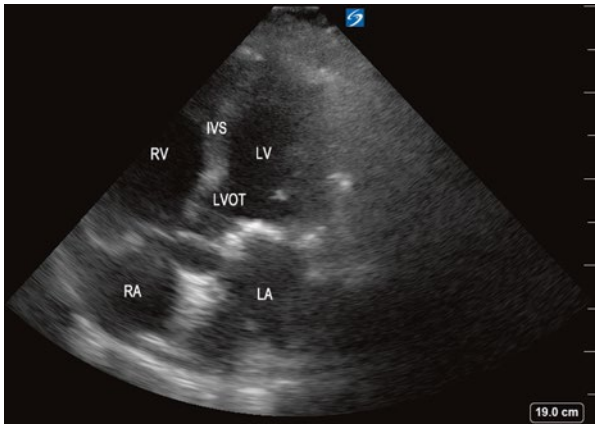

Fig. 5.17 Apical five-chamber view demonstrating the left ventricular outflow tract (*LVOT*), interventricular septum (*IVS*), left atrium (*LA*), left ventricle (*LV*), right atrium (*RA*), and right ventricle (*RV*). The circular structure in the center of the image is the aorta

Apical Five-Chamber (A5C) View

This view is obtained by slightly angling the probe upward or anteriorly from the A4C view to bring out the left ventricular outflow tract (LVOT) (Fig. 5.17). The aortic valve will be in the center of the image. Although this view may not be part of basic CCE, it is useful for calculating the velocity time integral (VTI) across the LVOT and for assessment of stroke volume. This view is also useful for assessing aortic stenosis and regurgitation.

Fig. 5.18 Transducer orientation in subcostal view with probe marker facing 3 o'clock position

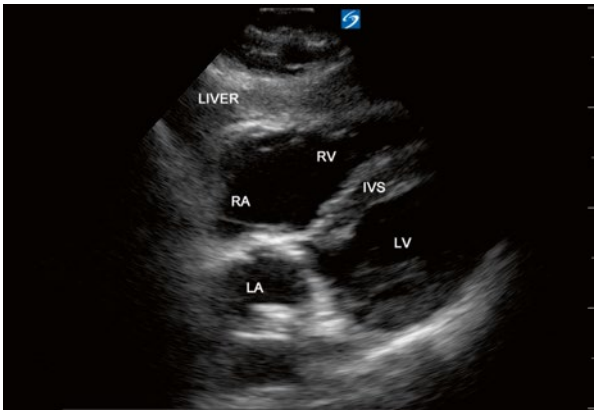

Fig. 5.19 Subcostal long axis view showing all four cardiac chambers and part of liver. Interventricular septum (*IVS*), left atrium (*LA*), left ventricle (*LV*), right atrium (*RA*), and right ventricle (*RV*)

Subcostal (SC) View

The "subcostal" view is especially useful in intubated patients and also in decompensating patients for a quick view of the cardiac chambers and pericardium. This view may often be the only adequate anatomical window available in patients with poor parasternal or apical views. In the supine position, the transducer is placed in the subcostal area, under the xiphoid process, and it should point to the patient's left shoulder (Fig. 5.18). The transducer should be held on its top surface so that it lies relatively flat on the patient's abdomen, with the marker pointing to 3'o clock position and angling cephalad. Imaging during deep inspiration or during a ventilator delivered breath will bring the diaphragm down and facilitate the subcostal approach. The four chambers and part of the liver are visualized in the SC view (Fig. 5.19). The entrance of the inferior vena cava (IVC) into the right atrium is visualized by angling the probe further posteriorly and rotating counterclockwise. Determination of the IVC diameter and its respiratory variation is helpful in the assessment of volume status—see Chap. 4 for further discussion (Fig. 5.20).

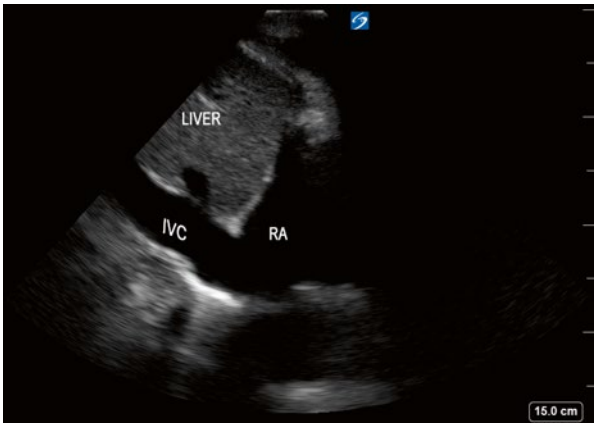

Fig. 5.20 Inferior vena cava (*IVC*) is visualized by angling the probe further posteriorly and rotating counterclockwise in the subcostal view. *RA* right atrium

Box 5.4. Questions to ask during basic CCE when suspecting LV or valvular dysfunction

- What is the size of the left ventricular cavity: small, normal, or severely dilated?
- Is the left ventricle adequately filled?
- How is the contractility of the left ventricle? Categorize as normal, hyperdynamic, moderate dysfunction, or severe dysfunction.
- Is there evidence of global or regional wall motion abnormalities?
- Can the hemodynamic compromise be explained on the basis of severe valvular regurgitation or stenosis?

Basic Competencies

Critical care physicians with basic training in CCE should be able to perform a goal-directed examination to answer specific questions related to patient management. Competence in obtaining the abovementioned four basic views and in interpretation is essential. The ACCP consensus statement identifies qualitative assessment of LV cavity size, LV systolic function, distinguishing homogeneous from heterogeneous patterns of LV contraction, and detecting severe valvular regurgitation using color Doppler as part of basic CCE practice [2]. Once other causes of acute hypotension such as cardiac tamponade and severe RV dysfunction are ruled out, the examiner should focus on the ventricular function and valve integrity (Box 5.4). All examinations should be performed in multiple views so as not to make erroneous conclusions from one tomographic plane. Global ventricular dysfunction is seen with conditions such as sepsis and myxedema, while acute cardiac ischemia may cause regional wall motion abnormalities. It is also important to repeat serial examinations to assess ventricular function at different loading conditions.

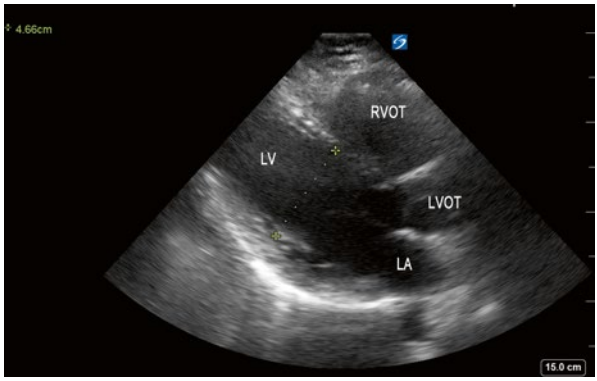

Fig. 5.21 Measurement of LV diameter in parasternal long-axis view. Note the measurements are made from the edge of the septal endocardium to the posterior wall, at the level of the mitral valve leaflet tips. *LA* left atrium, *LV* left ventricle, *LVOT* left ventricular outflow tract, *RVOT* right ventricular outflow tract

Assessment of Left Ventricular Size

Determination of LV chamber dimensions is a vital part of the assessment of systolic function. The LV diameter is assessed from the PLAX view as the ultrasound beam is perpendicular to the interface between blood and the myocardium. 2D imaging in long and short axis views can be used to evaluate the internal dimensions of the LV. M-mode is utilized to take advantage of the rapid sampling and accurate identification of the endocardium.

The LV end-diastolic diameter (EDD) measurement is made at the maximum chamber size, on the frame right before MV closure (at the onset of the QRS complex). LV end-systolic diameter (ESD) is measured at the minimum chamber size, right before AV closure. Measurements are made from the edge of the septal endocardium to the posterior wall, at the level of the MV leaflet tips (Fig. 5.21). When measured in M-mode, care must be taken to ensure that the ultrasound beam is cutting perpendicularly over the LV, otherwise dimensions will be overestimated. The LV chamber is considered to be severely enlarged when EDD is greater than 6.9 cm in men (normal <5.9 cm) or 6.2 cm in women (normal <5.3 cm).

Qualitative Assessment of LV Systolic Function

Global Visual Assessment

This is the most commonly used method to estimate LV systolic function by intensivists performing basic CCE [10, 11]. Although visual assessment is subjective and accuracy is influenced by the experience of the interpreter, adequate training makes

Box 5.5. Visual assessment of systolic function can be categorized as follows

- Hyperdynamic: >50 % excursion, >50 % thickening,
- Normal function: >25 % excursion and > 50 % wall thickening
- Moderate dysfunction: 10–25 % excursion and 30–50 % thickening
- Severe dysfunction: <10 % endocardial excursion and <30 % wall thickening

this method fast and easy to perform with reasonable correlation to quantitative measurement of EF.

Left ventricular ejection of blood depends on shortening of muscle fibers in three dimensions: the shortening of the distance from apex to base, the excursion and thickening of the chamber walls, and the spiral, rotational squeeze of the LV cavity. Visual assessment of this shortening largely relies on assessing wall segment excursion and thickening. Excursion refers to the movement of the endocardial borders toward each other; normally this distance shortening is at least 25–50 %. Thickening denotes the increase in diameter of the LV wall during systole, on average by approximately 40 % in multiple views [12]. Lack of thickening is the most sensitive method to detect presence of ischemia in that wall segment. Excursion and thickening should be assessed in multiple views, at multiple levels, looking at the different walls for any regional wall motion abnormalities. It is recommended to image from at least two views to increase the accuracy of assessment. Based on the above, LV systolic function can be categorized as being normal, hyperdynamic, moderate dysfunction, or severe dysfunction (Box 5.5). With normal systolic function, the ventricular wall demonstrates greater than 25 % excursion and 50 % wall thickening (Fig. 5.22). A hyperdynamic LV has greater than 50 % excursion and thickening, and the rotational squeeze often leads to full contact of the ventricular walls (Fig. 5.23). With moderate dysfunction, the LV wall has 10–25 % excursion and 30–50 % wall thickening (Fig. 5.24). Once there is severe LV dysfunction, the ventricular wall displays less than 10 % excursion and less than 30 % thickening (Fig. 5.25). Note our preference to avoid the categorization of "mildly" abnormal given its minimal clinical impact on the critically ill patient and its limitations in inter-observer variability [13].

There are several limitations to the global visualization or "eyeball" method. Adequate basic training in CCE is a prerequisite prior to assessing LV systolic function. Inadequate endocardial definitions may impair estimation and lead to erroneous measurements of systolic function [12]. A foreshortened A4C view can lead to incorrect assessment of global and regional LV function. In patients with conduction defects or pacemakers or who have had previous cardiac surgery, estimation of regional wall motion abnormality may be difficult. Both excursion and thickening of the myocardial segments should be noted for segmental asynchrony. Abnormal myocardial segments may be misdiagnosed as normal if the abnormal

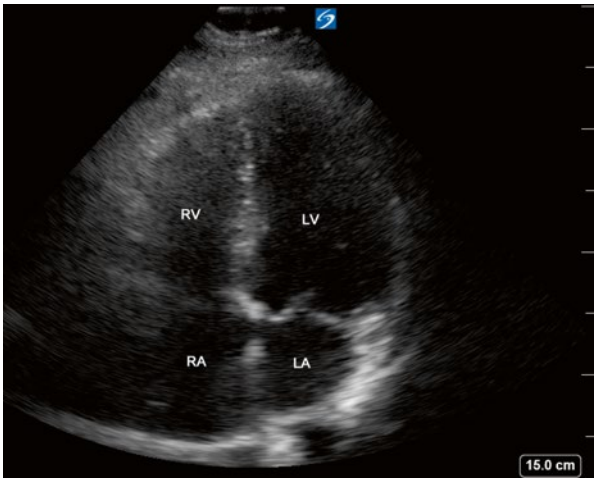

Fig. 5.22 Apical four-chamber view in a patient with normal left ventricular function. The ventricular wall demonstrates greater than 25 % excursion and 50 % wall thickening. Left atrium (*LA*), left ventricle (*LV*), right atrium (*RA*), and right ventricle (*RV*)

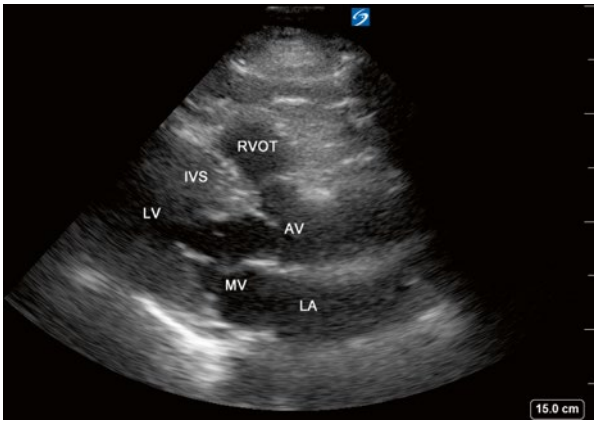

Fig. 5.23 Parasternal long-axis view in a patient with hyperdynamic LV. There is greater than 50 % excursion and thickening, and rotational squeeze with the ventricular walls touching each other. *LA* left atrium, *LV* left ventricle, *RVOT* right ventricular outflow tract, *MV* mitral valve, *AV* aortic valve

segment is moving or has excursion without thickening due to "tethering" by adjacent normal myocardium. Similarly, akinetic (i.e., no excursion or thickening seen) and dyskinetic segments (i.e., paradoxical movement of segments) are reflective of regional systolic dysfunction and should influence the interpretation of global systolic function assessment. Quantitative estimates of ejection fraction or LV function should be avoided by novice echocardiographers, and instead, they should rely on the categorical determination of global excursion and thickening for its simplicity and consistency [6].

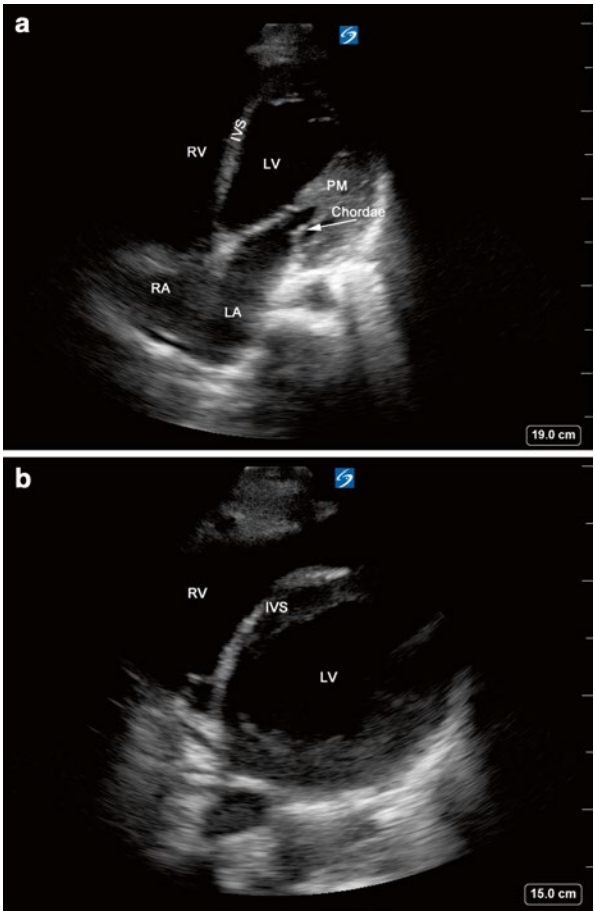

Fig. 5.24 (**a**) Apical four chamber and (**b**) Parasternal short axis view in a patient with moderate LV dysfunction. The LV wall has 10–25 % excursion and 30–50 % wall thickening. *LA* left atrium, *LV* left ventricle, *RA* right atrium, *RV* right ventricle, *IVS* interventricular septum, *PM* papillary muscle

Qualitative Assessment of Valve Integrity

Intensivists with basic training in CCE should be able to identify the apparent cause of acute hypotension due to ruptured chordae, papillary muscles, or flail leaflet. Preexisting severe stenosis or regurgitation can complicate other conditions such as severe sepsis or volume depletion, causing profound refractory hypotension, and can be recognized with basic CCE. Longstanding regurgitant or stenotic valve lesions cause corresponding chamber dilation and remodeling (i.e., left ventricle with aortic regurgitation and left atrium with mitral regurgitation), whereas acute lesions do not, except with preexisting cardiomyopathies.

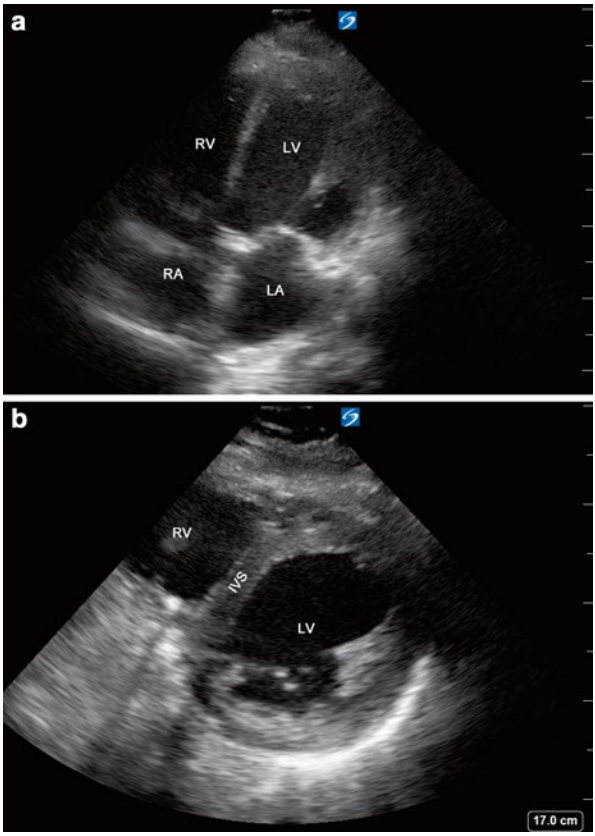

Fig. 5.25 (**a**) Apical four-chamber view in a patient with severe LV dysfunction. There is less than 10 % excursion and less than 30 % thickening of left ventricular wall. *LA* left atrium, *LV* left ventricle, *RA* right atrium, *RV* right ventricle. (**b**) Parasternal short axis view on the same patient with severe LV dysfunction. *IVS* interventricular septum, *LV* left ventricle, *RV* right ventricle

The focus with basic CCE is to identify major catastrophic causes of valve failure or valve dysfunction that would affect the hemodynamic status of the critically ill patient. A comprehensive assessment of valves, which requires advanced training in Doppler analysis, is neither practical nor time efficient in the ICU. Detailed examination of the tricuspid (TV) and pulmonic valves (PV) is generally not part of basic CCE, hence the focus is mainly on the AV and MV. Though color Doppler techniques are used in assessment with basic CCE, it should be done with the understanding that advanced training is required for knowing the complexities associated with the technique and may not be as straightforward as it appears. Consultation with colleagues in cardiology and a reference echocardiogram is recommended for advanced quantitative interrogation of valve function.

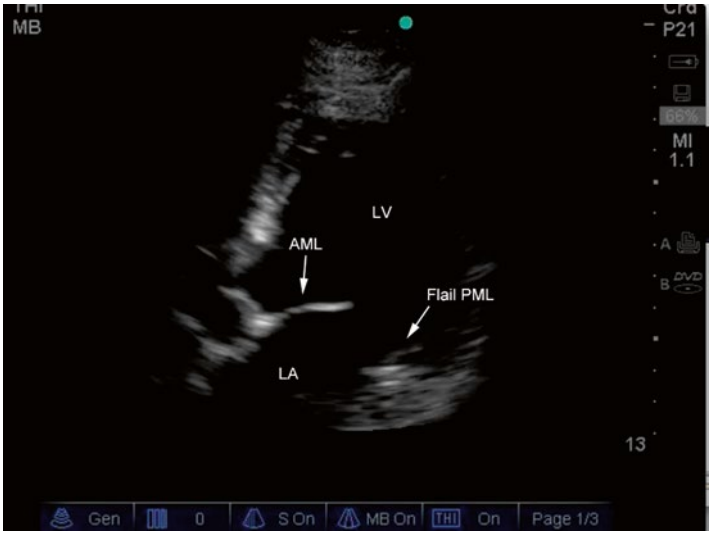

Fig. 5.26 Apical two-chamber view in a patient with flail posteromedial mitral leaflet. *AML* anterior mitral leaflet, *PML* posterior mitral leaflet, *LA* left atrium, *LV* left ventricle

2D Echocardiography and Color Doppler for Qualitative Assessment of Valve Integrity

Mitral Valve

Mitral stenosis (MS) is uncommon in the ICU and most patients arrive with an established diagnosis, usually from prior rheumatic fever. Mitral regurgitation (MR), on the other hand, is one of the common valve lesions encountered in the ICU, and the underlying cause can be identified by 2D echocardiography alone. Prompt recognition of acute MR due to structural abnormalities such as papillary muscle dysfunction, ruptured chordae, and destruction of valve leaflets from endocarditis can significantly impact management. Myocardial ischemia can cause acute MR from partial or complete papillary muscle rupture, usually affecting the posteromedial papillary muscle due to its single blood supply (Fig. 5.26). Acute MR can cause increased end diastolic volume (EDV) and reduction in stroke volume (SV) resulting in elevated LA pressure and pulmonary edema, whereas chronic severe MR can complicate resuscitative efforts in critically ill patients. Chronic MR, on the other hand, can occur due to chronic LV dilation and widening of the mitral valve annulus without structural changes in the valve leaflet itself.

The 2D examination should focus on identifying structural abnormalities such as ruptured chordae, flail mitral leaflet, papillary muscle rupture, mitral annulus calcification, endocarditis, and perforation. The valve should be imaged in multiple views including PLAX, PSAX, and A4C. In the PLAX view, the posterior mitral leaflet can be seen attached to the posterior LV wall and the anterior mitral leaflet is the closest to aorta. In the PSAX view, at level of mitral valve, the characteristic

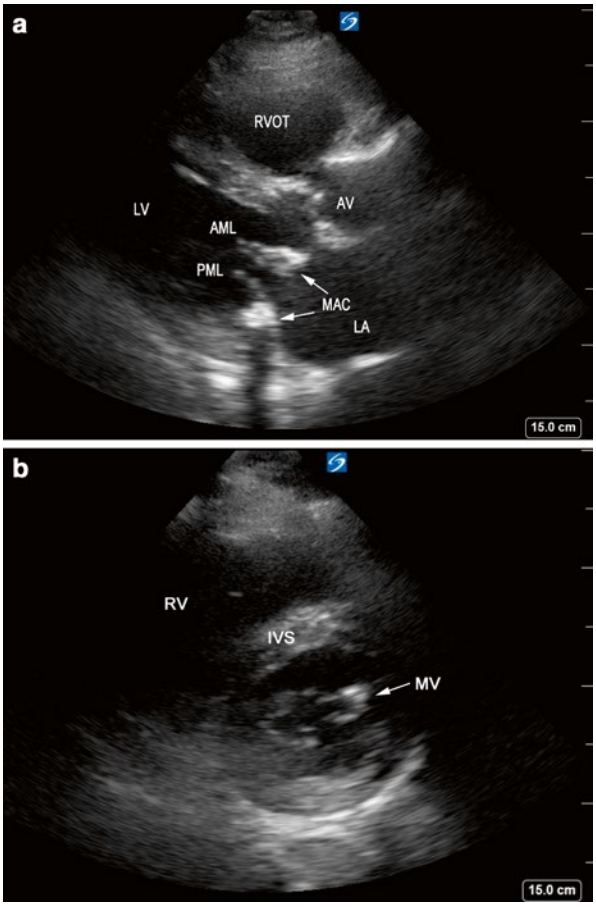

Fig. 5.27 Parasternal long-axis and short-axis views in a patient with moderate to severe mitral stenosis. Note the hyperechoic mitral annular calcification (*MAC*) of the anterior and posterior mitral leaflets. *LA* left atrium, *LV* left ventricle, *LVOT* left ventricular outflow tract, *RVOT* right ventricular outflow tract, *MV* mitral valve, *AV* aortic valve, *AML* anterior mitral leaflet, *IVS* interventricular septum, *MV* mitral valve, *PML* posterior mitral leaflet, *RVOT* right ventricle outflow tract

"fishmouth" appearance of mitral stenosis (MS) can be visualized, with the anterior leaflet on top, closer to the RV, and the posterior leaflet at the bottom (Fig. 5.27). In the A4C, the anterior leaflet is medial adjacent to the IVS and the posterior leaflet is attached to the lateral wall. The SC view is not the best view to image for MR.

Using color Doppler over the mitral valve, turbulent flow (yellow-green jet) can be seen over the MV, and a systolic blue jet indicating regurgitant flow from the left ventricle to the left atrium is seen with severe MR. Although the regurgitant jet can be directed either toward or away from the probe with PLAX view, color Doppler will show yellow-red (toward the probe) or green-blue (away from the probe). The amount of regurgitant flow back into the LA determines the severity of MR (Figs. 5.15 and 5.28). When the area of regurgitant jet is more than 40 % of the LA

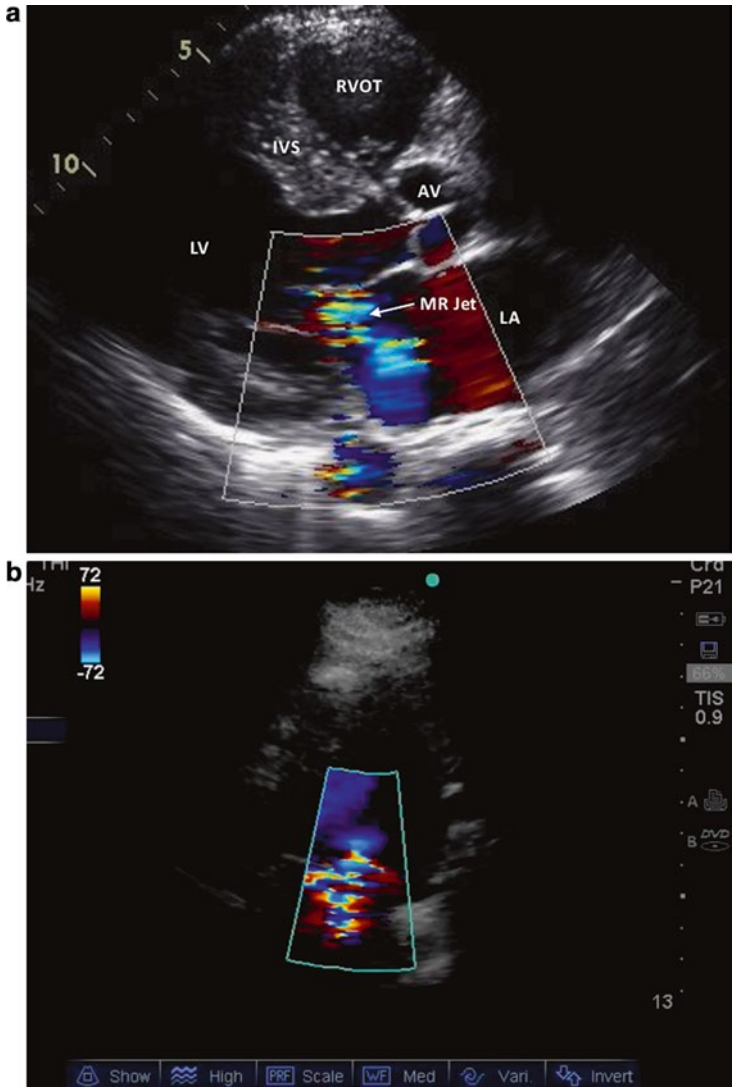

Fig. 5.28 (**a**) Color Doppler in parasternal long-axis view in a patient with mild mitral regurgitation (*MR*). *AV* aortic valve, *IVS* interventricular septum, *LA* left atrium, *LV* left ventricle, *RVOT* right ventricular outflow tract. (**b**) Apical four-chamber view in a patient with severe mitral regurgitation (*MR*). *MR* is considered severe, if the area of regurgitant jet is more than 40 % of the left atrial (*LA*) area or reaches the posterior wall of the LA

area or reaches the posterior wall of the LA, the MR is usually severe (Fig. 5.28) [14]. Keep in mind that color flow imaging of MR is dependent on many factors such as loading conditions, direction of jet, gain settings, depth, and pulsed repetition frequency.

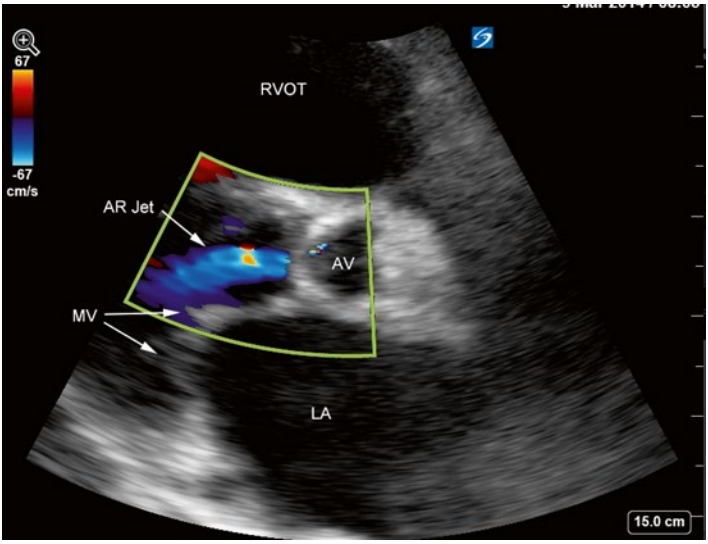

Fig. 5.29 Color Doppler in parasternal long-axis view in a patient with moderate aortic regurgitation (*AR*) and stenosis. Note the mitral valves are closed during systole. *LA* left atrium, *MV* mitral valve, *AV* aortic valve, *RVOT* right ventricular outflow tract

Aortic Valve

Severe aortic stenosis (AS) can cause significant hemodynamic impairment and can complicate other causes of hypotension. Acquired degenerative calcific valve stenosis is the commonest etiology, but other entities such as bicuspid aortic valve and rheumatic heart disease may also cause aortic stenosis. With basic CCE training, the 2D study echocardiogram will show calcified (hyperechoic), restricted aortic cusps and can be appreciated in PLAX view, PSAX view at level of aortic valve, or A5C view.

Acute severe aortic regurgitation (AR) can cause significant hemodynamic compromise and needs to be identified immediately. Acute AR can be caused by conditions such as aortic dissection and endocarditis, whereas chronic AR is from valve malformation or due to aortic root and annulus dilation from conditions like Marfan syndrome. 2D examination in the PLAX view, PSAX aortic valve view, and A5C view can show abnormalities of valve architecture, vegetation, and aortic root dilation. In cases with acute AR, the LV size will be normal with a hyperdynamic LV. With color Doppler in PLAX view, the regurgitant jet may be perpendicular and can be directed toward or away from the probe (Fig. 5.29). In A5C view AR appears as a yellow-red mosaic diastolic jet from the aorta to the LV.

Advanced Competencies

Advanced CCE requires a comprehensive evaluation of all hemodynamic parameters, mastery over all image acquisition techniques, and complete understanding of Doppler evaluation [2]. Competence entails ability to integrate the finding from CCE for bedside clinical management strategies. However, certain conditions like prosthetic valve function, complex congenital heart disease, cardiac source of systemic embolism, and stress echocardiography mandate cardiology consultation. Intensivists practicing advanced CCE should be able to measure the size of LV cavity, calculate stroke volume, LV ejection fraction, and LV fractional area change, and quantify LV regional wall motion abnormalities (Box 5.6). Also, proficiency in performing Doppler indexes to evaluate LV filling pressures, diastolic function, and assessing severity of valvular regurgitation and stenosis are an important skill set with advanced CCE.

Assessment of Left Ventricular Systolic Function

The ejection fraction is a number derived from the percentage of ventricular blood that is ejected during systole. The normal range is considered to be between 55 % and 65 % and is a crude measure of the amount of work of which the ventricle is capable. The ejection fraction, however, does not always correlate with the patient's stroke volume or cardiac output. EF can be quite low when the SV is normal in the setting of a compensatory dilated ventricle. Despite this limitation, the EF calculation is the most common reported index of LV function. LV function can be estimated qualitatively or quantitatively. EF estimated by global visual assessment as mentioned in the basic competency is a reliable index when performed by expert echocardiographers.

Although there are more than eight different echocardiographic indices for estimating LV function, intensivists largely rely on a discrete number of relatively straightforward ones with the most common method being the simplest, the "global visual assessment" [10, 11, 15]. Other intensivists have reported on using semiquantitative methods such as fractional area of change or fractional shortening measurements [16–18]. Advanced methods such as assessing the rate of pressure rise during mitral regur-

Box 5.6. Suggested questions when approaching a patient with LV or valve dysfunction with advanced CCE

- What is the size of the LV cavity?
- What is the ejection fraction?
- What is the calculated cardiac output?
- Are there segmental wall motion abnormalities?
- Is there presence of significant valvulopathy? Quantify severity.

gitant flow "dP/dt," annular motion velocity, or tissue Doppler measurements require either excellent views or more complex calculations. For these reasons, such measures will only be mentioned briefly given their limited applicability in the ICU by the majority of clinicians.

Qualitative Measurement of LV Function

Mitral Valve Leaflet Excursion Method

This is a simple, quantitative method for identifying decreased LV function and relies on assessing the amount of mitral valve leaflet opening by measuring the minimum distance between the anterior leaflet and the septum during diastole. This method is based on the observation that when LV systolic function decreases, there is a consequent decrease of left atrial filling and thus emptying into the LV. This decreased transmitral flow results in a decreased separation of the leaflets during diastole. Conversely, normal LV emptying and filling causes the anterior mitral valve leaflet to open almost to the septum, normally approaching within 5 mm. This septal separation, measured either by visual estimation or using 2D or M-mode measurements, has been shown to be one of the most accurate methods of identifying decreased LV function (Fig. 5.30). Cutoff points differentiating between normal and depressed EF have been reported between 4 mm and 7 mm, with the most commonly used being 6 mm [19, 20].

Traditionally, cardiologists have performed this measure using M-mode at the mitral valve leaflet tip in a parasternal long-axis view, denoting the tip of the mitral valve leaflet as the E' point and the leaflet tip to septum distance as the E' point-septal separation or EPSS. This distance can also be measured using 2D and simply

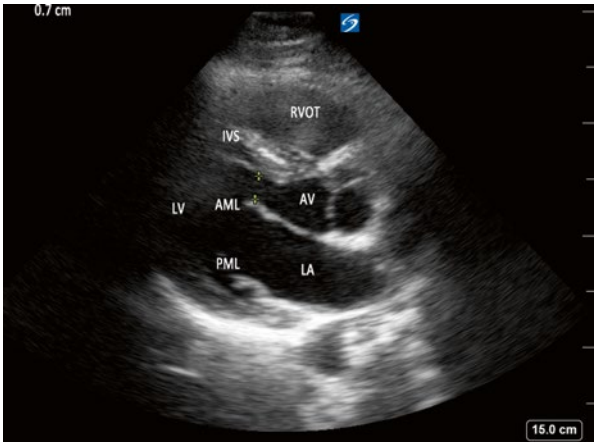

Fig. 5.30 Anterior mitral leaflet – septal separation in PLAX view. In patients with normal ejection fraction, this value ranges from 4 to 7 mm. *AML* anterior mitral leaflet, *AV* aortic valve, *IVS* interventricular septum, *LA* left atrium, *LV* left ventricle, *RVOT* right ventricular outflow tract, *MV* mitral valve, *PML* posterior mitral leaflet

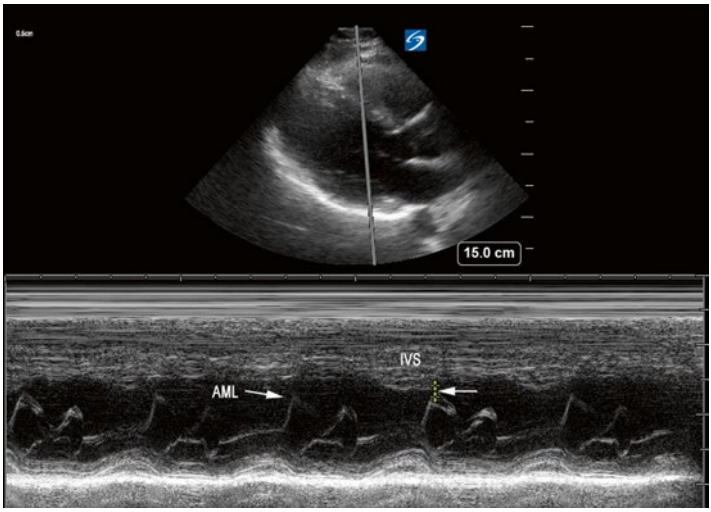

Fig. 5.31 E'point-septal separation (*EPSS*) with M-mode in a patient with normal ejection fraction. EF can be calculated using the formula: EF = 75.5 − 2.5 EPSS (mm). *AML* anterior mitral leaflet; *IVS* interventricular septum

advancing frame by frame to the point of maximal opening of the valve during diastole (Fig. 5.31). The mitral valve leaflet septum distance method is an attractive index of left ventricular function (LVF) because it can be obtained rapidly, requiring only a single view of the LV base or a single linear distance measurement, most commonly using the PLAX or A4C views. Moreover, it is a cumulative marker of function in that it reflects the net effect of wall motion throughout the ventricle, obviating the visualization and assessment of each myocardial segment, and it requires no geometric assumptions about ventricular shape.

Recent investigations have shown that the EPSS can also be used to quantify ejection fraction through the following formula: EF = 75.5 − 2.5 EPSS (mm) [21]. EPSS can be used as an adjunct to the global visual assessment to best identify the presence and degree of LV dysfunction. However, there are a few limitations with this technique to bear in mind, including the presence of valvular abnormalities such as aortic regurgitation (AR) or mitral stenosis (MS), septal or basal septal hypertrophy, and mechanical valves which may cause inaccurate measurement; oblique axis of echo beam to the LV can distort the leaflet-septum distance on M-mode; mistaking the mitral valve chord for the leaflet tip on M-mode can cause erroneous measurement.

Movement of Mitral Annulus

Although this method should be used by more experienced practitioners, it is prudent to discuss this method as it is easy to perform with 2D echocardiography. With systole, the mitral annulus moves toward the apex and this motion is

proportional to the ventricular shortening. Normally this movement is ≥8 mm and can be appreciated with A4C view. If it is less than 8 mm, the EF is usually less than 50 % [12, 22].

Quantitative Measurement of LV Function

Simpson's Method

EF can be directly calculated using the biplane method of discs or "Simpson's" method, as recommended by the American Society of Echocardiography [23]. This method requires tracing the LV endocardial borders in two orthogonal views. Calculation involves dividing the LV into cross-sectional disks. The total LV volume is then calculated from the summation of the cross-sectional disks. First, a good A4C view is obtained and the image is optimized. Tracings are done in both end-diastole (largest ventricular volume or first frame after MV closure; onset of QRS waves on EKG) and end-systole (smallest ventricular volume or frame just before MV opening; end of T-wave on EKG). These two areas, combined with the measured length of the ventricle, allow the machine software to estimate a volume of the ventricle.

$$\text{EF} = \frac{(\text{LV End Diastolic Volume} - \text{LV End Systolic Volume})}{\text{LV End Diastolic Volume}}$$

There are several limitations to this technique when performed in the ICU setting. It requires adequate visualization of the endocardium in at least two views and may be a technically difficult feat on ventilated patients. The operator has to avoid the inclusion of trabeculae and papillary muscles when "tracing" the borders. This requires considerable time to perform, rendering it somewhat impractical in a busy ICU.

Fractional Shortening (FS)

This is one of the more common quantitative measurements used in critical care and uses the parasternal long-axis view for a single measurement of LV diameter in systole and diastole. The measurement should be perpendicular to the long axis of the ventricle and centered in short axis. An M-mode beam perpendicular to ventricle at the mitral leaflet tip has a better resolution. The distance between the septal and inferior wall endocardium at end-systole (end of T wave or minimum distance) and end-diastole (beginning of the QRS wave or maximum distance) is measured (Fig. 5.32). Normal FS is between 25 % and 45 % [23].

$$\text{Fractional Shortening} = \frac{(\text{LV diameter end diastole} - \text{LV diameter end systole})}{\text{LV diameter end diastole}}$$

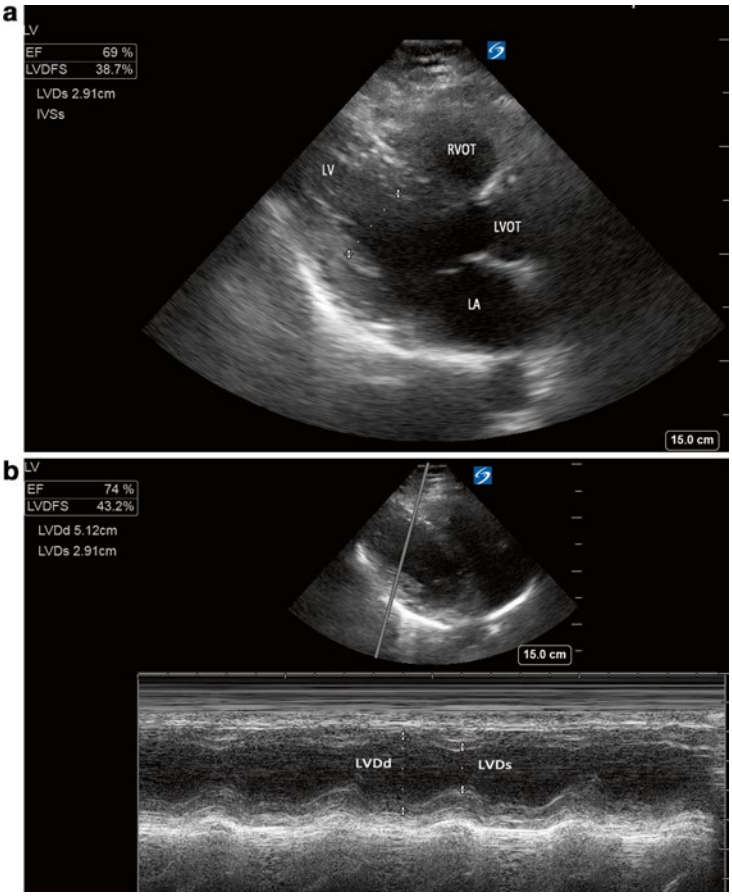

Fig. 5.32 Fractional shortening in (**a**) 2D and (**b**) M-mode in parasternal long-axis view. The measurement should be perpendicular to the long axis of the ventricle and centered in short axis in 2D mode. And in M-mode, the beam should be perpendicular to ventricle at the mitral leaflet tip. The distance between the interventricular septum and inferior wall endocardium at end-systole and end-diastole is measured. Normal values are between 25 % and 45 %. *LA* left atrium, *LV* left ventricle, *LVOT* left ventricular outflow tract, *LVDd* left ventricular diameter in diastole, *LVDs* left ventricular diameter in systole, *RVOT* right ventricular outflow tract

The main limitation of using FS as a measure of LV function is that it only measures myocardial excursion at the mid ventricle. Apical or basilar hypokinesis/akinesis may be missed and these areas can contribute significantly to EF. To avoid this limitation, simply assess for dysfunction in these areas using 2D imaging, and if they appear normal, then FS is likely a valid estimate of overall function.

Fractional Area of Change

Similar to the above methods measuring change in diameter (FS) or volume (EF), this method relies on measuring change in area during systole and diastole.

$$\text{Fractional Area of Change} = \frac{(\text{Area end diastole} - \text{Area end systole})}{\text{Area end diastole}}$$

The optimal view for measurement using the change in area is the parasternal short axis view at the papillary muscle level. The area can be traced using the ultrasound software and automatically calculated by the machine. Care should be given to avoid inclusion of papillary muscles when tracing. Limitation with using fractional area of change (FAC) is similar to that using FS in that function is only measured at mid-ventricle. Abnormal apical or basilar geometry will not be included in this measurement and can be a potential source of error. Additionally, the reliance on good endocardial visualization can limit its use in some cases.

Advanced Measures of LV Function

In summary, one or more of the five methods above methods (global visual assessment, mitral valve leaflet excursion/EPSS, Simpson's method, fractional shortening, and fractional area of change) are used by intensivists. Other methods have been developed and can be used, especially by the more advanced echocardiographer as they often times rely on the use of Doppler. These methods rely on various aspects of left ventricular function for quantification, and all have been shown to correlate with global estimates of LV function. Some examples include the measuring the rate of pressure rise of the mitral regurgitant flow ("dP/dt" method), or the velocity of mitral annulus descent or velocity of myocardial tissue (DTI method). These methods are of little use for intensivists, as they rely on high levels of expertise, are time consuming and require optimal imaging conditions, which are often not present in the ICU. In reality, practicing cardiologists also rarely use these methods and the global visual assessment is relied on as the most pragmatic method of assessment of LV function.

Estimation of Stroke Volume and Cardiac Output

The estimation of stroke volume (SV) and cardiac output (CO) by echocardiography is not routinely assessed in a standard exam, but can be a useful method for the assessment and monitoring of LV systolic function in the critically ill patient. Stroke volume (SV in cm^3 or mL) is defined as the volume of blood ejected into the aorta during a single cardiac cycle. Calculation of SV requires measuring the product of

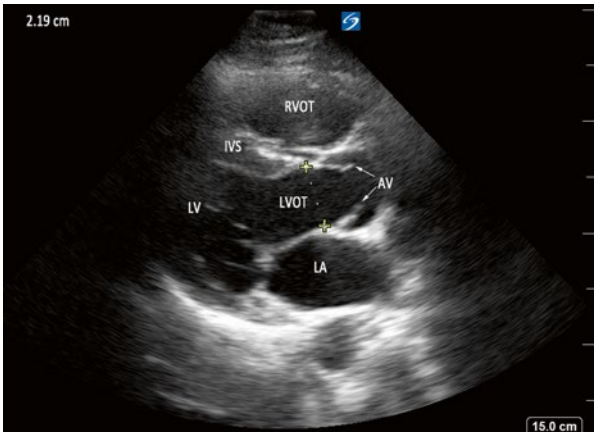

Fig. 5.33 Measurement of LVOT diameter in parasternal long-axis view. Measurement is done just proximal to the aortic valve (*AV*) leaflets. The left ventricular outflow tract (*LVOT*) diameter ranges from 1.8 to 2.2 cm. *AV* aortic valve, *IVS* interventricular septum, *LV* left ventricle, *LA* left atrium, *RVOT* right ventricular outflow tract

the cross-sectional area (CSA) of the left ventricular outflow tract (LVOT) multiplied by the distance the RBCs within the volume travel. This calculation of SV assumes that the LV pumps the blood into a cylindrical aorta, that the flow is laminar where all blood cells are moving in the same direction, and that the profile is flat:

$$SV = CSA \times VTI$$

Measurement of CSA

The measurement of the CSA is relatively straightforward given that the base of this cylinder is a circle formed by the LV outflow tract (LVOT). To calculate the area of this base, the following formula is used, requiring only the measurement of the LVOT diameter (D):

$$CSA = \pi\,(D/2)^2$$

Stroke volume can be calculated across any structure where one can measure CSA and velocity of blood flow. One must ensure that the site of flow velocity recording is the same as the anatomic measurement of the CSA [24]. In addition, CSA of the orifice can change based on loading conditions, requiring re-measurement of diameters to avoid erroneous measurements of SV. For this reason, the most preferred site for repeated SV measurements is the LVOT, given that the LVOT diameter changes very little through systole and diastole and is assumed to be constant and closely approximating a circle in shape [25].

When measuring LVOT CSA, the LVOT diameter is measured from the parasternal long-axis (PLAX) view, just proximal to the aortic valve (AV) leaflets (Fig. 5.33). The image should be optimized by decreasing the depth or zooming in on the image and adjusting gain. Placing a few beats in a cine-loop will allow measurement of the annulus diameter during mid-systole from the inner edge of the septal endocardium to the inner edge of the anterior mitral leaflet base. The LVOT diameter ranges from 1.8 to 2.2 cm. Additionally, M-mode can be used to ensure

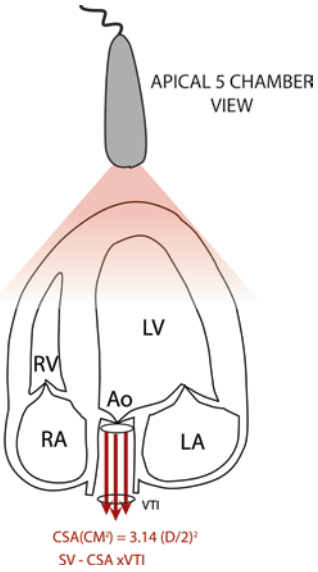

Fig. 5.34 Illustration of the red blood cell (*RBC*) column and calculation of velocity-time integral (*VTI*) using Doppler stroke volume calculation. It is important to have the Doppler beam orientation as parallel to the RBC column as possible and any angle higher than 20° would lead to underestimation of velocities and inaccurate calculation of hemodynamic parameters. Image courtesy of Guy Aristide, MD

further accuracy in measurement. Keep in mind that small inaccuracies in diameter measurement can lead to large errors in CSA and SV measurements as the radius is squared.

Velocity-Time Integral Measurement

The next step involves measuring the distance the column of blood travels during the cardiac cycle. This distance is derived from integrating the range of RBC velocities over time, a number called the velocity-time integral or (VTI) or time-velocity integral (TVI). In other words, VTI is the stroke distance that blood travels with each stroke. The velocities of this "column" of RBCs are measured using Doppler echocardiography (Fig. 5.34). The operator must gently position the ultrasound (US) transducer to align the Doppler beam with the most parallel angle in order to obtain the most accurate velocity (Fig. 5.35). Any angle higher than 20° would lead to underestimation of velocities and inaccurate calculation of hemodynamic parameters [12, 26]. For VTI measurements, pulsed-wave Doppler (PWD) of LVOT velocities is recorded from the apical five-chamber view, with the sample volume positioned just proximal to the AV. The AV closing click on the LVOT velocity recording ensures that the sample volume is located at the same site on the aortic annulus as the diameter measurement. It is best to trace the outer edge of the densest portion of the spectral tracing and ignore the dispersion that occurs near peak velocity. Normal LVOT VTI in adults range from 18 to 22 cm. For patients in sinus rhythm, data from 3 to 5 cardiac cycles may be averaged. However, in patients with irregular rhythms such as atrial fibrillation, 5–10 cycles may be required to ensure

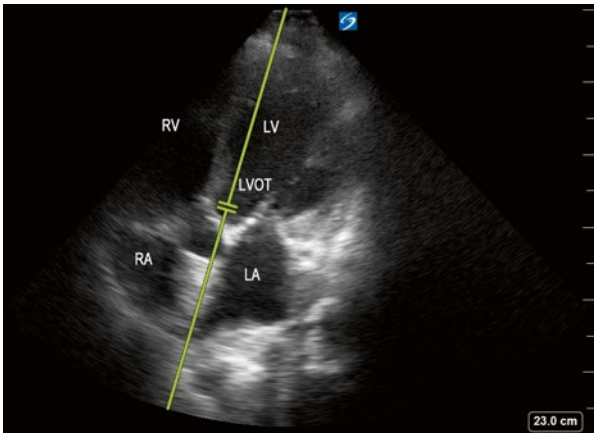

Fig. 5.35 Apical five-chamber view with Doppler beam orientation along the left ventricular outflow tract (*LVOT*). *LA* left atrium, *LV* left ventricle, *LVOT* left ventricular outflow tract, *RA* right atrium, *RV* right ventricle

accuracy of results. Performing measurements in at least two orthogonal planes and averaging several beats can reduce error, although the time investment required may not be feasible.

Cardiac Output

Cardiac output (L/min) is the effective volume of blood expelled per unit time and is calculated as the product of heart rate and stroke volume, divided by 1,000 mL/L. In adults, normal stroke volume ranges from 80 to 140 mL/beat and the normal cardiac output ranges from 4 to 7 L/min. The cardiac index (CI in L/min/m^2) is CO divided by body surface area (BSA in m^2), the normal values of which range from 2.8 to 4.5 L/min/m^2.

SV and CO are easily measured using Doppler echo and can aid in the management of the critically ill patient by assessing baseline CO and response to various interventions such as a fluid challenge, vasoactive agents, and medications that reduce the afterload. Stroke volume can be calculated at any site (i.e., mitral annulus, RVOT), where the diameter and VTI can be measured, but is most commonly measured at the LVOT (Fig. 5.36). As described above, the intricate calculations and assumptions necessary to derive these calculations can easily become inaccurate by small errors in measurement of LVOT diameter or tracing of VTI; hence, these measurements are operator dependent. Nevertheless, these measurements are underutilized and can be of high utility for noninvasive hemodynamic monitoring.

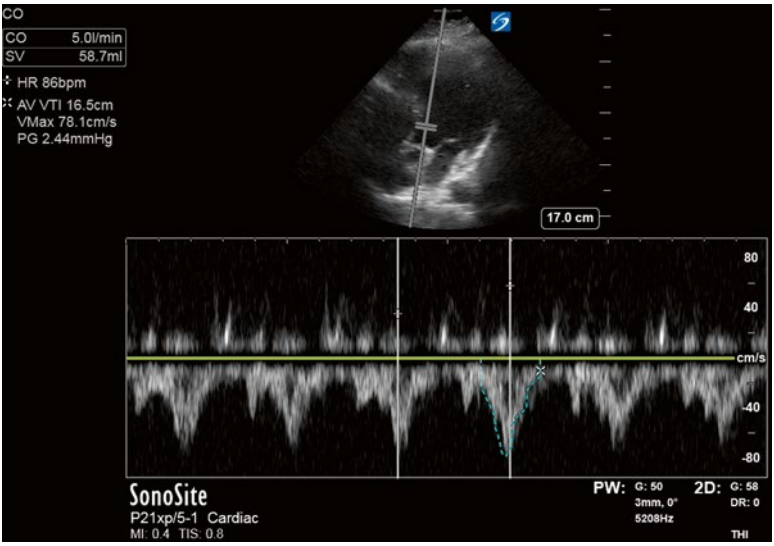

Fig. 5.36 Left ventricular outflow tract velocity time integral (*LVOT VTI*) measurement in apical five-chamber view using pulsed-wave Doppler (*PWD*). It is best to trace the outer edge of the densest portion of the spectral tracing and ignore the dispersion that occurs near peak velocity (indicated by *hashed lines*). Normal LVOT VTI in adults range from 18 to 22 cm. For patients in sinus rhythm, data from 3 to 5 cardiac cycles may be averaged

Assessment of Regional LV function

Whenever global systolic dysfunction is noted, a careful search for the active or prior sequelae of ischemic heart disease must be performed, done largely by identifying regional wall motion abnormalities (RWMA). The most common cause of RWMA is ischemia caused by partial or complete coronary arterial thrombotic obstruction in the vessel supplying that portion of the myocardium. This search for RWMA is particularly important in the patient who remains in a shock state despite vasoactive therapy, as classic signs and symptoms of acute coronary syndrome (ACS) may not be recognized due to sedation and unresponsiveness [27]. Patients with preexisting atherosclerosis often develop ischemia causing an inability to meet the myocardial demands from critical illness, resulting in supply–demand mismatch. Ischemic ST-segment changes and anginal symptoms are often late manifestations of ACS and are often preceded by diastolic dysfunction and RWMA. Myocardial ischemia is well described in patients with septic shock and may only become apparent after adequate fluid resuscitation and hemodynamic support [28].

Myocardial Segmentation

Evaluation of regional systolic function is based on careful observation of all myocardial segments for endocardial excursion and wall thickening. For proper documentation, monitoring, and guidance of interventions, the intensivists must learn the myocardial segment nomenclature developed by the American Heart Association (AHA), a 17-segment model [29]. In this system, the LV is divided into basal, mid-ventricular, and apical segments along the long axis to correspond to proximal, mid, and apical coronary lesions. The basal and mid-ventricular regions are further subdivided into 6 segments each, and the apical segment into 4 segments, with the apical cap being the 17th segment. In the short axis view, the LV is divided clockwise into 6 segments: anterior, anterior-lateral, inferior-lateral, inferior, inferior-septal, and anterior-septal. It should be noted that the apical cap can only be assessed by perfusion studies given that no excursion is normally seen in this area on echocardiography [23].

The above segmentation of the LV is based on its corresponding coronary artery blood supply. The left anterior descending artery (LAD) supplies the anterior wall, anterior septum, and the apex. The left circumflex artery (CX) supplies the anterior-lateral and inferior-lateral walls. The right coronary artery (RCA) supplies the inferior wall and the basal and mid-ventricular segments of the inferior septum. There is variability in the supply to the myocardial segments; however, segmental wall motion abnormalities generally correspond closely to the coronary artery supply to the impaired myocardial segment.

Regional Wall Motion Evaluation

It is recommended that each segment be analyzed individually and scored on the basis of its endocardial motion and systolic thickening. Normal contraction results in a spiral squeeze from the LV base to the apex. Excursion is measured by the amount of decrease in endocardial wall separation during systole, normally decreasing between 25 % and 50 %. Thickening is assessed by the degree to which the thickness of the myocardial wall segment increases during systole, normally doing so by greater than 40 %. A hyperdynamic LV has increased amplitude and velocity of endocardial excursion and thickening, whereas a hypokinetic LV has reduced endocardial motion and systolic wall thickening (see basic competencies section). Akinesis is characterized as the absence of endocardial excursion and wall thickening, and dyskinesis is defined by paradoxical outward motion of the thinned LV wall during systole. An aneurysmal segment is defined by thinning and bulging of the wall during both systole and diastole. Segmental wall motion abnormalities are visually assessed and scored as defined in Table 5.1. A wall motion score index is devised by adding the sum of individual segments and dividing this by the number of segments evaluated. Note that tethering of the myocardium can appear as normal endocardial excursion but not thickening [30]. M-mode can be a useful adjunct to further delineate normal endocardial excursion and thickening.

Table 5.1 Scoring of segmental wall motion abnormalities

Score	Wall motion	Definition
1	Normal	Normal endocardial excursion and thickening (or hyperdynamic)
2	Hypokinesis	Decreased endocardial excursion and thickening (<30 %)
3	Akinesis	Absence of endocardial excursion and negligible thickening (<10 %)
4	Dyskinesis	Paradoxical outward motion during systole; thin, scarred myocardium
5	Aneurysmal	Thinning and bulging during systole and diastole

$$\text{Wall Motion Score Index (WMSI)} = \frac{\text{Sum of segmental scores}}{\text{No. of segments visualized}}$$

Although this semiquantitative method is recommended for assessment of RWMA, this can be both challenging and impractical for the critical care physician. Nevertheless, a working knowledge of the coronary anatomy and the terminology to appropriately characterize regional abnormalities is essential for communication with other specialists and optimal multidisciplinary management of the patient. Moreover, the WMSI has clinical implications as a WMSI greater than 1.7 is associated with worse outcomes after a myocardial infarction [31].

Advanced Competencies Required for Assessment of Valve Function and Integrity

Qualitative and quantitative assessments of severity with valvular lesions are not routinely performed as part of routine CCE. Proficiency in advanced CCE necessitates ample training in Doppler techniques and understanding the limitations. There are several common principles to be cognizant of upon using Doppler in ICU. For instance, the presence of an obstruction to flow will result in a significant increase in velocity of blood across the valve in systole and can be used to calculate the pressure gradient between the two chambers using modified Bernoulli equation (pressure gradient = 4 V^2). The SV measured at one point in the heart should be equal to SV at another point, in the absence of valvular regurgitation or shunt (Box 5.7). In other words, what goes in must come out; this forms the basis of continuity equation. Other techniques, such as measurement of proximal isovelocity surface area (PISA), pressure half time, and vena contracta width, are laborious and time consuming in the ICU setting and hence not mentioned in detail.

Mitral Stenosis (MS)

MS can be caused by rheumatic heart disease, mitral annular calcification, and congenital malformation (parachute mitral valve). Increased LA pressure causes progressive atrial dilation, atrial fibrillation, and transmitted pressure to the pulmonary

Box 5.7. Continuity Equation

$$SV_1 = SV_2$$

$$A_1 \times VTI_1 = A_2 \times VTI_2$$

$$A_2 = \frac{A_1 \times VTI_1}{VTI_2}$$

SV stroke volume, *VTI* velocity time integral, *A* area

circuit causing pulmonary edema. 2D imaging shows a thickened mitral valve; thickening is seen at the tips and chordal level with rheumatic heart disease with a hockey stick appearance of anterior leaflet in the PLAX view. Thickening and fusion of the MV commissural edges and chordae can result in doming of the MV opening. Annular calcification, on the other hand, results in a hyperechoic lesion at the level of the mitral annulus. Left atrial enlargement and occasionally thrombus can be seen. Long standing MS can lead to secondary pulmonary hypertension and right ventricular enlargement.

An M-mode through the mitral valve in PLAX can show the anterior and posterior leaflets moving anteriorly, rather than moving in opposite directions. Color Doppler may not be optimal with severe calcification of the mitral valve causing ultrasound reflections. When not severely calcified there can be a narrow, forward jet with acceleration and spreading through the stenotic valve giving the appearance of a "candle flame." The severity of mitral stenosis can be assessed by measuring the pressure gradient across the mitral valve using CW Doppler in A4C view. CWD across the MV will determine the pressure gradient between the LA and LV. The peak pressure gradient can be obtained using the modified Bernoulli equation. The mean mitral gradient can be calculated by tracing the Doppler velocities above baseline. A mean gradient greater than 10 mmHg is considered severe. Additionally, the MV area can be calculated using the continuity equation. An MV area less than 1.0 cm^3 is considered severe. Pressure half time (PHT) is the time interval for the peak pressure gradient to reach its half level. MV area is equal to 220/PHT, hence a PHT greater than 220 milliseconds is consistent with severe MS.

Mitral Regurgitation

As mentioned above, MR is commonly encountered in ICU and can be due to acute conditions such as papillary muscle or chordae rupture and endocarditis or due to chronic conditions such as dilated cardiomyopathy. A 2D study will show,

depending on the etiology, mitral valve prolapse, thickening of the valve, chordae, mitral annular calcification, hyperechoic mass attached to mitral leaflet with endocarditis, or increased LA size. An M-mode in patients with MV prolapse shows >3 mm movement posteriorly. Color Doppler demonstrates the systolic regurgitation from the left ventricle to the left atrium in PLAX and A4C views as described above. MR can be graded as mild or severe based on the Doppler data. Color Doppler can be used to assess the jet size ratio to note if it is mild (MR/LA ratio <20 %; jet width <0.3 cm) or severe (MR/LA ratio >40 %; jet width >0.7 cm). The vena contracta is the narrowest portion of the MR jet downstream from the orifice. A vena contracta width greater than 0.7 cm is consistent with severe MR. Measurement of proximal isovelocity surface area (PISA) and vena contracta allows quantitative measurement of MR. CW Doppler uses jet density and jet profile to characterize MR into mild, moderate, and severe. PW Doppler on the other hand uses increased mitral inflow velocity and systolic pulmonary vein flow reversal to assess severity.

Aortic Stenosis

Etiology of AS is usually congenital, rheumatic, or degenerative. A 2D examination will show a hyperechoic valve with reduced excursion of the leaflet with severe valvular stenosis. Other features like number of cusps, systolic doming, and presence of supra- and subvalvular stenosis can be assessed at the same time. An M-mode shows decreased excursion of the cusps throughout the cardiac cycle. Instantaneous transvalvular gradient can be determined with CW Doppler. The peak velocity across the valve is calculated and using the Bernoulli equation mentioned above the average mean pressure between the aorta and left ventricle in systole is measured. Conversely, with continuity equation, the aortic valve area can be measured assuming the $CSA_{AV} \times VTI_{across\ AV} = CSA_{LVOT} \times VTI_{LVOT}$. However, one should know that mixed lesions (coexisting AS and AR) can affect LVOT velocities with continuity equation and mean gradient can be overestimated.

Aortic Regurgitation

Conditions such as flail leaflets, congenital defects, infections, and aortic root abnormalities can cause AR. A 2D examination can assess the anatomy of the cusps, vegetation, LV/LA size and function, and the size of ascending aorta. An M-mode will show MV diastolic fluttering, early closure of the MV, and presence of B wave (through MV). A Color Doppler can assess the direction of flow, jet size and configuration, or flow reversal in aorta. PW Doppler assessment at the descending aorta will show diastolic flow reversal and retrograde VTI >15 cm with severe AR. Pressure half time calculated with CW can detect severe AR (<200 ms), however is load-dependent and can be seen with a stiff noncompliant LV.

Evidence Review and Evidence-Based Use

Clinicians must acquire the requisite skill and experience for accurate assessment of LV function. Fortunately for the novice intensivists, the most commonly used and achievable measures require skills that can be acquired with focused training [13, 16]. A recent international consensus document recommended 30 fully supervised transthoracic echocardiographic examinations as a reasonable number to achieve competence, based on a review of the available literature [32]. A number of studies have been able to show both high accuracy and correct management decisions by intensivists after minimal training in basic echocardiography [16, 33]. Melamed and associates showed that intensivists could correctly make categorical assessments of LV function in 82 % of cases when compared to board-certified echocardiographers. Training in this study consisted of 2 h of didactics and 4 h of hands-on followed by unquantified independent study by the intensivists [13]. Manasia showed 84 % agreement in interpretation of LV function by surgical intensivists after ten 1 h tutorials on TEE, and Vignon recently validated a 12 h training program which showed trainees achieving a kappa of 0.84 when compared to experienced echocardiographers. It should be noted that one study showed a kappa of 0.7 between two experienced echocardiographers in a random sample of 20 hypotensive patients [10]. Studies among ED physicians also show similar accuracy after focused training [15]. In summary, the bulk of the literature demonstrates that intensivists can achieve acceptable accuracy after focused training, in amounts easily achievable in critical care training programs.

Pitfalls and Precautions

As mentioned above, when practiced in a standardized fashion, the use of goal-directed echocardiography can be an invaluable tool in the care of critically ill patients. However, it is extremely important to recognize some common situations where imaging errors may be introduced and how these missteps will lead to flawed interpretations. Listed below are selected common scenarios where one should recognize the possibility for such errors:

- Caution should be exercised when using PLAX view in the assessment of LV size, as off-axis views can lead to erroneous assessment of LV size and function.
- In the A4C view, an off-axis view will lead to foreshortening of the LV and incorrect conclusions in the assessment of LV wall thickness and EF.
- Global visual assessment of EF is highly operator dependent and requires formal, structured training.
- When examining for regional wall motion abnormalities, watch out for “tethering” where abnormal myocardium appears to have excursion but without thickening, as it is tethered to normal adjacent myocardium.

- When calculating LV dimensions using M-mode, if the ultrasound beam is not aligned perpendicular to the long axis, LV size can be overestimated.
- For fractional area of change measurements in PSAX view, oblique cuts make measurements more difficult.
- Fractional shortening assumes symmetric LV performance: hence, this is unreliable in the setting of regional wall motion abnormalities, specifically if apical or basilar hypokinesis/akinesis is present.
- EPSS measurements in the presence of valvular abnormalities such as aortic regurgitation (AR) or mitral stenosis (MS), septal or basal septal hypertrophy, and mechanical valves may cause inaccurate measurement.
- When using Simpson's method, improper tracing of the endocardium and foreshortening of the LV cavity can lead to erroneous measurements of LV volumes.
- For CO measurements, since the LVOT radius is squared, small errors in measurement can lead to erroneous measurements of stroke volume and cardiac output. Also, it is common to forget that one is measuring the diameter and thus must be divided by two prior to squaring it.

References

1. Beaulieu Y, Marik PE. Bedside ultrasonography in the ICU: part 1. Chest. 2005;128(2): 881–95.
2. Mayo PH, Beaulieu Y, Doelken P, Feller-Kopman D, Harrod C, Kaplan A, Oropello J, Vieillard-Baron A, Axler O, Lichtenstein D, Maury E, Slama M, Vignon P. American College of Chest Physicians/La Societe de Reanimation de Langue Francaise statement on competence in critical care ultrasonography. Chest. 2009;135(4):1050–60.
3. Mayo PH. Training in critical care echocardiography. Ann Intensive Care. 2011;1:36.
4. Oh JK. The echo manual. Philadelphia: Lippincott Williams and Williams; 2006.
5. Catherine M, Otto M. Textbook of clinical echocardiography. Philadelphia: Saunders Elsevier; 2009.
6. Spencer KT, Kimura BJ, Korcarz CE, Pellikka PA, Rahko PS, Siegel RJ. Focused cardiac ultrasound: recommendations from the american society of echocardiography. J Am Soc Echocardiogr. 2013;26(6):567–81.
7. Henry WL, DeMaria A, Gramiak R, King DL, Kisslo JA, Popp RL, Sahn DJ, Schiller NB, Tajik A, Teichholz LE, Weyman AE. Report of the American Society of Echocardiography Committee on nomenclature and standards in two-dimensional echocardiography. Circulation. 1980;62(2):212–7.
8. Mark DG, Ku BS, Carr BG, Everett WW, Okusanya O, Horan A, Gracias VH, Dean AJ. Directed bedside transthoracic echocardiography: preferred cardiac window for left ventricular ejection fraction estimation in critically ill patients. Am J Emerg Med. 2007;25(8): 894–900.
9. Culp BC, Mock JD, Chiles CD, Culp Jr WC. The pocket echocardiograph: validation and feasibility. Echocardiography. 2010;27(7):759–64.
10. Moore CL, Rose GA, Tayal VS, Sullivan DM, Arrowood JA, Kline JA. Determination of left ventricular function by emergency physician echocardiography of hypotensive patients. Acad Emerg Med. 2002;9(3):186–93.

11. Vignon P, Dugard A, Abraham J, Belcour D, Gondran G, Pepino F, Marin B, Francois B, Gastinne H. Focused training for goal-oriented hand-held echocardiography performed by noncardiologist residents in the intensive care unit. Intensive Care Med. 2007;33(10):1795–9.
12. Catherine M. Otto. Left and right ventricular systolic function. In: Textbook of clinical echocardiography. Philadelphia: Saunders Elsevier; 2009. p. 125–56.
13. Melamed R, Sprenkle MD, Ulstad VK, Herzog CA, Leatherman JW. Assessment of left ventricular function by intensivists using hand-held echocardiography. Chest. 2009;135(6): 1416–20.
14. Zoghbi WA, Enriquez-Sarano M, Foster E, Grayburn PA, Kraft CD, Levine RA, Nihoyannopoulos P, Otto CM, Quinones MA, Rakowski H, Stewart WJ, Waggoner A, Weissman NJ. American Society of Echocardiography: recommendations for evaluation of the severity of native valvular regurgitation with two-dimensional and Doppler echocardiography. Eur J Echocardiogr. 2003;4:237–61.
15. Randazzo MR, Snoey ER, Levitt MA, Binder K. Accuracy of emergency physician assessment of left ventricular ejection fraction and central venous pressure using echocardiography. Acad Emerg Med. 2003;10(9):973–7.
16. Manasia AR, Nagaraj HM, Kodali RB, Croft LB, Oropello JM, Kohli-Seth R, Leibowitz AB, DelGiudice R, Hufanda JF, Benjamin E, Goldman ME. Feasibility and potential clinical utility of goal-directed transthoracic echocardiography performed by noncardiologist intensivists using a small hand-carried device (SonoHeart) in critically ill patients. J Cardiothorac Vasc Anesth. 2005;19(2):155–9.
17. Vieillard-Baron A, Caille V, Charron C, Belliard G, Page B, Jardin F. Actual incidence of global left ventricular hypokinesia in adult septic shock. Crit Care Med. 2008;36(6):1701–6.
18. Vieillard-Baron A, Slama M, Cholley B, Janvier G, Vignon P. Echocardiography in the intensive care unit: from evolution to revolution? Intensive Care Med. 2008;34(2):243–9.
19. Child JS, Krivokapich J, Perloff JK. Effect of left ventricular size on mitral E point to ventricular septal separation in assessment of cardiac performance. Am Heart J. 1981;101(6): 797–805.
20. Ahmadpour H, Shah AA, Allen JW, Edmiston WA, Kim SJ, Haywood LJ. Mitral E point septal separation: a reliable index of left ventricular performance in coronary artery disease. Am Heart J. 1983;106(1 Pt 1):21–8.
21. Silverstein JR, Laffely NH, Rifkin RD. Quantitative estimation of left ventricular ejection fraction from mitral valve E-point to septal separation and comparison to magnetic resonance imaging. Am J Cardiol. 2006;97(1):137–40.
22. Picard MH, Popp RL, Weyman AE. Assessment of left ventricular function by echocardiography: a technique in evolution. J Am Soc Echocardiogr. 2008;21(1):14–21.
23. Lang RM, Bierig M, Devereux RB, Flachskampf FA, Foster E, Pellikka PA, Picard MH, Roman MJ, Seward J, Shanewise JS, Solomon SD, Spencer KT, Sutton MS, Stewart WJ. Recommendations for chamber quantification: a report from the American Society of Echocardiography's Guidelines and Standards Committee and the Chamber Quantification Writing Group, developed in conjunction with the European Association of Echocardiography, a branch of the European Society of Cardiology. J Am Soc Echocardiogr. 2005;18(12): 1440–63.
24. Zoghbi WA, Quinones MA. Determination of cardiac output by Doppler echocardiography: a critical appraisal. Herz. 1986;11(5):258–68.
25. Moulinier L, Venet T, Schiller NB, Kurtz TW, Morris Jr RC, Sebastian A. Measurement of aortic blood flow by Doppler echocardiography: day to day variability in normal subjects and applicability in clinical research. J Am Coll Cardiol. 1991;17(6):1326–33.
26. Quinones MA, Otto CM, Stoddard M, Waggoner A, Zoghbi WA. Recommendations for quantification of Doppler echocardiography: a report from the Doppler Quantification Task Force of the Nomenclature and Standards Committee of the American Society of Echocardiography. J Am Soc Echocardiogr. 2002;15(2):167–84.

27. Chockalingam A, Mehra A, Dorairajan S, Dellsperger KC. Acute left ventricular dysfunction in the critically ill. Chest. 2010;138(1):198–207.
28. Parker MM, Shelhamer JH, Bacharach SL, Green MV, Natanson C, Frederick TM, Damske BA, Parrillo JE. Profound but reversible myocardial depression in patients with septic shock. Ann Intern Med. 1984;100(4):483–90.
29. Cerqueira MD, Weissman NJ, Dilsizian V, Jacobs AK, Kaul S, Laskey WK, et al. Standardized myocardial segmentation and nomenclature for tomographic imaging of the heart: a statement for healthcare professionals from the Cardiac Imaging Committee of the Council on Clinical Cardiology of the American Heart Association. Circulation. 2002;105:539–42.
30. Lieberman AN, Weiss JL, Jugdutt BI, Becker LC, Bulkley BH, Garrison JG, Hutchins GM, Kallman CA, Weisfeldt ML. Two-dimensional echocardiography and infarct size: relationship of regional wall motion and thickening to the extent of myocardial infarction in the dog. Circulation. 1981;63(4):739–46.
31. Hillis GS, Moller JE, Pellikka PA, Gersh BJ, Wright RS, Ommen SR, Reeder GS, Oh JK. Noninvasive estimation of left ventricular filling pressure by E/e' is a powerful predictor of survival after acute myocardial infarction. J Am Coll Cardiol. 2004;43(3):360–7.
32. Cholley BP, Mayo PH, Poelaert J, Vieillard-Baron A, Vignon P, Alhamid S, Balik M, Beaulieu Y, Breitkreutz R, Canivet JL, Doelken P, Flaatten H, Frankel H, Haney M, Hilton A, Maury E, McDermid RC, McLean AS, Mendes C, Pinsky MR, Price S, Schmidlin D, Slama M, Talmor D, Teles JM, Via G, Voga G, Wouters P, Yamamoto T. International expert statement on training standards for critical care ultrasonography. Intensive Care Med 2011;37(7):1077–1083.
33. Vignon P, Mucke F, Bellec F, Marin B, Croce J, Brouqui T, Palobart C, Senges P, Truffy C, Wachmann A, Dugard A, Amiel JB. Basic critical care echocardiography: validation of a curriculum dedicated to noncardiologist residents. Crit Care Med. 2011;39(4):636–42.

Chapter 6
Critical Care Echocardiography: Right Ventricular Dysfunction

Johannes Steiner and Gaurav Choudhary

Introduction

Right heart failure (RHF) is a common and severe complication during perioperative and intensive care treatment. The most common causes are pulmonary hypertension, left heart failure, pulmonary embolism, sepsis, acute lung injury, right ventricular (RV) infarction, and thoraco-surgical procedures [1]. In the critical care setting, RV function is also altered by other conditions increasing RV afterload, including hypoxia and high levels of positive end-expiratory pressure [2]. Acute RHF is not only a major contributor to morbidity and mortality [3–5], it also influences efficacy and outcome of routinely used therapies, such as vasopressors [6], fluid loading [7], and thrombolytics [8]. In contrast to the left ventricle, the right ventricle's physiology and pathophysiology are understudied, and the diagnosis of acute RHF is frequently challenging.

Echocardiography is playing an increasingly important role in the intensive care unit to identify underlying right ventricular pathology and loading conditions. It provides rapid and important data for diagnosing RV failure, elucidating precipitating causes, monitoring hemodynamics, and triaging patients into three groups: RV failure with elevated pulmonary artery (PA) pressures (pulmonary embolus (PE), exacerbation of pulmonary hypertension (PH), respiratory or left ventricular failure), RV failure without elevated pressures (RV infarction, acute tricuspid regurgitation (TR)), and pericardial disease (tamponade, pericardial constriction).

J. Steiner, M.D. (✉)
Division of Cardiology, Alpert Medical School of Brown University/Rhode Island Hospital, 593 Eddy St., Providence, RI 02903, USA
e-mail: hannes.steiner@gmail.com

G. Choudhary, M.D.
Department of Medicine, Division of Cardiology, Alpert Medical School of Brown University/Providence VA Medical Center, 830 Chalkstone Ave, Providence, RI 02904, USA
e-mail: gaurav_choudhary@brown.edu

M. Jankowich, E. Gartman (eds.), *Ultrasound in the Intensive Care Unit*, Respiratory Medicine, DOI 10.1007/978-1-4939-1723-5_6

In this chapter, we will discuss the use of echocardiography in assessment of RV structure and function in the critical care settings, as well as describe commonly encountered intensive care unit (ICU) scenarios involving RV pathologies.

Pathophysiology of Right Heart Failure

The normal pulmonary circulation is a high-flow, low-pressure system. Unlike the left ventricle (LV), the thin-walled RV poorly tolerates acute increases in afterload. After an initial insult that increases pulmonary vascular resistance (PVR) (e.g., PE) or decreases RV function (e.g., RV infarct), RV dilation can increase the stroke volume of the RV by increasing preload and thus moving to a more favorable position on the Frank-Starling curve. However, this compensatory response of the RV to volume and pressure overload ultimately leads to an increase in myocardial oxygen consumption, reduction in contractility, and functional TR resulting in diminished cardiac output. Elevated pressure in the RV also compromises filling of the right coronary artery by decreasing the pressure gradient between the aorta and the RV. In addition, the dilated RV together with paradoxical intraventricular septal (IVS) movement can compromise filling of the LV and distort its geometry resulting in LV diastolic dysfunction and decreased stroke volume. In summary, the RV is particularly sensitive to changes in afterload and is prone to failure with acute elevations in PA pressure [1, 9].

Technical and Patient Considerations

The practical value of bedside ultrasonography in the management of critically ill patients is now widely accepted, despite its inherent limitations. These limitations are related mostly to the suboptimal imaging conditions that are often associated with the critically ill patient and as a consequence of the constrained physical environment of the ICU. In particular the RV can be difficult to image owing to its complex morphology, its thin wall with coarse trabeculations, its anterior position within the chest, and its marked load dependence [1]. For an ultrasound study to be deemed adequate, a good acoustic "window" is required to allow accurate analysis. Anything hindering the reflection of this acoustic signal, be it air, bone, calcium, a foreign body, or another interposed structure, will interfere with ultrasound transmission and will diminish the overall quality of the examination. In the critical care unit, up to one third of patients may be receiving mechanical ventilation, and adequate imaging is frequently limited due to interposition of the inflated lung between the heart and chest wall. Other important factors limiting data acquisition in critically ill patients are related to surgical wounds and dressings, tapes, tubing, surgical emphysema, obesity, and chronic obstructive pulmonary disease (COPD). In addition, lack of patient cooperation and the difficulty of moving patients into the

optimal position contribute to a high prevalence of technically inadequate studies. Although ultrasonography provides a window for the evaluation of structure and function of the heart and other important organs and structures, acquisition of data and interpretation of results are fraught with potential traps. Obtaining adequate images and knowledge of the limitations and pitfalls is key to the performance of ultrasonography in the ICU [10].

Image Acquisition and Interpretation

Adequate positioning of the patient is an important step in obtaining adequate image quality. For performance of transthoracic echocardiography (TTE) and transesophageal echocardiography (TEE), optimal imaging is usually obtained by having patients in the left lateral decubitus position. Apical four-chamber, modified apical four-chamber, left parasternal long-axis (PLAX) and parasternal short-axis (PSAX), left parasternal RV inflow, and subcostal views provide images for the comprehensive assessment of RV systolic and diastolic function and RV systolic pressure (Fig. 6.1).

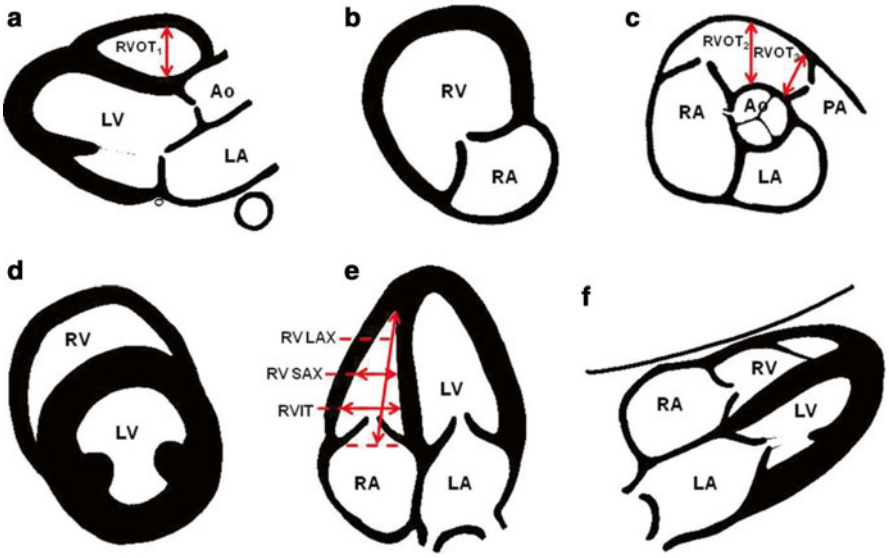

Fig. 6.1 Graphic representation of the echocardiographic views used for evaluating the right ventricle. (**a**) Parasternal long-axis view, (**b**) long-axis view of the inflow tract, (**c**) parasternal short-axis view at the base of the heart, (**d**) parasternal short-axis view at the level of the papillary muscles, (**e**) apical four-chamber view, and (**f**) subcostal view. *Ao* aorta, *LA* left atrium, *LV* left ventricle, *PA* pulmonary artery, *RA* right atrium, *RV* right ventricle, *RVIT* RV inflow tract, *RV LAX* RV long-axis, *RV SAX* RV short-axis, *RVOT* RV outflow tract (Reprinted with permission from Jurcut R, Giusca S, La Gerche A, Vasile S, Ginghina C, Voigt JU. The echocardiographic assessment of the right ventricle: what to do in 2010? Eur J Echocardiogr. 2010;11(2):81–96)

Dimensions and Right Ventricular Wall Thickness

In the ICU setting, the bedside RV echocardiography begins with an assessment of RV size. RV dimension is best estimated at end-diastole from a right ventricle-focused apical four-chamber view. In this view the RV normally has a triangular shape, which becomes more oval as its pathologic dilation occurs. The RV should appear smaller than the LV and usually no more than two thirds the size of the LV in the standard apical four-chamber view. There are many quantitative parameters that can help the intensivist evaluate the RV size. Diameter >42 mm at the base and >35 mm at the mid level indicates RV dilation [11] (Fig. 6.2). In all complete echocardiographic studies, at least the RV basal measurement should be reported. In practice however, the easiest way to do so is to compare the RV to the LV. The RV inner surface area at end-diastole should normally be no more than 0.6 that of the LV. Moderate RV dilation would elevate this ratio to 0.7–0.9 and severe dilation to >1 [12]. RV dimensions are highly dependent on probe rotation by the user, which can result in an underestimation of RV width. Care should be taken to obtain the image demonstrating the maximum diameter of the RV without foreshortening. Relative RV enlargement, as suggested by an RV to LV end-diastolic diameter ratio ≥0.9, is predictive of in-hospital mortality and may be useful in identifying which patients require more aggressive therapy in patients presenting with acute PE [13]. The distal right ventricular outflow tract (RVOT) diameter can be

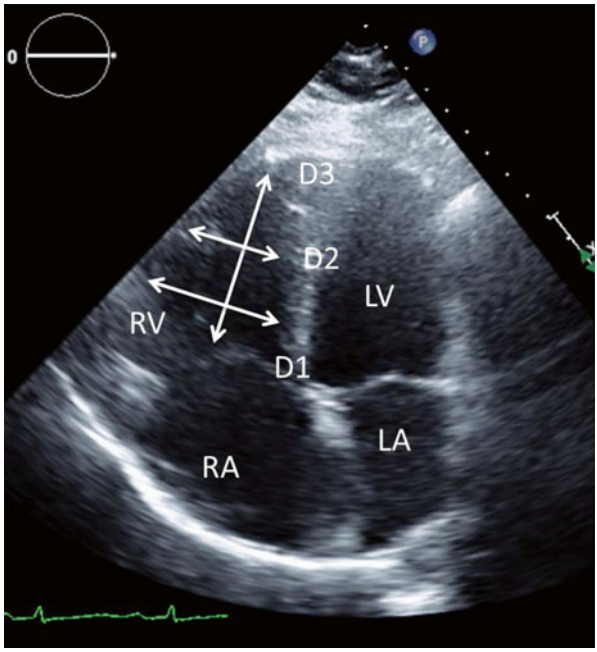

Fig. 6.2 Apical four-chamber view demonstrating measurements of the right ventricle obtained at end-diastole. *RV* right ventricle, *RA* right atrium, *LV* left ventricle, *LA* left atrium, *D1* basal RV measurement, *D2* mid-RV measurement, *D3* base-to-apex measurement

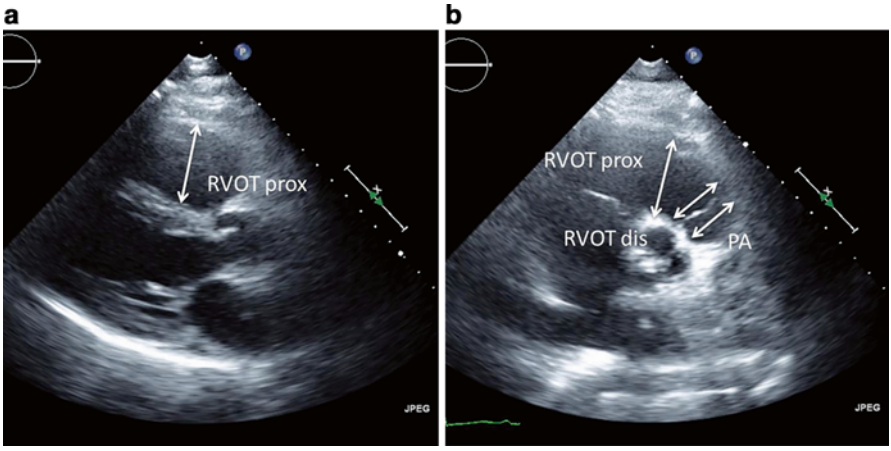

Fig. 6.3 Measurement of the right ventricular outflow tract. (**a**) The left parasternal long-axis view allows for the measurement of the proximal portion of the RVOT, also referred to as the "proximal diameter." (**b**) The left parasternal short-axis view demonstrating RVOT at the level of the pulmonic valve yields the "distal diameter." *RVOT prox* proximal right ventricular outflow tract, *RVOT dis* distal right ventricular outflow tract, *PA* pulmonary artery

visualized in the left PSAX view at the level of the pulmonic valve, while the left PLAX view allows for the measurement of the proximal diameter of the RVOT (Fig. 6.3).

In patients receiving mechanical ventilation adequate imaging from the parasternal view is frequently limited due to interposition of the inflated lung between the heart and chest wall. Alternatively, a comparison of the areas of the RV and LV cavities can be made from the subcostal four-chamber view as described in the apical four-chamber view, either by measurement or visual gestalt. Additionally, the subcostal four-chamber view affords a good look at the RV free wall. RV wall thickness is measured in diastole using either M-mode or two-dimensional imaging. Thickness >5 mm indicates RV hypertrophy (RVH) and may suggest more chronic RV pressure overload in the absence of other pathologies (Fig. 6.4) [14] (Table 6.1).

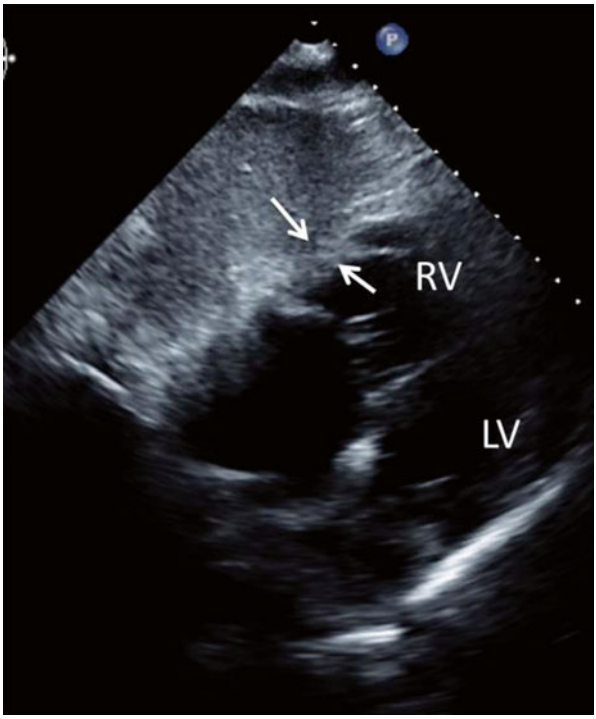

Fig. 6.4 Measurement of RV thickness. RV free wall thickness measurement obtained at end diastole at level of the tricuspid valve chordae tendineae in the subcostal four-chamber view. *RV* right ventricle, *LV* left ventricle

Table 6.1 Suggested measurements

Measurements	Suggested views	Brief description	Abnormal	Illustrations
Dimensions				
RV dimensions	Apical four chamber, alternatively subcostal views	Measurements of RV chamber dimensions in end diastole should include the diameters above the tricuspid valve annulus and in the mid-RV cavity, as well as the distance from the TV annulus to the RV apex	RV basal >42 mm RV mid >35 mm RV longitudinal >86 mm [11]	Fig. 6.2
RV outflow tract	Parasternal three chamber and short axis		RVOT PLAX Prox >33 mm RVOT PSAX Dist >27 mm [23]	Fig. 6.3
RV thickness	Subcostal views	Subcostal four-chamber view for measurements of RV free wall thickness has demonstrated a higher reproducibility than other views	RV wall thickness >5 mm [14]	Fig. 6.4

(continued)

Table 6.1 (continued)

Measurements	Suggested views	Brief description	Abnormal	Illustrations
RA dimension	Apical four chamber		RA end-systolic area >18 cm^2 [23]	Fig. 6.9
IVC dimension	Subcostal views	The subcostal view permits imaging and measurement of the IVC and also assesses inspiratory collapsibility. IVC diameter should be measured just proximal to the entrance of hepatic veins	Normal (3 mm Hg): <21 mm and >50 % collapsibility	Fig. 6.10
			Intermediate (8 mm Hg): <21 mm and <50 % collapsibility or >21 mm and >50 % collapsibility	
			High (15 mm Hg): >21 mm and <50 % collapsibility [32]	
RV function				
TAPSE	Apical four chamber	With the M-mode cursor aligned through the anterior tricuspid annulus in the apical four-chamber view, longitudinal displacement of the annulus toward the apex during systole can be recorded	<16 mm [28]	Fig. 6.8
RV S'	Apical four chamber	The sample volume is usually placed at or below the tricuspid annulus	<10 cm/s [25]	Fig. 6.7
FAC	Apical four chamber	Planimetry of the RV cavity area is traced across the TV annulus along the endocardium and then around the apex at the end-diastolic and end-systolic frames	<35 % [23]	Fig. 6.6
RV and pulmonary hemodynamics				
sPAP		4(TR velocity max)^2 + RAP [33]	>40 mm Hg	Fig. 6.11
mPAP		4(early PI velocity)^2 + RAP	>25 mm Hg	Fig. 6.11
PVR		TR velocity (m/s) / TVI RVOT (cm) x 10 + 0.16 (Woods units) [46]	>3 Wood units	

RV right ventricle, *RA* right atrium, *IVC* inferior vena cava, *TAPSE* tricuspid annular plane systolic excursion, *S'* tricuspid lateral annular systolic velocity, *FAC* fractional area change, *PLAX* parasternal long-axis, *PSAX* parasternal short-axis, *RVD* right ventricular diameter, *RVOT* right ventricular outflow tract, *sPAP* systolic pulmonary artery pressures, *mPAP* mean pulmonary artery pressures, *PVR* pulmonary vascular resistance, *TR* tricuspid regurgitation, *PI* pulmonic insufficiency, *RAP* right atrial pressure, *TVI* time-velocity integral

Interventricular Septal Morphology

The normal septal curvature is convexed toward the RV cavity, imparting a crescentic shape to the RV in cross section. An acute rise in the pulmonary pressure may frequently occur in critically ill patients. In such conditions, during systole, the RV faces an increased resistance in the pulmonary vasculature. As a result, the RV contraction time becomes prolonged and continues past the beginning of the LV diastole. The LV relaxes, and the pressure inside it falls, while the RV pressure remains high. This difference transiently pushes the IVS to the left, into the LV. Such paradoxical septal wall motion can be readily appreciated on echocardiography, and it represents a distinct sign of RV systolic failure. In the PSAX, the LV assumes a progressively more D-shaped cavity as the ventricular septum flattens and progressively loses its convexity with respect to the center of the RV cavity during diastole. Although patients with relatively isolated RV volume overload have the most marked shift of the ventricular septum away from the center of the RV at end-diastole (with relatively more normal septal geometry at end-systole), patients with relatively isolated RV pressure overload have leftward septal shift away from the center of the RV at both end-systole and end-diastole, with the most marked deformation at end systole (Fig. 6.5) [1].

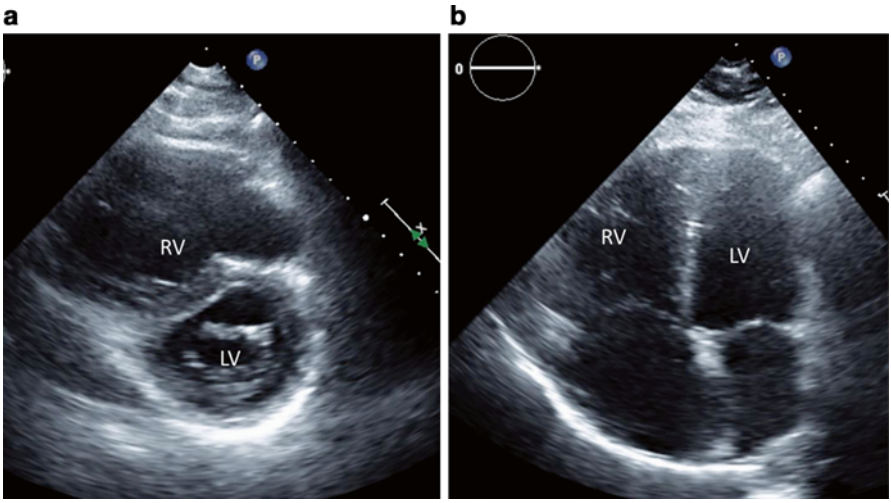

Fig. 6.5 Assessment of interventricular septum. (**a**) In the parasternal short-axis view, the left ventricle assumes a progressively more D-shaped cavity as the ventricular septum flattens and progressively loses its convexity with respect to the center of the RV cavity during diastole. (**b**) Paradoxical septal wall motion can be readily appreciated on apical four-chamber views, and it represents a distinct sign of RV systolic failure. *PSAX* parasternal long-axis, *RV* right ventricle, *LV* left ventricle

RV Systolic Function

A knowledge of RV systolic function may be essential in making hemodynamic decisions, considering thrombolysis in patients with PE and normal blood pressure [4], and in prognostication in RV infarction [15] and chronic cor pulmonale [16]. A visual gestalt of the contractility of the RV can be made by looking at the two major components of RV contraction: excursion of the free wall and the movement of the tricuspid annulus toward the apex. RV systolic function has been evaluated using several parameters, namely, myocardial performance (Right Ventricular Myocardial Performance Index or RIMP) [17], tissue Doppler velocity and tricuspid annular plane systolic excursion (TAPSE) [16], 2-D RV fractional area change (FAC) [18], 2-D RV ejection fraction (EF) [19], three-dimensional (3-D) RV EF [20], tissue Doppler-derived tricuspid lateral annular systolic velocity (S') [21], and longitudinal strain and strain rate [22]. However, few are convenient and reliable for everyday use. The RV has a complex geometry that makes calculation of RV volume (and thus RV EF) by 2-D echo challenging. However, this limitation does not preclude alternative, non-volumetric methods of RV function assessment.

Fractional Area Change (FAC)

Two-dimensional FAC, defined as (end-diastolic area – end-systolic area)/end-diastolic area × 100, provides an estimate of RV systolic function. FAC is obtained by tracing the RV endocardium both in systole and diastole from the annulus, along the free wall to the apex, and then back to the annulus, along the interventricular septum (Fig. 6.6). Two-dimensional FAC <35 % indicates RV systolic dysfunction

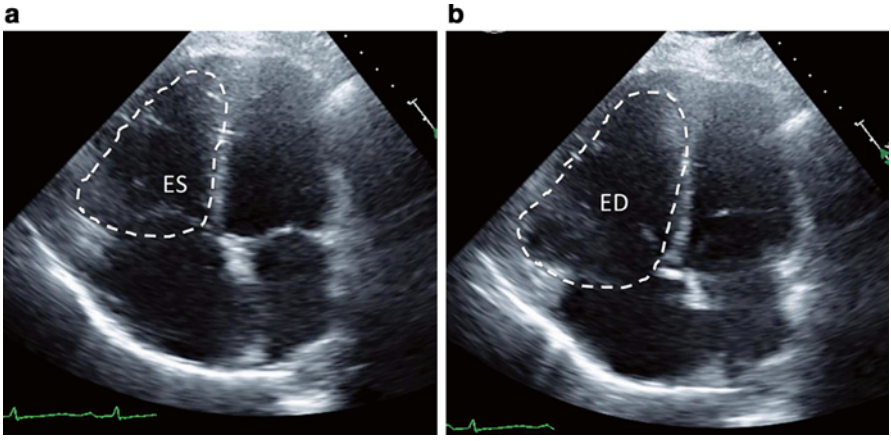

Fig. 6.6 Assessment of RV systolic function: fractional area change. Fractional area change is obtained by tracing the RV endocardium both in (**a**) end-systole and (**b**) end-diastole from the annulus, along the free wall to the apex, and then back to the annulus, along the interventricular septum. *ES* end-systole, *ED* end-diastole

[23]. The RV FAC does not require geometric assumptions and correlates with the RV EF. However, incomplete visualization of the RV cavity (more common in the setting of RV enlargement) as well as suboptimal endocardial definition leads to relatively high inter- and intra-observer variability [24]. Nevertheless, FAC was found to correlate best with the reference standard of MRI-derived RV EF [18]. Reduced FAC also represents an independent predictor of death in patients with acute myocardial infarction and evidence of LV dysfunction [15].

S' of the Tricuspid Annulus

Among the most reliably and reproducibly imaged regions of the right ventricle are the tricuspid annulus and the basal free wall segment. These regions can be assessed by pulsed tissue Doppler and color-coded tissue Doppler to measure the longitudinal velocity of excursion [25] (Fig. 6.7). This velocity has been termed the RV S' or systolic excursion velocity. To perform this measure, an apical four-chamber window is used with a tissue Doppler mode region of interest highlighting the RV free wall. Certain echo platforms also allow for color-coded Doppler-derived S' analysis offline.

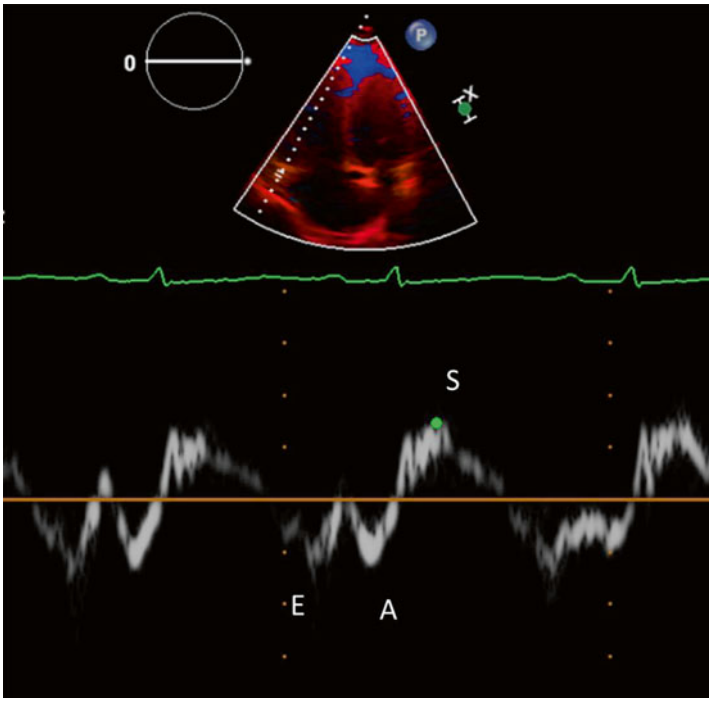

Fig. 6.7 Assessment of RV systolic function: RV S' or systolic excursion velocity. An apical four-chamber window is used with a tissue Doppler mode region of interest highlighting the RV free wall at tricuspid annulus. *S* tissue Doppler velocity during systole, *E* tissue Doppler velocity during early ventricular filling, *A* tissue Doppler velocity during atrial contraction

The pulsed Doppler sample volume is placed in either the tricuspid annulus or the middle of the basal segment of the RV free wall. A S' <10 cm/s should raise the suspicion for abnormal RV function [21]. However, these measurements assume that the function of a single basal segment represents the function of the entire RV, which can be misleading in conditions that include regional wall motion abnormalities, such as RV infarction or PE. S' appears to have prognostic value in different clinical scenarios including pulmonary hypertension [26] and inferior myocardial infarction [27].

Tricuspid Annular Plane Systolic Excursion (TAPSE)

The systolic movement of the base of the RV free wall provides one of the most visibly obvious movements on normal echocardiography. TAPSE is a method to measure the distance of systolic excursion of the RV annular segment along its longitudinal plane, from a standard apical four-chamber window. TAPSE is usually acquired by placing an M-mode cursor through the tricuspid annulus and measuring the amount of longitudinal motion of the annulus at peak systole (Fig. 6.8).

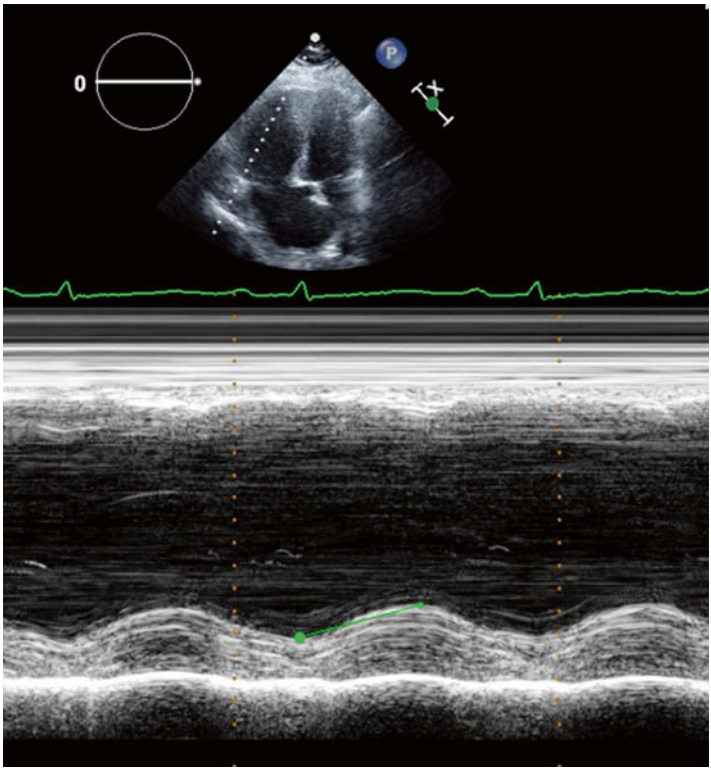

Fig. 6.8 Assessment of RV systolic function: tricuspid annular plane systolic excursion (TAPSE). TAPSE is acquired by placing an M-mode cursor through the tricuspid annulus and measuring the amount of longitudinal motion of the annulus at peak systole

TAPSE is simple, less dependent on optimal image quality, and reproducible, owing in part to the lack of reliance on RV endocardial definition or geometric assumptions, and it does not require sophisticated equipment or prolonged image analysis [28]. Therefore, it might represent the best validated tool to objectively assess RV function in the ICU setting with similar limitations concerning the assessment of possible regional dysfunction as described for S'. Current literature indicates that a TAPSE cutoff value <17 mm yielded a high specificity for diagnosis of RV dysfunction [29]. TAPSE has been shown to correlate well with MRI-derived RV EF [30], and values below 1.8 cm predict long-term mortality in patients with PH [16].

Right Atrium

The primary transthoracic window for imaging the right atrium (RA) is the apical four-chamber view. From this window, RA area is estimated by planimetry, using an upper reference limit of 18 cm^2 [23] (Fig. 6.9). Average indexed RA volume in healthy adults obtained by 2-D echo has been reported to be 16.76 ± 8.15 mL/m^2 [31]; however, validated cutoff values associated with adverse outcomes have not been defined as of yet.

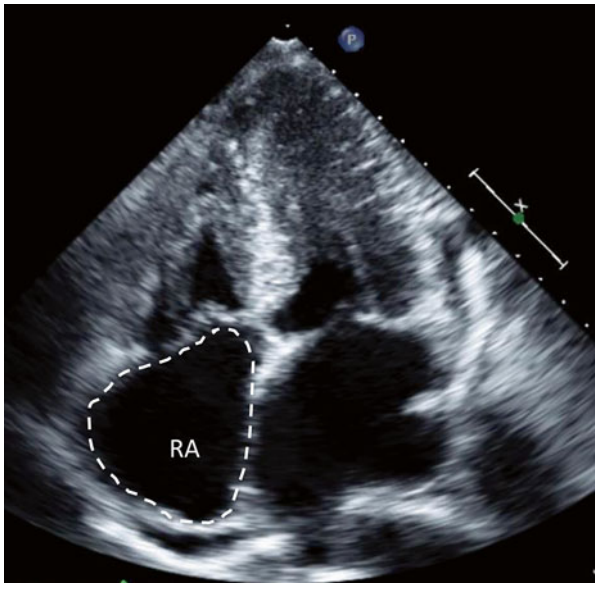

Fig. 6.9 Right atrial size measurement. RA area is estimated by planimetry in the apical four-chamber view. *RA* right atrium

Inferior Vena Cava (IVC) and RA Pressures

Estimation of right atrium pressure (RAP) is clinically relevant in many circumstances as an indicator of volume status and responsiveness to fluid challenge, as a sensitive diagnostic sign in patients with suspected cardiac tamponade, or as part of the echocardiographic estimation of PA pressures. The subcostal view permits imaging and measurement of the inferior vena cava (IVC) and also assesses inspiratory collapsibility. IVC diameter should be measured just proximal to the entrance of the hepatic veins (Fig. 6.10). For simplicity and uniformity of reporting, specific values of RA pressure, rather than ranges, should be used in the determination of systolic pulmonary artery pressure (SPAP). IVC diameter <2.1 cm that collapses >50 % with a sniff suggests a normal RA pressure of 3 mm Hg (range, 0–5 mm Hg), whereas IVC diameter >2.1 cm that collapses <50 % with a sniff suggests a high RA pressure of 15 mm Hg (range, 10–20 mm Hg) [32]. In scenarios in which IVC diameter and collapse do not fit this paradigm, an intermediate value of 8 mm Hg (range, 5–10 mm Hg) may be used. To accurately assess IVC collapse, the change in diameter of the IVC with a sniff and also with quiet respiration should be measured, ensuring that the change in diameter does not reflect a translation of the IVC into another plane.

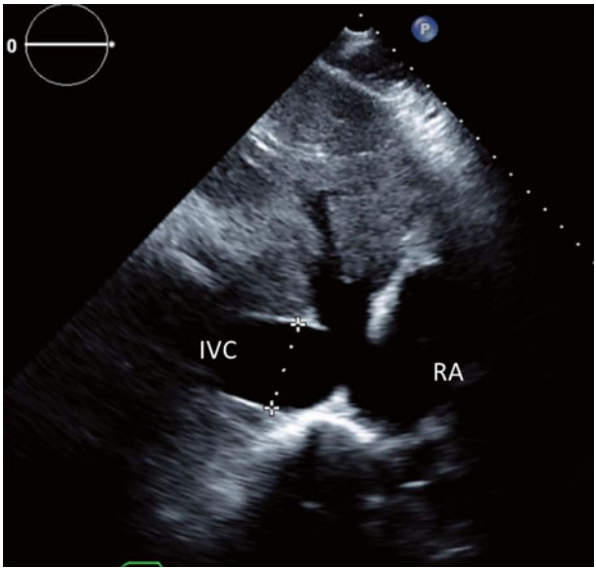

Fig. 6.10 Assessment of the inferior vena cava for estimating RA pressures. The subcostal view permits imaging and measurement of the IVC and also assesses inspiratory collapsibility. IVC diameter should be measured just proximal to the entrance of hepatic veins. *IVC* Inferior vena cava, *RA* right atrium

TV and RVOT Doppler

Pulmonary hypertension is common in the critically ill patient and can be a manifestation of various pulmonary, cardiac, and systemic processes. It is characterized hemodynamically as a mean pulmonary pressure >25 mm Hg. Systolic PA pressures are determined from TR velocities (some degree of regurgitation is essential to be able to obtain a Doppler signal and subsequently determine pulmonary artery pressure [PAP]). Peak TR velocity, usually obtained by continuous-wave Doppler from the RV inflow or the apical four-chamber view position, reflects the pressure difference during systole between the RV and the RA (Fig. 6.11a). Peak systolic RV pressure (which would be similar to PA systolic pressure in the absence of pulmonary stenosis or RVOT obstruction) is thus determined from the peak TR Doppler velocity using the modified Bernoulli equation and combining this value with an estimate of the RA pressure: PA systolic pressure = $4(V)^2$ + RA pressure, where V is the peak velocity (in meters per second) of the TR jet and RA pressure is estimated from IVC diameter and respiratory changes [33]. The tricuspid valve (TV) must be interrogated from multiple different views (i.e., RV inflow, short-axis, apical four-chamber, and subcostal views) to ensure that the ultrasound beam is parallel to the regurgitant signal, thus allowing optimal Doppler envelope quality and an accurate peak transtricuspid flow velocity.

The use of echocardiography in assessment and management of PH remains an area of much controversy [34, 35]. While echocardiography-derived PA systolic pressures have been shown to be inaccurate compared to right heart catheterization-derived PA systolic pressures, especially in more severe stages of PH [36, 37], the sensitivity and specificity of echo-derived PA systolic pressures (>39 mm Hg,) has been reported as 87 % and 81 %, respectively [38]. In general, echocardiographic estimation of PA systolic pressures can be used to determine the presence or absence of PH, but not necessarily the severity of disease.

Pulmonary artery diastolic pressure is frequently used as an estimate of LV filling pressure in the management of critically ill patients. Pulmonary artery diastolic pressure can be estimated by measuring the end-diastolic regurgitant flow velocity across the pulmonic valve (at the QRS complex on the electrocardiogram [ECG]), converting it to a pressure gradient, and then adding the gradient to the estimated RA pressure. Pulmonary flow velocity can be recorded by pulsed wave Doppler from the PSAX view, with the sample volume located in the PA at the level of the pulmonary valve (Fig. 6.11b).

Pulmonary artery acceleration time (PAAT) can be also used to estimate mean PA pressure. The pulsed Doppler echocardiography sample volume should be positioned in the main PA. PAAT is the time in milliseconds from the beginning of the Doppler envelope to the peak of the signal. On the basis of the formula 79–0.45 (× PAAT), the mean PA pressure can be estimated. In addition to the shortening of the PAAT in severe pulmonary arterial hypertension, the decreased compliance of the PA and the transmission of a reflected wave of blood result in a characteristic mid-systolic interruption of flow [39] (Fig. 6.12).

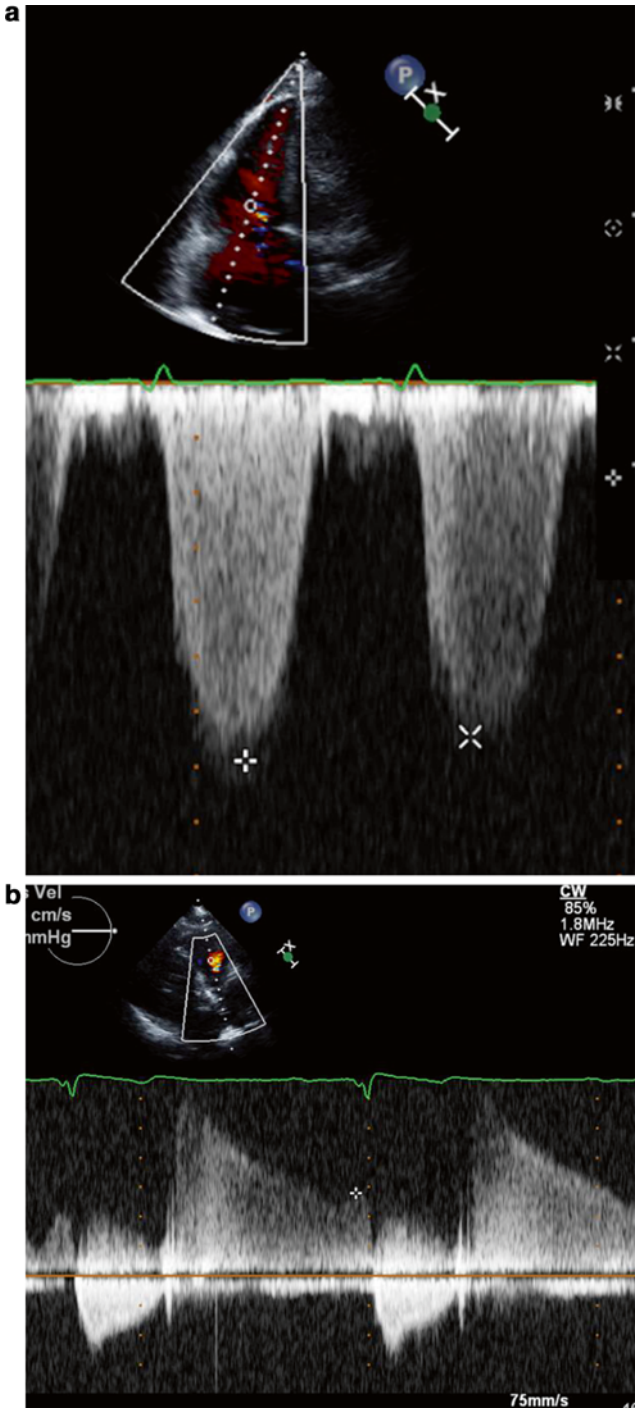

Fig. 6.11 Assessment of pulmonary artery pressures: tricuspid valve and RV outflow tract Doppler. (**a**) Peak tricuspid regurgitation velocity, usually obtained by continuous-wave Doppler from the RV inflow or the apical four-chamber view position, reflects the pressure difference during systole between the RV and the RA (marked with crosshairs). (**b**) Pulmonary artery diastolic pressure can be estimated by measuring the end-diastolic regurgitant flow velocity across the pulmonic valve (marked with a star)

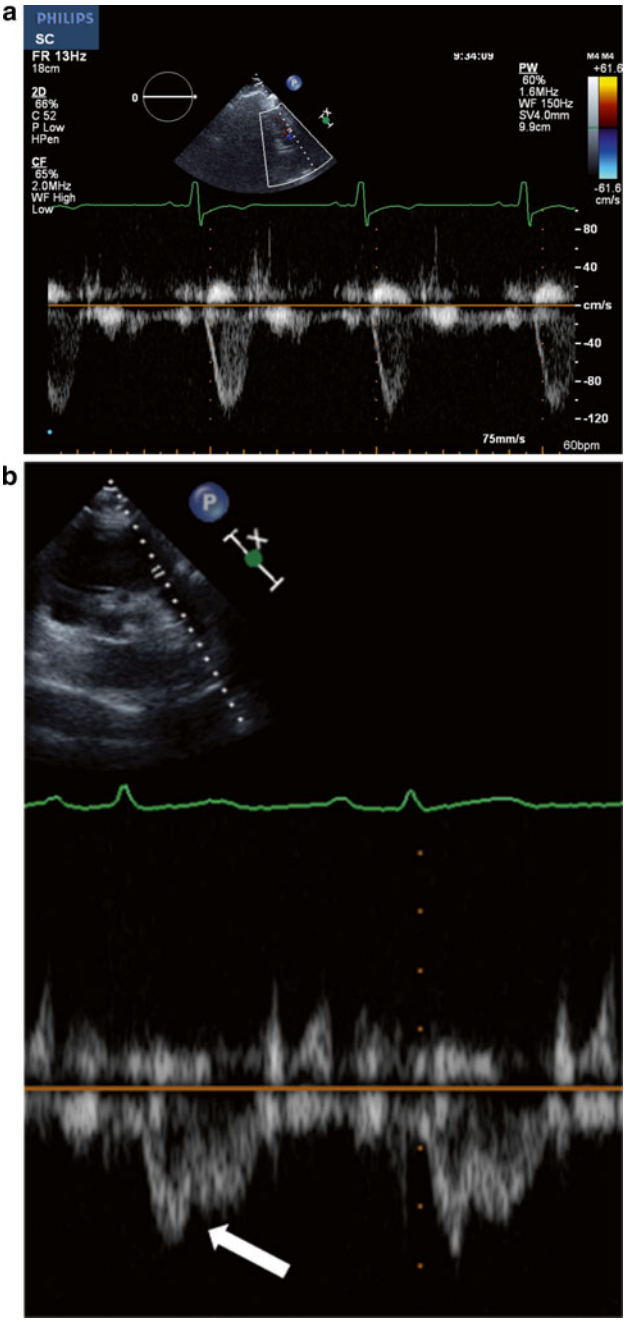

Fig. 6.12 Assessment of pulmonary artery pressures: shape of the right ventricular outflow tract Doppler envelope. Examples of the distinct patterns appreciated in the flow velocity envelope obtained from pulsed-wave Doppler interrogation from the right ventricular outflow tract. (**a**) Representative Doppler tracings in a patient with normal pulmonary artery pressure. (**b**) Doppler tracings with a late systolic notch, characterized by transient notching on the terminal aspect of the Doppler, suggestive of elevated pulmonary artery pressures (*arrow*)

Identifying Particular Clinical Scenarios

Volume Overload

RV volume overload results from tricuspid or pulmonary regurgitation or septal defects (Table 6.2). Volume overload results in RV dilation with little or no increase in free wall thickness. In RV volume overload, because the RV intracavitary pressure is higher than normal and the duration of systole is longer, RV pressure exceeds

Table 6.2 Clinical scenarios

Clinical scenarios	Brief description
RV volume overload	RV pressure exceeds LV pressure during end systole and early diastole, resulting in septal bowing and paradoxical motion; dilated inferior vena cava with reduced respiratory variations
RV pressure overload	Septal flattening through the cardiac cycle, PA systolic pressure rarely exceeds 50 mm Hg in the acute setting. In chronic pressure overload setting, septal flattening will be accompanied by RV hypertrophy
Pulmonary embolus	Similar to acute pressure overload described above. Additional supporting signs include small LV cavity size with normal LV systolic function and RV dysfunction (McConnell's sign). Typically, peak systolic pressures in the pulmonary artery do not exceed 50 mm Hg. One also needs to look for evidence of thrombi in transit, in the IVC, RA, RV, or main pulmonary artery
RV infarction	Regional wall motion abnormalities mainly affecting lateral wall and IVS; outward RV lateral wall dilation and displacement of papillary muscles resulting in (usually) low velocity TR. Very unlikely for PA pressures to be elevated
Acute severe dyspnea	Studies have demonstrated the high accuracy of ultrasonography in aiding differentiation between the common causes of acute respiratory failure; look for sonographic signs of cardiac tamponade (early diastolic RV collapse in setting of pericardial effusion), CHF (LV dysfunction), or signs of RV failure/pulmonary hypertension. Occasionally, a saddle embolus may be visualized by TTE at the proximal pulmonary arteries
Acute respiratory distress syndrome	ARDS patients have a high propensity to develop cor pulmonale, especially if they are on escalating PEEP [2]. If cor pulmonale patterns are detected on TTE, conservative volume management is indicated, as further fluid loading may worsen the RV strain and ischemia
Sepsis	Sepsis causes global myocardial suppression. The RV dysfunction seems well tolerated with adequate fluid loading, but with positive-pressure ventilation, the increased RV afterload may precipitate cor pulmonale [7]. If central venous pressures rise >10–14 mm Hg, additional volume loading may further exacerbate RV dysfunction, leading to a net decrease in cardiac output. In this setting, conservative fluid management is indicated, and inotropic agents may be superior to pure vasopressors

ARDS acute respiratory distress syndrome, *CHF* congestive heart failure, *IVC* inferior vena cava, *IVS* intraventricular septum, *LV* left ventricle, *PA* pulmonary artery, *PEEP* positive end-expiratory pressure, *RA* right atrium, *RV* right ventricle, *TTE* transthoracic echocardiography, *TR* tricuspid regurgitation

LV pressure during end systole and early diastole, leading to the IVS being pushed into the LV. However, at the onset of systole, the sudden increase in LV pressure produced by LV contraction restores the normal transseptal pressure gradient, pushing the IVS toward the RV cavity. This results in IVS flattening and a D-shaped LV only during early diastole [40].

Pressure Overload

RV pressure overload can be acute or chronic. Acute pressure overload is a result of massive PE or acute respiratory distress syndrome (both are forms of acute cor pulmonale) and is the most common pattern of RV overload seen in critically ill patients. Echocardiographically, it is indistinguishable from a volume overload picture. RA and RV enlargement is associated with flattening of the IVS in diastole and the absence of RV free wall thickening. As the RV has not had time to hypertrophy, the peak systolic pressures generated rarely exceed 50 mm Hg in acute cor pulmonale.

Chronic pressure overload is a result of chronic lung diseases such as COPD and interstitial lung disease (ILD), chronic thromboembolism, or chronic pulmonary venous hypertension secondary to left heart valvular or myocardial pathologies. In addition to demonstrating RV enlargement, thickening of the RV free wall is also apparent with increased trabeculation. Because RV adaptation has taken place, the RV is able to generate very high RV systolic pressures, usually exceeding 50 mm Hg, sometimes exceeding LV pressures. The IVS therefore is flattened into the LV cavity during the entire cardiac cycle. Because of the overlap of features with acute overload, it is difficult to diagnose acute or chronic cor pulmonale in the ICU using echocardiography, unless serial RV systolic pressures are available. All forms of RV overload also affect the LV, reducing diastolic function and resulting in higher filling pressures.

Pulmonary Embolism

Pulmonary embolism is not uncommon in critically ill patients. It is a complication with a high morbidity and mortality and needs rapid diagnosis and specific treatment [41]. The standard diagnostic algorithms for pulmonary thromboembolism may be difficult to follow in the ICU as they require the patient to be transported for computed tomography (CT) angiogram or ventilation-perfusion scans, which may not be feasible in the critical care setting. Therefore, we may have to rely on echocardiography to make a diagnosis before deciding on thrombolysis or catheter-based interventions. The echo picture of pulmonary embolism is that of acute pressure overload described above. Additional supporting signs include small LV cavity size with normal LV systolic function and RV dysfunction, sometimes with a particular pattern consisting of akinesis of the mid free wall but normal motion at

the apex (McConnell's sign) [42]. In addition, there may be a right-to-left shunt through a patent foramen ovale. Typically, peak systolic pressures in the PA do not exceed 50 mm Hg unless a PE has occurred on a background of chronic RV pressure overload. One also needs to look for evidence of thrombi in transit, in the IVC, RA, RV, or main PA. RV function assessment also has prognostic significance. In the International Cooperative Pulmonary Embolism Registry, RV dysfunction on echocardiography was an independent predictor of death [43].

Basic Competencies

Guidelines for competencies in critical care echocardiography have been published [44], emphasizing for the basic user the ability to acquire and interpret views, allowing an assessment of RV size and function and IVC size and variation. In these guidelines, it is recommended that the basic user should be able to recognize echocardiographic findings of acute cor pulmonale, including RV dilation and paradoxical septal motion, isolated RV dilation in the setting of RV infarct, and a dilated non-collapsible IVC consistent with right atrial hypertension. More advanced users are expected to have a competence in image acquisition and interpretation – similar to that required for cardiologists trained in echocardiography – consistent with the ability to perform and evaluate a complete echocardiography exam, including detailed assessment of RV function as outlined above, and to integrate their findings into the management of acute cardiopulmonary failure. According to American Society of Echocardiography guidelines [23], the parameters to be performed and reported in a comprehensive RV evaluation should include a measure of RV size, RA size, RV systolic function (at least one of the following: FAC, TAPSE, with or without RIMP), and SPAP with estimatation of RA pressure on the basis of IVC size and collapse. Additionally, this may include competence in TEE (see below).

Advanced Competencies

Pulmonary Vascular Resistance

An elevation in SPAP does not always imply an increased PVR, as can be seen from the relationship whereby Δ pressure = flow x resistance. PVR distinguishes whether increased afterload is due to pulmonary arterial hypertension, secondary PH, or hyperdynamic states [45]. PVR can be estimated using a simple ratio of peak TR velocity (surrogate of pressure) to the RVOT velocity-time integral (surrogate of flow) [46]. A normal invasively measured PVR is <1.5 Wood units (120 dyn • cm/s^2), and for the purpose of clinical studies in PH, significant PH is defined as a PVR >3 Wood units (240 dyn • cm/s^2). Previous literature showed that this echo-derived ratio closely correlates to PVR in a population of patients with an average PVR of 2 Wood units.

Transesophageal Echocardiography

In patients with suboptimal TTE images due to mechanical ventilation, surgical wounds, medications, or drainages, TEE can provide a valuable alternative. Although more difficult to study, the RV can be evaluated in terms of both systolic and diastolic function. Useful views include mid-esophageal four-chamber, mid-esophageal right ventricular inflow-outflow, transgastric mid-papillary short-axis, and transgastric right ventricular inflow view (Fig. 6.13) [1].

RV systolic function can be estimated by measuring TAPSE using M-mode analysis or 2-D measurement. The application of tissue Doppler imaging to the myocardial wall just below the tricuspid plane allows evaluation of systolic myocardial velocity (S'), which is a good estimate of global RV systolic performance. The tissue Doppler imaging also offers the opportunity to detect diastolic myocardial velocities, thus providing a prompt evaluation of RV diastolic function. TEE evaluation of RV function is crucial in many clinical scenarios when acute RV dysfunction, either primary (acute RV infarction) or secondary (PE, RV failure secondary to

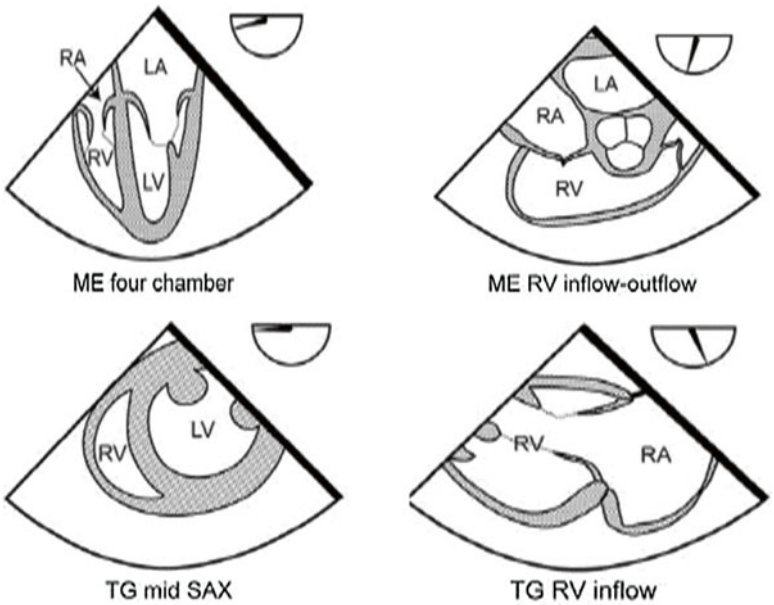

Fig. 6.13 Views useful in assessment of right ventricle by transesophageal echocardiography include mid-esophageal four-chamber view (*top left*), mid-esophageal right ventricular inflow-outflow view (*top right*), transgastric mid-papillary short-axis view (*bottom left*), and transgastric right ventricular inflow view (*bottom right*). *RA* right atrium, *RV* right ventricle, *PA* pulmonary artery, *LA* left atrium, *LV* left ventricle, *LVOT* left ventricle outflow tract, *RVOT* right ventricle outflow tract (Adapted with permission from Lippincott Williams and Wilkins/Wolters Kluwer Health: [Anesthesia & Analgesia] (Haddad et al, The right ventricle in cardiac surgery, a perioperative perspective: I. Anatomy, physiology, and assessment. 108 (2): copyright 2009))

pressure overload under mechanical ventilation), can influence the clinical course. The recognition of RV failure can guide diagnosis and treatment, leading to appropriate hemodynamic management.

TEE can also be used to detect thrombi in the pulmonary artery tree in patients with a suspected PE. The main and right PAs can be easily identified. The main PA can be followed until its division into two branches; often the left PA is not visualized because of the interposition of the left bronchus. TEE can be used to diagnose a PE through the direct detection of thrombi in the PAs rather than through the evaluation of indirect criteria of RV pressure overload (such as RV enlargement, paradoxical septal movement, TR, or loss of inspiratory collapse of the IVC).

Pitfalls and Precautions

- The study of the RV remains challenging due to its complex shape and marked load dependence. Hence, appropriate acquisition of standard echocardiographic windows is the key to evaluate RV size and function.
- Since qualitative assessments remain important in evaluating the RV and can be the basis of important therapeutic decisions, the experience and competency of the reader is important. It is advisable to seek consultation with experienced echocardiographer in most cases.

Conclusions

Integration of echocardiography into the clinical assessment of the critically ill is valuable in the assessment of right heart failure, allowing rapid assessment of RV dimensions, septal morphology, RV systolic function, and an estimation of RA pressures. Most quantitative echocardiographic measures outlined in this chapter are easy to obtain and should be measured routinely to gain insight into the underlying pathophysiology. In the near future, the use of novel tools including Speckle tracking and 3-D echocardiography may provide more objective assessments of the RV with higher inter- and intra-rater reliability.

References

1. Haddad F, Hunt SA, Rosenthal DN, Murphy DJ. Right ventricular function in cardiovascular disease, part I: anatomy, physiology, aging, and functional assessment of the right ventricle. Circulation. 2008;117(11):1436–48.
2. Vieillard-Baron A, Schmitt JM, Augarde R, Fellahi JL, Prin S, Page B, et al. Acute cor pulmonale in acute respiratory distress syndrome submitted to protective ventilation: incidence, clinical implications, and prognosis. Crit Care Med. 2001;29(8):1551–5.

3. Bogaard HJ, Abe K, Vonk Noordegraaf A, Voelkel NF. The right ventricle under pressure: cellular and molecular mechanisms of right-heart failure in pulmonary hypertension. Chest. 2009;135(3):794–804.
4. Konstantinides S. Clinical practice. Acute pulmonary embolism. N Engl J Med. 2008;359(26): 2804–13.
5. Chan CM, Klinger JR. The right ventricle in sepsis. Clin Chest Med. 2008;29(4):661–76. ix.
6. Kerbaul F, Rondelet B, Motte S, Fesler P, Hubloue I, Ewalenko P, et al. Effects of norepinephrine and dobutamine on pressure load-induced right ventricular failure. Crit Care Med. 2004;32(4):1035–40.
7. Berisha S, Kastrati A, Goda A, Popa Y. Optimal value of filling pressure in the right side of the heart in acute right ventricular infarction. Br Heart J. 1990;63(2):98–102.
8. Konstantinides S, Geibel A, Heusel G, Heinrich F, Kasper W, Management S, et al. Heparin plus alteplase compared with heparin alone in patients with submassive pulmonary embolism. N Engl J Med. 2002;347(15):1143–50.
9. Piazza G, Goldhaber SZ. The acutely decompensated right ventricle: pathways for diagnosis and management. Chest. 2005;128(3):1836–52.
10. Horton KD, Meece RW, Hill JC. Assessment of the right ventricle by echocardiography: a primer for cardiac sonographers. J Am Soc Echocardiogr. 2009;22(7):776–92. quiz 861–772.
11. Foale R, Nihoyannopoulos P, McKenna W, Kleinebenne A, Nadazdin A, Rowland E, et al. Echocardiographic measurement of the normal adult right ventricle. Br Heart J. 1986;56(1): 33–44.
12. Jardin F, Dubourg O, Bourdarias JP. Echocardiographic pattern of acute cor pulmonale. Chest. 1997;111(1):209–17.
13. Fremont B, Pacouret G, Jacobi D, Puglisi R, Charbonnier B, de Labriolle A. Prognostic value of echocardiographic right/left ventricular end-diastolic diameter ratio in patients with acute pulmonary embolism: results from a monocenter registry of 1,416 patients. Chest. 2008; 133(2):358–62.
14. Matsukubo H, Matsuura T, Endo N, Asayama J, Watanabe T. Echocardiographic measurement of right ventricular wall thickness. A new application of subxiphoid echocardiography. Circulation. 1977;56(2):278–84.
15. Zornoff LA, Skali H, Pfeffer MA, St John Sutton M, Rouleau JL, Lamas GA, et al. Right ventricular dysfunction and risk of heart failure and mortality after myocardial infarction. J Am Coll Cardiol. 2002;39(9):1450–5.
16. Forfia PR, Fisher MR, Mathai SC, Housten-Harris T, Hemnes AR, Borlaug BA, et al. Tricuspid annular displacement predicts survival in pulmonary hypertension. Am J Respir Crit Care Med. 2006;174(9):1034–41.
17. Tei C, Dujardin KS, Hodge DO, Bailey KR, McGoon MD, Tajik AJ, et al. Doppler echocardiographic index for assessment of global right ventricular function. J Am Soc Echocardiogr. 1996;9(6):838–47.
18. Anavekar NS, Gerson D, Skali H, Kwong RY, Yucel EK, Solomon SD. Two-dimensional assessment of right ventricular function: an echocardiographic-MRI correlative study. Echocardiography. 2007;24(5):452–6.
19. Lorenz CH, Walker ES, Morgan VL, Klein SS, Graham Jr TP. Normal human right and left ventricular mass, systolic function, and gender differences by cine magnetic resonance imaging. J Cardiovasc Magn Reson. 1999;1(1):7–21.
20. Grison A, Maschietto N, Reffo E, Stellin G, Padalino M, Vida V, et al. Three-dimensional echocardiographic evaluation of right ventricular volume and function in pediatric patients: validation of the technique. J Am Soc Echocardiogr. 2007;20(8):921–9.
21. Meluzin J, Spinarova L, Bakala J, Toman J, Krejci J, Hude P, et al. Pulsed Doppler tissue imaging of the velocity of tricuspid annular systolic motion; a new, rapid, and non-invasive method of evaluating right ventricular systolic function. Eur Heart J. 2001;22(4):340–8.
22. Kowalski M, Kukulski T, Jamal F, D'Hooge J, Weidemann F, Rademakers F, et al. Can natural strain and strain rate quantify regional myocardial deformation? A study in healthy subjects. Ultrasound Med Biol. 2001;27(8):1087–97.

23. Rudski LG, Lai WW, Afilalo J, Hua L, Handschumacher MD, Chandrasekaran K, et al. Guidelines for the echocardiographic assessment of the right heart in adults: a report from the American Society of Echocardiography endorsed by the European Association of Echocardiography, a registered branch of the European Society of Cardiology, and the Canadian Society of Echocardiography. J Am Soc Echocardiogr. 2010;23(7):685–713. quiz 786–688.
24. Lai WW, Gauvreau K, Rivera ES, Saleeb S, Powell AJ, Geva T. Accuracy of guideline recommendations for two-dimensional quantification of the right ventricle by echocardiography. Int J Cardiovasc Imaging. 2008;24(7):691–8.
25. Kukulski T, Hubbert L, Arnold M, Wranne B, Hatle L, Sutherland GR. Normal regional right ventricular function and its change with age: a Doppler myocardial imaging study. J Am Soc Echocardiogr. 2000;13(3):194–204.
26. De Castro S, Cavarretta E, Milan A, Caselli S, Di Angelantonio E, Vizza Carmine D, et al. Usefulness of tricuspid annular velocity in identifying global RV dysfunction in patients with primary pulmonary hypertension: a comparison with 3D echo-derived right ventricular ejection fraction. Echocardiography. 2008;25(3):289–93.
27. Alam M, Wardell J, Andersson E, Samad BA, Nordlander R. Right ventricular function in patients with first inferior myocardial infarction: assessment by tricuspid annular motion and tricuspid annular velocity. Am Heart J. 2000;139(4):710–5.
28. Miller D, Farah MG, Liner A, Fox K, Schluchter M, Hoit BD. The relation between quantitative right ventricular ejection fraction and indices of tricuspid annular motion and myocardial performance. J Am Soc Echocardiogr. 2004;17(5):443–7.
29. Tamborini G, Pepi M, Galli CA, Maltagliati A, Celeste F, Muratori M, et al. Feasibility and accuracy of a routine echocardiographic assessment of right ventricular function. Int J Cardiol. 2007;115(1):86–9.
30. Sato T, Tsujino I, Ohira H, Oyama-Manabe N, Yamada A, Ito YM, et al. Validation study on the accuracy of echocardiographic measurements of right ventricular systolic function in pulmonary hypertension. J Am Soc Echocardiogr. 2012;25(3):280–6.
31. Moreno J, Perez de Isla L, Campos N, Guinea J, Dominguez-Perez L, Saltijeral A, et al. Right atrial indexed volume in healthy adult population: reference values for two-dimensional and three-dimensional echocardiographic measurements. Echocardiography. 2013;30(6):667–71.
32. Beigel R, Cercek B, Luo H, Siegel RJ. Noninvasive evaluation of right atrial pressure. J Am Soc Echocardiogr. 2013;26(9):1033–42.
33. Yock PG, Popp RL. Noninvasive estimation of right ventricular systolic pressure by Doppler ultrasound in patients with tricuspid regurgitation. Circulation. 1984;70(4):657–62.
34. Rudski LG. Point: can Doppler echocardiography estimates of pulmonary artery systolic pressures be relied upon to accurately make the diagnosis of pulmonary hypertension? Yes. Chest. 2013;143(6):1533–6.
35. Rich JD. Counterpoint: can Doppler echocardiography estimates of pulmonary artery systolic pressures be relied upon to accurately make the diagnosis of pulmonary hypertension? No. Chest. 2013;143(6):1536–9.
36. Rich JD, Shah SJ, Swamy RS, Kamp A, Rich S. Inaccuracy of Doppler echocardiographic estimates of pulmonary artery pressures in patients with pulmonary hypertension: implications for clinical practice. Chest. 2011;139(5):988–93.
37. Farber HW, Foreman AJ, Miller DP, McGoon MD. REVEAL Registry: correlation of right heart catheterization and echocardiography in patients with pulmonary arterial hypertension. Congest Heart Fail. 2011;17(2):56–64.
38. Bech-Hanssen O, Karason K, Rundqvist B, Bollano E, Lindgren F, Selimovic N. Can pulmonary hypertension and increased pulmonary vascular resistance be ruled in and ruled out by echocardiography? J Am Soc Echocardiogr. 2013;26(5):469–78.
39. Arkles JS, Opotowsky AR, Ojeda J, Rogers F, Liu T, Prassana V, et al. Shape of the right ventricular Doppler envelope predicts hemodynamics and right heart function in pulmonary hypertension. Am J Respir Crit Care Med. 2011;183(2):268–76.

40. Ryan T, Petrovic O, Dillon JC, Feigenbaum H, Conley MJ, Armstrong WF. An echocardiographic index for separation of right ventricular volume and pressure overload. J Am Coll Cardiol. 1985;5(4):918–27.
41. Scridon T, Scridon C, Skali H, Alvarez A, Goldhaber SZ, Solomon SD. Prognostic significance of troponin elevation and right ventricular enlargement in acute pulmonary embolism. Am J Cardiol. 2005;96(2):303–5.
42. McConnell MV, Solomon SD, Rayan ME, Come PC, Goldhaber SZ, Lee RT. Regional right ventricular dysfunction detected by echocardiography in acute pulmonary embolism. Am J Cardiol. 1996;78(4):469–73.
43. Goldhaber SZ, Visani L, De Rosa M. Acute pulmonary embolism: clinical outcomes in the International Cooperative Pulmonary Embolism Registry (ICOPER). Lancet. 1999;353(9162): 1386–9.
44. Mayo PH, Beaulieu Y, Doelken P, Feller-Kopman D, Harrod C, Kaplan A, et al. American College of Chest Physicians/La Societe de Reanimation de Langue Francaise statement on competence in critical care ultrasonography. Chest. 2009;135(4):1050–60.
45. Hoeper MM, Barbera JA, Channick RN, Hassoun PM, Lang IM, Manes A, et al. Diagnosis, assessment, and treatment of non-pulmonary arterial hypertension pulmonary hypertension. J Am Coll Cardiol. 2009;54(1 Suppl):S85–96.
46. Abbas AE, Fortuin FD, Schiller NB, Appleton CP, Moreno CA, Lester SJ. A simple method for noninvasive estimation of pulmonary vascular resistance. J Am Coll Cardiol. 2003;41(6): 1021–7.

Chapter 7
Critical Care Echocardiography: Pericardial Disease, Tamponade, and Other Topics

Girish B. Nair and Joseph P. Mathew

Introduction

Echocardiography is a valuable tool in the comprehensive evaluation of critically ill patients with suspected pericardial effusion and cardiac tamponade. Cardiac tamponade is a life-threatening condition which requires timely identification and treatment. In recent years, conclusive data has emerged on adverse outcomes related to invasive hemodynamic monitoring in critically ill patients [1]. As a result, critical care physicians have increasingly been relying on noninvasive techniques, particularly ultrasonography, as preferred modalities for the hemodynamic assessment and management of critically ill patients [2]. Advances in ultrasound imaging and device portability have made bedside applications readily available in recent years [3]. Critical care echocardiography (CCE) provides real-time visualization of anatomic structures and also provides an assessment of functional parameters [4, 5]. CCE is increasingly being adopted by both intensivists and emergency medicine physicians and is particularly helpful in the acute diagnosis of pericardial effusion and tamponade [6, 7], allowing time-sensitive, lifesaving interventions to be performed at a rapid pace compared to traditional cardiologist-driven echocardiography [8, 9].

In this chapter, we will review the technical considerations, image acquisition techniques, and basic and advanced competencies required by intensivists when approaching a patient with suspected pericardial effusion or tamponade.

G.B. Nair, M.D., FCCP (✉)
Division of Pulmonary and Critical Care Medicine,
Winthrop University Hospital, 222 Station Plaza, Suite 400, Mineola, NY 11501, USA
e-mail: gbnair@winthrop.org

J.P. Mathew, M.D., FCCP
Department of Medicine, Division of Pulmonary and Critical Care Medicine,
Winthrop-University Hospital, 222 Station Plaza North, Suite 400, Mineola, NY 11501, USA
e-mail: jpmathew@winthrop.org

M. Jankowich, E. Gartman (eds.), *Ultrasound in the Intensive Care Unit*,
Respiratory Medicine, DOI 10.1007/978-1-4939-1723-5_7

Technical and Patient Considerations

Ultrasound Principles

The improvements in transducer technology and miniaturization of the ultrasound probe size have helped bedside echocardiography become feasible and accessible to non-cardiologists. For optimal cardiac visualization, "microconvex" or phased array probes with smaller footprints and lower frequencies are commonly used (1–5 MHz). Phased array probes are more compact, allowing for easier imaging and maneuverability within the intercostal space. The commonly used ultrasound modes are "B-mode" or brightness mode, where structures are displayed in two-dimensional (2D) images. This is the default mode on most ultrasound machines and is optimal for evaluation of cardiac anatomy and function. A pericardial effusion can be seen in B-mode as a black, echo-free space surrounding the cardiac chambers (Fig. 7.1). The "M-mode" or motion mode displays images over time on a single plane when a scan line is placed over the point of interest in the 2D-mode. M-mode is better for assessing the rapid movements and excursion of cardiac structures in a single plane (Fig. 7.2). Although this is especially useful in diagnosing a pericardial effusion, advanced training is required to determine findings consistent with tamponade physiology in M-mode. The Doppler mode utilizes the "Doppler shift" resulting from interactions of the ultrasound waves with constantly moving particles to determine the direction and speed of tissue motion and blood flow. Doppler echocardiography is useful to measure respirophasic variations in blood flow velocities through right- and left-sided heart valves to diagnose cardiac tamponade.

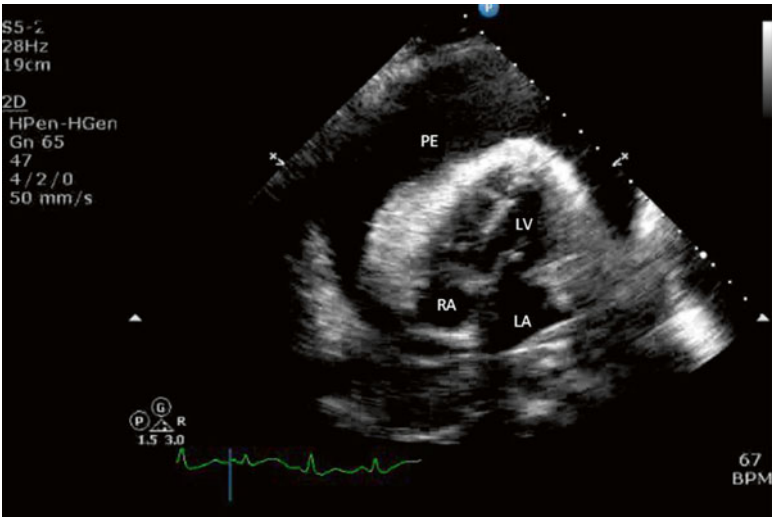

Fig. 7.1 Apical four-chamber view, showing complete ventricular collapse in a patient with large pericardial effusion and cardiac tamponade. *RA* right atrium, *PE* pericardial effusion, *LA* left atrium, *LV* left ventricle

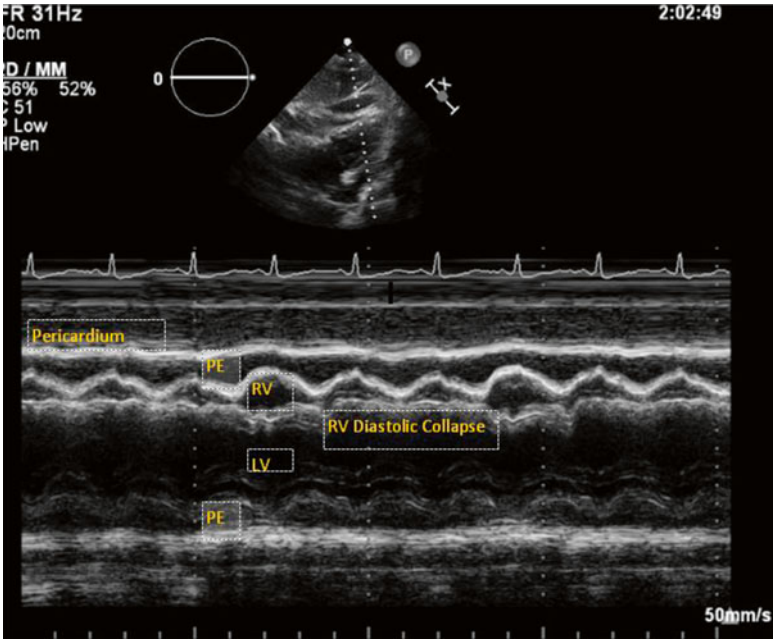

Fig. 7.2 M-mode from parasternal long axis view in a patient with cardiac tamponade. Note the right outflow tract collapse in diastole. *PE* pericardial effusion, *LV* left ventricle, *RV* right ventricle

Basic Anatomy of the Pericardium

The pericardium is normally 1–2 mm thick and consists of an outer parietal layer and an inner visceral layer. The parietal pericardium is a thicker fibrous layer that surrounds the heart and the visceral pericardium and is contiguous with the epicardium. The enclosed space between the two layers forms the pericardial sac, which normally contains around 5–10 mL of fluid. The parietal pericardium meets with the visceral pericardium around the great vessels to form the pericardial reflections. The pericardium encases all four chambers of the heart and extends 1–2 cm up the great vessels. The pericardial layers provide an enclosed chamber effectively isolating the heart from the rest of the structures in the mediastinum, allowing dynamic movements during the cardiac cycle, aiding cardiac filling during diastole, and providing lubrication [10]. Usually, the pericardial pressure reflects the pleural pressure and varies between – 5 cm H_2O during inspiration and + 5 cm H_2O during expiration [11, 12].

Table 7.1 Various etiologies causing pericardial effusion

Infection
• Viral infections (Coxsackie, Echo, Adeno, Cytomegalovirus) • Bacterial (Staphylococcus, Pneumococcus, Salmonella, Mycobacteria) • Parasitic (amoebiasis, Echinococcus)
Malignant
• Metastatic (primary lung, breast, lymphoma, leukemia) • Primary cardiac tumors (rhabdomyosarcoma, angioma)
Inflammation
• Autoimmune (SLE, rheumatoid arthritis) • Uremia • Post-myocardial infarction
Traumatic
• Blunt trauma • Penetrating injuries
Radiation
Drugs
Procedure related
• Post-cardiac surgery • Pacemaker and catheter related • Cardiopulmonary resuscitation
Idiopathic
Catastrophic causes
• Aortic dissection • Post infarction LV rupture • Penetrating chest trauma

Pericardial Effusion and Tamponade Physiology

Pericardial effusions can result from various causes including, but not limited to, inflammatory or infectious etiologies, trauma, or malignancy (Table 7.1). Normally, the pericardium can stretch up to a point, termed the reserve volume, to accommodate changes in pericardial fluid volume; however, once the reserve volume is exceeded, pericardial compliance decreases. Further increases in the pericardial volume will then result in dramatic increases in pericardial pressure and hence affect atrioventricular filling, as described in detail below, with resultant hemodynamic effects.

Pericardial Compliance

When pericardial fluid accumulates, the compliance of the parietal pericardium initially increases, resulting in a stable intrapericardial pressure. When the pericardial reserve volume is exceeded, pericardial compliance begins to fall and the

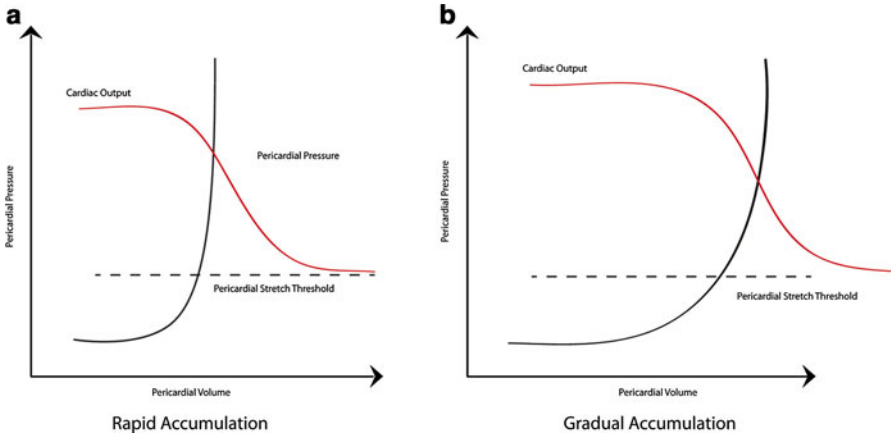

Fig. 7.3 Pericardial pressure-volume curves in relation to cardiac output. (**a**) Rapid accumulation of pericardial fluid leads to a rise in the pericardial pressure. Once the fluid overcomes the pericardial reserve volume and reaches the pericardial stretch threshold, the pressure in the pericardial space increases dramatically causing chamber collapse and impairing cardiac output. (**b**) With gradual accumulation of pericardial fluid, the pericardium is able to acclimate and stretch to a further extent prior to reaching the pericardial stretch threshold where cardiac output falls. Image courtesy of Guy Aristide, MD

intrapericardial pressure rises, and the central venous pressure must increase to maintain a gradient that allows cardiac filling. When the stretch threshold of the pericardium is exceeded, pericardial compliance markedly decreases, resulting in rapid increases in pericardial pressure with increasing volume (Fig. 7.3). At this point, the intrapericardial pressure may first equalize with the right ventricular diastolic pressure, and then with the left ventricular diastolic pressure. Critical tamponade occurs when all cardiac chambers have equal diastolic pressure. At this inflection point, there is collapse of the right-sided cardiac chambers and the cardiac output can suddenly drop (Fig. 7.3). Circulation at this point is maintained only through an increase in heart rate, contractility, and peripheral arteriolar vasoconstriction. Left untreated, this can result in circulatory failure and death [13].

Rate of Accumulation

The rate of accumulation of pericardial fluid and the total fluid volume determine the relative hemodynamic impairment caused by excess fluid in the pericardial space (Fig. 7.3). Conditions like uremic pericarditis or malignancy-related effusion can cause gradual accumulation of a large volume (>2 L) of fluid in the compliant pericardium, potentially causing minimal symptoms and no hemodynamic effects. However, in acute conditions, such as cardiac free wall rupture from pacemaker lead placement, rapid accumulation of even small amounts of pericardial fluid (50–80 mL) can exceed the pericardium's ability to stretch and can cause hemodynamic compromise [14].

Interventricular Dependence

As the pericardial pressure exceeds the central venous and pulmonary venous pressure, diastolic filling is impaired and becomes increasingly influenced by the respiratory variation in intrathoracic pressures. During inspiration, as the intrathoracic pressure becomes more negative, central venous blood flow to the right atrium and right ventricle (RV) is augmented; at the same time, there is pooling of blood in the pulmonary veins, thereby reducing flow to the left atrium. As the RV is preferentially filled during inspiration, the interventricular septum bows into the left ventricle (LV), causing a drop in cardiac output and hence a drop in blood pressure with inspiration (Fig. 7.4). The opposite holds true with expiration, when the intrathoracic pressure increases and causes diminished return of blood from the vena cava to the right side of the heart and increased flow from the pulmonary veins into the left side of the heart. As more blood is accommodated in the LV, the ventricular septum bows toward the RV. This over-filling and under-filling of the heart with respect to respiration forms the basis for "pulsus paradoxus," a classic clinical finding associated with cardiac tamponade. Although not specific for cardiac tamponade, an inspiratory drop in blood pressure of more than 10 mmHg in patients with pericardial effusion has a pooled sensitivity of 82 % for cardiac tamponade [13]. Moreover, the severity of the pulsus paradoxus correlates with the severity of hemodynamic compromise in cardiac tamponade [15]. However, caution should be used when interpreting this finding in patients with severe obstructive lung disease,

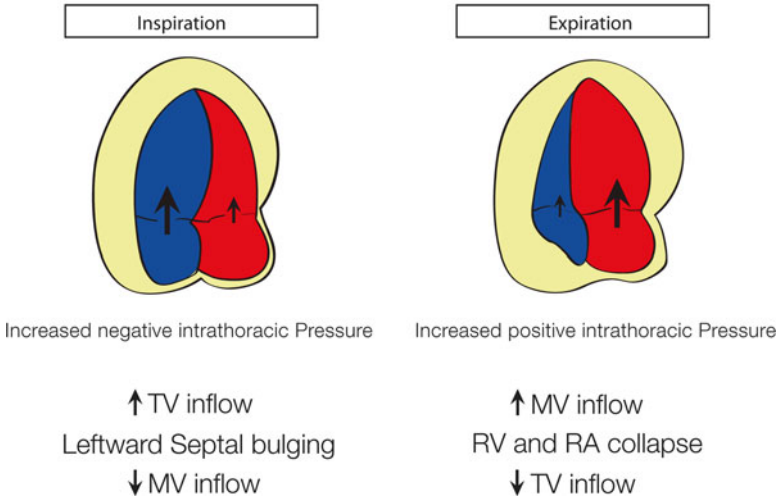

Fig. 7.4 Illustration of respirophasic cardiac physiology in a spontaneously breathing patient with pericardial effusion and tamponade. With inspiration, the intrathoracic pressure becomes more negative leading to increased right heart filling and bulging of the interventricular septum into the left ventricle and decreased left ventricular filling and stroke volume. The converse is true with expiration where the left heart filling is increased, leading to septal bowing into the right ventricle. Image courtesy of Guy Aristide, MD

Fig. 7.5 Note the phased array transducer is held steadily like a pencil and stabilized by resting the hand on the patient's body. A steady hold with subtle manipulations is required for optimal cardiac images

severe volume depletion, right or left ventricular hypertrophy, or in those on invasive positive pressure ventilation. The clinician must be cognizant that cardiac tamponade is a clinical diagnosis and that neither presence of an elevated pulsus paradoxus nor an echocardiography finding of a pericardial effusion establishes the diagnosis of tamponade.

Patient Considerations

The patient should be examined in the supine or left lateral decubitus position. Suboptimal positioning of the patient will result in unsatisfactory images, especially in critically ill patients who are often on ventilatory support. It is worthwhile for the intensivist to take the time to reposition the patient in a left lateral decubitus position if adequate images are not obtained in a supine position. This position will move the cardiac structures away from the sternum, allowing for improved imaging. The ultrasound machine itself should be positioned such that the machine controls can be easily adjusted by the intensivist. The transducer should be held like a pencil and stabilized by resting the hand holding the transducer on the patient's body (Fig. 7.5). If the patient is able to follow directions, the left arm should be positioned under the patient's head when in the lateral decubitus position. Although electrocardiographic (EKG) monitoring is helpful in determining timing of systole and diastole, it is not an absolute necessity while performing emergency point-of-care ultrasonography, when time is of the essence.

Image Acquisition and Interpretation

Image acquisition and interpretation requires an awareness of the plane in which sound waves are transmitted by the footprint, or surface, of the ultrasound probe and the resulting orientation of the 2-D images of the cardiac structures that are

generated by the reflected waves. On the monitor, structures closest to the transducer appear at the top of the screen (or near field) and deep structures appear on the bottom (or far field). The leading edge of the beam is marked on the probe and corresponds to the mark on the monitor. By convention, for cardiac imaging the marker is typically on the upper right-hand corner of the screen. The gain can be adjusted to amplify the sound beam and obtain a clearer view. Pericardial fluid can be visualized in a long axis, or sagittal, plane as well as in short axis, or transverse, plane.

Image Acquisition

The cardiac and pericardial structures must be visualized in multiple echocardiographic views to confidently rule out the presence of a pericardial effusion. The pericardial layers appear as a thin, bright, echogenic line around the myocardium (Fig. 7.6). The normal thickness of the pericardium is 1–2 mm. In the normal pericardium, there is less than 25 mL of serous fluid in the pericardial sac formed by the visceral and parietal pericardium. A simple pericardial effusion is visualized as an anechoic (black) area on B-mode, contiguous to the adjacent cardiac structures and separating the echogenic layers of the pericardium (Fig. 7.7). With advanced practice, M-mode and pulsed wave Doppler can be utilized to assess for findings of cardiac tamponade.

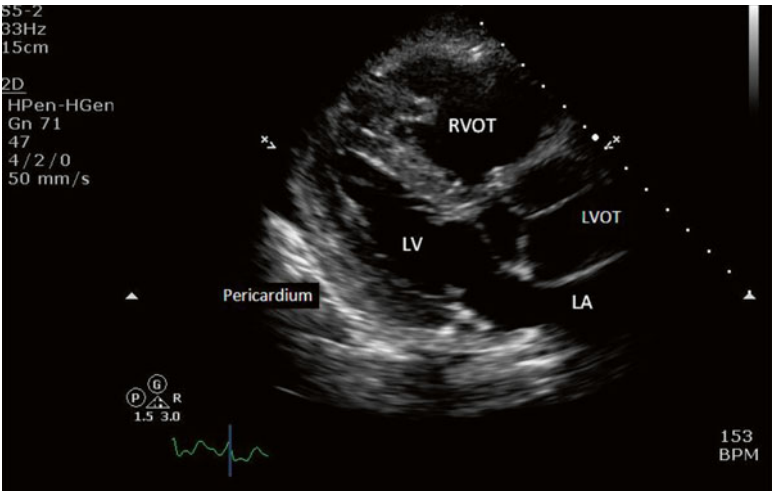

Fig. 7.6 Parasternal long axis view showing the pericardium and adjacent structures. The pericardium appears as a thin, bright, echogenic line around the myocardium. *LV* left ventricle, *LA* left atrium, *RVOT* right ventricular outflow tract, *LVOT* left ventricular outflow tract

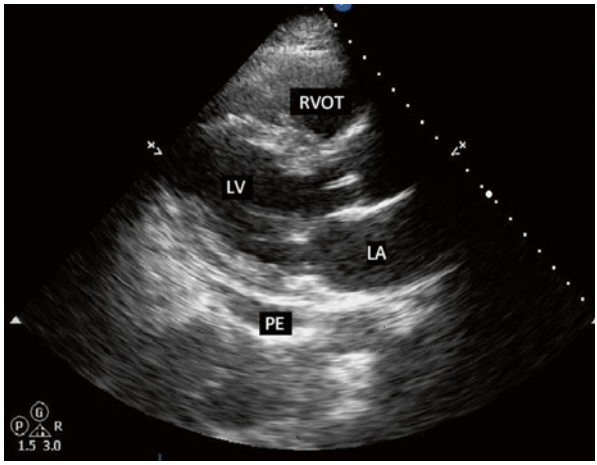

Fig. 7.7 Parasternal long axis view in a patient with small pericardial effusion. Note the *black*, echo-free space adjacent to the left ventricle. *PE* pericardial effusion, *LV* left ventricle, *LA* left atrium, *RVOT* right ventricular outflow tract

Fig. 7.8 Parasternal long axis view. The transducer is placed in the third or fourth intercostal space along the left parasternal region. The probe marker (*arrow*) should be facing the 10 o' clock position toward the patient's right shoulder

Parasternal Long Axis (PLAX)

In the parasternal long axis view, the transducer is placed on the third or fourth intercostal space along the left parasternal region with the probe marker pointing toward the patient's right shoulder (Fig. 7.8). If the views are suboptimal in the supine position, the patient should be examined in left lateral decubitus position.

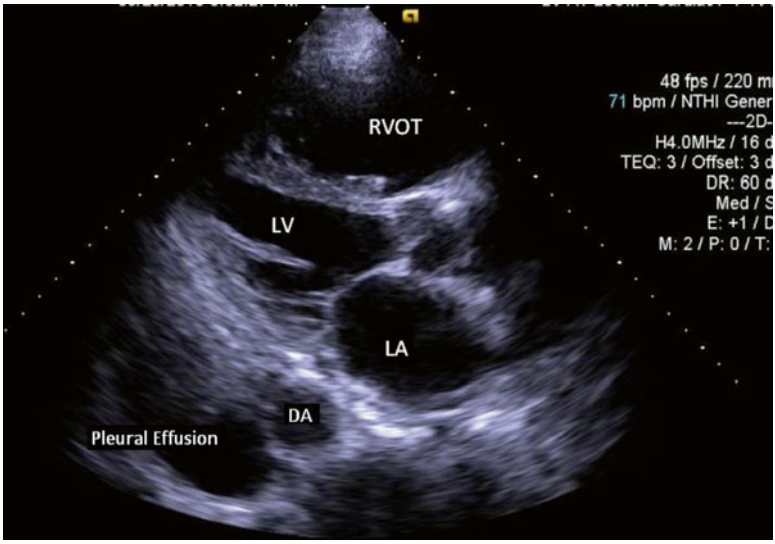

Fig. 7.9 Parasternal long axis view in a patient with a pleural effusion. Note the *black*, echo-free space located posterior to the descending aorta. *LV* left ventricle, *LA* left atrium, *RVOT* right ventricular outflow tract, *DA* descending aorta

The depth and gain should be adjusted to optimize the image. Subtle rotation and angling of the probe will ensure that the heart is visualized as a horizontal, elliptical-shaped structure in this view (Fig. 7.7). The normal pericardium is a highly reflective, bright echogenic layer surrounding the cardiac chambers. A pericardial effusion is visualized as a black, anechoic, or echo-free space within the pericardium, separating the two echogenic layers (Fig. 7.7). When the volume of fluid is small, it can be seen as an anechoic space present posterior to the left ventricle and may be seen only in systole. Using the caliper feature, the pericardial fluid can be measured both anteriorly and posteriorly. The right ventricular outflow tract (RVOT), which is seen in the near field, can display diastolic chamber collapse with tamponade physiology. This view is also useful to differentiate pericardial from pleural effusion, which appears posterior to the descending aorta (Fig. 7.9). Localized pericardial effusions, which sometimes can cause hemodynamic instability, can be seen with the PLAX view. Echogenic material with stranding between the pericardial layers may also be seen in this view, indicating the presence of an exudative pericardial effusion from malignant, infectious, or inflammatory etiologies. Additionally, M-mode can be employed from the PLAX 2-D view to closely assess for chamber collapse.

Parasternal Short Axis (PSAX)

From the PLAX view, the transducer is turned 90°, so that the probe marker is now pointing toward the patient's left shoulder to achieve the PSAX (Fig. 7.10). A cross-sectional image of the left ventricle, with all four walls and part of the right

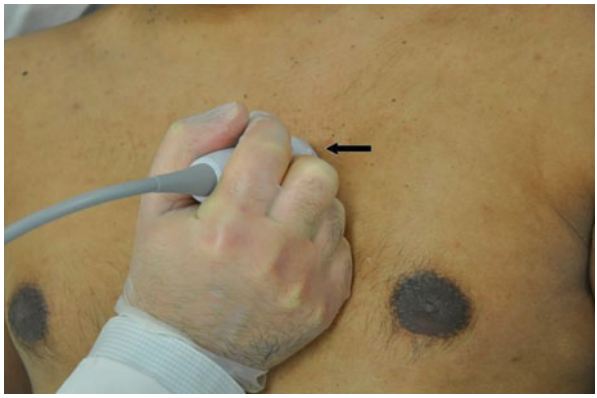

Fig. 7.10 Parasternal short axis view. From the parasternal long axis view, the transducer is turned clockwise to the 2 o' clock position such that the probe marker (*arrow*) is now pointing toward the patient's left shoulder. Angling the probe up and down allows one to scan up and down from apex to base

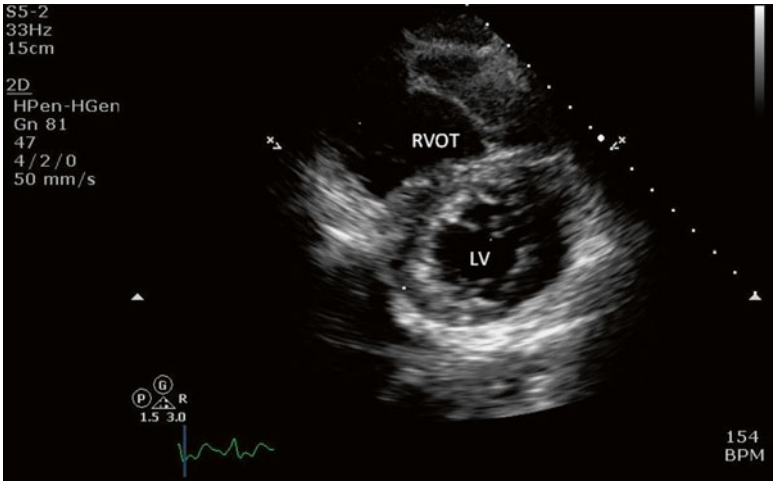

Fig. 7.11 Parasternal short axis view showing left ventricle, right ventricle, and the interventricular septum. *LV* left ventricle, *RVOT* right ventricular outflow tract

ventricle, can be seen in this view (Fig. 7.11). The PSAX view is particularly useful to study respirophasic movements of the interventricular septum. The dynamic movements of the septum with respiratory variation should alert the clinician to the possibility of increased pressure in the pericardial space. By gently angling anteriorly to the aortic valve level such that the probe is facing the right shoulder, the RVOT, aortic, tricuspid, and pulmonic valves can be visualized. The RVOT can be seen at the top of the screen and can be assessed for diastolic chamber collapse.

Apical Four Chamber (A4C)

In the apical four-chamber view, the footprint of the probe is placed near the apex of the heart or point of maximum impulse with the probe marker pointing to the left shoulder (Fig. 7.12). A left lateral decubitus position and subtle adjustment of the

Fig. 7.12 Apical four-chamber view. The transducer is placed at the apex or point of maximal impulse. The probe marker (*arrow*) is placed at the 2–3 o' clock facing the patient's left shoulder

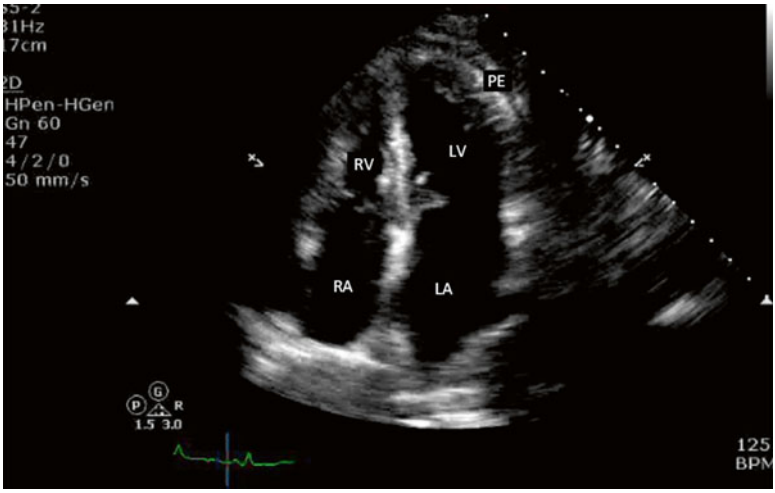

Fig. 7.13 Apical four-chamber view in a patient with small pericardial effusion. Note that the anechoic space adjacent to the LV apex. Note that the right ventricle is collapsed in diastole (mitral valves are open in diastole). *RA* right atrium, *RV* right ventricle, *LA* left atrium, *LV* left ventricle, *PE* pericardial effusion

probe will further optimize this view such that the heart appears elliptical and not foreshortened (Fig. 7.13). Both the PLAX and the A4C views are optimal for visualizing pericardial effusions. The A4C view can demonstrate RA and RV diastolic collapse and the paradoxical movement of the interventricular septum that occurs with tamponade physiology. The Doppler sample box can be placed over the mitral and tricuspid valves to assess Doppler velocities.

Apical Five Chamber (A5C)

This view is obtained by slightly angling the probe anteriorly from the A4C view to bring out the left ventricular outflow tract (LVOT). Pulsed wave Doppler (PWD) recordings can reveal exaggerated respiration-dependent phasic changes in the LVOT outflow velocities reflecting changes in stroke volume.

Subcostal (SC)

The subcostal (or subxiphoid) view is especially useful in intubated patients. In the supine position, the probe is placed in the subxiphoid area with the marker pointing to the 3 o' clock position and the probe angled at 15° cephalad (Fig. 7.14). The four chambers and part of the liver are visualized in the SC view (Fig. 7.15). Occasionally

Fig. 7.14 Subcostal view. With the patient in the supine position, the probe is held on the top surface and placed in the subxiphoid area at a 15° angle with the marker (*arrow*) pointing to the patient's left at the 3 o' clock position

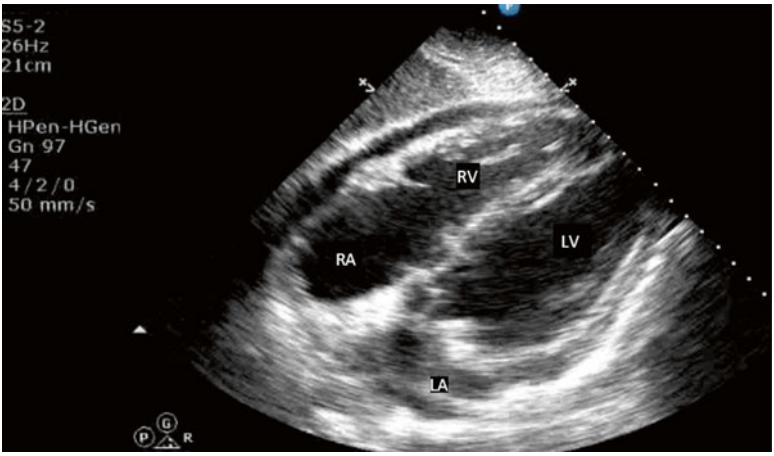

Fig. 7.15 Subcostal view in a patient with moderate pericardial effusion (seen as a *black* space interposed between the right atrium/right ventricle and liver). *RA* right atrium, *LA* left atrium, *LV* left ventricle

a pericardial cyst or epicardial fat pad can be seen and should be distinguished from an effusion. The entrance of the inferior vena cava (IVC) into the right atrium is seen by angling the probe further posteriorly and rotating counterclockwise. This view is critical when ruling out tamponade, as it is a quick and easy way to assess for inspiratory collapse of the IVC [16]. The SC view is of high utility in evaluating the right atrium for chamber collapse. Additionally, the SC view can be utilized for real-time echocardiographic guidance for pericardiocentesis via the subxiphoid approach.

Image Interpretation

Identification of Pericardial Effusion

Pericardial fluid is seen as an anechoic, or echo-free, space adjacent to the heart (Fig. 7.15). When evaluating for the presence of an effusion, using multiple echocardiographic views is prudent. In the absence of a prior history of cardiac surgery or pericardial disease, the effusion is usually diffuse and circumferential, separating the parietal and visceral pericardium. Small effusions are located posteriorly and, as the size increases, an echo-free space forms around the entire heart. Catastrophic causes of pericardial effusion, such as ventricular wall rupture or post-cardiac surgery effusions, can cause an echogenic effusion due to thrombus or fibrinous debris in the pericardial space. Effusions can also appear as a grayish, hypoechoic layer around the cardiac chambers. An isolated anterior, hypoechoic area should raise the possibilities of either epicardial fat or a loculated effusion. Other conditions such as a pericardial cyst or a pleural effusion can mimic pericardial fluid and should be ruled out in the hypotensive patient (Table 7.2). Pleural effusions are very common and are located posterior to the descending aorta in the PLAX view, whereas pericardial effusions are visualized anterior to the descending aorta and are contained within the echogenic pericardium. Pleural effusions can be further confirmed by dedicated ultrasonography of the thorax. Congenital pericardial cysts, on the other hand, are uncommon and can be unilocular or multilocular. Inflammatory pericardial cysts often present as a loculated pericardial effusion and are a result of connective tissue diseases, infections, or trauma. Chest radiography will often show

Table 7.2 Mimics of pericardial effusion on echocardiography

• Large pleural effusion
• Epicardial cyst
• Anterior epicardial fat
• Foramen of Morgagni hernia
• Inferior left pulmonary vein
• Left ventricular pseudoaneurysm
• Subphrenic abscess
• Pericardial thickening
• Pericardial tumors

loculated fluid in the right cardiophrenic angle. Computed tomography (CT) scan or magnetic resonance imaging can be used to further confirm this finding. Lastly, pericardial fat may also be seen on echocardiography, especially in patients with increased abdominal fat. Pericardial fat pads are usually localized anterior to the right ventricular outflow tract. Some clues to the diagnosis of a fat pad are absence of fluid posteriorly, a normal motion of the pericardium, and low intensity echoes or speckles in the pericardium.

Measuring the Size of a Pericardial Effusion

The separation between the heart and the parietal pericardium can be used to gauge the size of effusion. Pericardial effusions should be measured both in anterior and posterior dimensions. Different schemes have been used to quantify the volume of pericardial effusion. In general, a pericardial effusion is described as small if it is less than 1 cm; moderate, if 1 cm to 2 cm; and large, if greater than 2 cm in size [17, 18]. A trace pericardial effusion can be seen even with as little as 25 mL of pericardial fluid. It will appear as a small echo-free space in the posterior atrioventricular groove and may be visible only in systole, when the heart has pulled away from the pericardium. In a small effusion, as much as 1 cm of posterior fluid can be seen with or without fluid accumulation elsewhere. Moderate effusions have 1–2 cm of echo-free space (Fig. 7.16). Large effusions have more than 2 cm of maximal separation, and the heart may be seen swinging within the pericardial fluid (Fig. 7.1). Cardiac tamponade can be seen with moderate to large pericardial effusions but can also be present with small and/or loculated effusions.

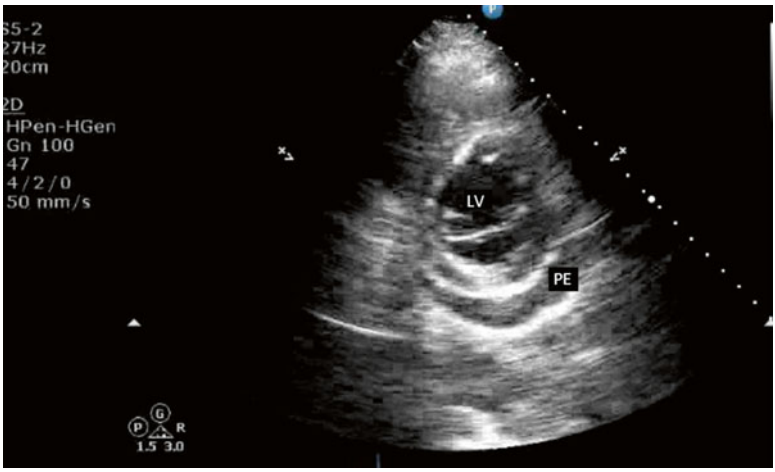

Fig. 7.16 Parasternal short axis view in a patient with moderate pericardial effusion. *PE* pericardial effusion, *LV* left ventricle

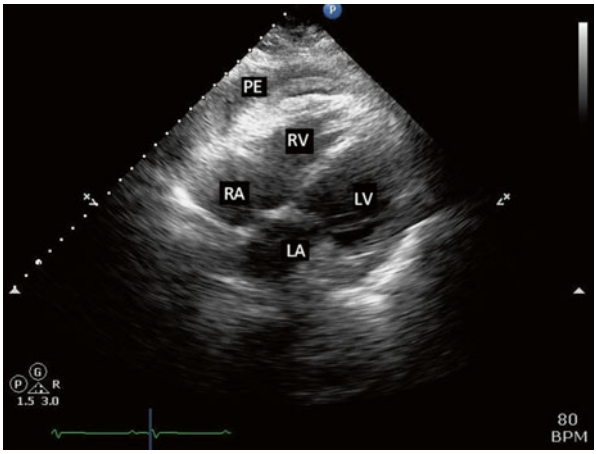

Fig. 7.17 Subcostal view in a patient with anteriorly loculated moderate pericardial effusion. Note the echogenic material in the pericardial space. *RA* right atrium, *RV* right ventricle, *LA* left atrium, *LV* left ventricle, *PE* pericardial effusion

Distribution of Pericardial Fluid

Pericardial effusions are usually diffuse, but in instances of prior inflammation or surgery, the effusion can be loculated. Identifying these effusions is important, as loculated effusions can cause hemodynamic compromise. Evaluation from multiple acoustic windows is fundamental in ruling out a loculated effusion (Fig. 7.17). The parasternal views help with excluding fluid collection at the base of the heart. In apical views, lateral, medial, and apical fluid collections can be observed.

Differentiating Pleural from Pericardial Effusion

A left pleural effusion results in an echo-free space posterior to the heart and can be easily confused with a pericardial effusion. Pericardial reflections surround the pulmonary veins and tend to limit the potential space behind the left atrium. Hence, fluid appearing exclusively behind the left atrium is more likely to represent pleural rather than pericardial effusion. The pericardial reflection is typically anterior to the descending thoracic aorta, and therefore, fluid appearing anterior to the aorta is likely to be pericardial; whereas fluid appearing posterior to the descending thoracic aorta is more likely to be pleural (Fig. 7.9; see also Fig 14.16 in Chap. 14).

Basic Competencies

In the evaluation of patients with dyspnea and hypotension, detecting an anechoic area separating the pericardial layers on any of the basic echocardiographic views will establish the diagnosis of a pericardial effusion. However, the characteristic

findings of pericardial tamponade may not always be present on echocardiography, and correlation with clinical findings is essential. Hence, the first step is always to obtain vital signs and to check for jugular venous distention and pulsus paradoxus in a patient suspected to have pericardial effusion and/or tamponade. Critical care echocardiography can then be correlated with the clinical findings. The critical care physician with basic echocardiographic training should be able to identify a pericardial effusion, to distinguish a pericardial effusion from mimics, to assess the distribution of the effusion, and to determine if the effusion is associated with echocardiographic signs of hemodynamic impairment (see Box 7.1). The basic assessment of hemodynamic compromise by CCE is discussed below.

Determining Hemodynamic Impairment

Bedside CCE can be performed to determine if a pericardial effusion is causing hemodynamic impairment (Box 7.2). However, patients with pericardial effusion and hypotension but without typical tamponade physiology findings on CCE should still be considered for pericardial effusion drainage, if no other explanation for the hypotension is felt to be present.

Box 7.1 Suggested approach with suspected pericardial effusion

The critical care physician with the help of CCE should attempt to answer the following questions:

- Is this pericardial effusion or a mimic?
- Can the etiology of the effusion be determined with CCE?
- Is the effusion localized or diffuse?
- Is the effusion small, moderate, or large in size?
- Is the effusion causing hemodynamic compromise?
- Can it be safely drained percutaneously?

Box 7.2 basic critical care echocardiographic findings suggestive of cardiac tamponade physiology

- Moderate or large pericardial effusion
- Right atrial collapse or inversion
- Right ventricular diastolic collapse
- Respiratory paradoxical septal motion
- Respiratory variation of left and right ventricular size
- IVC dilation and loss of respiratory variation

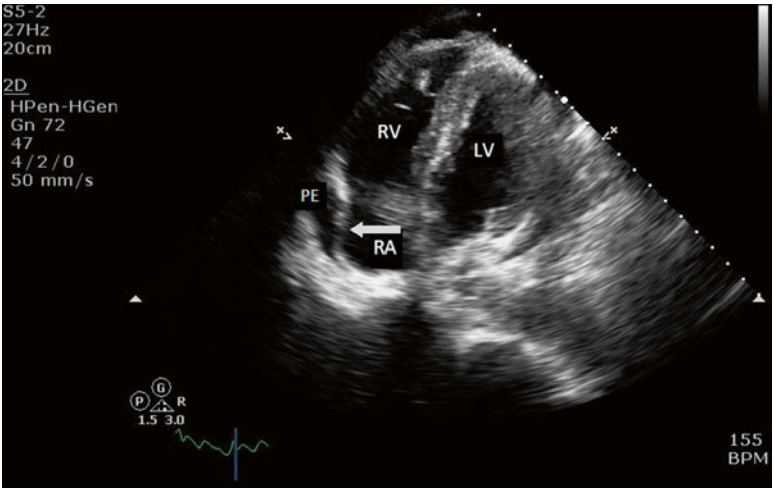

Fig. 7.18 Apical four-chamber view in a patient with moderate effusion. Note that the right atrium is inverted (*arrow*) in diastole (mitral valves are open in diastole). *PE* pericardial effusion, *RA* right atrium, *RV* right ventricle, *LA* left atrium, *LV* left ventricle

Right Atrial (RA) Systolic Collapse

The RA is a low pressure chamber, and the RA free wall is relatively thin. When the pericardial pressure surpasses the atrial pressure, the free wall may collapse during atrial systole (ventricular diastole) (Fig. 7.18). RA systolic collapse is best assessed in the A4C and SC views. The RA wall can remain collapsed through atrial diastole. This *inversion* of the RA, when present for more than a third of the cardiac cycle, has a very high sensitivity and specificity for diagnosis of tamponade [19]. RA collapse typically occurs at lower intrapericardial pressures than will cause right ventricular collapse. It may be seen as a lone finding in the absence of tamponade physiology, hence other echocardiographic features of tamponade must also be present to confirm cardiac tamponade [20].

Right Ventricular Diastolic Collapse

As the pericardial pressure exceeds the RV diastolic pressure, the free wall of the RV, which is less thick than the LV free wall, may collapse. This can be appreciated with PLAX, PSAX, A4C, or SC views. The RV outflow tract is the more compressible area of the RV and tends to collapse earlier with increasing intrapericardial pressure (Fig. 7.19). Diastolic collapse can be identified following the T wave by employing real-time EKG monitoring. Using echocardiography, the frames can be scanned back and forth to observe for the opening of the mitral or tricuspid valve to estimate the onset of diastole and to assess for RV collapse at that time point [4].

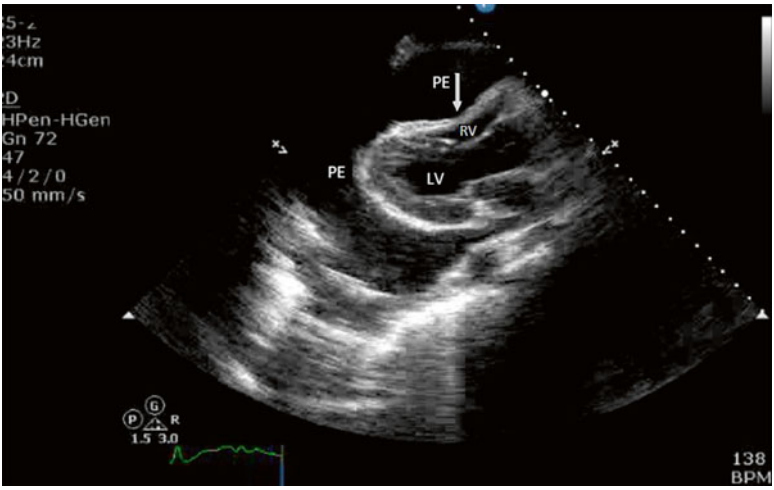

Fig. 7.19 Parasternal long axis view in a patient with large pericardial effusion. Note the right ventricular outflow tract collapse (*arrow*) with cardiac tamponade. *PE* pericardial effusion, *LV* left ventricle, *RV* right ventricle

In the PLAX view, an M-mode recording through the RV free wall and anterior mitral valve leaflet helps with visualization and timing of the free wall collapse (Fig. 7.2). RV collapse may be absent in conditions causing RV hypertrophy, such as long-standing pulmonary hypertension. While the finding of RA systolic collapse is highly sensitive, diastolic collapse of the right ventricle is highly specific for diagnosing cardiac tamponade [10, 21].

Reciprocal Respiratory Changes

With cardiac tamponade, the total pericardial volume is fixed and there is an equalization of diastolic pressures within the pericardium and the cardiac chambers. As filling in the right-sided chambers increases with inspiration, there is a reciprocal decrease in the left-sided volume. This is best appreciated in the four-chamber view. During inspiration, there is a shift in the interventricular septum toward the LV and vice versa with expiration (Fig. 7.4). An M-mode tracing can be obtained from the PLAX view to delineate the movement of the septum.

IVC Plethora

Elevated right atrial pressures are reflected by a dilation of the IVC. In a spontaneously breathing patient, a dilated IVC without an inspiratory decrease in size, along with dilated hepatic veins, is termed *IVC plethora*. This can be visualized best on the SC view (Fig. 7.20). An M-mode tracing of the IVC shows the change in

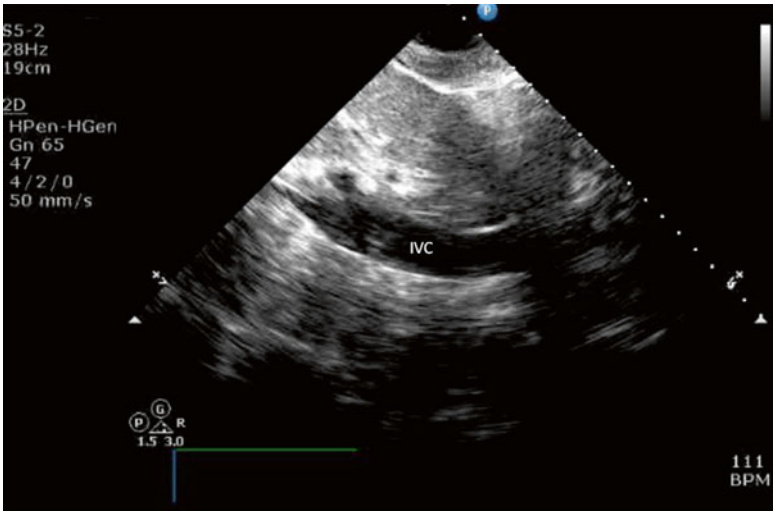

Fig. 7.20 A subcostal view of the point of entry of the inferior vena cava (*IVC*) into the right atrium. There is IVC plethora with a size of more than 2 cm; loss of respiratory variation would also be seen

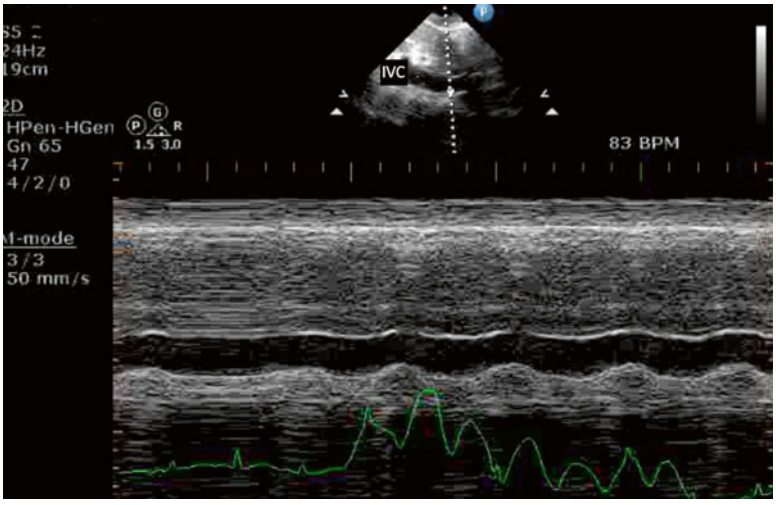

Fig. 7.21 An M-mode tracing through the inferior vena cava (*IVC*) in a patient with cardiac tamponade. With inspiration, there is loss of respiratory variation in the size of the IVC

diameter with the respiratory cycle (Fig. 7.21). Less than 50 % inspiratory reduction in the IVC diameter within 2 cm of the entrance into the RA is very sensitive but not specific for diagnosing tamponade [22]. For other causes of IVC plethora, see Pitfalls and Precautions below.

Advanced Competencies

Advanced critical care echocardiography involves the use of Doppler recordings to assess the volume of inflow across the mitral and tricuspid valves and RV/LV diastolic filling to exclude tamponade physiology (see Box 7.3). During inspiration, early diastolic filling velocity in the RV is augmented, while LV diastolic filling is reduced. Normally, there is some variation in flow across the valves due to respiration. In cardiac tamponade, this respiratory variation in blood flow across the valves is exaggerated. If the respiratory variation in flow across the mitral or tricuspid valve is more than 25 %, tamponade is suggested. The tissue Doppler through the mitral annulus will show a reduced E′ when tamponade is present. Additionally, analysis of Doppler flow provides information regarding velocities and direction of flow. Velocities toward the transducer are displayed above the baseline, and velocities away from the transducer are displayed below the baseline. The returning Doppler signal is a spectral tracing of velocity against time. The area under the curve of the spectral trace is known as the Velocity Time Integral (VTI). In tamponade, the VTI in the pulmonary artery increases with inspiration, while the stroke volume and VTI of aortic velocity decrease. Once the diagnosis of tamponade is established, the management should focus on maintaining hemodynamics while preparing for percutaneous or surgical drainage.

Box 7.3 Advanced CCE features of cardiac tamponade

2-D Assessment
- Moderate or large pericardial effusion
- Right atrial collapse or inversion (>1/3 cardiac cycle)
- Right ventricular diastolic collapse
- Respiratory "paradoxical" septal motion
- Respiratory variation of left and right ventricular size
- Inferior vena cava plethora

M-Mode
- Interventricular septal shift with respiration
- Diastolic collapse of RVOT/RV
- IVC dilation (>2 cm) with no respiratory variation

Pulsed-Wave Doppler
- Increased respiratory variation of inflow across mitral valve >25 % or tricuspid >35 %
- Phasic variation of LVOT and RVOT outflow velocities
- IVC with low-velocity flow

Doppler Flow Velocities Across Mitral and Tricuspid Valve

Proceeding with the Doppler tracing, the ventricular inflow velocities are traced across the tricuspid and mitral valve. A 2D image on A4C view is recorded for several beats to correctly align the intercept angle of the Doppler beam parallel to the direction of inflow [10]. Note that as the Doppler intercept angle increases from the direction of inflow, Doppler flow velocities may potentially be underestimated. Inflow velocities can be calculated using the caliper feature of the machine. With cardiac tamponade, there is an increased respiratory variation in flow across the mitral valve of >25 % and across the tricuspid valve of >35 % (Figs. 7.22 and 7.23).

Velocity Time Integral Across the Left Ventricular Outflow Tract

VTI is measured with PWD of LVOT velocities and is recorded from the apical five-chamber view, with the sample volume positioned just proximal to the AV. It denotes the distance that blood travels with each stroke. In patients with cardiac tamponade, VTI across the LVOT is reduced with inspiration. However, measurement of VTI may be time consuming and difficult in the critically ill patient.

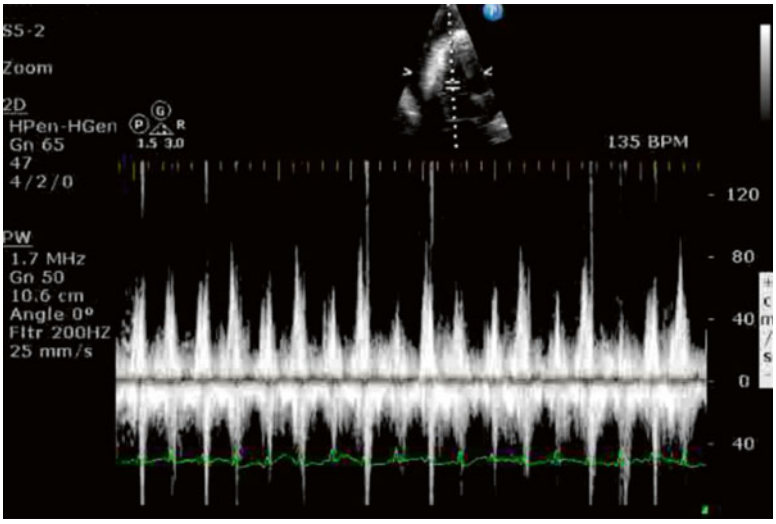

Fig. 7.22 Pulsed wave Doppler velocities through the tricuspid valve in a patient with a large pericardial effusion and tamponade. Note the large variation in Doppler flow across the tricuspid valve. Respiratory variation of more than 35 % is indicative of cardiac tamponade

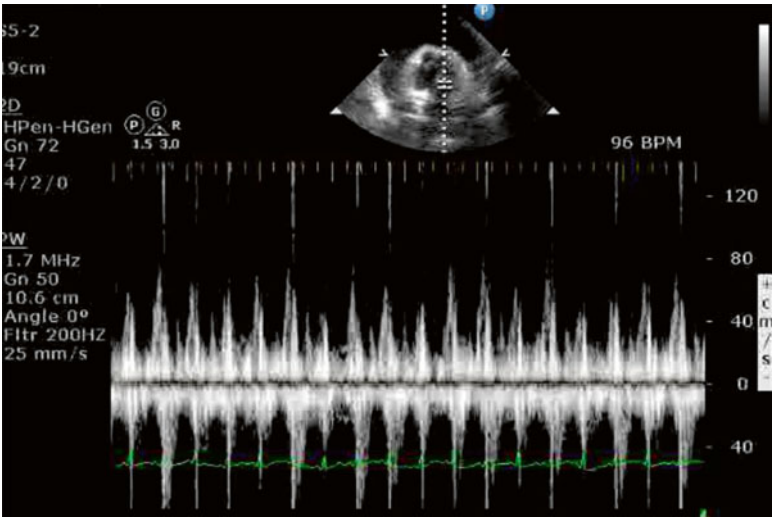

Fig. 7.23 Pulsed wave Doppler velocities through the mitral valve in a patient with a large pericardial effusion and tamponade. Respiratory variation of more than 25 % is indicative of cardiac tamponade

Echocardiography-Guided Pericardiocentesis

With the patient in supine position, 2-D echo is performed in multiple views. The angle and depth of penetration to reach the fluid is measured, and a site is marked. Most physicians use the subcostal approach with the needle placed between the xiphoid process and the left costal margin and advanced toward the left scapula in the same orientation as the probe. Real-time echocardiography, using a sterile probe cover, has been used for pericardiocentesis via other approaches including apical and left parasternal, with a 97 % success rate [23]. Care must be taken to avoid the internal mammary artery when using these alternative approaches. Visualization of the needle tip may be difficult, so agitated saline can be injected to confirm that the needle is in the pericardial space prior to insertion of the catheter. Post-procedure echocardiography should be performed to determine residual fluid volume or complications from the procedure.

Transesophageal Echocardiography (TEE)

TEE has a limited role in the spontaneously breathing patient with cardiac tamponade, who may be decompensating. However, patients on positive pressure ventilation, particularly those who are post-sternotomy and have suboptimal 2-D views, may be good candidates for TEE. Postoperative effusions can be loculated and

localized to the posterior and lateral aspects of the heart. Postoperative effusions are by definition hemorrhagic in the immediate postoperative setting. An intrapericardial hematoma will have an echogenic appearance similar to the myocardium. They can cause isolated compression of one or more chambers. Transesophageal echocardiography may be the best imaging modality of pericardial effusion or hematoma in these circumstances.

Evidence Review and Evidence-Based Use

Goal-directed critical care echocardiography in the intensive care unit (ICU) setting is increasingly performed at the bedside to determine the cause of hemodynamic impairment and to provide critical information about the cardiovascular status of the patient [24]. In many instances, pocket/handheld devices can only provide 2-D images and may not be able to perform Doppler studies [25]. Newer devices available on the market have overcome this limitation and are increasingly being used by intensivists to perform goal-directed CCE.

Many common presentations of ICU patients, including shock, dyspnea, respiratory failure, and suspected pericardial effusion, are listed by the American Society of Echocardiography as indications for transthoracic echocardiography [26]. Major professional societies such as the American College of Chest Physicians, European Society of Intensive Care Medicine, and networks such as WINFOCUS (World Interactive Network Focused on Critical UltraSound) ECHO-ICU Group all recommend that intensivists obtain necessary echocardiographic training such that they are able to practice this anatomical and physiological investigation at a high level [27–29]. Training in ultrasound techniques for intensivists should aim to achieve competencies in three main areas: general critical care ultrasound, basic critical care echocardiography, and advanced CCE [28]. The training in focused echocardiographic techniques should be adopted as part of fellowship training or, if not available at the time of fellowship training, through training from relevant endorsing professional societies.

A significant number of patients admitted to the medical ICU with noncardiac illness can have cardiac abnormalities. In one series, up to 77 % of patients who had surveillance echocardiography had cardiac abnormalities, including 5 % who had moderate to large pericardial effusions [30]. In another series by Joseph et al., up to 63 % of patients who presented with shock were found to have a cardiac etiology. After severe systolic dysfunction, cardiac tamponade was the second most common cause of shock (17 %) in this series and prompted therapeutic intervention. Of note, transthoracic echocardiography provided adequate imaging in nearly all the cases [31]

Vignon and colleagues studied the use of handheld echocardiography performed by critical care physicians and compared the exam to conventional transthoracic echocardiography (TTE) interpreted by a cardiologist in 103 intubated patients [32]. The diagnostic capacity of the 2-D imaging and the therapeutic impact based on imaging were similar in both groups (44 % vs. 46 %, p = 0.9). However, the mean time required for completing the examination was shorter with the portable device (5 ± 4 min vs. 9 ± 5 min, P = 0.001). Both the portable device and conventional TTE had similar capability in diagnosing pericardial effusion and tamponade (75 % each). In another study involving 515 patients at high risk for pericardial effusion, emergency medicine physicians trained in bedside echocardiography, as compared to trained cardiologists, were able to identify patients with pericardial effusion with a sensitivity of 96 %, specificity of 98 %, and overall accuracy of 97.5 % (95 % CI 95.7–98.7 %) [5].

Biais and associates performed a single-center, prospective study to compare the diagnostic ability of ultra-miniaturized handheld ultrasound devices used by intensivists to conventional TTE, read by a cardiologist blinded to the initial study [33]. Focused examinations showed a high concordance with conventional TTE and adequately identified RV dilation, RV dysfunction, pericardial effusion, and tamponade with good to excellent agreement (κ values 0.63 – 1).

Pitfalls and Precautions

There are several potential pitfalls while performing CCE in diagnosing pericardial effusion and tamponade [34].

- Diastolic chamber collapse can be seen with severe hypovolemia and large pleural effusion. On the other hand, patients with right ventricular hypertrophy, such as with longstanding pulmonary hypertension, may not demonstrate diastolic chamber collapse even in the presence of cardiac tamponade.
- An echo-free space limited to the anterior surface is a pericardial fat pad, which appears as an isolated dark area with brighter speckles.
- A pleural effusion is usually located posterior to the descending thoracic aorta and unlike a pericardial effusion, would not surround the heart on all sides.
- In post-surgical patients, a loculated or eccentric effusion may cause regional cardiac compression and hemodynamic compromise.
- Rapid accumulation of even relatively small effusions can cause tamponade physiology and should not be discounted based on size alone.
- Intrapericardial hematoma arising as a complication of cardiac surgery or procedures may not be apparent on the initial examination, and serial echocardiographic evaluations may be necessary to determine the cause of hypotension.
- IVC plethora may be seen with other loading conditions causing elevated right atrial pressure such as pulmonary embolism and volume overload states.
- Cardiac tamponade is ultimately a clinical diagnosis established by a combination of physical exam and echocardiographic findings.

References

1. Wheeler AP, Bernard GR, Thompson BT, Schoenfeld D, Wiedemann HP, deBoisblanc B, et al. Pulmonary-artery versus central venous catheter to guide treatment of acute lung injury. N Engl J Med. 2006;354(21):2213–24.
2. Moore CL, Copel JA. Point-of-care ultrasonography. N Engl J Med. 2011;364(8):749–57.
3. Beaulieu Y. Bedside echocardiography in the assessment of the critically ill. Crit Care Med. 2007;35(5 Suppl):S235–49.
4. Nagdev A, Stone MB. Point-of-care ultrasound evaluation of pericardial effusions: does this patient have cardiac tamponade? Resuscitation. 2011;82(6):671–3.
5. Mandavia DP, Hoffner RJ, Mahaney K, Henderson SO. Bedside echocardiography by emergency physicians. Ann Emerg Med. 2001;38(4):377–82.
6. Melamed R, Sprenkle MD, Ulstad VK, Herzog CA, Leatherman JW. Assessment of left ventricular function by intensivists using hand-held echocardiography. Chest. 2009;135(6): 1416–20.
7. Vignon P, Dugard A, Abraham J, Belcour D, Gondran G, Pepino F, et al. Focused training for goal-oriented hand-held echocardiography performed by noncardiologist residents in the intensive care unit. Intensive Care Med. 2007;33(10):1795–9.
8. Labovitz AJ, Noble VE, Bierig M, Goldstein SA, Jones R, Kort S, et al. Focused cardiac ultrasound in the emergent setting: a consensus statement of the American Society of Echocardiography and American College of Emergency Physicians. J Am Soc Echocardiogr. 2010;23(12):1225–30.
9. Kaplan A, Mayo PH. Echocardiography performed by the pulmonary/critical care medicine physician. Chest. 2009;135(2):529–35.
10. Catherine M, Otto M. Pericardial Disease. In: Catherine M, Otto M, editors. Text book of clinical echocardiography. 4th ed. Philadelphia: Saunders Elsevier; 2009. p. 242–58.
11. Schairer JR, Biswas S, Keteyian SJ, Ananthasubramaniam K. A systematic approach to evaluation of pericardial effusion and cardiac tamponade. Cardiol Rev. 2011;19(5):233–8.
12. Bodson L, Bouferrache K, Vieillard-Baron A. Cardiac tamponade. Curr Opin Crit Care. 2011;17(5):416–24.
13. Roy CL, Minor MA, Brookhart MA, Choudhry NK. Does this patient with a pericardial effusion have cardiac tamponade? JAMA. 2007;297(16):1810–8.
14. Spodick DH. Acute cardiac tamponade. N Engl J Med. 2003;349(7):684–90.
15. Curtiss EI, Reddy PS, Uretsky BF, Cecchetti AA. Pulsus paradoxus: definition and relation to the severity of cardiac tamponade. Am Heart J. 1988;115(2):391–8.
16. Himelman RB, Kircher B, Rockey DC, Schiller NB. Inferior vena cava plethora with blunted respiratory response: a sensitive echocardiographic sign of cardiac tamponade. J Am Coll Cardiol. 1988;12(6):1470–7.
17. Maisch B, Seferovic PM, Ristic AD, Erbel R, Rienmuller R, Adler Y, et al. Guidelines on the diagnosis and management of pericardial diseases executive summary; The Task force on the diagnosis and management of pericardial diseases of the European society of cardiology. Eur Heart J. 2004;25(7):587–610.
18. William F, Armstrong TR. Feigenbaum's echocardiography. Philadelphia: Lippincott Williams & Wilkins; 2009.
19. Gillam LD, Guyer DE, Gibson TC, King ME, Marshall JE, Weyman AE. Hydrodynamic compression of the right atrium: a new echocardiographic sign of cardiac tamponade. Circulation. 1983;68(2):294–301.
20. Merce J, Sagrista-Sauleda J, Permanyer-Miralda G, Evangelista A, Soler-Soler J. Correlation between clinical and Doppler echocardiographic findings in patients with moderate and large pericardial effusion: implications for the diagnosis of cardiac tamponade. Am Heart J. 1999;138(4 Pt 1):759–64.
21. Kerber RE, Gascho JA, Litchfield R, Wolfson P, Ott D, Pandian NG. Hemodynamic effects of volume expansion and nitroprusside compared with pericardiocentesis in patients with acute cardiac tamponade. N Engl J Med. 1982;307(15):929–31.

22. Kircher B, Himmelman R. Non invasive estimation of right atrial pressure from the inspiratory collapse of the inferior vena cava. Am J Cardiol. 1990;66:493–6.
23. Tsang TS, Enriquez-Sarano M, Freeman WK, Barnes ME, Sinak LJ, Gersh BJ, et al. Consecutive 1127 therapeutic echocardiographically guided pericardiocenteses: clinical profile, practice patterns, and outcomes spanning 21 years. Mayo Clin Proc. 2002;77(5): 429–36.
24. Schmidt GA, Koenig S, Mayo PH. Shock: ultrasound to guide diagnosis and therapy. Chest. 2012;142(4):1042–8.
25. Spevack DM, Tunick PA, Kronzon I. Hand carried echocardiography in the critical care setting. Echocardiography. 2003;20(5):455–61.
26. Douglas PS, Garcia MJ, Haines DE, Lai WW, Manning WJ, Patel AR, et al. ACCF/ASE/AHA/ASNC/HFSA/HRS/SCAI/SCCM/SCCT/SCMR 2011 Appropriate Use Criteria for Echocardiography. A Report of the American College of Cardiology Foundation Appropriate Use Criteria Task Force, American Society of Echocardiography, American Heart Association, American Society of Nuclear Cardiology, Heart Failure Society of America, Heart Rhythm Society, Society for Cardiovascular Angiography and Interventions, Society of Critical Care Medicine, Society of Cardiovascular Computed Tomography, Society for Cardiovascular Magnetic Resonance American College of Chest Physicians. J Am Soc Echocardiogr. 2011;24(3):229–67.
27. Price S, Via G, Sloth E, Guarracino F, Breitkreutz R, Catena E, et al. Echocardiography practice, training and accreditation in the intensive care: document for the World Interactive Network Focused on Critical Ultrasound (WINFOCUS). Cardiovasc Ultrasound. 2008;6:49.
28. Cholley B. International expert statement on training standards for critical care ultrasonography. Intensive Care Med. 2011;37(7):1077–83.
29. Mayo PH, Beaulieu Y, Doelken P, Feller-Kopman D, Harrod C, Kaplan A, et al. American College of Chest Physicians/La Societe de Reanimation de Langue Francaise statement on competence in critical care ultrasonography. Chest. 2009;135(4):1050–60.
30. Bossone E, DiGiovine B, Watts S, Marcovitz PA, Carey L, Watts C, et al. Range and prevalence of cardiac abnormalities in patients hospitalized in a medical ICU. Chest. 2002; 122(4):1370–6.
31. Joseph MX, Disney PJ, Da Costa R, Hutchison SJ. Transthoracic echocardiography to identify or exclude cardiac cause of shock. Chest. 2004;126(5):1592–7.
32. Vignon P, Chastagner C, Francois B, Martaille JF, Normand S, Bonnivard M, et al. Diagnostic ability of hand-held echocardiography in ventilated critically ill patients. Crit Care. 2003;7(5): R84–91.
33. Biais M, Carrie C, Delaunay F, Morel N, Revel P, Janvier G. Evaluation of a new pocket echoscopic device for focused cardiac ultrasonography in an emergency setting. Crit Care. 2012; 16(3):R82.
34. Saito Y, Donohue A, Attai S, Vahdat A, Brar R, Handapangoda I, et al. The syndrome of cardiac tamponade with “small” pericardial effusion. Echocardiography. 2008;25(3):321–7.

Chapter 8
Ultrasound and Airway Management

Alan Šustić and Alen Protić

Introduction

Ultrasound (US) offers an extensive number of attractive advantages when compared to the competitive imaging techniques or endoscopy for critically ill patients. Some of the most important advantages of using bedside US are its broad availability, repeatability, portability, relatively affordable price, safety, and painless applicability. Even though some of the earliest reports on the US applications in clinical medicine deal with the description of soft-tissue imaging of the pretracheal structures and anterior tracheal wall [1, 2], the first thorough reports of using US as an assistance tool in multiple applications in airway management have been supplied within the last few years [3, 4]. What directly determines the usage of ultrasonography in airway management in anesthesia and intensive care unit (ICU) is the availability of portable and low-cost US capacities in daily practice in operative theaters and ICU. Clinicians initially described US-guided central venous and arterial catheterization, followed by US-guided regional anesthesia techniques, which led to the emergence of increasing experience with the application of US toward airway management. In this chapter, we will describe the sonographic anatomy of the upper respiratory organs and highlight the crucial potential applications of ultrasonography in the airway management of the critically ill patient.

A. Šustić, M.D., Ph.D. (✉)
Department of Anesthesiology and Intensive Care Unit, University Hospital Rijeka,
T. Strižića 3, Rijeka, Croatia
e-mail: alan.sustic@medri.uniri.hr

A. Protić, Ph.D.
Department of Anesthesiology and Intensive Care Unit, University Hospital Rijeka,
Tome Strizica 3, Rijeka, Croatia 385, Croatia
e-mail: alen.protic@medri.uniri.hr

M. Jankowich, E. Gartman (eds.), *Ultrasound in the Intensive Care Unit*,
Respiratory Medicine, DOI 10.1007/978-1-4939-1723-5_8

Technical and Patient Considerations

Ultrasound Anatomy of the Upper Airway

Ultrasound Examination of Upper Airway

The upper airway is a complex air-filled structure made of bones, cartilaginous, muscular, and soft tissue, which can only be partially visualized by ultrasound (US). US waves strongly reflect when meeting air, and the structures below the air compartment are therefore impossible to visualize. When adjoining the bones, US waves are mostly absorbed or reflected by them, not allowing any further visualization of the underlying structures. If a bony structure is present, US will show it in the form of a bright hyperechoic line on the bone surface with acoustic shadow underneath. On the other hand, cartilage and muscle have very similar impedances and are well visualized by US as hypoechoic, well-distinguished structures, which allow the underlying structures to be assessed by US. Additionally, muscles appear as heterogeneous, striated, and hypoechoic structures. Fat and connective soft tissue mostly appear as hypoechoic signet-ring shape structure under the skin, not as well defined as cartilages or muscles.

Anatomy of the Upper Airway

The upper airway starts with the pyramid of the nasal cavity, a bony and cartilaginous structure divided into two nostrils and separated by septum nasi. Each nasal cavity contains three nasal conchae forming superior, middle, and inferior nasal meati that communicate with frontal, maxillary, sphenoidal, and ethmoidal sinuses. The nasal cavity is mostly made by bones filled with air and therefore is not very suitable for US analysis.

Through the nasal choanae, the nasal cavity communicates with the pharynx, a cone-shaped muscular organ conventionally divided into three sections: superior (epipharynx), middle (mesopharynx), and inferior (hypopharynx). The pharynx is a part of the respiratory and digestive systems. The muscular structure of the pharynx makes US assessment favorable, but its position prohibits a routine approach with the US probe.

The succeeding part of the upper respiratory airway includes the larynx, a cartilaginous and muscular organ positioned between the fourth and sixth cervical vertebrae. The larynx connects the pharynx with the trachea and consists of four cartilages (thyroid, cricoid, arytenoid cartilage, epiglottis) [which form two pairs of joints (crico-thyroid and crico-arytenoid)] and several muscles (two posterior and two anterior crico-arytenoid muscles, transverse arytenoid muscle, crico-thyroid muscle, and two vocal muscles). US approach to the frontal and lateral parts of the larynx is very good since these parts of the larynx lie closely under the skin. The lower part of the larynx extends to the trachea, which is a cartilaginous and

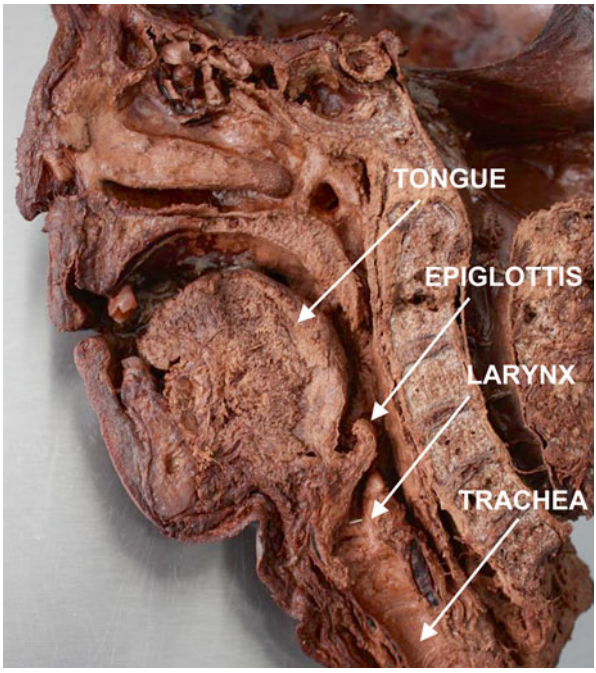

Fig. 8.1 Anatomic view of the upper respiratory system (cadaver model)

membranous tube measuring approximately 12 cm in length. The trachea starts at the level of sixth cervical vertebra and ends at the level of fourth or fifth thoracic vertebrae. The trachea is composed of imperfect rings of hyaline cartilage, which are C-shaped, dorsally incomplete, and connected to each other by elastic tissue. The ends of the rings are joined by the muscular tissue (Fig. 8.1).

Technique of the Upper Airway US Examination

The optimal positioning of the patient for US examination of the upper airway is the "sniffing" position, which includes head extension and neck flexion. If this position is not possible to perform due to reasons such as a cervical spine injury, the mandible needs to be moved into protrusion. This maneuver requires the help of an assistant. Two main planes are usually used for the US examination: horizontal, also called transverse view, and sagittal plane, called longitudinal view. Transverse view is mostly used for the US assessment of the mouth floor, posterior part of the tongue (Fig. 8.2), and supra- and infra-hyoid bone regions. For the US assessment from larynx to the suprasternal notch, both views can be used, depending on the clinical needs. According to the anatomy of the patient, any other plane can be used as long as the structures under the US probe are discerned. Besides the planes where the US probe should be at 90° in relation to skin (e.g., transverse and longitudinal), there

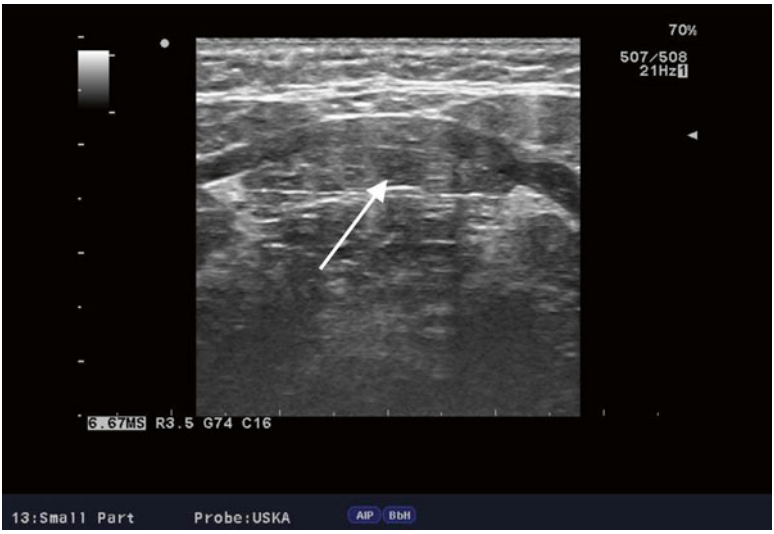

Fig. 8.2 Tongue ultrasound view—posterior part. *White arrow* (tongue)

are four different movements of the US probe which can be useful to get a better view on the screen:

- *Sliding*—longitudinal or transverse US probe movement over the skin surface without changing angle of the US probe in relation with the skin surface.
- *Rotation*—around the vertical axis of the US probe without any lateral movement. Usually used to distinguish muscles, tendons, blood vessels, and nerves from other structures.
- *Tilting*—manipulating the US probe about its horizontal axis thereby changing the angle of the US wave in relation to the skin surface, but without longitudinal or transversal movement across the skin surface. The best US screen view usually appears when the US wave comes at a 90° angle to the skin surface; it nevertheless does not mean that all structures in the neck are parallel with skin. Therefore, tilting is the maneuver which corrects the entrance of the US wave into target organs, intending to get the best US screen view.
- *Pressure*—moderate force applied with the US probe on the underlying tissue at 90° angle to the skin surface. This maneuver can be helpful to differentiate arteries from veins.

A short linear US probe with a frequency of more than 7.5 MHz is appropriate for the upper airway US examination, due to the higher frequency, which gives a better resolution of the superficial organs and tissues. For this examination, the best selected setting on ultrasound apparatus is the small parts or vascular setting.

Image Acquisition and Interpretation

US Anatomy of the Upper Airway

An US probe with a frequency of more than 7.5 MHz is appropriate for the upper airway US examination, due to the higher frequency, which gives a better resolution of the superficial organs and tissues. In spite of the high impedance of air-filled spaces, analysis of the soft tissue and cartilages of the upper airway is possible, including: the floor of the mouth, posterior part of the tongue, supra- and infrahyoid bone region, larynx, and trachea. The US examination of the floor of the mouth usually includes the posterior part of the tongue and its base, which presents the tongue as an iso- to hypoechoic organ (Fig. 8.2). Epiglottic vallecula is well visualized from both sides of the tongue base, and it is considered to be a margin to hypopharynx (Fig. 8.3). Moving the US probe from the mouth floor caudally (sliding) in the transverse view, the hyoid bone with characteristically inverted U-shaped hyperechoic line (reflection of the US wave) and the acoustic shadow underneath can be assessed (Fig. 8.4). The hyoid bone and nearby laryngeal cartilages are clearly visible due to its bony structure. By further sliding of the US probe caudally, the main laryngeal cartilages (cricoid and thyroid) can be assessed. Although a median approach of the US probe is the best one for the US examination of the upper airway anatomy, para-medial approach would be preferable in the area of the laryngeal prominence, since there is no perfect contact between the US probe and skin. Thyroid and cricoid cartilages are visible as homogeneous, hypoechoic

Fig. 8.3 Ultrasound view of the vallecula epiglottica (*arrows*)

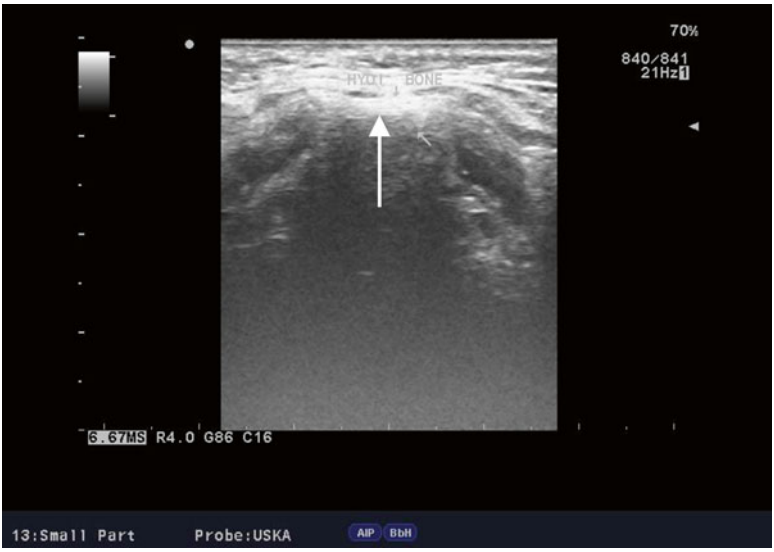

Fig. 8.4 Ultrasound view of the hyoid bone (*arrow*)

well-defined structures, connected with iso-echoic crico-thyroid ligament. Vocal cords can be assessed by the transverse view by positioning the US probe on the distal part of the thyroid cartilage or on the crico-thyroid membrane caudally and tilting the US probe (Fig. 8.5). Vocal cords are visible as hypoechoic structures and appear as triangle movement during phonation. Approximately half of the length of the trachea is positioned in the neck and is available for US analysis. Caudally from the cricoid cartilage, imperfect tracheal cartilage rings appear and can be assessed by longitudinal and transversal view. Cartilage rings are clearly visible as hypoechoic, well-defined, lens-shaped structures. Between tracheal cartilages and tracheal air-filled space, there is a hyperechoic line, which is called the air-mucosa interface. Sliding in a caudal direction, anterior to the trachea at the level of second to fourth tracheal cartilage, a homogeneous hyperechoic structure (in comparison with adjacent strap muscles) can be seen. This structure serves as a bridge connecting two identical echoic oval structures anterolateral to the trachea, which represent the isthmus and two lobes of the thyroid gland. Transverse view of the trachea is usually used to examine the width of the air space at different levels of the view and also to measure the width of the soft tissue from trachea to the skin surface (Fig. 8.6). The longitudinal view in the median or para-median plane is suitable for showing the line of tracheal cartilages, and their number as well (Fig. 8.7). Via the longitudinal midline view, the distance from the skin surface to the anterior cartilage, as well as the distance from the posterior cartilage to the tracheal air space, can be estimated.

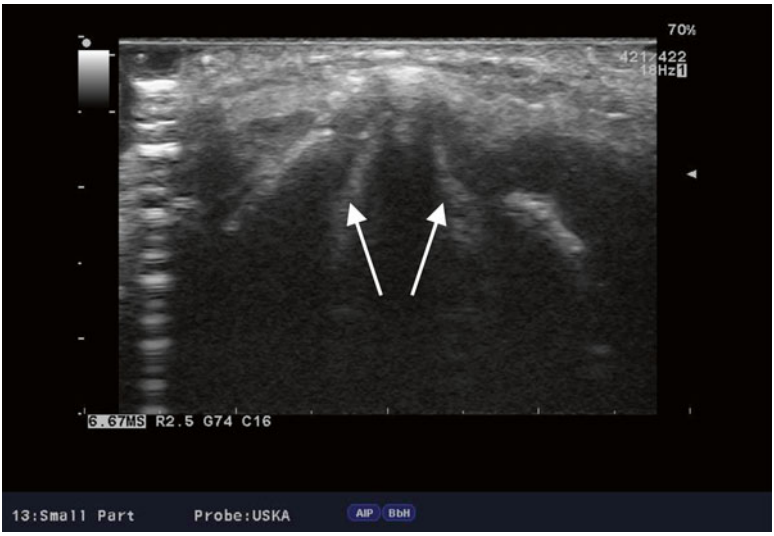

Fig. 8.5 Ultrasound view of the vocal cords (*arrows*)

Fig. 8.6 The air space of the trachea and the pretracheal soft tissue—transverse view

Fig. 8.7 Tracheal cartilage rings—longitudinal view

Verification of Endotracheal and Double-Lumen Tube Position

When focusing on methods of definitive airway protection and control in critically ill patients, endotracheal tube (ETT) insertion persists as the primary one. In order to exclude esophageal or endobronchial intubation, with respect to the Advanced Cardiac Life Support guidelines from 2000, a confirmatory procedure should be undertaken after the insertion of the ETT [5]. Furthermore, the position of the ETT tube must be constantly supervised during patients' stay in ICU so that incidental endobronchial intubation, with subsequent atelectasis, is forestalled. Even though the physical examination comprising mainly auscultation of the left thoracoabdominal area is advised to be the firsthand and everyday method of ETT positioning confirmation, its sensitivity is nevertheless considerably low, which consequently points out the necessity of a secondary method of confirmation. The end-tidal CO_2 detection and esophageal suction device are the most often used bedside ones, but both of these secondary methods are firstly limited in detecting endobronchial intubation, and secondly they do not render direct anatomic evidence of accurate ETT position [6].

On the other hand, US provides indirect but proper dynamic anatomic evidence of the correct physiologic function of the ETT in paralyzed or apneic patients during and after resuscitation; moreover, it effectively and quickly images the movement of the diaphragm and pleura, both of them being the indirect quantitative and qualitative indicators of lung expansion [3, 7]. If the ETT is in the correct position

(i.e., trachea), bilateral and equal motions of the diaphragm toward the abdomen are likely to be visible on ultrasound, representing equal bilateral expansion of the lungs [7, 8] (see Chap. 10 for a complete discussion of diaphragm ultrasound imaging). When using the intercostal ultrasonographic view, it is also easy to identify the "sliding lung" sign at the lung-chest wall interface, a sort of "to-and-fro" movements of the hyperechoic pleura synchronized with ventilation (see Chap. 9) [9]. If the aforementioned sign is imaged on the left, or on both sides of the chest, it should correspond to appropriate bilateral lung ventilation, thus verifying correct ETT position. In contrast, if the ETT is in the esophagus, expansion of the lungs will not occur as a result of mechanically delivered breath, but diaphragmatic movement may be seen if the patient continues to spontaneously breathe. Furthermore, when the patient is paralyzed or apneic, an esophageal intubation will result in an immobile diaphragm or paradoxical movement of the diaphragm (due to the instillation of positive pressure into the abdomen). An intercostal view in paralyzed or apneic patients with an intra-esophageal ETT will result in absence of motion of the pleura on both sides of the chest (i.e., absence of "lung sliding") with assisted ventilation. When the "lung sliding" sign is absent, the vibrations of the pleura will occur in rhythm with the heartbeat, a sign known as the "lung pulse" (see Chap. 9) [10]. Finally, it will be either impossible to see the movements of the left diaphragm—or the movement is significantly minimized—when the tube is in the right main bronchus; the movements of pleura ("lung sliding)," on the other hand, will occur only on the right side of the chest, while the "lung pulse" should be visible on the left side. As an important reminder, the presence of lung sliding indicates lung inflation and the absence of pneumothorax, but, as is evident in these examples, the absence of lung sliding does not necessarily indicate the presence of a pneumothorax.

In adults, successful imaging of the ETT correctly placed in the trachea can be variable (Fig. 8.8). There have been limited reports of additional methods that can augment one's ability to capture the ETT position with US, such as increasing the echogenicity of the tube by retaining a stylet in the tube or by filling the ETT cuff with fluid and air bubbles. In contrast, in children, and especially in infants, correct anatomic position of ETT can be visualized by bedside US in almost all cases [11]. Furthermore, in emergency settings US is highly useful in detection of the esophageal malposition of ETT, since it is possible to verify esophageal position of ETT in nearly all patients within just a few seconds [12].

In the case of a thoracic procedure or one-lung ventilation, the purpose of using double-lumen tubes (DLT) is to both isolate and/or collapse a given lung. The placement of a DLT must always be accurate in order to prevent injury to a patient or endangerment of the procedure. The current methods used to confirm the DLT placement are auscultation and fiberoptic bronchoscopy (FOB)—neither of which is optimal. Auscultation is not fully dependable and appropriate to confirm the correct position of the DLT, and FOB is not always available in clinical practice, particularly for the narrow DLTs used for children or small stature patients. Moreover, blood or mucus in the airway and anatomical distortion complicate the confirmation of DLT position, making visualization more difficult or even impossible. In these, albeit rare, cases, the FOB fails to guarantee success and positioning problems and

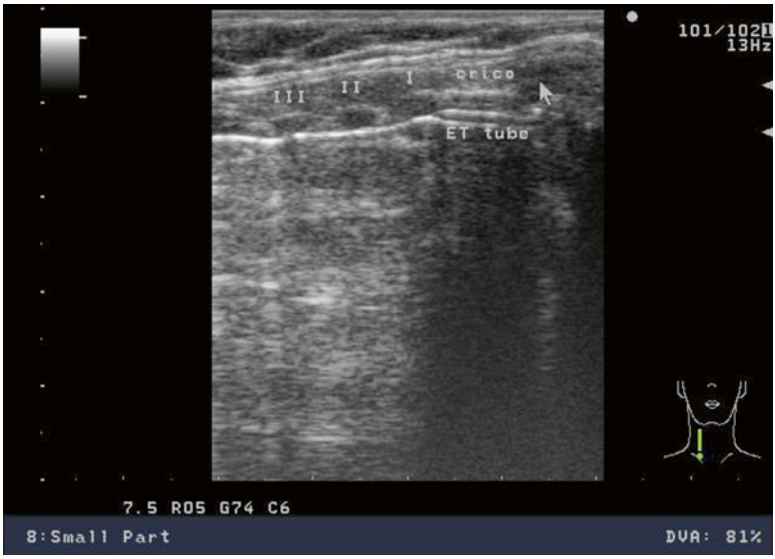

Fig. 8.8 Endotracheal tube placement in the trachea

severe complications can occur; therefore, US is a new and highly useful tool for confirming the proper DLT placement. The utility of US in confirming the proper DLT position is identical to the verification of endotracheal position of ETT. Movements of the right diaphragm will not be visible or will be significantly reduced if the left DLT has been placed in the correct position (i.e., left main bronchus). The pleural movements ("lung sliding") will be seen only on the left side of the chest, while the "lung pulse" will be visible on the right. If the DLT is placed in the trachea, bilateral equal movements of the diaphragm toward the abdomen and bilateral "lung sliding" can be observed [13].

Basic and Advanced Competencies

Basic Competences:

- Visualization and measurement of the air space in trachea (transverse view)
- Measurement and evaluation of the tissue in front of the trachea (transverse or longitudinal view)
- Doppler control during evaluation of the pretracheal tissue
- Identification and numbering of tracheal ring cartilages

Advanced Competences:

- Endotracheal tube identification
- Ultrasound-guided percutaneous tracheostomy
- Ultrasound-guided upper airway anesthesia

Evidence Review and Evidence-Based Use

Ultrasound and Endotracheal Intubation

Preintubation Assessment

Unsuccessful intubation of a pharmacologically paralyzed patient leads to devastating consequences, and since it can be challenging to predict a difficult airway with surety, other methods have to be considered. For instance, while one of the most well-known independent predictors of a difficult intubation is obesity, increased body mass index (BMI) does not sufficiently predict difficult laryngoscopy [14]. Interesting studies have recently been published regarding the usage of US in the assessment of the upper airways in prediction of difficult intubation in obese patients and particularly in patients with obstructive sleep apnea. Within the chosen group of obese patients, Ezri et al. found that an abundance of fat tissue at the anterior neck region, as measured by ultrasound, was a satisfactory independent predictor of difficult laryngoscopy, rather than BMI [15]. Hyomental distance, measured by US, in the neutral- and head-extended positions (low hyomental distance ratio) is also considered as an excellent predictor of a difficult intubation in obese and morbidly obese patients with a large neck circumference (Fig. 8.9) [16]. In the early nineties, Siegel and coworkers had moreover concluded that, when analyzing patients with sleep apnea, the upper airway US is a simple, reliable, and comfortable method to identify the airway obstruction mechanism [17]. The role of a preintubation US assessment elsewhere in the upper airway is also important, and there recently has

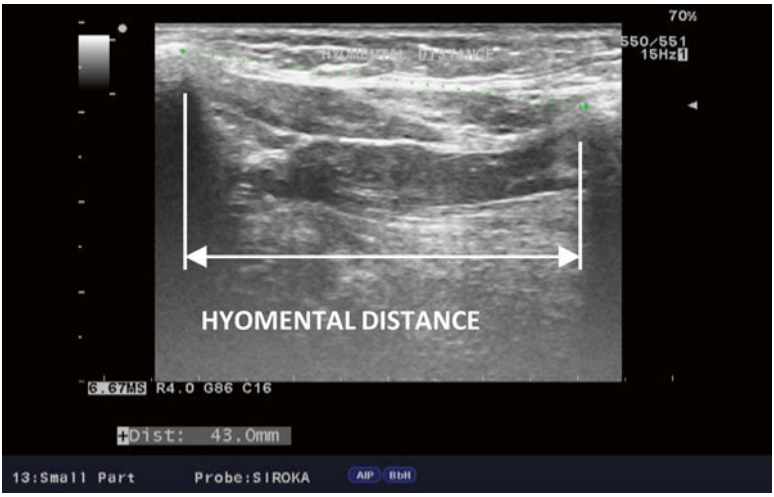

Fig. 8.9 Hyomental distance measurement by ultrasound

Fig. 8.10 Gastric ultrasound examination. Gaster = stomach

been great interest in this subject [3]. For example, US can detect pharyngeal or laryngeal pathology with a relevant impact on the airway management—e.g., tumors, trauma (e.g., aerodigestive tract injury), abscesses, or epiglottitis. Finally, in the case of emergent preintubation assessment, a brief gastric US examination is highly useful, since it can provide necessary information about gastric fullness and the risk of vomiting and aspiration (Fig. 8.10) [18].

Proper ETT and Left Double-Lumen (LDL) Tube Selection

Within the framework of pediatric and neonatologic anesthesia and critical care management, the selection of a proper dimension ETT is crucial and there are studies suggesting US as a useful tool for this. Recently, Shibasaki and coworkers found that subglottic upper airway diameter measured by ultrasonography was an excellent predictor of correct cuffed and uncuffed ETT sizes for pediatric patients [19].

In addition, one of the relevant parts of the lung separation procedure (e.g., one-lung ventilation) is determining the proper size of the (left) DLT. The tube must be the right size; otherwise, if too large, it will cause trauma and cuff over-inflation, and if too small, it will be dislocated, consequently assuming the wrong position. Brodsky and associates underline the usage of the measurement of the tracheal width from a chest radiograph as a useful guideline in predicting which size left DLT is appropriate [20]. US is also considered to be a highly functional method for specifying the proper left-sided DLT size, and there is a statistically significant correlation between

US measurement of the outer tracheal width and the inner tracheal and bronchial width measured by multi-slice computed tomography (MSCT) scan [21]. The US measurement of tracheal width is thus a simple noninvasive bedside method, which additionally should be used for determining the proper left-sided DLT.

Extubation Failure

One of the most common and severe complications of the management of mechanically ventilated patients is extubation failure, and therefore methods to predict extubation failure are important. Extubation outcome is directly correlated with respiratory muscle endurance, where diaphragmatic function has primary role (see Chapter 10). Respiratory motions and excursions of the diaphragm, liver, and spleen, which are easily detected by US, are in straightforward correlation with respiratory muscular strength. Jung-Rern and associates discovered in their research that a substantially larger displacement of liver and spleen (i.e., diaphragmal movement) occurred in patients with successful extubation, compared to those in whom extubation failure occurred [22]. The authors concluded that ultrasonographic measurement of liver and spleen displacement during a spontaneous breathing trial (SBT) before extubation is a highly important method for a good and successful prediction of the extubation outcome. The evaluation of diaphragmatic motions by US is thus likely to become a relevant tool when it comes to the evaluation of the respiratory muscle endurance in critically ill patients [8]. Moreover, lung US provides critical information about aeration during the SBT, which is very important and highly relevant in predicting postextubation distress [23].

Finally, it is worth mentioning that the US evaluation of vocal cords and laryngeal morphology in intubated patients is perceived as a useful method in identifying patients facing high risk of postextubation stridor and laryngeal edema [24].

Percutaneous Tracheostomy and Cricothyrostomy

Percutaneous dilational tracheostomy (PDT) is a well-founded and safe tool for gaining tracheal access in intensive care, but it nevertheless can lead to serious complications, and bronchoscopic or US guidance is recommended for the procedure [25]. Even though bronchoscopic guidance provides the best visualization and is used frequently, there are certain disadvantages when compared to US. Firstly, potential complications of bronchoscopy are compromised ventilation and significant hypercarbia with resultant elevated intracranial pressure—which is not tolerated well by patients with severe head or spinal cord injury. Secondly, bronchoscopy potentially can induce pulmonary hyperinflation and pneumothorax, since airway resistance is significantly increased. Therefore, an alternative method for guidance using airway US has been developed to guide the puncture of the trachea, and this has been a highly successful method applicable even in difficult cases [26].

The trachea and paratracheal soft tissues of the neck, due to their superficial position, are easily examined at the highest resolution with high-frequency US probes (e.g., 7–12 MHz). The anterior tracheal wall, thyroid and cricoid cartilages, tracheal rings, and pretracheal tissue are also well imaged, enabling the clinician to choose the optimal intercartilaginous space for tracheostomy tube placement [27]. Furthermore, the diagnostic US shows the relationship between the thyroid gland and the vascular structures of the neck to the trachea as well. Pre-procedural US plays a large role in patient safety, since if the US demonstrates unfavorable anatomy for PDT, open tracheostomy should be suggested.

The trachea is visualized in vertical medial section using a linear transducer, prepared in a sterile sheath (short vascular probe, 5–10 MHz), with concurrent activation of a constant Doppler signal over the trachea on the level of the second ring (or pulsed Doppler signal with sample volume in trachea). The endotracheal tube is then withdrawn until the cuff is just underneath the vocal cords. After the tip of the tube passes the second tracheal ring, the intensity of the Doppler signal is heavily increased due to an enhanced signal from unencumbered, turbulent air, which at the same time implies the confirmation of a proper position of the endotracheal tube. The site of the puncture is normally selected between the second and third tracheal rings, following a clear US verification of anatomy of the thyroid and cricoid cartilage and tracheal rings (Fig. 8.7). It is not mandatory to avoid the thyroid isthmus, if situated alongside the planned puncture canal, since isthmus penetration is frequent but generally harmless in PTD. The distance between the probe and the echo of the anterior tracheal wall can be measured and marked on the cannula, for the purpose of the puncture. The correct position of tracheostomy tube can ultimately be confirmed using US, at the same time excluding a potential pneumothorax [9]. If the tracheostomy tube assumes the proper position (i.e., in the trachea), "lung sliding" signs can be identified with intercostal US view. In addition, when the aforementioned sign is seen on the both sides of the chest, it corresponds to bilateral lung ventilation and correct tracheostomy tube position, thus excluding pneumothorax.

Miscellaneous

Laryngeal Mask Airway

The laryngeal mask airway (LMA) is an adjunctive airway device, which consists of a tube with a cuffed mask-like projection of the distal end. The precise position of the cuff, sealing the larynx, is highly relevant for adequate ventilation through the LMA. When the cuff is filled with fluid, the position of the LMA cuff is visible by US from the lateral approach on the larynx, and if US fails to image LMA equally on both sides of the larynx, repositioning should be performed. This application of US as a quality control measure is significantly useful during clinical training in the use of the LMA [28].

Ultrasound-Guided Upper Airway Anesthesia

Airway management during laryngoscopy or endotracheal intubation in awake critically ill patients is often associated with laryngospasm, coughing, and undesirable cardiovascular reflexes, which can be either abolished or blunted by anesthetizing the upper airway, including the superior laryngeal nerve. The precise position of superior laryngeal nerve block, located between the hyoid bone and thyroid cartilage, can be seen with ultrasonography, and a guided block is therefore possible to perform [4].

Pitfalls and Precautions

As in all other applications, the use of US in airway management is a skill that requires training, practice, and expertise. One of the most common and important mistakes of inexperienced operator during ultrasound examination of pretracheal soft tissue before or during ultrasound percutaneous tracheostomy is excessively strong pressure with transducer. Such pressure causes collapses of the pretracheal vessels, especially veins, which lead to a failure to detect them.

Conclusion

There is a growing body of literature supporting the relevance of bedside ultrasonography in critical care, including its use in airway management. A broader access to portable and affordable ultrasound devices with high resolution has resulted in the increased use of ultrasound in the intensive care setting. Ultrasound can be especially useful in the examination of the superficial structures of the upper airway, with potential roles in the preintubation assessment, confirmation of endotracheal and laryngeal mask airway placement, and performance of bedside percutaneous tracheostomy. These airway ultrasound techniques are highly likely to become routine practice in the future of airway management, particularly when it comes to teaching and the management of difficult cases.

References

1. Katz AD. Midline dermoid tumors of the neck. Arch Surg. 1974;109:822–3.
2. Bohme G. Clinical contribution to ultrasound diagnosis of the larynx (echolaryngography). Laryngorhinootologie. 1989;68:504–8.
3. Šustić A. Role of ultrasound in the airway management of critically ill patients. Crit Care Med. 2007;35:S173–7.
4. Kristensen MS. Ultrasonography in the management of the airway. Acta Anaesthesiol Scand. 2011;55:1155–73.

5. The American Heart Association in collaboration with the International Liasion Committee on Resuscitation. Guidelines 2000 for cardiopulmonary resuscitation and emergency cardiovascular care: Part 6. Advanced cardiovascular life support: Section 3. Adjuncts for oxygenation, ventilation and airway control. Circulation 2000;102(Suppl 8):I95–104
6. Knapp S, Kofler J, Stoiser B, et al. The assessment of four methods to verify tracheal tube placement in the critical care setting. Anesth Analg. 1999;88:766–70.
7. Hsieh KS, Lee CL, Lin CC, et al. Secondary confirmation of endotracheal tube position by ultrasound image. Crit Care Med. 2004;32(suppl):S3 74–77.
8. Matamis D, Soilemezi A, Tsagourias M, et al. Sonographic evaluation of the diaphragm in critically ill patients. Technique and clinical application. Intensive Care Med. 2013;39:801–10.
9. Lichtenstein D, Menu Y. A bedside ultrasound sign ruling out pneumothorax in the critically ill; lung sliding. Chest. 1995;108:1345–8.
10. Lichtenstein D, Lascols N, Prin S, Meziere G. The lung pulse: en early ultrasound sign of complete atelectasis. Intensive Care Med. 2003;29:2187–92.
11. Dennington D, Vali P, Finer NN, Kim JH. Ultrasound confirmation of endotracheal tube position in neonates. Neonatology. 2012;102:185–9.
12. Muslu B, Sert H, Kaya A, et al. Use of sonography for rapid identification of esophageal and tracheal intubations in adult patients. J Ultrasound Med. 2011;30:671–6.
13. Šustić A, Protić A, Cicvarić T, Župan Ž. The addition of brief ultrasound examination to clinical assessment increases the ability to confirm placement of double-lumen endotracheal tubes. J Clin Anesth. 2010;22:246–9.
14. Bond A. Obesity and difficult intubation. Anaesth Intensive Care. 1993;21:828–30.
15. Ezri T, Gewűrtz G, Sessler DI, et al. Prediction of difficult laryngoscopy in obese patients by ultrasound quantification of anterior neck soft tissue. Anaesthesia. 2003;58:1111–4.
16. Wojtczak JA. Assessment of hyomental distances and ratio, tongue size, and floor of the mouth musculature using portable sonography. J Ultrasound Med. 2012;31:523–8.
17. Siegel HE, Sonies BC, Vega-Bermudez F, et al. The use of simultaneous ultrasound and polysomnography for diagnosis of obstructive sleep apnea. Neurology. 1999;52 suppl 2:A110–1.
18. Shiver SA, Blaivas M. Gastric outlet obstruction secondary to linitis plastica of the stomach as shown on transabdominal sonography. J Ultrasound Med. 2004;23:289–992.
19. Shibasaki M, Nakajima Y, Ishii S, et al. Prediction of pediatric endotracheal tube size by ultrasonography. Anesthesiology. 2010;113:819–24.
20. Brodsky JB, Malott K, Angst M, et al. The relationship between tracheal width and left bronchial width: implication for left-sided double-lumen tube selection. J Cardiothorac Vasc Anesth. 2001;15:216–7.
21. Šustić A, Miletić D, Protić A, et al. Can ultrasound be useful for predicting the size of a left double-lumen bronchial tube? Tracheal width as measured by ultrasonography versus computed tomography. J Clin Anesth. 2008;20:247–52.
22. Jung-Rern J, Tzu-Hsiu T, Jih-Shuin J, et al. Ultrasonographic evaluation of liver/spleen movements and extubation outcome. Chest. 2004;126:179–85.
23. Summer A, Perbet S, Brisson H, et al. Ultrasound assessment of lung areation loss during a successful weaning trial predicts postextubation distress. Crit Care Med. 2012;40:2064–72.
24. Ding LW, Wang H-C, Wu H-C, et al. Laryngeal ultrasound: a useful method in predicting postextubation stridor. A pilot study. Eur Respir J. 2006;27:384–9.
25. Bardell T, Drower JW. Recent developments in percutaneous tracheostomy: improving techniques and expanding roles. Curr Opin Crit Care. 2005;11:326–32.
26. Šustić A, Krstulović B, Eškinja N, et al. Percutaneous dilatational tracheostomy vs. surgical tracheostomy in patients with anterior cervical spine fixation: preliminary report. Spine. 2002;27:1942–5.
27. Šustić A, Kovač D, Žgaljardić Z, et al. Ultrasound-guided percutaneous dilatational tracheostomy: a safe method to avoid cranial misplacement of the tracheostomy tube. Intensive Care Med. 2000;26:1379–81.
28. Takeyama K, Kobayashi H, Suzuki T. Optimal puncture site of the right internal jugular vein after laryngeal mask airway placement. Anesthesiology. 2005;103:1136–41.

Chapter 9
Lung Ultrasound in Respiratory Failure and Pneumonia

Keith P. Guevarra

Introduction

The extensive availability of high-quality bedside ultrasound machines in intensive care units (ICUs) provides the ability to acquire real-time diagnostic information that was not previously available, and has fostered a new era in clinical decision-making with bedside ultrasound's incorporation into daily clinical practice. As discussed in other chapters in this textbook, in addition to the diagnostic data that one can derive from scanning a patient's thorax, ultrasound significantly augments the safety and accuracy of bedside procedures in the ICU. The use of lung ultrasonography is well suited for the ICU setting, given the restrictions that are often encountered when traditional imaging is desired in our patients (e.g., safety of moving very critically ill patients off the unit, loss of nursing staff due to traveling, safety issues with transferring patient from bed to scanner, etc.). Lung ultrasound may be performed repeatedly and comparatively over time to document the evolution of a patient's clinical problem – without any further exposure to radiation or need to transfer off the ICU. Lung ultrasound will not replace traditional imaging modalities, but rather it provides data to augment one's bedside clinical decision-making and possesses the benefits of real-time performance.

Lung ultrasonography has become an important tool in obtaining information regarding the etiology of respiratory distress and respiratory failure in patients in the intensive care unit. This field was pioneered and developed extensively through the work of Dr. Daniel Lichtenstein, and has evolved into a powerful modality that may be used repeatedly to follow one's patient at the bedside in the ICU. As discussed below, it has been shown that a composite of lung ultrasonographic findings can

K.P. Guevarra, DO, FCCP (✉)
Division of Pulmonary & Critical Care Medicine, New Jersey Medical School- Rutgers, The State University of New Jersey, 150 Bergen Street, UH I-354, Newark, NJ 07103, USA
e-mail: kpguevarr@yahoo.com

M. Jankowich, E. Gartman (eds.), *Ultrasound in the Intensive Care Unit*, Respiratory Medicine, DOI 10.1007/978-1-4939-1723-5_9

help determine the cause of respiratory failure, and has been reported to provide immediate guidance on the etiology of acute respiratory failure in over 90 % of cases [1]. This chapter will guide the reader through the process of acquiring quality images for interpretation, how to identify the findings on lung ultrasound that support various potential causes of respiratory distress/failure, and how to ensure the reader recognizes the common pitfalls and limitations of lung ultrasonography.

Technical and Patient Considerations

Similar to other facets of goal-directed critical care ultrasonography, the selection of the proper equipment and appropriate positioning of the patient are crucial in obtaining valuable images for interpretation. As discussed in previous chapters, the availability of several probes of varying frequencies allows one to choose the correct probe for the desired ultrasound task. In general, given that most of the structures of interest in the thorax are relatively deep structures, a low frequency probe with a convex tip should be selected for the majority of lung ultrasounds. Exceptions to this are the use of a linear high frequency probe for ultrasonography of the pleura before and after placing a central venous catheter to assess for presence of iatrogenic pneumothorax [2] (Figs. 9.1 and 9.2) (also discussed in other chapters in this book).

ICU patients frequently present challenges regarding proper positioning for clinical tasks, which can be due to many factors such as external devices (e.g., intra-aortic balloon pump, intravenous lines, monitor leads, endotracheal tubes with mechanical ventilator support), patient body habitus, and hemodynamic instability. However, lung ultrasound can be adapted to the patient, and can be performed with the patient sitting up or in the supine position. In mechanically ventilated patients, the only possible way to scan the chest is often in a supine or semi-recumbent

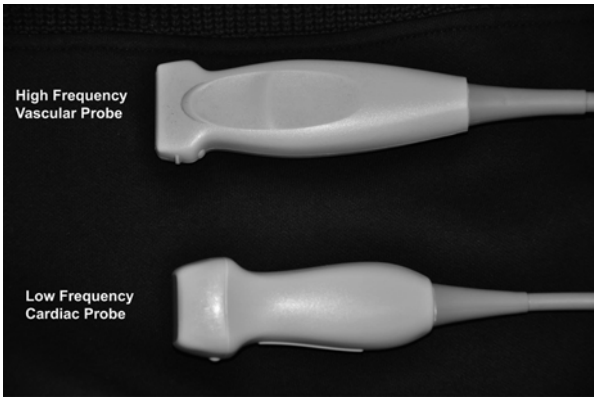

Fig. 9.1 A low frequency probe is normally used for depth imaging but has less resolution compared to a high frequency probe. High frequency probes are optimal for imaging relatively superficial structures like the pleura

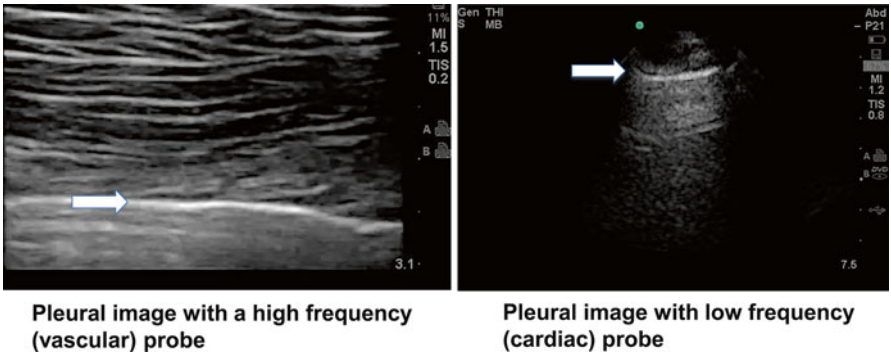

Fig. 9.2 Contrast of pleural images obtained using a high frequency versus low frequency probe. *Arrow* indicated hyperechoic pleural line

position. If a patient is able to maintain an upright position, the posterior aspect of the chest can be readily scanned. When scanning the axillary area of the chest, the patient's arm on the ipsilateral side can be abducted away from the patient's chest or moved across the body to increase the viewing area. This maneuver also can be performed in intubated patients provided that there is no restriction of movement (e.g., arm injury, arm restraints/sling).

Patience is key in obtaining images using ultrasound. Oftentimes, minute movements of the probe are necessary to improve image quality. Increasing gain does not automatically improve the image caliber but may even worsen image quality by increasing noise. Caution should also be observed when applying excessive pressure on the chest with the probe since this may not improve image quality, but may inflict pain on the patient.

The probe must sometimes be placed on the most posterior part of the thorax to scan for consolidation, atelectasis, or pleural effusion in intubated patients. While this can be uncomfortable for patient and operator, since these patients are typically supine these findings are more likely to be found in the most dependent part of the chest. A complete examination of the recumbent patient therefore necessitates posterior scanning.

Image Acquisition and Interpretation

Lung ultrasound can be performed with the patient in a variety of positions, and as such, approaching the patient systematically to ensure thorough scanning of the entire thorax is important. The ultrasound transducer should be held like a pen to allow for the ultrasound beam to be manipulated readily in all planes. The probe marker should be oriented cephalad, and the marker dot should be oriented on the

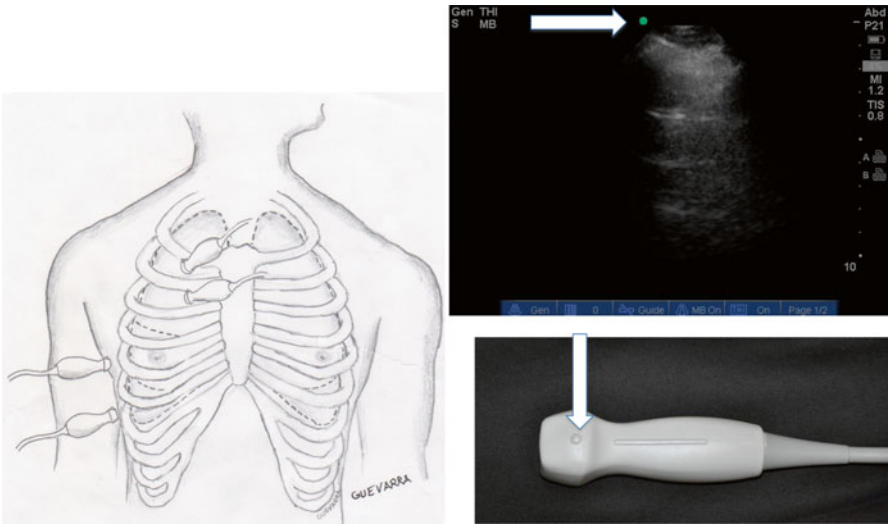

Fig. 9.3 Diagram of ultrasound scanning approach. Note that the transducer is placed in between the ribs. The *arrows* correspond to the marker on the screen and on the transducer, which should normally be oriented cephalad

left side of the ultrasound screen (i.e., the left side of the screen should correspond to the cephalad part of the patient). The transducer is placed in between the ribs and angled medially and laterally in a rib interspace, continuing to the next interspace from cephalad to caudad (Fig. 9.3). Subtle changes in the rotation, tilt, and angle of the probe are helpful in obtaining quality images – especially underneath the rib since bone prevents ultrasound transmission.

In order to thoroughly scan a patient's thorax, the chest wall is divided into four zones to ensure systematic scanning. Zone 1 corresponds to the anterior part of the chest, zone 2 to the lateral part of the chest, and zone 3 to the posterior and most dependent part of the chest. [1] Zone 4 (not shown) corresponds to the posteromedial part of the thorax, which can be scanned if the supine patient is placed in lateral decubitus position (Fig. 9.4). Scanning the thorax completely is important, especially including the most basal portion of the thorax bringing images of the liver or spleen into view. Finally, understand that the nature of the ICU patient population often presents limitations to obtaining adequate lung ultrasound images for various reasons; these are listed in Table 9.1.

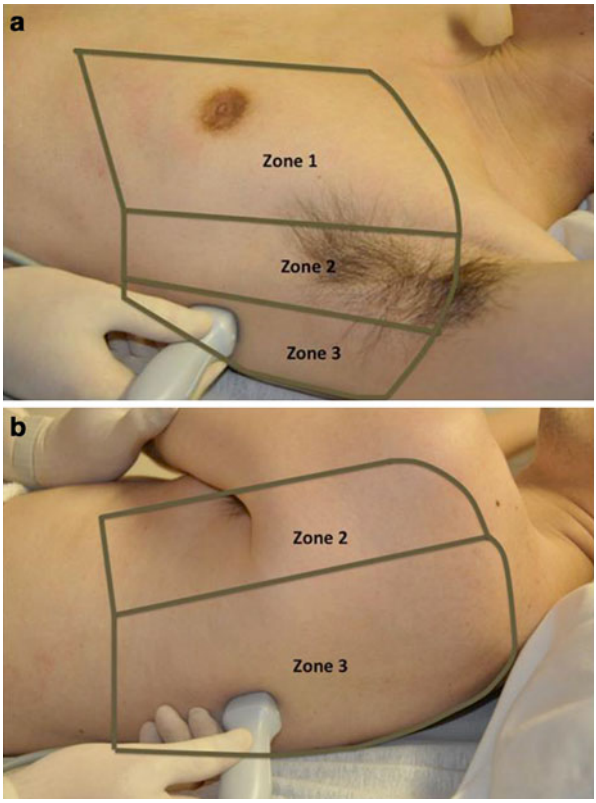

Fig. 9.4 (**a**) Ultrasound scanning zones (anterior view). (**b**) Ultrasound scanning zones (posterior view). Zone 4 not shown

Table 9.1 Challenges in ultrasound image acquisition [4, 19]

• Morbid obesity with excessive pannus
• Subcutaneous emphysema
• Cachexia (unable to place U/S probe in the rib interspace)
• Chest wall dressings
• Lines, tubings, and electrocardiogram leads
• Inability to properly position the patient
• Inability to place ultrasound probe in the posterior aspect of the chest
• Pneumothorax
• Shotgun pellets
• Pleural calcifications

Basic Competencies

Normal Lung and A-Lines

As is the case with many facets of medicine, a firm grasp of "normal" is important – and the image of the normal lung under ultrasound is no exception. Air prevents ultrasound wave transmission, while fluid promotes it. Therefore, ultrasound waves cannot transmit through organs that are gas-filled, and the waves that are reflected in gas-filled organs, such as the lung, produce amorphous gray images on the screen. Bones, such as the ribs, do not transmit ultrasound waves and appear as anechoic "shadows." A normally aerated lung ultrasound is depicted in Fig. 9.5, showing first the hyperechoic pleural line, followed by amorphous gray parenchyma (due to lung being filled with air). The anechoic black images running longitudinally on the right side of the image are the normal appearance of rib shadows. Finally, the regularly spaced echogenic horizontal lines (termed "A-lines") are produced as reverberation artifacts reflecting the sliding pleural line and appear at multiples of the distance from the body surface to the pleural line, appearing to project into the air-filled lung [3].

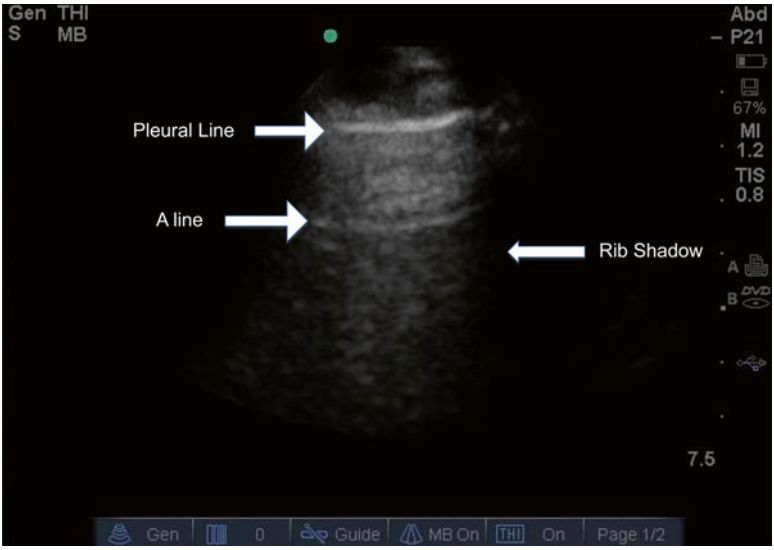

Fig. 9.5 Ultrasound image of a normal fully aerated lung. The *black* veil-like structure that borders the lateral segments of the image corresponds to the rib shadow resulting from reflection of the ultrasound beam. An A-line corresponding to a reverberation artifact is indicated. Repeated A-lines may be seen at multiples of the distance to the pleural line

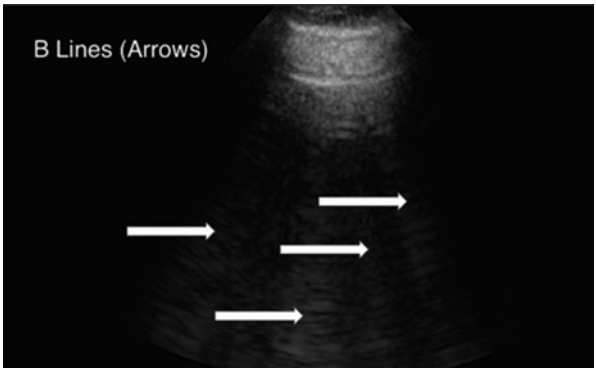

Fig. 9.6 B-Lines (*white arrows*) in a patient with pulmonary edema. In the presence of B-lines, A-lines will be abolished

B-Lines

An interruption or alteration in the normal aeration of the lung leads to abnormal findings on lung ultrasound. The presence of fluid or other material in the lung interstitium can be determined using ultrasonography. This can be seen as an increased number of vertical artifacts arising from the pleural line called "B-lines" (also referred to as "comet tails" or as "lung rockets" if several are present in a group) (Fig. 9.6; also see, e.g., Figs. 14.25 and 15.33) [3]. B-lines begin at the pleural line as a narrow hyperechoic beam that broadens as it goes deeper, extends the entire depth of the image, and effaces the normally appearing A-lines (since there is a loss of normal aeration of the lung) [4]. The intensity of B-lines increases with inspiratory movements. Random B-lines can be a normal finding at the lung bases due to small areas of atelectasis in that region [5]. Therefore, when scanning for pathologic B-lines or B-lines that have clinical relevance, start scanning at the least-dependent part of the thorax first. In other words, start the scan at the apical part of the thorax in an upright patient, or at the most anterior part of the chest in a supine patient. The variations in the number and spacing of B-lines can be used in conjunction with other findings to provide diagnostic relevance, as discussed in the sections below. Z-lines should not be confused with B-lines – these are comet-tail-like artifact that do not extend the entire depth of the imaging, are not as echoic as the pleural line, and do not efface the A-lines [3]. They are of uncertain clinical significance and may be present in healthy individuals [3].

Lung Sliding and Lung Pulse

A fully inflated lung, or more specifically the pleural surface of the inflated lung in contact with the chest wall, can be visualized through ultrasonography. The pleura appears as a hyperechoic shimmering linear structure (pleural line) that moves back

and forth in concordance to the respiratory cycle (called "lung sliding") [6] or the cardiac cycle (called "lung pulse") [7]. Lung sliding can be absent in the setting of pneumothorax, but also with severe hyperinflation resulting in impaired diaphragm excursion and poor lung ventilation. The presence of a lung pulse, not normally visualized when ventilation is normal, indicates that pneumothorax is not present, as the cardiac pulsation is being transmitted through the lung to the pleural surface. These findings are further discussed in the chapter on pleural ultrasound, but the presence or absence of these findings is important in the complete interpretation of lung ultrasound for respiratory failure.

Alveolar-Interstitial Syndrome

As stated earlier, normal lung is air-filled with a very small amount of fluid. Air has different acoustic impedance characteristics compared to fluid, and the image produced is different once there is alteration of the air-fluid interface of the lung interstitium (e.g., in cases such as pulmonary edema or inflammation). B-lines or comet tail artifacts are seen when a small water-rich structure, such as an edematous interlobular septa, is surrounded by air, resulting in a high impedance gradient. It is absent under normal conditions and present in alveolar-interstitial syndromes [8]. The alveolar-interstitial syndromes refer to a collection of disorders that result in interstitial and/or alveolar fluid accumulation producing increased B-lines on lung ultrasound and resulting in the impairment of the alveolocapillary gas exchange capacity of the lungs and acute, subacute, or chronic respiratory failure. Examples include acute conditions, such as congestive heart failure, acute respiratory distress syndrome, or other causes of pulmonary edema, and chronic conditions such as pulmonary fibrosis [8]. The alveolar-interstitial syndrome is therefore not a diagnosis itself, and the clinician must distinguish the underlying cause of the alveolar-interstitial process. B-lines arising from alveolar-interstitial syndrome with thickening of interlobular septa appear as *regularly spaced* B-lines, on average a distance of 7 mm apart. B-lines that are positioned *closer* to each other (generally less than 3 mm), are more typically seen in a generalized alveolar-filling process or in the setting of subpleural ground glass lesions [8]. More *irregularly spaced* B-lines are from disseminated foci of pneumonia [2]. B-lines are more clinically relevant if there are more than three B-lines per single field and they present all over the surface of the lung, especially in the most apical portion, or in the anterior part of the thorax in a supine patient [2, 8, 9]. Presence of B-lines, in addition to the presence of lung sliding, also rules out the possibility of pneumothorax when assessing for the cause of respiratory distress [10, 11].

Pneumonia and Consolidation

Pneumonia is a clinical diagnosis supplemented by radiographic findings. It is sometimes difficult to make the diagnosis when the symptoms and/or the radiographic findings are vague, such as in the setting of faint interstitial findings or retrocardiac opacities on chest radiography. Lung ultrasonography can help elucidate lung pathology that otherwise can be difficult to interpret on standard radiographic testing. In general, consolidated lung can be visualized via ultrasonography due to the loss of normal lung aeration, and will appear similar to other "tissue" images (similar to the liver, i.e., "hepatization" or to the spleen) [2]. A consolidated lung with persistent aeration of the airways will have the added appearance of hyperechoic small round structures – representing sonographic air bronchograms (Fig. 9.7). The consolidated lung has an irregular border delineated by a normal lung or by an effusion. This is called the "shred sign," and the asymmetric border is called the "shred line" [1]. If the consolidated lung moves with the respiratory cycle, it is likely the airway leading towards the affected segment is nonobstructed [2].

A-lines and lung sliding are preserved unless concomitant pulmonary edema (i.e., acute respiratory distress syndrome) is also present, which would abolish A-lines. Recruitment maneuver effect in the lungs of intubated patients who have acute lung injury or acute respiratory distress syndrome can be seen as transformation of consolidation to B-lines in the anterior and lateral parts of the chest wall [12, 13].

If there is a mucous plug or an endobronchial blockage affecting the part of the lung being scanned, lung sliding may not exist but lung pulse is preserved. In this scenario, lung sliding is minimal since the lung does not have full excursion in relation to the breathing cycle. On the other hand, lung pulse is a motion that can be

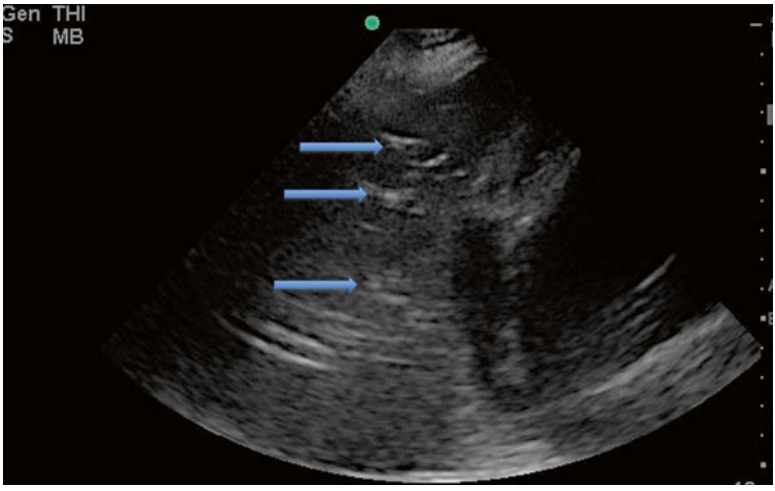

Fig. 9.7 Ultrasound image of PLAPS – posterolateral alveolar and/or pleural syndrome. The hyperechoic white specks (*blue arrows*) in the consolidated lung are sonographic air bronchograms

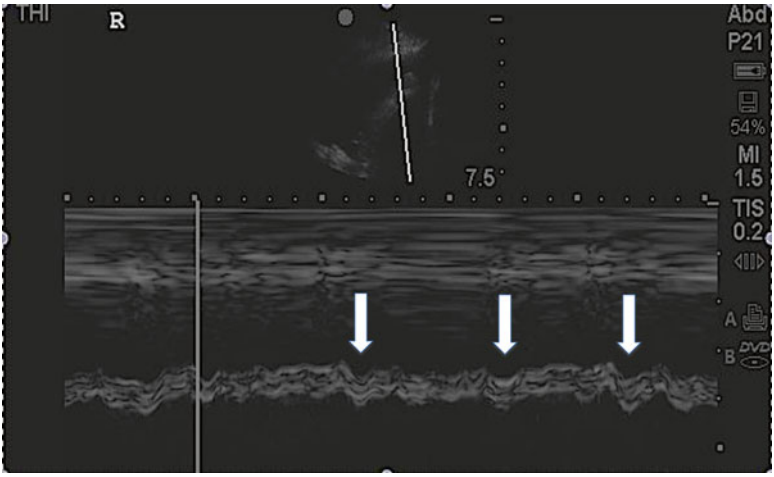

Fig. 9.8 M-mode imaging of a lung surrounded by a pleural effusion. The "sinusoid" sign is the movement of the lung during breathing excursion in relation to the pleura. *White arrows* indicate expiratory phase

observed in this scenario since the lung remains in close proximity to the chest wall, and while not being ventilated ("lung sliding" absent or minimal) it does moves in sequence with the cardiac motion ("lung pulse" present). The non-affected/contralateral normal lung should still have the normal findings such as A-lines, lung sliding, and lung pulse, while the lung with consolidation may have B-lines. Posterolateral alveolar and/or pleural syndrome (PLAPS) is seen as alveolar consolidation with a concominant pleural effusion in the posterior lateral aspect of chest in a supine or semirecumbent patient (Fig. 9.7). It has a high specificity for pneumonia (close to 96 %) if seen in conjunction with A-lines [1].

There may be times when consolidation from pneumonia may be difficult to distinguish from complex pleural effusion, or the presence of an effusion may be hard to identify when in close proximity to a consolidation especially if the effusion is small in size. The "sinusoid sign" is an M-mode imaging sign that shows movement of the lung surrounded by pleural effusion in relation to the pleura in real time (Fig. 9.8). The lung movement occurs during breathing excursion when the lung approximates with the pleura during inspiration [6].

Assessment of Failure to Wean of the Ventilator and Diaphragm Function

Respiratory muscle weakness and dysfunction occurs quickly in controlled ventilation patients, and ultrasound of the diaphragm potentially can be very helpful in detecting this problem [14]. This subject is covered thoroughly in Chap. 11.

Pneumothorax and Pleural Effusion

The expedient and accurate evaluation for a pneumothorax in an ICU patient is a valuable utility of bedside ultrasound. This is discussed fully in Chap. 10.

Advanced Competencies

Parenchymal Lung Disease

Lung abscesses can be detected using ultrasound. They appear as round structures with a hypoechoic center and irregular hyperechoic sharp borders within a consolidated lung. Peripheral abscesses contiguous with the pleura are easier to visualize and can be better delineated using a high frequency (vascular probe) although depending on the size of the abscess, a low frequency probe might be necessary to measure the size of the abscess. Lung masses bordering the pleura can also be seen with ultrasound. If close to the visceral pleura, ultrasound guided needle biopsy can be performed almost comparable to the computed tomography (CT) guided type. Ultrasound can help find a safe site for placement of the needle. However, these advanced imaging techniques and procedures are usually outside the bounds of goal-directed, urgent critical care ultrasound of the lung.

Evidence Review and Evidence-Based Use

Over the past 10–15 years, there has been expanding evidence on the utility and performance of bedside lung ultrasonography. As stated previously, the intended purpose of this modality is not to replace traditional imaging with lung ultrasound, but rather to offer an evidence-based addition to the clinical data available to the ICU team. Below is a summary of the available literature on the performance of lung ultrasound and a summary of how to interpret the constellation of imaging findings that may support a particular pulmonary pathology. Keep in mind that many of these studies were single-center studies performed by highly experienced operators.

Lung ultrasound has been reported to be highly accurate in detecting alveolar consolidation from acute respiratory distress syndrome (ARDS) or pneumonia. In a study published by Lichtenstein et al. [1], the sensitivity, specificity, and diagnostic accuracy of ultrasonography in diagnosing alveolar consolidation in a group of 32 patients with ARDS, using computed tomography as the gold standard, was 93 %, 100 %, and 97 %, respectively, vs. chest radiography that had a sensitivity of 68 % and diagnostic accuracy of 75 %. In a multicenter study of patients with suspected community-acquired pneumonia by Reissig et al. [15], lung ultrasonography for

detection of pneumonia had a sensitivity of 93.4 %, specificity of 97.7 %, and likelihood ratios of 40.5 for positive and 0.07 for negative results, compared to two-plane chest radiography supplemented by low-dose CT in inconclusive cases. In combination with auscultation, the positive likelihood ratio increased to 42.9 and decreased the negative likelihood ratio to 0.04. In addition, the authors found that resolution of pneumonia could also be followed sonographically with bigger lesions showing a greater change. These results suggest that lung ultrasonography can be a useful bedside tool for the diagnosis of alveolar consolidation as in pneumonia or ARDS.

Lung ultrasonography may be used to assess for the presence of lung edema, with the presence of B-lines/comet tail artifacts indicating edema. In a single-center study, in distinguishing pulmonary edema from chronic obstructive pulmonary disease (COPD) exacerbation [1] presence of multiple disseminated or laterally located B-lines had 100 % sensitivity and 92 % specificity for pulmonary edema. Lichtenstein et al. [3], in a prospective study of mechanically ventilated patients, found that bilateral A-lines in the anterior part of the thorax, without bilateral "lung rockets" (a so-called A-predominance profile), indicating presence of dry lungs, corresponded to a pulmonary arterial occlusion pressure (PAOP) $\leq$ 13 mmHg with a 90 % specificity, 67 % sensitivity, 91 % (positive predictive value) PPV, and 65 % NPV (negative predictive value). For PAOP $\leq$ 18 mmHg, A-predominance showed 93 % specificity, 50 % sensitivity, 97 % PPV, and 24 % NPV. Volpicelli et al. [9] found multiple and diffuse B-lines to be relatively sensitive and specific for the presence of the "alveolar-interstitial syndrome" in emergency department patients, as compared to chest radiography. They noted a sensitivity of 85.7 % and a specificity of 97.7 % with a positive predictive value of 93.0 % and a negative predictive value of 95.1 % for lung ultrasound showing multiple B-lines. Lung ultrasound took less than 3 min when performed. When "comet tails" were compared to pulse contour cardiac output monitoring (PiCCO), a negative ultrasound (rare or absent comet tails, or present only just above the diaphragm) was 90 % sensitive and 89 % specific for extravascular lung water < 500 mL. The sensitivity and specificity of "comet tails" were 90 % and 86 % when the extravascular lung volume water is > 500 mL [16]. These studies suggest a role for noninvasive diagnosis and monitoring of pulmonary edema using lung ultrasonography.

Utility of lung ultrasound may extend to conditions other than pneumonia and pulmonary edema, but requires the imaging and accurate interpretation of the presence or absence of multiple ultrasonographic signs and artifacts. A lung ultrasound profile consisting of anterior A-lines without PLAPS and with presence of lung sliding (or if lung sliding was absent, no evidence of a lung point) had a 89 % sensitivity and 97 % specificity for asthma/COPD exacerbation [1]. B-lines were noted to be absent in 92 % of patients with suspected COPD exacerbation [1]. For pulmonary embolism, presence of A-lines plus venous thrombosis had a 81 % sensitivity and 99 % specificity [8]. In a study by Reissig et al. [15], 80 % of patients with a pulmonary embolism had one or more lung parenchymal lesions detectable by ultrasound. These consisted of wedge-shaped or rounded lesions, hypoechoic lesions extending to the pleural surface, occasionally with a single echo in the

center. In this study, ultrasound had a sensitivity of 80 % and a specificity of 92 % for detection of pulmonary embolism. These studies highlight the potential for lung ultrasound in clinical diagnosis, but indicate a need for experience in imaging acquisition and interpretation.

Clinical Applicability

Ultrasound findings can potentially be used to determine possible causes of respiratory distress or respiratory failure. Due to the portability of ultrasound machines, scanning can be done quickly [16, 9] and in real time especially during medical emergencies including rapid response calls or medical codes. Table 9.2 lists clinical scenarios in which associated ultrasound findings can be helpful [1, 9, 17, 18]. Keep in mind that ultrasound profiles may overlap between different conditions, highlighting the need to interpret lung ultrasound, as one would chest radiography, in the appropriate clinical context.

In pulmonary edema, there will be an anterior-predominant B-lines that are found in the bilateral chest. Lung sliding is preserved, but with the disappearance of A-lines. PLAPS may be present. This profile can also be observed in pneumonia.

In COPD and status asthmaticus, there will be A-lines, but B-lines are usually not present to a significant degree. Loss of lung sliding may occur especially if there is hyperinflation that would prevent pleural excursion, but no lung point should be present, as would occur in pneumothorax. Consolidation and/or effusion can also be found if there is concomitant pneumonia, again indicating potential for overlap of profiles.

In pneumothorax, disappearance of lung sliding in the anterior chest with preservation of bilateral A-lines is visualized. If meticulous scanning of the chest is performed, a lung point can be found where the separation between the parietal and visceral pleura is precisely located. This sign appears to be relatively specific for pneumothorax.

In pulmonary embolism, A-lines are found bilaterally while lung sliding can be found in most. PLAPS can also be seen at times. Note that this type of profile can overlap with that seen in COPD/asthma or pneumonia. Ultrasound findings in the lung parenchyma related to pulmonary embolism are normally found as peripheral lesions [18]. Typical parenchymal findings include hypoechoic lesions that can also be seen in the pleural surface, wedge-shaped or rounded and at times contain a single echo detected in the center of the lesion. Concomitant ultrasound examination of the lower venous system presenting as an echoic intraluminal thrombosis or absence of compressibility in a venous vessel can help increase diagnostic accuracy.

Table 9.2 Ultrasonographic findings of the lungs and corresponding disease process [1, 9, 17, 18]

Diagnosis	Ultrasound finding	Sensitivity (%)	Specificity (%)	Positive predictive value (%)	Negative predictive value (%)	Diagnostic accuracy (%)
Alveolar consolidation	–	93–94	98–100	–	–	97
Pulmonary edema	Diffuse B-lines	86–97	94–98	93	95	–
COPD/asthma	Anterior A-lines	97	89	–	–	–
	B/L lung sliding					
	No PLAPS					
Pulmonary embolism	A-lines (+) venous embolism	81	99	–	–	–
	Peripheral lesions	80	92	95	72	84
Pneumonia	PLAPS A-lines	42	96	–	–	–
	B-lines + disappearance of lung sliding	11	100	–	–	–
	A-lines in affected lung + B-lines in contralateral lung	14	100	–	–	–
	Anterior alveolar consolidation	11	99	–	–	–
	Anterior alveolar consolidation + PLAPS + A-lines	89	94	–	–	–

Pitfalls and Precautions

- Meticulous scanning or minute movement may help find an ideal spot to visualize the lungs.
- There are certain modifiable and nonmodifiable factors that can obstruct or hinder imaging of the lungs such as body habitus, dressings/lines, or bony structures such as the ribs or the scapula, so scanning the entire lung surface is not possible.
- When scanning for lung sliding or A-lines, decreasing the gain, the depth, or both may improve the image quality on the screen.
- It is sometimes necessary to place the probe to the most dependent part of the thorax between the patient and the bed to accurately scan for consolidation, atelectasis, or pleural effusion on intubated patients. Since these patients are typically supine, these findings are more likely to be seen on the most dependent part of the chest.
- As mentioned earlier, B-lines separated by more than 7 mm or single B line seen in the dependent parts of the lungs is normal variant and is considered non-pathologic.
- Z-lines are comet-tail-like artifacts of unclear significance that are shorter than B-lines and do not erase A-lines, and so should not be confused with B-lines [3].
- Keep in mind the potential for overlapping ultrasound profiles in different clinical conditions, and use ultrasound only as an additional piece of data when formulating the clinical diagnosis and plan.
- When scanning for consolidation, the liver can be mistaken for a consolidated portion of the lungs hence the term "hepatization" [15]. Hence identifying the diaphragm as a hyperlucent structure below the consolidated lung and above the liver may help prevent confusion. In addition, the kidney is located right below the liver or in close proximity to the liver.
- When scanning with a high frequency probe, certain linear hyperechoic structures can be mistaken for non-sliding pleura. It is important that the scanning part of the probe is angled to face towards the thorax caudally until the sliding pleura can be identified.

Summary

Lung ultrasonography is a useful imaging tool in assessment of causes of hypoxemia and respiratory disease. The presence of pulmonary edema, alveolar-interstitial syndrome, lung consolidation/pneumonia, pleural effusion, or pneumothorax can be determined with this diagnostic modality, and it can be performed quickly at the bedside and can be easily repeated. Besides providing diagnostic data, it can help guide with procedures and interventions, adding cost-effectiveness and safety. In patients with pneumonia, ultrasonography may have better diagnostic ability than regular chest radiography. Image acquisition and interpretation requires professional training and repetition in order to avoid poor image quality and misinterpretation.

References

1. Lichtenstein D, Mezière G. Relevance of Lung ultrasound in the diagnosis of acute respiratory failure: the BLUE protocol. Chest. 2008;134(1):117–25.
2. Koenig SJ, Narasimhan M, Mayo PH. Thoracic ultrasonography for the pulmonary specialist. Chest. 2011;140(5):1332–41.
3. Lichtenstein D, Mezie`re G, Lagoueyte J, Biderman P, Goldstein I, Gepner A. A-lines and B-lines: lung ultrasound as a bedside tool for predicting pulmonary artery occlusion pressure in the critically ill. Chest. 2009;136(4):1014–20.
4. Lichtenstein D, Mezière G. A lung ultrasound sign allowing bedside distinction between pulmonary edema and COPD: the comet-tail artifact. Intensive Care Med. 1998;24(12):1331–4.
5. Bouhemad B, Zhang M, Lu Q, Rouby JJ. Clinical review: bedside lung ultrasound in critical care practice. Crit Care. 2007;11(1):205.
6. Lichtenstein DA, Menu YA. Bedside ultrasound sign ruling out pneumothorax in the critically ill. Lung sliding. Chest. 1995;108(5):1345–8.
7. Lichtenstein DA, Lascols N, Prin S, Mezière G. The "lung pulse": an early ultrasound sign of complete atelectasis. Intensive Care Med. 2003;29(12):2187–92.
8. Lichtenstein D, Mézière G, Biderman P, Gepner A, Barré O. The comet-tail artifact. An ultrasound sign of alveolar-interstitial syndrome. Am J Respir Crit Care Med. 1997;156(5):1640–6.
9. Volpicelli G, Mussa A, Garofalo G, Cardinale L, Casoli G, Perotto F, Fava C, Frascisco M. Bedside lung ultrasound in the assessment of alveolar-interstitial syndrome. Am J Emerg Med. 2006;24(6):689–96.
10. Lichtenstein D, Mezière G, Biderman P, Gepner A. The comet-tail artifact: an ultrasound sign ruling out pneumothorax. Intensive Care Med. 1999;25(4):383–8.
11. Lichtenstein DA, Mezière G, Lascols N, Biderman P, Courret JP, Gepner A, Goldstein I, Tenoudji-Cohen M. Ultrasound diagnosis of occult pneumothorax. Crit Care Med. 2005; 33(6):1231–8.
12. Bouhemad B, Brisson H, Le-Guen M, Arbelot C, Lu Q, Rouby JJ. Bedside ultrasound assessment of positive end-expiratory pressure-induced lung recruitment. Am J Respir Crit Care Med. 2011;183(3):341–7.
13. Stefanidis K, Dimopoulos S, Tripodaki ES, Vitzilaios K, Politis P, Piperopoulos P, Nanas S. Lung sonography and recruitment in patients with early acute respiratory distress syndrome: a pilot study. Crit Care. 2011;15(4):R185.
14. Matamis D, Soilemezi E, Tsagourias M, Akoumianaki E, Dimassi S, Boroli F, Richard JC, Brochard L. Sonographic evaluation of the diaphragm in critically ill patients. Technique and clinical applications. Intensive Care Med. 2013;39(5):801–10.
15. Reissig A, Copetti R, Mathis G, Mempel C, Schuler A, Zechner P, Aliberti S, Neumann R, Kroegel C, Hoyer H. Lung ultrasound in the diagnosis and follow-up of community-acquired pneumonia: a prospective, multicenter, diagnostic accuracy study. Chest. 2012;142(4):965–72.
16. Agricola E, Bove T, Oppizzi M, Marino G, Zangrillo A, Margonato A, Picano E. "Ultrasound comet-tail images": a marker of pulmonary edema: a comparative study with wedge pressure and extravascular lung water. Chest. 2005;127(5):1690–5.
17. Lichtenstein D, Goldstein I, Mourgeon E, Cluzel P, Grenier P, Rouby JJ. Comparative diagnostic performances of auscultation, chest radiography, and lung ultrasonography in acute respiratory distress syndrome. Anesthesiology. 2004;100(1):9–15.
18. Reissig A, Heyne JP, Kroegel C. Sonography of lung and pleura in pulmonary embolism: sonomorphologic characterization and comparison with spiral CT scanning. Chest. 2001; 120(6):1977–83.
19. Mayo P, Doelken P. Pleural ultrasonography. Clin Chest Med. 2006;27:215–27.

Chapter 10
Pleural Ultrasound

Samuel K. Evans and Matthew Jankowich

Introduction

The use of ultrasound for the two major disorders affecting the pleural space in the critically ill, pleural effusion and pneumothorax, is appealing due to the frequency with which these conditions occur, the proximity of the pleural space to the body surface, and the clear need for more effective imaging than extant portable chest radiography for diagnosis and procedural guidance. Application of ultrasound to these disorders also satisfies a basic tenet of point of care ultrasound that the bedside practitioner is interested in obtaining through ultrasound a rapid diagnosis of a specific condition to augment clinical knowledge and enhance medical decision making. The ease of serial bedside ultrasound examinations is also a unique strength of this technology. Application of ultrasound to pleural effusions in the intensive care unit (ICU) has become widespread and is often an entry point for the training of the novice critical care practitioner in point of care ultrasound. Sonography for pneumothorax is also becoming more widely accepted, though this application requires a relatively deeper understanding of thoracic anatomy and technical aspects of

Electronic supplementary material Supplementary material is available in the online version of this chapter at 10.1007/978-1-4939-1723-5_10. Videos can also be accessed at http://www.springerimages.com/videos/978-1-4939-1722-8.

S.K. Evans, M.D. (✉)
Division of Pulmonary, Critical Care and Sleep Medicine, Providence VA Medical Center, 830 Chalkstone Ave Building 35, Room 222, Providence, RI 02908, USA
e-mail: sevans2@lifespan.org

M. Jankowich, M.D.
Division of Pulmonary, Critical Care and Sleep Medicine, Alpert Medical School of Brown University, Providence VA Medical Center, 830 Chalkstone Ave., Office 158 L, Providence, RI 02908, USA
e-mail: matthew_jankowich@brown.edu

M. Jankowich, E. Gartman (eds.), *Ultrasound in the Intensive Care Unit*, Respiratory Medicine, DOI 10.1007/978-1-4939-1723-5_10

ultrasound, and has significant potential pitfalls if images are not acquired and interpreted appropriately. In this chapter, we will systematically examine the use of critical care ultrasound in the setting of pleural effusion and pneumothorax separately, recognizing the two conditions may coexist at times. Bedside ultrasound of pleural tumors or masses will not be discussed, as this application is not routinely needed by the critical care physician and is better served by comprehensive, nonurgent ultrasonography.

Ultrasound for Pleural Effusion

Introduction

Pleural effusions are caused by imbalances in hydrostatic and oncotic forces and/or alterations in permeability within the pleural space. They are common findings in critically ill patients and may portend a worse prognosis [1, 2]. Systemic diseases such as sepsis, hypoalbuminemia, and volume overload states frequently cause bilateral effusions. Local disease processes such as pneumonia, pulmonary infarct, trauma, and malignancy are also commonplace and tend to cause unilateral effusions. Timely diagnosis and management is particularly important in critically ill patients. Expansion of effusions can lead to atelectasis and resultant respiratory compromise, and pleural infection must be promptly addressed.

Conventional imaging modalities of portable chest radiography and computed tomography (CT) scan have limitations in the critically ill patient. The cost, exposure to ionizing radiation, and risk of transporting critically ill patients make routine CT scanning a suboptimal diagnostic test when pleural disease (including effusion) is suspected. Additionally, chest x-ray (CXR) has poor sensitivity in the diagnosis of pleural effusion [3–5]. Pleural fluid volumes of 100–200 cc have been traditionally cited as the minimum amount needed to cause blunting of the costophrenic angle on standard upright chest radiography [4]. However, imaging patients in the supine or semi-supine position can cause free-flowing pleural fluid to track up the posterior wall of the thoracic cavity and diminish the radiographic appearance of a fluid collection. This can lead to underestimation of the volume of an effusion. Additionally, portable radiography, with its lack of a lateral view, poorly discriminates loculated pleural effusion from pleural or parenchymal mass, atelectasis, or consolidation [6].

Stationary thoracic ultrasound (US) has been used since the 1960s for evaluation of pleural effusions [7]. Bedside US is a safe, inexpensive, portable, and highly accurate modality for rapid and longitudinal evaluation of pleural effusion in the critically ill patient. It can also help to evaluate other processes such as consolidation, interstitial disease, and atelectasis that may coexist with effusions [5, 8]. Methods have been described to quantify the volume of a pleural effusion, which may be particularly helpful in the management of effusions that warrant sampling

or tube thoracostomy [4–10]. Characteristics of the pleural fluid itself (e.g., simple fluid, presence of septations or cellularity) can also be assessed ultrasonographically [11–13]. Many effusions in the ICU warrant diagnostic or therapeutic intervention, and ultrasound can increase the yield and decrease the rate of complications associated with thoracentesis [3, 14–19].

Technical and Patient Considerations

The absence of air adjacent to the parietal pleura is necessary for effective visualization of the pleural space; any degree of pneumothorax will reflect sound waves and prevent imaging of deeper structures and fluid collections. The presence of chest wall or parietal pleural disease (scar, metastatic disease, calcification) may completely attenuate sound waves and complicate visualization of a deeper effusion [20].

Given the greater depth of imaging required, a low frequency probe (1–5 MHz) is needed for analysis of pleural effusions and imaging of relevant anatomic structures (e.g., diaphragm, liver, spleen, heart). A phased array cardiac probe (Fig. 10.1a) or a curvilinear probe (Fig. 10.1b) should be used since they are better suited than linear probes for directing sound waves through the narrow window of an intercostal space. As with other pleural US applications, by convention the probe indicator should be aimed cephalad and the marker on the left side of the US screen. Depth should be adjusted to see the relevant structures listed above and the distance measurements carefully noted prior to pleural fluid sampling.

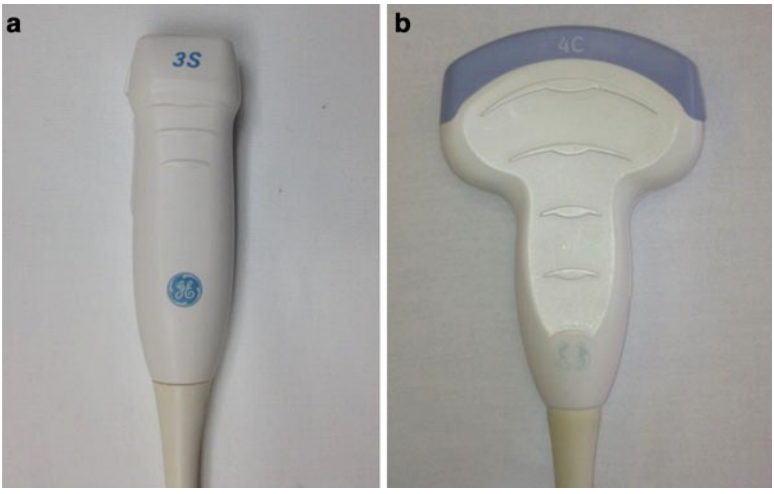

Fig. 10.1 Cardiac probe (**a**) and curvilinear probe (**b**). Both are low frequency probes (2–5 MHz) which allow for adequate visualization of pleural effusions and deeper thoracic structures

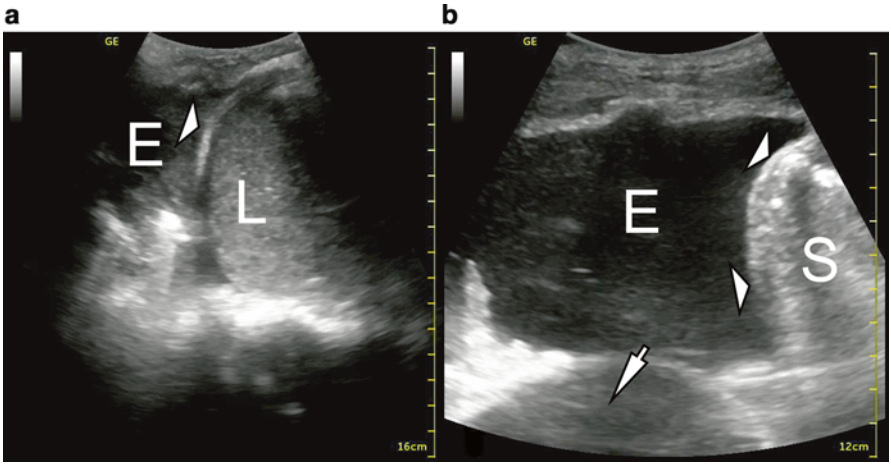

Fig. 10.2 B-mode image of pleural effusions. *L* liver, *S* spleen, *E* effusion. Standard gain for appropriate imaging of the liver (**a**) or spleen (**b**). Diaphragm (*white arrowheads*). In image **b**, a pericardial effusion can be seen (*white arrow*)

Unlike in the abdomen, there are no cystic structures in the chest to assist in optimizing gain on the US machine for visualizing fluid densities [6]. The liver and the spleen may instead serve as reference structures for determining the gain needed to image heterogeneous structures clearly (Fig. 10.2). At that level of gain, increasingly anechoic findings will more likely represent fluid. Under normal conditions, air-filled lung has high acoustic impedance that facilitates the distinction between subcutaneous tissue, pleura, and pulmonary parenchyma. A free-flowing pleural effusion (transudates, noncomplicated exudates) represents a homogeneous, anechoic media compared to surrounding structures. Tissue-specific acoustic profiles are frequently blurred in the presence of exudative effusions, particularly when the pleural space contains pus, cells (inflammatory or malignant), clot, or other relatively echoic materials.

Scanning of the most dependent regions of the thorax is usually indicated in order to evaluate an effusion. If a patient can be positioned upright, all areas of the chest may be scanned for effusions. A short-handled probe may be wedged between a supine or semi-recumbent, nonmobile patient and the bed in order to visualize posterior collections, though this technique may be uncomfortable for both the patient and the sonographer. Alternatively, patients may be situated in a lateral decubitus position to facilitate ultrasound evaluation, especially for moderate to large effusions. Patients with previously established pleural space infections may warrant a more comprehensive examination of less dependent regions to maximize the likelihood of locating clinically relevant and potentially drainable pleural fluid collections. As is the case with other point of care ultrasound applications, "ruling in" a pleural fluid collection with bedside ultrasound tends to be easier than comprehensively ruling out the presence of a pleural fluid collection, especially a loculated, nondependent one.

Patients on mechanical ventilation, particularly those on high levels of positive end expiratory pressure (PEEP), may be at higher risk of complications from thoracentesis. Particular care must be taken in this population to avoid iatrogenic pneumothorax. A minimum amount of pleural fluid for thoracentesis in mechanically ventilated patients is not known, but effusions 15 mm thick have been safely sampled using US [17]. An experienced proceduralist using US guidance should be required for pleural fluid sampling in patients on mechanical ventilation.

Image Acquisition and Interpretation

With the probe indicator pointing cephalad and the orientation marker on the upper left corner of the US display screen, superior structures will be oriented screen-left. The same superficial structures seen in pneumothorax evaluation (discussed below) should be seen in pleural effusion analysis, but due to the deeper field of view, they will often appear closer to the top of the screen (more superficially) and appear smaller in comparison. These include subcutaneous tissue, ribs and rib shadows, sliding lung (apposed parietal and visceral pleura), and B-lines.

A key anatomic landmark in the analysis of an effusion is the hemidiaphragm on the side of interest. When imaging the lower thoracic area, the diaphragm appears as a curved, band-like, smooth-bordered structure originating superficially and inferiorly and arching deep and superiorly (Fig. 10.3). Respirophasic motion of this structure, particularly in the spontaneously breathing patient, should aid in

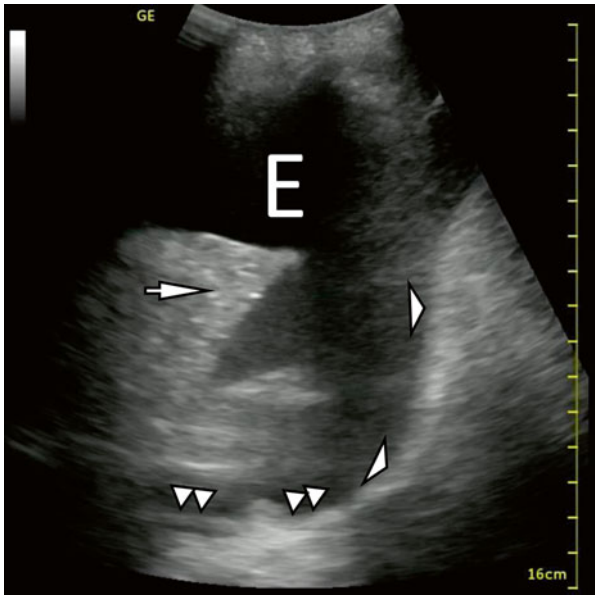

Fig. 10.3 B-mode imaging of diaphragm (*white arrowheads*), effusion (*E*), and atelectatic lung (*white arrow*). The V-line, a sonographic representation of the thoracic spine (*double white triangles*) is also demonstrated

differentiating the diaphragm from aerated lung. Identifying the diaphragm with confidence will help the proceduralist locate an appropriate site for thoracentesis or tube thoracostomy. As free fluid (e.g., ascites and cystic fluid collections) can also be located below the diaphragm, identifying anechoic fluid while scanning the lower thorax is insufficient to diagnose a pleural effusion. The hemi-diaphragm must first be identified to ensure that the apparent fluid identified is cephalad to the hemidiaphragm, thus preventing nondiagnostic or erroneous sub-diaphragmatic punctures with potentially serious complications.

On the left side, concurrent pericardial effusion can sometimes be seen (Fig. 10.2). When imaging the thorax from the mid-axillary line, Atkinson et al. [21] reported that the ultrasonographic signature of the thoracic spine – a densely echoic line extending cephalad from the deep portion of the diaphragm – is only visible when pleural fluid has displaced the normally interposed lung. They argue that visualization of the deep and posterior spine (termed V-line) is strongly supportive of the presence of pleural fluid (Fig. 10.3).

Heterogeneously echoic structures below the diaphragm are the spleen (left side) or the liver (right side). Ultrasonographic characteristics of pleural fluid can lend clues to the etiology of the fluid itself. Pleural fluid will generally appear anechoic, though the presence of cells, septations, clot, or air in the pleural space can cause a heterogeneous appearance (Figs. 10.4 and 10.5). Free-flowing fluid usually appears homogeneously anechoic. Complex fluid due to hemopneumothorax, parapneumonic, or malignant effusions can assume a range of ultrasonographic appearances. However, for reasons discussed below (see Evidence Review and Evidence-Based Use), use of the ultrasound appearance of pleural fluid alone to guide decision-making regarding whether diagnostic sampling or other procedures should occur should generally be avoided.

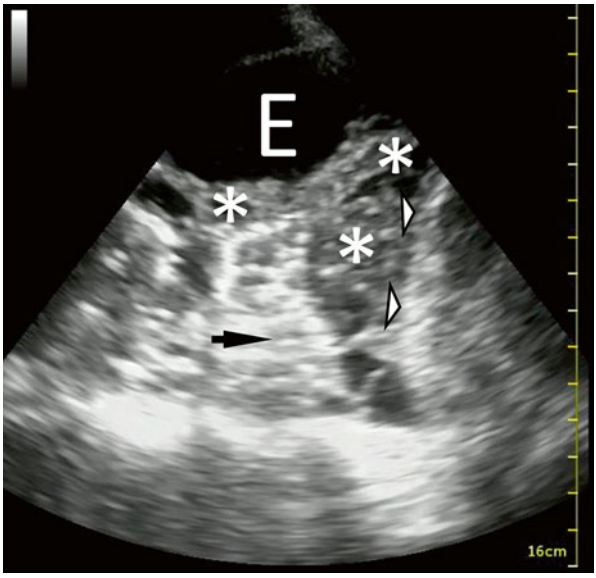

Fig. 10.4 B-mode image of a complex pleural effusion with visible loculations. *E* effusion. Diaphragm (*white arrowheads*), lung (*black arrow*), complex loculated effusion (*asterisks*)

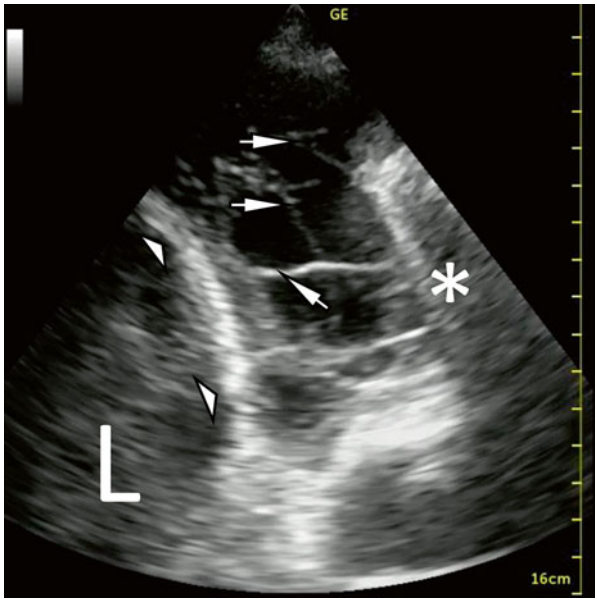

Fig. 10.5 B-mode picture of septated (complex) pleural effusion imaged with cardiac probe. Note that cephalad is to the *right* in this image. Diaphragm (*white arrowheads*), septations in the pleural space (*white arrows*). A single B-line (*white asterisk*) can also be seen projecting deep from the visceral pleura. *L* liver

Basic Competencies

The principle goals for point of care US in the evaluation of pleural effusion should be to identify the presence or absence of pleural fluid and to determine the feasibility of diagnostic or therapeutic thoracentesis. The initial ultrasonographic approach to the patient should consider patient positioning and identification of key anatomic landmarks. If a patient can sit up in bed and lean forward over a table, a detailed examination of the lower posterior thorax can be performed to more thoroughly assess dependent fluid collections.

The area from the mid-axillary line to approximately mid-scapular line should be systematically scanned with a curvilinear or cardiac probe, and the diaphragm should be clearly identified on the right side (inferior) of the screen. The probe should be applied firmly to the skin, with adequate interposed gel, and oriented perpendicularly to the skin at all times. Inspiration, either patient or ventilator-driven, can help to identify the diaphragm through its downward motion. Inferior to the diaphragm, the spleen or liver should be identified. We often mark with a sterile marker the level of the diaphragm, keeping in mind that diaphragm motion will change that level slightly during the respiratory cycle. Scanning above the level of the diaphragm can then be performed to identify relatively anechoic collections consistent with pleural effusion. Observation of atelectatic or consolidated lung in the far field is helpful in confirming the presence of interposed pleural fluid between the parietal and visceral pleura (Fig. 10.2). If pleural fluid is identified, the depth of

the effusion should be measured with the gradations on the screen. The approximate thickness of subcutaneous tissue should be noted and needle length adjusted accordingly if instrumentation is being considered. We then typically scan superiorly, identifying the vertical height of the effusion; the interface where the effusion diminishes in depth and eventually disappears, replaced by the bright reflection of air-filled lung, marks the superior edge of the effusion. This upper border of the effusion can also be marked with a sterile marker for reference.

Since images will only be obtained through intercostal windows, a skin mark may be made superficially just above the superior border of the lower rib of the appropriate intercostal space in order to guide subsequent thoracentesis or tube thoracostomy. The ribs should be palpated, and marking the course of the ribs above and below the procedural mark with a sterile marker can be helpful for orientation. We usually identify a relatively dependent site to maximize ability to extract pleural fluid while maintaining a margin of safety above the dome of the diaphragm. Keep in mind that the diaphragm level may rise during the course of pleural fluid drainage.

Pleural procedures should be carried out immediately following the ultrasound and site marking, and should be performed in the same patient position and directional orientation as the ultrasound (perpendicular to the skin surface). Excessively medial posterior (i.e., towards the spine) puncture sites for thoracentesis should be avoided due to the risk of puncture or laceration of the intercostal artery, which is more likely to be exposed below the rib in this region [22]. The site identified for thoracentesis should be above the diaphragm, in a relatively lateral position, and identified as having an adequate depth of fluid.

For chest tube placement, lateral positions in the "triangle of safety" should be considered, depending on patient circumstance and fluid location. The "triangle of safety" is denoted by the lateral border of the pectoralis major anteriorly, by the lateral border of the latissimus dorsi posteriorly, and by a line extended along the 5th intercostal space inferiorly (Fig. 10.6) [23]. The chosen area should be cleaned, then sterilely prepped and draped after ultrasound. We find that real-time ultrasound using a sterile probe cover is sometimes beneficial but is typically not necessary during most pleural procedures.

The volume of pleural fluid can be estimated with one of the several published techniques. Balik et al. [9] found the maximal distance between the diaphragm and the base of the lung at end-expiration correlates with the volume of effusion according to the following equation: volume of effusion (in mL) = 20 × distance of separation (in mm). Another group [24] found that end-expiratory intrapleural distances > 45 mm may reliably predict larger (around 800 mL) effusions. Remerand et al. [10] calculated pleural fluid volume by multiplying the area of the effusion (as measured in two ultrasonographic planes) in supine patients with free-flowing effusions at the midpoint between caudal and apical limits of the effusion. No one method has been exhaustively validated, but the method by Balik is frequently cited in the literature [4, 9–11].

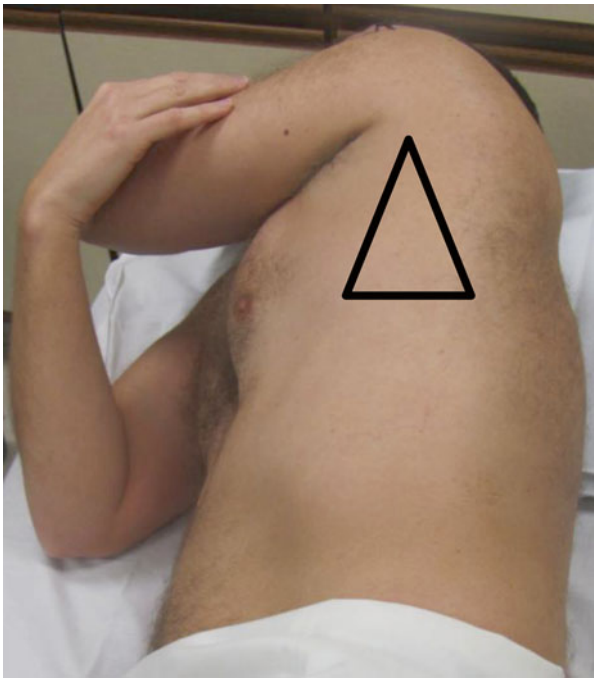

Fig. 10.6 The "triangle of safety" is the recommended location for safe performance of tube thoracostomy. The *triangle* is demarcated anteriorly by the lateral border of pectoralis major, posteriorly by the lateral border of latisimus dorsi, and inferiorly by the 5th intercostal space

Advanced Competencies

Different disease processes of the pleura and pleural space may be elucidated sonographically based on varying acoustic profiles [20, 25]. Four patterns have been described to categorize the effusion in a manner that suggests a specific disease process. Anechoic fluid is homogeneously dark and is most consistent with transudative fluid. Complex nonseptated fluid contains more cellular debris, fibrin, blood, and is more likely to be exudative. Complex septated fluid may have organized locules, septations, and pleural adhesions, and is consistent with exudative fluid that likely requires tube thoracostomy [26]. Homogeneously echogenic fluid is generally consistent with empyema. Establishing appropriate gain settings is crucial to the correct interpretation of complex pleural fluid images, since overgain may cause relatively anechoic fluid to appear more echogenic.

Color Doppler has been reported as a means to distinguish small effusions from pleural thickening [27]. In patients suspected of having effusion based on radiography, Doppler analysis can be performed in addition to standard B-mode imaging. When B-mode images suggest the presence of effusion, a positive Doppler signal suggests the presence of fluid (dynamic) rather than pleural thickening (static). M-mode identification of the pleural fluid sinusoid sign can also be helpful in distinguishing small effusions from pleural thickening [28]. As most

point-of-care pleural ultrasound in the intensive care unit is done to determine an optimal site for thoracentesis or tube thoracostomy, making a fine distinction based on ultrasound between a very small pleural effusion that is unlikely to be clinically significant and pleural thickening is not likely to be excessively important in the critical care setting.

Evidence Review and Evidence-based Use

A growing body of evidence supports the use of US in routine evaluation and management of pleural effusions in the critically ill. As a diagnostic tool, US outperforms conventional chest radiography. Diacon et al. [3] prospectively compared clinical exam and CXR to US for identifying a site of at least 10 mm of fluid for thoracentesis in 255 cases for possible instrumentation. US increased the number of accurate sites detected by 26 % and prevented possible organ puncture in 15 % of clinically and radiographically determined sites. Kocijancic et al. [25] determined that US had a positive predictive value of 92 % for detecting small effusions. In the surgical intensive care unit, a focused thoracic US examination demonstrated 83.6 % sensitivity, 100 % specificity, and 93.6 % accuracy for detecting pleural effusion [29].

In another study of pleural effusion in ICU patients the sensitivity of handheld US and standard radiography was 91 % and 74 %, respectively (not statistically significant). Specificity was 100 % for US versus 73 % for CXR ($p = .008$). The authors attribute three cases of US false negative to the inability to diagnose a small effusion (<50 mL) in patients with higher body mass indices (BMIs) [30]. Additionally, the ability of US to differentiate effusion from consolidation was demonstrated in a study of 97 ICU patients with findings suggestive of effusion on CXR. Effusion was better predicted by US ($R^2 = 0.74$, ROC 0.99) compared to CXR ($R^2 = 0.51$, ROC 0.70). The lack of lateral chest radiography in the ICU may weaken the ability of CXR to reliably identify pleural effusion [24].

Quantitation of pleural fluid volume by US has been well studied. Rothlin et al. [31] used portable handheld US in trauma patients to quickly rule in the presence of pleural fluid, which in that setting helped to diagnose traumatic hemothorax. More specific techniques to ascertain the precise volume of pleural fluid have been described by Balik et al. (discussed above) and Vignon et al. [24]. The latter group found that end-expiratory intrapleural distances of > 45 mm on the right and > 50 mm on the left predicted effusions > 800 mL with sensitivity of 94 % and 100 % and specificity of 76 % and 67 %, respectively, for each hemithorax. Their model was less robust for larger effusions. Roch et al. [32] conducted a prospective study of 42 ICU patients on mechanical ventilation who had effusion identified on CXR and in whom drainage was considered. An ultrasound-measured distance of 5 cm between the posterior chest wall and the lung base correlated with > 500 mL effusions with sensitivity 83 %, specificity 90 %, positive predictive value (PPV) 91 %, and negative predictive value (NPV) 82 %.

US has been shown to be a useful but imperfect diagnostic adjunct to clinical exam and standard radiography in the assessment of pleural fluid characteristics prior to thoracentesis. In a study of 118 thoracenteses in febrile medical ICU patients with effusions, 43 % of collections characterized as either complex septated, homogeneously echogenic, or complex nonseptated and relatively hyperechoic turned out to be empyema on initial or follow-up thoracentesis [12]. Ultrasonographic pleural fluid characteristics must be considered in the overall clinical context, however. Hirsch et al. evaluated 50 patients (24 % in the ICU) and, in 46 aspirations, 16 were complex septated, of which one was a transudate. Anechoic effusions were mixed (6 transudates, 5 exudates, 1 hematoma) [33]. Chen et al. [11] reviewed the US findings of 149 Light's criteria-confirmed transudates and demonstrated that greater than half had a complex nonseptated appearance. Kearney et al. [13] found that US can better identify septations than CT scan, but that US characteristics did not reliably predict the nature of fluid in empyema. The authors found that some stage I exudates (pH > 7.2, lactate dehydrogenase [LDH] < 1,000 IU/l, glucose > 2.2 mmol/l, no organisms) contained septations and that some anechoic collections turned out to be frank pus when aspirated. These studies have considerable variation in the US protocol used, timing of imaging, and sampling. Further study is needed before US can be used as an effective prognostic tool for pleural effusion in ICU patients.

There is strong evidence that US increases the safety and yield of thoracentesis. Safety has been addressed in small retrospective studies of patients on antiplatelet medications (Abouzgheib 2012, $n = 24$; Dammert 2013, $n = 43$) who underwent US-guided pigtail catheter placement and suffered no complications [15, 18]. A larger study of 450 thoracenteses (67.8 % performed with US, 32.2 % performed without) revealed a significantly higher pneumothorax and tube thoracostomy rate of 4.1 % in the non-US group compared to 0.7 % in the US-guided group [17]. Lichtenstein et al. [16] prospectively studied 40 mechanically ventilated patients with effusions at least 15 mm and found no complications (pneumothorax or hemoptysis) in 45 procedures. However, in a prospective, randomized study, Kohan et al. [34] found no difference in the rate of complications in 205 patients who underwent thoracentesis with or without chest ultrasound. Most current studies of thoracentesis or tube thoracostomy involve US guidance in their protocols, reflecting that routine use of ultrasonography in this setting is effectively the standard of care.

The sensitivity and specificity of US operated by newly trained providers is variable, however. After an 8.5 h multimodality training session in US-naïve ICU residents, Chalumeau-Lemoine et al. demonstrated in 23 patients with confirmed pleural effusions a sensitivity of 58.3 % and specificity of 70 % [35]. This suggests the need for adequate and protocolized training in the use of point-of-care US. A questionnaire-based study of pulmonary and critical care fellowship directors identified significant interest in nonvascular applications of US (including evaluation of pleural effusion). Insufficient faculty expertise, lack of knowledge of the data supporting its use, and financial considerations were cited as barriers to more widespread use of US in critical care medicine fellowships [36]. There is also evidence that bedside US may facilitate care of patients with pleural effusion in nonindustrialized countries [37].

Pitfalls and Precautions

- User proficiency in both pleural ultrasound and associated pleural procedures must be optimized for effective and safe performance. Guidelines for minimal competencies in pleural ultrasound have not been published, but regular training and use of this technology under the instruction of experienced operators is vital.
- Technical proficiency with the US machine will help to avoid errors in depth and gain selection as well as probe orientation. Overgain will mischaracterize pleural fluid as more complex than it really is. Undergain can lead to poor visualization of the lung and overestimation of the size of an effusion.
- An assessment of the integrity of the subcutaneous tissue across which the US waves must project is important. Subcutaneous air will rapidly attenuate sound waves and impair visualization of deeper structures, which can lead to false-negative examinations [31].
- Always start a pleural ultrasound exam by identifying the hemidiaphragm to avoid subdiaphragmatic punctures. Marking the levels of both the diaphragm and the superior extent of the effusion, as well as careful marking of the chosen site for a procedure, can aid in orientation following sterile draping of the patient.
- Noting the depth of the subcutaneous tissues and the relative depth of the pleural fluid pocket on ultrasound can help increase operator confidence and allow for appropriate anesthesia infiltration prior to procedures.
- Carry out pleural procedures in the same positioning and orientation as the ultrasound. Avoid excessive time delay between ultrasound and pleural procedure, and rescan if delays or patient movement do occur.
- Certain pleural diseases may mimic effusion. Lymphomas and neurogenic neoplasms transmit US with the production of few or little echoes [20].
- The stage at which an effusion is imaged is an important consideration. In empyema, for example, fluid at the early exudative stage will appear different than during the late organizing phase [12]. Care must always be taken to interpret US findings in the context of the clinical situation and the established natural history of various pleural effusions [13].
- Serial US exams are readily performed and may help to better characterize the evolution of disease processes within the pleural space.
- Avoid overreliance on pleural fluid US characteristics to guide decision-making about sampling and drainage – simple-appearing effusions may be exudative in nature, and transudative effusions may appear complex in the setting of preexisting pleural or parenchymal lung disease.
- Some pleural fluid may simply abut the lung and not be walled off in a discrete locule. The relatively higher attenuation of lung tissue relative to fluid could lead to misinterpretation of the fluid-lung interface as a septation [6].

Ultrasound for Pneumothorax

Introduction

In the critically ill patient, pneumothorax (PTX) is associated with high morbidity and mortality and can be readily treated. Despite an incidence of only 3–6 %, mortality ranges from 22 % to 68 % [38–40], hence timely diagnosis and management are essential. Under the best of circumstances, diagnosing pneumothorax can be difficult. The ICU setting imposes additional challenges including comorbid hemodynamic instability, patient positioning limitations, inaccessibility of advanced imaging modalities due to patient transport safety concerns, staffing limitations, and others [40].

Historically, the gold standard for diagnosing pneumothorax has been non-contrast enhanced computed tomography (CT). However, the cost, exposure to ionizing radiation, and safety of ICU patient transport make routine CT scanning a suboptimal diagnostic test when PTX is suspected. Chest radiography, usually performed in the supine or semi-recumbent position, has been shown to lack diagnostic accuracy [41–45].

Bedside thoracic ultrasound (US) has been increasingly reported in the literature as a safe, inexpensive, portable, and highly accurate modality for rapid evaluation of PTX in the critically ill patient. First described in the veterinary literature for the assessment of horses with suspected thoracic disease [7], thoracic US has been subjected to increasingly rigorous study in the setting of PTX in humans since the 1980s. Expansion of provider awareness and skill in obtaining and correctly interpreting US images has created a powerful new tool for the ICU provider. Additionally, portable US machines have become commonplace for use in vascular access, hence many ICUs are already equipped with the necessary technology for US evaluation of PTX.

Pneumothorax in the ICU is generally due to iatrogenic causes (mechanical ventilation, post-procedure) or secondary to a range of conditions, including blunt or penetrating trauma, or rupture of preexisting bullous disease [46]. Air enters the pleural space and occupies the least dependent location in the thorax, most commonly anteromedial and subpulmonic recesses based on retrospective studies of PTX in supine and semi-recumbent ICU patients [41]. Still, a significant number of pneumothoraces are missed by portable chest radiography. Particularly in the setting of mechanical ventilation, many progress to exhibit tension physiology, a high mortality yet generally treatable condition if addressed early [40, 41].

Technical and Patient Considerations

Of overarching importance is the fact that ultrasound waves do not penetrate air, thus air in the pleural space will create a characteristic ultrasound image based on the differing acoustic impedance characteristics of aerated or nonaerated tissue. This aspect of pleural ultrasound will be revisited in greater detail in the subsequent discussion of normal and abnormal findings that are key to accurate diagnosis of PTX.

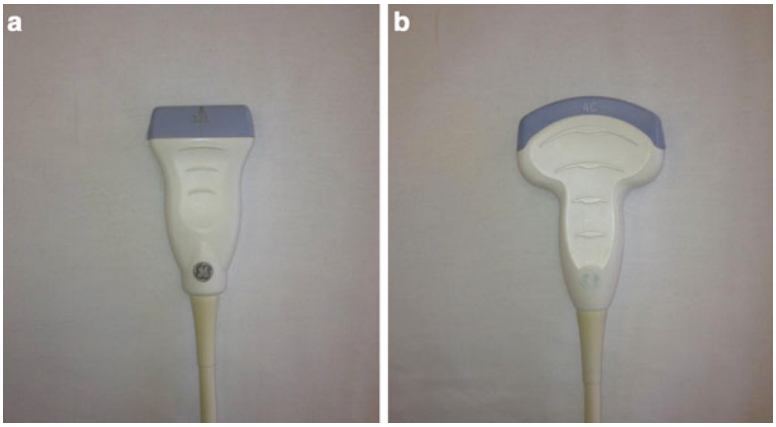

Fig. 10.7 Standard US probes for evaluation for pneumothorax. High frequency linear probe (5–13 MHz) (**a**), 2.5–5 MHz curvilinear probe (**b**). The higher frequency enables greater resolution of pleural and other superficial structures and may be preferred

The thoracic ribcage enables only small windows for sonographic visualization of the pleural space. Probe selection must account for this window as well as for the depth of structures of interest. Convex/curved or linear array transducers in the 5–9 MHz range are frequently used for pleural analysis (Fig. 10.7). Freestanding portable US units are most commonly reported in the literature. Handheld units are being increasingly studied in the trauma setting [47].

The supine or semi-recumbent position of most ICU patients dictates that pleural air commonly settles in an anteromedial location [41, 48]. Therefore, attention to this area is important when searching for PTX. Preexisting pleural abnormalities such as scarring, adhesions, or plaques may alter the expected anatomic distribution of PTX. A systematic approach to thoracic US has not been firmly established in the literature, however, Lichtenstein et al. [42, 49] outline a method that evaluates the most likely locations in which to identify PTX.

As shown in Fig. 10.8, the anterior and posterior axillary lines divide the thorax into roughly three areas: anteromedial (area 1), lateral (area 2), and posterolateral (area 3). The paraspinal and apical regions have been termed “area 4” and are involved in more comprehensive US examinations of the chest than are routinely performed in clinical practice. The examiner should begin in the second intercostal space in area 1, with the probe marker oriented cephalad (Fig. 10.9). Appropriate anatomic and pleural landmarks (soft tissue, ribs, rib shadows, and pleura – Fig. 10.10) should be identified in this area. If these findings are not seen, the probe should be moved inferiorly until an adequate window is achieved. Scanning of areas 2 and 3 may be performed based on the clinical suspicion for PTX. Imaging of areas 3 and 4 in the supine patient requires the patient to be placed in the lateral decubitus position and/or the use of a short probe to access the chest between patient and hospital bed.

Fig. 10.8 The three zones of the chest recommended for routine evaluation of pneumothorax. Area 1 is on the anterior chest and is demarcated medially by the sternum and laterally by the anterior axillary line. Area 2 covers the lateral chest and is demarcated medially by the anterior axillary line and postero-laterally by the posterior axillary line. Area 3 covers the posterior chest and is defined laterally by the posterior axillary line and medially by the mid-scapular line

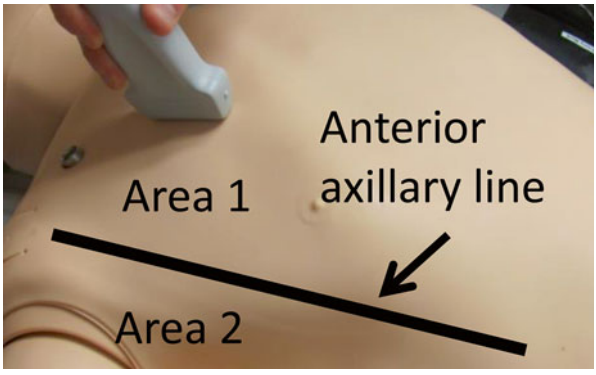

Fig. 10.9 A linear probe oriented cephalad on the upper anteromedial chest, with areas 1 and 2 demarcated by the anterior axillary line. In the supine or semi-recumbent patient, area 1 should be scanned carefully for lung sliding and B-lines, as air in the pleural space will typically settle in the least dependent region of the chest

Image Acquisition and Interpretation

Accurate evaluation of PTX requires detailed understanding of the normal and abnormal findings of thoracic and pleural ultrasound. Conceptualization of the relevant anatomy is best achieved by progressing stepwise from the most superficial to the deeper structures. In the normal state, soft tissue and superficial musculature is first seen on the top of the screen (Fig. 10.10). This zone contains the ribs, which cast widening columns of shadow distally due to periosteal reflection of sound

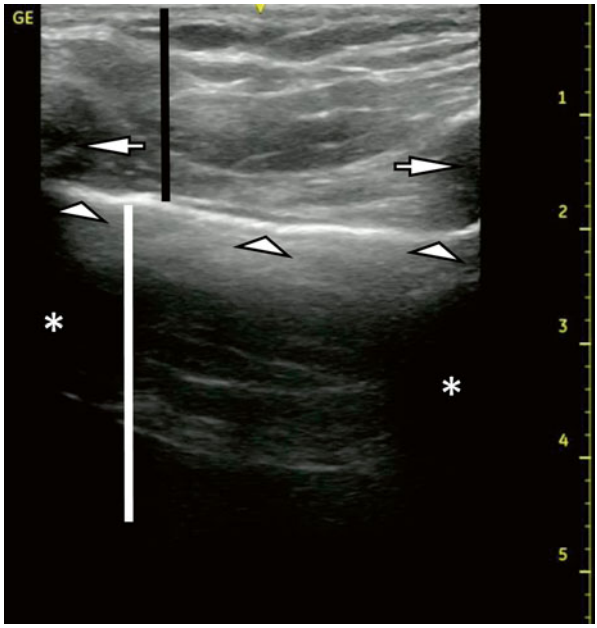

Fig. 10.10 B-mode image of normal pleura acquired with linear probe. Centimeters indicated at *right*. Subcutaneous tissue (*dark bar*), pleural interface (*white arrowheads*), lung (*white bar*), ribs (*white arrows*), and rib shadows (*white asterisks*)

waves. Subcutaneous emphysema and foreign bodies (e.g., shotgun pellets) in the chest wall can significantly affect image acquisition and complicate the interpretation of pleural findings; care must be taken in such circumstances [50].

The visceral and pleural surfaces appear as a hyperechoic line running parallel to the body surface, between adjacent rib shadows, just distal to the zone of soft tissue (Fig. 10.10). A respirophasic motion of these apposed pleural surfaces, visualized sonographically as a horizontal shimmering, is a key finding called "lung sliding," which is universally present in the absence of PTX (Video 10.1 – sliding lung). Physiologically, lung sliding is due to the differential echoprofiles of the static parietal pleura and the dynamic visceral pleura during spontaneous respiration or mechanical ventilation. Entry of air into the pleural space creates a barrier to sound wave transmission, and as a result, lung sliding disappears in the presence of PTX. Doppler mode can be used to enhance US sensitivity to detect subtle differences in motion of the two pleural surfaces.

B-mode assessment of lung sliding can be confirmed in M-mode (motion mode). The static subcutaneous tissues and the moving lung create different sonographic signals that are easily interpreted: the former as a zone of tight horizontal parallel lines, the latter as a zone of homogeneous granular densities (Fig. 10.11). This pattern has been dubbed the "seashore sign" – the parallel lines resemble waves, and the aerated lung the shore. An intact pleural interface allows this sign to be seen in the absence of PTX. This sign is lost when air has entered the pleural space and the image assumes an appearance resembling a "barcode" (see Basic Competencies below).

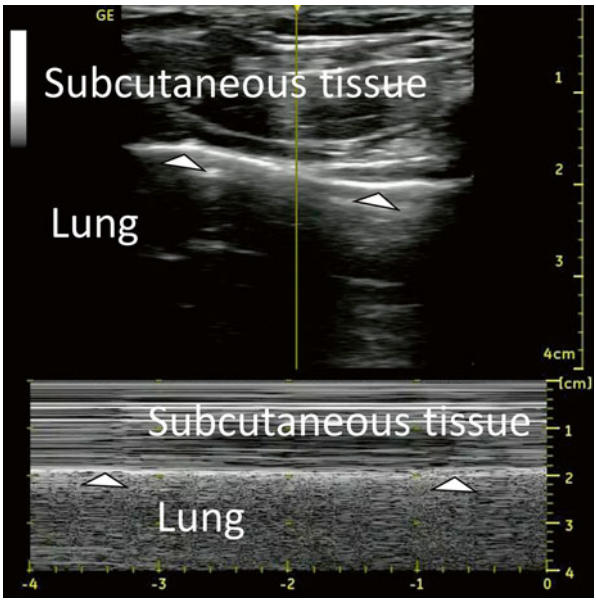

Fig. 10.11 Simultaneous B-mode (*upper panel*) and M-mode (*lower panel*) images of normal pleura obtained with a linear probe. The M-mode image (seashore sign) is obtained in the plane selected by the indicator in the center of the B-mode image. In the M-mode image, the boundary between subcutaneous tissue (horizontal lines – waves) and lung (granular – seashore) is the white horizontal line representing an intact pleural interface (*white arrowheads*). The seashore sign has a high negative predictive value for ruling out PTX

Two ultrasonographic artifacts are important in the interpretation of images obtained during an evaluation for PTX. A-lines are roughly parallel, horizontal hyperechoic-appearing lines that appear in the lung at intervals equal to multiples of the distance between the probe and the parietal pleura. They result from reverberation of sound waves from the pleural interface and an artifactual projection of similarly shaped echodensities in the far (lung) field. These reverberation artifacts can be found in the presence or absence of PTX (Fig. 10.12).

B-lines are sharp vertical projections of echodensity projecting distally from the pleural line, which usually reach the bottom of the screen. Though sometimes visible at the bases of normal lungs (due to greater perfusion), they are usually evidence of subpleural interstitial disease that may or may not be clinically related to the scenario prompting investigation for PTX. Based on a linear and outwardly spreading pattern (Fig. 10.13), the terms "lung rockets" and "comet-tail artifact" have been used to describe any collection of vertically oriented artifacts (including but not limited to B-lines) projecting from the pleura. B-lines can only be seen when the parietal-visceral pleural interface is intact. As a result, B-lines disappear in PTX [50, 51]. The comet-tail artifact, lung rockets, and B-lines are functionally synonymous in the evaluation of PTX, as all require an intact pleural interface to be visualized.

It is important to note that the absence of lung sliding and B-lines/comet-tail artifact is suggestive, but not diagnostic of PTX. Other conditions in which the motion of the adjacent pleural surfaces is compromised can lead to the disappearance of these findings. Right main stem bronchus intubations, severe hyperinflation as in chronic obstructive pulmonary disease (COPD) or asthma, and pleural scarring

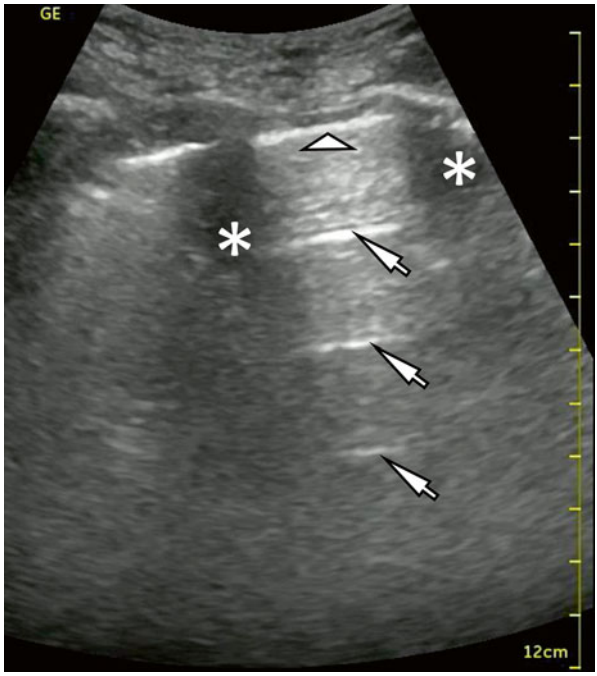

Fig. 10.12 B-mode image of pleural surface acquired with curvilinear probe. Rib shadows (*white asterisks*). A-lines (*white arrows*) are horizontal artifacts caused by sound wave reverberation between the US probe and parietal pleura (pleura marked by *white arrowheads*). Since A-lines are reverberation artifacts generated by a structure superficial to the pleural space, they may be seen in the absence or presence of PTX

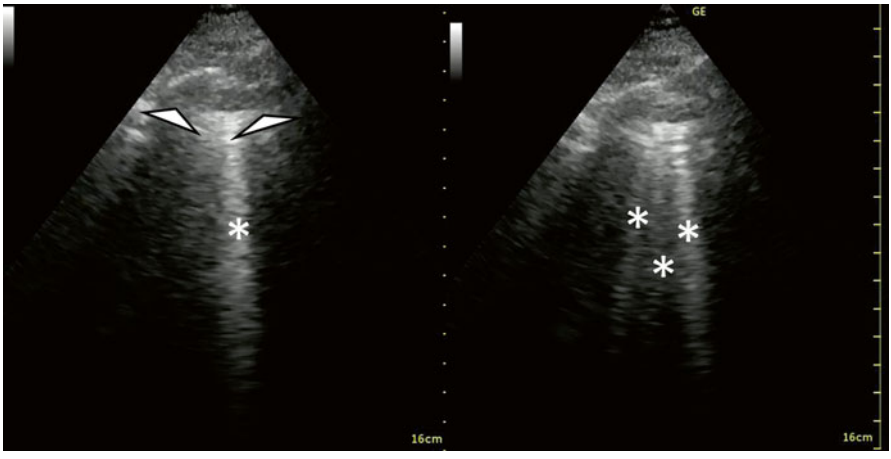

Fig. 10.13 B-mode image acquired with phased array cardiac probe. (**a**) *White asterisk* denotes a B-line, a vertical artifact caused by subpleural interstitial disease, which projects from the pleura (*white arrowheads*) to the *bottom* of the screen. (**b**) *White asterisks* indicate a collection of B-lines which together are termed "lung rockets" or the "comet-tail artifact." The presence of the comet-tail artifact essentially rules out pneumothorax

can mimic PTX ultrasonographically. In the setting of lung collapse, such as in a main stem intubation, the ultrasonographic "lung pulse" may be seen in the collapsed lung. The "lung pulse" describes pulsatile pleural movement, seen in B- or M-mode, caused by the transmission of cardiac activity through completely atelectatic lung [52].

Other ultrasonographic artifacts have been described and may help to minimize confusion about the artifacts most salient to the evaluation of PTX. Lichtenstein et al. discuss Z-lines, which, in contradistinction to B-lines, are ill-defined, vanish 2–5 cm into the field, do not abolish A-lines, and are independent of lung sliding. They are found in normal and in abnormal lungs. E-lines describe a heterogeneous array of vertical artifacts of differing depths that arise *superficial* to the pleural line. E-lines are seen in the setting of subcutaneous or parietal emphysema (E for emphysema), which will frequently abolish the normal anatomy (rib shadows, clear pleural window) needed to evaluate PTX. Assessing for PTX in the presence of E-lines is therefore not feasible [42].

A full pleural US examination has been reported to take different amounts of time depending on the experience of the user and the positioning of the patient. In the most experienced hands a comprehensive bedside US study may take as little as 3–5 min [42, 53]. When performed by ICU residents newly trained in pleural US, a full examination was reported to take 35+/−34 min [44]. Learning effective bedside critical care US of the pleura involves an initial learning curve which, once surpassed, leads to rapid, accurate, and repeatable evaluations. Even in more experienced hands, care must be taken to ensure that key anatomic areas suggested by the patient's clinical scenario are studied rigorously and that all relevant ultrasonographic findings are found.

Basic Competencies

The ultrasonographic approach to the patient with possible PTX should first consider the patient's position in the hospital bed. Since air will rise to the least dependent area of the thorax, attention should be paid to the more superior regions in the upright or semi-upright patient. In the supine patient consideration of the lower chest is also warranted. Sufficient ultrasound gel should be used to ensure efficient transmission of sound waves into the body. The correct probe frequency (5–10 MHz usually allows adequate resolution of pleural structures) and shape (a convex probe may help to focus the beam in the intercostal space) should be selected. As in the analysis of pleural effusions, the probe is oriented with the indicator pointed cephalad and placed on the anteromedial chest wall, in or near the second intercostal space. A clear window between adjacent ribs should be obtained.

Lung sliding should be determined to be present or absent. If lung sliding is not identified (Video 10.2), suspicion of PTX should increase, and there should be prompt consideration of alternate causes of absent lung sliding [54]. For example, if sliding only is absent on the left side of a recently intubated patient, a right main

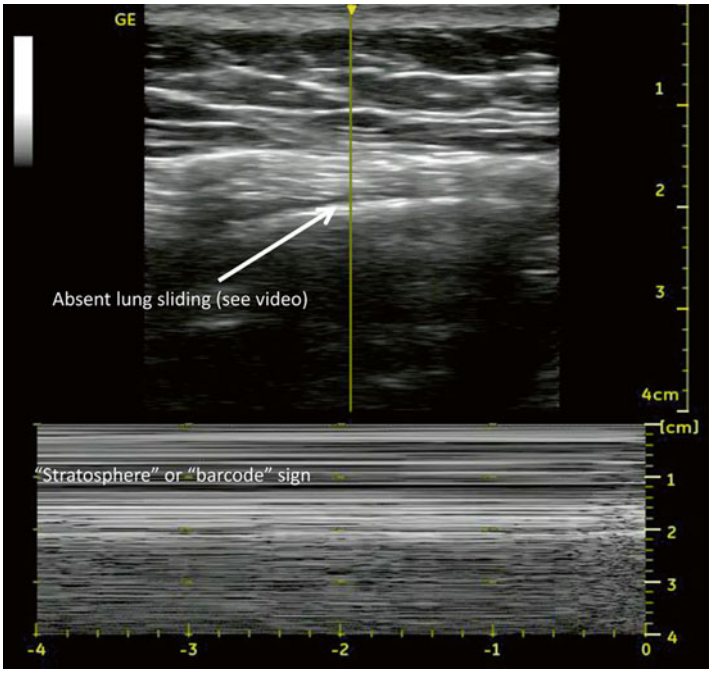

Fig. 10.14 B-mode (*above*) and M-mode (*below*) of patient with CT-confirmed pneumothorax. The M-mode image is termed the "stratosphere sign" or "barcode sign" and indicates pneumothorax

stem intubation should be ruled out (See Image Acquisition and Interpretation). Doppler function may also be used to better assess differential motions of the pleural surfaces (helping to rule out PTX), but this technique has not been studied as thoroughly as simple lung sliding and presence or absence of B-lines.

M-mode should next be employed to correlate the pleural findings seen on B-mode. In a single sagittal plane, the "seashore sign" should be identified. In the presence of a PTX, the proximal parallel lines (the waves in the seashore) should be seen uninterrupted throughout the depth of the image (Fig. 10.14). This has been dubbed the "stratosphere sign" or "barcode sign." This pattern can be repeated in areas 2 and 3 depending on the patient's known pleural history (i.e., presence of mesothelioma, adhesions, or pleural plaques) and the clinical suspicion of PTX.

A-lines and B-lines should next be identified. A-lines may be seen in normal or diseased states, and should be differentiated from pleura, but otherwise may be largely ignored in the evaluation for PTX. B-lines ("lung rockets" or "comet-tail artifact"), however, are a key finding which, when present, effectively rule out PTX [50].

Advanced Competencies

Identifying lung sliding and B-lines is necessary and sufficient for the bedside ultrasonographic evaluation of PTX in the critically ill patient. However, additional techniques have been reported to better characterize PTX. The "lung point" is a sign that delineates the boundary between PTX and normal lung. The location of the transition from normally apposed pleura to PTX moves with respiratory motion. Visualization of the lung point requires an assessment of both lung sliding and the B-line artifact. In one image, sliding lung and B-lines (PTX absent) and nonsliding lung and absent B-lines (PTX present) are seen. This sign can be identified in either B-mode or M-mode (Video 10.3; see also Fig. 14.29 in Chap. 14). The lung point sign is highly specific for PTX [55].

Lung point can also be employed to evaluate the extent of a PTX [55, 56]. A small anteromedial PTX will likely be seen with US in the second intercostal space in area 1 (see above). Identifying the lung point can give a graphic representation of the underlying lung and pleural pathology. Lung that has collapsed more extensively might demonstrate a lung point sign farther down the lateral and posterior reaches of the chest wall. This information might be useful for assessing the clinical relevance of a PTX and may prompt more urgent intervention (e.g., tube thoracostomy) [42, 55–57]. The size of a PTX has been estimated using the location at which lung sliding disappears (i.e., a more posterior location indicates a larger PTX). Good agreement has been demonstrated between the location of absent lung sliding and size of PTX [45].

Routine US examinations (as opposed to examinations driven by a specific clinical question) are performed in some institutions. Another potential adaptation of bedside US in the ICU is the serial examination in certain patients at risk of developing or known to have PTX. This might include patients with severe acute respiratory distress syndrome (ARDS), poor lung compliance and high airway pressures, and severe bullous disease at risk of rupture [46]. Serial US examinations for PTX have not been reported, but the portability and feasibility of bedside US make it an appealing approach to monitoring for the development of a deadly yet treatable condition.

Evidence Review and Evidence-Based Use

Bedside thoracic US in the evaluation of PTX has been well studied since the technique first appeared in the literature in the mid-1980s [58]. Research on the accuracy of this imaging modality has been carried out predominantly in two overlapping but distinct critically ill patient populations: ICU patients and Emergency Department trauma cases. Overall, US outperforms CXR in the diagnosis of PTX, though CT scan remains the gold standard for determining the presence and extent of PTX.

Early small studies have shown that lung sliding, B-lines, and the lung point are the most robust diagnostic signs for PTX [43, 50, 54, 55]. In a comparison of US (5 MHz) findings in patients with occult pneumothoraces (missed by CXR but diagnosed on CT scan), lung sliding alone has a sensitivity of 100 %, specificity 78 %, NPV 100 %, and PPV 40 %. For ruling in PTX, the presence of A-lines and the complete absence of B-lines, (termed the A-line sign) when combined with lung sliding, had a sensitivity of 95 %, specificity 94 %, NPV 99 %, and PPV 71 % [42]. The lung point alone is a uniquely specific marker for PTX: while less sensitive (79 %, NPV 97 %), specificity and PPV were 100 %. Interestingly, the authors note that the location of the lung point correlated with the need for chest tube placement. As a proxy for the volume of PTX, the more lateral the location of the lung point, the greater the volume of air in the pleural space and the higher likelihood of chest tube placement: 90 % of patients (n = 10) with a lateral lung point received a tube thoracostomy compared to 8 % (n = 24) with an anterior lung point [42, 55].

Xirouchaki et al. [57] compared lung US with bedside CXR in ICU patients, with CT scan as the gold standard. In a prospective study of 42 mechanically ventilated patients, the authors used US (5–9 MHz) to evaluate lung consolidation, effusion, PTX, and interstitial disease. Using the A-line sign (horizontal reverberation artifacts without B-lines), stratosphere sign (M-mode finding of uninterrupted horizontal lines), and lung point to diagnose PTX, US showed sensitivity of 75 %, specificity 93 %, and diagnostic accuracy of 92 %. CXR was 0 % sensitive, 99 % specific, and 89 % accurate. The two missed PTXs in the US group were small and apical, highlighting the need to consider this region in the examination. There were five false-positive US exams, attributed to subcutaneous emphysema in three and severe COPD/hyperinflation in two. This highlights the need for caution and clinical synthesis of ultrasound findings to avoid hastily pursuing tube thoracostomy based on a false-positive test.

A systematic review and meta-analysis of eight studies including 1,048 patients, mostly trauma victims (73 %), compared US findings to CXR. Using lung sliding and comet-tail artifacts, they found the overall sensitivity for US was 90.9 % (95 % confidence interval [CI]: 86.5–93.9 %), specificity 98.2 % (95 % CI: 97.0–99.0 %), PPV 94.4 %, and NPV 97.0 %. CXR performed poorly in comparison, with sensitivity 50.2 % (95 % CI: 43.5–57.0 %), specificity 99.4 % (95 % CI: 98.3–99.8 %), PPV 96.5 %, and NPV 85.6 %. Their findings differed minimally when limited to analysis of the trauma subgroup. These results highlight the inability of CXR to reliably detect PTX [43] and the need to consider alternative diagnostic modalities.

In the emergency department (ED) population, US outperforms CXR and offers considerable practical advantages compared to CT scan. However, the ED setting poses additional challenges. Kirkpatrick et al. prospectively evaluated a handheld US system (5–10 MHz) for identifying traumatic PTXs in 208 patients. Comparison was made to CT, which was not always performed, CXR, or aspiration of air on tube thoracostomy. They assessed lung sliding (including Doppler) imaging and B-lines. Interestingly, the overall performance for US in this population was less

robust than in the ICU, with sensitivity of 59 %, specificity 99 %, PPV 92 %, NPV 94 %, accuracy 94 %, likelihood ratio (LR) of positive test 69.7, and LR of negative test 0.41. They reported false-positive results in three cases of US-diagnosed PTX: one was due to initially inapparent subcutaneous air and two in right main stem intubations. The authors attribute their lower NPV compared to previous studies to the difficulty in trauma scenarios of differentiating a normal from an abnormal lung. Whereas bilateral pneumothoraces are less common in the ICU population, where the uninvolved hemithorax can serve as an individual patient's negative control, comparison of a diseased to a healthy lung was not always available in this population [47].

Bedside thoracic US has been studied in the post-procedural setting. Since many patients in the ICU require invasive interventions (e.g., central line placement, thoracentesis), better understanding of US performance after instrumentation may be useful. In a prospective study of 285 patients who underwent US-guided biopsy of peripheral lung lesions, Sartori et al. [59] observed PTX in 2.8 % of patients. Sensitivity, specificity, PPV, NPV, and overall accuracy were 100 % for US (5–7.5 MHz), and 87.5, 100, 100, 99.6, and 99.6, respectively, for CXR. The authors also performed serial assessments to determine worsening or resolution of the initial PTX. Given the high morbidity and mortality in patients with iatrogenic PTX, these results may suggest a role in the longitudinal management of patients at risk of or with known PTX [60].

A prospective observational study compared CXR and US to evaluate for residual PTX after evacuation of pneumothorax (70.5 % primary spontaneous, 15.9 % trauma, 13.6 % emphysema and iatrogenic) in ICU patients. In the primary spontaneous group US had a PPV of 100 %. In the other groups the overall PPV was 90 % and improved to 100 % with the utilization of the lung point sign. CXR missed 39 % of pneumothoraces that were identified by US. Interestingly, US examinations were performed by both an experienced user and newly trained ICU residents. A two-hour training was given, and the overall K value was .78 for agreement between the primary investigator and the residents. This suggests that bedside US for evaluation of PTX can be learned quickly and effectively [44].

Pitfalls and Precautions

- As in the setting of ultrasound imaging of pleural effusion, user proficiency must be optimized. In the studies reviewed herein, operators included ED physicians, ICU physicians, and radiologists. Specific guidelines for minimal competencies have not been published, though several professional societies have issued consensus statements advocating the training and routine use of US in the ICU [61–63].
- Simple breath holding can abolish lung sliding, as can ARDS, extensive pneumonia, or severe hyperinflation due to COPD [42].

- In the ED, chaotic trauma scenarios and handheld US machines may introduce opportunities for device or user error [47]. There may be difficulty interpreting contralateral lung findings in the setting of bilateral pneumothoraces, and chest wall trauma, subcutaneous air, or foreign bodies in the chest wall or parietal pleura may complicate image acquisition or interpretation.
- In the ICU, caution must be used in patients with preexisting pleural disease, such as adhesions, plaques, and loculated pneumothoraces, or in patients with severe parenchymal or airways disease including ARDS and severe emphysema [64]. The absence of lung sliding or B-lines in these situations must prompt careful thought about potential coexisting diseases before invasive treatments are undertaken.
- Assessment of the left lung pulse may be useful if right main stem intubation is suspected and lung sliding is absent on the left.
- Patients with preexisting pleural disease may warrant more detailed US evaluation of the chest wall. Searching for the lung point sign and examining the lateral and posterior reaches of the chest should be considered in these patients.

Conclusions

Pleural effusion and pneumothorax are common problems in critically ill patients. Bedside US performs better than clinical exam or standard radiography for the diagnosis and quantitation of pleural effusion, and it allows accurate site marking for subsequent thoracentesis and tube thoracostomy when indicated. Ability to use US for thoracentesis guidance is "strongly recommended" by the American Board of Internal Medicine guidelines for trainees in Critical Care Medicine [63]. British Thoracic Society guidelines published in 2010 make a grade B recommendation for the routine use of US in indwelling chest catheter placement [65]. Training of intensivists in the use of bedside US in critically ill patients will be helpful in optimizing the safe management of pleural effusions in the ICU.

Bedside ultrasound for evaluation of PTX is increasingly being used for rapid and accurate diagnosis of a high mortality condition that is readily treatable. Since its inception in the mid-1980s in the veterinary literature, US has been studied and validated in several critically ill patient populations. Traditional means of diagnosing PTX lack sensitivity (CXR) and feasibility (CT scan) compared to US. The portability, low cost, reproducibility, and lack of ionizing radiation make US a more appealing modality for assessing PTX. The primary US artifacts needed to assess for PTX are lung sliding and B-lines, which are easily recognized with a reasonable amount of practice. In summary, while caution must be used in certain clinical scenarios, bedside US is on aggregate a powerful tool for the point-of-care evaluation of two major categories of pleural disease in the ICU setting.

References

1. Fartoukh M, et al. Clinically documented pleural effusions in medical ICU patients: how useful is routine thoracentesis? Chest. 2002;121(1):178–84.
2. Mattison LE, et al. Pleural effusions in the medical ICU: prevalence, causes, and clinical implications. Chest. 1997;111(4):1018–23.
3. Diacon AH, Brutsche MH, Soler M. Accuracy of pleural puncture sites: a prospective comparison of clinical examination with ultrasound. Chest. 2003;123(2):436–41.
4. Eibenberger KL, et al. Quantification of pleural effusions: sonography versus radiography. Radiology. 1994;191(3):681–4.
5. Lichtenstein D, et al. Comparative diagnostic performances of auscultation, chest radiography, and lung ultrasonography in acute respiratory distress syndrome. Anesthesiology. 2004;100(1): 9–15.
6. Rosenberg ER. Ultrasound in the assessment of pleural densities. Chest. 1983;84(3):283–5.
7. Joyner Jr CR, et al. Reflected ultrasound in the study of diseases of the chest. Trans Am Clin Climatol Assoc. 1967;78:28–37.
8. Rocco M, et al. Diagnostic accuracy of bedside ultrasonography in the ICU: feasibility of detecting pulmonary effusion and lung contusion in patients on respiratory support after severe blunt thoracic trauma. Acta Anaesthesiol Scand. 2008;52(6):776–84.
9. Balik M, et al. Ultrasound estimation of volume of pleural fluid in mechanically ventilated patients. Intensive Care Med. 2006;32(2):318–21.
10. Remerand F, et al. Multiplane ultrasound approach to quantify pleural effusion at the bedside. Intensive Care Med. 2010;36(4):656–64.
11. Chen HJ, et al. Sonographic appearances in transudative pleural effusions: not always an anechoic pattern. Ultrasound Med Biol. 2008;34(3):362–9.
12. Tu CY, et al. Pleural effusions in febrile medical ICU patients: chest ultrasound study. Chest. 2004;126(4):1274–80.
13. Kearney SE, et al. Computed tomography and ultrasound in parapneumonic effusions and empyema. Clin Radiol. 2000;55(7):542–7.
14. Gryminski J, Krakowka P, Lypacewicz G. The diagnosis of pleural effusion by ultrasonic and radiologic techniques. Chest. 1976;70(1):33–7.
15. Abouzgheib W, et al. Is chest tube insertion with ultrasound guidance safe in patients using clopidogrel? Respirology. 2012;17(8):1222–4.
16. Lichtenstein D, et al. Feasibility and safety of ultrasound-aided thoracentesis in mechanically ventilated patients. Intensive Care Med. 1999;25(9):955–8.
17. Barnes TW, et al. Sonographically guided thoracentesis and rate of pneumothorax. J Clin Ultrasound. 2005;33(9):442–6.
18. Dammert P, Pratter M, Boujaoude Z. Safety of ultrasound-guided small-bore chest tube insertion in patients on clopidogrel. J Bronchol Interv Pulmonol. 2013;20(1):16–20.
19. Sandweiss DA, et al. Ultrasound in diagnosis, localization, and treatment of loculated pleural empyema. Ann Intern Med. 1975;82(1):50–3.
20. McLoud TC, Flower CD. Imaging the pleura: sonography, CT, and MR imaging. AJR Am J Roentgenol. 1991;156(6):1145–53.
21. Atkinson P, et al. The V-line: a sonographic aid for the confirmation of pleural fluid. Crit Ultrasound J. 2012;4(1):19.
22. Salamonsen M, et al. Thoracic ultrasound demonstrates variable location of the intercostal artery. Respiration. 2012;83(4):323–9.
23. Mahmood K, Wahidi MM. Straightening out chest tubes: what size, what type, and when. Clin Chest Med. 2013;34(1):63–71.
24. Vignon P, et al. Quantitative assessment of pleural effusion in critically ill patients by means of ultrasonography. Crit Care Med. 2005;33(8):1757–63.
25. Kocijancic I, Vidmar K, Ivanovi-Herceg Z. Chest sonography versus lateral decubitus radiography in the diagnosis of small pleural effusions. J Clin Ultrasound. 2003;31(2):69–74.

26. Yang PC, et al. Value of sonography in determining the nature of pleural effusion: analysis of 320 cases. AJR Am J Roentgenol. 1992;159(1):29–33.
27. Wu RG, et al. Image comparison of real-time gray-scale ultrasound and color Doppler ultrasound for use in diagnosis of minimal pleural effusion. Am J Respir Crit Care Med. 1994;150(2): 510–4.
28. Lichtenstein D. Pleural effusion and introduction to the lung ultrasound technique. In: Lichtenstein D, editor. General ultrasound in the critically ill. Springer: Berlin; 2005. p. 96–100.
29. Rozycki GS, Pennington SD, Feliciano DV. Surgeon-performed ultrasound in the critical care setting: its use as an extension of the physical examination to detect pleural effusion. J Trauma. 2001;50(4):636–42.
30. Schleder S, et al. Bedside diagnosis of pleural effusion with a latest generation hand-carried ultrasound device in intensive care patients. Acta Radiol. 2012;53(5):556–60.
31. Rothlin MA, et al. Ultrasound in blunt abdominal and thoracic trauma. J Trauma. 1993;34(4): 488–95.
32. Roch A, et al. Usefulness of ultrasonography in predicting pleural effusions > 500 mL in patients receiving mechanical ventilation. Chest. 2005;127(1):224–32.
33. Hirsch JH, Rogers JV, Mack LA. Real-time sonography of pleural opacities. AJR Am J Roentgenol. 1981;136(2):297–301.
34. Kohan JM, et al. Value of chest ultrasonography versus decubitus roentgenography for thoracentesis. Am Rev Respir Dis. 1986;133(6):1124–6.
35. Chalumeau-Lemoine L, et al. Results of short-term training of naive physicians in focused general ultrasonography in an intensive-care unit. Intensive Care Med. 2009;35(10):1767–71.
36. Eisen LA, et al. Barriers to ultrasound training in critical care medicine fellowships: a survey of program directors. Crit Care Med. 2010;38(10):1978–83.
37. Shah S, et al. Development of an ultrasound training curriculum in a limited resource international setting: successes and challenges of ultrasound training in rural Rwanda. Int J Emerg Med. 2008;1(3):193–6.
38. de Lassence A, et al. Pneumothorax in the intensive care unit: incidence, risk factors, and outcome. Anesthesiology. 2006;104(1):5–13.
39. Chen KY, et al. Pneumothorax in the ICU: patient outcomes and prognostic factors. Chest. 2002;122(2):678–83.
40. Kollef MH. Risk factors for the misdiagnosis of pneumothorax in the intensive care unit. Crit Care Med. 1991;19(7):906–10.
41. Tocino IM, Miller MH, Fairfax WR. Distribution of pneumothorax in the supine and semirecumbent critically ill adult. AJR Am J Roentgenol. 1985;144(5):901–5.
42. Lichtenstein DA, et al. Ultrasound diagnosis of occult pneumothorax. Crit Care Med. 2005;33(6):1231–8.
43. Alrajhi K, Woo MY, Vaillancourt C. Test characteristics of ultrasonography for the detection of pneumothorax: a systematic review and meta-analysis. Chest. 2012;141(3):703–8.
44. Galbois A, et al. Pleural ultrasound compared with chest radiographic detection of pneumothorax resolution after drainage. Chest. 2010;138(3):648–55.
45. Blaivas M, Lyon M, Duggal S. A prospective comparison of supine chest radiography and bedside ultrasound for the diagnosis of traumatic pneumothorax. Acad Emerg Med. 2005; 12(9):844–9.
46. Weg JG, et al. The relation of pneumothorax and other air leaks to mortality in the acute respiratory distress syndrome. N Engl J Med. 1998;338(6):341–6.
47. Kirkpatrick AW, et al. Hand-held thoracic sonography for detecting post-traumatic pneumothoraces: the Extended Focused Assessment with Sonography for Trauma (EFAST). J Trauma. 2004;57(2):288–95.
48. Kiley S, et al. Retrospective computed tomography mapping of intrapleural air may demonstrate optimal window for ultrasound diagnosis of pneumothorax. J Intensive Care Med. 2013. PubMed ID is 23753251.
49. Lichtenstein DA, et al. Ultrasound diagnosis of alveolar consolidation in the critically ill. Intensive Care Med. 2004;30(2):276–81.

50. Lichtenstein D, et al. The comet-tail artifact: an ultrasound sign ruling out pneumothorax. Intensive Care Med. 1999;25(4):383–8.
51. Husain LF, et al. Sonographic diagnosis of pneumothorax. J Emerg Trauma Shock. 2012; 5(1):76–81.
52. Lichtenstein DA, et al. The "lung pulse": an early ultrasound sign of complete atelectasis. Intensive Care Med. 2003;29(12):2187–92.
53. Dulchavsky SA, et al. Prospective evaluation of thoracic ultrasound in the detection of pneumothorax. J Trauma. 2001;50(2):201–5.
54. Lichtenstein DA, Menu Y. A bedside ultrasound sign ruling out pneumothorax in the critically ill. Lung sliding. Chest. 1995;108(5):1345–8.
55. Lichtenstein D, et al. The "lung point": an ultrasound sign specific to pneumothorax. Intensive Care Med. 2000;26(10):1434–40.
56. Targhetta R, et al. Ultrasonic signs of pneumothorax: preliminary work. J Clin Ultrasound. 1993;21(4):245–50.
57. Xirouchaki N, et al. Lung ultrasound in critically ill patients: comparison with bedside chest radiography. Intensive Care Med. 2011;37(9):1488–93.
58. Wernecke K, et al. Pneumothorax: evaluation by ultrasound–preliminary results. J Thorac Imaging. 1987;2(2):76–8.
59. Sartori S, et al. Accuracy of transthoracic sonography in detection of pneumothorax after sonographically guided lung biopsy: prospective comparison with chest radiography. AJR Am J Roentgenol. 2007;188(1):37–41.
60. Despars JA, Sassoon CS, Light RW. Significance of iatrogenic pneumothoraces. Chest. 1994;105(4):1147–50.
61. Expert Round Table on Ultrasound in, I.C.U. International expert statement on training standards for critical care ultrasonography. Intensive Care Med. 2011;37(7):1077–83.
62. The Royal College of Radiologists. Ultrasound training recommendations for medical and surgical specialties. 2nd ed. London: The Royal College of Radiologists; 2012.
63. American Board of Internal Medicine. American Board of Internal Medicine, training policy for critical care medicine. Philadelphia: American Board of Internal Medicine; 2013. Available from: http://www.abim.org/pdf/publications/Policies-and-Procedures-Certification.pdf. Accessed 29 August 2014.
64. Murphy M, Nagdev A, Sisson C. Lack of lung sliding on ultrasound does not always indicate a pneumothorax. Resuscitation. 2008;77(2):270.
65. Havelock T, et al. Pleural procedures and thoracic ultrasound: British thoracic society pleural disease guideline 2010. Thorax. 2010;65 Suppl 2:ii61–76.

Chapter 11
Diaphragm Ultrasound in the Intensive Care Unit

F. Dennis McCool and Taro Minami

Introduction

Knowledge of diaphragm function is crucial when caring for patients with respiratory failure and determining the optimal time to discontinue mechanical ventilation. However, unlike most skeletal muscles, the diaphragm is relatively inaccessible to direct study. Diaphragm strength can be determined by measuring transdiaphragmatic pressure, but this requires the positioning of gastric and esophageal catheters. By contrast, diaphragm ultrasound utilizes a technology which is noninvasive and can provide information regarding diaphragm position, mass, and motion; all parameters which reflect diaphragm function. Ultrasound can be readily used at the bedside, requires minimal to no patient effort, and delivers no ionizing radiation. This technology is available in most intensive care units and physicians are quickly gaining familiarity with its use for line placement, evaluating volume status, and for other utilities such as those discussed in this textbook [1]. This chapter reviews the principles of ultrasonography in reference to the diaphragm and the practicalities of using ultrasound to evaluate diaphragm function in the intensive care unit.

F.D. McCool
Division of Pulmonary, Critical Care and Sleep Medicine, Memorial Hospital of Rhode Island, 111 Brewster Street, Pawtucket, RI 02860, USA
e-mail: F_McCool@Brown.edu

T. Minami, M.D., FACP, FCCP (✉)
Division of Pulmonary, Critical Care and Sleep Medicine, Memorial Hospital of Rhode Island, 111 Brewster Street, Pawtucket, RI 02860, USA
e-mail: taro_minami@brown.edu

M. Jankowich, E. Gartman (eds.), *Ultrasound in the Intensive Care Unit*, Respiratory Medicine, DOI 10.1007/978-1-4939-1723-5_11

Technical and Patient Considerations

The ultrasound transducer is comprised of a transmitter and receiver. It transmits high frequency (typically 3.5–15 MHz) bursts of sound through the body surface to underlying structures [2]. As the sound waves penetrate into the body, they encounter tissue boundaries with different impedances. When there is an abrupt change in acoustic impedance, sound is partially reflected back to the receiver. Acoustic impedance is determined by tissue mass, density, and elastance. These properties differ sufficiently between muscle, serous membranes, fat, and fluids such that partial reflections occur at boundaries between these tissues. The ultrasound receiver analyzes the returning echo for its time delay and for the direction from which it comes. The time delay and direction, respectively, indicate the depth and direction of the reflected boundaries. This data is used to construct an image which can be displayed using two different methods. With the Brightness (B)-mode technique, the sound path is swept through an arc, by an electronically controlled linear array of transmitter/receivers. With this mode, the information is displayed as a two-dimensional image with the brightness of the image representing the intensity of the reflected signal. With the Motion (M)-mode technique, the depths of reflecting boundaries along a selected sound path are recorded as a one-dimensional tracing against time (Fig. 11.1). Studies of diaphragm function in the critically ill have been performed using both M- and B-modes with high- and low-frequency transducers.

Differences in acoustic impedance between tissue interfaces can be exploited in the zone of apposition (ZAP) of the diaphragm to the rib cage to visualize the diaphragm and its adjacent structures. As the sound wave penetrates into body tissues, differences in acoustic impedance at boundaries between the parietal pleura, diaphragm, peritoneum, and liver are used to identify these structures. Muscles, such as the intercostals and diaphragm, will scatter sound and appear as a speckled image at higher ultrasound frequencies. A collection of homogenous fluid, such as a simple pleural effusion, has no internal boundaries and, therefore, no changes in acoustic impedance. Therefore, it is not echogenic, and appears featureless (black on B-mode). By contrast, air is so echogenic that the sound wave is nearly completely reflected back to the transducer and does not penetrate into deeper structures. Such differences in acoustic impedance have been used to distinguish the diaphragm from its adjacent structures such as the pleura and peritoneum (Fig. 11.2). Because the lung contains air, structures lying deep to it do not appear on the image. When imaging the diaphragm, the unique acoustic-reflective characteristics of the lung can be used to identify the location of the lower border of the air-containing lung. As the lung inflates, its lower border moves caudally and can be used to identify the pleural boundary of the diaphragm. The pleural boundary appears as a thin, echogenic structure inferior to the lung border and deep to the chest wall, which is then masked by the lung as it descends during inspiration. The peritoneal boundary of the diaphragm can be recognized as a second, somewhat thicker, echogenic boundary deep to and separated from the pleura by the diaphragm itself, which appears in between these two membranes as a less echogenic, speckled structure (Fig. 11.2).

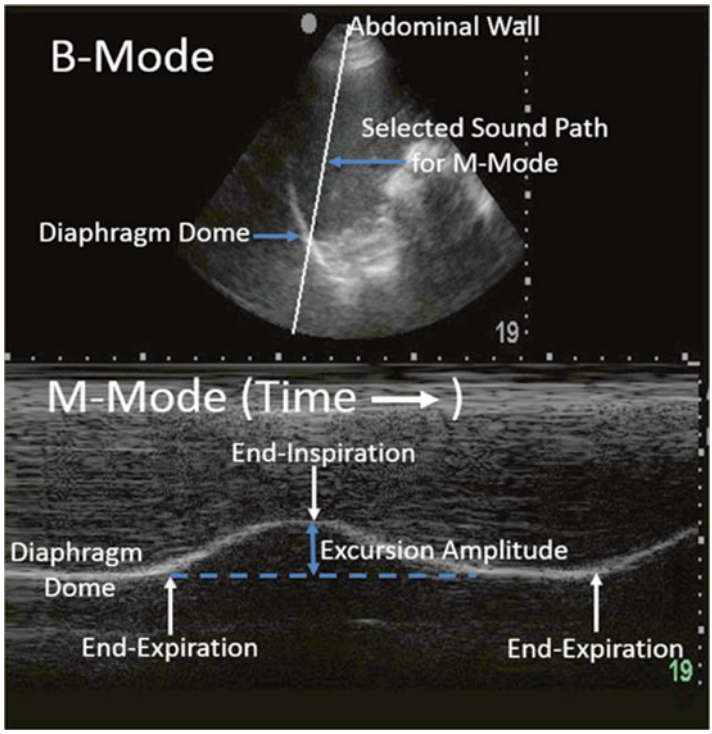

Fig. 11.1 B-Mode and M-Mode images of the diaphragm dome. With B-Mode, a 2-dimensional image is constructed. With M-Mode, a single sound path is used to follow changes in diaphragm dome position over time

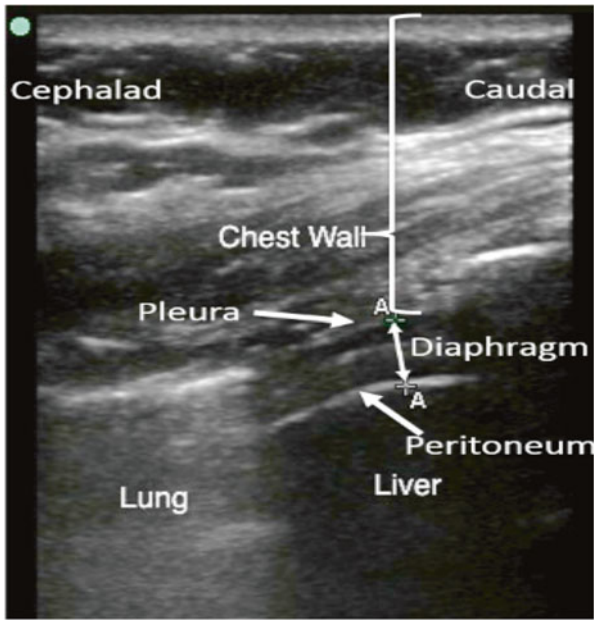

Fig. 11.2 Image of the diaphragm in the zone of apposition demonstrating chest wall, diaphragm, liver, and lung

Image Acquisition and Interpretation

Diaphragm Zone of Apposition

The ZAP of the diaphragm refers to the area where the diaphragm abuts the lower rib cage (Fig. 11.3). In this region the diaphragm is a relatively superficial structure. Since structures close to the body surface can be imaged with high frequencies, a transducer in the range of 5–15 MHz is typically used to image the diaphragm in the ZAP and has a resolution of 0.1 to 0.2 mm. This higher frequency-range transducer provides an image of greater resolution than lower frequency transducers. Once obtained, the image can be displayed in either the M-mode or B-mode (Fig. 11.4). The advantage of using the B-mode is the ability to visualize the diaphragm in two dimensions rather than as a point in time.

To visualize the diaphragm in the ZAP, the transducer is placed on the skin surface in the coronal plane [3, 4] (Fig. 11.3). The diaphragm in the ZAP is best visualized in the mid-axillary line in the region of the lower rib cage, usually in the 8th or 9th intercostal space. Typically the B-Mode is used to create a two-dimensional coronal image of the ZAP. The diaphragm is identified as a three-layered structure just superficial to the liver, comprised of two parallel echogenic lines (peritoneal and diaphragmatic pleura) sandwiching a relatively non-echogenic layer, the diaphragm muscle itself (Fig. 11.5). On occasion, a 4th noncontinuous line may be seen within the diaphragm muscular layer which may represent a neural or vascular structure. The diaphragm can be further identified dynamically as the most superficial structure which is obliterated by the leading edge of the lung during inspiration. On occasion, the transducer may have to be moved cephalad to the 6th or 7th intercostal space to identify the leading edge of the lung, especially when the diaphragm is elevated. However, obliteration of the diaphragm by the leading edge of lung may not be present when the diaphragm is paralyzed or during mechanical ventilation.

Once the diaphragm is identified, the image is frozen at end-expiration and the thickness of the diaphragm (tdi) measured as the distance from the middle of the diaphragmatic pleura to the middle of the peritoneum to the nearest 0.1 mm.

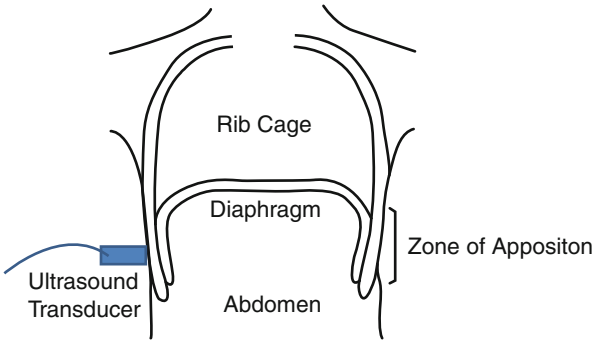

Fig. 11.3 Schematic illustrating ultrasound transducer placement for visualizing the diaphragm in the zone of apposition

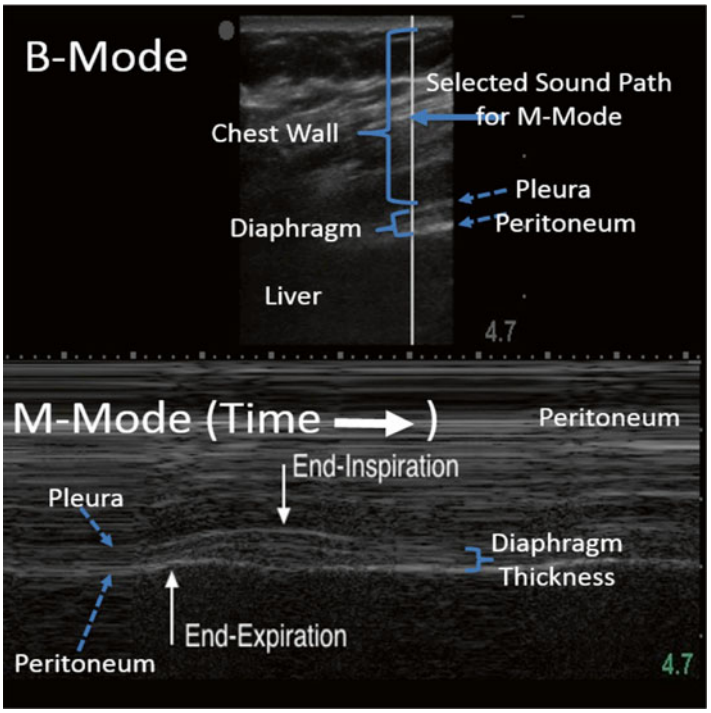

Fig. 11.4 B-Mode and M-Mode of the diaphragm in the zone of apposition. With B-Mode, the diaphragm muscle is visualized as the minimally echogenic structure "sandwiched" between the pleura and peritoneum. Similar information can be displayed using M-Mode

A subsequent image is obtained at end-inspiration, and tdi is measured at this lung volume (Fig. 11.6). The change in diaphragm thickness between end-inspiration and end-expiration (Δtdi) is then calculated along with a thickening fraction (Δtdi% = Δtdi/tdi end-expiration × 100). The thickening fraction can be measured over a range of inspired volumes and tends to be alinear with more thickening at higher lung volumes [4]. The change in diaphragm thickness during inspiration can be measured either using B-mode or M-mode, with subjects in the standing, seated, supine, or prone positions. Normal values for diaphragm thickness at end-expiration generally fall between 2.0 and 3.5 mm. Normal values for diaphragm thickening with inspiration (Δtdi%) fall between 20 % and 100 %. Because the inherent thickness of the diaphragm in this region varies only slightly from place to place, thickening of the diaphragm in the ZAP is representative of general thickening of the diaphragm muscle and not movement of an adjacent relatively thicker part of the diaphragm under the transducer [4].

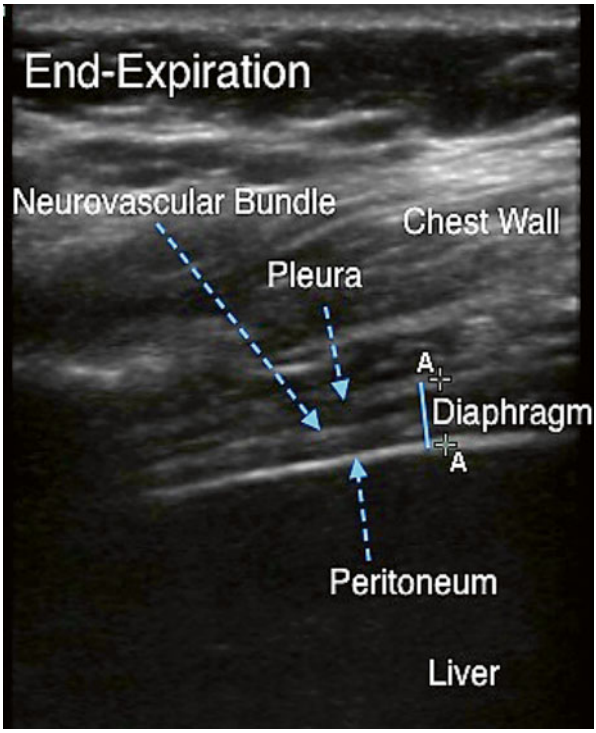

Fig. 11.5 Diaphragm at end-expiration in the zone of apposition. The diaphragm on ultrasound appears as a relatively hypoechoic structure sandwiched between the bright echogenic lines of pleura and peritoneum. The echogenic line contained within the diaphragm is the neurovascular bundle. *Solid blue line* indicates diaphragm thickness. The calipers adjacent to the *solid blue line* can be used to measure diaphragm thickness on a frozen image

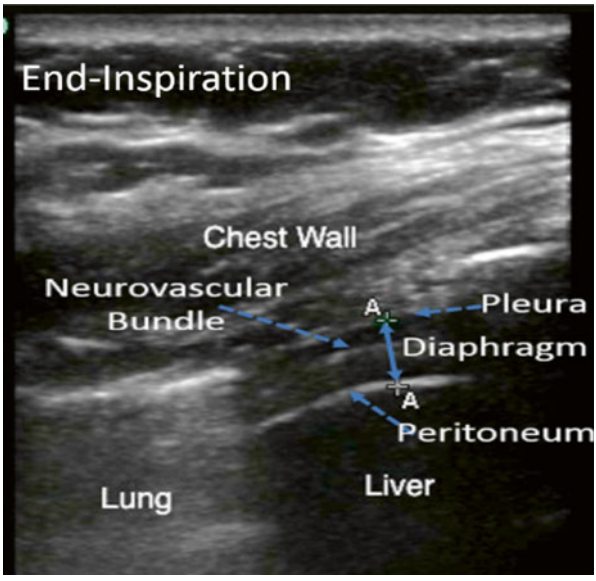

Fig. 11.6 Diaphragm at end-inspiration. The *double-arrowed line* indicates diaphragm thickness. Note the relative thickening of the muscle compared with Fig. 11.5. Note the bright echogenic curtain to the *left* of the screen indicating air-filled lung that has descended caudally with inspiration

Diaphragm Dome

A subcostal approach is typically used to visualize the diaphragm dome (Fig. 11.7). The distance from the anterior abdominal wall to the posterior diaphragm is much greater than the distance from the skin surface to the diaphragm in the ZAP. Because sound penetrates further at lower frequencies, the dome of the diaphragm typically is visualized using a 3.5–5 MHz transducer. The longer wavelength of sound in this frequency range allows for deeper penetration of the ultrasound beam, but the resolution of the lower frequency transducer is reduced to approximately 0.3 to 0.6 mm. When using a subcostal approach to visualize the dome, the liver provides a good acoustic window allowing one to assess movement of the right hemidiaphragm. Unfortunately, air in the gastrointestinal tract may interfere with visualization of the left hemidiaphragm when using a subcostal approach. This can be circumvented, in part, by using the spleen as an acoustic window. Motion of the diaphragm dome towards the transducer during inspiration is generally assessed using the M-mode but also can be viewed using B-mode [5–8].

Note that when imaging the dome, the diaphragm muscle itself is not visualized. As previously discussed, air is strongly echogenic. Since the lung reflects all sound transmitted towards it, the image of the diaphragm dome is comprised of the intensely reflected sound at the interface of the diaphragm and lung and not the diaphragm muscle itself. The motion of the diaphragm can be inferred from movement of the lung–diaphragm interface but the thickness of diaphragm muscle cannot be measured. When using this approach, the diaphragm muscle can only be seen when there is a pleural effusion between the dome and the lung.

Motion of the diaphragm dome is not uniform from region to region. Normally, there is greater displacement in the middle and posterior regions than in the anterior region in supine subjects during large inspirations [9]. Similar findings have been described in children [10]. These differences in regional motion in the supine position have been attributed to the larger abdominal pressure that acts on the posterior diaphragm, which passively displaces the posterior diaphragm higher into the

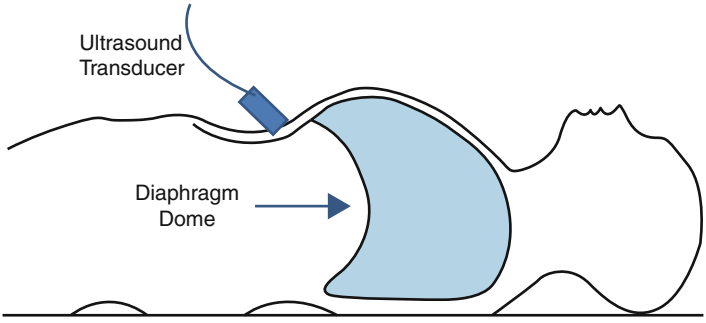

Fig. 11.7 Schematic illustrating ultrasound transducer placement for visualizing the diaphragm dome using a subcostal approach

thoracic cavity at end-expiration than the anterior hemidiaphragm. Consequently the posterior portion of the diaphragm has to descend further during inspiration to move towards its relatively flattened configuration at full inspiration.

To visualize the diaphragm dome, a low frequency ultrasound transducer (3.5–5 MHz) is placed on the right or left side in the subcostal region well below the lower border of the lung and angled upward [11, 12]. The right or left mid-clavicular lines or the right or left anterior axillary lines can be used for transducer placement depending on the quality of image. The transducer is directed cephalad and dorsally towards the posterior third of the hemidiaphragm. With this approach, the dome is viewed in a sagittal (longitudinal) plane with the liver or spleen providing acoustic "windows." Alternatively the diaphragm dome can be visualized by placing a low frequency transducer (3.5–5 MHz) over the xiphoid process and scanning in the transverse plane. This placement may allow both hemidiaphragms to be viewed simultaneously. The diaphragm typically is initially identified with the B-mode as a two-dimensional structure, then M-mode is used to follow the motion of a single point in time (Fig. 11.1). Note that this point does not represent a single anatomic point on the diaphragm but several points of the diaphragm as they cross the path of the ultrasound beam.

Normal values for diaphragm motion have been reported for quiet breathing and deep inspiration. During quiet breathing, the posterior dome of the diaphragm is displaced anteriorly and caudally with a mean displacement of 1.6 cm [11, 13]. With deeper breaths, the mean displacement was 4.8 cm with about two-thirds of the diaphragm movement occurring by the time of mid-inspiration [9]. An M-mode tracing of diaphragm motion allows for calculation of the inspiratory and expiratory times, the amplitude of diaphragm motion (maximum height in cm), and the speed of diaphragm contraction (slope in cm/s).

A number of pathologic processes affect motion of the diaphragm dome. Subphrenic fluid accumulations or developmental defects, such as eventration, may reduce regional or global diaphragm motion. In patients with ascites, diaphragm excursion may be decreased, especially if the ascites is due to a malignant process. In this instance, motion may be reduced secondary to splinting from pain or fixation of the diaphragm from the malignant process [2]. With a subphrenic abscess, diaphragm motion may be impaired, absent, or even paradoxical in the presence of inflammation [14]. Overall diaphragm displacement is less with passive mechanical ventilation than is seen during an active breath, and the posterior displacement is no longer dominant over the anterior displacement [10]. The lesser diaphragmatic displacement during passive inspiration may reflect more symmetrical action of the positive inflation pressure on rib cage/diaphragm partitioning or differences in diaphragm tension between active and passive breaths.

Basic and Advanced Competencies

Imaging of the diaphragm in the ZAP using B-mode, with measurement and interpretation of tdi, Δtdi, and Δtdi%, is the basic core competency in diaphragm ultrasound. Mastery of this competency will allow for the most straightforward

assessment of suspected diaphragm paralysis and dysfunction. Imaging of the diaphragm dome using M-mode, with both quiet breathing and with performance of maneuvers such as a sniff test (see below), and the appropriate interpretation of diaphragm motion with these maneuvers, should be viewed as more advanced competencies in diaphragm ultrasound. This is due to the technical challenges of image acquisition, especially of the left hemidiaphragm, and also to the challenges in appropriate interpretation of diaphragm motion discussed below.

Evidence Review and Evidence-Based Use

Functional Correlates

Measurements of diaphragm thickness at end-expiration and diaphragm thickening during inspiration reflect diaphragm strength and shortening, respectively. In general, the resting cross-sectional area of skeletal muscle is proportional to the maximal tension it can develop. Similarly, the resting thickness of the diaphragm (tdi at end-expiration) should be proportional to the maximal transdiaphragmatic pressure (Pdimax) it can develop. Both Pdimax and maximal inspiratory pressure (PImax) were significantly correlated with diaphragm thickness measured at end-expiration in the ZAP in healthy subjects ($R = 0.94$ and 0.76, respectively) [15]. Further evidence supporting the notion that measures of tdi reflect diaphragm strength is derived from studies of longitudinal measures of changes in diaphragm thickness and strength following recovery from diaphragm paralysis [16], studies of strength-training activities and diaphragm thickness [17–19], and calculations of specific tension which are similar to those reported for other skeletal muscle groups [20, 21]. Recovery from diaphragm paralysis and strength training of the diaphragm lead to significant increases in diaphragm thickness, Pdimax, and PImax.

A second functional correlate is that between diaphragm thickening during inspiration and diaphragm muscle shortening [4]. The volume of diaphragm muscle mass (vdi) is related to its width (wdi), thickness, and length (ldi) as follows: vdi = ldi x wdi x tdi. With the assumptions that vdi is constant and wdi varies little with inspiration (wdi is related to the perimeter of the thoracic cavity), ldi will vary inversely with tdi. This relationship can be applied to ultrasound measures of diaphragm thickening as follows: $\Delta tdi \approx 1/\Delta ldi$. Using this relationship, calculation of Δldi from measures of Δtdi during a breath to total lung capacity (TLC) is in the range of what has been measured in humans [22]. A very practical application derived from measures of Δtdi relates to determining the presence or absence of diaphragm paralysis [23]. A paralyzed diaphragm does not thicken and a normally functioning diaphragm thickens by more than 20 % during inspiration. Measures of resting diaphragm thickness and thickening during inspiration provide powerful tools to assess serial changes of diaphragm function and should give insights into identifying factors that are myopathic or myotrophic to the diaphragm.

Diaphragm Paralysis

Ultrasound can be of diagnostic value when assessing the presence of unilateral or bilateral diaphragm paralysis [24]. Unilateral diaphragm paralysis results in paradoxical motion of the affected hemidiaphragm during inspiration. This paradoxical motion can be appreciated using M-mode imaging of the diaphragm dome and is a consequence of the normal action of the contralateral hemidiaphragm raising intra-abdominal pressure and displacing the passive paralyzed diaphragm cephalad. It can be elicited by instructing the patient to sniff or to forcefully inhale. Ultrasound is more sensitive than fluoroscopy in diagnosing unilateral paralysis [11]. However, false positive results occur in as many as 6 % of patients without diaphragmatic paralysis [25], and false negative tests occur when recruitment of rib cage muscles produce caudal displacement of the paralyzed hemidiaphragm [26]. These limitations may be circumvented by directly visualizing the diaphragm muscle in the ZAP in either the B- or M-mode. A paralyzed diaphragm will not thicken, whereas a normally functioning diaphragm will thicken by > 20 % [23].

Bilateral diaphragm paralysis may be difficult to diagnose when using M-mode to assess motion of the diaphragm dome. Normal caudal motion of the paralyzed diaphragm can be seen and is a consequence of strategies employed by patients to compensate for diaphragm paralysis. Specifically, actively contracting the abdominal muscles will displace the paralyzed diaphragm cephalad. When the abdominal muscles are "turned off," the passive recoil of the respiratory system results in inspiration and caudal motion of the paralyzed diaphragm. Alternatively, using the rib cage muscles to inhale will generate negative pressure in the sub-diaphragmatic regions displacing the passive diaphragm caudally [27]. By contrast, visualizing the diaphragm muscle itself in the ZAP will circumvent issues related to diaphragm motion and allow the clinician to determine if the muscle is contracting or not with more accuracy.

Diaphragm Dysfunction in the ICU

Diaphragm dysfunction may be seen following upper abdominal, neck, or cardiothoracic surgery [28–30]. Damage to the phrenic nerve may be due to transection, stretching, crushing, or hypothermia. With cardiac surgery, the use of cold saline solutions containing ice chips or slush to lower myocardial temperature may directly injure the phrenic nerve [31]. The use of cardiac insulating pads has minimized the risk of phrenic frostbite [32]. Diaphragm dysfunction may be seen in patients with sepsis, multiorgan failure, hyperglycemia, critical illness polyneuropathy and myopathy, undernutrition, and with the use of aminoglycosides and other medications which interfere with neuromuscular transmission [33]. Metabolic abnormalities such as hypokalemia, hypocalcemia, hypophosphatemia, hypomagnesemia, and thyroid disturbances also can contribute to diaphragmatic dysfunction.

Ultrasound evaluation of the diaphragm dome has been used to document abnormal motion of the diaphragm in the intensive care unit in patients without a prior history of diaphragmatic disease [30]. Diaphragm dysfunction was present in 29 % of medical patients that required mechanical ventilation for a duration of 48 h or more. Patients with diaphragm dysfunction had higher rates of weaning failure and required a greater duration of mechanical ventilation than patients without diaphragmatic dysfunction.

Weaning from Mechanical Ventilation

Diaphragm ultrasound has been used to predict weaning success or failure [34, 35]. Caudal motion of the diaphragm dome during spontaneous breaths of more than 1.1 cm had a sensitivity and specificity of 84.4 % and 82.6 %, respectively, in predicting successful extubation. Because diaphragm motion is influenced by breath size and differs from region to region, direct measures of diaphragm thickening using B-mode in the ZAP may enhance the utility of M-mode in predicting extubation outcomes.

Disuse Atrophy

Atrophy of the diaphragm has been described following periods of mechanical ventilation as brief as 24 h. Both fast-twitch and slow-twitch myofibers are involved in the mypopathic process which leads to a reduction in muscle force [36–40]. Accordingly, ventilator-induced diaphragm atrophy may be expected to impede weaning from mechanical ventilation. Other conditions that contribute to diaphragm dysfunction which are commonly encountered in the critically ill include administration of paralyzing agents, undernutrition, and metabolic abnormalities. B-mode ultrasound in the ZAP has been used to identify the presence of ventilator-induced diaphragm injury [37]. Progressive thinning of the diaphragm occurred in 7 patients within 48 h of the initiation of mechanical ventilation. These findings indicate that ultrasound may be used to identify patients with ventilator-induced diaphragm dysfunction and has the potential to be used to monitor the efficacy of interventions designed to prevent atrophy. Ultrasound was used to demonstrate that 20 min of phrenic nerve stimulation was sufficient to prevent atrophy in a C-2 tetraplegic individual [18].

Pitfalls and Precautions

A 3.5–5 MHz transducer is used to image the diaphragm dome. This frequency transducer will penetrate further but has less resolution than a higher frequency (7.5–10 MHz) transducer, which is typically used to image the diaphragm in the zone of apposition.

The diaphragm dome and the diaphragm in the zone of apposition may be difficult to visualize in patients who are obese.

The diaphragm can be visualized using either the M-Mode or B-Mode. B-Mode enables the operator to visualize the diaphragm in 2 dimensions. M-mode enables the operator to visualize one region of the diaphragm over time. The distances displaced by the diaphragm are more easily measured using M-Mode, whereas the thickness of the diaphragm is more easily measured using B-Mode.

The image of a single point on M-mode does not represent a single point on the diaphragm but represents multiple points on the diaphragm passing through the ultrasound beam.

An observation which can be used to help identify the diaphragm in the zone of apposition is the obliteration of the diaphragm by the leading edge of lung during inspiration. This helpful observation may not be seen with diaphragm paralysis or during mechanical ventilation.

The image of the diaphragm dome is comprised of sound that is intensely reflected from the lung-diaphragm interface. Measurements of diaphragm thickness using such images are not representative of thickness of the diaphragm muscle itself. When visualizing the dome, a true image of the diaphragm muscle itself will only be present when there is a pleural effusion between the diaphragm dome and the lung.

The caudal movement of the diaphragm is not uniform from region to region and differs between passive ventilation and active breathing. In addition, pathologic processes due to inflammation or malignancy may alter regional or global diaphragm motion.

Diaphragm paralysis may be difficult to diagnose when only evaluating diaphragm motion. False negatives and false positives may occur. These limitations may be circumvented by directly visualizing thickening of the diaphragm in the zone of apposition using a higher frequency transducer either in the B- or M-mode.

Conclusion

Ultrasound provides a promising new approach to study the diaphragm in the intensive care setting. It is particularly attractive in that it is noninvasive, can be used at the bedside, and delivers no ionizing radiation. Ultrasound can be used in the B-mode, which provides a 2-dimensional image, or in the M-mode, which tracks one point in time. The diaphragm can be assessed by measuring the caudal displacement of the dome during inspiration or by measuring its thickness in the zone of apposition. Diaphragm ultrasound provides a real-time image and a permanent record of function. It can be applied to address questions of diaphragm structure, configuration, and motion in health and disease and may allow us to assess biological determinants of diaphragm structure and structural change with disease. Diaphragm ultrasound has been applied to diagnose diaphragm paralysis and the presence of diaphragm dysfunction and to predict extubation success.

References

1. Matamis D, Soilemezi E, Tsagourias M, Akoumianaki E, Dimassi S, Boroli F, Richard J-CM, Brochard L. Sonographic evaluation of the diaphragm in critically ill patients. Technique and clinical applications. Intensive Care Med. 2013;39:801–10.
2. McCool FD, Hoppin FG. Ultrasonography of the diaphragm. In: Roussos C, editor. Thorax, vol. 85. New York: Marcel Dekker; 1995. p. 1295–309.
3. Wait JL, Nahormek PA, Yost WT, et al. Diaphragmatic thickness–lung volume relationship in in vivo. J Appl Physiol. 1989;67:1560–8.
4. Cohn D, Benditt JO, Eveloff S, McCool FD. Diaphragm thickening during inspiration. J Appl Physiol. 1997;83:291–6.
5. Houston JG, Morris AD, Howie CA, et al. Technical report: quantitative assessment of diaphragmatic movement – a reproducible method using ultrasound. Clin Radiol. 1992;46: 405–7.
6. Gerscovich EO, Cronan M, McGahan JP, et al. Ultrasonographic evaluation of diaphragmatic motion. J Ultrasound Med. 2001;20:597–604.
7. Lloyd T, Tang YM, Benson MD, et al. Diaphragmatic paralysis: the use of M mode ultrasound for diagnosis in adults. Spinal Cord. 2006;44:505–8.
8. Boussuges A, Gole Y, Blanc P. Diaphragmatic motion studied by M-mode ultrasonography: methods, reproducibility, and normal values. Chest. 2009;135:391–400.
9. Harris RS, Giovannetti M, Kim BK. Normal ventilatory movement of the right hemidiaphragm studied by ultrasonography and pneumotachography. Radiology. 1983;146:141–4.
10. Laing IA, Teele RL, Stark AR. Diaphragmatic movement in newborn infants. J Pediatr. 1988;112(4):638–43.
11. Houston JG, Angus RM, Cowan MD, et al. Ultrasound assessment of normal hemidiaphragmatic movement: relation to inspiratory volume. Thorax. 1994;49:500–3.
12. Epelman M, Navarro OM, Daneman A, et al. M-mode sonography of diaphragmatic motion: description of technique and experience in 278 pediatric patients. Pediatr Radiol. 2005;35: 661–7.
13. Drummond GB, Allan PL, Logan MR. Changes in diaphragmatic position in association with the induction of anaesthesia. Br J Anaesth. 1986;58(11):1246–51.
14. Miller WT, Talman EA. Subphrenic abscess. Am J Roentgenol Radium Ther Nucl Med. 1967;101(4):961–9.
15. McCool FD, Conomos P, Benditt JO, Cohn D, Sherman CB, Hoppin Jr FG. Maximal inspiratory pressures and dimensions of the diaphragm. Am J Resp Crit Care Med. 1997;155(4): 1329–34.
16. Summerhill EM, El-Sameed YA, Glidden TJ, McCool FD. Monitoring recovery from diaphragm paralysis with ultrasound. Chest. 2008;133:737–43.
17. Summerhill EM, Angov N, Garber C, McCool FD. Respiratory muscle strength in the physically active elderly. Lung. 2007;185(6):315–20.
18. Ayas NT, McCool FD, Gore RL, Lieberman SL, Brown R. Prevention of diaphragm atrophy with brief periods of electrical stimulation. Am J Resp Crit Care Med. 1999;159:2018–20.
19. DePalo VD, Parker AL, Al-Bilbeisi F, McCool FD. Respiratory muscle strength training with non-respiratory maneuvers. J Appl Physiol. 2004;96(2):731–4.
20. Rehan VK, Laiprasert J, Wallach M, Rubin LP, McCool FD. Diaphragm dimensions of the healthy preterm infant. Pediatrics. 2001;108(5):91–5.
21. McCool FD, Benditt JO, Conomos P, Anderson L, Sherman CB, Hoppin Jr FG. Variability of diaphragm structure among healthy individuals. Am J Respir Crit Care Med. 1997;155: 1323–8.
22. Rochester DF, Farkas GA, Lu J. Contractility of the in situ diaphragm: assessment based on dimensional analysis. In: Respiratory muscles and their neuromotor control. New York: Liss; 1987. p. 327–36.

23. Gottesman E, McCool FD. Ultrasound evaluation of the paralyzed diaphragm. Am J Respir Crit Care Med. 1997;155:1570–4.
24. McCool FD, Tzelepis GE. Current clinical aspects of diaphragm dysfunction. N Engl J Med. 2012;366:932–42.
25. Alexander C. Diaphragm movements and the diagnosis of diaphragmatic paralysis. Clin Radiol. 1966;17:79–83.
26. Scillia P, Cappello M, De Troyer A. Determinants of diaphragm motion in unilateral diaphragmatic paralysis. J Appl Physiol. 2004;96:96–100.
27. McCool FD, Mead J. Dyspnea on immersion: mechanisms in patients with bilateral diaphragm paralysis. Am Rev Resp Dis. 1989;39:275–6.
28. Fedullo AJ, Lerner RM, Gibson J, et al. Sonographic measurement of diaphragmatic motion after coronary artery bypass surgery. Chest. 1992;102:1683–6.
29. Diehl JL, Lofaso F, Deleuze P, Similowski T, Lemaire F, Brochard L. Clinically relevant diaphragmatic dysfunction after cardiac operations. J Thorac Cardiovasc Surg. 1994;107: 487–98.
30. Kim SH, Na S, Choi JS, Na SH, Shin S, Koh SO. An evaluation of diaphragmatic movement by M-mode sonography as a predictor of pulmonary dysfunction after upper abdominal surgery. Anesth Analg. 2010;110:1349–54.
31. Merino-Ramirez MA, Juan G, Ramón M, et al. Electrophysiologic evaluation of phrenic nerve and diaphragm function after coronary bypass surgery: prospective study of diabetes and other risk factors. J Thorac Cardiovasc Surg. 2006;132:530–6.
32. Wheeler WE, Rubis LJ, Jones CW, Harrah JD. Etiology and prevention of topical cardiac hypothermia-induced phrenic nerve injury and left lower lobe atelectasis during cardiac surgery. Chest. 1985;88:680–3.
33. Chawla J, Gruener G. Management of critical illness polyneuropathy and myopathy. Neurol Clin. 2010;28:961–77.
34. Kim WY, Suh HJ, Hong SB, Koh Y, Lim CM. Diaphragm dysfunction assessed by ultrasonography: influence on weaning from mechanical ventilation. Crit Care Med. 2011;39:2627–30.
35. DiNino EK, Gartman EJ, Sethi JM, McCool FD. Diaphragm ultrasound as a predictor of successful extubation from mechanical ventilation. Thorax. 2014;69:423–7.
36. Jaber S, Petrof BJ, Jung B, et al. Rapidly progressive diaphragmatic weakness and injury during mechanical ventilation in humans. Am J Respir Crit Care Med. 2011;183:364–71.
37. Grosu HB, Lee YI, Lee J, Eden E, Eikermann M, Rose K. Diaphragm muscle thinning in mechanically ventilated patients. Chest. 2012. PMID: 22722229
38. Hudson MB, Smuder AJ, Nelson WB, Bruells CS, Levine S, Powers SK. Both high level pressure support ventilation and controlled mechanical ventilation induce diaphragm dysfunction and atrophy. Crit Care Med. 2012;40:1254–60.
39. Vassilakopoulos T. Ventilator-induced diaphragm dysfunction: the clinical relevance of animal models. Intensive Care Med. 2008;34:7–16.
40. Levine S, Nguyen T, Taylor N, et al. Rapid disuse atrophy of diaphragm fibers in mechanically ventilated humans. N Engl J Med. 2008;358:1327–35.

Chapter 12
Abdominal Ultrasound and Genitourinary Ultrasound in the Intensive Care Unit

Taro Minami

Introduction

Ultrasound of the abdomen in critical care can be valuable in the assessment of the critically ill patient. A few examples of how ultrasound can assist in the bedside evaluation of the critically ill patient are rapid assessment of kidneys and bladder in patients with acute kidney injury to rule out obstruction; evaluation of the urinary tract in patients with urinary tract infections; imaging and guidance for drainage of ascites in liver disease or abdominal sepsis; assessment of volume status by examination of the inferior vena cava (IVC) in the patient with shock; and scanning of the abdominal aorta in patients with back or abdominal pain to assess for possible aneurysm rupture.

While a computed tomography (CT) scan of the abdomen provides detailed information to assess abdominal pathologies in the critically ill and thus prevails in a global assessment of acute abdominal pathology, ultrasound of the abdomen has its own unique advantages in the intensive care unit (ICU). In fact, ultrasound examination of the abdomen in the critically ill is superior to CT scan in some respects. First, it can be performed at the bedside; thus, there is no need for transportation, avoiding potentially compromised safety during the transfer. Second, the examination, if needed, can be repeated as many times as desired without the risk of radiation or contrast-induced nephropathy. This can be especially important for young patients or patients with renal failure. Third, the information can be obtained and clinically acted upon immediately. As is the case with all other aspects of critical care ultrasound, the bedside ultrasound imaging needs to be appropriately acquired and interpreted – a skill that comes with systematic practice and supervision.

T. Minami, M.D., FACP, FCCP (✉)
Division of Pulmonary, Critical Care and Sleep Medicine, Memorial Hospital of Rhode Island, 111 Brewster Street, Pawtucket, RI 02860, USA
e-mail: taro_minami@brown.edu

M. Jankowich, E. Gartman (eds.), *Ultrasound in the Intensive Care Unit*,
Respiratory Medicine, DOI 10.1007/978-1-4939-1723-5_12

General Technical and Patient Considerations

Learning to utilize ultrasound is similar to learning to use a stethoscope. Not only must one master the knowledge of where to place the instrument, variations in positioning, anatomy, or body habitus may alter how sounds are produced or images are created. The experience with ultrasound additionally requires one to be comfortable manipulating the rotation, angle, and tilt of the probe, as well as sonographic parameters of gain and depth, to obtain the optimal image. In the end, as with the use of a stethoscope, once accustomed to these prerequisites and well practiced in technique, ultrasound images can be acquired, interpreted, and incorporated into the clinical assessment within minutes.

Technical Considerations for Abdominal Ultrasound Examination

Ultrasound Transducer

Given that most of the abdominal structures are deeply located, a lower frequency transducer should be used to allow the sound waves to penetrate into deeper structures. A 1–5 Mhz phased array probe is recommended for abdominal ultrasound (Fig. 12.1).

Fig. 12.1 Transducer suitable for abdominal examination. 1–5 MHz phased array transducer; note the orientation marker

Machine Setup

Orientation

The orientation marker on the probe should be directed toward the patient's head (cephalad: sagittal or coronal section; Fig. 12.2), but sometimes you may want to put the marker to the patient's right to scan the body horizontally (transverse section; Fig. 12.3). On the screen, an orientation marker should be on the left upper corner of the screen.

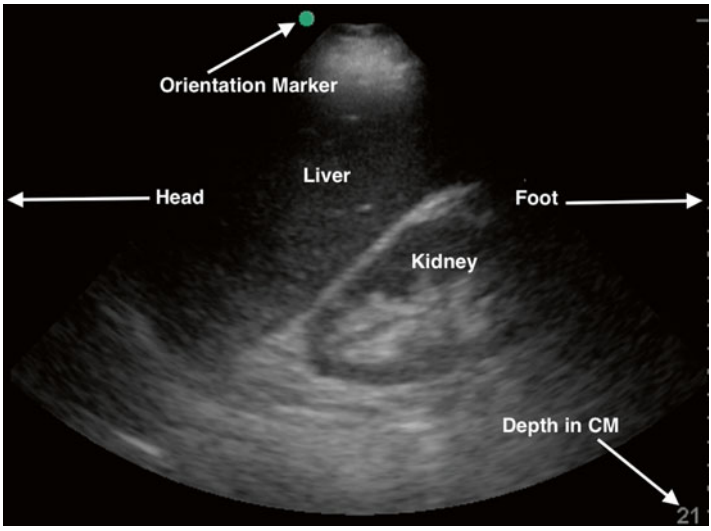

Fig. 12.2 Sagittal view of the *right upper* quadrant. The transducer is oriented with the probe marker toward the patient's head (cephalad), corresponding to the *left* side of the screen (*green-blue orientation dot*). Also pay attention to the depth, which is 21 cm in this image

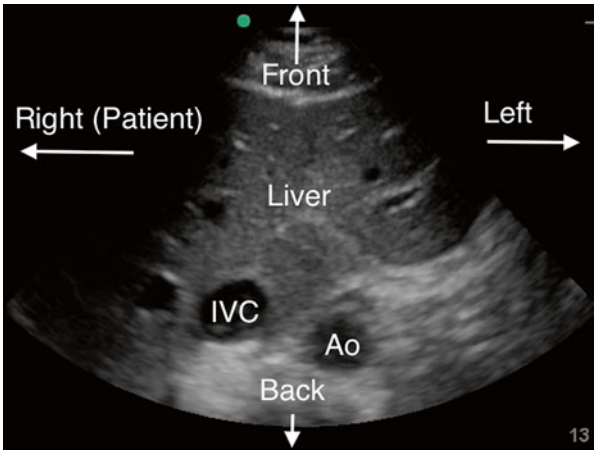

Fig. 12.3 Transverse view of the *right upper* quadrant. This time, the orientation marker on the transducer is facing patient's right. This image is analogous to a transverse image on a CT scan of the abdomen. *IVC* inferior vena cava, *Ao* aorta. Note depth is 13 cm in this image

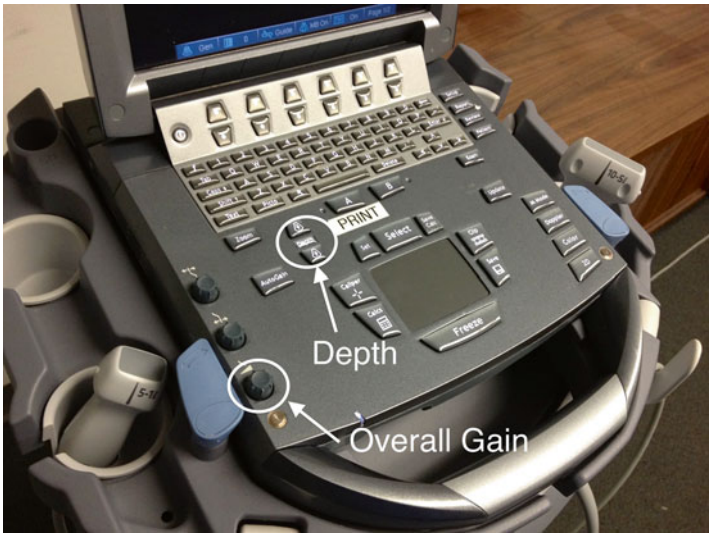

Fig. 12.4 Depth and gain controls. Though there are so many buttons on a console as shown above, important ones are very few (pictured: SonoSite M-Turbo, SonoSite Inc., Bothell, Washington, USA). Note each console (key layout) varies between machines

Depth

Start with the depth set at 13–19 cm, and, occasionally, even more depth is required. Always start with sufficient depth so that important structures or pathology located deep in the abdomen are not missed.

Gain

Overgain is another common error made by the novice ultrasonographer. Try to undergain as much as possible.

Figure 12.4 illustrates control layout on a typical portable ultrasound machine.

Patient Considerations for Abdominal Ultrasound in the ICU

The nature of the ICU patient may present several challenges to obtaining quality ultrasound images. Oftentimes, many of these obstacles can be overcome by technical or operator adaptations, and examples of such strategies are presented below.

The Obese Patient

If abdominal subcutaneous tissue is preventing an effective examination of the anterior abdomen, depth may be increased. If the machine function allows selection of different frequencies, choose a lower frequency for better penetration. Some structures, such as the inferior vena cava (IVC) or aorta, occasionally are better observed from a lateral approach.

Abdominal Gas

Gas has a high attenuation coefficient, meaning abdominal gas will prevent ultrasound from penetrating deep to a gas-filled viscus to examine other intra-abdominal structures. Performing ultrasound from a frontal approach is difficult in patients with abdominal gas. In such a setting, important vascular structures, such as the IVC and aorta, may not be well examined from a frontal examination, and laterally placing the probe in the anterior to mid-axillary line can prove helpful.

Supine Patients

Very few people in the ICU are not supine. The diaphragm may therefore be higher than expected in these patients. Therefore, identifying the diaphragm is of particular importance when you are planning procedures, such as thoracentesis or paracentesis. Scan higher in the thorax to definitively identify the diaphragm level prior to deciding on a spot for a procedure.

When examining the retroperitoneal organs, particularly the kidneys (especially the left one), a supine position makes the ultrasound more difficult. Place the transducer deep into the small space between the patient's back and the bed. Sometimes help from other members of the critical care team in lifting the subcutaneous tissue or repositioning the patient is needed so that a space to scan can be created.

Other Patient Considerations: Age, Gender, and Body Size

Age, gender, and body size have to be taken into consideration as the size of organs is affected by the patient's age, gender, or height. For example, longitudinal length of the kidney is longer in men and in younger or taller patients [1].

Competencies in Critical Care Abdominal Ultrasound

No definitive qualification or certification currently exists to dictate full competency in abdominal ultrasonography in the critically ill. In order to begin to help guide training programs and practicing critical care physicians, the American College of Chest Physicians (ACCP) and La Societe de Reanimation de Langue Française (SRLF) together published a statement on competence in critical care ultrasonography in 2009 [2].

Image Acquisition and Interpretation: A Location-Specific Approach to Abdominal Ultrasound in the ICU

Points of Interests: FAST Examination and the Location-Specific Approach

When imaging the abdomen, an ultrasonographer can take an organ-specific or a location-specific approach. A so-called organ-specific approach will focus on one specific organ at a time and then move, if desired, to the next organ. This is the typical approach taken in comprehensive abdominal ultrasounds performed in the radiology suite. Focused Assessment with Sonography for Trauma (FAST) examination [3] (see Chap. 14) is an example of a context-driven, location-specific ultrasound approach that was introduced to assess rapidly for the presence of free fluid as a sign of intraperitoneal injury following trauma. In the FAST exam, the examination is limited to a few key points of interest to allow a quick, stereotyped examination that can be carried out in the chaotic trauma bay. The concept of limiting the number of points of interest can be applied to the general critical care abdominal ultrasound as well.

A location-specific approach focuses on one specific point of examination, and all of the important organs are visualized from that location. This approach is efficient, and provides a logical and consistent framework to follow, so that with repeated examinations the ultrasonographer will gain confidence and experience in obtaining and interpreting a few critical views. There are inherent limitations in the comprehensiveness of this approach, and this must be kept in mind when assessing for specific pathologies, such as possible abdominal aortic aneurysm, in which imaging of a more complete extent of the organ is needed.

Point A: Right Upper Quadrant

Right mid- to anterior axillary line at the 8–10th intercostal space. What can be evaluated: right hemidiaphragm, liver, pleural effusion, ascites, right kidney, IVC, and aorta.

Point B: Subcostal Point

Common structures to be evaluated: IVC, aorta, pancreas, liver, gallbladder, common bile duct, ascites, and stomach.

Point C: Left Upper Quadrant

Left mid-axillary line at the 8–10th intercostal space.

Common structures to be evaluated: left hemidiaphragm, spleen, left kidney, and ascites.

Point D: Suprapubic Window

Structures to be evaluated: bladder, prostate gland, uterus, and ascites.

Point A: Right Upper Quadrant

Point A should be the starting point of an abdominal ultrasound examination in the critically ill. Not only can the diaphragm, liver, and right kidney be examined, but the IVC and aorta can also be imaged from this view. Below, I will describe each organ accessible from this viewpoint.

Right Hemidiaphragm

Examination of the diaphragm is important for two reasons [1]. The diaphragm is an important landmark that separates the abdomen from the thorax [2]. Evaluation of the diaphragm itself gives you important information in the critically ill. By observation of how much it thickens during inspiration, inspiratory muscle function can be assessed. Evaluation of diaphragmatic function is discussed in detail in Chap. 10.

Locating the diaphragm is of primary importance since this is the major structure that separates the abdomen from the thorax (Fig. 12.5). Since free fluid may be located above or below the diaphragm, failure to identify this structure may lead to preventable errors during procedures, such as an inadvertent sub-diaphragmatic puncture during a thoracentesis.

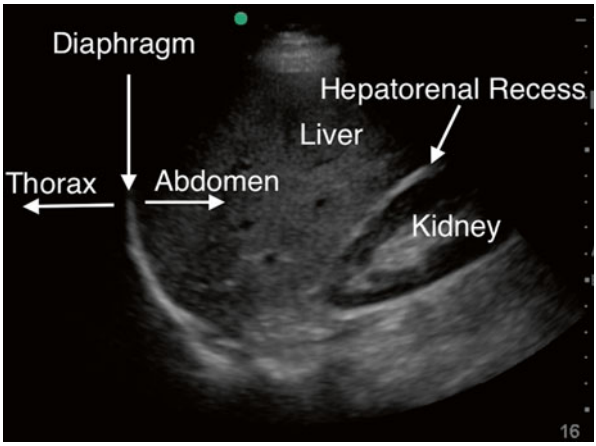

Fig. 12.5 Ultrasound image: right diaphragm, liver, and kidney. The diaphragm in this ultrasound image is the hyperechoic *curved line*. Do not confuse the diaphragm with the hyperechoic line in the hepatorenal recess (Morison's pouch)

Fig. 12.6 Position of the transducer at Point A. Start scanning at this point in a critical care abdominal ultrasound examination. Place the transducer in the right anterior to midaxillary line at the 8th–10th intercostal space to examine the right hemidiaphragm. Note the orientation marker is facing up (cephalad). The liver and kidney can be imaged here, as well as the diaphragm. Rotate the transducer (orientation marker) to 10–11 o'clock to minimize artifact from the rib cage (acoustic shadowing). Carefully select the depth (usually 16–19 cm) so that you do not miss important structures

Technical Aspects: How to Locate the Diaphragm

When using the phased array 1–5 MHz transducer at Point A, the orientation marker should be facing cephalad (Fig. 12.6) or directed toward the right shoulder, thus slightly rotated to the back (parallel to rib). Place the transducer at the mid-axillary line at the level of the 8th to 10th intercostal space. The probe may be rotated so that the acoustic shadow of the rib does not interfere with the image.

Pitfalls and Precautions

- Do not confuse the right hemidiaphragm with the hyperechoic line between liver and kidney representing Gerota's fascia.
- Supine patients usually have their diaphragm in higher position. Where you normally expect lung, there may be liver or kidney. Move the transducer cephalad and caudad freely to make sure you identify the diaphragm. If you have trouble finding the diaphragm, usually there are a few specific reasons:

  1. The transducer is positioned either too high (imaging the lung) or too low (imaging part of the liver or kidney).
  2. The transducer is placed too far anteriorly.
  3. The transducer rotation is suboptimal.

Right Kidney

With rare exception, every patient who comes to the ICU with acute renal failure or low urine output should have ultrasound scanning of the genitourinary system rapidly carried out to rule out obstruction (hydronephrosis, full bladder with outlet obstruction, etc.) and to assess for evidence of chronic kidney disease. When a UTI is suspected, look for fluid collections around the kidney and/or signs of hydronephrosis. Pathology can subsequently be confirmed with a comprehensive ultrasound, but early identification of these findings can allow appropriate early interventions, further imaging, and consultations to be initiated quickly.

Technical Aspects: Imaging the Right Kidney

To scan the kidney, start the scan from the mid- to posterior axillary line, moving slowly forward to the anterior axillary line. Start scanning from the back so that the hand holding the transducer is almost touching the bed when the patient is in a supine position. If orientation is lost, look for the diaphragm, an important landmark. Placing the patient in the left lateral decubitus position, if possible, may be helpful. The transducer may be rotated slightly to minimize the effect of the acoustic artifact from the rib cage. Novice examiners may find it difficult to locate the kidney; this is often due to the fact that they start scanning too far anteriorly. Because the kidney is a retroperitoneal organ, scanning from back to front allows the sonographer to identify the kidney more easily (this is particularly the case with the left kidney). Angulation is also important: angle the transducer so that the beam is aimed posteriorly, almost scanning in a sagittal plane, i.e., not with the beam in a perpendicular position (coronal view), which is more suitable for assessment of

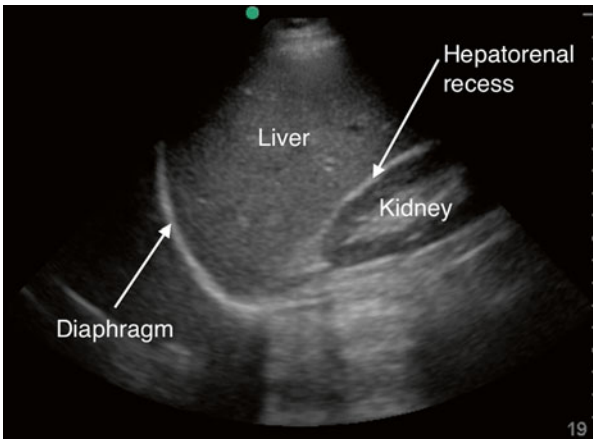

Fig. 12.7 The hepatorenal recess (Morison's pouch). The potential space that exists between the kidney and the liver constitutes the hepatorenal recess, or Morison's pouch. The echogenic line of Gerota's fascia should not be confused with the echogenic pleural line of the diaphragm. Fluid accumulation in the hepatorenal recess will result in a relatively hypoechoic space forming between the liver and the kidney (see also Fig. 12.11 below)

IVC and aorta. Look for free fluid in the hepatorenal recess (Fig. 12.7) between the right kidney and the liver (Morison's pouch). Be sure to image the kidney through its inferior pole to avoid inadvertently missing free fluid in the most inferior aspect of Morison's pouch.

Basic Competencies: Kidney

Goals when scanning the kidney include an assessment of kidney size, observation of the pelvis for evidence of hydronephrosis, and qualitative examination of renal cortex echogenicity. First, assess kidney size. Freezing an image and using calipers may be helpful. The size of the normal kidney usually ranges from 9 to 12 cm [1]. Reduction in kidney size typically indicates chronic/irreversible renal pathology, i.e., chronic kidney disease with atrophy [4]. Next, observe the renal pelvis to see if there is any sign of hydronephrosis (dilation of renal pelvis and collecting system) (Fig. 12.8). This will appear as hypoechoic regions that communicate and coalesce in the renal pelvis and drain into the ureter. More subtle evidence of early hydronephrosis may require comprehensive abdominal ultrasound for confirmation. Finally, assess the renal cortex. The normal renal cortex appears thick; a thin cortex suggests the presence of chronic kidney disease. In acute kidney injury, the cortex is usually hyperechoic. By contrast, in chronic kidney disease the renal cortex is usually thin and hypoechoic.

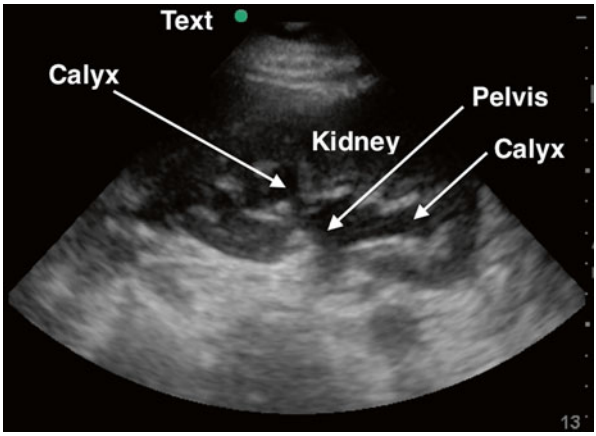

Fig. 12.8 Hydronephrosis: Note hypoechoic lesions which are dilated calyces connected to the renal pelvis. Unlike renal cysts, these structures can be shown to be connected. Move the transducer carefully to observe and document connectivity and drainage into the renal pelvis

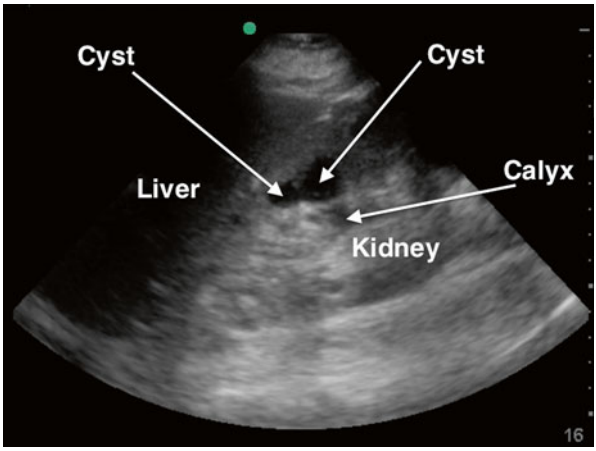

Fig. 12.9 Renal cysts: Though this image looks similar to the one with hydronephrosis, the hypoechoic regions are cysts, as the structures have a clear boundary and no connection to the calyx. To confirm this, the transducer must be moved carefully by the sonographer to confirm that there is no connection between these two structures and no connection to the renal pelvis

Pitfalls and Precautions

Avoid mistaking renal cysts (Fig. 12.9) for dilation of the collecting system. Dilated elements of the collecting system should join together in the renal pelvis, so change the transducer tilt and angulation for comprehensive assessment of any hypoechoic region visualized in the kidney.

Inferior Vena Cava and Aorta

Images of both the IVC and aorta can be obtained from Point A. The IVC in this position will appear as a tubular structure deep to the liver (Fig. 12.10). The aorta will also be visualized, in a deeper position still. If there is any confusion regarding whether the IVC or aorta is being visualized, the use of Doppler signaling may be helpful. Following the drainage of the hepatic veins into the IVC can also be helpful in identifying the IVC. Imaging of the IVC, useful in the assessment of volume status and fluid responsiveness, is more fully discussed in Chap. 4. Examination of the IVC from Point A is not extensively examined from an evidence-based point of view. Thus, the evidence is not sufficient to state that measurement of the IVC from this approach can be substituted for the measurement of the IVC from the anterior abdomen or from the subcostal view. However, since imaging of the IVC from an anterior or subcostal position may be technically difficult, owing to factors such as patient body habitus or presence of intra-abdominal gas, gaining experience in imaging the IVC from Point A is important.

Imaging of the abdominal aorta with ultrasound can be critical in the rapid triage of the patient with back or abdominal pain and hypotension/shock. The goal is to assess for abdominal aortic aneurysm (dilation of the aorta to a size greater than 3 cm) [5, 6]. Imaging from Point A can offer a valuable initial reference point in the assessment of the aorta, but for more comprehensive imaging of the aorta, see the discussion of aortic imaging under Point B below.

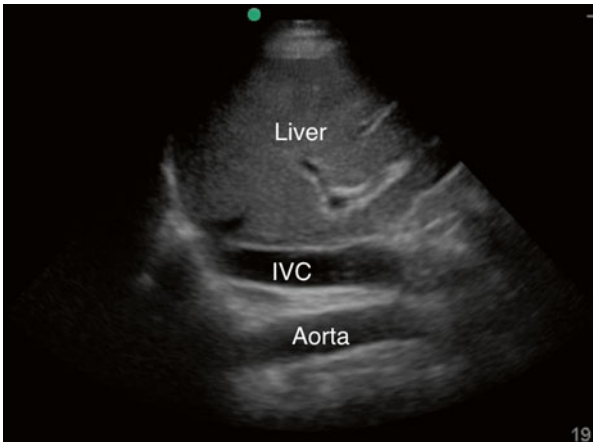

Fig. 12.10 IVC and aorta from Point A (coronal view). The transducer is placed in the same position as in imaging of the liver and the right kidney. The only difference is that the transducer is angled so that it is more perpendicular (coronal view). This approach is particularly useful for obese or ventilated patients as the IVC or aorta may not be visible from the frontal approach because of abdominal fat or gas. (*IVC* inferior vena cava)

Technical Aspects

The transducer is placed in the same position as described above for the kidney. The angulation of the transducer should be more perpendicular to image the inferior vena cava and aorta, i.e., a coronal view. Carefully change the angle of the transducer so that the plane is not off-axis. Complete examination of the aorta to rule out aneurysm cannot be performed solely from Point A, but the aorta may be imaged both proximally and distally with angulation changes.

Pitfalls and Precautions

- The IVC may be confused with the aorta, as both structures can be observed from the same point but typically with slightly different angulations of the ultrasound beam. Note that there should be pulsatile Doppler flow in the aorta, but not the IVC, and that the aorta should be located deeper than the IVC.
- The draining hepatic veins can be followed to their entrance into the IVC to confirm that the IVC is correctly identified.

Ascites/Pleural Effusion

From Point A, both a right pleural effusion and ascites may be identified.

Ascites

Identification of ascites is a key goal of critical care abdominal ultrasonography. From Point A, you can assess the hepatorenal recess, or Morison's pouch, an important dependent area where ascites or free fluid first gathers in the abdomen. This is therefore an excellent location to assess for the presence of early ascites. Ascites typically appears as an anechoic space surrounding the normal organs (Figs. 12.11 and 12.12). Complicated ascites, as in infection, may have some internal or swirling/scintillating echogenicity (the so-called plankton sign) or even contain internal septations (Fig. 12.13). Therefore, recording an assessment of the qualitative appearance of the fluid may be helpful. Again, do not confuse ascites in Morison's pouch with a pleural effusion. Confirmation of the location of the diaphragm is critical. Keep in mind that fluid may be present both above and below the diaphragm (see Fig. 12.12); therefore, simply locating anechoic fluid from this viewpoint is not sufficient to determine whether the fluid is intrathoracic or intra-abdominal.

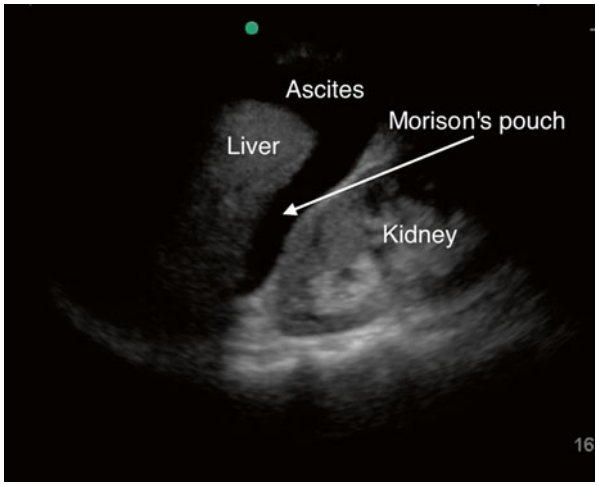

Fig. 12.11 Ascites in Morison's pouch (the hepatorenal recess). Note that in large volume ascites, as in this case, fluid is easily recognized in Morison's pouch, but in small volume ascites, signs may be more subtle and ascites may be only visualized as the presence of a slit-like line in Morison's pouch (see also Fig. 14.5 in Chap. 14)

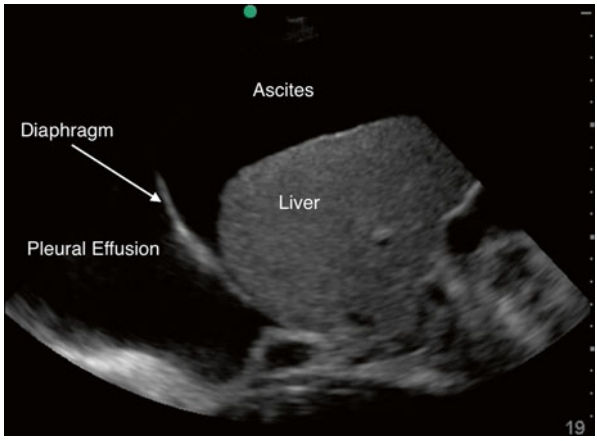

Fig. 12.12 Large volume ascites and hepatic hydrothorax. Note the simultaneous presence of pleural effusion above the diaphragm, illustrating the importance of identifying the diaphragm

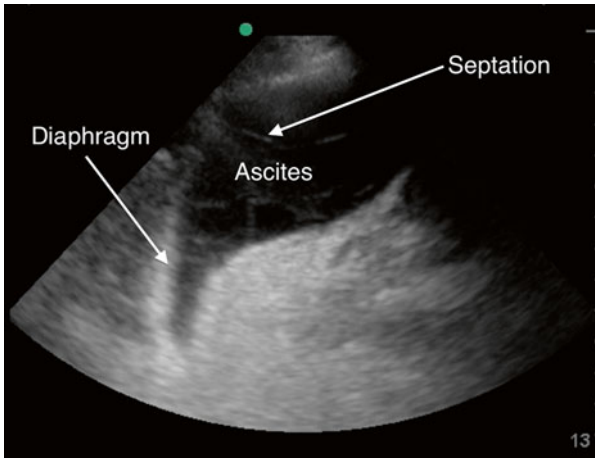

Fig. 12.13 Complex ascites. The hemidiaphragm (in this case, the left hemidiaphragm) is a critical landmark to distinguish ascites from pleural effusion. Note the internal septations, indicating complex fluid. Complex features typically implies inflammation, but an absence of apparent fluid complexity does not always rule out inflammation

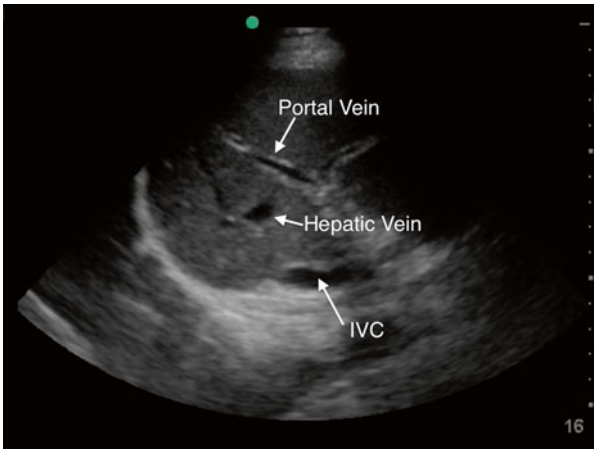

Fig. 12.14 Portal and hepatic veins. Note the highly echogenic wall of the portal vein, in contrast to the non-discernible wall of the hepatic vein. The hepatic veins will be observed to drain into the IVC with transducer manipulation

Liver and Biliary Tree

Examination from Point A also enables examination of the liver and biliary structures. A comprehensive analysis of the liver is beyond the scope of our discussion; however, a few important structures are worth mentioning.

There are three vessels or vessel-like structures within the liver: the hepatic veins, portal vein, and the intrahepatic biliary tree. Of these three structures, the intrahepatic biliary ducts are usually not discernable by ultrasound unless there is specific pathology (dilation). Distinguishing hepatic vein from portal vein is typically easy, as the hepatic vein usually does not have a discernable vessel wall, whereas the portal vein has a highly echogenic vessel wall (Fig. 12.14). Anatomically, the hepatic veins flow into the IVC; thus, vascular structures in the liver without discernible walls that are connected to IVC are hepatic veins. If the splenic vein, which runs behind the pancreas, is carefully followed, this structure should lead to the portal vein, but this technique is beyond the scope of this chapter.

The intrahepatic biliary ducts run parallel to the portal veins, but usually they are hard to detect in ultrasonographic examination. If two vascular structures are imaged running in parallel, and one set of these structures is the portal veins with highly echogenic walls, the parallel set of structures are likely to be dilated intrahepatic biliary ducts.

Point B: Subcostal

From Point B, several structures important in the assessment of hemodynamics can be imaged, such as the heart and pericardium, the inferior vena cava (IVC), and the aorta. The gallbladder may also be visualized from this position with tilting and

angulation of the probe. Assessment of the heart/pericardium from the subcostal view will be discussed in Chaps. 5, 6, 7, but here I would like to primarily discuss the technical aspects of how the IVC and aorta can be imaged from this viewpoint.

Inferior Vena Cava

Technical Aspects: Identification of the Inferior Vena Cava

Many novice examiners spend excessive amounts of time struggling to locate the IVC. A common misconception is that the IVC will be located in the middle of the abdomen. Rather, the IVC is located slightly to the right of midline. The other common technical pitfall is placing the transducer perpendicular to the abdominal wall. The transducer should be tilted up almost 45° (Fig. 12.15) so that the beam is aimed at the diaphragm dome. Simply placing the transducer slightly to the patient's right and tilting the transducer upwards makes the examination of this vascular structure much easier. A basic approach is to start by finding the heart from the subcostal approach, then rotating the transducer counterclockwise until you see the IVC flowing into the right atrium. Manipulate the transducer angle until the hepatic vein entrance is visualized.

For uniformity, the IVC diameter should be assessed proximal to the entrance of the hepatic veins. As discussed in Chap. 6, an IVC diameter <2.1 cm that collapses >50 % with inspiration suggests a normal right atrial pressure (range 0–5 mmHg), while an IVC diameter greater than 2.1 cm that fails to collapse at least 50 % with inspiration suggests a high right atrial pressure (range 10–20 mmHg).

Fig. 12.15 Transducer placement to examine the IVC. Note the transducer is slightly shifted to the patient's right from midline. Also note it is tilted almost 45° to cephalad

Pitfalls and Precautions

- Abdominal gas can complicate IVC visualization. Use the liver as an imaging window. Follow the hepatic veins to the IVC if localization is difficult.
- Avoid imaging the midline, where the IVC won't be found. Place the probe just to the right of midline and tilt the transducer upwards 45°.
- Be sure that movement of the IVC into a different imaging plane is not mistaken for diameter change or collapsibility.

Aorta

Technical Aspects: Identification of Abdominal Aorta

With a similar approach to imaging the IVC, the aorta can be localized. Place the transducer in the midline of the abdomen with the transducer slightly tilted cephalad, and the probe marker oriented cephalad to catch the aorta in a longitudinal view (Fig. 12.16). Rotation of the probe counterclockwise, with the probe marker oriented to the patient's right, will reveal a transverse view (Fig. 12.17). The spine will be visualized as a hyperechoic line adjacent and posterior to the aorta with posterior acoustic shadowing. The IVC will be visualized to the patient's right. The ultrasonographic image of the aorta is similar to the IVC, but different in that [1] the aorta has a thicker wall; [2] the aorta has pulsatile flow on Doppler; and [3] the IVC will have a respirophasic variation in diameter. For a complete examination of the length of the intra-abdominal aorta, the ultrasound transducer should be moved caudad toward the umbilicus. The celiac axis and superior mesenteric artery will be observed as branches off the aorta when the transducer is moved distally. The aorta should be

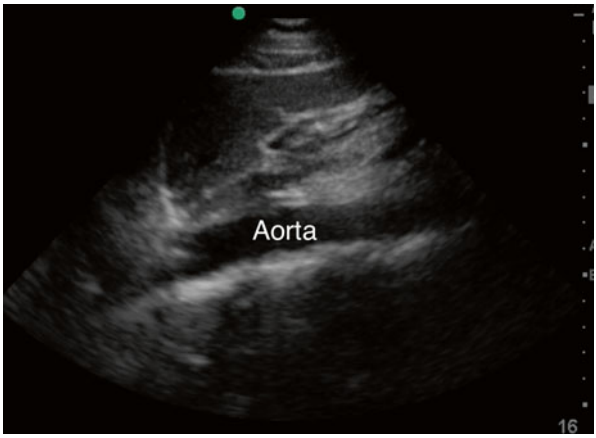

Fig. 12.16 Abdominal aorta, longitudinal view. Carefully note the diameter of the aorta, with a diameter greater than 3 cm indicating aneurysmal dilation. Freeze an image and use calipers for accurate measurement

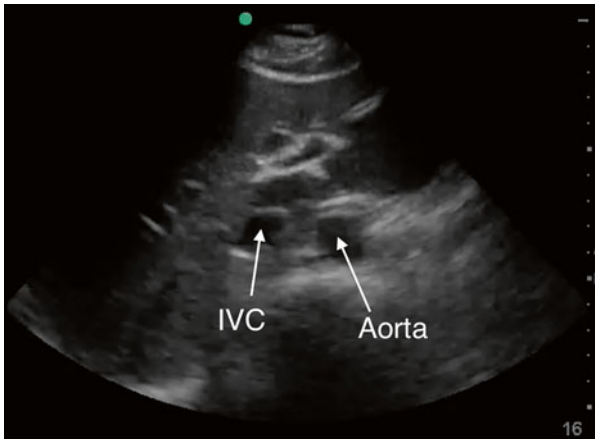

Fig. 12.17 Abdominal aorta, transverse view. Again, note the diameter from the outer wall to outer wall, using image freeze and calipers for accurate measurement

followed until it branches into the iliac arteries. This should be done in both the transverse view and longitudinal view. A transverse view avoids the problems of shifting off-axis as can occur in the longitudinal view.

Basic Competency: Identification of Abdominal Aortic Aneurysm

Detecting abdominal aortic aneurysm by ultrasound scanning is sensitive and specific, and may improve patient care [7, 8]. External wall diameter (from outer wall to outer wall) of more than 3 cm was considered aneurysmal in these studies. Imaging the aorta from Point B alone is insufficient to rule out an aneurysm. If aneurysm is in the differential, the aorta should be followed caudally along its length to its bifurcation into the iliac arteries to ensure a comprehensive examination.

Pitfalls and Precautions

- Avoid confusing the aorta and the IVC. A few tips to tell IVC from aorta: the visualized structure is the IVC if it flows into the right atrium; the hepatic veins flow into the IVC; and the IVC is just adjacent to the liver. The aorta is located to the left of midline, with IVC to the right, thus location can be helpful; but above all, the aorta is a pulsatile structure with a thicker wall. Use Doppler imaging to assess for pulsatile flow if there are any doubts.
- Similarly, don't mistake the spine for the aorta. Again, Doppler flow measurement can be helpful.
- Assessing the aorta in a longitudinal view can underestimate the size of the aorta if the aorta is imaged off the central axis.
- Measure the aorta from the outer wall to outer wall, not across the inner lumen of the aorta, to assess for aneurysm. Measuring the inner lumen will result in underestimation of aortic size.

Pancreas

While the pancreas can potentially be imaged from this point [5], it has been suggested that "Not too much energy should be devoted to this organ by the intensivist who has not full mastery of priority targets (lungs, veins, basic heart, etc.)" [5], a statement with which I agree. The ACCP/SRLF statement by Mayo et al. [2] also does not include imaging of the pancreas as a competency in abdominal ultrasonography.

Point C: Left Upper Quadrant

Observation of organs from this point is technically more challenging because their anatomic locations are more posterior than the liver or the right kidney. Locating the left hemidiaphragm is also more challenging because the landmark of the liver is not present. The organs to be identified from Point C are the left hemidiaphragm, spleen, and left kidney. As with imaging from Point A, identification of the hemidiaphragm allows classification of free fluid as pleural or peritoneal, and thus this structure should be identified first. Figure 12.18 shows the typical structures visualized from this imaging window.

Left Hemidiaphragm

The left hemidiaphragm is usually better imaged from the posterior axillary line than from the mid-axillary line, thus the hand holding the transducer should be touching the bed (i.e., "knuckles on the stretcher") if the patient being imaged is in

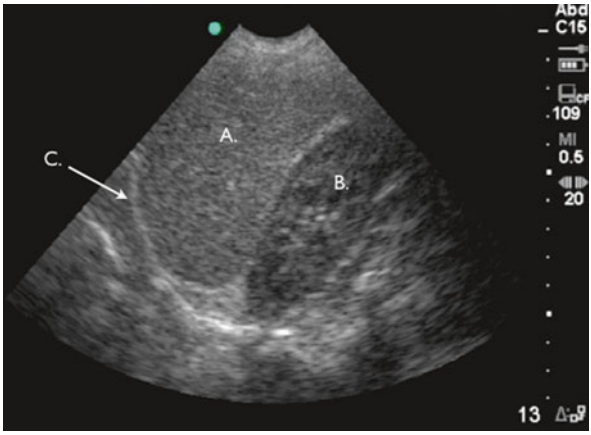

Fig. 12.18 Normal view of *left upper* quadrant structures from Point C. *A* spleen, *B* left kidney, *C* left hemidiaphragm (Image courtesy of Amie H. Woods, MD)

the supine position. The probe marker should be oriented cephalad, with the probe at the level of the 8th to 10th intercostal space. Carefully rotate the transducer to minimize the effects of rib shadow. The left hemidiaphragm will be visualized as a curving hyperechoic line (Fig. 12.18).

Spleen

The spleen can be imaged at the same time as the left hemidiaphragm. Spleen echogenicity is almost the same as the liver. It will be more posteriorly located and smaller than the liver. The spleen is mainly utilized as a guide to locate the left kidney or the diaphragm and to identify fluid in the adjacent splenorenal recess. Examination of the spleen itself is of less utility to the intensivist compared to other organs; however, the splenorenal recess should be carefully imaged to assess for the presence or absence of free fluid/ascites.

Left Kidney

Technical Aspects: Identification of the Left Kidney

Ultrasound of the left kidney is technically more challenging than the right kidney due to its more posterior anatomical position. The ultrasound probe needs to be positioned more posteriorly than on the right. First, locate the spleen, which should be located just beneath the left diaphragm. Carefully move the transducer caudally to see if you can visualize the left kidney, normally just beneath the spleen. Observe closely the splenorenal space for ascites/free fluid. Be sure to image the entire length of the kidney to its inferior pole.

Basic Competencies: Left Kidney

The basic competencies when examining the left kidney are identical to the right kidney outlined above. Kidney size should be measured, the renal pelvis should be examined for hydronephrosis, and a qualitative evaluation of the renal cortex, especially its echogenicity, should be done systematically, as on the right.

Ascites and Pleural Effusion

Analogous to Point A, Point C is a convenient window to rapidly assess for the presence of ascites (in the splenorenal space) and for a left pleural effusion (an anechoic space above the left hemidiaphragm).

Point D: Suprapubic

The Bladder

Technical Aspects: Imaging the Bladder

When scanning the bladder, the transducer should be placed just above the pubic symphysis, with the probe orientation marker positioned facing the patient's right for a transverse view of the bladder (Fig. 12.19). The transducer should be angled very low, almost parallel to the body surface. A common mistake is that the examiner will angle the transducer too high or perpendicular to the body surface. The bladder will be visualized as a rectangular structure with a hypoechoic internal space and hyperechoic wall. By rotating the probe marker cephalad, a longitudinal view of the bladder can be obtained.

Note that the seminal vesicles and prostate (in men) can be visualized deep to the bladder on the transverse view, with the seminal vesicles appearing as paired hypoechoic structures deep to the hyperechoic far bladder wall. The prostate appears more echogenic, and may indent the posterior bladder wall if hypertrophic; and the rectum may be visualized deep to the prostate. On longitudinal view, the prostate will be seen along the caudad aspect of the bladder. The uterus (in women) can similarly be visualized from the suprapubic view relatively deep and superior to the bladder.

Basic Competencies: Assessment of Bladder Filling and Free Fluid

If a patient is oliguric or anuric, assessment of the bladder by ultrasound may help to determine the cause of the lack of urine output. In an anuric patient with a full or overdistended bladder, the point of urinary tract obstruction is likely distal, at the

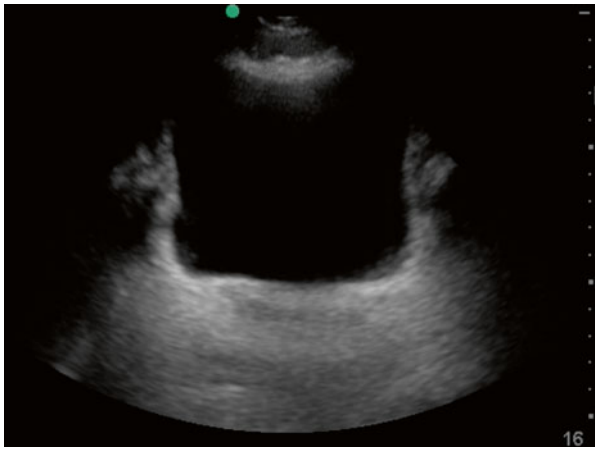

Fig. 12.19 Full Bladder (transverse view). The full bladder can be seen as a rectangular structure with hyperechoic walls and a hypoechoic internal space

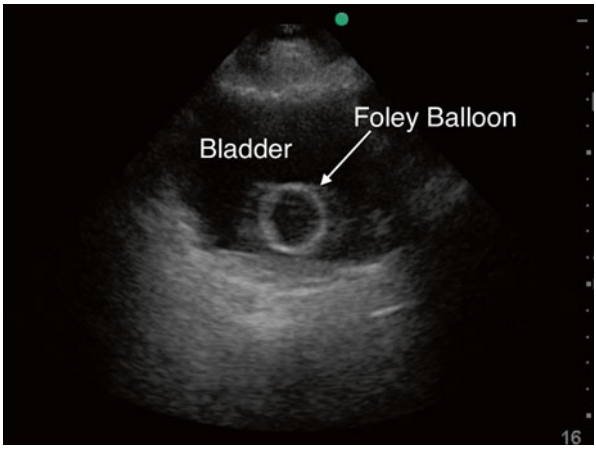

Fig. 12.20 Blocked Foley catheter in bladder (transverse view). Note that the bladder is full of urine despite the presence of the Foley catheter. Changing the Foley catheter relieved the obstruction, allowing urine flow

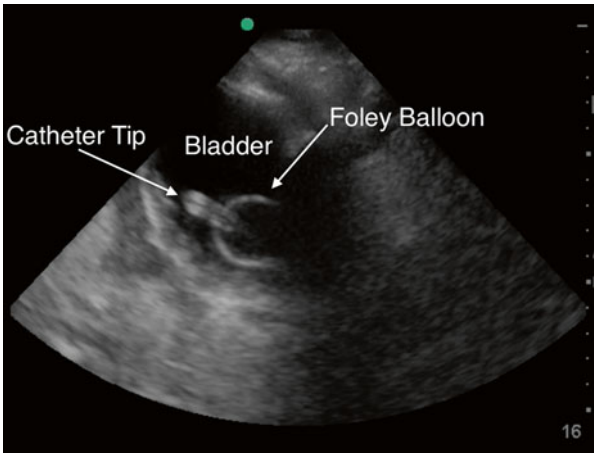

Fig. 12.21 Blocked Foley catheter (sagittal view). Same view of Foley catheter in the bladder from a different orientation

bladder outlet or urethra. When a Foley catheter is visualized surrounded by hypoechoic urine in the bladder, that means the catheter itself is obstructed and should be flushed or replaced (Figs. 12.20 and 12.21). However, if the bladder is collapsed in an anuric patient, this indicates either more proximal obstruction(s) or simply a lack of urine production. Imaging information from this view should thus be correlated with the views of the kidneys at Points A and C in this imaging schema. Stones may be seen as bright structures within the bladder lumen with acoustic shadowing. When imaging from point D, also assess for anechoic spaces posterior to the uterus and between uterus and bladder (in women) or between the bladder and rectum (in men) indicating the presence of free intraperitoneal fluid. Larger amounts of free fluid may also be observed to collect superior to the bladder.

Evidence Review and Evidence-Based Use of Critical Care Abdominal Ultrasound

The use of the FAST exam in trauma has been the most well-studied application of emergency abdominal ultrasound. This evidence is reviewed in Chap. 14. While there is agreement that aspects of abdominal ultrasound should be incorporated into the assessment of the nontrauma critically ill patient [3], a generalized approach to this aspect of critical care ultrasound has not been well studied. A combined abdominal and cardiac evaluation for patients with shock has been proposed, and is intuitively appealing, though without systematic supportive evidence [8] (approaches such as the Abdominal and Cardiac Evaluation with Sonography in Shock [ACES] evaluation and this location-specific approach require validation through further study.

However, there are studies to support specific aspects of the proposed critical care abdominal ultrasound exam. For example, there is relatively extensive data on the use of point-of-care abdominal ultrasound in the emergency setting in symptomatic patients to assess for abdominal aortic aneurysm. A systematic review of studies of emergency department bedside ultrasound for suspected abdominal aortic aneurysm showed very high pooled sensitivity and specificity (99 %, 95 % CI 96–100 % and 99 %, 95 % CI 97–99 %, respectively) [9]. Additionally, emergency physicians have been shown to attain reasonable sensitivity (86.8 %, 78.8–92.3 %) [10] and specificity (92 %, 84–100 %) [11] for the diagnosis of hydronephrosis. These studies suggest that aspects of abdominal ultrasound carried out in an emergency setting and focused on specific diagnostic problems can be highly successful. However, incorporating a more systematic examination into the daily care of the intensive care unit patient may pose different challenges, and the diagnostic and clinical return on the investment of time deserves further examination.

Conclusions

The proposed location-specific approach to abdominal ultrasound in the critically ill allows for a systematic framework for an intensivist-driven bedside ultrasound evaluation of intra-abdominal pathology. This approach provides an extensive, though not comprehensive, evaluation of numerous organ systems and potential pathologies to supplement the clinical examination and may aid in the rapid diagnosis and triage of specific conditions in the ICU.

References

1. Miletic D, Fuckar Z, Sustic A, Mozetic V, Stimac D, Zauhar G. Sonographic measurement of absolute and relative renal length in adults. J Clin Ultrasound. 1998;26:185–9.
2. Mayo PH, Beaulieu Y, Doelken P, et al. American college of chest physicians/La Societe de Reanimation de Langue Francaise statement on competence in critical care ultrasonography. Chest. 2009;135:1050–60.

3. Scalea TM, Rodriguez A, Chiu WC, et al. Focused assessment with sonography for trauma (FAST): results from an international consensus conference. J Trauma. 1999;46:466–72.
4. KDOQI. Clinical practice guidelines for chronic kidney disease: evaluation, classification, and stratification. 2004. http://www.kidney.org/professionals/kdoqi/guidelines_ckd/p5_lab_g6.htm. Accessed 22 May 2014.
5. Lichtenstein D, Lichtenstein D. Whole body ultrasonography in the critically ill. Heidelberg/New York: Springer; 2010.
6. Atkinson PR, McAuley DJ, Kendall RJ, Abeyakoon O, Reid CG, Connolly J, Lewis D. Abdominal and cardiac evaluation with sonography in shock (ACES): an approach by emergency physicians for the use of ultrasound in patients with undifferentiated hypotension. Emerg Med J. 2009;26:87–91.
7. Dent B, Kendall RJ, Boyle AA, Atkinson PR. Emergency ultrasound of the abdominal aorta by UK emergency physicians: a prospective cohort study. Emerg Med J. 2007;24:547–9.
8. Bentz S, Jones J. Towards evidence-based emergency medicine: best BETs from the Manchester Royal Infirmary. Accuracy of emergency department ultrasound scanning in detecting abdominal aortic aneurysm. Emerg Med J. 2006;23:803–4.
9. Rubano E, Mehta N, Caputo W, Paladino L, Sinert R. Systematic review: emergency department bedside ultrasonography for diagnosing suspected abdominal aortic aneurysm. Acad Emerg Med. 2013;20(2):128–38.
10. Gaspari RJ, Horst K. Emergency ultrasound and urinalysis in the evaluation of flank pain. Acad Emerg Med. 2005;12:1180–4.
11. Torres-Macho J, Antón-Santos JM, García-Gutierrez I, de Castro-García M, Gámez-Díez S, de la Torre PG, Latorre-Barcenilla G, Majo-Carbajo Y, Reparaz-González JC, de Casasola GG, Working Group of Clinical Ultrasound, Spanish Society of Internal Medicine. Initial accuracy of bedside ultrasound performed by emergency physicians for multiple indications after a short training period. Am J Emerg Med. 2012;30:1943–9.

Chapter 13
Intensive Care Unit Ultrasound for Venous Thromboembolism

Genese Lamare and Chee M. Chan

Introduction

Venous thromboembolism (VTE) remains a major concern for the intensivist, both de novo in the form of a massive pulmonary embolus (PE) leading to intensive care unit (ICU) admission and when VTE is acquired within the ICU as a complication of other critical illness. Nonspecific symptoms associated with PE render it difficult to diagnose. Symptoms can range from simple shortness of breath to syncope to shock to cardiac arrest. The vague clinical presentation of PE requires astuteness on the part of the clinician to pursue diagnostic testing, particularly in those patients who are unable to express their symptoms. Adding to this diagnostic conundrum are limitations in available testing modalities and in the critically ill patient's ability to travel due to hemodynamic derangements. For example, computed tomography (CT) of the chest with PE protocol is often not feasible in those who suffer from impaired renal function, while intubated patients are unable to make conscious inspiratory efforts, thus precluding much meaningful information to be gained from ventilation perfusion scintigraphy (V/Q scan).

Further complicating this equation is the high incidence of deep vein thrombosis (DVT) and PE among critically ill patients. Despite numerous available options for thromboprophylaxis, up to 12 % of patients in a mixed medical-surgical ICU [1, 2] and approximately 30 % of trauma patients still develop DVT [3]. More concerning

G. Lamare, M.D. (✉)
Department of Pulmonary & Critical Care Medicine, MedStar Washington Hospital Center,
110 Irving St. NW #2A-68, Washington, DC 20010, USA
e-mail: genese.lamare@gmail.com

C.M. Chan, M.D., MPH, FCCP
Department of Pulmonary & Critical Care Medicine, Washington Hospital Center,
110 Irving Street NW #2B-39, Washington, DC 20010, USA
e-mail: chee262@hotmail.com

M. Jankowich, E. Gartman (eds.), *Ultrasound in the Intensive Care Unit*,
Respiratory Medicine, DOI 10.1007/978-1-4939-1723-5_13

is the close relationship between DVT and PE, whereby the majority of PEs originate from a lower extremity (LE) DVT [4]. This worrisome nexus between undiagnosed DVT leading to subsequent PE is a critical missed opportunity when PE is massive and compromises hemodynamic stability, as this situation is associated with mortality rates of approximately 25 % [5]. This illustrates the need to maintain a high clinical suspicion for VTE, since limitations in the cardiopulmonary reserve of critically ill patients will result in substantial morbidity and mortality from undiagnosed VTE. Exemplifying this point are multiple autopsy reports documenting that PE is the most commonly missed major diagnosis in the ICU [6, 7]. Conversely, coagulopathy associated with critical illness contributes to the need to definitely diagnose VTE so that the risk-benefit ratio of bleeding from full dose anticoagulation can be carefully weighed in this high-risk population. Since timely treatment has been demonstrated to affect vital outcome for VTE, timely diagnosis is imperative.

The many limitations to obtaining definitive imaging for VTE in critically ill patients underscore the need for portable, bedside tests to aid in making a diagnosis. The increasing use and accessibility of ultrasonography in the ICU setting provide an ideal opportunity to improve VTE diagnosis. Although ultrasound may be unable to provide a definitive diagnosis of PE, the presence of a DVT strengthens clinical suspicion and allows the clinician to initiate treatment for VTE. In conjunction with the appropriate clinical setting, other ultrasonographic findings, such as thrombus in the right atrium (RA) or right ventricle (RV), RV strain, and McConnell's sign, assist in the diagnosis and management of VTE in the critically ill patient. Furthermore, in patients already diagnosed with PE, ultrasound will assist in determining both the level of care required by the patient as well as whether more aggressive therapy is necessary.

One of the most appealing characteristics of ultrasound is the ability to acquire crucial information rapidly, at the bedside, and in a noninvasive fashion. For the diagnosis of DVT, venous ultrasononography is already the first-line modality. With a sensitivity of 97 % and specificity of 94 % in symptomatic patients, clinicians should not hesitate in initiating treatment when a DVT is found by ultrasound or in withholding treatment for DVT if the examination is negative [8–10]. Currently, the biggest rate-limiting step associated with LE ultrasonography is the availability of skilled technicians to perform such studies 24 h a day and 7 days a week. Furthermore, a radiologist is typically required to review and interpret the ultrasound images. However, waiting for others to perform this test can cause substantial delays in therapy or can needlessly subject critically ill patients to the bleeding risk of full dose empiric anticoagulation. It therefore behooves the intensivist to become proficient at performing a focused bedside vascular ultrasound. With proper training and experience in using portable handheld ultrasound devices, rapidly obtained and interpreted images can be applied in combination with clinical factors to expedite VTE diagnosis and treatment.

Technical and Patient Considerations

The first bedside test used to diagnose VTE in the ICU is LE ultrasonography. Complete color-flow duplex ultrasonography, combining B-mode with Doppler flow analysis, is the most common examination performed when DVT is suspected. However, a full duplex ultrasound of the LEs is time consuming, taking approximately 30 min to complete. Also, color flow analysis has not been shown to improve sensitivity or specificity when compared to limited compression ultrasonography (CUS), which is just as accurate, sensitive, and specific for diagnosing DVT [11–13]. In fact, the sensitivity and specificity of a limited compression exam is 100 % and 98 %, respectively [12]. The trained practitioner can perform a limited CUS in 5 min and at any time of the day or night at the bedside, precluding the need to wait for vascular technicians and/or radiologists when the diagnosis is time sensitive. The CUS exam is performed while the patient is lying supine, with the head of the bed raised at 30–45° to maximize venous return (consider also reverse Trendelenburg position in patients who have spinal precautions), making this examination ideal for the intubated or hemodynamically compromised patient.

A high-resolution linear array transducer is needed to examine the peripheral vascular system. Probe frequencies typically range from 7 to 10 MHz, with higher frequencies allowing for better resolution and more detail, at the price of decreased depth of penetration. Occasionally, lower frequency 5 MHz probes can be considered for obese patients or in the presence of significant LE edema to overcome depth limitation. Although color and pulse-wave Doppler are not required for the examination, most portable machines currently have these capabilities, which can aid in delineating vasculature. Applying color allows the sonographer to view color pulsations indicating an arterial pattern of blood flow when placed over an artery. When placed over a vein, some color might be seen in the vessel, but flow will not be pulsatile (Fig. 13.1). Similarly, when pulse-wave Doppler is placed over an artery, a pulsatile flow tracing is seen.

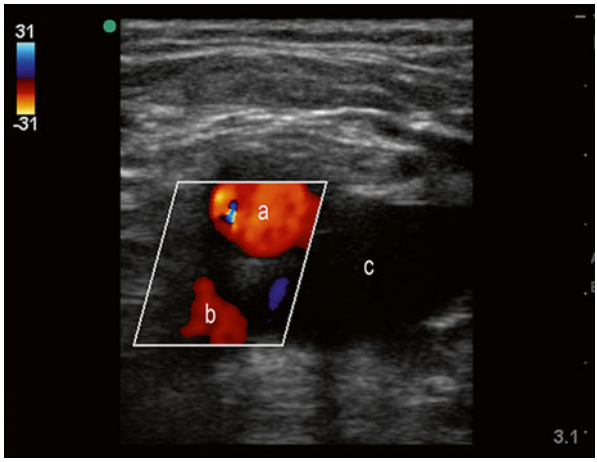

Fig. 13.1 Color Doppler is used to distinguish the superficial (**a**) and deep (**b**) femoral arteries from the common femoral vein (**c**)

In situations where PE is a major concern, identification of a DVT allows the clinician to institute immediate anticoagulant therapy. However, caution must be exercised when no DVT is identified as up to 40 % of patients with a PE do not have a DVT [14]. Additionally, it is important to remember that the diagnosis of PE cannot be made explicitly with ultrasound. The utility of bedside echocardiography in the evaluation of PE augments clinical suspicion in hemodynamically unstable patients who cannot safely undergo a definitive test. Thus, ultrasonographic testing for PE is most helpful when typical findings of RV strain are absent, so that massive PE can be ruled out as part of a differential for shock of unknown etiology. Conversely, when submassive or massive PE is suspected in someone already known to have VTE, the presence of RV strain confers higher mortality.

Limited bedside echo performed to evaluate for signs consistent with PE is done using a phased-array, 2–4 MHz probe. The standard echo views are the parasternal long, parasternal short, subcostal long, and apical four-chamber. These views are easiest to obtain with the patient lying on the left side; however, this positioning is often not feasible for critically ill patients who cannot follow commands. Thus, these views are frequently obtained with the patient lying supine.

Image Acquisition and Interpretation

Sonographic diagnosis of a DVT is made by visualizing echogenic material within the lumen of a vein and/or by identifying a non-compressible venous segment. Determination of venous compressibility (visualizing complete collapse of the vessel lumen when adequate pressure is applied) or incompressibility (absence of venous collapse with adequate pressure) is the most reliable diagnostic sign when determining the presence or absence of a DVT [13]. Pressure is considered adequate when the walls of the adjacent artery become mildly deformed when attempting to compress the vein.

Lower Extremity

Examination of the LE venous system begins proximally at the common femoral vein and ends distally at the trifurcation of the popliteal vein, covering the entire proximal deep vein system. Vessels should be compressed every 1–2 cm between these two points while traveling down the leg. For symptomatic patients, a shorter exam with compression at only two separate points (the common femoral and popliteal veins) is adequate to identify most DVTs (sensitivity: 100 %; specificity: 99 % [15]; PPV 94 % [16]). However, clear evidence to demonstrate the diagnostic accuracy of this shorter examination when screening for asymptomatic DVT is insufficient. One study consisting of 2,704 symptomatic and asymptomatic subjects who required LE ultrasounds found that approximately 20 % of DVTs were missed

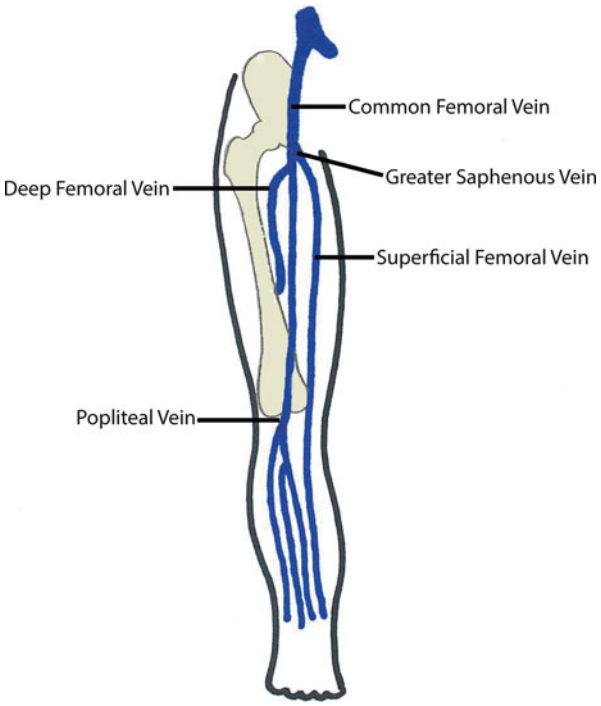

Fig. 13.2 Deep venous anatomy of the lower extremity

when using the shorter exam compared to standard testing [17]. It remains unclear if this high rate of missed DVT was due to the inclusion of asymptomatic patients. Given that the critically ill patient is often unable to communicate, and missing a DVT in this population can have devastating consequences, compressive ultrasonography of the entire proximal venous system of the lower limb is recommended.

Veins in the proximal deep venous system that should be visualized include the common femoral, greater saphenous, superficial and deep femoral and popliteal veins (Fig. 13.2). Of note, the misleadingly named superficial femoral vein is a part of the deep venous system, and thrombus identified in this vein must be treated. Moving from proximal to distal the external iliac artery and vein become the common femoral vessels, with the common femoral vein generally seen medial to the artery. Continuing distally, the greater saphenous vein enters the common femoral vein from the superficial plane. There is no artery accompanying the greater saphenous vein. After this junction, the common femoral vessels divide into the superficial and deep femoral vessels, with all four vessels visible in the transverse ultrasound plane (Fig. 13.3). The superficial femoral artery and vein then become the popliteal artery and vein. Even more distal examination reveals the trifurcation of the popliteal vein into the anterior tibial, posterior tibial and peroneal veins.

Typically, the superficial greater saphenous vein traverses the medial aspect of the leg from ankle to proximal thigh, emptying into the common femoral vein near the inguinal ligament. Because thrombus in the greater saphenous vein has a high

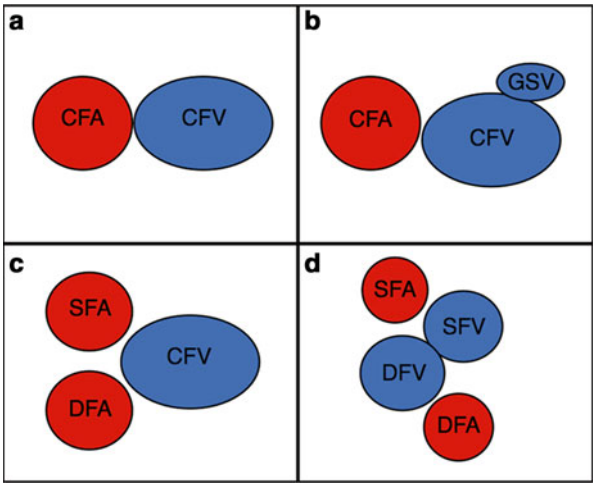

Fig. 13.3 Venous anatomy moving from proximal to distal lower extremity. (**a**) Typical relationship of the common femoral artery (CFA) and common femoral vein (CFV), in inguinal region. (**b**) Moving distally, the greater saphenous vein (GSV) enters the CFV medially. (**c**) Continuing down the leg, first the CFA bifurcates into the superficial femoral artery (SFA) and deep femoral artery (DFA). (**d**) After the artery bifurcates, the CFV bifurcates into the superficial femoral vein (SFV) and deep femoral vein (*DFV*)

likelihood of extending into the common femoral vein, this vein should be carefully evaluated and considered part of the deep venous system [18].

Deep veins of the calf include the anterior tibial, posterior tibial, and peroneal veins; however, debate exists regarding the management of calf DVTs, since the risk of embolization or extension into the proximal system is variable [19]. Routine full examination of the calf is not considered a necessary component of the bedside examination. In moderate to high-risk patients who have a negative initial study for proximal DVT, repeat CUS at a one-week interval is recommended [20]. This allows evaluation for any missed DVT that might have extended from the less concerning distal region into the more dangerous proximal region.

Lower Extremity Image Acquisition and Interpretation

The LE should be exposed from the inguinal region to the popliteal fossa. The leg should be externally rotated and the knee slightly flexed (Fig. 13.4). On the rare occasion when a barrier, such as a dressing, is obscuring the ability to perform an ideal exam, consider removing the barrier and using a sterile probe cover to create a clean interface between the probe and the patient's skin.

A high-resolution ultrasound machine with grayscale imaging and a high-frequency 7–10-MHz linear probe are needed for the examination. Place the transducer just below the inguinal ligament, holding the transducer in a transverse

Fig. 13.4 Proper positioning of the lower extremity: the leg is externally rotated and flexed at the knee

orientation with the indicator pointing toward the operator's left. The common femoral vein and artery should be immediately visible where the vein is typically more medial than the artery (Fig. 13.5). Apply downward pressure until the vein completely collapses to the extent that the walls touch each other. When adequate pressure is applied (demonstrated by visualizing simultaneous deformity of the artery with downward pressure) and the vessel lumen does not collapse or if echogenic material is noted within the vein, the study is diagnostic for a thrombus. If the walls of the vein are seen to completely collapse, pressure is released, and the probe is moved distally by 1–2 cm to find the junction of the greater saphenous vein with the common femoral vein. The greater saphenous vein will be seen entering the common femoral vein medially. When compressed, the lumen of both the greater saphenous and the common femoral veins should completely disappear (Fig. 13.6).

After inspecting the greater saphenous vein, the next important landmark is the bifurcation of the common femoral artery into the superficial and deep femoral arteries, adjacent to the accompanying common femoral vein (Fig. 13.1). The common femoral vein then divides into the deep femoral and superficial femoral veins (Fig. 13.7). In this region distinguishing artery from vein may be difficult, especially

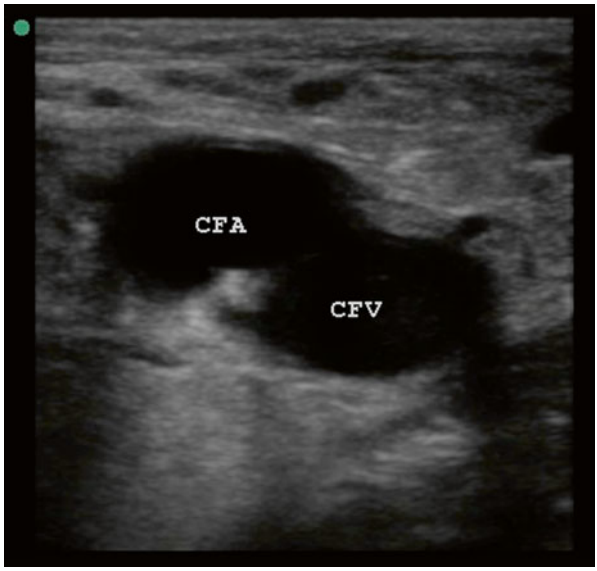

Fig. 13.5 Common femoral artery (CFA) and common femoral vein (CFV) with typical relationship of vein medial to artery in the groin region. Lateral designated by *green dot* in the *left* corner

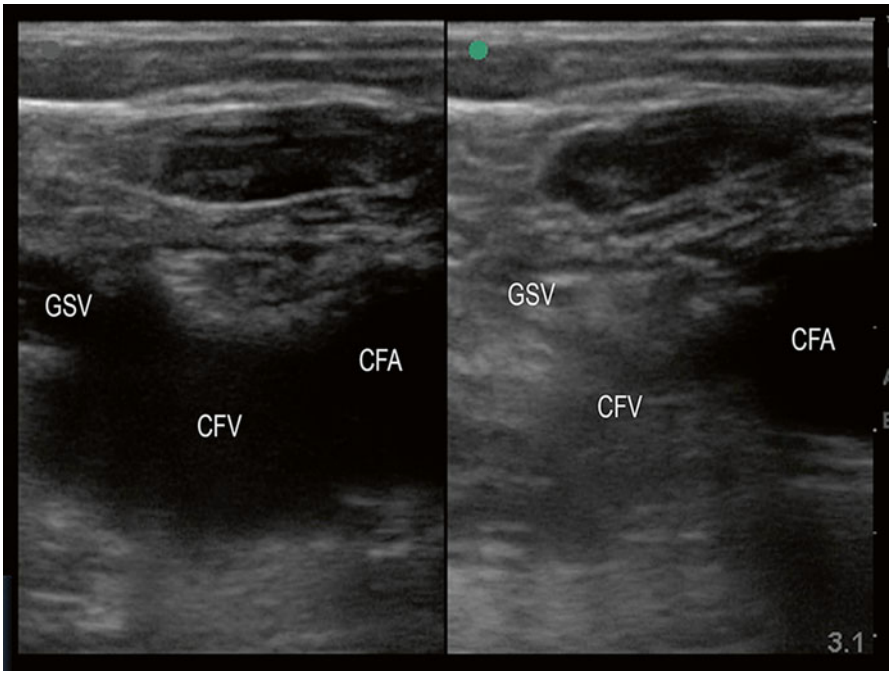

Fig. 13.6 Dual screen mode. *Left*: greater saphenous vein (GSV) enters the common femoral vein (CFV). *Right*: With compression, there is complete obliteration of the GSV and CFV lumen

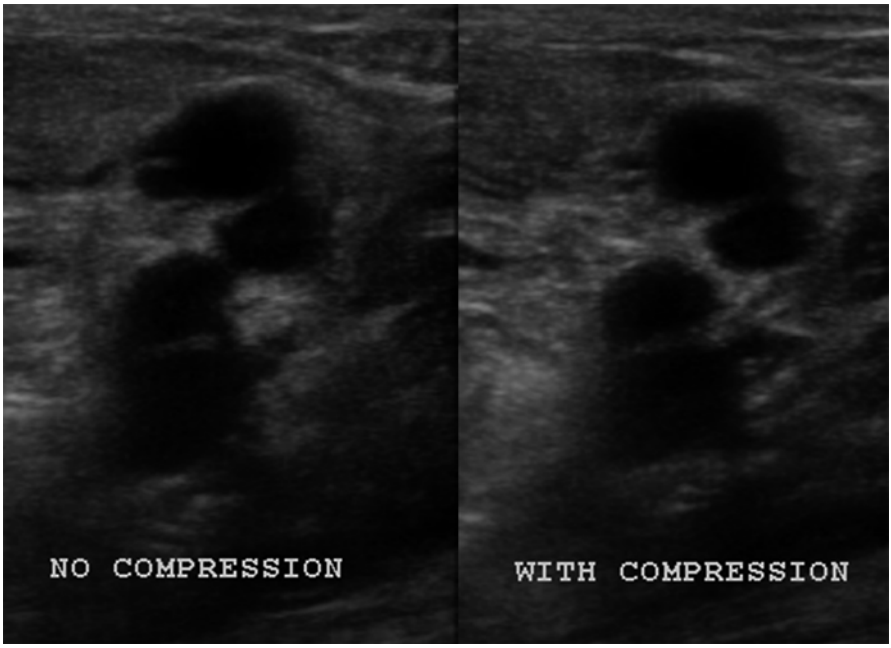

Fig. 13.7 Superficial femoral artery (SFA), superficial femoral vein (SFV), deep femoral artery (DFA), and deep femoral vein (DFV). With compression, none of the vessels collapse in this patient with a DVT in both the SFV and DFV

with larger legs. Use of pulse wave and/or color Doppler is extremely helpful in distinguishing the superficial and deep arteries from the veins. Next, the superficial and deep femoral veins are evaluated in 1–2 cm segments until the deep femoral vein disappears, leaving the superficial femoral vein to be followed as distally as possible.

With the knee flexed 45°, place the transducer in the popliteal fossa to begin examination of the lower leg and popliteal region. After the popliteal artery and vein are identified, and compression of the vein is demonstrated (Fig. 13.8), move down the leg slightly until the veins just distal to the trifurcation of the popliteal vein are visualized and compressed. Though identification of a DVT in the calf veins (distal to the popliteal vein) does not mandate automatic treatment, knowledge of its presence warrants close follow-up with repeat CUS. The consideration to initiate full dose anticoagulation must be carefully weighed in high-risk ICU patients found to have a distal DVT [20].

Once transverse imaging is complete, longitudinal views of the veins serve as a quick check and balance. Returning to the common femoral vein and rotating the ultrasound probe 90°, scan through the common femoral, superficial femoral, and popliteal veins in the longitudinal plane to ensure no intraluminal thrombus is seen. Just like with transverse views, compress the vessels with the probe to ensure that the vessels collapse completely. If thrombus was previously found in the transverse plane, the longitudinal view helps visualize the extent of intraluminal thrombus.

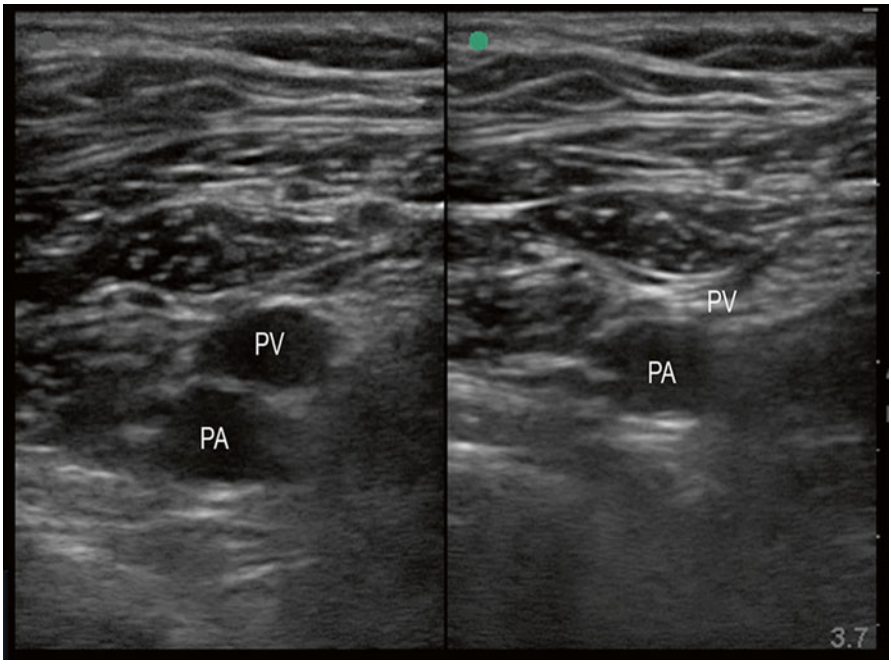

Fig. 13.8 Popliteal artery (PA) and popliteal vein (PV). *Left* screen shows no compression; *right* screen shows disappearance of lumen with compression

Augmentation can sometimes be used in difficult cases (e.g., morbid obesity or edema) to distinguish vasculature. This maneuver requires the application of color Doppler to the vein being visualized, then squeezing the leg at any area distal to the placement of the probe. Augmentation results in a rush of increased venous flow at the level of the probe. Theoretically, greater flow in the vessel rules out thrombus between the level of the vessel being visualized and where the leg is squeezed. However, augmentation does not provide additional meaningful information to the compression study [21] and 17–35 % of patients with DVT still show augmentation [22, 23]. For these reasons, augmentation is not a required part of the LE evaluation and should only be reserved for use when standard LE ultrasonography is inconclusive.

Upper Extremity

Upper extremity (UE) DVTs are not as rare or harmless as once thought. Though less common than LE DVT, they comprise between 10 % and 18 % of all DVTs and carry a risk of embolization, prompting current guidelines from the American College of Chest Physicians to recommend treatment of all proximal (axillary vein or higher) UE DVTs [24–26]. The incidence appears to be rising [27, 28], likely

due to the association between UE DVTs and central venous catheters and an increased recognition that these DVTs are not benign. Because of frequent central venous catheterization, the critically ill population is particularly susceptible to UE DVT, and the possibility of an UE DVT must be given careful consideration in these patients.

The deep venous system of the UE begins with the radial and ulnar veins which meet in the antecubital fossa to become the brachial vein. This vein comprises of two vessels that travel on either side of the accompanying brachial artery throughout the upper arm. Continuing proximally, the basilic vein (a superficial vein) joins the brachial vein and forms the axillary vein; vessels proximal to and including the axillary vein encompass the proximal UE deep venous system. After passing under the clavicle the axillary vein becomes the subclavian vein, which joins the internal jugular (IJ) vein to become the brachiocephalic vein. Similar to the LE deep venous system, ultrasound examination of the UE system requires 1–2 cm compressions between the brachial and IJ veins.

Upper Extremity Image Acquisition and Interpretation

Starting in the supine position, identify the IJ in the transverse plane, sitting adjacent to the carotid artery. Evaluate the lumen of the IJ for visible thrombus, and perform compression. Typically, the IJ can be traced starting at the mastoid and progressing distally to its entry into the brachiocephalic vein. Since compression of the brachiocephalic is not possible because of the overlying clavicle, place color Doppler over the vein and watch for luminal filling from wall to wall. Pulse wave Doppler is then applied to look for presence of flow. Absence or reduction in flow is considered positive for the presence of a DVT. The subclavian vein is then found and traced toward the shoulder above the clavicle, but similar to the brachiocephalic vein, it is not compressible. Doppler interrogation with both pulse wave and color should be used throughout the course of the subclavian vein. Not only will pulse wave Doppler help to identify an area of the vein with clot, it will help to distinguish artery from vein in a confusing and difficult region. Small pulsations will be seen when pulse wave Doppler is applied to the vein, but these pulsations are generally less pronounced than in the artery. Further assisting in differentiation between artery and vein is the demonstration of respiratory variation with venous pulsations. Nearing the shoulder, the proximal portion of the axillary vein will also be obscured by the clavicle, therefore necessitating the continued use of Doppler interrogation of the vessel. Consider elevating and extending the arm outward to help engorge the veins if the distal subclavian and axillary veins are not visualized [29]. Once in the axilla, the brachial vein is compressible as it runs distally toward the antecubital fossa before splitting into the radial and ulnar veins. Throughout the UE examination, visible clot, a non-compressible segment, or lack of Doppler flow is diagnostic for a DVT.

Right Ventricular Evaluation

Limited echocardiography is used to risk-stratify a patient already diagnosed with PE or to determine whether PE might be causing shock. The basic four echocardiographic views to assess RV function are the subcostal long axis, parasternal long axis, parasternal short axis, and apical four-chamber views. On each of these views, the focus is on the RV to evaluate its function, appearance (dilation), and whether the interventricular septum intrudes into the left ventricle (LV), causing obstructive shock. Additionally, visible clot seen swirling in the RA or RV would further strengthen the case for an acute PE.

Right Ventricle Image Acquisition and Interpretation

A 2–4-MHz phased-array transducer is used to find four standard echocardiography windows: parasternal long axis, parasternal short axis, apical four-chamber, and subcostal long axis. Though all four windows should always be obtained, the most helpful windows are the parasternal short axis and the apical four-chamber. A good parasternal short view is generally created after successfully obtaining a clear parasternal long picture. The transducer is placed just to the left of the sternum in the 3rd–4th intercostal space, with the indicator facing toward the patient's right shoulder. Once a clear parasternal long view is obtained showing the RV, LV, mitral valve, aortic outflow tract, and aortic valve (Fig. 13.9), the probe is then rotated 90° clockwise in the same position to produce the parasternal short axis view. This view provides a clear picture of the LV (typically round in appearance) with the RV seen to the top left of the image screen (Fig. 13.10). The transducer should be adjusted until the papillary muscles are clearly seen in the LV. The presence of RV strain is demonstrated by a dilated RV as it wraps around the LV. In cases where a PE is causing obstructive shock secondary to RV pressure overload, the septum between

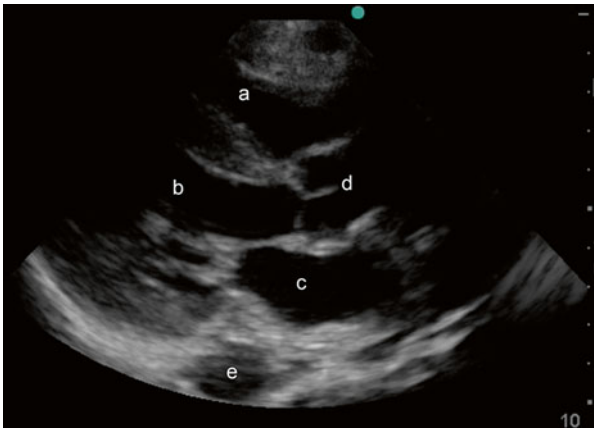

Fig. 13.9 Parasternal long axis view showing the right ventricle (**a**), left ventricle (**b**), left atrium (**c**), aortic valve and aortic outflow tract (**d**), and descending thoracic aorta (**e**)

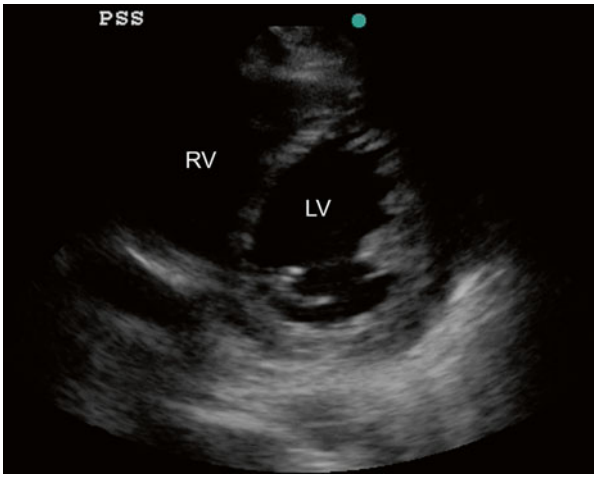

Fig. 13.10 Parasternal short axis view at the level of papillary muscles showing the right ventricle (RV) and circular left ventricle (LV)

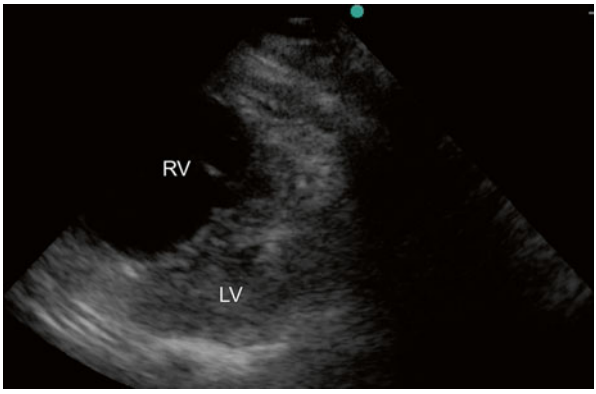

Fig. 13.11 Parasternal short axis view showing a large and dilated right ventricle (RV) with a flattened D-shaped septum and an almost obliterated left ventricle (LV) cavity during systole, due to pressure overload

the RV and LV will be pushed into the LV lumen. The LV will then lose its round appearance and adapt a flattened shape, commonly referred to as a "D-shaped septum" (Fig. 13.11). The apical four-chamber view is obtained by sliding the probe laterally to the apex of the LV, at the point of maximum impulse, with the indicator facing the patient's left side. This view shows the RA, RV, left atrium, and LV with the corresponding valves (Fig. 13.12). Knowing that the RV is normally approximately 60 % of the size of the LV, evidence of a large, dilated RV or an interventricular septum that pushes into the LV suggests hemodynamically significant PE in undifferentiated shock. This view also allows for evaluation of McConnell sign (normal apical movement with decreased RV free wall contractility) and for presence of abnormal echogenic densities within the RA or RV signifying the presence of clot. Absence of all of these findings makes PE an unlikely cause of shock.

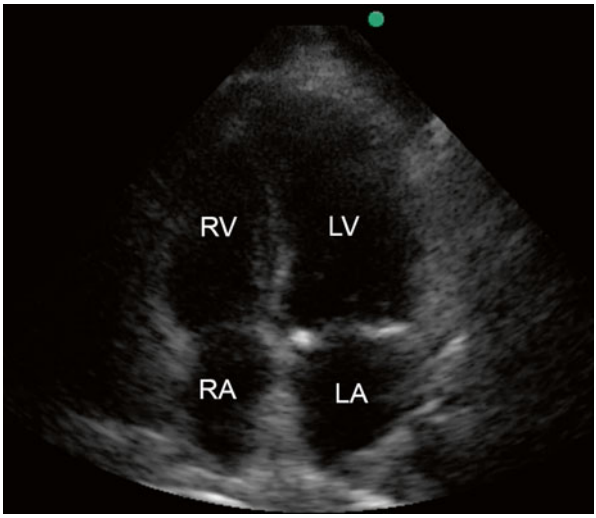

Fig. 13.12 Apical four-chamber view showing the left atrium (LA), left ventricle (LV), right atrium (RA), and right ventricle (RV)

Basic Competencies

Examination of the LE deep venous system with compression ultrasonography remains the most rapid and straightforward evaluation for deep vein thrombi. This technique should be mastered prior to moving on to more advanced evaluations for VTE, such as upper extremity ultrasonography and right heart echocardiography. These more advanced evaluations require additional time, knowledge, training, and technical skill.

Advanced Competencies

Evaluation of the Upper Extremity Venous System

Though an important consideration in the ICU patient, ultrasound examination of UE veins is more challenging than the LE evaluation, and is less accurate with a sensitivity and specificity of 82 % and 82 %, respectively [30]. Much of the examination's difficulty arises because the axillary and subclavian veins are not easily compressible. This is in contrast to the LE examination where all veins are easily compressed throughout the leg. Indirect confirmation of vein patency becomes much more important in this study, and the use of color and pulse wave Doppler to assist with determining blood flow is key.

Evaluation of the Right Ventricle

The role of echocardiography for PE is twofold. In the ideal and classic scenario, it is used to risk stratify those who have already been diagnosed with PE. In the more difficult scenario, this modality of testing is used to augment the clinical suspicion for PE. Echocardiography to evaluate for PE is reserved for the subset of patients who are acutely hemodynamically unstable. The intent is not to definitively diagnose PE via ultrasound but rather to rule out PE as the immediate cause of shock. Evidence of clot within the RA, RV, or pulmonary artery and/or the presence of RV pressure overload or dysfunction are the key echocardiographic findings associated with hemodynamically significant PE. Absence of any RV abnormality essentially excludes PE as the etiology for hemodynamic instability [31]. The combined approach of evaluating the LEs and the RV for signs consistent with thrombus will allow the clinician to more confidently rule out VTE as a cause of shock.

Lung Evaluation for PE

Thoracic ultrasound is an additional potential bedside modality that can aid in the diagnosis of PE. In cases of pulmonary infarction after PE, typical round- or wedge-shaped pleural lesions can develop as rapid breakdown of surfactant causes atelectasis, transudation of fluid, and cell infiltration of the affected lung [32]. This examination requires the provider to carefully scrutinize the pleura for well-demarcated, triangular- or circular-, hypoechoic lesions, and is considered positive for PE when one or more pleural-based lesions are appreciated. In approximately 42–50 % of cases, a concomitant pleural effusion is also noted [32, 33]. Studies evaluating the utility of thoracic ultrasound in diagnosing PE resulted in sensitivities between 74 % and 90 % and specificities ranging from 60 % to 95 %. In these studies, individuals suspected of having PE received thoracic ultrasonography while undergoing confirmatory testing for their PE. Complicating the feasibility of this modality is that experienced thoracic sonographers performed testing in these studies [32–34]. Thus, the variation in sensitivity and specificity, the experience of the bedside clinician, and the clinical suspicion for PE must be considered carefully when using thoracic ultrasound to look for PE.

Evidence Review and Evidence-Based Use

Accuracy and Speed

The cornerstone of peripheral venous system DVT evaluation hinges on venous compressibility. Much of the data comparing CUS with gold-standard venography was compiled using symptomatic patients. In these patients, CUS had a high

sensitivity and specificity (97 % and 94 %, respectively) [8]. Some caution must be exercised in asymptomatic patients, as the sensitivity of CUS in this group decreases to 62 %, though the specificity is similar (94 %) [8]. Few studies have specifically looked at CUS in ICU patients, but current evidence demonstrates that specificity is maintained (>95 %) [35, 36]. For example, Kory and colleagues performed a multicenter, retrospective study on 128 critically ill patients with physical examination findings concerning for DVT or in whom there was a high clinical suspicion for PE [36]. These patients had bedside CUS by pulmonary and critical care fellows and attending physicians. When compared to formal vascular ultrasound studies, bedside CUS yielded a sensitivity of 86 %, a specificity of 96 %, and a diagnostic accuracy of 95 %. A recent systematic review further confirms the accuracy of bedside CUS among emergency physicians. In a pooled analysis consisting of 16 studies ($n = 2{,}379$ subjects suspected of having DVT), the mean sensitivity was 96.1 % (95 % confidence interval [CI]: 90.5–98.5 %) and the mean specificity was 96.8 % (95 % CI: 94.6–98.1 %) [37]. Further, after proper training and experience, CUS of the LE can be performed accurately in less than 4 min. In a prospective study that included 112 emergency department patients suspected of being high risk for having a DVT, physicians were timed while performing color duplex ultrasound examinations of the LEs [22]. Median examination time was 3:28 min (95 % CI: 2:45–4:02; interquartile range: 3:09). There was minimal interobserver variability between examinations performed by these physicians and official studies performed by the vascular laboratory with 98 % agreement (95 % CI: 95.4–100 %; kappa = 0.90).

UE CUS has comparable sensitivity and specificity for the detection of DVT. A systematic review evaluated the ability of CUS, Doppler ultrasonography, and Doppler ultrasonography with compression to accurately diagnose UE DVT when compared to venography [38]. A total of 17 studies were included yielding a sample size of 793 subjects. Sensitivity estimates were 97 % (95 % CI: 90–100 %) for CUS, 84 % (95 % CI: 72–97 %) for Doppler ultrasonography, and 91 % (95 % CI: 85–97 %) for combined Doppler ultrasonography with compression. The estimated specificities were 96 % (95 % CI: 87–100 %), 94 % (95 % CI: 86–100 %), and 93 % (95 % CI: 80–100 %), respectively. However, there were substantial limitations to the studies included in this analysis. The operators were radiologists or vascular technicians, many of the studies included outpatients, and the methodological quality was often poor. Presently, there is a lack of data pertaining to this topic in critically ill patients, and the accuracy of clinician-performed ultrasonography for upper extremity DVT in the ICU is therefore unknown.

Right Ventricular Evaluation

Echocardiographic evidence of clot in the RA, RV, or pulmonary artery is the most helpful sign. Unfortunately, this finding is extremely rare (4 %), necessitating further evaluation for signs of RV strain [39]. The evidence base for the following RV strain signs is the most robust: (1) signs of RV overload such as increased RV

diastolic dimension or systolic flattening of the intraventricular septum; (2) the "60/60 sign" which describes a RV ejection acceleration time of <60 ms in the setting of a tricuspid insufficiency jet of <60 mmHg; and (3) the McConnell sign. RV strain indicating massive or submassive PE, as demonstrated by echocardiography, is a poor prognostic sign. In a randomized, controlled trial where subjects with submassive PE were randomized to unfractionated heparin (UFH) and alteplase versus UFH alone, the overall mortality ranged from 2.2 % to 3.4 % [40]. More concerning, the mortality rates for those with massive PE were found to be even higher in a systematic review that compared the use of thrombolytic therapy versus placebo [41]. When thrombolytic therapy was administered, the mortality rate in this pooled analysis of 5 trials ($n=254$) was 6.2 % but was as high as 12.7 % for those who received placebo. Moreover, approximately 20 % of patients with RV strain at the time of diagnosis of PE will die within 3 months [42, 43]. Thus, the use of echocardiography is essential to risk stratify patients with acute PE.

When echocardiography is used to facilitate the diagnosis of PE, its use is most helpful in the setting of hemodynamic instability. Kucher and colleagues determined that PE can safely be ruled out when signs of RV strain are absent for these subjects [43]. In a prospective intervention study, 204 consecutive patients suspected of having PE were risk stratified according to the shock index and clinical pretest probability for PE. Of the 21 subjects who were in shock, all 7 subjects who had preserved RV function were excluded from PE with confirmatory spiral CT of the chest. The remaining 14 subjects who had echocardiographic evidence of RV dysfunction had confirmatory testing diagnostic for PE. Hence, the absence of signs of RV dysfunction safely rules out VTE as the cause of undifferentiated shock.

In patients who are hemodynamically stable, echocardiogram findings of RV dysfunction are insensitive for VTE. Of the above signs, the McConnell sign and the 60/60 sign have the highest specificity, but both tests have very low sensitivity [44, 45]. Among 100 consecutive patients with acute PE, the sensitivity and specificity for the McConnell sign was 19 % and 100 %, respectively, and 25 % and 94 % for the 60/60 sign [44]. In the setting of patients with known cardiorespiratory disease, the specificity and PPV of the 60/60 sign decrease to 89 % and 82 %, respectively. In this same study, RV overload signs had better sensitivity (81 %) but poor specificity (45 %) for PE. Though the sensitivity of RV overload signs for PE is better than that seen with the McConnell sign or the 60/60 sign, this sensitivity also decreases dramatically in patients with known cardiopulmonary disease [31]. Furthermore, presence of the McConnell sign is also often noted in patients with RV infarction. In a retrospective study of 201 patients with either massive or submassive PE or RV infarction, two experienced echocardiographers who were blinded to diagnosis reviewed cardiac ultrasound images for McConnell sign [46]. The sensitivity, specificity, positive, and negative predictive values of the McConnell sign for the diagnosis of PE were 70 %, 33 %, 67 %, and 36 %, respectively. Thus, given the limitations associated with these echocardiographic findings to diagnose PE when shock is absent, these findings must be used in combination with the appropriate clinical scenario when definitive testing for PE is not possible.

Pitfalls and Precautions

There are many benefits to focused bedside ultrasound, but the limitations of this test must also be appreciated. First, it is oftentimes difficult to distinguish the artery from the vein. This can be due to the patient's body habitus, the presence of anasarca, or clinician inexperience. In these cases, consider the use of color or pulse wave Doppler to assist in differentiating the vasculature.

Second, proficiency and confidence using the ultrasound machine requires a substantial amount of time and experience. With practice, the technical aspects of the examination will become much easier. Small adjustments in the probe angle lead to major changes in the picture obtained. Thus, nuanced manipulation of the probe has higher yield than large movements. For example, in a DVT study, if the probe is not perpendicular to the vein during compressions, the vessel may not fully flatten. Conversely, when using color Doppler over a vessel, flow will not be seen unless the probe is angled.

A third potential pitfall for ultrasound is the need to perform the same steps systematically for each exam. Incomplete studies will produce more false negative results. For a LE DVT study, the entire proximal deep venous system must be adequately visualized with compression of the common femoral vein, greater saphenous junction, and then continuously down the leg and through the superficial femoral vein in 1–2 cm increments. This should be completed with an evaluation of the popliteal vein. Similarly, for the UE, visualization of the IJ, brachiocephalic, subclavian, axillary, and brachial veins must be diligently obtained. When assessing the heart for signs of PE, all four cardiac images should be performed. A single view that appears to show RV dilation is not sufficient to claim the presence of PE. Abnormal images must be confirmed with additional views. Given the sensitivity and specificity of the 60/60 and McConnell signs, the presence of these signs should not automatically conclude a diagnosis of PE but must be carefully correlated to the clinical scenario.

Finally, visualization of a clot is challenging. Slow-flowing blood has a wispy echogenic appearance that may easily be mistaken for clot. Artifact caused by body habitus or technical issues with the connection of the ultrasound transducer can create bright reflections leading to misidentification of thrombus. In each of these situations, the vessel should still be compressible if clot is absent. Further complicating this issue is that lymph nodes are often confused as clots within a vessel. They typically have a classic hypoechoic rim with a hyperechoic center. Comprehensive knowledge of the anatomy and clearly identifying the expected vessels will help avoid this pitfall. More importantly, it is crucial to remember that absence of visualization of clot does not rule out DVT, as many clots are anechoic. When no clot is visualized, venous compressibility or Doppler flow must be performed to confirm vessel patency. Regardless of any of the above limitations, when inadequate or unclear images are obtained leading to uncertainty regarding the study results, additional confirmatory testing should be performed to ensure patient safety.

Conclusion

The use of ultrasound in the ICU is becoming increasingly more common. With dedicated hands-on practice and an understanding of anatomy, bedside sonography assessing for VTE can be incorporated into the routine assessment of patients in the ICU. The ability to obtain immediate, noninvasive information on DVT and to rule out RV dysfunction from PE as a cause of undiagnosed shock using bedside sonography is invaluable and exciting. This useful skill can save time and allow for safe and appropriate treatment of critically ill patients.

References

1. Marik PE, Andrews L, Maini B. The incidence of deep venous thrombosis in ICU patients. Chest. 1997;111(3):661–4.
2. Cook D, Meade M, Guyatt G, Walter S, Heels-Ansdell D, Warkentin TE, et al. Dalteparin versus unfractionated heparin in critically ill patients. N Engl J Med. 2011;364(14):1305–14.
3. Geerts WH, Jay RM, Code KI, Chen E, Szalai JP, Saibil EA, et al. A comparison of low-dose heparin with low-molecular-weight heparin as prophylaxis against venous thromboembolism after major trauma. N Engl J Med. 1996;335(10):701–7.
4. Cook D, Attia J, Weaver B, McDonald E, Meade M, Crowther M. Venous thromboembolic disease: an observational study in medical-surgical intensive care unit patients. J Crit Care. 2000;15(4):127–32.
5. Kasper W, Konstantinides S, Geibel A, Olschewski M, Heinrich F, Grosser KD, et al. Management strategies and determinants of outcome in acute major pulmonary embolism: results of a multicenter registry. J Am Coll Cardiol. 1997;30(5):1165–71.
6. Landefeld CS, Chren MM, Myers A, Geller R, Robbins S, Goldman L. Diagnostic yield of the autopsy in a university hospital and a community hospital. N Engl J Med. 1988;318(19): 1249–54.
7. Tejerina E, Esteban A, Fernandez-Segoviano P, Maria Rodriguez-Barbero J, Gordo F, Frutos-Vivar F, et al. Clinical diagnoses and autopsy findings: discrepancies in critically ill patients*. Crit Care Med. 2012;40(3):842–6.
8. Kearon C, Julian JA, Newman TE, Ginsberg JS. Noninvasive diagnosis of deep venous thrombosis. McMaster diagnostic imaging practice guidelines initiative. Ann Intern Med. 1998; 128(8):663–77.
9. Johnson SA, Stevens SM, Woller SC, Lake E, Donadini M, Cheng J, et al. Risk of deep vein thrombosis following a single negative whole-leg compression ultrasound: a systematic review and meta-analysis. JAMA. 2010;303(5):438–45.
10. Birdwell BG, Raskob GE, Whitsett TL, Durica SS, Comp PC, George JN, et al. The clinical validity of normal compression ultrasonography in outpatients suspected of having deep venous thrombosis. Ann Intern Med. 1998;128(1):1–7.
11. Lensing AW, Doris CI, McGrath FP, Cogo A, Sabine MJ, Ginsberg J, et al. A comparison of compression ultrasound with color Doppler ultrasound for the diagnosis of symptomless postoperative deep vein thrombosis. Arch Intern Med. 1997;157(7):765–8.
12. Poppiti R, Papanicolaou G, Perese S, Weaver FA. Limited B-mode venous imaging versus complete color-flow duplex venous scanning for detection of proximal deep venous thrombosis. J Vasc Surg. 1995;22(5):553–7.
13. Bernardi E, Camporese G, Buller HR, Siragusa S, Imberti D, Berchio A, et al. Serial 2-point ultrasonography plus D-dimer vs whole-leg color-coded Doppler ultrasonography for

diagnosing suspected symptomatic deep vein thrombosis: a randomized controlled trial. JAMA. 2008;300(14):1653–9.
14. Girard P, Sanchez O, Leroyer C, Musset D, Meyer G, Stern JB, et al. Deep venous thrombosis in patients with acute pulmonary embolism: prevalence, risk factors, and clinical significance. Chest. 2005;128(3):1593–600.
15. Crisp JG, Lovato LM, Jang TB. Compression ultrasonography of the lower extremity with portable vascular ultrasonography can accurately detect deep venous thrombosis in the emergency department. Ann Emerg Med. 2010;56(6):601–10.
16. Heijboer H, Buller HR, Lensing AW, Turpie AG, Colly LP, ten Cate JW. A comparison of real-time compression ultrasonography with impedance plethysmography for the diagnosis of deep-vein thrombosis in symptomatic outpatients. N Engl J Med. 1993;329(19):1365–9.
17. Maki DD, Kumar N, Nguyen B, Langer JE, Miller Jr WT, Gefter WB. Distribution of thrombi in acute lower extremity deep venous thrombosis: implications for sonography and CT and MR venography. AJR Am J Roentgenol. 2000;175(5):1299–301.
18. Chengelis DL, Bendick PJ, Glover JL, Brown OW, Ranval TJ. Progression of superficial venous thrombosis to deep vein thrombosis. J Vasc Surg. 1996;24(5):745–9.
19. Masuda EM, Kistner RL, Musikasinthorn C, Liquido F, Geling O, He Q. The controversy of managing calf vein thrombosis. J Vasc Surg. 2012;55(2):550–61.
20. Bates SM, Jaeschke R, Stevens SM, Goodacre S, Wells PS, Stevenson MD, et al. Diagnosis of DVT: antithrombotic therapy and prevention of thrombosis, 9th ed: American college of chest physicians evidence-based clinical practice guidelines. Chest. 2012;141 Suppl 2:e351S–418.
21. Lockhart ME, Sheldon HI, Robbin ML. Augmentation in lower extremity sonography for the detection of deep venous thrombosis. AJR Am J Roentgenol. 2005;184(2):419–22.
22. Blaivas M, Lambert MJ, Harwood RA, Wood JP, Konicki J. Lower-extremity Doppler for deep venous thrombosis–can emergency physicians be accurate and fast? Acad Emerg Med. 2000; 7(2):120–6.
23. McQueen AS, Elliott ST, Keir MJ. Ultrasonography for suspected deep vein thrombosis: how useful is single-point augmentation? Clin Radiol. 2009;64(2):148–55.
24. Kearon C, Akl EA, Comerota AJ, Prandoni P, Bounameaux H, Goldhaber SZ, et al. Antithrombotic therapy for VTE disease: antithrombotic therapy and prevention of thrombosis, 9th ed: American college of chest physicians evidence-based clinical practice guidelines. Chest. 2012;141 Suppl 2:e419S–94.
25. Mustafa S, Stein PD, Patel KC, Otten TR, Holmes R, Silbergleit A. Upper extremity deep venous thrombosis. Chest. 2003;123(6):1953–6.
26. Prandoni P, Polistena P, Bernardi E, Cogo A, Casara D, Verlato F, et al. Upper-extremity deep vein thrombosis. Risk factors, diagnosis, and complications. Arch Intern Med. 1997;157(1):57–62.
27. Spence LD, Gironta MG, Malde HM, Mickolick CT, Geisinger MA, Dolmatch BL. Acute upper extremity deep venous thrombosis: safety and effectiveness of superior vena caval filters. Radiology. 1999;210(1):53–8.
28. Gaitini D, Beck-Razi N, Haim N, Brenner B. Prevalence of upper extremity deep venous thrombosis diagnosed by color Doppler duplex sonography in cancer patients with central venous catheters. J Ultrasound Med. 2006;25(10):1297–303.
29. Blaivas M. Ultrasound in the detection of venous thromboembolism. Crit Care Med. 2007;35 Suppl 5:S224–34.
30. Baarslag HJ, van Beek EJ, Koopman MM, Reekers JA. Prospective study of color duplex ultrasonography compared with contrast venography in patients suspected of having deep venous thrombosis of the upper extremities. Ann Intern Med. 2002;136(12):865–72.
31. Torbicki A, Perrier A, Konstantinides S, Agnelli G, Galie N, Pruszczyk P, et al. Guidelines on the diagnosis and management of acute pulmonary embolism: the Task Force for the Diagnosis and Management of Acute Pulmonary Embolism of the European Society of Cardiology (ESC). Eur Heart J. 2008;29(18):2276–315.
32. Reissig A, Heyne JP, Kroegel C. Sonography of lung and pleura in pulmonary embolism: sonomorphologic characterization and comparison with spiral CT scanning. Chest. 2001; 120(6):1977–83.

33. Mathis G, Blank W, Reissig A, Lechleitner P, Reuss J, Schuler A, et al. Thoracic ultrasound for diagnosing pulmonary embolism: a prospective multicenter study of 352 patients. Chest. 2005;128(3):1531–8.
34. Comert SS, Caglayan B, Akturk U, Fidan A, Kiral N, Parmaksiz E, et al. The role of thoracic ultrasonography in the diagnosis of pulmonary embolism. Ann Thorac Med. 2013;8(2): 99–104.
35. Tomkowski WZ, Davidson BL, Wisniewska J, Malek G, Kober J, Kuca P, et al. Accuracy of compression ultrasound in screening for deep venous thrombosis in acutely ill medical patients. Thromb Haemost. 2007;97(2):191–4.
36. Kory PD, Pellecchia CM, Shiloh AL, Mayo PH, DiBello C, Koenig S. Accuracy of ultrasonography performed by critical care physicians for the diagnosis of DVT. Chest. 2011;139(3): 538–42.
37. Pomero F, Dentali F, Borretta V, Bonzini M, Melchio R, Douketis JD, et al. Accuracy of emergency physician-performed ultrasonography in the diagnosis of deep-vein thrombosis: a systematic review and meta-analysis. Thromb Haemost. 2013;109(1):137–45.
38. Di Nisio M, Van Sluis GL, Bossuyt PM, Buller HR, Porreca E, Rutjes AW. Accuracy of diagnostic tests for clinically suspected upper extremity deep vein thrombosis: a systematic review. J Thromb Haemost. 2010;8(4):684–92.
39. Torbicki A, Galie N, Covezzoli A, Rossi E, De Rosa M, Goldhaber SZ. Right heart thrombi in pulmonary embolism: results from the International Cooperative Pulmonary Embolism Registry. J Am Coll Cardiol. 2003;41(12):2245–51.
40. Konstantinides S, Geibel A, Heusel G, Heinrich F, Kasper W. Heparin plus alteplase compared with heparin alone in patients with submassive pulmonary embolism. N Engl J Med. 2002; 347(15):1143–50.
41. Wan S, Quinlan DJ, Agnelli G, Eikelboom JW. Thrombolysis compared with heparin for the initial treatment of pulmonary embolism: a meta-analysis of the randomized controlled trials. Circulation. 2004;110(6):744–9.
42. Goldhaber SZ, Visani L, De Rosa M. Acute pulmonary embolism: clinical outcomes in the International Cooperative Pulmonary Embolism Registry (ICOPER). Lancet. 1999;353(9162): 1386–9.
43. Kucher N, Luder CM, Dornhofer T, Windecker S, Meier B, Hess OM. Novel management strategy for patients with suspected pulmonary embolism. Eur Heart J. 2003;24(4):366–76.
44. Kurzyna M, Torbicki A, Pruszczyk P, Burakowska B, Fijalkowska A, Kober J, et al. Disturbed right ventricular ejection pattern as a new Doppler echocardiographic sign of acute pulmonary embolism. Am J Cardiol. 2002;90(5):507–11.
45. Goldhaber SZ. Echocardiography in the management of pulmonary embolism. Ann Intern Med. 2002;136(9):691–700.
46. Casazza F, Bongarzoni A, Capozi A, Agostoni O. Regional right ventricular dysfunction in acute pulmonary embolism and right ventricular infarction. Eur J Echocardiogr. 2005;6(1):11–4.

Chapter 14
Ultrasound in Trauma Critical Care

Amie Hall Woods

Introduction

Some of the earliest descriptions of ultrasound as a rapid and noninvasive tool in the evaluation of the trauma patient date back to the early 1970s [1]. By 1976, Asher and colleagues had published data describing reliable use of ultrasound in the diagnosis of splenic injury [2]. Widespread adoption of ultrasound in the American medical and surgical communities progressed quickly in the 1990s [3, 4]. An earlier example of the role of ultrasound in triage and patient management occurred in 1988 during a major earthquake in Armenia, highlighting the utility and significance of this evolving diagnostic tool. During this mass casualty event, death toll estimates reached 25,000 with an additional 150,000 injured. Medical centers left standing were overwhelmed. In an attempt to triage those needing immediate surgical intervention, screening ultrasounds were performed in the reception area of one hospital on 400 patients within the first 72 h after the quake. The average time spent on each patient was 4 min. Trauma-related pathology of the abdomen and/or retroperitoneal space was identified, correctly, in 12.8 % of patients, with only 1 % false negatives and no false positives [5]. False negative cases included solid organ hematomas and retroperitoneal injury, highlighting important limitations that must be considered when using ultrasound as an examination or diagnostic tool.

In current practice, point of care ultrasound training is recommended for residents by both the American College of Surgeons and the American College of Emergency Physicians [6]. The Focused Assessment with Sonography in Trauma exam, or FAST exam, has existed in the curriculum for the advanced trauma life

A.H. Woods, MD, FACEP, ARDMS (✉)
Department of Emergency Medicine, Inova Fairfax Hospital,
3300 Gallows Road, Falls Church, VA 22042, USA
e-mail: amiehwoods@gmail.com

M. Jankowich, E. Gartman (eds.), *Ultrasound in the Intensive Care Unit*,
Respiratory Medicine, DOI 10.1007/978-1-4939-1723-5_14

support (ATLS) course since 1997 [7], and has become standard of care for evaluating the unstable trauma patient. In the transition from the trauma bay to the medical, surgical, or trauma critical care unit, trauma patients continue to remain ideal candidates for this portable, noninvasive, and rapid technology. Patients in the intensive care unit (ICU) frequently require ventilatory support, may be hemodynamically unstable, and are difficult to transport. The ability to perform serial ultrasound exams provides valuable clinical information without adding additional radiation risk to the patient. Furthermore, ultrasound assists in the monitoring of patients for whom nonoperative management of traumatic abdominal injuries is preferred, e.g., splenic lacerations.

In this chapter, we will examine the use of ultrasound in the setting of trauma, both in the initial patient evaluation and the critical care setting. We will illustrate and discuss both normal and abnormal images of the abdomen, heart, and lung. We will also explain standard techniques of image acquisition and comment briefly on evolving uses of ultrasound in trauma. The extended FAST (eFAST) exam asks the additional questions of whether fluid is visible above the diaphragm, or if a pneumothorax is present. At the chapter's conclusion, we will illustrate a sample clinical protocol for integrating the FAST and eFAST exams into the management of the trauma critical care patient.

Technical and Patient Considerations

Successful diagnostic ultrasonography results from a combination of operator skill and the right equipment. Similar to computers and smartphones, companies producing ultrasound machines have responded to increased consumer demand for miniaturization and have created handheld ultrasound machines which may to be carried in the pocket of a white coat. While these devices are attractive in their advanced design and portability, their diminutive size makes theft or misplacement a costly possibility in the busy environments of trauma and critical care. Additionally, the small screen size can make image interpretation difficult for other team members, decreasing its utility as a teaching tool for early learners. In contrast, older ultrasound machines of significantly larger size may be difficult to maneuver in the crowded trauma bay and limited space of the ICU. A compromise of size, durability, and quality will ultimately guide an appropriate machine selection. For probe selection, a phased array or curvilinear probe ranging in frequency from 2 to 5 MHz (Fig. 14.1) is most commonly used to acquire images in the FAST exam. The lower frequency sacrifices some resolution but improves penetrance, a critical component in the search for deeper visceral injury.

The target patient population for the eFAST exam is any patient with a history of blunt or penetrating thoracoabdominal trauma and/or any patient with unexplained hypotension or shortness of breath in a known or suspected trauma. Other accurate modalities exist for detecting pathologic thoracoabdominal free fluid, such as computed tomography, but ultrasound is ideal in that it may be performed at the bedside

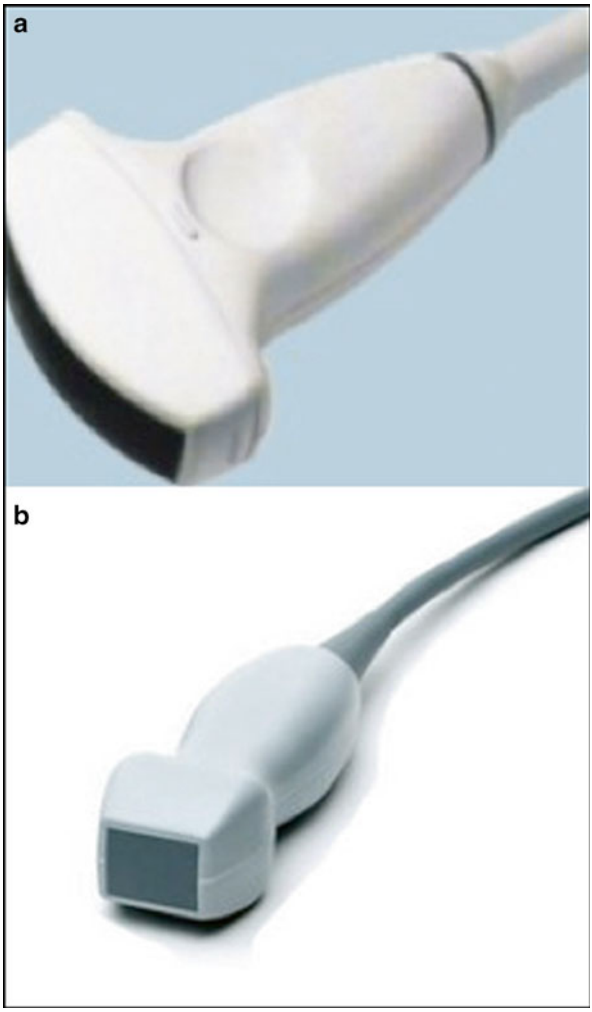

Fig. 14.1 (**a**) Curvilinear probe, (**b**) phased array probe

of the unstable patient for whom transport to radiology poses too great a risk. Previous gold standard diagnostic methods, such as peritoneal lavage, have an extremely high sensitivity for detecting abdominal free fluid (98 %) [8], but pose the risk of exposing the patient to a nontherapeutic laparotomy [9]. For this reason, their use in practice has waned in favor of less invasive methods [10]. Both morbid obesity and the presence of subcutaneous air dramatically reduce the sensitivity of the FAST exam. Patients with these conditions should be approached with caution when the suspicion for the presence of abdominal or pericardial free fluid is high. One method of increasing the sensitivity of the FAST exam is placing the patient in the Trendelenburg position, a feasible maneuver as most trauma patients arrive supine with cervical spine immobilization [11]. Further limitations of the FAST exam will be discussed later in the chapter.

Image Acquisition and Interpretation

The traditional FAST exam is performed with a goal of obtaining three views of the abdomen and a single view of the pericardial space, or four views in total:

1. Right upper quadrant (RUQ) or Morison's pouch/hepatorenal space
2. Left upper quadrant (LUQ) or splenorenal space
3. Pelvic view
4. Subxiphoid or other pericardial view

The exam addresses the focused question of whether free fluid is present in the abdomen and/or pericardium. Some authors have traditionally taught that the first view acquired is the subxiphoid or other pericardial view, with a goal of allowing the operator to adjust the gain based on the appearance of intracardiac fluid. Our current discussion will focus on the patient with blunt or penetrating abdominal trauma, for whom the first view obtained should be that of the most dependent space in the peritoneum, known as Morison's pouch.

A discussion of orientation is important, as this component of ultrasonography may be difficult for the novice and is crucial for accurate image interpretation. Figure 14.2 illustrates the relationship between the probe marker, the orientation mark on the screen, and the operator. Understanding that the probe uses a credit card thin beam to create a two-dimensional image from three-dimensional structures takes some practice; one analogy used is that of "shining a flashlight in a dark room." What is visible on the screen is only that which is present in the probe beam's path; once the beam moves beyond the object, the image is no longer visible, but it does not mean that the object does not exist.

Fig. 14.2 The *yellow star* denotes the corresponding direction between the screen, the probe, and the operator

Varying clinical circumstances and space availability hinder the practice of performing the FAST exam on a dedicated side of the patient and require flexibility on the part of the operator. Therefore, while the exam may be performed from either side of the patient and with either hand, depending on the operator's comfort, the image planes should remain consistent. Images will then be dutifully replicated with attention to marker consistency and operator orientation to patient. We recommend one-handed scanning, whether right or left, with the operator's other hand free to adjust the gain, depth, and other components of the image. All images should be obtained by the operator from the same side of the patient, with skilled ultrasonographers dividing their attention among the screen, the probe, and the patient as needed.

Due to its higher specificity than sensitivity the FAST exam is suited for use only as a screening tool for thoracoabdominal free fluid, and should be interpreted accordingly – negative exams should be regarded with caution. Trauma patients with abdominal pain and an absence of abdominal free fluid on ultrasound should be observed with serial exams and undergo a repeat ultrasound or be further evaluated with an additional imaging modality such as CT scan [12].

RUQ View

Each patient will bring unique anatomic characteristics to the clinical scenario; thus, accurate images will be obtained using slightly different movements each time. A starting point for the RUQ view begins at the intersection of the anterior- to mid-axillary line and the horizontal subxiphoid line or at the seventh to tenth intercostal rib spaces on most patients (Fig. 14.3). The probe marker is oriented toward

Fig. 14.3 Probe position for RUQ view. The marker is oriented toward the patient's head

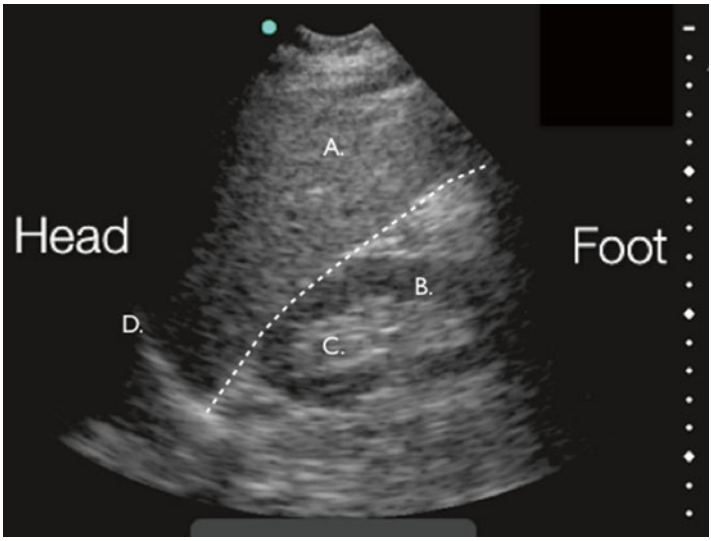

Fig. 14.4 A normal RUQ view. *A* liver, *B* renal cortex, *C* renal medulla, *D* diaphragm. Note the *dashed line* indicating the potential space between the echogenic liver and hypoechoic renal cortex, or Morison's pouch

the patient's head, and the image created is a coronal plane. The lateral aspect of the body correlates with the near field of the image, while the far field of the image demonstrates medial structures. In other words, Images at the top of the screen represent structures closest to the skin's surface, and images at the bottom of the screen represent structures deeper in the body. Recognizing that the ribs run obliquely across the body, the probe may be rotated slightly so that the thin ultrasound beam is able to penetrate through the narrow rib space. Figure 14.4 demonstrates the normal RUQ FAST view. Visible here is the normal homogenous, echogenic liver, the hyperechoic (compared to liver, which serves as the reference for echogenicity) renal medulla, the hypoechoic renal cortex, and the hyperechoic diaphragm. Morison's pouch, the most dependent space in the peritoneum and the potential space between the liver and the right kidney, is the visual zone on which the operator should focus, searching for a hypo- or anechoic area between the two organs which represents free fluid (Fig. 14.5). Vigilance must be maintained to ensure that the entirety of Morison's pouch is evaluated, lest a small amount of free fluid "hide" near the inferior portion of the liver. Visualization of the inferior pole of the right kidney is an effective way to do this. After the liver, the superior pole of the right kidney, and the bright respirophasic diaphragm are visualized, the probe may be slid caudally to reveal the kidney's inferior pole. Figure 14.6 demonstrates how free fluid may be missed in absence of attention to this fact.

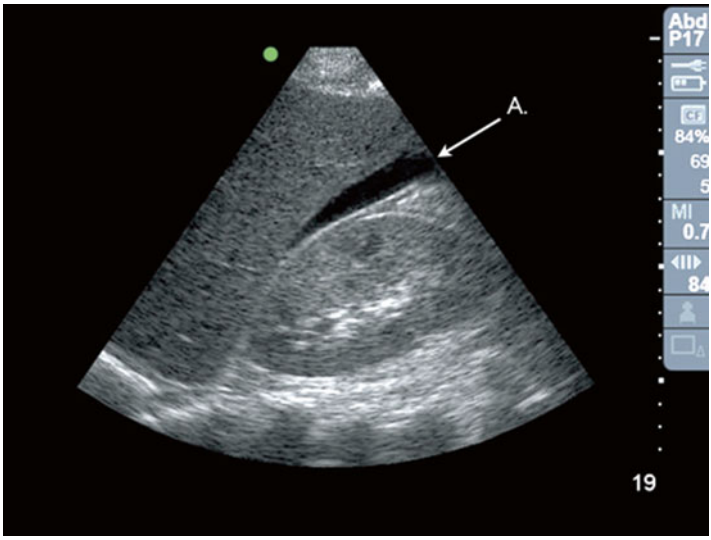

Fig. 14.5 *A* Free fluid in Morison's pouch, indicated by the *black*, or anechoic stripe of fluid in the hepatorenal space

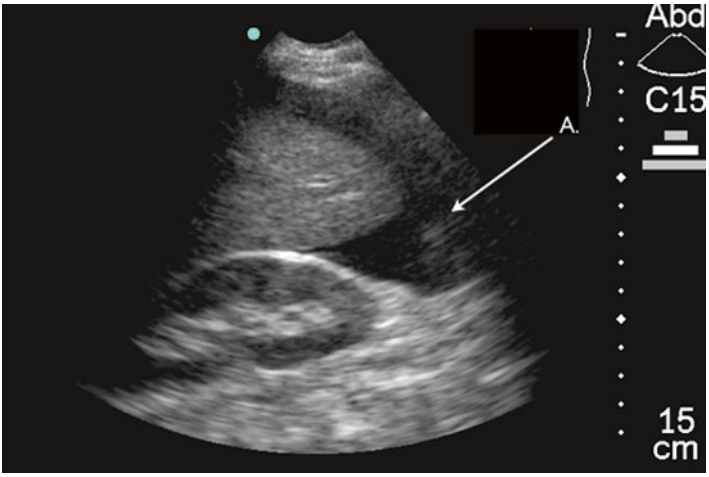

Fig. 14.6 *A* Free fluid in the RUQ at the inferior kidney pole, which may be missed without a complete survey of the right kidney

LUQ View

The splenorenal space is visualized in similar fashion to Morison's pouch, with the probe marker toward the patient's head and the probe placed in the horizontal subxiphoid line, with the corresponding intersecting line as the middle to posterior

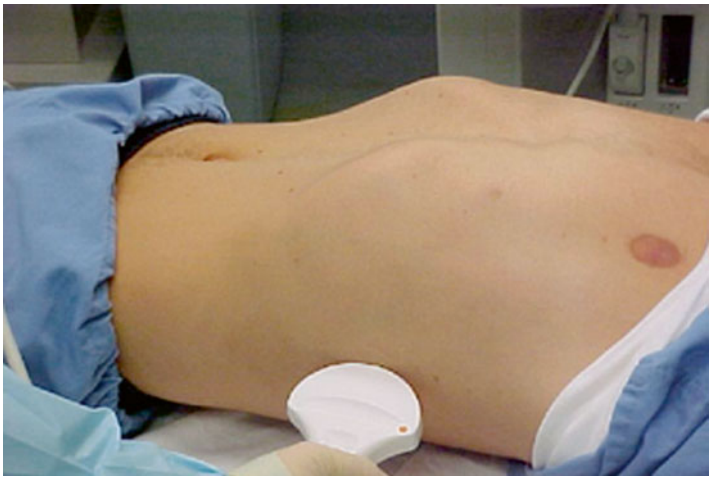

Fig. 14.7 Probe position for the LUQ view. The probe marker is oriented toward the patient's head

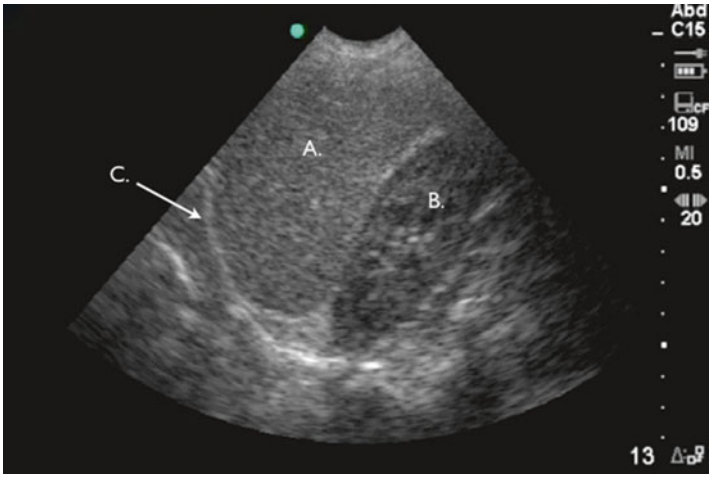

Fig. 14.8 Normal LUQ view. *A* spleen, *B* left kidney, *C* diaphragm

axillary line (Fig. 14.7). The smaller size of the spleen provides less of an acoustic window than the liver, and the more posterior position of the left kidney requires positioning adjustment. A direction frequently given to trainees standing on the right side of the patient performing this component of the FAST exam is to put their "knuckles on the stretcher," extending the probe-holding hand posteriorly enough to orient the probe beam in a retroperitoneal direction, which will adequately visualize the splenorenal space. Figure 14.8 demonstrates the normal LUQ view; note the echogenic spleen, left kidney, and diaphragm. Because the phrenicocolic ligament creates a barrier to the splenorenal space, fluid generally accumulates in the

subphrenic space prior to the splenorenal space. For this reason, attention should be paid to adequately visualize the border of the spleen and diaphragm, where free fluid may be missed (Fig. 14.9). After this, the search for free fluid continues to the splenorenal space (Fig. 14.10).

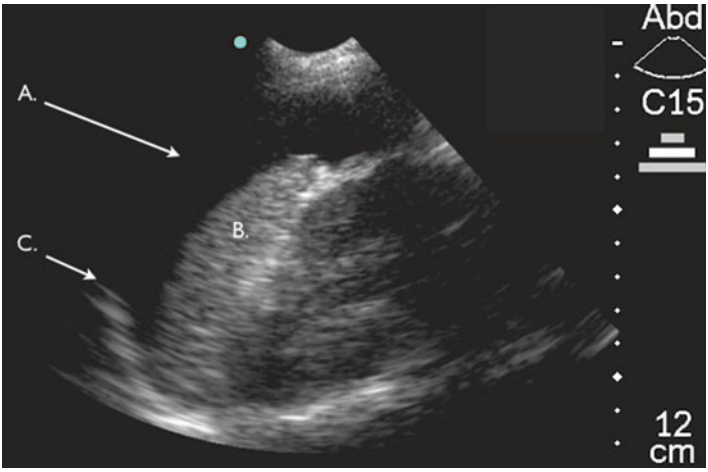

Fig. 14.9 *A* Free fluid in LUQ in subdiaphragmatic space, *B* spleen, *C* diaphragm. Fluid accumulates here before the splenorenal recess due to the phrenicocolic ligament

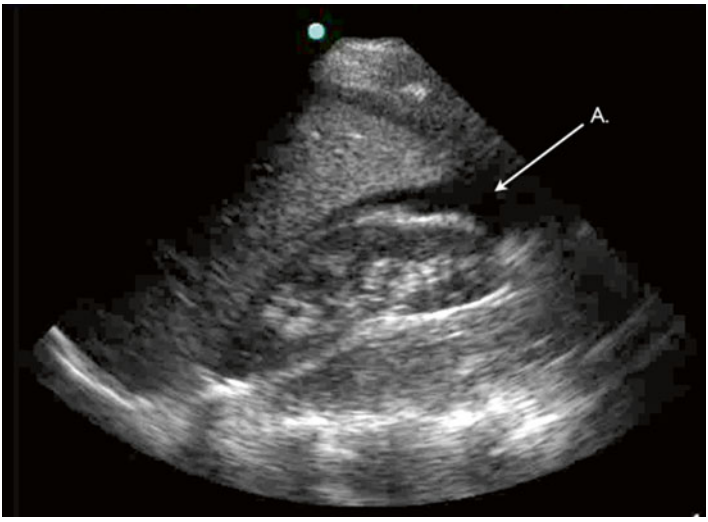

Fig. 14.10 *A* Free fluid in splenorenal recess

Pericardial View

Due to the anatomic position of the heart, penetrating trauma to the chest wall often injures the right ventricle. The classic pericardial image obtained in a FAST exam is that of a subxiphoid image. On initial positioning, the probe marker is on the patient's right, and the probe itself is aimed toward the patient's head or slightly toward the patient's left shoulder (Fig. 14.11). An overhand grip of the probe is encouraged here, as the probe must be angled closely to the body to provide an adequate view into the thoracic space, and an underhand grip may inhibit this. The normal subxiphoid view of the heart uses the liver as an acoustic window and demonstrates the hyperechoic pericardium and cardiac septum and the four anechoic chambers of the heart (Fig. 14.12). The border of the liver and the right side of the heart, found in the near field of the image, is the focal zone in the search for anechoic fluid (Fig. 14.13). In some cases, the subxiphoid view may not be attainable either due to cutaneous abdominal or chest trauma or patient anatomy (e.g., those with a long thoracic cage or narrow subxiphoid space). An alternative view in the search for pericardial free fluid is the parasternal long view. Teaching varies in regard to screen and probe marker orientation, but probe placement is consistent in that it is placed in the left mid-clavicular line at the second through fourth intercostal space, in plane with a sagittal cut through the heart. Care should be taken to decrease the depth of the image, as the parasternal long heart is much more shallow than the subxiphoid image previously described. Obtained is the image seen in Fig. 14.14; visible is the left atrium and ventricle, the aortic outflow tract, the right ventricle, and the descending thoracic aorta in cross section. This last structure is crucial, as

Fig. 14.11 Probe position for the subxiphoid view. The probe marker is toward the patient's *right side*. An overhand grip is used to flatten the probe against the xiphoid process

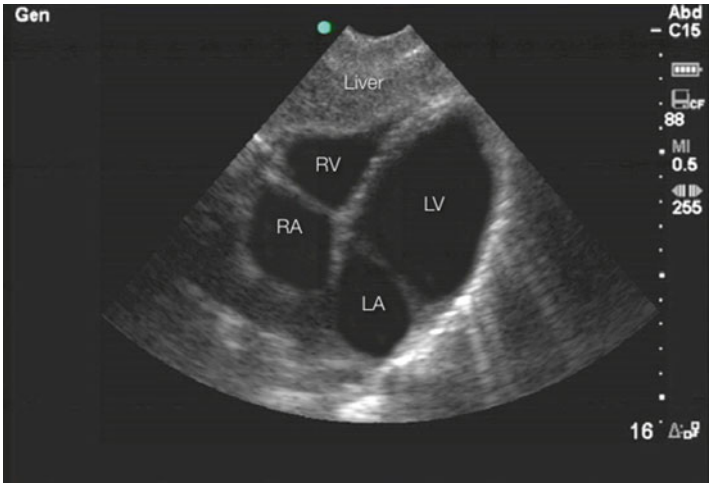

Fig. 14.12 Normal subxiphoid view of the heart. *RA* right atrium, *RV* right ventricle, *LA* left atrium, *LV* left ventricle

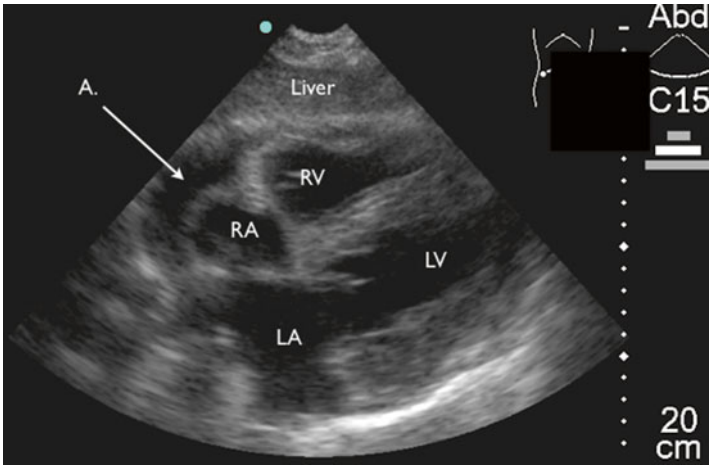

Fig. 14.13 Subxiphoid view of fluid in pericardium. The liver is used as an acoustic window to visualize the echo-free stripe of fluid (*A*) shown between the liver and right side of the heart

the anechoic stripe seen in Fig. 14.15 between the descending thoracic aorta and the posterior pericardium represents pericardial fluid, whereas Fig. 14.16 also shows an anechoic stripe of fluid, but its location behind the descending thoracic aorta indicates that this is a pleural effusion or hemothorax. Further discussion of echocardiography is available in Chaps. 5, 6, and 7. We will discuss the search for fluid above the diaphragm in the description of the eFAST exam in the "advanced competencies" section of this chapter.

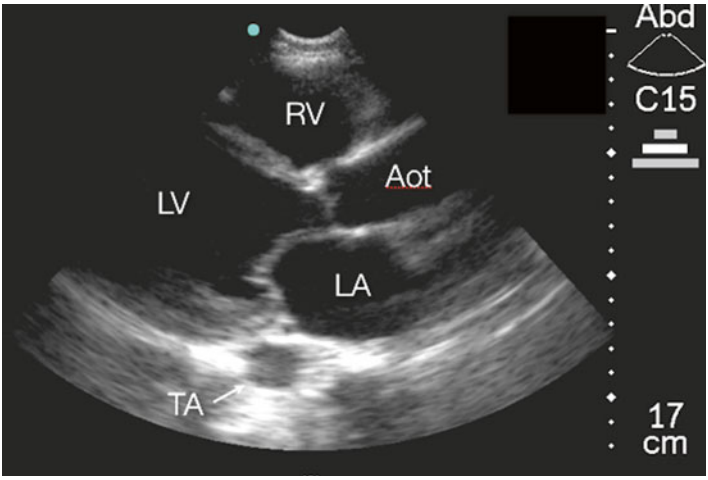

Fig. 14.14 Normal parasternal long view. *LA* left atrium, *LV* right ventricle, *RV* right ventricle, *Aot* aortic outflow tract, *TA* descending thoracic aorta in cross section

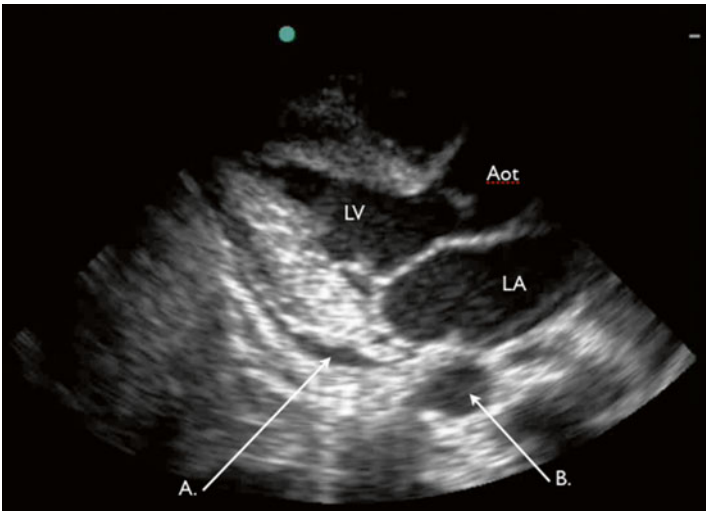

Fig. 14.15 Parasternal long view with pericardial fluid. Note the location of fluid (*A*) between the descending thoracic aorta (*B*) and the posterior pericardium, indicating that the effusion is pericardial

Pelvic View

The pelvic view is obtained by placing the probe in the midline just superior to the symphysis pubis, angled 30° caudal with the probe marker toward the patient's right side; this provides an axial view of the bladder. An additional view is obtained by

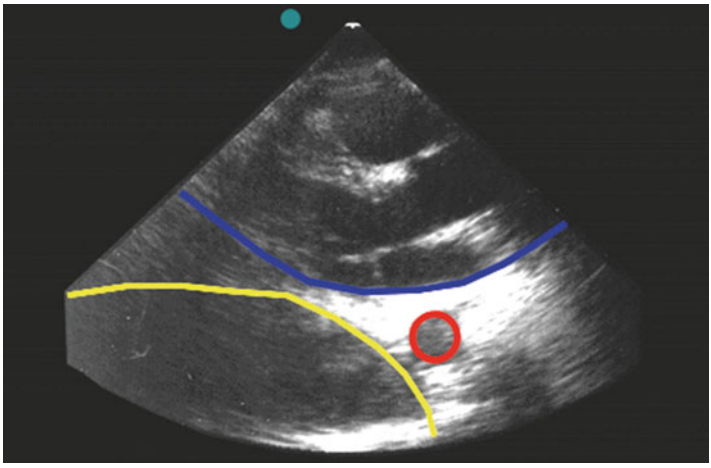

Fig. 14.16 Parasternal long view with pleural fluid. Note the location of fluid (*yellow*) behind the descending thoracic aorta (*red*), rather than the pericardium (*blue*), indicating that the effusion is pleural

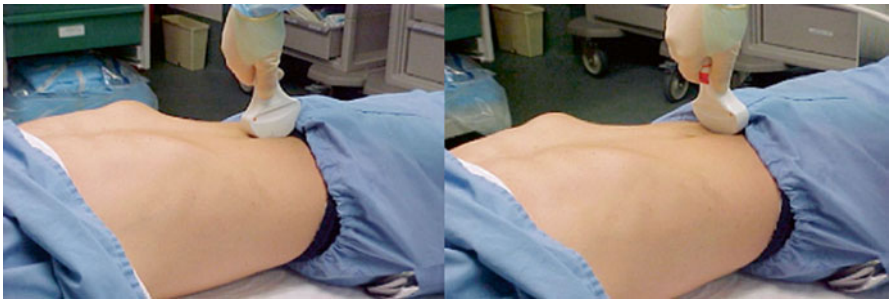

Fig. 14.17 Probe position for pelvic view. The *left* image shows the probe marker oriented toward the patient's head, producing a sagittal pelvic view. The *right* image shows the probe marker oriented toward the patient's right side, producing an axial pelvic view

placing the probe in the same location and position with the probe marker oriented toward the patient's head; this provides a sagittal view (Fig. 14.17). In the axial view, the probe is fanned cranially and caudally, visualizing the superior and inferior portions of the bladder and, in women, the uterus in cross section (Fig. 14.18). In the sagittal view, the bladder and uterus are visualized in sagittal or long-view (Fig. 14.19). In women, the search for fluid should include the space posterior to the bladder and uterus, and among loops of bowel. In men, views should include the posterior bladder and anterior rectal space. The paired, hypoechoic seminal vesicles may be noted posteriorly to the bladder. In contrast to the pericardial view just obtained, adjustments of both gain and depth are often necessary to obtain a

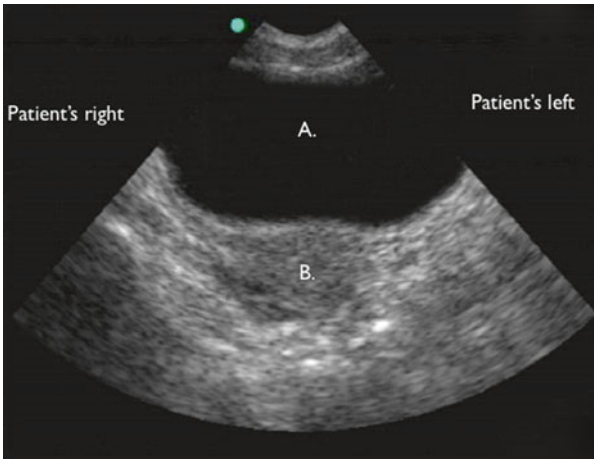

Fig. 14.18 Normal transverse view of the female pelvis with the anechoic bladder in the near field (*A*) and the uterus in the far field (*B*). The probe is oriented so that the marker is pointed toward the patient's *right*

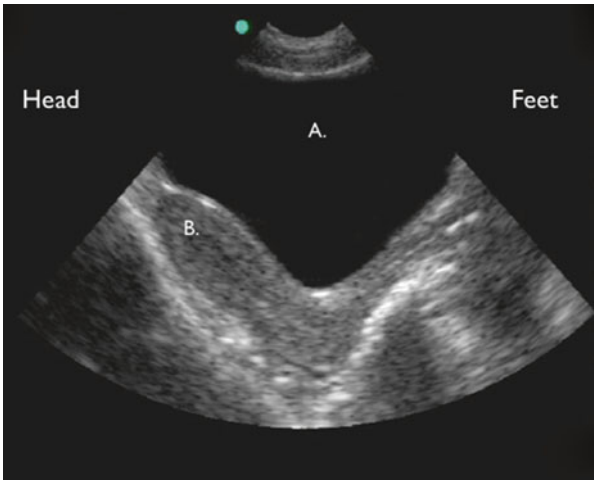

Fig. 14.19 Normal sagittal view of the female pelvis. Again seen is the anechoic bladder in the near field (*A*) and the uterus in the far field (*B*). The probe is oriented so that the marker is toward the patient's head

satisfactory search for pelvic free fluid. If the preceding view obtained was of the subxiphoid heart, minimal depth increase may be needed. However, if the image obtained was that of the parasternal long heart, a depth increase will likely be required to properly search for pelvic free fluid. A full urinary bladder provides an excellent acoustic window through which pelvic free fluid may be visible (Fig. 14.20). Posterior enhancement, an artifactual phenomenon which causes structures deep to an area of anechogenicity to appear bright, may result in a need for gain adjustment. A greater challenge is the patient with an empty bladder who lacks an acoustic window through which free fluid may be visible. Gain adjustment may be necessary in this scenario to find small pockets of anechogenicity among the surrounding structures. Free fluid located adjacent to the bladder may also be indicative of traumatic bladder rupture, especially in the patient with gross hematuria and suprapubic abdominal trauma or a high clinical likelihood of pelvic fractures [13].

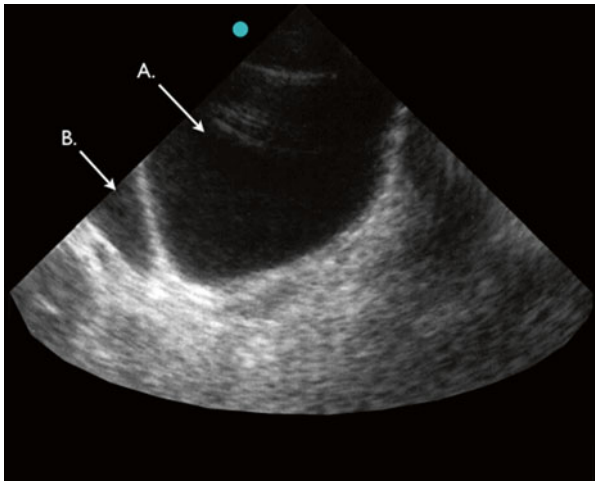

Fig. 14.20 This transverse view of the bladder (*A*) shows a small area of free fluid (*B*) on the *left* side of this image, which is the patient's *right* side

Basic Competencies

The FAST exam is approached from the standpoint of whether or not free fluid is present in the peritoneal or pericardial space. As described above, while free fluid in Morison's pouch may be easily noted by an experienced sonographer, free fluid in other locations such as the pelvis or LUQ may be more difficult to visualize and will require careful technique. Once the exam is performed, the appropriate use of the information gained is crucial. Figure 14.21 illustrates an algorithm for use of the FAST exam in the setting of blunt abdominal trauma, with the hinge point for action resting on hemodynamic stability. In the hemodynamically unstable patient with a history of trauma and free fluid visible on FAST exam, operative management is indicated. A notable and complex exception here is the patient with a past medical history significant for ascites (e.g., patients with a history of liver disease, cancer, or dialysis). These patients may also have a baseline low blood pressure, and this clinical information must be integrated into their management. One solution is a brief and small volume diagnostic paracentesis, using ultrasound in real time or for marking the fluid's location. If straw-colored fluid is retrieved, clinical management may be redirected accordingly; if blood is obtained, the pathway described above stands [14].

In the hemodynamically stable patient, some trauma and critical care providers may elect to perform a FAST exam; others may not. However, as systemic hypotension has been validated as a late marker of shock [15], we recommend the FAST exam for all patients with a history of blunt abdominal trauma as long as it does not interfere with the primary/secondary survey. The stable patient with a positive FAST exam may be directed for expedited CT; the stable patient with a negative FAST exam may be managed with serial exams, CT as indicated, or observation.

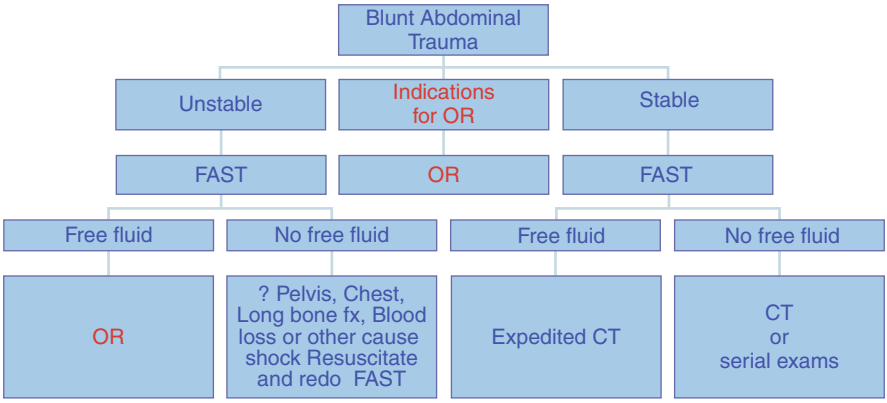

Fig. 14.21 Blunt abdominal trauma algorithm

The unstable patient with a negative FAST exam and a history of blunt abdominal trauma is one who requires clinical problem solving on the part of the providers. Has the patient suffered a long bone injury and lost blood into an extremity? Was blood loss significant enough on the scene of the event that tachycardia and/or hypotension has resulted? Is there another cause of shock that must be considered given the patient's medical history? In these cases, resuscitation is continued and the FAST exam may be repeated as needed. A trauma patient for whom immediate operative management is indicated based on primary/secondary survey alone is a patient for whom management should never be delayed for purposes of ultrasound examination. In such cases, the FAST exam does not add any information that will help guide patient management further, and therefore should not be performed.

Recommendations for teaching and establishment of competency vary by specialty, but a combination of didactic and hands-on instruction has been demonstrated to be an effective teaching tool for the clinician sonographer [16]. While no established competency exam exists, the use of an objective structured clinical examination (OSCE) is one effective method of evaluating knowledge base and ultrasound interpretation skills [17], while others direct competency assessments and clinical privileges to the institution's designated ultrasound or medical director [6]. For a further discussion of educational issues, see Chap. 2.

Advanced Competencies

The extended FAST, or eFAST exam, expands the purpose of the FAST exam in its search for intra-abdominal injury to ask the questions "is there fluid above the diaphragm?" and "is there a pneumothorax?" These advanced competencies add minimal time to that required to complete the FAST exam and may aid the clinician in the diagnostic evaluation of a patient, as well as enhance understanding of the patient's risk for morbidity/mortality.

Evaluation of the thoracic cavity for fluid above the diaphragm may be seamlessly incorporated into the FAST exam, and is a reliable method of diagnosing traumatic hemothorax [18]. In obtaining the first two FAST views, the RUQ and LUQ views, respectively, the operator identifies the hyperechoic, respirophasic line of the diaphragm, slides the probe cephalad, and looks for an anechoic stripe of fluid. An absence of fluid above the diaphragm will not reveal lung tissue in the image, but rather the echogenic appearance of liver or spleen above the diaphragm. This is because of the phenomenon of mirror image artifact. In the absence of fluid, the bright reflective surface of the diaphragm causes the ultrasound beam to produce a mirror image of the solid organ on the opposite side (Fig. 14.22). Thus, in the normal FAST exam, mirror image artifact will be present in both the upper quadrant views, and absent in the presence of thoracic free fluid (Fig. 14.23).

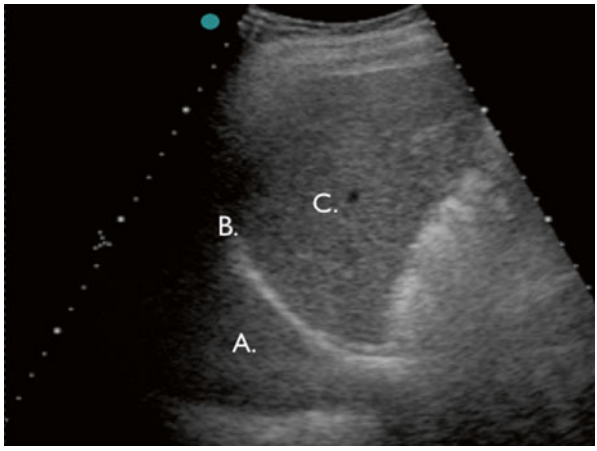

Fig. 14.22 Normal RUQ image with mirror image artifact. *A* mirror image, *B* diaphragm, *C* liver

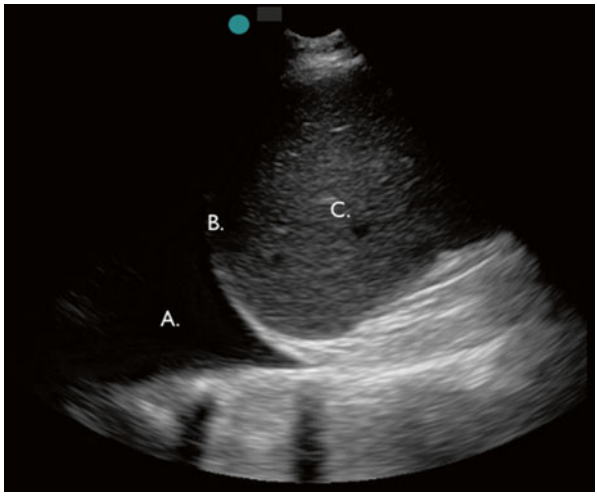

Fig. 14.23 Traumatic pleural effusion. Note the echo-free fluid (*A*) above the diaphragm (*B*) and liver (*C*), with absence of mirror image artifact

Fig. 14.24 Probe placement for pneumothorax (PTX) at 2nd/3rd intercostal space. The probe marker is oriented toward the patient's head. *Black lines* denote additional locations for probe placement during a complete evaluation for PTX

A component of the eFAST exam performed separately from the abdominal/diaphragmatic evaluation is the search for a pneumothorax (see Chap. 10 for a complete discussion of ultrasound for pneumothorax). Portable chest x-ray is traditionally used for this purpose, but due to the supine position of most trauma patients and variability of air location in the setting of pneumothorax, the sensitivity of supine chest x-ray is exceeded by lung ultrasound when performed correctly [19]. A higher frequency, lower penetration probe (a probe used for vascular access is typical) is optimal for this exam, although a curvilinear or phased array probe will also work. The exam is begun with the probe placed anteriorly in the mid-clavicular line, at the second or third intercostal space (Fig. 14.24), the probe marker oriented toward the patient's head. Note that this location is toward the lung's apex. The goal is identification of the intercostal pleura. The probe may be rotated 10–20° clockwise when evaluating the right lung, or counterclockwise when evaluating the left lung, to assume a position perpendicular to the rib/pleural complex. Once the intercostal space is identified, the image produced is that of the bright, hyperechoic pleura midscreen, with the two rib shadows on either side. In the normal lung, the movement of the visceral and parietal pleura creates the appearance of "sliding" or movement of the hyperechoic pleural lines on the screen. At times, the normal sliding pleura will produce several bright, vertical, artifactual lines extending from the pleura, referred to as "comet tails" or "B-lines" (Fig. 14.25). These lines are reverberation artifacts produced by the ultrasound beam moving rapidly between two fixed structures and, while not always seen, are a marker of normalcy if present. The presence of a pneumothorax will reveal the hyperechoic pleura in the intercostal space, with no sliding evident, as air has separated the visceral and parietal pleura (Fig. 14.26). While the absence of pleural sliding is highly suggestive of a pneumothorax, an additional technique to confirm this finding is the use of motion mode (M)-mode. In this technique, the M-mode cursor is placed through the pleura in question and either detects pleural motion (Fig. 14.27, commonly referred to as a "sandy seashore" sign) or not (Fig. 14.28, commonly referred to as a "barcode" sign). The anterior

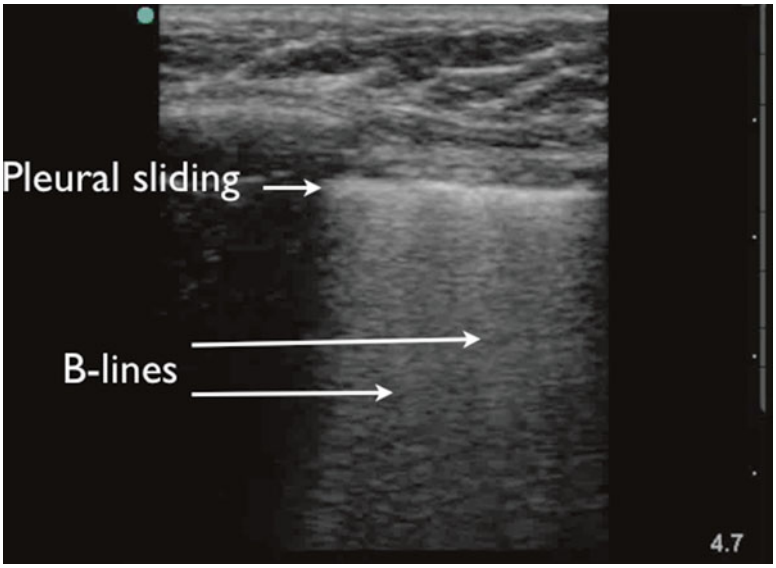

Fig. 14.25 Normal pleural sliding next to rib shadow with comet tails or B-lines

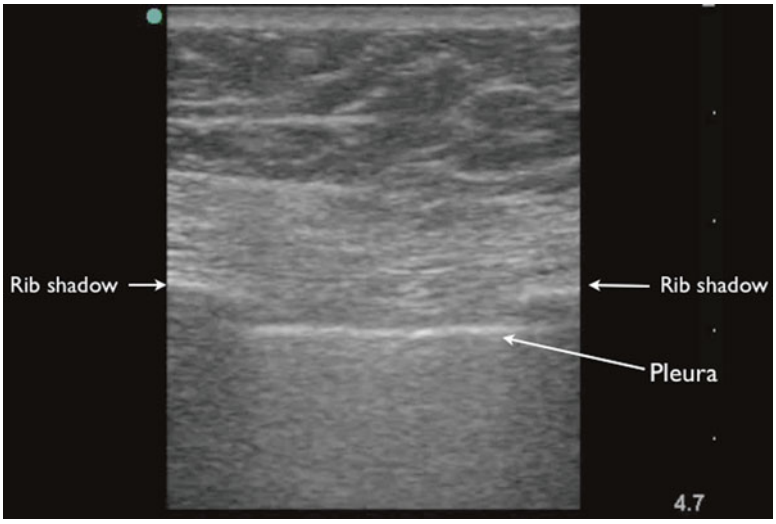

Fig. 14.26 Pneumothorax. Note the two rib shadows and the absence of lung sliding and B-lines seen beneath the bright pleural line. This finding is seen best during a clip or real-time scanning

chest wall must be evaluated at two to four additional intercostal spaces bilaterally, as a pneumothorax may not be present at the apex of the lung in the supine patient. Additional views also increase the likelihood of identifying the junction of pneumothorax and normal lung, known as the "lung point," where the sliding pleura abuts a

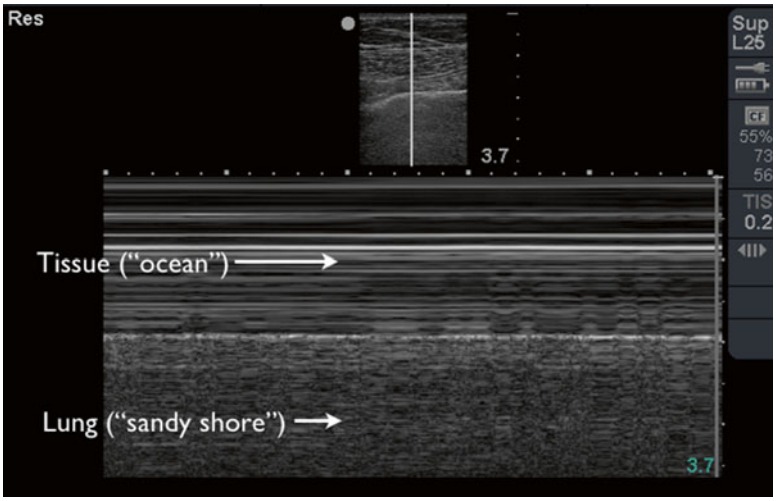

Fig. 14.27 M-mode image of normal lung ("sandy shore") with tissue in the near field ("ocean")

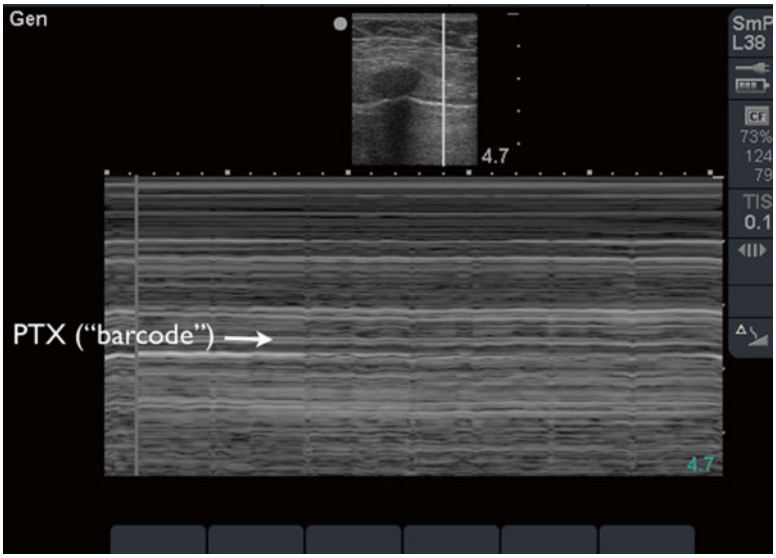

Fig. 14.28 M-mode image of a pneumothorax. The absence of pleural sliding creates a continuous "barcode" sign

non-sliding region (the pneumothorax) in the intercostal space. M-mode may also be used to confirm the finding, producing an image with both the "sandy shore" and the "barcode" present, meeting at the "lung point" (Fig. 14.29). The absence of the lung point increases the sensitivity of the exam, and its presence has been found to be 100 % specific for pneumothorax in the supine patient [20]. Potential limitations of ultrasound for pneumothorax are discussed in Chap. 10.

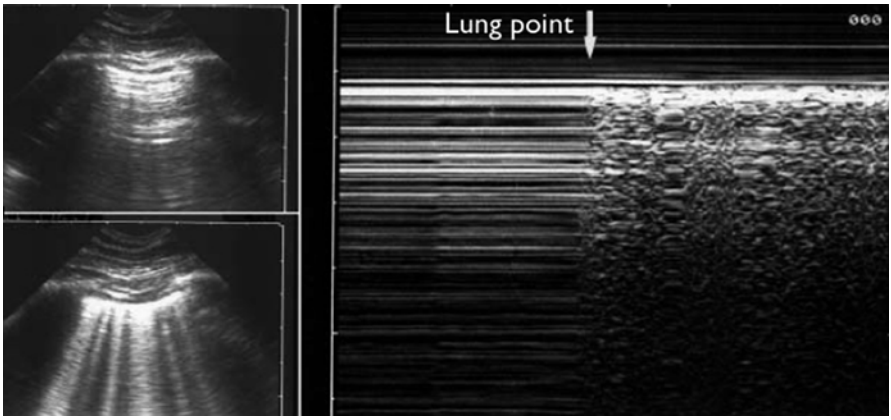

Fig. 14.29 M-mode image of lung point

Diaphragmatic rupture from blunt abdominal trauma, while relatively infrequent, is difficult to diagnose via the conventional methods of chest radiography or computed tomography (CT). Magnetic resonance imaging is more sensitive and specific but may not be obtainable in a timely fashion. One case series describes three cases of diaphragmatic rupture diagnosed on initial evaluation with FAST exam, using the M-mode cursor directed through the diaphragmatic line [21]. In all three cases, when diaphragmatic excursion was noted to be minimal or absent on FAST exam, the M-mode cursor confirmed lack of movement and correctly identified diaphragmatic rupture. Of these three cases, one was unstable on initial evaluation and unable to receive imaging outside the trauma bay, and one had a normal CT scan. The third's diagnosis was confirmed via abnormal appearance of NG tube on post-placement chest x-ray. This report represents a small number of cases, and further studies with a greater number of patients are required to validate this technique.

The pregnant trauma patient represents a unique challenge to providers. In cases where viability is confirmed or suspected, the number of patients requiring treatment has now become two. Assessment of the fetus, legally considered viable between 24 and 28 weeks [22] is beyond the scope of this discussion, but the mother remains a valid candidate for FAST evaluation due to the limitations of imaging in pregnancy. Accurate images are often obtained by probe adjustment with allowances made for the space-occupying uterus; at 28 weeks fundal height is found approximately 3 fingerbreadths above the umbilicus. Both RUQ and LUQ views should therefore be obtained with probe adjustment superiorly and posteriorly, and the pelvic view just above the symphysis pubis and angled caudal. Often the subxiphoid cardiac view will be impossible due to the gravid abdomen, and a parasternal long view is recommended. Limited data is available validating the accuracy of the FAST exam in the pregnant trauma patient, but initial reports suggest that as a test it performs less well on the pregnant than the nonpregnant trauma patient [23].

Evidence Review and Evidence-Based Use

Lessons learned from early success in European centers of the utility of bedside ultrasound in management of the trauma patient began populating the North American literature in the 1990s. In a large early study, Tiling et al. found a sensitivity of 89 % and a specificity of 99 % with an accuracy of 99 % for the detection of free intraperitoneal fluid in a prospective study of 808 blunt trauma patients [24]. With these results validated in future studies [25–27], ultrasound quickly became a viable and widespread tool used in the trauma evaluation, with the term "FAST" cemented as the accepted term describing the exam by Rozycki and colleagues in 1996 [28]. With a growing body of data supporting the use of ultrasound in the setting of blunt abdominal trauma, the utility of ultrasound in the setting of the patient with penetrating abdominal trauma remained less quantified. Udobi and colleagues prospectively evaluated 75 patients presenting with either stab or gunshot wounds to the abdomen, flank, or back, comparing results of the FAST exam with diagnostic peritoneal lavage (DPL), triple-contrast CT, or laparotomy. The sensitivity of FAST was 46 % and the specificity was 94 %, concluding that while ultrasound exam plays a role in the evaluation of penetrating abdominal trauma, negative results should be interpreted with caution [29].

On average, a FAST exam of the abdominal and thoracic cavities can be performed with the accuracy described above in an average of 4 min [30]. While identification of free fluid has been demonstrated with a single RUQ view in less than 20 s [31], the standard four-view FAST exam has retained higher sensitivity and accuracy for detection of free fluid when compared to a single-view technique [32] and remains the currently recommended method. In 2006, Melniker and colleagues performed a randomized controlled trial to assess the use of a protocol which included point of care ultrasound to evaluate patients with suspected torso trauma. The study was conducted during a 6-month period at two Level I trauma centers. The primary outcome measure was time from emergency department arrival to transfer to operative care; secondary outcomes included CT use, length of stay, complications, and charges. For patients whose trauma evaluation included bedside ultrasound, time to operative care was 64 % less, days spent in the hospital were reduced by 27 %, and hospital charges were reduced by 35 %. Those patients also underwent fewer CTs and had fewer complications when compared to control patients who did not receive an ultrasound inclusive protocol [33].

Patients presenting with penetrating cardiac trauma are at a distinct disadvantage in that the physical diagnosis of effusion or tamponade can be difficult and unreliable. The use of ultrasound in the diagnosis of serious cardiac injury resulting in acute hemopericardium has been shown to be effective, with a sensitivity approaching 100 % and a specificity of 97 % [34, 35]. Plummer and colleagues retrospectively evaluated patients with penetrating cardiac injury who received a cardiac ultrasound compared to controls who were not evaluated with ultrasound. Time to operative management and survival was compared between the two groups. Patients with penetrating cardiac injury who received an ultrasound arrived in the

operating room in 15 min and had a 100 % survival rate, compared to 57 % survival in control patients who did not receive an ultrasound, who arrived in the operating room in 42 min [36].

To assess the utility of ultrasound in the diagnosis of hemothorax, Ma and colleagues compared clinician-performed trauma ultrasound with the results of the initial plain chest radiograph in 245 patients at a level I trauma center. Findings indicated that both modalities were comparably sensitive and specific in the diagnosis of hemothorax but that ultrasound may provide the diagnosis faster [37]. Sisley and colleagues addressed this question in their evaluation of 360 patients with blunt and penetrating torso injuries. All patients had a surgeon-performed thoracic ultrasound in addition to supine portable chest radiography. Sensitivity and specificity of x-ray versus ultrasound were comparable, but the standout data point was performance time: an average of 1.3 min for ultrasound versus 14.2 min for x-ray for the detection of traumatic effusion [38]. Further comparisons of ultrasound to traditional chest imaging were made when Rowan and colleagues prospectively compared the accuracy of ultrasonography with that of supine chest x-ray in the detection of traumatic pneumothoraces. Using CT as the reference standard, ultrasound was more sensitive than supine chest x-ray and as sensitive as CT, in the detection of traumatic pneumothoraces [39].

The use of ultrasound in the triage and assessment of trauma lies not only in the identification of injury but also in the incorporation of that knowledge into the clinical picture of the patient. Free fluid may be identified on the initial trauma evaluation but may not warrant immediate surgical intervention, as seen by the increasing prevalence of nonoperative management of intra-abdominal injuries [40]. Two scoring systems have been developed and prospectively evaluated in an attempt to correlate ultrasound findings with need for surgical intervention. The first assigned a score based on presence (one point), depth of fluid (two points for fluid > 2 mm in either upper quadrant), and floating bowel loops (one point). Scores ranged from zero to 8. Investigators found that 96 % of patients with a score greater than or equal to three required therapeutic laparotomy, while only 38 % of those with a score of less than three received operative management [41]. A later study also assigned a score based on presence and depth of fluid but compared that score with initial systolic blood pressure and base deficit to assess the ability of sonography to predict the need for a therapeutic laparotomy. McKenney and colleagues concluded that sonography was 83 % sensitive in determining the need for therapeutic laparotomy, compared to 28 % for systolic blood pressure and 49 % for base deficit [42].

As future studies continue to work toward investigating and validating known data regarding the utility of ultrasound in the management of the acutely ill trauma patient, current consensus guidelines and expert opinions have remained consistent. In the hemodynamically unstable patient with abdominal, thoracic, or pericardial free fluid noted on ultrasound, procedural/operative management is usually indicated. The stable patient with free fluid is directed toward further imaging studies, such as CT, while the unstable patient without abdominal or pericardial free fluid requires further clinical problem solving. The stable patient who receives a FAST exam without significant findings, but remains symptomatic, may undergo varying routes of management, including serial exams and observation, repeat ultrasound, or CT [12].

Pitfalls and Precautions

- Obesity and subcutaneous air greatly decrease both the sensitivity and specificity of the exam.
- Findings that may mimic free fluid in the RUQ due to their anechogenicity include the gallbladder, duodenum, inferior vena cava, and hepatic vessels.
- Failure to visualize the inferior pole of the right kidney may cause small pockets of free fluid to be missed.
- In the LUQ, knowledge of movement patterns of free intraperitoneal fluid will prevent inadequate visualization of the subphrenic space, which is more dependent than the splenorenal recess.
- The slightly superior and posterior position of the left kidney requires concomitant probe adjustment; directing the probe cephalad and posterior usually solves this issue.
- An accessory splenic lobule or more commonly a fluid-filled stomach may be mistaken for free fluid as well. Figure 14.30 depicts the LUQ view of a 30-year-old woman presenting with a history of pregnancy, vaginal bleeding, and hemorrhagic shock. On initial evaluation the picture may suggest subphrenic free fluid, but closer inspection reveals the well-circumscribed nature of the fluid collection, which was indeed a fluid-filled stomach. The presumptive diagnosis of ruptured ectopic pregnancy was avoided with knowledge of this ultrasonographic pitfall; rather than receiving a subtherapeutic laparotomy, she was resuscitated and underwent successful dilation and curettage for an incomplete abortion.
- Both ascites and bladder rupture can mimic hemoperitoneum and can fool the unaware clinician. In the case of the former, we discussed bedside paracentesis as a branch point in diagnostic decision making [14]. In the latter, the finding should be correlated clinically and operative management directed accordingly, as most extraperitoneal ruptures can be safely managed with simple catheter drainage [43], while most intraperitoneal bladder injuries require surgical exploration [44].

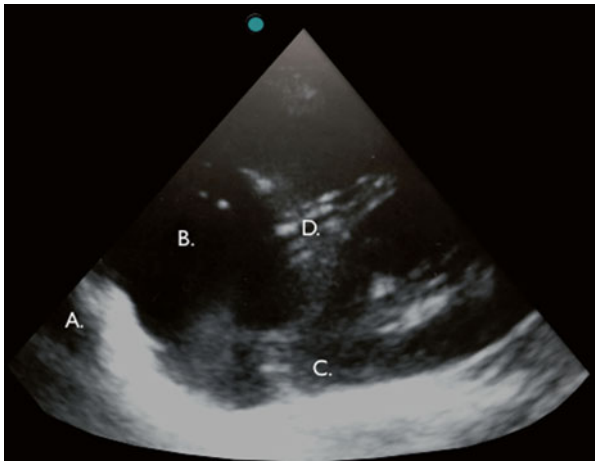

Fig. 14.30 Fluid-filled stomach mimicking free fluid in the LUQ. *A* diaphragm, *B* stomach, *C* superior pole of the left kidney, *D* spleen

- Fluid-filled loops of bowel, the seminal vesicles, and ovarian cysts can also mimic the anechogenicity of free fluid; adjusting the gain and depth may help.
- A full bladder is a significant aid in improving acoustic throughput. If empty, improved results may be obtained by instilling 250 mL of normal saline through an inserted Foley catheter and repeating the exam if pelvic free fluid is suspected. This is contraindicated in patients for whom urethral injury may be present.
- In a prior section we discussed the evaluation of a pericardial versus pleural effusion. A large left hemothorax can either prevent visualization of a pericardial effusion due to displacement of the pericardial sac or be confused with a pericardial effusion due to its proximity. The parasternal long view is especially helpful in this scenario, as visualization of the descending thoracic aorta and subsequent identification of fluid anterior (pericardial) or posterior (pleural) to this structure can help differentiate the two findings.
- Another common pitfall is incorrectly labeling an epicardial fat pad as a pericardial effusion [45]. This common anatomic variant, which will not be visualized posteriorly, is an accumulation of fat between the parietal pericardium and the parietal pleura. The ability to differentiate a fat pad versus a potential effusion in multiple views will aid an operator's diagnostic abilities.

Like any diagnostic tool, ultrasonography in the setting of trauma and critical care must be used and interpreted correctly to add successfully to the trauma evaluation. While the FAST exam has been shown to reliably identify as little as 250 mL of free fluid in Morison's pouch [46], it has not been shown to be a reliable indicator of solid organ injury [47]. Additionally, in patients with penetrating torso trauma, the specificity for the FAST exam remains high, but the sensitivity drops significantly [48]. Clinicians are cautioned to avoid overreliance on an initially negative FAST exam and to perform repeat exams on patients with evolving symptoms or a changing hemodynamic profile. Bearing these principles in mind, skilled clinician sonographers can use the FAST and e-FAST exam(s) to greatly improve diagnostic accuracy and thereby improve patient care.

References

1. Kristensen JK, Buemann B, Keuhl E. Ultrasonic scanning in the diagnosis of splenic haematomas. Acta Chir Scand. 1971;137:653–7.
2. Asher WM, Parvin S, Virgilio RW, Haber K. Echographic evaluation of splenic injury after blunt trauma. Radiology. 1976;118:411–5.
3. Tso P, Rodriguez A, Cooper C, Militello P, Mirvis S, Badellino M, et al. Sonography in blunt abdominal trauma: a preliminary progress report. J Trauma. 1992;33(1):39–45.
4. Bode PJ, Niezen RA, Van Vugt AB, Schipper J. Abdominal ultrasound as a reliable indicator for conclusive laparotomy in blunt abdominal trauma. J Trauma. 1993;34(1):27–31.
5. Sarkisian AE, Khondkarian RA, Amirbekian NM, Bagdasarian NB, Khojayan RL, Oganesian YT. Sonographic screening of mass casualties for abdominal and renal injuries following the 1988 Armenian earthquake. J Trauma. 1991;31(2):247–50.
6. American College of Emergency Physicians. Emergency ultrasound guidelines 2008. Available at: www.acep.org. Accessed 28 Apr 2013.

7. American College of Surgeons (ACS). Advanced trauma life support for physicians. Chicago: ACS; 1997.
8. Catre MG. Diagnostic peritoneal lavage versus abdominal computed tomography in blunt abdominal trauma: a review of prospective studies. Can J Surg. 1995;38(2):117–22.
9. Henneman PL, Marx JA, Moore EE, Cantrill SV, Ammons LA. Diagnostic peritoneal lavage: accuracy in predicting necessary laparotomy following blunt and penetrating trauma. J Trauma. 1990;30:1345–55.
10. Kam CW, Lai CH, Lam SK, So FL, Lau CL, Cheung KH. What are the ten new commandments in severe polytrauma management? World J Emerg Med. 2010;1(2):85–92.
11. Abrams BJ, Sukumvanich P, Seibel R, Moscati R, Jehle D. Ultrasound for the detection of intraperitoneal fluid: the role of Trendelenburg positioning. Am J Emerg Med. 1999;17: 117–20.
12. Scalea TM, Rodriguez A, Chiu WC, Brenneman FD, Fallon Jr WF, Kato K. Focused assessment with sonography for trauma (FAST): results from an international consensus conference. J Trauma. 1999;46(3):466–72.
13. Wu T, Pearson TC, Meiners S, Daugharthy J. Bedside ultrasound diagnosis of traumatic bladder rupture. J Emerg Med. 2011;41(5):520–3.
14. Blaivas M. Emergency diagnostic paracentesis to determine intraperitoneal fluid identity discovered on bedside ultrasound of unstable patients. J Emerg Med. 2005;29(4):461–5.
15. Parks JK, Elliott AC, Gentilello LM, Shafi S. Systemic hypotension is a late marker of shock after trauma: a validation study of Advanced Life Support principals in a large national sample. Am J Surg. 2006;192:727–31.
16. Salen PN, Melanson SW, Heller MB. The focused abdominal sonography for trauma (FAST) examination: considerations and recommendations for training physicians in the use of a new clinical tool. Acad Emerg Med. 2000;7(2):162–8.
17. Sisley AC, Johnson SB, Erickson W, Fortune JB. Use of an objective structured clinical examination (OSCE) for the assessment of physician performance in the ultrasound evaluation of trauma. J Trauma. 1999;47(4):627–31.
18. Ma OJ, Mateer JR. Trauma ultrasound examination vs chest radiography in the detection of hemothorax. Ann Emerg Med. 1997;29(3):312–5.
19. Volpicelli G. Sonographic diagnosis of pneumothorax. Int Care Med. 2011;37(2):224–32.
20. Lichenstein DA, Meziere G, Lascols N, Biderman P, Courret JP, Gepner A, et al. Ultrasound diagnosis of occult pneumothorax. Crit Care Med. 2005;33(6):1231–8.
21. Blaivas M, Brannam L, Hawkins M, Lyon M, Sriram K. Bedside emergency ultrasonographic diagnosis of diaphragmatic rupture in blunt abdominal trauma. Am J Emerg Med. 2004; 22(7):601–4.
22. Roe v. Wade, 410 U.S. 113, 160, 93 S.Ct. 705, 730 (1973).
23. Svinos H. Best BETS from the Manchester Royal Infirmary. BET 1 Using ultrasound to detect peritoneal fluid in a pregnant patient with abdominal trauma. Emerg Med J. 2009;26(3): 201–2.
24. Tiling T, Bouillon B, Schmid A. Ultrasound in blunt abdomino-thoracic trauma. In: Border JR, Allgoewer M, Hansen ST, Ruedi TP, editors. Blunt multiple trauma: comprehensive pathophysiology and care. New York: Marcel Dekker; 1990. p. 415–33.
25. Rozycki GS, Ochsner MG, Jaffin JH, Champion HR. Prospective evaluation of surgeons' use of ultrasound in the evaluation of trauma patients. J Trauma. 1993;34(4):516–26.
26. Tso P, Rodriguez A, Cooper C, Militello P, Mirvis S, Badellino M, et al. Sonography in blunt abdominal trauma: a preliminary progress report. J Trauma. 1992;33(1):39–44.
27. Jehle D, Guarino J, Karamanoukian H. Emergency department ultrasound in the evaluation of blunt abdominal trauma. Am J Emerg Med. 1993;11(4):342–6.
28. Rozycki GS, Ochsner MG, Schmidt JA, Frankel HL, Davis TP, Wang D, Champion HR. A prospective study of surgeon-performed ultrasound as the primary adjunct modality for injured patient assessment. J Trauma. 1995;39(3):492–500.
29. Udobi KF, Rodriguez A, Chiu WC, Scalea TM. Role of ultrasonography in penetrating abdominal trauma: a prospective clinical study. J Trauma. 2001;50(3):475–9.

30. Ma OJ, Mateer JR, Ogata M, Kefer MP, Wittmann D, Aprahamian C. Prospective analysis of a rapid trauma ultrasound examination performed by emergency physicians. J Trauma. 1995; 38:879–85.
31. Rozycki GS, Ochsner MG, Feliciano DV, Thomas B, Boulanger BR, Davis FE, et al. Early detection of hemoperitoneum by ultrasound examination of the right upper quadrant: a multicenter study. J Trauma. 1998;45(5):878–83.
32. Ma OJ, Kefer MP, Mateer JR, Thoma B. Evaluation of hemoperitoneum using a single- vs multiple-view ultrasonographic examination. Acad Emerg Med. 1995;2:581–6.
33. Melniker LA, Leibner E, McKenney MG, Lopez P, Briggs WM, Mancuso CA. Randomized controlled clinical trial of point-of-care, limited ultrasonography for trauma in the emergency department: the first sonography outcomes assessment program trial. Ann Emerg Med. 2006; 48(3):227–35.
34. Rozycki GS, Feliciano DV, Ochsner MG, Knudson MM, Hoyt DB, Davis F, et al. The role of ultrasound in patients with possible penetrating cardiac wounds: a prospective multicenter study. J Trauma. 1999;46:543–52.
35. Meyer DM, Jessen ME, Grayburn PA, et al. Use of echocardiography to detect occult cardiac injury after penetrating thoracic trauma: a prospective study. J Trauma. 1995;39:902–9.
36. Plummer D, Brunett D. Emergency department echocardiography improves outcomes in penetrating cardiac injury. Ann Emerg Med. 1992;21(5):709–12.
37. Ma OJ, Mateer JR. Trauma ultrasound examination versus chest radiography in the detection of hemothorax. Ann Emerg Med. 1997;29(3):312–6.
38. Sisley AC, Rozycki GS, Ballard RB. Rapid detection of traumatic effusion using surgeon-performed ultrasonography. J Trauma. 1998;44:291–7.
39. Rowan KR, Kirkpatrick AW, Liu D, Forkheim KE, Mayo JR, Nicolaou S. Traumatic pneumothorax detection with thoracic US: correlation with chest radiography and CT–initial experience. Radiology. 2002;225(1):210–4.
40. Bose SM, Mazumdar A, Gupta R, Giridhar M, Lal R, Praveen BV. Expectant management of haemoperitoneum. Injury. 1999;30(4):269–73.
41. Huang MS, Liu M, Wu JK, Shih HC, Ko TJ, Lee CH. J Trauma. Ultrasonography for the evaluation of hemoperitoneum during resuscitation: a simple scoring system. 1994;36(2):173.
42. McKenney KL, McKenney MG, Cohn SM, Compton R, Nunez DB, Dolich M. Hemoperitoneum score helps determine need for therapeutic laparotomy. J Trauma. 2001;50(4):650–6.
43. Kotkin L, Koch MO. Morbidity associated with nonoperative management of extraperitoneal bladder injuries. J Trauma. 1995;38(6):895–8.
44. Al-Aghbari S, Al-Harthy A, Ahmed M, Al-Reesi A, Al-Wahaibi K, Al-Qadhi H. Laparoscopic repair of traumatic intraperitoneal bladder rupture. Sultan Qaboos Univ Med J. 2011;11(4): 515–8.
45. Blaivas M, DeBehnke D, Phelan MB. Potential errors in the diagnosis of pericardial effusion on trauma ultrasound for penetrating injuries. Acad Emerg Med. 2000;7(11):1261–6.
46. Branney SW, Wolfe RE, Moore EE, Albert NP, Heinig M, Mestek M, et al. Quantitative sensitivity of ultrasound in detecting free intraperitoneal fluid. J Trauma. 1995;39(2):375–80.
47. Kendall JL, Faragher J, Hewitt GJ, Burcham G, Haukoos JS. Emergency department ultrasound is not a sensitive detector of solid organ injury. West J Emerg Med. 2009;10(1):1–5.
48. Quinn AC, Sinert R. What is the utility of the focused assessment with sonography in trauma (FAST) exam in penetrating torso trauma? Injury. 2011;42(5):482–7.

Chapter 15
Ultrasound in the Neurointensive Care Unit

Venkatakrishna Rajajee

Introduction

Bedside ultrasound has long played an important role in the neurointensive care unit, although mostly in the form of transcranial Doppler (TCD) for the detection of cerebral vasospasm following subarachnoid hemorrhage (SAH) [1]. More recently, however, the range of potential clinical applications for bedside ultrasound in the neurointensive care unit has greatly expanded. Optic nerve ultrasound (ONUS) has been extensively investigated as a noninvasive tool for the detection of raised intracranial pressure (ICP) [2–6]. Similar to patients in any other unit, bedside ultrasound is also invaluable for the assessment of shock, acute hypoxic respiratory failure, suspected deep venous thrombosis, and for the performance of several common bedside procedures. Patients with aneurysmal subarachnoid hemorrhage (aSAH) may particularly benefit from the use of bedside ultrasound: in addition to the risk of cerebral vasospasm, they are at considerable risk for severe left ventricular dysfunction and neurogenic pulmonary edema. While cranial ultrasound in the neonate and carotid ultrasound in ischemic cerebrovascular disease are among the most common applications of ultrasound relevant to neurological disease, they are beyond the scope of this chapter, which will focus on common applications of multipurpose point-of-care (POC) ultrasound in the adult neurointensive care unit.

V. Rajajee, M.D. (✉)
Departments of Neurosurgery & Neurology, University of Michigan Health System,
3552 Taubman Health Care Center, SPC 5338, 1500 E. Medical Center Drive,
Ann Arbor, MI 48109-5338, USA
e-mail: vrajajee@yahoo.com

M. Jankowich, E. Gartman (eds.), *Ultrasound in the Intensive Care Unit*,
Respiratory Medicine, DOI 10.1007/978-1-4939-1723-5_15

Transcranial Color-Coded Sonography

Technical and Patient Considerations

Transcranial Doppler vs Transcranial Color-Coded Sonography

Transcranial Doppler sonography has traditionally been performed using dedicated portable machines and transducers that display a spectral Doppler waveform only. Acquisition of the Doppler signal from intracranial vessels with these machines requires "blind" manipulation of the probe and adjustment of depth of the sample volume. "Blind" TCD can therefore be technically challenging, particularly for inexperienced operators. While traditional TCD is an established and well-validated tool, this technique requires dedicated equipment separate from the multipurpose point-of-care machines typically available in the intensive care unit (ICU). The angle of insonation of vessels cannot be known, and an insonation angle of greater than 60° may easily occur, leading to marked inaccuracy in measured velocities.

Transcranial color-coded sonography (TCCS) is performed using multipurpose machines with standard phased array probes to obtain grayscale images of cerebral parenchyma and duplex images of intracranial vessels, permitting rapid acquisition and identification of multiple intracranial vessels. The pulse Doppler spectral waveform is obtained guided by the duplex images, with appropriate consideration for the angle of insonation. More recently, TCCS capability in hand-carried POC ultrasound machines more familiar to intensive care professionals has become more widely available, obviating the need for dedicated TCD equipment. Image-guided acquisition of Doppler waveforms with TCCS can be much easier than "blind" acquisition of Doppler signal using traditional TCD, particularly for trainees and inexperienced sonographers. For these reasons, this chapter will focus on the use of TCCS instead of "blind" TCD. Potential disadvantages of TCCS are the relatively larger footprint of the probe and the relative insensitivity of duplex ultrasound for low flow signals.

Equipment

A phased array (5–1 MHz) transducer (Fig. 15.1) is used, and the transcranial preset (Fig. 15.2) selected. Transcranial imaging cannot be performed with the cardiac and abdominal presets available on most multipurpose POC machines.

Patient Factors

The patient is positioned supine with the head resting comfortably back on the bed during transtemporal insonation. During transforaminal insonation the patient is ideally positioned sitting up with the head flexed forward; however, the patient can also be positioned on his/her side with the chin in contact with the chest. While no specific adverse effects have been reported with the diagnostic use of standard

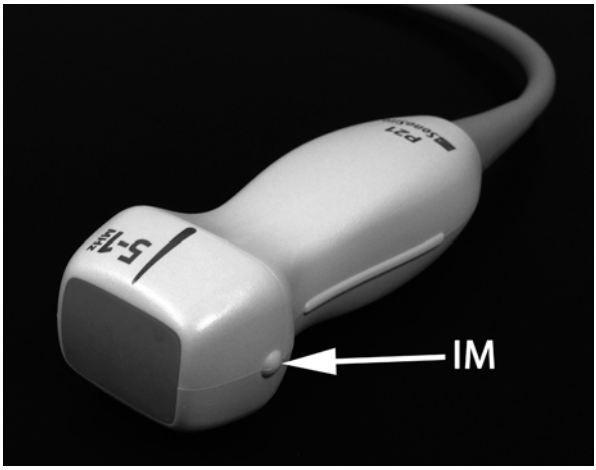

Fig. 15.1 Phased array transducer used for TCCS. *IM* index mark on the probe corresponds to index mark on the screen

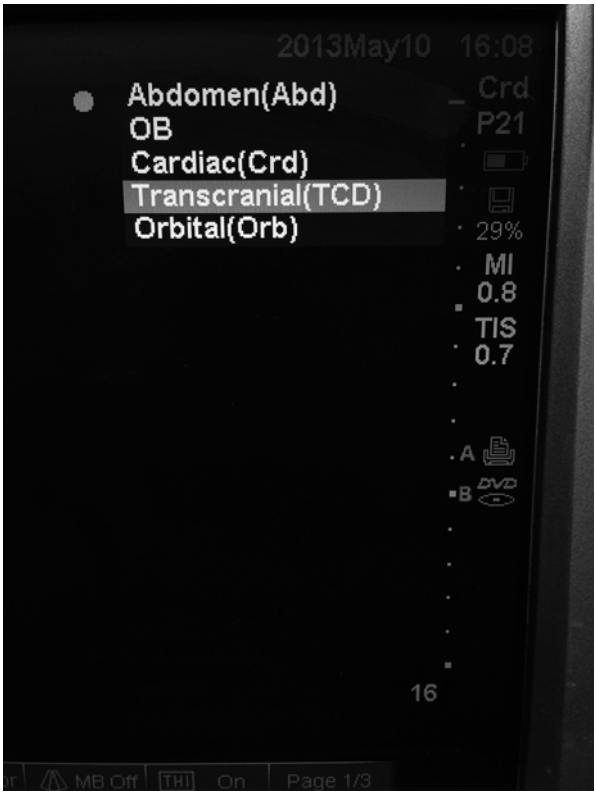

Fig. 15.2 Selection of transcranial preset. Select "Transcranial" from the l ist of presets available for the phased array transducer probe

TCD/TCCS probes, the general principle of ALARA (as low as reasonably achievable) must be kept in mind, with the duration of insonation restricted to that which is clinically essential. This is particularly true because transcranial insonation typically requires maximal acoustic power output. About 5–20 % of patients have an inadequate transtemporal window for performance of TCCS [7, 8]. Risk factors for absence of transtemporal window include older age, female sex, and measured skull thickness [7, 8].

Image Acquisition and Interpretation

Image Acquisition

The sector-shaped image on the screen obtained from the phased array probe is oriented with the index mark on the upper left aspect of the image. The examiner ideally stands behind the patient's head, although any position that allows the elbow to rest on the patient's bed or be held close to the examiner's side is acceptable; arm fatigue can be expected to develop rapidly. Insonation is initially performed through the transtemporal acoustic window, with the transducer placed immediately anterior to the upper border of the tragus and superior to the posterior zygomatic arch (Fig. 15.3). The index mark on the probe is directed anteriorly and rotated at a 10–20° angle superior to the axial plane (Fig. 15.4) with the transducer itself tilted at a 10–20° angle cephalad to the axial plane (Fig. 15.5). If the desired image is not obtained, the probe can be moved within the approximate area delineated by the circle in Fig. 15.3 until the desired initial grayscale image is obtained. If no recognizable anatomical features are seen, it is possible that the patient does not have an acoustic window on that side.

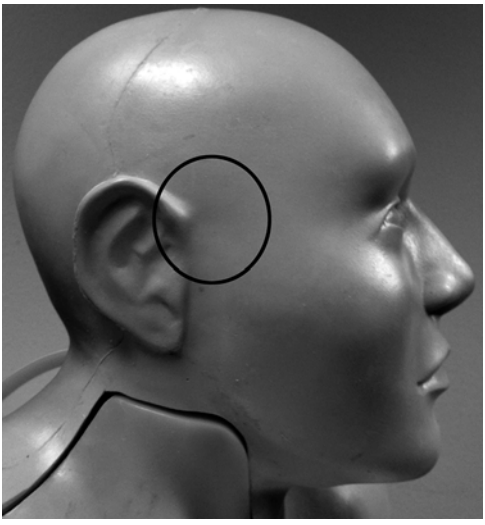

Fig. 15.3 Transtemporal window. The phased array probe can be moved within the *circle* until the midbrain is identified on B-mode

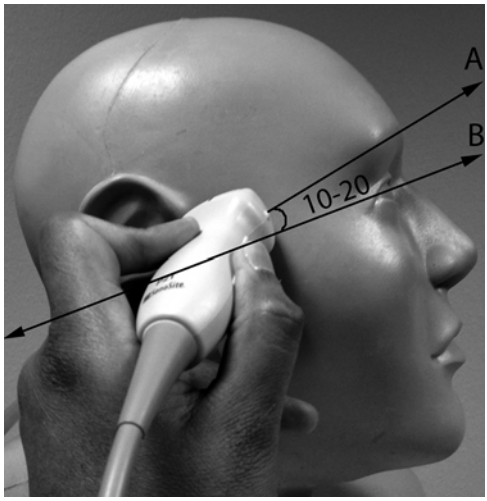

Fig. 15.4 Probe position for TCCS – lateral view of transtemporal insonation. The transducer is rotated slightly so the index mark on the phased array probe points in the direction A, which is at about a 10–20° angle to the anatomical axial plane, depicted by line B

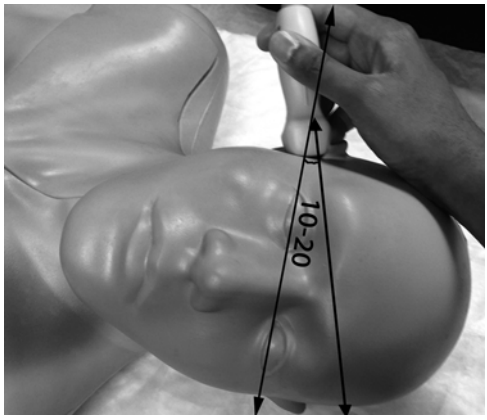

Fig. 15.5 Probe position for TCCS – anteroposterior view of transtemporal insonation. The transducer is tilted slightly cephalad, at a 10–20° angle to the anatomical axial plane

The single most important anatomical feature to identify at this point is the *midbrain* (Fig. 15.6), at a depth of about 5–8 cm, with the "Mickey Mouse ears" of the crus cerebri seen turned on their side. This is comparable, but not identical, to the image obtained with computed tomography (CT) imaging at this level (Fig. 15.7). Once this plane of imaging is obtained, other prominent anatomical features can be rapidly identified, including the *lesser sphenoid wing of the temporal bone* and the *basal cisterns*, particularly the interpeduncular and quadrigeminal cisterns (Figs. 15.6 and 15.7). The normal anatomical distribution of the major intracranial arteries and the circle of Willis is shown in Fig. 15.8. Once the midbrain is identified on the grayscale image, the color box is positioned over the expected anatomical location of the vessel(s) of interest, with "red" typically depicting flow toward and "blue" flow away from the probe. The most important intracranial artery to identify

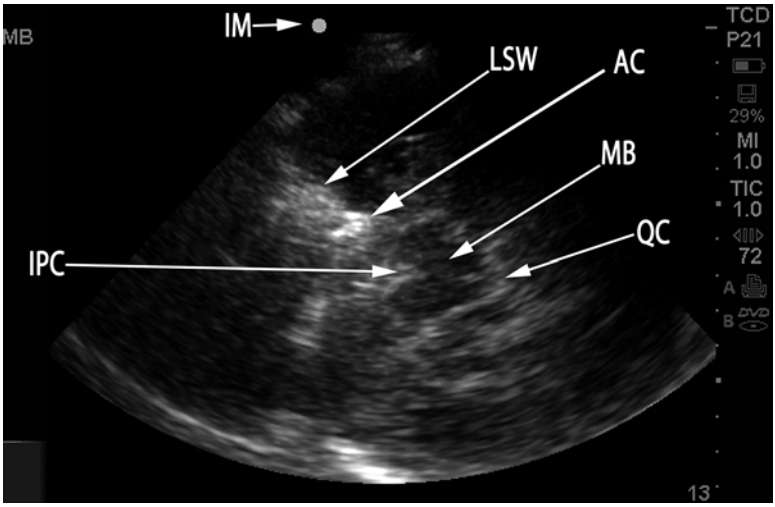

Fig. 15.6 B-mode image at level of the midbrain. Compare to Fig. 15.7, which depicts CT imaging at the same level in the same aSAH patient, with the same anatomical features labeled. *IM* index mark (corresponds to Index Mark on transducer), *MB* midbrain, *LSW* lesser sphenoid wing, *AC* aneurysm clip, *QC* quadrigeminal cistern, *IPC* interpeduncular cistern

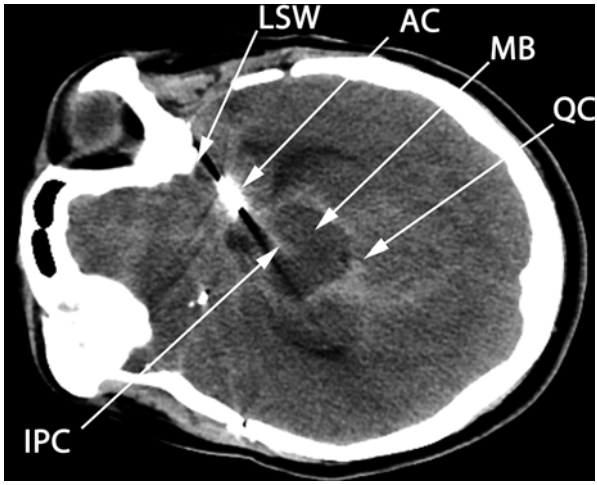

Fig. 15.7 CT axial image at level of midbrain. Compare to Fig. 15.6, which depicts B-mode image at the same level in the same aSAH patient, with the same anatomical features labeled. The CT image has been rotated 90° to the *left* for easier comparison to the ultrasound image. *MB* midbrain, *LSW* lesser sphenoid wing, *AC* aneurysm clip, *QC* quadrigeminal cistern, *IPC* interpeduncular cistern

is the *middle cerebral artery (MCA)*, seen as a curved vessel extending out toward the probe with flow directed toward the probe (depicted in red in Fig. 15.9) from a point anterior and lateral to the midbrain that is the point of bifurcation of the internal carotid artery, at about 4–6 cm depth. The A1 segment of the *anterior cerebral artery* (ACA) is seen extending from the *internal carotid artery* (ICA) bifurcation in the opposite direction, anteriorly, and toward the midline, with flow away from

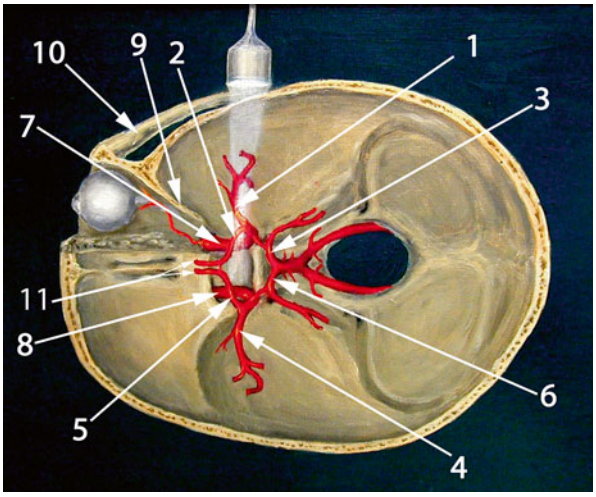

Fig. 15.8 Normal anatomical distribution of intracranial arteries. Compare to Fig. 15.9, which is a duplex image of the circle of Willis in approximately the same anatomical plane with the same labeling. *1* Ipsilateral MCA, *2* ipsilateral ACA A1 segment, *3* ipsilateral PCA P1 segment, *4* contralateral MCA, *5* contralateral ACA A1 segment, *6* contralateral PCA P1 segment, *7* ipsilateral ICA, *8* contralateral ICA, *9* lesser sphenoid wing, *10* zygomatic arch, *11* bilateral ACA A2 segments (This figure was adapted from http://en.wikipedia.org/wiki/File:Transcranial_doppler.jpg under the terms of GNU Free Documentation License, Version 1.3 by Rune Aaslid)

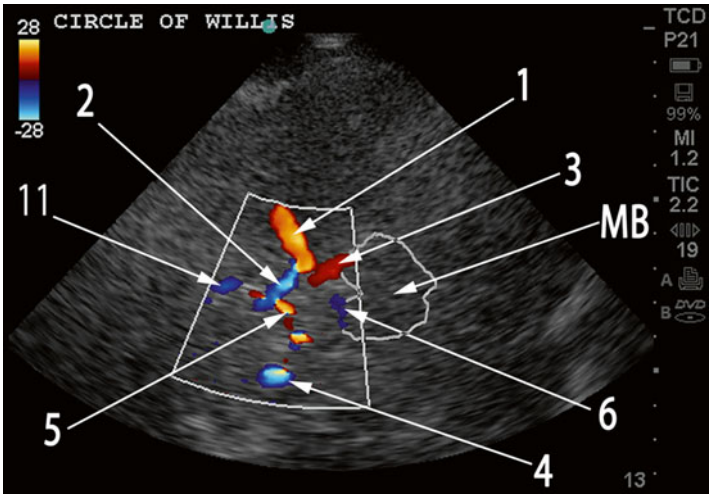

Fig. 15.9 TCCS duplex image of the circle of Willis. Compare to Fig. 15.8 which depicts normal anatomical distribution of intracranial vessels in approximately the same anatomical plane with the same labeling. *1* ipsilateral MCA, *2* ipsilateral ACA A1 segment, *3* ipsilateral PCA P1 segment, *4* contralateral MCA, *5* contralateral ACA A1 segment, *6* contralateral PCA P1 segment, *11* bilateral ACA A2 segments (cannot be distinguished on TCCS)

the probe (depicted in blue in Fig. 15.9). The ipsilateral (blue) and contralateral (red) A1 segments appear to meet in the midline (where the anterior communicating artery is typically *not* visualized) with the two A2 segments (which can often not be individually distinguished) extending anteriorly from this point, in the midline, with flow away from the probe (blue in Fig. 15.9). Minimal downward (caudal) angulation of the probe from this plane will reveal the distal internal carotid artery (ICA) following its entry into the skull, in continuity with proximal MCA, with flow directed toward the probe. Placing the color box around the midbrain itself, in the original plane of insonation, will reveal the *posterior cerebral artery* (PCA) curving around the crus cerebri and the midbrain from its point of origin (the bifurcation of the basilar artery) in the interpeduncular cistern. The ipsilateral PCA P1 segment demonstrates flow toward the probe (red in Fig. 15.9), which changes to flow away from the probe (blue) in the P2 segment following the completion of the bend in the PCA around the crus cerebri.

Increasing the depth of insonation to 13 cm or greater and extending the color box will sometimes reveal the contralateral intracranial vessels, depending on the quality of the acoustic window. This is most feasible when performing insonation through a large decompressive craniectomy defect. When visible, the contralateral ACA A1 segment and PCA P2 segments are seen with flow toward the probe (red), while the contralateral MCA and PCA P1 segment are seen with flow away from the probe (blue), as seen in Fig. 15.9. An attempt at interrogation of the contralateral vessels may be the only recourse when a patient has a viable transtemporal acoustic window on only one side.

To visualize the vertebrobasilar circulation, the patient's head is flexed forward and the transducer firmly positioned in the suboccipital region with use of copious conductive gel to permit acoustic transmission through the hair at the nape of the neck. The probe is angled so that the long axis of the probe passes through the *nasion*, permitting insonation through the foramen magnum (Fig. 15.10). The most important structure seen on the grayscale image will be the *foramen magnum*, a large circular hypoechoic structure in the midline between about 2–7 cm of depth (Fig. 15.11). The color box is placed so that it covers the foramen magnum and the

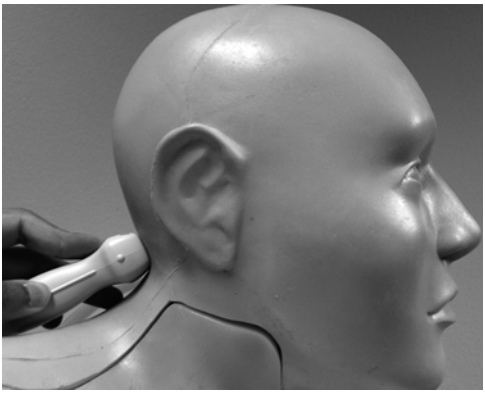

Fig. 15.10 Probe position for TCCS – transforaminal (suboccipital) window. Probe is placed below occipital protuberance with head flexed (head flexion not demonstrated in this image), probe points toward the nasion

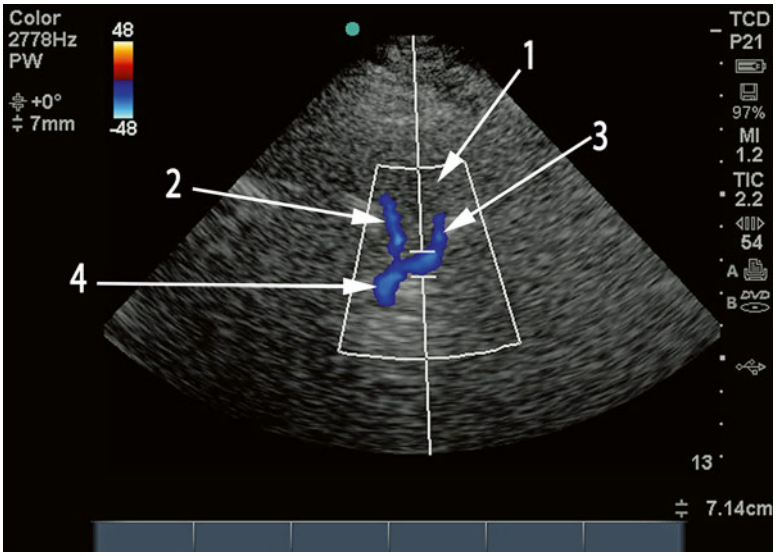

Fig. 15.11 Transforaminal view of vertebral and basilar arteries. The hypoechoic circular structure labeled 1 is the foramen magnum. *Right* (*2*) and *left* (*3*) vertebral arteries meet to form the basilar artery (*4*), producing the characteristic Y shape on duplex imaging

expected location of the *basilar artery* deeper to the foramen, within the cranial vault. The two *vertebral arteries* are visualized on either side of the foramen magnum, with flow away from the probe (blue in Fig. 15.11), extending intracranially to a point of confluence at about 6–8 cm of depth, beyond which the basilar artery is seen extending distally into the cranial vault, also with flow away from the probe (blue in Fig. 15.11). This confluence typically results in the "Y" shape seen in Figs. 15.11 and 15.12. The distal bifurcation of the basilar artery is typically not visualized with TCCS.

Once the vessels of interest are identified, pulse Doppler is selected with a sample volume size of about 3–10 mm. The sample volume is then placed on the arterial segment of interest (Fig. 15.13). Since the anatomical orientation of the artery can be clearly visualized, an effort must be made to obtain an insonation angle as close as possible to zero degrees for flow toward the probe and 180° for flow away from the probe (Figs. 15.13 and 15.14). When this is not possible, most POC machines with TCCS capability permit angle correction through manual delineation of the direction of flow within the vessel. The machine then corrects the calculated velocity using a formula that includes the angle of insonation. Using angle correction is generally not recommended when the angle of insonation is greater than 60° or when a sufficiently long arterial segment is not available to accurately depict the direction of flow. Once the sample volume is appropriately positioned (and angle correction performed if so desired), the spectral Doppler reading is obtained (Fig. 15.15). The Doppler frequency shift recorded within the sample volume is converted to flow velocity, depicted on the y-axis, against time, on the x-axis.

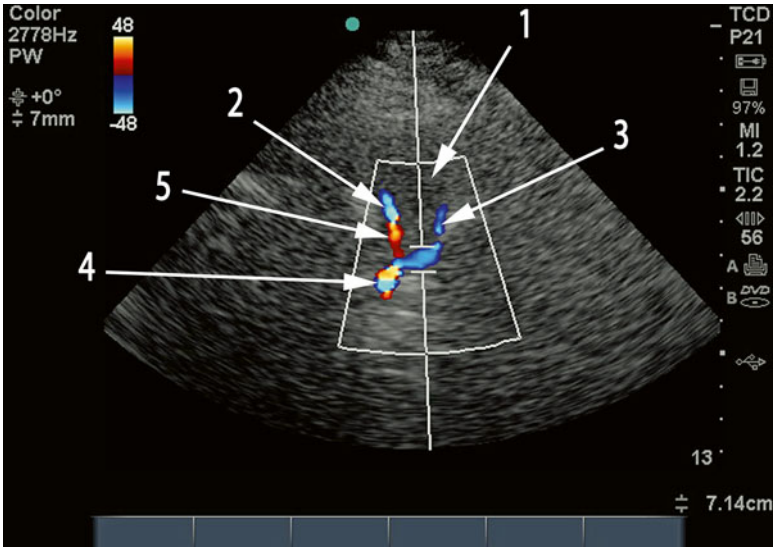

Fig. 15.12 Aliasing in the vertebrobasilar circulation. Repeat TCCS performed on the same patient with aSAH several days following Fig. 15.11. Identical image to Fig. 15.11, except aliasing is seen in the distal right vertebral (*5*) and proximal basilar (*4*) arteries. *1* foramen magnum, *2* right vertebral artery with aliasing in the distal segment labeled 5, *3* left vertebral artery, *4* basilar artery now with aliasing

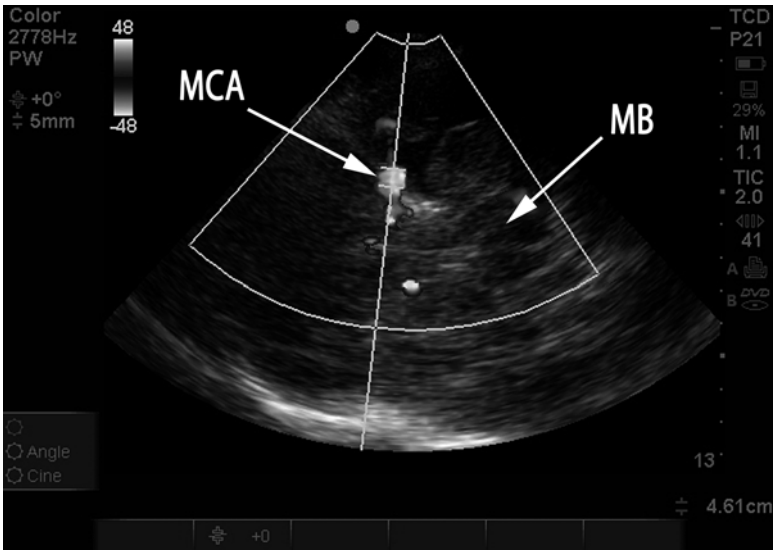

Fig. 15.13 Placement of sample volume on MCA, good angle of insonation. Duplex color image rendered in *black* and *white*. The sample volume has been placed in the MCA M1 segment. Note excellent angle of insonation, in-line with direction of flow in the MCA. *MB* midbrain, *MCA* middle cerebral artery

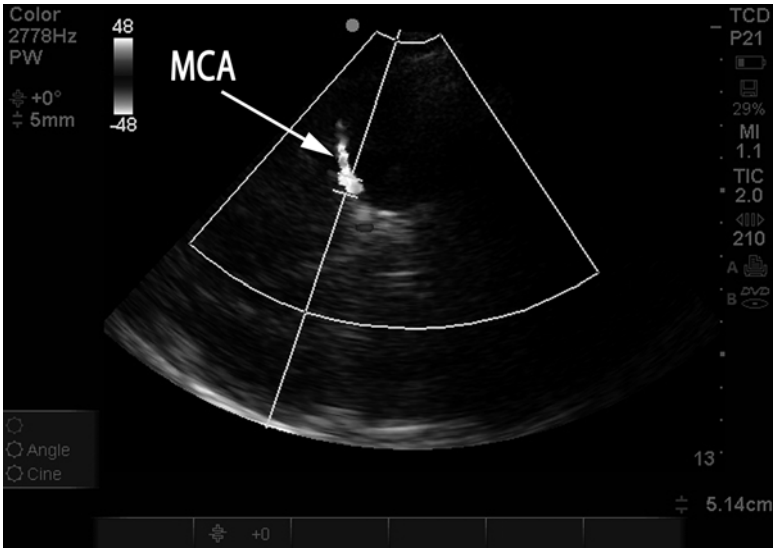

Fig. 15.14 Placement of sample volume on MCA, suboptimal angle of insonation. Duplex color image rendered in *black* and *white*. Same patient and examination as in Fig. 15.13. Probe has been moved slightly and the sample volume is again placed on the MCA M1 segment; however, there is now a relatively steep angle of insonation to the direction of flow in the MCA, which will artificially lower the measured mCBFV. Probe position needs to be altered slightly to optimize angle of insonation, seen in Fig. 15.13

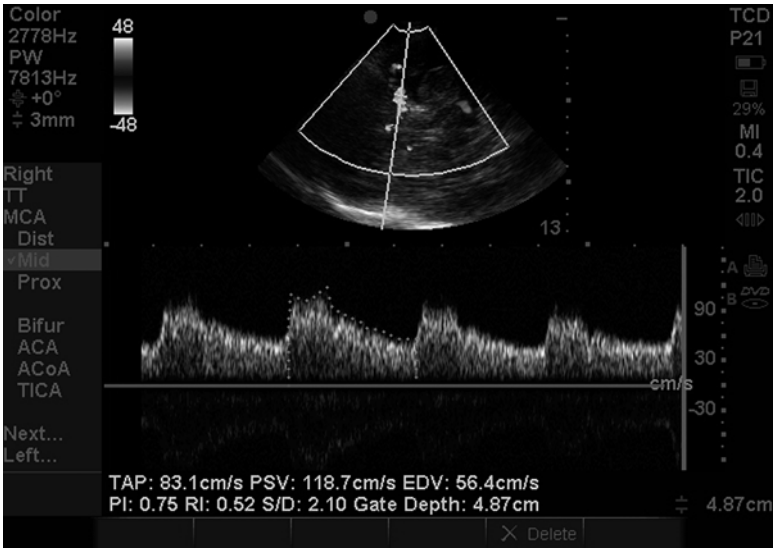

Fig. 15.15 Spectral Doppler waveform. Spectral Doppler waveform obtained from sample volume placement on MCA shown in Fig. 15.13. The mCBFV is depicted here as the time averaged peak (TAP). *PSV* peak systolic velocity, *EDV* end-diastolic velocity, *PI* pulsatility index

One complete cardiac cycle on the spectral Doppler waveform is then traced out and the machine calculates the parameters of interest, including the peak systolic velocity (PSV), end-diastolic velocity (EDV), the mean cerebral blood flow velocity (mCBFV – otherwise known as the time averaged peak or TAP), and the pulsatility index {PI = (PSV-EDV)/mean flow velocity or MFV}.

When the blood flow velocity within an arterial segment is relatively high relative to the set color scale, aliasing may occur. Aliasing is visible as an abrupt change in color duplex examination within a segment of the artery (but not the entire artery) from the expected color appropriate to the direction of flow to the opposite color: red to blue or vice versa. The presence of aliasing can be clinically useful, since regions of aliasing are more likely to represent higher velocities and can be preferentially sampled when looking for vasospasm (Fig. 15.12). Most aliasing does NOT represent vasospasm; however, and if so desired, aliasing can be eliminated by increasing the range of the color scale.

Once the intracranial vessels have been interrogated, measuring the velocities in the distal cervical internal carotid arteries, immediately prior to their entry into the skull, should be performed when evaluating for vasospasm. These extracranial ICA (exICA) velocities are used to calculate the *Lindegaard ratio* ($mCBFV_{MCA}/mCBFV_{exICA}$). The transducer is placed in the submandibular region at the angle of the jaw and directed upward and slightly medially, toward the ipsilateral eye (Fig. 15.16). The exICA is a linear (sometimes tortuous) vessel with flow away from the probe (blue in Fig. 15.17) and is typically medial to the internal jugular vein, which is distinguished by the presence of flow toward the probe (red) and a venous pattern of pulsation. The most important distinguishing feature of the exICA, compared to the

Fig. 15.16 Probe position for TCCS – submandibular insonation. Probe is placed below angle of the jaw and directed upward and slightly medially

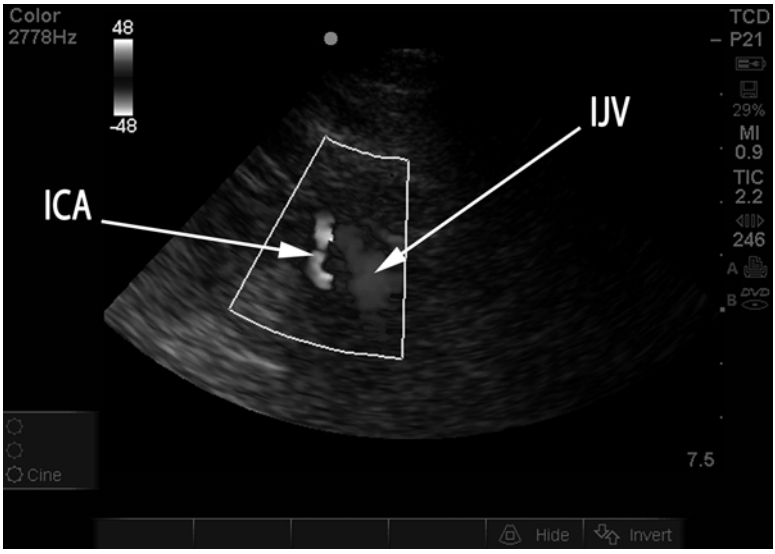

Fig. 15.17 Extracranial ICA and IJV seen on submandibular insonation. Duplex color image rendered in *black* and *white. ICA* internal carotid artery, was *blue* in original duplex image depicting flow away from probe. *IJV* internal jugular vein, was *red*, with flow toward the probe

external carotid artery, is the presence of substantial diastolic flow in the exICA. As with intracranial vessels, obtaining an angle of insonation as close to 0° or 180° as possible is important; otherwise, perform angle correction.

Image Interpretation

The most important parameter obtained from TCCS is the mCBFV, since most angiographic correlation to vessel caliber has been performed with this parameter. The range of "normal" velocities used at the University of Michigan is shown in Table 15.1.

1. Cerebral vasospasm after aSAH
   Reduction in vessel caliber caused by cerebral vasospasm following aSAH will result in an elevation in mCBFV, since velocity of blood flow is inversely proportional to the square of the vessel radius [9]. A mCBFV <120 cm/s in the MCA is reliable for the exclusion of hemodynamically significant vasospasm and mCBFV >200 cm/s is specific for severe vasospasm [1, 10]. Elevations in velocity between 120 and 200 cm/s may be caused by either hyperdynamic flow or vasospasm. Hyperdynamic flow frequently results from factors such as the catecholamine surge following aSAH, anxiety, pain, fever, anemia, and the use of inotropic agents. The Lindegaard ratio ($mCBFV_{MCA}/mCBFV_{exICA}$) can be used to differentiate hyperdynamic flow from vasospasm [1, 10]. A ratio >3 likely

Table 15.1 Normal range of mean cerebral blood flow velocities

Intracranial artery	Normal range of mCBFV (cm/s)
Middle cerebral artery (MCA)	37–81
Anterior cerebral artery (ACA)	25–77
Posterior cerebral artery (PCA)	18–58
Intracranial internal carotid artery (ICA)	19–69
Vertebral artery	16–56
Basilar artery	21–57
Extracranial internal carotid artery (ExICA)	28–48

represents mild vasospasm and a ratio >6 severe vasospasm. Thresholds for the identification of vasospasm have been validated primarily in the MCA. However, normal MCA velocities are almost always higher than ipsilateral normal ACA, ICA, and PCA velocities. Therefore, an elevation in the velocity (or corresponding ratio to ipsilateral exICA velocity) in any of these other arteries above thresholds validated for vasospasm in the MCA are very likely to represent vasospasm in those vessels as well; this is especially true when the mCBFV in any of these other arteries exceeds 200 cm/s. Normal velocities in the posterior circulation are typically lower than in the anterior circulation. In one study, a basilar velocity >85 cm/s and a ratio of basilar to extracranial (measured in the neck, not transforaminal) vertebral mCBFV >3 had 92 % sensitivity and 97 % specificity for basilar narrowing of more than 50 % on angiography [11]. While mCBFV identifies large vessel vasospasm and not tissue ischemia, a PI $\leq$ 0.58 may identify patients with large vessel vasospasm at higher risk for subsequent clinical neurological decline [12].

2. Determination of brain death
   The American Academy of Neurology's Quality Standards Subcommittee requires that the determination of brain death using TCD/TCCS be made on the basis of reverberating flow (Fig. 15.18) or short systolic spikes (Fig. 15.19) recorded in the anterior circulation (typically the MCA) bilaterally as well as in the posterior circulation (basilar) [1]. While the presence of such diffuse reverberating flow or short systolic spikes is considered incompatible with clinical recovery, the absence of flow signal cannot be used to determine brain death, since the inability to detect signal is commonly the result of inadequate windows or other technical factors.
3. Recanalization following acute ischemic stroke
   The spectral Doppler waveform obtained from the vessel targeted by reperfusion therapy, either intravenous tissue plasminogen activator (tPA) or endovascular therapy, may be used to assess the degree of recanalization. The consensus on grading intracranial flow obstruction (COGIF) score has been proposed as a tool for assessment of recanalization in clinical trials of acute ischemic stroke using TCCS and is shown in Table 15.2 [13].

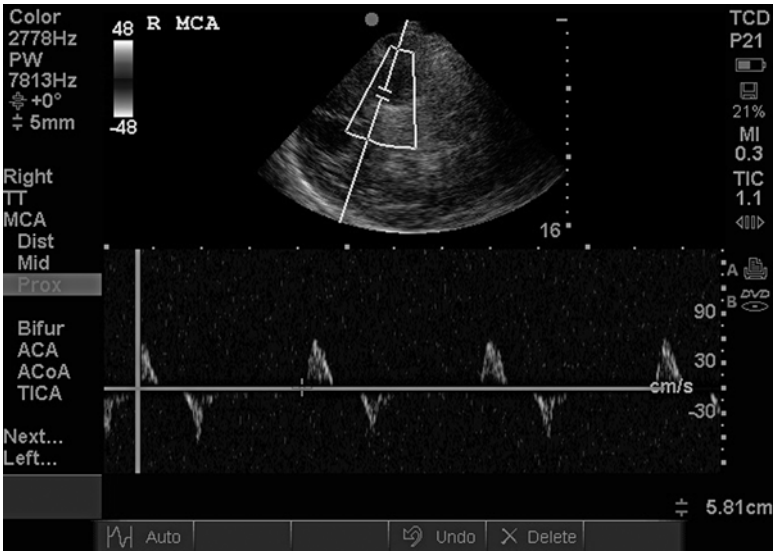

Fig. 15.18 Reverberating flow in brain death. Reverberating systolic/diastolic flow seen in the MCA. When present in both MCAs and the basilar, this is incompatible with clinical recovery

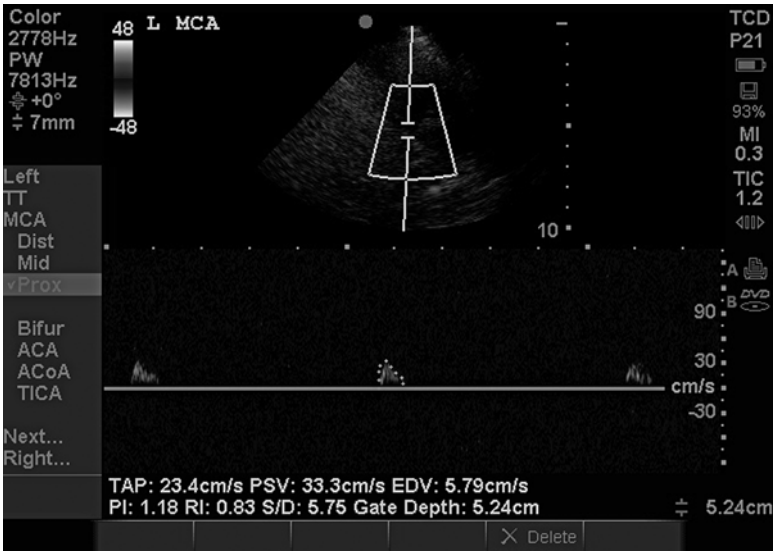

Fig. 15.19 Short systolic spikes in brain death. Short systolic spikes with no diastolic flow in the MCA. When present in both MCAs and the basilar, this is incompatible with clinical recovery

Table 15.2 Consensus on grading intracranial flow obstruction (COGIF) scale for assessment of recanalization following thrombolysis for acute ischemic stroke

COGIF grade	Hemodynamic pattern on TCCS	Clinical significance
1	No flow	Absent recanalization OR suboptimal acoustic window
2	Low systolic flow velocities, absent diastolic flow	Minimal recanalization OR downstream/ upstream severe narrowing or obstruction
3	Low systolic flow velocities with some diastolic flow	Partial recanalization OR downstream/ upstream severe narrowing or obstruction
4 Established perfusion		Established perfusion
(a) Flow velocities equal to contralateral side		Normal flow
(b) High focal flow velocities		Focal intracranial stenosis
(c) High segmental flow velocities		Hyperperfusion

Basic and Advanced Competencies in TCCS

There is, as yet, no consensus on what may constitute basic or core competencies in the performance and interpretation of TCCS in the neurointensive care unit. As the most common and well-established indication for TCCS in the neuroICU, the detection of vasospasm following aSAH would likely be considered a core competency, while the use of TCCS for brain death determination and assessment of recanalization are used less commonly than vasospasm monitoring and may therefore be considered relatively advanced competencies.

Evidence Review and Evidence-Based Use

Vasospasm of the large intracranial arteries evaluated by TCCS occurs in up to 70 % of patients with aneurysmal subarachnoid hemorrhage (aSAH) in a time window between 3 and 14 days following ictus (peak 8–10 days), although a majority of these patients remain asymptomatic [14–16]. About 20–30 % of patients will, however, develop delayed cerebral ischemia (DCI), presumably from severe vasospasm resulting in compromised distal flow to the brain, with 15–20 % of patients progressing to death or cerebral infarction [17–19]. Delayed infarction can result in severe morbidity and long-term functional disability [19].

The evidence that the use of TCD/TCCS is useful, although not definitive, for the prediction of large vessel (angiographic) vasospasm in the MCA following a SAH is robust [1, 10, 14, 15]. The predictive value appears to be substantially lower for vessels other than the MCA [10]. In one meta-analysis of 26 studies assessing the predictive value of TCD for vasospasm, sensitivity was 67 % (95 % CI 48–87 %), specificity 99 % (98–100 %), positive predictive value (PPV) 97 % (95–98 %), and

negative predictive value (NPV) 78 % (65–91 %) for the MCA. For the ACA, however, sensitivity was 42 % (11–72 %), specificity 76 % (53–100 %), PPV 56 % (27–84 %), and NPV 69 % (43–95 %) [10]. The frequency at which TCD/TCCS should be performed following aSAH is unclear, although many institutions perform daily TCD/TCCS evaluation while the patient is within the risk period for vasospasm.

In 2004, the Therapeutics and Technology Assessment Subcommittee of the American Academy of Neurology specified clinical indications for which the use of TCD/TCCS is well established on the basis of the existing evidence [1]. Detection and monitoring of large vessel vasospasm following aSAH was found to be a "setting in which TCD is able to provide information and in which its clinical utility is established," based on a moderately high level of evidence. In contrast, confirmation of cerebral circulatory arrest in the patient with suspected brain death was determined to be a "setting in which TCD is able to provide information, but in which its clinical utility, compared with other diagnostic tools, remains to be determined," while the monitoring of thrombolysis of acute MCA occlusions was determined to be a "setting in which TCD is able to provide information, but in which its clinical utility remains to be determined."

Pitfalls and Precautions

While considering the evidence base for the use of TCD/TCCS in prediction and monitoring of vasospasm following aSAH, several factors must be taken into account. While accurate at predicting large vessel vasospasm, TCD/TCCS is not consistently accurate at predicting the development of DCI and delayed infarction [20]. It is now recognized that DCI and angiographic vasospasm are distinct entities – patients with even severe angiographic vasospasm may continue to perfuse cerebral tissue adequately and DCI may occur in the absence of severe vasospasm [21]. The treatment of cerebral vasospasm with either hemodynamic augmentation or endovascular therapy, although widely performed, has not been evaluated in clinical trials with meaningful outcome measures. The presence of severe angiographic vasospasm, however, is strongly *correlated* with the subsequent occurrence of DCI [19], and the expectation that a severe reduction in luminal diameter will eventually compromise tissue perfusion is reasonable. The presence of TCCS evidence of severe vasospasm should, therefore, be a "red flag" that warrants close monitoring of the patient's hemodynamic and neurological condition, with hemodynamic and endovascular intervention considered for any neurological decline.

As previously mentioned, an important limitation in the use of TCCS is the relatively frequent (5–20 %) absence of adequate acoustic windows [7, 8]. As with any other ultrasound examination, TCCS is an operator-dependent tool and is prone to error in the hands of less experienced operators. The ACA in particular is often challenging to detect on duplex examination. Angle-corrected velocities obtained from

TCCS are significantly higher than those obtained from TCD and may lead to overestimation of vasospasm when using criteria established using "blind" TCD. Therefore, in the absence of large studies correlating angle corrected velocities to angiographic vasospasm, the University of Michigan protocol is to attempt to obtain as narrow an angle of insonation as possible using image guidance but not to perform angle-correction.

B-Mode Imaging of the Cerebral Parenchyma

While transcranial ultrasound is routinely used for the detection of intracranial hemorrhage in neonates, there has been interest more recently in the use of B-mode imaging of the cerebral parenchyma in adults, particularly when a decompressive craniectomy defect permits adequate acoustic transmission. Imaging of the cerebral parenchyma can be performed by first identifying the plane of the midbrain, as described above, then tilting the probe minimally upward/cephalad until the *third ventricle* and *lateral ventricles* are seen. This is typically possible only in the patients with the very best temporal acoustic windows, primarily patients with decompressive craniectomy and a large skull defect. While the lateral ventricles are hypoechoic from their fluid content, in the absence of hydrocephalus, it is the hyperechoic *choroid plexus* within the ventricles that is often visualized (Figs. 15.20 and 15.21).

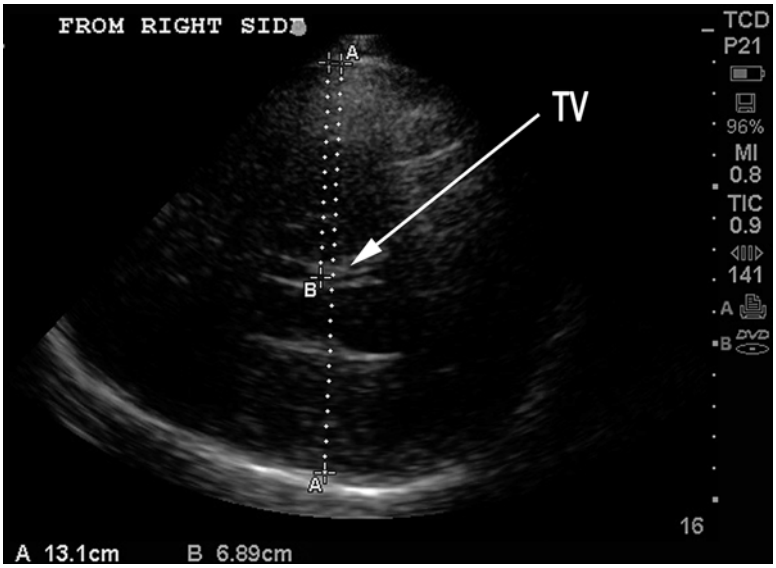

Fig. 15.20 B-mode measurement of midline shift – measurement from *right*. Patient with large right MCA infarction. Third ventricle (TV) is identified by the presence of the hyperechoic *double line* ("tram track") of the choroid plexus and marks the midline. Distance from surface to TV is 6.89 cm from the *right* and (see Fig. 15.21) 6.19 cm from the *left*. Midline shift is therefore (6.89–6.19)/2 = 0.35 cm, almost identical to the midline shift measured on CT (see Fig. 15.22)

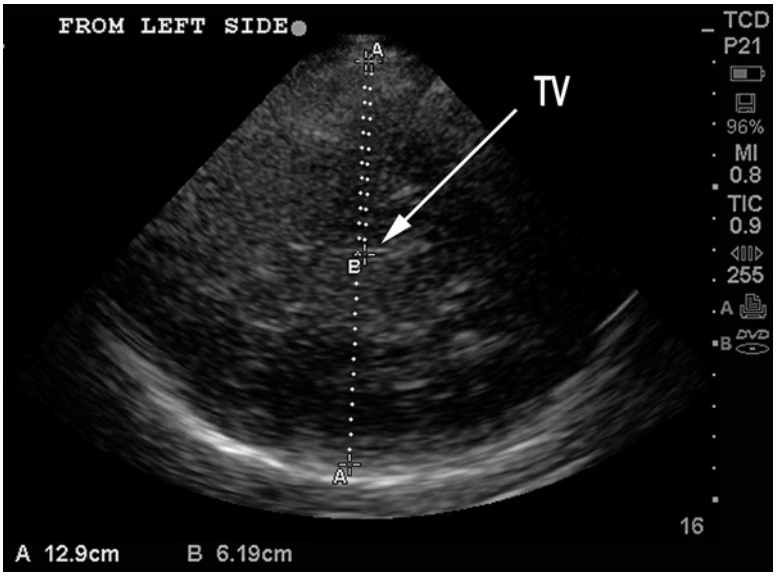

Fig. 15.21 B-mode measurement of midline shift – measurement from *left*. Patient with large right MCA infarction. Third ventricle (TV) is identified by the presence of the hyperechoic *double line* ("tram track") of the choroid plexus and marks the midline. Distance from surface to TV is 6.19 cm from the *left* and 6.89 cm from the *right* (see Fig. 15.20). Midline shift is therefore (6.89–6.19)/2 = 0.35 cm, almost identical to the midline shift measured on CT (see Fig. 15.22)

The third ventricle can be used to identify the *midline*, and *midline shift* in the setting of space-occupying lesions (such as malignant MCA infarction) is calculated as the difference in the distance from the probe to the midline from each side, divided by two (Figs. 15.20 and 15.21) with good correlation to measurement using CT (Fig. 15.22) [22]. Assessment using B-mode also has good correlation to CT imaging for determination of lateral ventricular size in hydrocephalus (Figs. 15.23 and 15.24) as well as for the detection and measurement of intraparenchymal hematomas (Figs. 15.25 and 15.26) [23, 24]. While B-mode imaging of the brain appears to hold significant promise, it is considered investigational at this time, and its clinical role not yet defined.

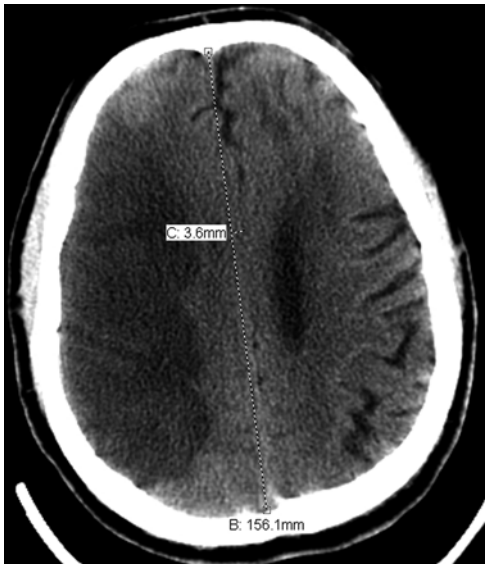

Fig. 15.22 CT measurement of midline shift. Same patient as in Figs. 15.20 and 15.21, same day as B-mode evaluation. Midline shift on CT (3.6 mm) is almost identical to midline shift calculated from B-mode imaging (see Figs. 15.20 and 15.21)

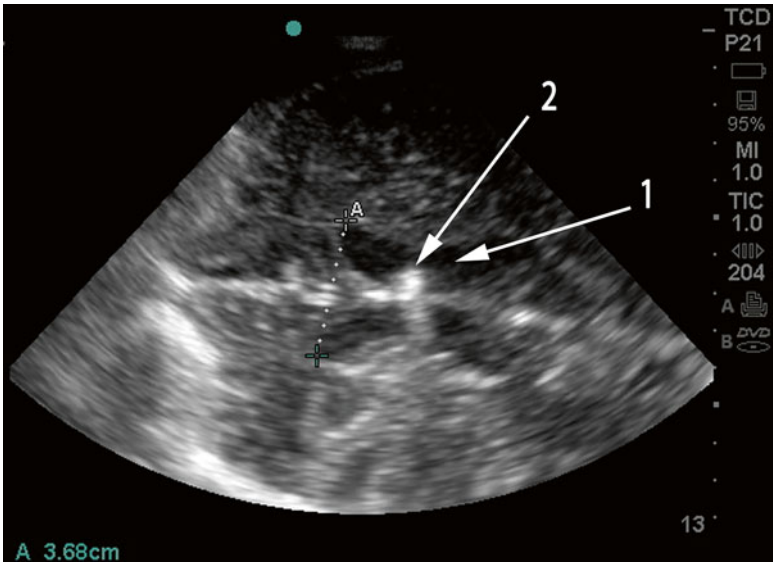

Fig. 15.23 Measurement of lateral ventricular size through craniectomy defect. Measurement of frontal horns for quantification of lateral ventricular size. Distance measured (3.68 cm) is almost identical to distance measured on CT (3.69 cm) in Fig. 15.24. *1* Right lateral ventricle, *2* external ventricular drain

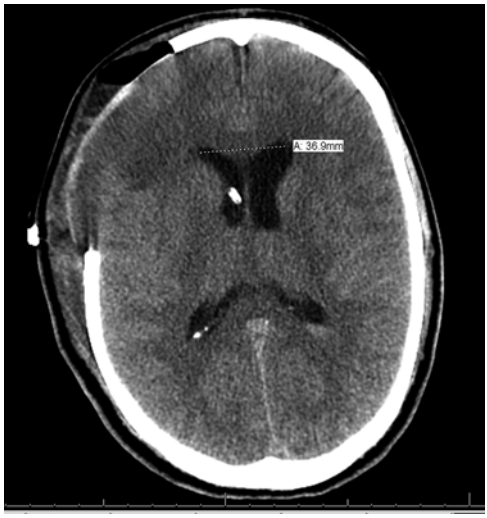

Fig. 15.24 Measurement of lateral ventricular size on CT. Same patient as in Fig. 15.23, on same day as B-mode examination. Distance measured (3.69 cm) is almost identical to distance measured on B-mode (3.68 cm) in Fig. 15.23. The external ventricular drain is seen in the same position in the right lateral ventricle as in Fig. 15.23

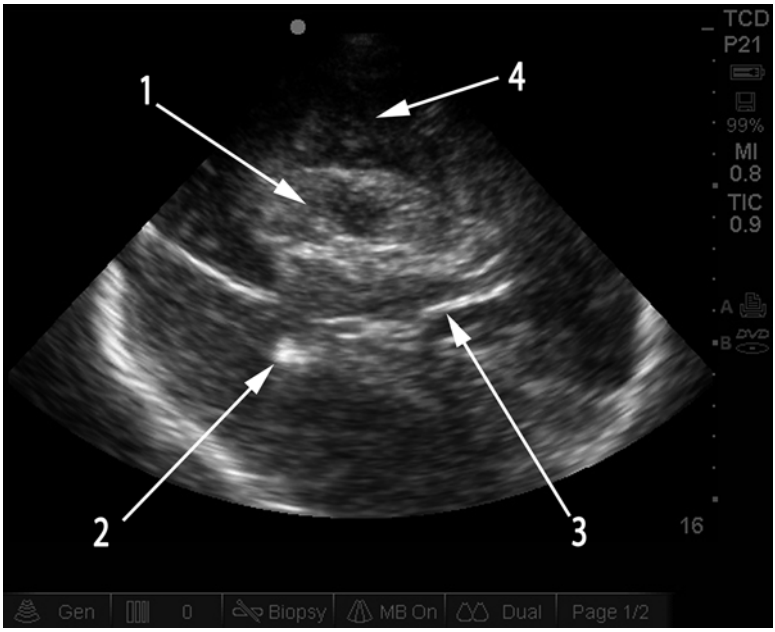

Fig. 15.25 B-mode for imaging of intracerebral hematoma through craniectomy defect. Large left hemispheric intracerebral hematoma (*1*). Compare to CT in Fig. 15.26 – same patient, same labeling. *2* External ventricular drain, *3* hyperechoic choroid plexus in left lateral ventricle, *4* skull defect

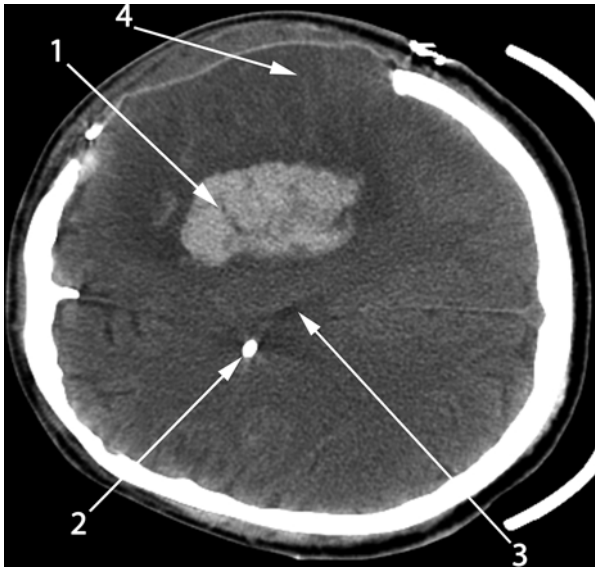

Fig. 15.26 Intracerebral hematoma on CT. Same patient as in Fig. 15.25, same day as B-mode evaluation. Same labeling. *1* hematoma, *2* external ventricular drain, *3* left lateral ventricle, *4* skull defect

Optic Nerve Ultrasound

Management of raised intracranial pressure is a cornerstone of patient management in the neuroICU. The assessment of ICP in a variety of acute neurological conditions typically requires the placement of an invasive monitor, either an external ventricular drain or a parenchymal catheter. Since there is expense and risk associated with the placement of invasive catheters, there is significant interest in potential techniques for the noninvasive detection of raised ICP. Of the available noninvasive techniques, ONUS appears to be among the most promising. The optic nerve sheath is a continuation of the dura and contains the subarachnoid space. An elevation in the ICP is transmitted down the subarachnoid space and results in distension of the optic nerve sheath (ONS), which can be detected using ocular ultrasound. While the same mechanism eventually results in papilledema, this can take hours or days, and papilledema can persist for hours to days following return of ICP to normal levels.

Technical and Patient Factors

Equipment

A linear array (13–6 MHz) transducer probe (Fig. 15.27) with an ophthalmic preset (Fig. 15.28) is recommended for this application, since not all probes and settings meet the Food and Drug Administration (FDA) requirements for ultrasound

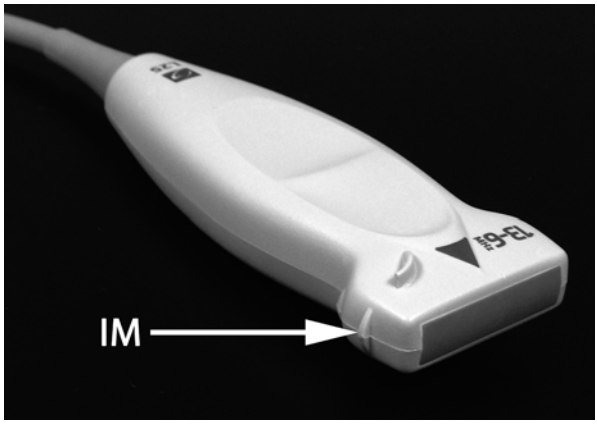

Fig. 15.27 Linear array transducer used for ONSD measurement. *IM* index mark on the probe, corresponds to index mark on the screen

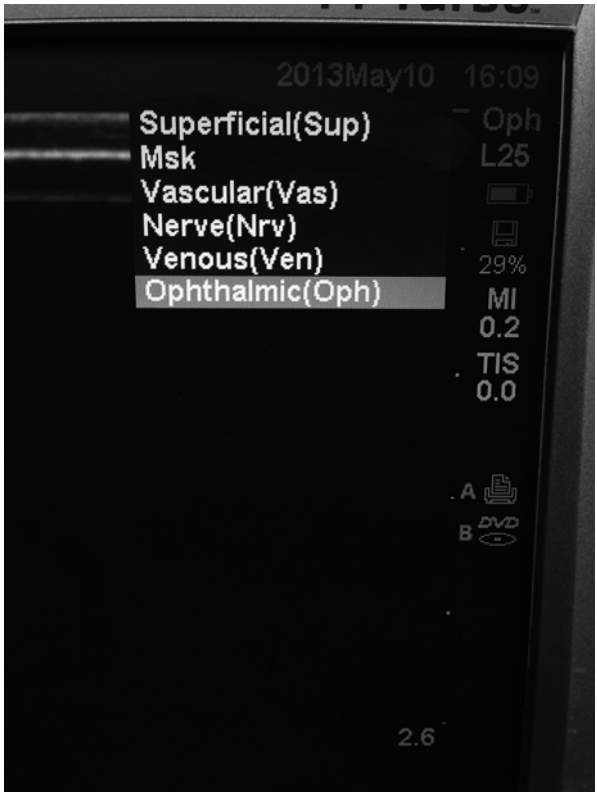

Fig. 15.28 Selection of ophthalmic preset. Select "Ophthalmic" from the list of presets available for the 13–6 MHz linear array transducer

examination of the eye. Theoretical concerns for thermal injury to the eye have led the FDA to limit the acoustic exposure during ocular ultrasound to a derated spatial-peak temporal-average intensity ($I_{SPTA.3}$) of $\leq$17 mW/cm^2 and mechanical index $\leq$0.23 [25].

Patient Factors

Patients with known optic nerve pathology or evident injury to the globe have typically been excluded from studies of ONUS [2–6].

Image Acquisition and Interpretation

Image Acquisition

The probe is placed on the superior and lateral aspect of the orbit against the upper eyelid, with the eye closed. The transducer is angled slightly caudally and medially (Fig. 15.29) until the *optic nerve* is visualized as a linear hypoechoic structure with clearly defined margins posterior to the globe (Fig. 15.30). The probe is never placed in direct contact with the cornea or sclera to avoid corneal abrasion. Contact with the eye must be gentle at all times, as excess pressure can result in nausea, vomiting, and a vagal response. The University of Michigan protocol is then to perform magnification and to use calipers to identify a point 3 mm behind the retina. The optic nerve sheath diameter (ONSD) is measured at this level using a second set of calipers. Very careful probe manipulation is performed to obtain clear margins of the ONS, distinct from the hypo- and hyper-echoic artifacts that are common posterior to the globe.

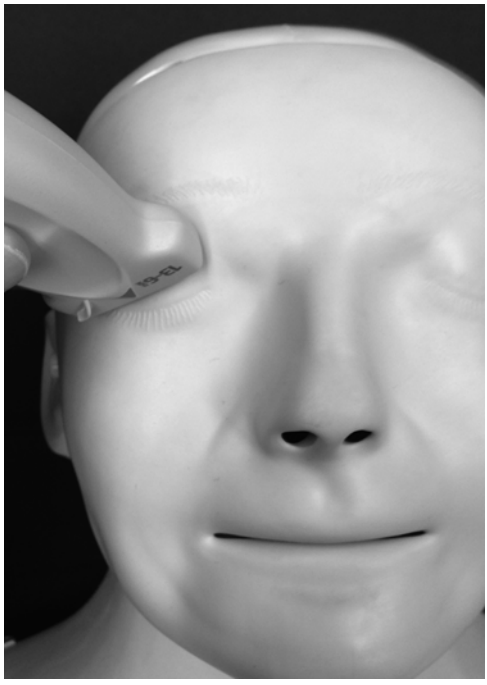

Fig. 15.29 Probe position for ONSD measurement. Transducer is placed on the *upper outer* margin of the orbit with the eye closed and angled slightly downward and medially

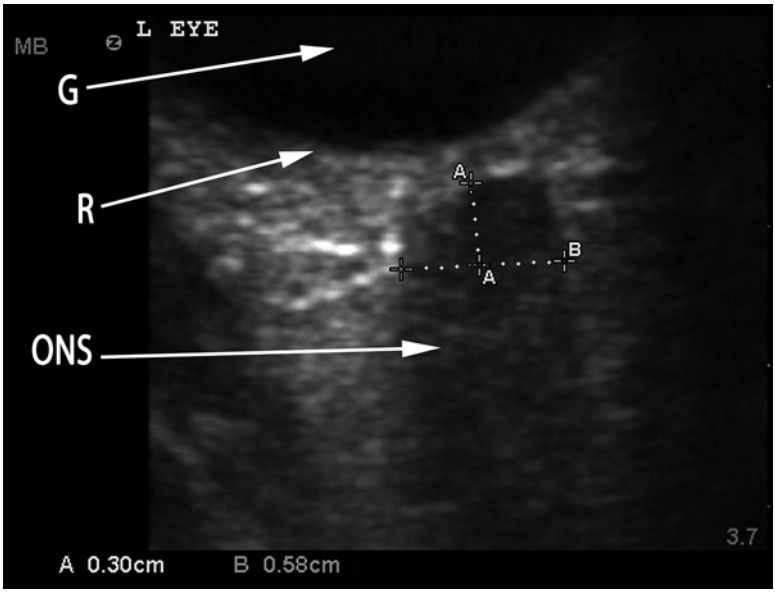

Fig. 15.30 ONSD measurement. The optic nerve sheath (ONS) is seen as a linear hypoechoic structure extending posterior to the globe (G). Caliper A measures a standard distance 3 mm behind the retina (R). Caliper B measures the ONSD at this level. ONSD is 0.58 cm, higher than the 0.50 cm cutoff. This patient was found to have ICP>40 mmHg following placement of an external ventricular drain

Image Interpretation

The optimal ONSD cutoff for the identification of raised intracranial pressure (ICP), typically defined as >20 mmHg, is a matter of debate. The validation study performed at the University of Michigan identified an optimal ONSD cutoff ≥0.50 cm for the detection of intracranial hypertension (defined as ICP>20 mmHg) with sensitivity 90 % (95 % CI 79–97 %), specificity 98 % (94–99 %), PPV 92 % (95 % CI 81–98 %), and NPV 97 % (93–99 %). For patients not on mechanical ventilation the optimal ONSD cutoff was ≥0.48 cm with sensitivity 99 % (93–100 %), specificity 95 % (91–97 %), PPV 85 % (76–92 %), and NPV 100 % (98–100 %).

Evidence Review and Evidence-Based Use

Several investigators have performed blinded correlation of ONSD measurement to the gold standard of simultaneous invasive ICP measurement [2–6]. These studies, as well as a subsequent meta-analysis, concluded that ONSD measurement was an accurate tool for the detection of raised ICP (>20 mmHg) [26]. The sensitivity of

this tool has ranged from 74 % to 96 % and specificity 74–99 % in different studies [2–6]. Agreement does NOT exist, however, on the optimal ONSD threshold for identification of raised ICP (>20 mmHg), with the suggested cutoff ranging from 0.48 cm to 0.58 cm. This variability may be related to variations in techniques of measurement and the presence of artifacts. In view of the discrepancy in the optimal ONSD threshold across studies, significant caution must be used in the interpretation of this test, unless validation of the specific technique being used at the clinician's institution against invasive ICP monitoring has been performed. Based on such a validation study [6] we use the cutoffs mentioned in the earlier section but always integrate ONSD measurement into a comprehensive clinical evaluation that includes history, physical examination, and imaging before decisions are made to treat intracranial hypertension. The presence of an ONSD above the threshold value should lead to consideration for the placement of an invasive ICP monitor.

Pitfalls and Precautions

The variation in optimal ONSD threshold for detection of elevated ICP has been discussed above. While this variation may be partly related to technique, it may also be related to the frequent presence of linear hypoechoic and hyperechoic artifacts posterior to the globe, which can significantly confound ONSD measurement. Figures 15.31 and 15.32 illustrate how inclusion of hypoechoic signal beyond the

Fig. 15.31 Artifact and ONSD – incorrect measurement. Inclusion of hyperechoic structures posterior to the globe other than the content of the optic nerve sheath can lead to serious error. In this case, ONSD is mistakenly measured at 0.64 cm, which would suggest a very high ICP. The ICP recorded from the external ventricular drain was only 11 mmHg

Fig. 15.32 Artifact and ONSD – correct measurement. Same examination as in Fig. 15.31. More careful measurement of only the content of the optic nerve sheath reveals ONSD is 0.38 cm, consistent with the normal ICP (11 mmHg) measured from the external ventricular drain

content of the ONS may result in misidentification of raised ICP. A delay in reversibility of ONS distension following a period of raised ICP may also possibly result in a decreased PPV in the setting of active treatment of raised ICP [27, 28]. Remember that ONUS is a qualitative (high vs normal) and not a quantitative assessment of ICP. Also, it is a snapshot assessment in time and not a continuous measure of ICP.

Cardiopulmonary Evaluation in Subarachnoid Hemorrhage

Technical considerations, image acquisition and interpretation of bedside echocardiography, and thoracic ultrasound have been described in detail elsewhere in this book. This section will briefly detail considerations specific to the neurointensive care unit.

Cardiomyopathy

Up to 30 % of patients with aSAH develop significant cardiac injury, with more severe grades of aSAH incrementally associated with more severe cardiac injury [29]. This injury may be a consequence of the catecholamine surge that accompanies

aSAH, leading to both acute endocardial and myocardial injury [30]. While cardiac injury can manifest as transient electrocardiogram changes or troponin elevation, severe left ventricular (LV) failure can occur, leading to cardiogenic shock and pulmonary edema. The occurrence of cardiac injury is also predictive of DCI, poor functional outcomes, and death [31].

Patients with aSAH and LV failure typically demonstrate a pattern similar to Takotsubo cardiomyopathy, with apical and/or mid-ventricular hypokinesia or akinesia and sparing of the basal segments [32]. Left ventricular dysfunction is typically maximal soon after ictus and almost always resolves over a period of days to weeks. Rapid identification of the severity and pattern of LV dysfunction in the setting of cardiogenic shock permits the initiation of appropriate therapy, including the addition of inotropic agents such as dobutamine or vasopressors such as norepinephrine.

Pulmonary Edema

Neurogenic pulmonary edema is relatively common following aSAH but may also occur in a range of acute neurological conditions [33]. Neurogenic edema is thought to result from an abrupt increase in pulmonary hydrostatic pressure and capillary permeability and can result in severe hypoxic respiratory failure but is transient and typically resolves over several days. Similar to cardiac injury, the incidence and severity is highest at admission. The use of thoracic ultrasound can be very valuable for the diagnosis of acute pulmonary edema. Using the "BLUE" (bedside lung ultrasound in emergency) protocol for assessment of respiratory failure, the presence of bilateral B-lines in the anterior fields in the patient with aSAH likely suggests the presence of aSAH (Fig. 15.33) [34].

Hemodynamic Augmentation for DCI

The mainstay of treatment of DCI along with endovascular therapy is hemodynamic augmentation to promote perfusion of ischemic cerebral tissue. The use of ultrasound can be helpful in this regard, allowing for assessment of volume status and optimization of cardiac output. The presence of complete end-systolic obliteration of the left ventricular cavity implies significant hypovolemia and the need for fluid resuscitation (Fig. 15.34) [35]. Respiratory variation in the inferior vena cava (IVC) diameter is a useful predictor of fluid responsiveness in the patient on the ventilator without respiratory effort [36]. When severe LV dysfunction is identified on echocardiography, the addition of dobutamine to vasopressors may be valuable in promoting cerebral perfusion [37]. Inotropic therapy and fluid resuscitation can be titrated to the measured stroke volume, obtained either by the fractional shortening

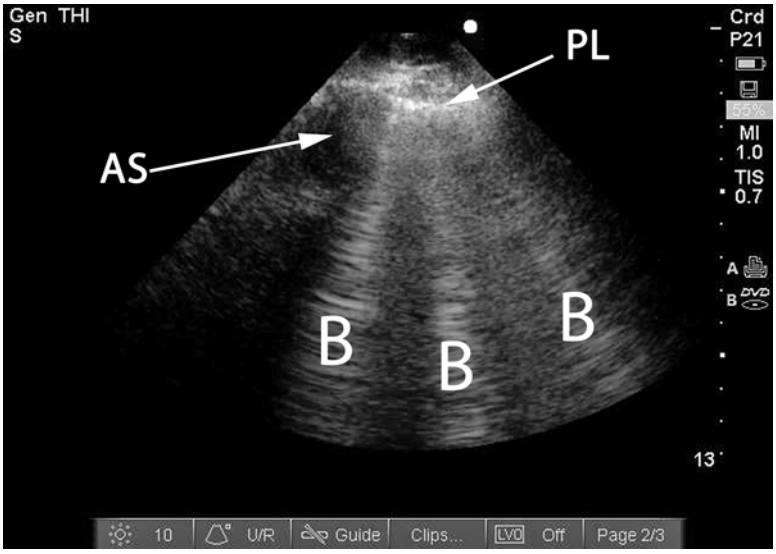

Fig. 15.33 B-lines on thoracic ultrasound. Patient with SAH and severe neurogenic pulmonary edema. *PL* pleural line, *AS* acoustic shadow of rib, *B* B-lines, extending from pleural line to edge of screen

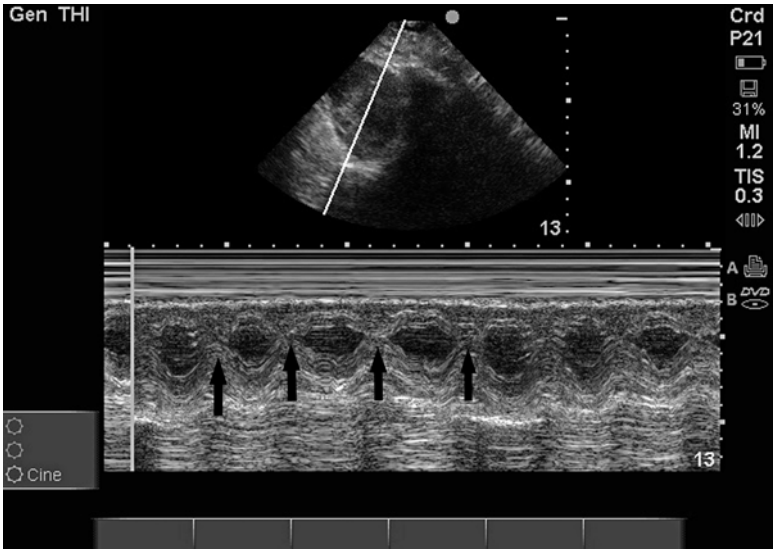

Fig. 15.34 Echocardiography M-mode demonstrating hypovolemia. Patient with aSAH, cerebral salt wasting, and delayed cerebral ischemia. M-mode examination performed in the parasternal short axis view at the papillary muscle level. *Black vertical arrows* demonstrate end-systolic obliteration of the left ventricular cavity, suggesting significant hypovolemia and the need for fluid resuscitation

method or by measurement of LV outflow tract diameter and aortic valve Doppler, both of which are described elsewhere in this book. While performing fluid resuscitation for DCI, the appearance of new B-lines bilaterally on thoracic ultrasound may be useful in the early identification of fluid overload and pulmonary edema.

Other Applications of Ultrasound in the Neuro-ICU

Similar to their use in other ICUs, the following applications of bedside ultrasound find common use in the neuroICU:

1. Echocardiography for assessment of shock and preload
2. Measurement of IVC for assessment of fluid responsiveness
3. Thoracic ultrasound for the assessment of acute respiratory failure ("BLUE" protocol)
4. Extended focused assessment with sonography in trauma (eFAST) for patients with severe traumatic brain injury and multisystem injuries
5. Diagnosis of deep vein thrombosis
6. Real-time guidance for bedside procedures: central venous and arterial catheterization, thoracentesis, paracentesis, and percutaneous tracheostomy

Conclusion

While TCD has long been an integral part of evaluation and management of patients with acute brain injury, more recently the range of applications of ultrasound in the ICU have greatly expanded. Gaining proficiency in all aspects of critical care ultrasound is likely to empower the neurointensivist to significantly enhance the range and depth of clinical care provided to patients in the neuroICU.

References

1. Sloan MA, Alexandrov AV, Tegeler CH, Spencer MP, Caplan LR, Feldmann E, Wechsler LR, Newell DW, Gomez CR, Babikian VL, Lefkowitz D, Goldman RS, Armon C, Hsu CY, Goodin DS, Therapeutics and Technology Assessment Subcommittee of the American Academy of Neurology. Assessment: transcranial Doppler ultrasonography: report of the therapeutics and technology assessment subcommittee of the American academy of neurology. Neurology. 2004;62(9):1468–81.
2. Geeraerts T, Launey Y, Martin L, Pottecher J, Vigué B, Duranteau J, Benhamou D. Ultrasonography of the optic nerve sheath may be useful for detecting raised intracranial pressure after severe brain injury. Intensive Care Med. 2007;33(10):1704–11. Epub 2007 Aug 1.
3. Kimberly HH, Shah S, Marill K, Noble V. Correlation of optic nerve sheath diameter with direct measurement of intracranial pressure. Acad Emerg Med. 2008;15(2):201–4.

4. Soldatos T, Karakitsos D, Chatzimichail K, Papathanasiou M, Gouliamos A, Karabinis A. Optic nerve sonography in the diagnostic evaluation of adult brain injury. Crit Care. 2008;12(3):R67. Epub 2008 May 13.
5. Moretti R, Pizzi B, Cassini F, Vivaldi N. Reliability of optic nerve ultrasound for the evaluation of patients with spontaneous intracranial hemorrhage. Neurocrit Care. 2009;11(3):406–10.
6. Rajajee V, Vanaman M, Fletcher JJ, Jacobs TL. Optic nerve ultrasound for the detection of raised intracranial pressure. Neurocrit Care. 2011;15(3):506–15.
7. Krejza J, Swiat M, Pawlak MA, Oszkinis G, Weigele J, Hurst RW, Kasner S. Suitability of temporal bone acoustic window: conventional TCD versus transcranial color-coded duplex sonography. J Neuroimaging. 2007;17(4):311–4.
8. Wijnhoud AD, Franckena M, van der Lugt A, Koudstaal PJ, Dippel ED. Inadequate acoustical temporal bone window in patients with a transient ischemic attack or minor stroke: role of skull thickness and bone density. Ultrasound Med Biol. 2008;34(6):923–9. doi:10.1016/j.ultrasmedbio.2007.11.022. Epub 2008 Feb 20.
9. Alexandrov AV, Neumyer MM. Practical models of cerebral hemodynamics and waveform recognition. In: Alexandrov A, editor. Cerebrovascular ultrasound in stroke prevention and treatment. 1st ed. Elmsford: Blackwell publishing; 2004. p. 66.
10. Lysakowski C, Walder B, Costanza MC, Tramer MR. Transcranial Doppler versus angiography in patients with vasospasm due to a ruptured cerebral aneurysm: a systematic review. Stroke. 2001;32:2292–8.
11. Sviri GE, Ghodke B, Britz GW, Douville CM, Haynor DR, Mesiwala AH, Lam AM, Newell DW. Transcranial Doppler grading criteria for basilar artery vasospasm. Neurosurgery. 2006;59(2):360–6; discussion 360–6.
12. Rajajee V, Fletcher JJ, Pandey AS, Gemmete JJ, Chaudhary N, Jacobs TL, Thompson BG. Low pulsatility index on transcranial Doppler predicts symptomatic large-vessel vasospasm after aneurysmal subarachnoid hemorrhage. Neurosurgery. 2012;70(5):1195–206; discussion 1206.
13. Nedelmann M, Stolz E, Gerriets T, Baumgartner RW, Malferrari G, Seidel G, Kaps M, TCCS Consensus Group. Consensus recommendations for transcranial color-coded duplex sonography for the assessment of intracranial arteries in clinical trials on acute stroke. Stroke. 2009;40(10):3238–44.
14. Connolly Jr ES, Rabinstein AA, Carhuapoma JR, Derdeyn CP, Dion J, Higashida RT, Hoh BL, Kirkness CJ, Naidech AM, Ogilvy CS, Patel AB, Thompson BG, Vespa P, American Heart Association Stroke Council, Council on Cardiovascular Radiology and Intervention, Council on Cardiovascular Nursing, Council on Cardiovascular Surgery and Anesthesia, Council on Clinical Cardiology. Guidelines for the management of aneurysmal subarachnoid hemorrhage: a guideline for healthcare professionals from the American Heart Association/American Stroke Association. Stroke. 2012;43(6):1711–37.
15. Diringer MN, Bleck TP, Claude Hemphill 3rd J, Menon D, Shutter L, Vespa P, Bruder N, Connolly Jr ES, Citerio G, Gress D, Hänggi D, Hoh BL, Lanzino G, Le Roux P, Rabinstein A, Schmutzhard E, Stocchetti N, Suarez JI, Treggiari M, Tseng MY, Vergouwen MD, Wolf S, Zipfel G, Neurocritical Care Society. Critical care management of patients following aneurysmal subarachnoid hemorrhage: recommendations from the Neurocritical Care Society's Multidisciplinary Consensus Conference. Neurocrit Care. 2011;15(2):211–40.
16. Fisher CM, Roberson GH, Ojemann RG. Cerebral vasospasm with ruptured saccular aneurysm: the clinical manifestations. Neurosurgery. 1977;1:245–8.
17. Haley Jr EC, Kassell NF, Torner JC. The international cooperative study on the timing of aneurysm surgery: the North American experience. Stroke. 1992;23:205–14.
18. Longstreth Jr WT, Nelson LM, Koepsell TD, van Belle G. Clinical course of spontaneous subarachnoid hemorrhage: a population-based study in King County, Washington. Neurology. 1993;43:712–8.
19. Frontera JA, Fernandez A, Schmidt JM, Claassen J, Wartenberg KE, Badjatia N, Connolly ES, Mayer SA. Defining vasospasm after subarachnoid hemorrhage: what is the most clinically relevant definition? Stroke. 2009;40:1963–8.

20. Carrera E, Schmidt JM, Oddo M, Fernandez L, Claassen J, Seder D, Lee K, Badjatia N, Connolly Jr ES, Mayer SA. Transcranial Doppler for predicting delayed cerebral ischemia after subarachnoid hemorrhage. Neurosurgery. 2009;65:316–23.
21. Dankbaar JW, Rijsdijk M, van der Schaaf IC, Velthuis BK, Wermer MJ, Rinkel GJ. Relationship between vasospasm, cerebral perfusion, and delayed cerebral ischemia after aneurysmal subarachnoid hemorrhage. Neuroradiology. 2009;51:813–9.
22. Stolz E, Gerriets T, Fiss I, Babacan SS, Seidel G, Kaps M. Comparison of transcranial color-coded duplex sonography and cranial CT measurements for determining third ventricle midline shift in space-occupying stroke. AJNR Am J Neuroradiol. 1999;20(8):1567–71.
23. Becker G, Bogdahn U, Strassburg HM, Lindner A, Hassel W, Meixensberger J, Hofmann EJ. Identification of ventricular enlargement and estimation of intracranial pressure by transcranial color-coded real-time sonography. Neuroimaging. 1994;4(1):17–22.
24. Kukulska-Pawluczuk B, Książkiewicz B, Nowaczewska M. Imaging of spontaneous intracerebral hemorrhages by means of transcranial color-coded sonography. Eur J Radiol. 2012;81(6):1253–8.
25. Guidance for industry and FDA staff – information for manufacturers seeking marketing clearance of diagnostic ultrasound systems and transducers. 2008. http://www.fda.gov/medicaldevices/deviceregulationandguidance/guidancedocuments/ucm070856.htm
26. Dubourg J, Javouhey E, Geeraerts T, Messerer M, Kassai B. Ultrasonography of optic nerve sheath diameter for detection of raised intracranial pressure: a systematic review and meta-analysis. Intensive Care Med. 2011;37(7):1059–68.
27. Hansen HC, Lagrèze W, Krueger O, Helmke K. Dependence of the optic nerve sheath diameter on acutely applied subarachnoidal pressure – an experimental ultrasound study. Acta Ophthalmol. 2011;89(6):e528–32.
28. Rajajee V, Fletcher JJ, Rochlen LR, Jacobs TL. Comparison of accuracy of optic nerve ultrasound for the detection of intracranial hypertension in the setting of acutely fluctuating vs stable intracranial pressure: post-hoc analysis of data from a prospective, blinded single center study. Crit Care. 2012;16(3):R79.
29. Hravnak M, Frangiskakis JM, Crago EA, Chang Y, Tanabe M, Gorcsan 3rd J, Horowitz MB. Elevated cardiac troponin I and relationship to persistence of electrocardiographic and echocardiographic abnormalities after aneurysmal subarachnoid hemorrhage. Stroke. 2009;40(11):3478.
30. Hinson HE, Sheth KN. Manifestations of the hyperadrenergic state after acute brain injury. Curr Opin Crit Care. 2012;18(2):139–45.
31. van der Bilt IA, Hasan D, Vandertop WP, Wilde AA, Algra A, Visser FC, Rinkel GJ. Impact of cardiac complications on outcome after aneurysmal subarachnoid hemorrhage: a meta-analysis. Neurology. 2009;72(7):635.
32. Lee VH, Connolly HM, Fulgham JR, Manno EM, Brown Jr RD, Wijdicks EF. Tako-tsubo cardiomyopathy in aneurysmal subarachnoid hemorrhage: an underappreciated ventricular dysfunction. J Neurosurg. 2006;105(2):264.
33. Baumann A, Audibert G, McDonnell J, Mertes PM. Neurogenic pulmonary edema. Acta Anaesthesiol Scand. 2007;51:447.
34. Lichtenstein DA, Mezière GA. Relevance of lung ultrasound in the diagnosis of acute respiratory failure: the BLUE protocol. Chest. 2008;134(1):117–25. Epub 2008 Apr 10.
35. Leung JM, Levine EH. Left ventricular end-systolic cavity obliteration as an estimate of intraoperative hypovolemia. Anesthesiology. 1994;81(5):1102–9.
36. Barbier C, Loubières Y, Schmit C, Hayon J, Ricôme JL, Jardin F, Vieillard-Baron A. Respiratory changes in inferior vena cava diameter are helpful in predicting fluid responsiveness in ventilated septic patients. Intensive Care Med. 2004;30(9):1740–6. Epub 2004 Mar 18.
37. Joseph M, Ziadi S, Nates J, Dannenbaum M, Malkoff M. Increases in cardiac output can reverse flow deficits from vasospasm independent of blood pressure: a study using xenon computed tomographic measurement of cerebral blood flow. Neurosurgery. 2003;53(5):1044–51; discussion 1051–2.

Chapter 16
Ultrasound in the Neonatal Intensive Care Unit

Hussnain S. Mirza, Gregory Logsdon, and James Padbury

Part I: Practice and Training Guidelines

Introduction

Point-of-care ultrasound is a routine practice in neonatal intensive care units (NICUs) in many parts of the world, including Australia, New Zealand, United Kingdom, and many other countries in Asia and Europe. In North America, point-of-care ultrasound has been adopted in clinical practice in emergency rooms, adult intensive care units, obstetrics and gynecology. Recently it has gained some acceptance in NICUs as well [1]. The potential for medicolegal problems and lack of uniform training for different applications of point-of-care ultrasound in the NICU are the biggest challenges to more widespread adoption of this valuable practice. It is important to emphasize that clinical sonography performed by providers in the NICU entails limited, goal-directed ultrasound imaging at the bedside for a rapid assessment of an acute or subacute clinical problem. It is intended to be an extension and augmentation of the clinical examination, and should not be considered a replacement for formal clinical imaging.

H.S. Mirza, M.D. (✉)
Center for Neonatal Care/Florida Hospital for Children, UCF College of Medicine,
2501 N. Orange Ave., Suite 446, Orlando, FL 32804, USA
e-mail: Hussnain.Mirza.MD@flhosp.org

G. Logsdon, M.D.
Department of Pediatric Radiology, Florida Hospital for Children,
601 E. Rollins St., Orlando, FL 32803, USA
e-mail: Gregory.Logsdon.MD@flhosp.org

J. Padbury, M.D.
Department of Neonatal-Perinatal Medicine, Women & Infants Hospital,
101 Dudley Street, Providence, RI 02905, USA
e-mail: JPadbury@Wihri.org

M. Jankowich, E. Gartman (eds.), *Ultrasound in the Intensive Care Unit*,
Respiratory Medicine, DOI 10.1007/978-1-4939-1723-5_16

The utility of point-of-care ultrasound in the NICU lies in its portability, reliability, and lack of invasiveness or radiation exposure. Point-of-care ultrasound can be adopted in NICU for a wide range of indications, such as research, procedural guidance, and rapid assessment of critical emergencies like cardiac tamponade. Similar to other intensive care settings, ultrasound guidance can improve the safety and success rate of clinical procedures, such as umbilical vein catheter (UVC) placement, and other lifesaving interventions, such as pericardiocentesis to relieve cardiac tamponade. Given its availability and reliability, ultrasound can be used frequently and longitudinally to follow-up subacute or evolving problems, such as monitoring the progress of post-hemorrhagic hydrocephalus. Point-of-care ultrasound can decrease the use of and dependence on x-rays to confirm the appropriate placement of umbilical lines, central venous lines, endotracheal tubes, or feeding tubes.

A basic requirement for point-of-care ultrasound in NICU is the easy availability of a suitable machine with the required hardware and the application-specific software. Every machine is different, and the required specifications differ depending upon the application of ultrasound. Due to the extremely small size of infants in NICU, high frequency (>8 MHz) and smaller size transducers are required for neonatal point-of-care ultrasound. Depending upon the spectrum of clinical practice, two separate transducers are preferable (6–10 MHz and 12–18 MHz). Oftentimes, two-dimensional (2-D) imaging is not sufficient to offer a complete exam, so the addition of pulse wave (PW), continuous wave (CW), and color Doppler modes are also helpful. Doppler imaging is particularly important for the study of cerebral or mesenteric blood flow and for other hemodynamic studies. M-mode is required for targeted neonatal echocardiography (TnECHO). If point-of-care ultrasound is intended for use in sterile field (e.g., for securing central venous access), a foot switch with programmable pedal should be added to the device. Similarly, for neonatal ultrasound, NICU-specific software packages should be installed on the machine including a comprehensive software application for annotation, measurements, and calculations. An automatic image optimization package will help for reliable imaging by the providers who are not well versed with sonographic optimization techniques.

Indications for Ultrasound in the NICU

Ultrasound can be valuable in the evaluation of life-threatening emergencies, screening and monitoring for certain subacute clinical conditions, to guide clinical procedures, and for research purposes. The breadth of available indications for point-of-care ultrasound in the NICU are summarized in Table 16.1. We highly recommend developing local guidelines to define the limitations for any particular application based on local experience, training, and proficiency. The Australian Society for Ultrasound in Medicine (ASUM) has recently published a policy statement for safe and proficient practice of point-of-care ultrasound in NICU. These

Table 16.1 Indications for point-of-care ultrasound in NICU

Critical assessment	Screening and monitoring	Clinical procedures	Research
Pericardial tamponade	Intraventricular hemorrhage	Thoracocentesis	SVC blood flow
Pleural effusion	Periventricular leukomalacia	Peritoneal tap	Cerebral blood flow
Ascites or hemoperitoneum Intraventricular hemorrhage	Hydrocephalus	Suprapubic tap	Mesenteric blood flow
	Patent ductus arteriosus	Confirmation of normal placement	Miscellaneous
	Pulmonary hypertension	UVC/UAC	
	Hemodynamic studies	Central venous line	
	Necrotizing enterocolitis	ETT	
		Gastric/jejunal feeding tube	

Abbreviations: *ETT* endotracheal tube, *SVC* superior vena cava, *UAC* umbilical arterial catheter, *UVC* umbilical vein catheter

guidelines can be helpful to develop a new point-of-care ultrasound program in the NICU. With appropriate boundaries in place, the introduction of point-of-care ultrasound into clinical practice should not be delayed until full competencies are reached in all facets, given that many of its applications are relatively simple and can dramatically improve care. In turn, as experience builds and local clinicians gain experience and expertise, a more expanded service can evolve over time.

Training Recommendations

Multiple ultrasound applications are available in the NICU for different clinical indications, and each application has unique training requirements. Ultrasound applications in the NICU can be broadly classified into four categories: head ultrasound, targeted neonatal echocardiography (TnECHO), general sonography, and critical imaging. For certain applications, detailed training and practice guidelines are available, e.g., TnECHO [2]. On the other hand, some applications have been adopted less formally into clinical practice over many decades based on local experience and expertise (e.g., general sonography and critical imaging). The Australian Society for Ultrasound in Medicine has developed a standard curriculum for point-of-care ultrasound training and certification for neonatology trainees, accessible online at ASUM's website: http://www.asum.com.au/newsite/Education.php?p=CCPU

In the United States, formal training or certification for point-of-care ultrasound in NICU is not available. It is of paramount importance to develop local guidelines before adopting this new practice in NICU. To establish a new program,

collaboration with an advanced-level user (e.g., a pediatric radiologist or a pediatric cardiologist) is essential to ensure adequate training and supervision of NICU providers. Furthermore, as more advanced competencies are sought by the NICU clinician, the involvement of trained neonatologists becomes increasingly important. Ultimately, in the future the goal of all training programs should be to create and adopt a uniform set of core competencies that should be attained while completing a critical care training program, perhaps through national consensus or specialty organizations like the American Academy of Pediatrics.

Proposed Training Model

The basic training for any ultrasound application begins with an introduction to the required hardware and software, basic ultrasound physics, point-of-care ultrasound indications and limitations. Hands-on training starts in the 2nd phase, followed by the consolidation of skills in the 3rd phase (Fig. 16.1). After demonstrating

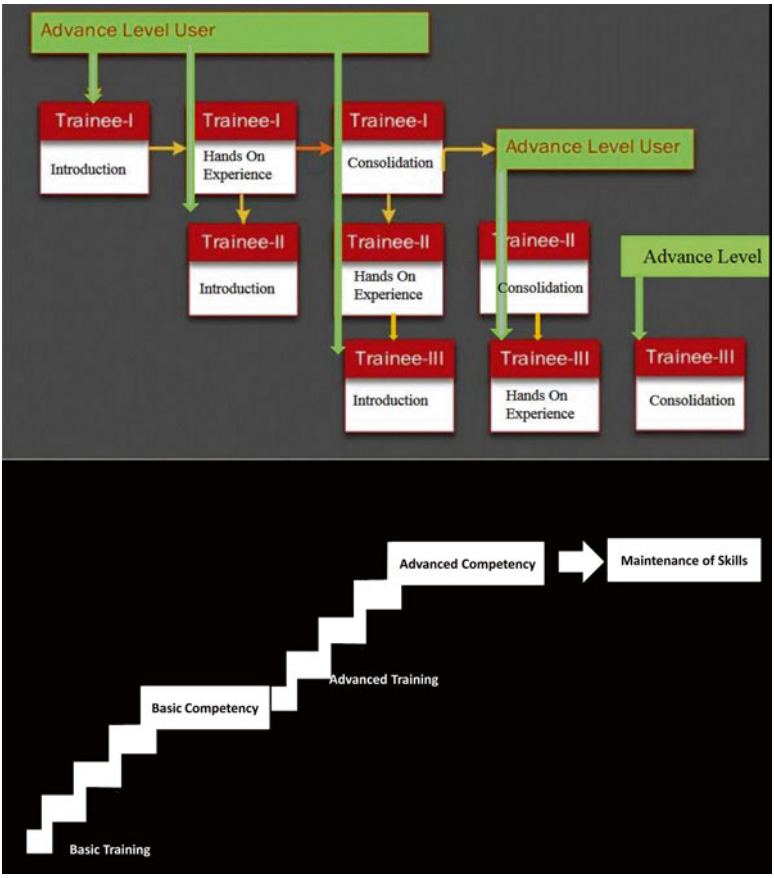

Fig. 16.1 Proposed training model for the point-of-care ultrasound in NICU

proficiency with all core competencies, a provider may be upgraded to an advanced level user. Training requirements and duration of each phase are different depending upon the application of point-of-care ultrasound. Proposed training guidelines and suggestions for different applications are summarized in Table 16.2. We recommend to maintain a log book for all trainees during the basic and advanced level training.

Maintenance of skill should be ensured for advanced level users by performing a minimum required number of scans for any particular application, continued medical education or CME (courses and workshops), peer review, and quality assurance (review by consultants) of acquired images and interpretation. Requirements and

Table 16.2 Training guidelines and suggestions for different applications of point-of-care ultrasound

Application	Basic training	Advanced training	Maintenance of skill	Remarks
[a]Echocardiography (TnECHO)	150 studies performed	150 additional studies performed	100 studies/year	Normal studies should be < 20 % of the total
	150 studies reviewed	150 additional studies reviewed	CME: 24–48 h/year	
	Duration: 4–6 months	Duration: additional 4–6 months	Peer review: once/week	
			Consultant review: once/month	
[b]Head ultrasound	25–50 studies performed	25–50 additional studies performed	50 studies/year	Normal studies should be 30–40 % of total
	25–50 studies reviewed	25–50 additional studies reviewed	CME: 6–12 h/year	
	Duration: 2–4 weeks	Duration: additional 1–2 months	Peer review: once/week	
			Consultant review: once/month	

(continued)

Table 16.2 (continued)

Application	Basic training	Advanced training	Maintenance of skill	Remarks
[b]General sonography for placement confirmation of UVC, PICC line, ETT, NGT and for suprapubic tap	15–25 studies performed	15–25 additional studies performed	25 studies/year	Training should separately focus on each skill, e.g., confirming UVC or PICC position
	15–25 studies reviewed	15–25 additional studies reviewed	CME: 6–12 h/year	
	Duration: 2–4 weeks	Duration: additional 1–2 months	Peer review: once/week	
			Consultant review: once/month	
[b]Critical imaging for cardiac tamponade or pleural effusion	Basic or advanced level training in functional echocardiography or general sonography applications		Peer and consultant review after every incidence in practice	Simulation for lifesaving procedures can also be helpful

[a]Adapted from: Mertens L, Seri I, Marek J, et al. Targeted neonatal echocardiography in the neonatal intensive care unit: practice guidelines and recommendations for training. Eur J Echocardiogr. 2011;12:715–36

[b]Local guidelines or author's suggestions

suggestions for maintenance of skills for different applications are also given in Table 16.2.

After basic or advanced training, certain competencies are expected for each application of point-of-care ultrasound. Basic and advanced competencies for different applications are summarized in Table 16.3. Like training guidelines, competencies have thus far only been defined for targeted neonatal echocardiography. For other applications, most institutions depend upon the local guidelines, developed in collaboration with pediatric diagnostic imaging consultants.

Table 16.3 Basic and advanced competencies for different applications of point-of-care ultrasound

Application	Competencies		Remarks
	Basic	Advanced	
[a]**Echocardiography (TnECHO)**	**Imaging** 1. Initial comprehensive study 2. Initial focused study 3. Follow-up comprehensive study 4. Follow-up focused study	**Imaging** Basic competencies	Functional echocardiography is not recommended in the presence of clinical suspicion for congenital heart disease
	Interpretation No independent interpretation except for follow-up focused studies	**Interpretation** All types of functional echocardiography	Initial comprehensive studies should be considered for review by a pediatric cardiologist
[b]**Head ultrasound**	**Imaging** 1. Initial comprehensive study 2. Initial focused study 3. Follow-up comprehensive study 4. Follow-up focused study	**Imaging** Basic competencies	Initial comprehensive studies and all other studies with any clinically significant finding on interpretation by an advanced user should be considered for review by a pediatric radiologist
	Interpretation No independent interpretation	**Interpretation** All types of head ultrasound	
[b]**General sonography** (UVC/PICC line/pericardial or pleural effusion, ascites, and suprapubic tap)	**Imaging** 1. Initial focused study 2. Follow-up focused study	**Imaging** Basic competencies	Studies with any significant finding on interpretation by an advanced user should be considered for review by a pediatric radiologist
	Interpretation No independent interpretation except for suprapubic tap	**Interpretation** All or few variants of initial or follow-up studies; determined by the training in all or few variants of general sonography	
[b]**Critical imaging**	Basic or advanced level competency in functional echocardiography or general sonography and appropriate clinical training for lifesaving intervention		All images should be considered for review by a pediatric radiologist

[a]Adapted from: Mertens L, Seri I, Marek J, et al. Targeted neonatal echocardiography in the neonatal intensive care unit: practice guidelines and recommendations for training. Eur J Echocardiogr. 2011;12:715–36

[b]Local guidelines or author's suggestions

Part II: Common Applications in Clinical Practice

Neonatal Head Ultrasound

Introduction and Patient Considerations

The diagnosis of severe intraventricular hemorrhage (IVH), especially with extreme prematurity, may impact the decision for redirection of medical care. Due to the significant clinical implications of diagnosing severe IVH in extremely premature infants, their head ultrasounds should be interpreted by a pediatric radiologist. After a diagnosis is made by the radiologist, point-of-care ultrasound can be utilized for follow-up imaging. However, in critical circumstances where imaging by a sonographer or a radiologist is not immediately available, neonatologists may need to evaluate for severe IVH [3] and in this situation a limited head sonography can be performed using point-of-care ultrasound in the NICU. However, all interpretations should be verified either by a pediatric radiologist or an advanced-level user, especially when severe IVH is suspected. This may be facilitated during off-hours by transferring the images via secure email or, in some instances, images can be directly uploaded onto the radiology department's server.

Post-hemorrhagic hydrocephalus (PHH) is a common complication of IVH. Close monitoring of the ventricular size helps to guide the need for clinical interventions (e.g., serial lumber puncture, ventricular taps, or need for a temporary or permanent ventricular shunt). Daily measurement and plotting of the head circumference on a centile chart is a common practice. However, the increase in head circumference lags behind the development of persistently elevated intracranial pressure. This elevated intracranial pressure can induce brain parenchymal injury before a provider recommends any clinical intervention based on an enlarging head circumference. Point-of-care ultrasound can be adopted to monitor the progress of PHH. Ventricular dimensions can be plotted on a nomogram, and frequent and objective evaluation of ventricular size may better guide timely intervention and may improve the clinical outcome of PHH.

Periventricular leukomalacia (PVL) is a selective white matter injury to the developing brain. Incidence of PVL varies between 1.2 % and 1.5 % [4, 5]. Although magnetic resonance imaging (MRI) brain is indicated to evaluate the presence and severity of white matter injury when the index of suspicion is high, MRI brain is not recommended to screen for white matter injury in all preterm infants. Head ultrasound is a suitable test for evaluation and screening of cystic PVL. Depending upon the timing of brain injury, PVL can be evident at birth or as late as 4–6 weeks of postnatal life. Routine screening for PVL is carried out at 4–6 weeks of age. However, point-of-care head ultrasound can be helpful for more frequent screening and early diagnosis. Additional possible indications for point-of-care head ultrasound may include Doppler studies performed for research on cerebral blood flow changes during transition after delivery or, rarely, for another clinical indication (e.g., middle cerebral artery resistive index for assessing the severity of hypoxic ischemic encephalopathy).

Discussing the clinical status of the infant with the bedside nurse is of utmost importance before imaging. Sick and extremely preterm infants are prone to instantaneous desaturation and bradycardia just by touching them. In such an event, one should stop scanning and wait until the infant is completely recovered from the acute event before resuming the imaging. One should be able to perform head ultrasound in an open crib, radiant warmer, or through the portholes in an isolette. For head ultrasound, ideally an infant should be supine on a flat bed with the head kept in midline position. However, most sonographers are trained to scan in any position and still acquire standard images. This flexibility allows head ultrasound to be performed in critically sick or extremely preterm infants without changing their position in the isolette. One should be careful about the endotracheal tube, arterial and venous lines while performing sonography.

Technical Considerations

The following are technical considerations in point-of-care head ultrasound in neonates:

- During the procedure these high-risk infants shall be handled gently. Avoid procedure-related hypothermia, and follow standard asepsis protocol in the unit.
- A sector or curved linear probe of appropriate size to fit the anterior fontanelle should be used.
- Commonly, the 5–8 MHz transducer is used for best combination of penetration and resolution. For extremely premature infants, the 8–12 MHz transducer also can be used to achieve a higher resolution image.
- For standard imaging, the reference point on the transducer should be facing right for a coronal view and anteriorly for a sagittal view.
- Image orientation: The standard orientation of the coronal image is that the baby's right side is on the left side as you face the image. For the sagittal plane, anterior or rostral is on the left as you face the image.
- Focus point: The focus point should be at the depth of the ventricles or the periventricular region. In individual cases it may be useful to adapt the focus point, aiming at a region of interest (e.g., on PVL or cerebellar hemorrhage). Also, many transducers have multiple focal zones that can be adjusted to examine a larger region of interest.
- Compatible software for neonatal head ultrasound should be installed
- Doppler studies and additional imaging from posterior, temporal, and mastoid fontanelle are optional depending upon the expertise and indications for the point-of-care ultrasound.
- Some experts recommend saving point-of-care ultrasound in a video format. This will facilitate the interpretation of the scan as the frame-by-frame review will be possible in video format.

Image Acquisition and Interpretation

Several windows are used to perform a comprehensive head ultrasound to look into various parts of the brain. The anterior, posterior, mastoid, and temporal fontanelle views are recommended for comprehensive imaging. However, for a point-of-care ultrasound, conventional views via the anterior fontanelle may be sufficient.

Conventional views are obtained through the anterior fontanelle as shown in Fig. 16.2. Start imaging with the coronal planes: the reference point on the transducer should be on the right side for coronal views. Both Sylvian fissures, frontal horns of both lateral ventricles, and the third ventricle should be clearly visible in the midline coronal view. Sweep from orbits to occiput; save 5–6 images in coronal view as shown in Fig. 16.2. Appropriately mark the frontal and occipital views while performing an anteroposterior sweep in the coronal plane.

Subsequently switch to the sagittal plane. The reference point on the transducer should be anterior for the sagittal views. The corpus callosum, basal ganglia, fourth ventricle, anterior portion of cerebellum, and part of the brain stem should be visible in the midline sagittal view. In the midline sagittal plane, tilt the transducer slightly to either side to examine the caudothalamic groove, a linear echogenic line between the head of the caudate and thalamus for evaluation of Grade 1 hemorrhages. Sweep

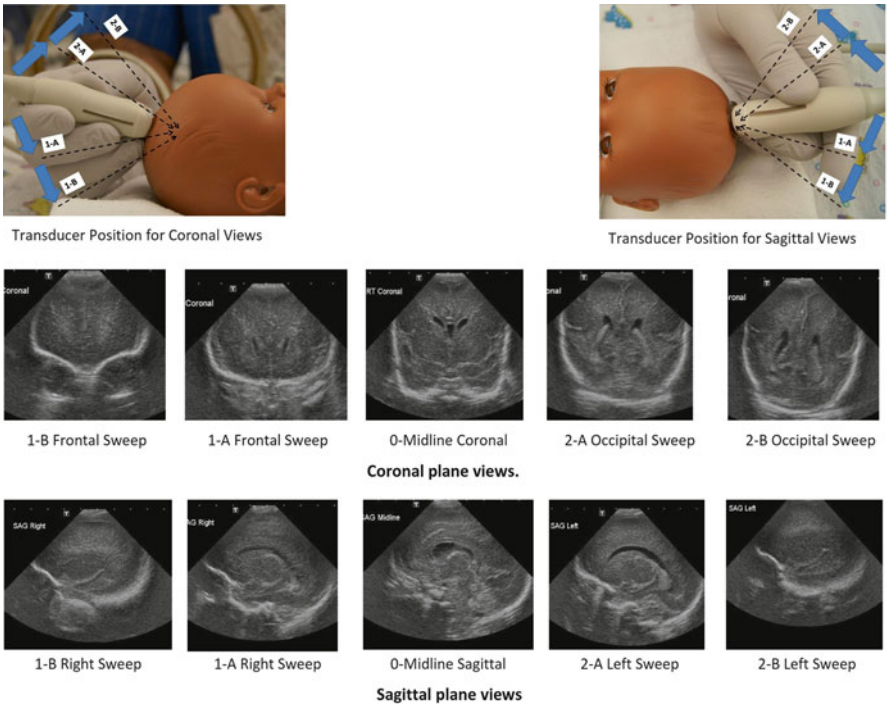

Fig. 16.2 Transducer position and sonographic views for the point-of-care head ultrasound

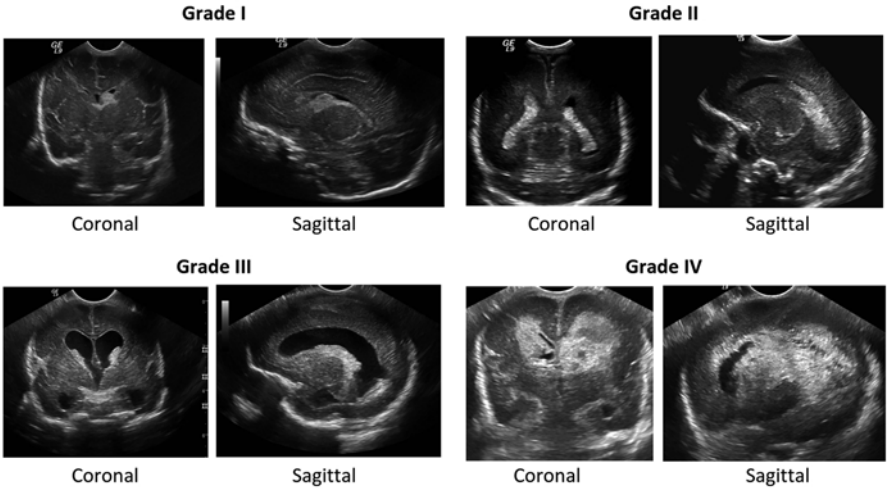

Fig. 16.3 Sonographic imaging and IVH grading

from midline to either side until the Sylvian fissures and insulae are visible. The posterior part of probe is angled slightly laterally to get a complete view of the lateral ventricles. A midline image and two views on either side are recorded as shown in Fig. 16.2. Appropriately mark right and left on the lateral ventricle sagittal views.

The widely accepted classification of IVH is described in Fig. 16.3. Post-hemorrhagic hydrocephalus (PHH) and ventriculomegaly are the most common sequelae of severe IVH. Ventricular size can be subjectively assessed by looking at the lateral ventricle from multiple sonographic views. However, objective assessment is preferable for point-of-care head ultrasound. There are many ventricular parameters that may be assessed using ultrasound (Fig. 16.4). *Ventricular index (VI)* is defined as the distance between the falx and the lateral wall of the anterior horn in the coronal plane. Other parameters are *anterior horn width (AHW)*, which is the diagonal width of the anterior horn measured at its widest point in the coronal plane, and the *thalamo-occipital distance (TOD)*, defined as the distance between the outermost point of the thalamus at its junction with the choroid plexus and the outermost part of the occipital horn in the parasagittal plane. Different ranges of normal values in association with the gestational age have been described for all these parameters. We recommend to plot these measurements on the new cross-sectional and longitudinal reference value curves published by Brouwer et al. [6]. Quantitative assessment of ventricular size provides an opportunity for accurate and timely intervention for infants with progressive hydrocephalus.

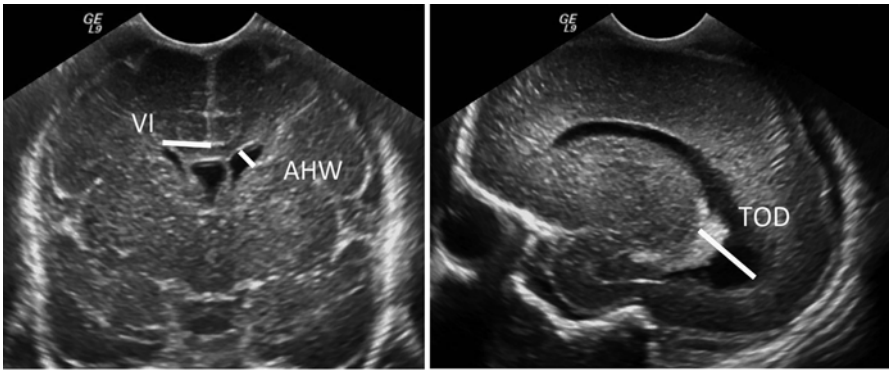

Fig. 16.4 Assessing ventricular size and dilatation

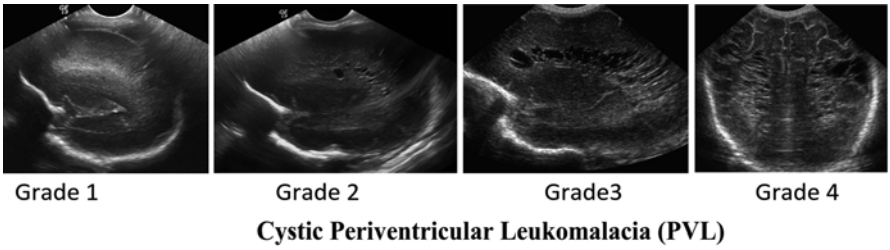

Fig. 16.5 Sonographic imaging and grading of periventricular leukomalacia (*PVL*)

Point-of-care ultrasound for PVL screening can be used for early identification or to document interval changes in the cystic lesions. PVL grading is described in Fig. 16.5 [7, 8].

Image interpretation depends upon the quality of the images, anatomical knowledge of different parts of the brain, and the training and experience of the NICU provider to review neonatal head ultrasounds at different gestational ages. For structured reporting of point-of-care head ultrasounds, we recommend adopting a template for interpretation of the studies. The following components should be included in all reports:

(i) Are the anatomical structures distinguishable and do they appear normal? It is essential to identify the following structures – ventricular system, interhemispheric fissure, corpus callosum, Sylvian fissure, thalamus, and basal ganglia.

(ii) Does the maturation of the brain appear appropriate for the gestation?
(iii) Does the size, lining, and echogenicity of the ventricular system appear normal? Is there any evidence of IVH?
(iv) If the ventricles are enlarged, size of the ventricles should be measured and compared with the nomogram.
(v) Is there a midline shift?
(vi) Is there any evidence of PVL?

Basic Competencies

Any NICU provider with basic level training in point-of-care head ultrasound should be able to scan and save conventional images in coronal and sagittal planes through the anterior fontanelle. However, at the basic level, interpretation of the imaging is restricted to follow up studies only (Table 16.3).

Advanced Competencies

In addition to all skills required at the basic level, an advanced level user should be able to interpret all initial and follow-up head ultrasounds with precision comparable to a pediatric radiologist. Imaging through the posterior, temporal, and mastoid fontanelles can be performed by the advanced level user to screen for cerebellar hemorrhage. Training for cerebral Doppler studies to calculate resistive index in anterior or middle cerebral arteries for research or clinical indications (hypoxic ischemic encephalopathy or HIE) is optional at the advanced level (Table 16.3).

Evidence Review and Evidence-Based Use

Head ultrasound is an optimal test for screening and diagnosis of IVH, PVL, hydrocephalus, and other structural anomalies of the brain [9, 10]. Following an adequate period of training, NICU providers reliably can produce quality head ultrasound images that are equivalent to those obtained in the traditional manner [4]. Furthermore, the utility of the point-of-care head ultrasound for rapid diagnosis of IVH in newborns has been shown in different clinical settings [11].

Pitfalls and Precautions

Head ultrasound is the most common screening test for diagnosis of brain injury in preterm infants. However, several common errors or misinterpretations can occur:

– Due to their similar sonographic appearances, differentiating between Grade 1 IVH and simply a bulky normal choroid plexus may be difficult even in very

experienced hands. Follow-up sonography is required to make the correct diagnosis.
- Due to the variable angle of insonation, inter-observer and intra-observer variability exists in sonographic measurements of the ventricular size. Depending upon changes in head circumference, follow-up ultrasound may be needed up to twice a week if ventricular dilation is suspected.
- For assessment of cerebellar hemorrhage, posterior fontanelle and mastoid views are needed, which require advanced level expertise.
- Several brain pathologies are not well visualized with ultrasound, such as extracerebral hemorrhage, cerebral ischemia, and damage to the basal ganglia, and diffuse PVL. Alternative imaging should be considered if such conditions are included in the list of differential diagnoses.
- Sonographic findings in PVL can at times be very subtle and easily missed – especially the non-cystic variant of PVL. MRI has been shown to be more sensitive in detection of PVL due to white matter signal changes and better ability to detect white matter volume loss.

Umbilical Venous Line (UVC) Placement

Introduction and Patient Considerations

Insertion of an umbilical venous catheter (UVC) is a routine procedure in the clinical care of extremely premature infants or sick term or near-term infants, and assurance of proper placement is key. UVC placement in the hepatic venous channels can cause liver abscess, hepatic parenchymal injury, or portal vein thrombosis [12]. Potential complications of UVC tip placement in the cardiac chambers include cardiac arrhythmias, endocarditis, and myocardial perforation leading to pericardial effusion and cardiac tamponade. Possible pulmonary complications may be pleural effusion, embolism, infarction, or hemorrhage. Due to the spectrum of possible complications, ensuring the optimal position of UVC tip at the junction of right atrium and inferior vena cava (IVC) is extremely important.

Most providers rely on single-view x-ray imaging to confirm UVC placement, although some centers perform both AP and lateral views to enhance the accuracy of this method. X-ray assessment of the UVC tip is not very precise. Since x-ray imaging is not done in real time, multiple images are necessary if the UVC has to be repositioned. In contrast, compared to conventional radiography, sonographic evaluation of UVC positioning is superior, more precise, and reliable [13]. For UVC placement, ultrasound can be performed in real time to make necessary adjustments, avoiding multiple x-rays.

UVC placement is carried out under sterilized conditions in NICU. Infants are lying supine on a flat bed and covered by sterile drapes. The transducer can be placed in a sterilized plastic bag along with some ultrasound gel. These bags are specifically designed for use with ultrasound for central venous access. An assistant can help to control the machine settings during the procedure or a foot pedal with control panel can be used.

Technical Considerations

- Avoid procedure related hypothermia and follow standard asepsis protocol.
- Generally, the convex probe (8–12 MHz) or a linear probe (12–18 MHz) can be used for UVC placement. For extremely premature infants, a high resolution transducer (>10 MHz) is preferable to achieve a clear image of smaller umbilical catheters (2.5 or 3.5 Fr G).
- Focus point: It is best to have the focus point on the IVC (subcostal sagittal view) or on the heart for echocardiography (subcostal/parasternal short axis or four-chamber view).
- Acoustic window: Use the liver as the acoustic window to enhance image quality and avoid interference from gas in adjacent bowel.
- Software: Although an abdominal point-of-care ultrasound can be used to identify the UVC tip, a cardiac package for neonatal echocardiography is preferable to view the UVC tip in the heart chambers. A cardiac package can be installed on a point-of-care ultrasound device for basic echocardiography.

Image Acquisition and Interpretation

Multiple views are helpful to confirm the optimal position of UVC tip. Echocardiography with saline contrast injection has been described as a gold standard to confirm the anatomical location of the UVC tip [14]. However, conventional sonography results are comparable for assessment of UVC position [15]. In extremely premature infants, saline injections for imaging should be avoided if possible due to the risk for IVH or fluid overload.

A basic scan can be performed by conventional sonography via the subcostal acoustic window. The transducer should be placed in the midline, just below the xiphoid sternum. For subcostal imaging in newborns, vertically inverting the image orientation (upside down) is preferred for easy recognition of structures as shown in Fig. 16.6a, b. For sagittal views, the transducer should be held vertically with the

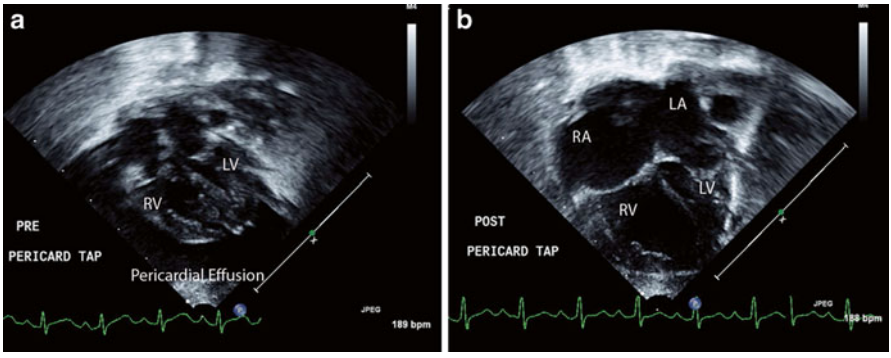

Fig. 16.6 (**a**) Four-chamber view showing pericardial effusion/cardiac tamponade. (**b**) Four-chamber view showing minimal pericardial effusion after pericardiocentesis

reference point facing upwards, and, with slight right to left tilting, the IVC and pulsating descending aorta can be identified. The IVC entering into the right atrium can be visualized in the sagittal plane. For the subcostal short axis view, hold the transducer vertically with the reference point toward the umbilicus. Pressing the tail of the transducer toward the left will bring the bicaval view of the right atrium, sweeping the transducer in the opposite direction can show the atrial septum, foramen ovale, AV valves, and both ventricles up to the apex. Optimal positioning of the UVC tip is at the junction of right atrium and IVC. Usually the UVC tip can be easily identified in the abovementioned two views by conventional sonography. The benefits of ultrasound are demonstrated in Fig. 16.7a, b – showing a malpositioned UVC that was not detected on x-ray, but shown by ultrasound.

However, if the UVC tip is not visible from the subcostal views, imaging can be shifted to echocardiography by initiating the installed cardiac package on the point-of-care ultrasound machine. A more comprehensive imaging by echocardiography includes 2 additional views – the parasternal short axis view and apical four-chamber view. Techniques to acquire additional images by echocardiography are described in Chaps. 5, 6, and 7.

Basic Competencies

Basic competency will enable a provider to perform conventional sonography from two different views to identify the tip of the catheter, i.e., subcostal sagittal and subcostal short axis. If initial assessment of catheter tip position is made by an advanced level user, the UVC can then be used for IV infusions. If an advanced level user is not available for interpretation of sonographic imaging, an x-ray should be performed prior to using the UVC for IV fluids. Ultrasound images should be verified by a radiologist, cardiologist, or an advanced level user within 24 h.

Advanced Competencies

At advanced levels, the ability to scan and to locate reliably the position of UVC is expected. If an infant has poor acoustic windows, both conventional point-of-care ultrasound and neonatal echocardiography may be required.

Evidence Review and Evidence-Based Use

Training of NICU providers to assess UVC positioning by ultrasound may be possible in 2–4 weeks [16]. Studies have shown that an acceptable position of a UVC on x-ray does not exclude an intra-cardiac placement [14, 15, 17]. The benefits of ultrasound over conventional X-ray imaging for more accurate and reliable UVC placement have been shown [14].

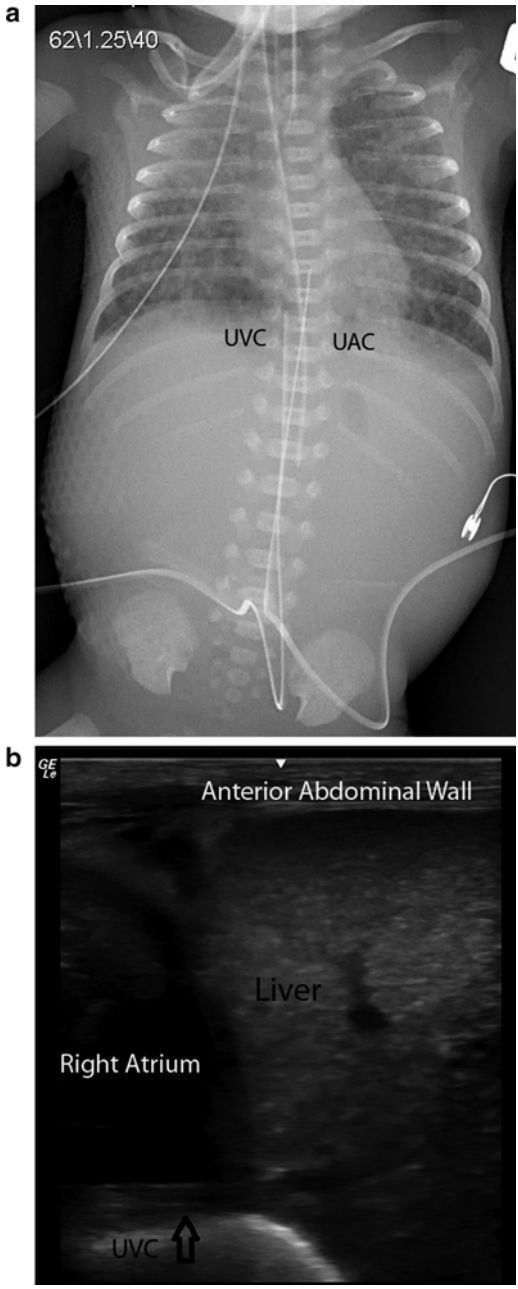

Fig. 16.7 (**a**) Abdominal x-ray for UVC placement; catheter tip is at the diaphragm level. (**b**) Subcostal sagittal sonography view showing the UVC catheter in the right atrium

Pitfalls and Precautions

- Many comorbid problems inherent to critically ill neonates may prohibit optimal visualization of the UVC. Given the lack of ultrasound transmission through air, gaseous intestinal distension or free air in the abdominal cavity poses a barrier in sonography via the subcostal view. When this is the case, reliance on echocardiographic views is needed. Similarly, echocardiographic imaging may be limited via the parasternal or apical four-chamber acoustic windows due to the hyperinflation of lungs, and reliance on the subcostal view is necessary.
- If the UVC has deviated into the hepatic lobes, it can be difficult to visualize on ultrasound since the echogenicity of adjacent liver more closely matches the catheter, decreasing contrast and making it more difficult to visualize. In such a circumstance, going back and locating the catheter in the umbilical vein and then following it into the liver to better identify any aberrant course are advisable.

Evaluation and Aspiration of Pericardial or Pleural Effusion

Introduction and Patient Considerations

A rare but fatal complication of central venous access in newborns is pericardial effusion leading to cardiac tamponade. The reported incidence of percutaneous line-related pericardial effusion or tamponade is 0.1–2 % of total line placements [18, 19]. Line-related cardiac tamponade is not always due to the perforation of a vein or myocardium, but leak can occur through micro-tears in the vessel intima which are not visible – even at autopsy. Other rare causes of pericardial effusion in neonates include hydrops fetalis and pericarditis. Not all pericardial effusions require aspiration; however, cardiac tamponade presenting as an acute emergency will need prompt lifesaving intervention. A typical scenario is an infant with central venous access who suddenly develops oxygenation failure, worsening of respiratory distress, bradycardia, or cardiac arrest. Infants with cardiac tamponade may not respond to resuscitation without evacuation of the fluid. The typical clinical signs of cardiac tamponade – hypotension, muffled heart sounds, and pulsus paradoxus – are not easily discernible in sick preterm infants. A clinician managing infants with central venous lines in place should have a high index of suspicion to make the diagnosis of cardiac tamponade [20–22]. Sonography can confirm the diagnosis and can also guide the needle aspiration [23]. Given the unpredictable nature of such events and likely lack of immediate availability of a cardiologist or a pediatric radiologist, readily available point-of-care ultrasound by an NICU provider can be extremely helpful in making the diagnosis of cardiac tamponade and guiding lifesaving needle aspiration.

Neonatal pleural effusion can occur secondary to pneumonia, sepsis, capillary leak syndrome, chylothorax, hydrops fetalis, myocardial dysfunction, persistent pulmonary hypertension of the newborn (PPHN), renal failure with volume over-

load, and intravenous (IV) fluid leak from central venous lines. Not all pleural effusions require aspiration; however, rapid accumulation of pleural effusion secondary to leak from central venous lines may cause significant respiratory distress and necessitate emergency evacuation. Traditionally, a chest X-ray has been used to make the diagnosis, and needle thoracocentesis was performed blindly. Bedside ultrasound guidance for thoracentesis is a well-accepted and widely used procedure in both the pediatric and adult settings. Ultrasound can help determine the best route for needle thoracentesis by localizing the largest pocket of fluid. Pertinent anatomy such as the diaphragm, lung, abdominal contents, and vascular structures can be identified with ultrasound, thereby improving success and safety. For assessing pediatric pleural effusions, ultrasound is superior to computed tomography (CT) for the detection of septations in complex fluid collections [24]. Therefore, aspiration of loculated effusions can be aided by ultrasound-guided needle placement. In the supine position, pleural effusions accumulate posteriorly and can be difficult to access, but, with the addition of ultrasound guidance, aspiration from posterior pleural effusions can be safely and effectively achieved. A radiologist can help during elective indications for ultrasound-guided thoracocentesis, however, in acute emergencies, point-of-care ultrasound can guide a lifesaving thoracentesis in NICU.

Technical Considerations

- Echocardiography or conventional point-of-care ultrasound device can be used.
- For point-of-care ultrasound, a convex (4–8 MHz) or linear probe (8–12 MHz) may be used. A convex or sector transducer (8–12 MHz) is required for echocardiography.
- Focus point: The focus point should be at the heart for pericardial effusion.
- Software: Abdominal imaging on point-of-care ultrasound can be sufficient. However, a cardiac package should be installed on point-of-care ultrasound devices to perform echocardiography.
- Doppler modes are not required.

Image Acquisition and Interpretation

To assess pericardial effusion, the most common and suitable view for sonography is via the subcostal acoustic window or a four-chamber echocardiography view, as shown in Fig. 16.6. See Chap. 7 for detailed discussion of these views. Depending upon the size, the pericardial effusion can appear like a thin rim or a huge cavity around the cardiac chambers as shown in Fig. 16.6. The depth of the pericardial effusion can be measured to quantify the pericardial fluid volume, although it should be noted that cardiac tamponade does not always depend upon the pericardial fluid volume. A slowly developing pericardial effusion can stretch the pericardial membrane to accommodate a large volume as compared to a rapid accumulation which can cause cardiac tamponade even with a moderate volume of pericardial

fluid. Restricted ventricular filling during diastole is a more reliable sign of the functional impact of cardiac tamponade than the volume of pericardial effusion.

For assessment of pleural effusion, start scanning anteriorly from the midclavicular point on the anterior chest to the lower margins of the rib cage, and slide laterally in the midaxillary line to screen for any fluid collection in the lateral or posterior pleural cavity. The reference point of the transducer is pointed toward the head for longitudinal scanning. For transverse scanning, the reference point should be pointed anteriorly. When recording longitudinal scans, the standard orientation is for the patient's head to be on the left of the image. Transverse images should be oriented, so the patient's right side is on the left as you face the image. Longitudinal and transverse images should be obtained documenting the site for needle thoracentesis. It is vital that the diaphragm be localized to avoid intra-abdominal structures. The diaphragm is typically readily identifiable as a curvilinear echogenic structure with the liver or spleen often visualized below the diaphragm. Note also should be made of the heart and descending thoracic aorta for left-sided thoracentesis. Color Doppler can be of assistance to evaluate these and other vascular structures to improve safety. Figure 16.8 shows a posterior pleural effusion in a 27-week premature infant lying supine due to a leak from a percutaneous central venous line. The image was obtained from the 4th intercostal space in the right midaxillary line. Using digital calipers, the pleural fluid volume can be estimated by measuring the dimensions of the fluid collection in the chest.

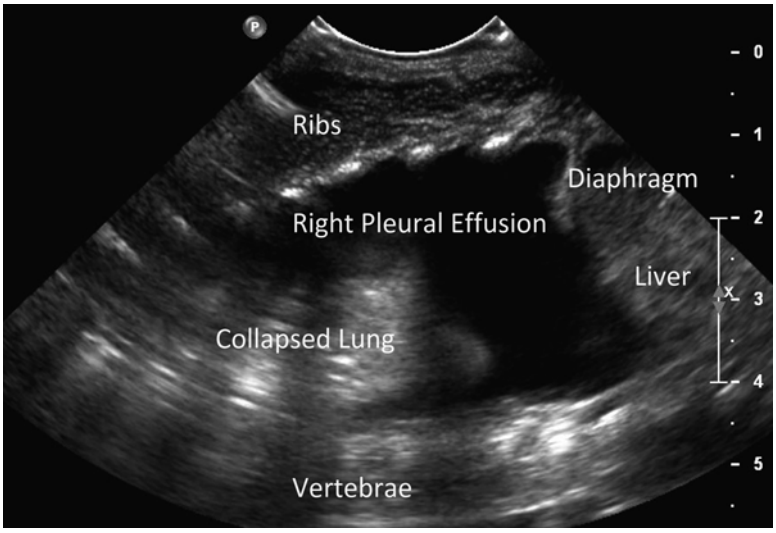

Fig. 16.8 Right pleural effusion (Sagittal view)

Basic Competencies

A basic level user should be able to perform and interpret point-of-care ultrasound imaging for the presence or absence of a pericardial effusion. In addition, in the event of cardiac tamponade, a basic level user is expected to perform pericardiocentesis efficiently.

Advanced Competencies

An advanced level user should be able to assess a pericardial effusion, cardiac tamponade, and pleural effusion using point-of-care ultrasound or echocardiography. An advanced level user should be an expert to support ultrasound-guided pericardiocentesis or thoracentesis in order to help another provider to perform the aforementioned procedures.

Evidence Review and Evidence-Based Use

Fluid leak from central venous catheters can lead to a fatal pericardial or pleural effusion which requires instant sonographic evaluation and intervention in NICU [22, 25, 26]. Timely recognition and subsequent intervention can significantly reduce the risk of death [23, 25, 27], and the immediate availability of ultrasound in the NICU has the potential to improve outcomes.

Pitfalls and Precautions

- It is important to recognize that every pericardial or pleural effusion does not need to be drained. Sonographic findings therefore should be interpreted with clinical correlation.
- A provider should be adequately trained to perform clinical procedures like pericardiocentesis and thoracentesis.
- Although ultrasound-guided thoracentesis is safer compared to the conventional blind procedure, it is an operator-dependent skill [28, 29].
- Needle injury to the underlying tissue causing pneumothorax, hemorrhage, or chylothorax is possible due to failure to identify the deepest pocket of fluid or to recognize that lung volume change with inspiration/expiration will affect the depth of fluid. To decrease the risk of intrathoracic injury, one must allow enough room for lung expansion, and one must perform a thorough ultrasound imaging of the entire pleural space to select the largest pocket of fluid [30].
- Failure to recognize and identify the diaphragm may lead to complications from unintended intra-abdominal puncture.

References

1. Evans N, Gournay V, Cabanas F, Kluckow M, Leone T, Groves A, et al. Point-of-care ultrasound in the neonatal intensive care unit: international perspectives. Semin Fetal Neonatal Med. 2011;16:61–8.
2. Mertens L, Seri I, Marek J, Arlettaz R, Barker P, McNamara P, et al. Targeted neonatal echocardiography in the neonatal intensive care unit: practice guidelines and recommendations for training. Writing Group of the American Society of Echocardiography (ASE) in collaboration with the European Association of Echocardiography (EAE) and the Association for European Pediatric Cardiologists (AEPC). J Am Soc Echocardiogr. 2011;24:1057–78.
3. Burdjalov V, Srinivasan P, Baumgart S, Spitzer AR. Handheld, portable ultrasound in the neonatal intensive care nursery: a new, inexpensive tool for the rapid diagnosis of common neonatal problems. J Perinatol. 2002;22:478–83.
4. Klebermass-Schrehof K, Wald M, Schwindt J, Grill A, Prusa AR, Haiden N, et al. Less invasive surfactant administration in extremely preterm infants: impact on mortality and morbidity. Neonatology. 2013;103:252–8.
5. Resch B, Resch E, Maurer U, Mueller W. Periventricular leukomalacia and neurodevelopmental outcome. J Pediatr. 2011;159:1049; author reply −50.
6. Brouwer MJ, de Vries LS, Groenendaal F, Koopman C, Pistorius LR, Mulder EJ, et al. New reference values for the neonatal cerebral ventricles. Radiology. 2012;262:224–33.
7. de Vries LS, Eken P, Dubowitz LM. The spectrum of leukomalacia using cranial ultrasound. Behav Brain Res. 1992;49:1–6.
8. Rennie JM. Neonatal cerebral ultrasound. Cambridge: Cambridge University Press; 1997.
9. Mack LA, Wright K, Hirsch JH, Alvord EC, Guthrie RD, Shuman WP, et al. Intracranial hemorrhage in premature infants: accuracy in sonographic evaluation. AJR Am J Roentgenol. 1981;137:245–50.
10. Pape KE, Bennett-Britton S, Szymonowicz W, Martin DJ, Fitz CR, Becker L. Diagnostic accuracy of neonatal brain imaging: a postmortem correlation of computed tomography and ultrasound scans. J Pediatr. 1983;102:275–80.
11. Halm BM, Franke AA. Diagnosis of an intraventricular hemorrhage by a pediatric emergency medicine attending using point-of-care ultrasound: a case report. Pediatr Emerg Care. 2011;27:425–7.
12. Bayhan C, Takci S, Ciftci TT, Yurdakok M. Sterile hepatic abscess due to umbilical venous catheterization. Turk J Pediatr. 2012;54:671–3.
13. Simanovsky N, Ofek-Shlomai N, Rozovsky K, Ergaz-Shaltiel Z, Hiller N, Bar-Oz B. Umbilical venous catheter position: evaluation by ultrasound. Eur Radiol. 2011;21:1882–6.
14. Ades A, Sable C, Cummings S, Cross R, Markle B, Martin G. Echocardiographic evaluation of umbilical venous catheter placement. J Perinatol. 2003;23:24–8.
15. Michel F, Brevaut-Malaty V, Pasquali R, Thomachot L, Vialet R, Hassid S, et al. Comparison of ultrasound and X-ray in determining the position of umbilical venous catheters. Resuscitation. 2012;83:705–9.
16. Pulickal AS, Charlagorla PK, Tume SC, Chhabra M, Narula P, Nadroo AM. Superiority of targeted neonatal echocardiography for umbilical venous catheter tip localization: accuracy of a clinician performance model. J Perinatol. 2013;33:950–3.
17. Haase R, Hein M, Thale V, Vilser C, Merkel N. Umbilical venous catheters – analysis of malpositioning over a 10-year period. Z Geburtshilfe Neonatol. 2011;215:18–22.
18. Ohki Y, Maruyama K, Harigaya A, Kohno M, Arakawa H. Complications of peripherally inserted central venous catheter in Japanese neonatal intensive care units. Pediatr Int. 2013;55:185–9.
19. Nowlen TT, Rosenthal GL, Johnson GL, Tom DJ, Vargo TA. Pericardial effusion and tamponade in infants with central catheters. Pediatrics. 2002;110:137–42.
20. Arya SO, Hiremath GM, Okonkwo KC, Pettersen MD. Central venous catheter-associated pericardial tamponade in a 6-day old: a case report. Int J Pediatr. 2009;2009:910208.

21. Megha M, Jain N, Pillai R. Pericardial tamponade in a newborn following umbilical catheter insertion. Indian Pediatr. 2011;48:404–5.
22. Jacobson Z, Strom J. Pericardial tamponade complicating central venous catheterization in an infant with very low birth weight: the role of echocardiography in diagnosis and treatment. Heart Dis. 1999;1:133–5.
23. Pizzuti A, Parodi E, Abbondi P, Frigerio M. Cardiac tamponade and successful pericardiocentesis in an extremely low birth weight neonate with percutaneously inserted central venous line: a case report. Cases J. 2010;3:15.
24. Kim OH, Kim WS, Kim MJ, Jung JY, Suh JH. US in the diagnosis of pediatric chest diseases. Radiographics. 2000;20:653–71.
25. Haass C, Sorrentino E, Tempera A, Consigli C, De Paola D, Calcagni G, et al. Cardiac tamponade and bilateral pleural effusion in a very low birth weight infant. J Matern Fetal Neonatal Med. 2009;22:137–9.
26. Traen M, Schepens E, Laroche S, van Overmeire B. Cardiac tamponade and pericardial effusion due to venous umbilical catheterization. Acta Paediatr. 2005;94:626–8.
27. Weil BR, Ladd AP, Yoder K. Pericardial effusion and cardiac tamponade associated with central venous catheters in children: an uncommon but serious and treatable condition. J Pediatr Surg. 2010;45:1687–92.
28. Patel PA, Ernst FR, Gunnarsson CL. Ultrasonography guidance reduces complications and costs associated with thoracentesis procedures. J Clin Ultrasound. 2012;40:135–41.
29. Mercaldi CJ, Lanes SF. Ultrasound guidance decreases complications and improves the cost of care among patients undergoing thoracentesis and paracentesis. Chest. 2013;143:532–8.
30. Koh DM, Burke S, Davies N, Padley SP. Transthoracic US of the chest: clinical uses and applications. Radiographics. 2002;22:e1.

Index

A
Abdomen. *See also* Genitourinary system
  aortic aneurysm, 260, 266
  competencies, 254
  evidence-based review, 271
  FAST examination, 254
  location-specific approach, 254
  patient considerations, 252–253
  right hemidiaphragm, 255–257
  technical considerations
    machine setup, 251–252
    transducer, 250
  ultrasound, 27
Abdominal and Cardiac Evaluation with Sonography in Shock protocol, 66, 67
Absorption, sound waves, 5–6
ACCP. *See* American College of Chest Physicians (ACCP)
Accreditation, 20, 22
Accreditation Council for Graduate Medical Education (ACGME), 23
Acute coronary syndrome (ACS), 113
Acute respiratory distress syndrome (ARDS)
  clinical scenarios, 139, 140
  description, 201–202
Acute severe dyspnea, 139
Air-mucosa interface, 180
Airway management
  impact, 186
  during laryngoscopy/endotracheal intubation, 189
  ultrasound usage, 175
  upper airway examination (*see* Upper airway examination)
A-lines, lung ultrasound, 196
Alveolar-interstitial syndrome, 198
American College of Chest Physicians (ACCP), 94
American Society of Anesthesiologists Task Force on Central Venous Access, 40
American Society of Cardiovascular Anesthesiologists, 59
American Society of Echocardiography (ASE), 84, 86
Anterolateral papillary muscle (APM), 81, 82, 90
Aorta
  abdominal ultrasound, 260–261, 265–266
  undifferentiated shock, 67–68
Aortic regurgitation (AR), 103, 117
Aortic stenosis (AS), 103, 117
Aortic valve (AV), 81
  LVOT and, 83
  parasternal short axis view, 83
  PLAX view, 87–89
  2D echocardiography/color Doppler, 103
Apical five-chamber (A5C) view
  left ventricular/valvular dysfunction, 92–93
  pericardial effusion, 159–160
Apical four-chamber (A4C) view
  left ventricular/valvular dysfunction, 90–91, 97–99
  pericardial effusion, 148, 157–158, 164
  transducer in, 90, 158
Apical two-chamber (A2C) view, left ventricular dysfunction, 91–92
AR. *See* Aortic regurgitation (AR)
Arterial lines, 59

M. Jankowich, E. Gartman (eds.), *Ultrasound in the Intensive Care Unit*,
Respiratory Medicine, DOI 10.1007/978-1-4939-1723-5

Artifacts
bayonet, 17–18
enhancement, 12
mirror image, 16
reflection, 15
refraction, 16–17
reverberations, 12–14
ring-down, 15
shadowing, 11–12
AS. *See* Aortic stenosis (AS)
Ascites, 242, 261–262, 268
ASE. *See* American Society of Echocardiography (ASE)
Atrioventricular valves, 81
Atrophy, 245
Auscultation, 182, 183, 202
AV. *See* Aortic valve (AV)

B
Bayonet artifacts, 17–18
Bladder, genitourinary system, 269–270
B-lines, lung ultrasound, 197
Brightness (B)-mode technique, 236–238

C
Calcified structures, 11
Cardiac output (CO)
definitions, 84
estimation, 109
measurement, 72
pericardial pressure-volume curves, 151
stroke volume and, 112–113
Cardiac tamponade, 147
apical four-chamber view, 148
CCE features, 167
interventricular dependence, 152–153
M-mode, 149
pericardial effusion and (*see* Pericardial effusion)
TEE, 169
ultrasound principles, 148–149
Cardiomyopathy, 349–350
Caval index, IVC, 70, 71, 73
CCE. *See* Critical care echocardiography (CCE)
Central venous access, 35
complications, 36
risk factors, 42–43
Central venous catheter (CVC), 25
Central venous pressure (CVP), 69
Cerebral parenchyma
B-mode imaging, 340–344
CT imaging, 341–343
intracerebral hematoma, 343, 344
third ventricle, 341
transcranial ultrasound, 340
Certification
and accreditation, 22
and critical care ultrasound, 21
in echocardiography, 21–22
principles, 20–21
CFD. *See* Color flow Doppler (CFD)
Chronic obstructive pulmonary disease (COPD), 202, 203, 228
CO. *See* Cardiac output (CO)
Color Doppler, 80, 374
A4C view, 91
aortic regurgitation, 117
aortic valve, 103
mitral regurgitation, 117
mitral valve, 100–103
PLAX view, 103
techniques, 99
Color flow Doppler (CFD), 80
Computed tomography (CT)
abdomen, 269
pleural effusion, 373
Continuous wave Doppler (CWD), 80, 116
COPD. *See* Chronic obstructive pulmonary disease (COPD)
Critical care echocardiography (CCE), 147
bedside applications, 77
cardiac function, 28
cardiac tamponade, 147
apical four-chamber view, 148
features, 167
interventricular dependence, 152–153
M-mode, 149
TEE, 169
ultrasound principles, 148–149
certification, 21–22
competencies, 78, 141
left ventricular/valvular dysfunction (*see* Left ventricular/valvular dysfunction)
pericardial effusion (*see* Pericardial effusion)
right ventricular dysfunction (*see* Right ventricular system)
Critical care ultrasound education
certification and (*see* Certification)
components
learning curve, 23–24
longitudinal curricula, 25
simulation, 24–25
web-based/computer, 24

comprehensive approach
faculty development, 26–27
introductory didactic course, 26
ongoing assessment, 26
core competencies
abdomen, 27
echocardiography, 28–29
thoracic, 27
vascular, 27
difficulties, 30
goals, 19
objectives, 19
roles, 20
training
barriers, 29–30
requirements, 23
Curvilinear array, 3
CWD. *See* Continuous wave Doppler (CWD)

D
Deep vein thrombosis (DVT), 24. *See also* Venous thromboembolism (VTE)
lower extremity, 276–278
sonographic diagnosis, 276
upper extremity, 282–283
Delayed cerebral ischemia (DCI), 350–352
Depth control, images modulation, 9
Diaphragm
B-mode technique, 236, 237
competencies, 242–243
complications, 245–246
discontinuity artifact, 17
evidence-based review
disuse atrophy, 245
dysfunction, 244–245
functional correlates, 242
paralysis, 242
weaning, mechanical ventilation, 245
image acquisition/interpretation
diaphragm dome, 241–242
end-expiration, 238, 240
end-inspiration, 239, 240
subcostal approach, 241
ZAP, 238–240
M-mode technique, 237
motion, 241–242
patient considerations, 236–237
precautions, 245–246
technical considerations, 236–237
zone of apposition, 236
Diffraction, sound waves, 6
DLT. *See* Double-lumen tubes (DLT)
Doppler echocardiography, 111, 136, 148
Doppler techniques
pleural effusion, 215–216
sound frequency, 78
Doppler velocity, 79
Double-lumen tubes (DLT), 182–184, 186–187

E
Echocardiography, 86, 123, 153, 164
CCE (*see* Critical care echocardiography (CCE))
competence levels, 22
echocardiography-guided pericardiocentesis, 169
goal-directed, 66
goal-oriented, 28
pulmonary embolus, 284, 287, 289
simulators, 25
Echolocation, 2
Edge shadow artifacts, 16, 17
Education. *See* Critical care ultrasound education
Ejection fraction (EF), 84, 104, 105, 107
Endotracheal intubation, 185–187, 189
Endotracheal tube (ETT)
and DLT, 182–184
esophagus, 183
and LDL tube, 186–187
Epiglottic vallecula, 179
E'point-septal separation (EPSS), 105–106
Esophagus, endotracheal tube, 183
ETT. *See* Endotracheal tube (ETT)
Extended FAST (eFAST) exam, 310, 312

F
FAC. *See* Fractional area change (FAC)
Femoral vein, 59
cannulation, 57
anatomy, 52–53
procedure, 53–54
thrombosis, 42
Fiberoptic bronchoscopy (FOB), 183–184
Fluid responsiveness (FR), 69
competencies, 71–74
complications, 74
definition, 73
image acquisition/interpretation, 70–71
patient considerations, 69–70
precautions, 74
technical considerations, 69–70

Focused assessment with sonography for trauma (FAST) exam
abdominal ultrasounds, 254, 271
trauma
blunt abdominal trauma, 309, 310
hemodynamically stable patient, 309–310
left upper quadrant, 301–303
pelvic view, 306–309
pericardial image, 304–306
pregnant trauma patient, 315
right upper quadrant, 299–301
undifferentiated shock, 67
Fractional area change (FAC), 109, 131–132
Fractional shortening (FS), 107–108

G
Gain, images modulation, 10
Genitourinary system. *See also* Abdomen
left upper quadrant
left hemidiaphragm, 267–268
left kidney, 268
spleen, 268
right kidney
ascites, 261–262
competencies, 258–259
complications, 259
hepatorenal recess, 258
hydronephrosis, 258, 259
inferior vena cava and aorta, 260–261
liver and biliary tree, 263
precautions, 259
technical aspects, 257–258
subcostal
aorta, 265–266
inferior vena cava, 264–265
pancreas, 267
suprapubic, 269–270
Guidelines for Prevention of Intravascular Catheter-Related Infections, 37

H
Hemodynamic impairment, 163
IVC plethora, 165–166
RA systolic collapse, 164
reciprocal respiratory changes, 165
right ventricular diastolic collapse, 164–165
High-frequency micro-ultrasound (HFMU), 57
High-frequency Ultrasound in Kids Study (HUSKY), 57
Hockey-stick probes, 38, 39, 57
Hyoid bone, 179, 180

I
Images modulation, 9–10
Inferior vena cava (IVC)
and aorta, 260
caval index, 70, 71, 73
complications, 265
and CVP, 69
demonstration, 71
dIVC and cIVC, 73
image acquisition/interpretation, 70–71
M-mode, 71, 72, 166
precautions, 265
and RAP, 135
subcostal view, 93–94, 165–166
technical aspects, 264
transducer, 70
undifferentiated shock, 67
Internal jugular vein, 59
cannulation, 56
anatomy, 45
freehand access, 45
procedure, 46–47
longitudinal/transverse view, 46
Interventricular septum (IVS), 81, 87–88, 130, 140
Intraventricular hemorrhage (IVH)
classifications, 365
neonatal head ultrasound, 362, 367
IVC. *See* Inferior vena cava (IVC)

L
Laryngeal mask airway (LMA), 188
Learning curve, critical care ultrasound, 23–24
Left double-lumen (LDL) tube, 186–187
Left upper quadrant (LUQ)
FAST exam, 301–303
left hemidiaphragm, 267–268
left kidney, 268
spleen, 268
Left ventricular outflow tract (LVOT), 81
aortic valve, 83
CSA, 110
measurement, 110
PWD, 111
VTI, 72, 111–113, 168
Left ventricular/valvular dysfunction
aortic regurgitation, 117
aortic stenosis, 117
aortic valve (*see* Aortic valve (AV))
apical five-chamber view, 92–93
apical four-chamber view, 90–91, 97–99
apical two-chamber view, 91–92
complications, 118–119

- end-diastolic diameter, 95
- end-systolic diameter, 95
- evidence-based review, 118
- mitral regurgitation, 116–117
- mitral stenosis, 115–116
- mitral valve (*see* Mitral valve (MV))
- myocardial segmentation, 114
- parasternal long-axis view, 87–89, 95, 97
- parasternal short axis view, 89–90, 98
- precautions, 118–119
- RWMA, 113, 115
- stroke volume
  - cardiac output, 112–113
  - CSA measurement, 110–111
  - definitions, 84, 109
  - velocity-time integral measurement, 111–112
- subcostal view, 93–94
- systolic dysfunction, 28, 113
- systolic function, 95–98, 104–105

Linear probe, 4, 38
Linear transducer, 3–4, 46
Longitudinal curriculum, critical care ultrasound, 25
Lung pulse, 197–198
Lung sliding, 197–198
Lung ultrasound
- A-lines, 196
- alveolar-interstitial syndrome, 198
- B-lines, 197
- complication, 205
- evidence-based review, 201–204
- high *vs.* low frequency probe, 192–193
- lung sliding and lung pulse, 197–198
- parenchymal lung disease, 201
- patient considerations, 192–193
- pneumonia and consolidation, 199–200
- pneumothorax and pleural effusion, 201
- precautions, 205
- technical considerations, 192–193
- uses, 191

LVOT. *See* Left ventricular outflow tract (LVOT)

M

Magnetic resonance imaging (MRI), 315, 362
Marfan syndrome, 103
McConnell's sign, 274, 285, 289
Medical simulation, 24–25
Mirror image artifacts, 16
Mitral annulus, 106–107, 109, 116, 167
Mitral regurgitation (MR)
- acute *vs.* chronic, 100
- etiology, 116–117
- severity, 101–102

Mitral stenosis (MS), 100, 115–116
Mitral valve (MV), 81
- apical two-chamber view, 100
- Doppler velocities, 169
- excursion method, 105–106
- left ventricular/valvular dysfunction, 100–102
- parasternal long-axis view, 81–82, 88, 116
- and tricuspid valve, 168
- 2D echocardiography/color Doppler, 100–103
- valvular dysfunction, 100–102

Morison's pouch, 261–262, 298, 300
Motion (M)-mode technique, 237
MR. *See* Mitral regurgitation (MR)
MS. *See* Mitral stenosis (MS)
Multi-slice computed tomography (MSCT) scan, 187
Myocardial ischemia, 81, 100, 113

N

Nasal cavity, 176
Neonatal head ultrasound
- competencies, 367
- complication, 367–368
- evidence-based review, 367
- image acquisition/interpretation, 364–367
- patient considerations, 362–363
- precautions, 367–368
- technical considerations, 363

Neonatal intensive care units (NICUs)
- indications, 356, 357
- neonatal head ultrasound
  - competencies, 367
  - complication, 367–368
  - evidence-based review, 367
  - image acquisition/interpretation, 364–367
  - patient considerations, 362–363
  - precautions, 367–368
  - technical considerations, 363
- pleural effusion
  - competencies, 375
  - complication, 375
  - evidence-based review, 375
  - image acquisition/interpretation, 373–374
  - patient considerations, 372–373
  - precautions, 375
  - technical considerations, 373

Neonatal intensive care units (NICUs) (*cont.*)
practice and training
competencies, 360, 361
guidelines and suggestions, 359–361
indications, 356–357
point-of-care ultrasound, 355–356
proposed training model, 358–361
training recommendations, 357–358
requirements, 356
utility, 356
UVC placement
competencies, 370
complication, 372
evidence-based review, 370
image acquisition/interpretation, 369–371
patient considerations, 368
technical considerations, 369
Neonates
pericardial effusion, 372
point-of-care head ultrasound, 363
ultrasound-guided venous access (*see* Ultrasound-guided venous access)
Neurointensive care unit
cerebral parenchyma
B-mode imaging, 340–344
CT imaging in hydrocephalus, 341–343
intracerebral hematoma, 343, 344
third ventricle, 341
transcranial ultrasound, 340
optic nerve ultrasound
complications, 348–349
equipment, 344–345
evidence-based review, 347–348
image acquisition, 346–347
image interpretation, 347
intracranial pressure, 344
patient factors, 345
precautions, 348–349
subarachnoid hemorrhage
cardiomyopathy, 349–350
cardiopulmonary evaluation, 349–352
hemodynamic augmentation, 350–352
pulmonary edema, 350
transcranial color-coded sonography
competencies, 338
complication, 339–340
equipment, 324, 325
evidence-based review, 338–339
image acquisition, 326–335
image interpretation, 335–338
patient factors, 324, 326
precautions, 339–340
vs. transcranial Doppler, 324

O

Optic nerve ultrasound (ONUS)
complications, 348–349
equipment, 344–345
evidence-based review, 347–348
image acquisition, 346–347
image interpretation, 347
intracranial pressure, 344
patient factors, 345
precautions, 348–349

P

Papillary muscle, 12, 81–82
Paralysis, diaphragm, 242
Parasternal long-axis (PLAX) view
color Doppler, 103
left ventricular/valvular dysfunction, 87–89, 95, 97
mitral valve, 81, 82, 88, 116
pericardial effusion, 154, 155–156, 161, 165
transducer in, 87–88, 155
Parasternal short axis (PSAX) view
aortic valve, 83
left ventricular/valvular dysfunction, 89–90, 98
pericardial effusion, 156–157
transducer in, 89–90, 156, 157
Parenchymal lung disease, 201
Pediatric patients, 59
peripheral vascular access, 57
ultrasound-guided venous access (*see* Ultrasound-guided venous access)
Percutaneous dilational tracheostomy (PDT), 187–188
Pericardial effusion
apical five chamber view, 159–160
apical four-chamber view, 148, 157–158, 164
competencies, 162, 163
advanced, 167–170
IVC plethora, 165–166
RA systolic collapse, 164
reciprocal respiratory changes, 165
right ventricular diastolic collapse, 164–165

complications, 171
distribution, 162
etiologies causing, 150
evidence-based review, 170–171
image acquisition, 154–155
interventricular dependence, 152–153
mimics on echocardiography, 160
PLAX, 154, 155–156, 161, 165
pleural effusion *vs.*, 162
precautions, 171
PSAX, 156–157
rate of accumulation, 151
size measurement, 161
subcostal view, 159–160, 162
and tamponade physiology, 150–153
ultrasound principles, 148–149
Pericardiocentesis, 169
Pericardium
anatomy, 149
compliance, 150–151
pressure-volume curves, 151
Peripherally inserted central catheters (PICC), 36, 57–58
Peripheral venous access, 57, 59
Periventricular leukomalacia (PVL)
neonatal head ultrasound, 362
point-of-care ultrasound, 366
sonographic imaging and grading, 366
PH. *See* Pulmonary hypertension (PH)
Pharynx, 176
Phased array probes, 70, 147, 148, 297, 312
Piezoelectricity
crystals, 78
principle, 2
PLAPS. *See* Posterolateral alveolar and/or pleural syndrome (PLAPS)
PLAX. *See* Parasternal long-axis (PLAX) view
Pleural effusion. *See also* Pneumothorax (PTX)
B-mode image, 210
cardiac and curvilinear probe, 209
competencies
anechoic fluid, 215
complex nonseptated and septated fluid, 215
Doppler analysis, 215–216
evaluation, 213
homogeneously echogenic fluid, 215
triangle of safety, 214–215
volume of effusion, 214
evidence-based review, 216–217
hemidiaphragm, 211–212
heterogeneously echoic structures, 212
identification, 160
image acquisition/interpretation, 211–213
M-mode, 200
NICUs
competencies, 375
complication, 375
evidence-based review, 375
image acquisition/interpretation, 373–374
patient considerations, 372–373
precautions, 375
technical considerations, 373
patient considerations, 209–211
vs. pericardial effusion, 162
PLAX, 156
pneumothorax and, 201
stationary thoracic ultrasound, 208–209
technical considerations, 209–211
thoracentesis, 211, 214
Pneumonia
clinical diagnosis, 199–200
lung ultrasound (*see* Lung ultrasound)
Pneumothorax (PTX)
clinical applicability, 203
competencies, 225–227
complications, 229–230
computed tomography, 219
diagnosis, 219
eFAST exam, 312
evidence-based review, 227–229
image acquisition/interpretation
B-lines, 223, 224
comet-tail artifact, 223
E-lines, 225
lung rockets, 223
lung sliding, 225, 226
ribs zone, 221–222
seashore sign, 222
ultrasonographic artifacts, 223, 224
visceral and pleural surfaces, 222
Z-lines, 225
patient considerations, 219–221
and pleural effusion, 201
precautions, 229–230
probes, 220
technical considerations, 219–221
thoracic ultrasound, 219
Point-of-care ultrasound, 19, 362
applications, 359–361
competencies, 360, 361
conventional views, 364
errors, 30
guidelines and suggestions, 359–360
indications, 356–357

Point-of-care ultrasound (*cont.*)
intraventricular hemorrhage, 362
NICUs (*see* Neonatal intensive care units (NICUs))
periventricular leukomalacia, 362, 366
post-hemorrhagic hydrocephalus, 362
programs, 30
requirements, 356
Posterolateral alveolar and/or pleural syndrome (PLAPS), 199, 200, 202, 203
Posteromedial papillary muscle, 81, 82
Post-hemorrhagic hydrocephalus (PHH), 362
Preintubation US assessment, 185–186
Pressure overload, right ventricle, 139, 140
PRF. *See* Pulse repetition frequency (PRF)
Protocolized Care for Early Septic Shock (ProCESS), 69
PSAX view. *See* Parasternal short axis (PSAX) view
Pulmonary arterial occlusion pressure (PAOP), 202
Pulmonary artery acceleration time (PAAT), 136
Pulmonary artery pressure (PAP), 136–138
Pulmonary edema, 116, 350
B-lines in patient, 197
clinical applicability, 203
subarachnoid hemorrhage, 350
Pulmonary embolism (PE), 139, 140–141
clinical presentation, 273
computed tomography, 273
echocardiography, 284, 287, 289
lung evaluation, 287
right ventricle evaluation, 287
Pulmonary hypertension (PH), 136, 141
Pulmonary vascular resistance (PVR), 124, 141
Pulsed-wave Doppler (PWD), 275
limitation, 80
LVOT, 111, 159, 168
Pulse repetition frequency (PRF), 2, 80
Pulsus paradoxus, 152–153, 163
PVR. *See* Pulmonary vascular resistance (PVR)

R

RA. *See* Right atrium (RA)
RAP. *See* Right atrium pressure (RAP)
Rapid Ultrasound for Shock and Hypotension (RUSH) protocol, 66, 67
Red blood cells (RBCs), 80, 110, 111
Reflection
artifacts, 15
sound waves affect, 6–7
Refraction
artifacts, 16–17
sound waves affect, 6
Regional wall motion abnormalities (RWMA), 113, 115
Respiratory system
failure, 190–191
lung ultrasound (*see* Lung ultrasound)
reciprocal changes, 165
upper, 177
Reverberation artifacts, 12–14
RHF. *See* Right heart failure (RHF)
Right atrium (RA), 134–135, 164
Right atrium pressure (RAP), 135
Right heart failure (RHF), 123, 124
Right kidney
ascites, 261–262
competencies, 258–259
complications, 259
hydronephrosis, 258, 259
inferior vena cava and aorta, 260–261
liver and biliary tree, 263
precautions, 259
technical aspects, 257–258
Right upper quadrant (RUQ)
FAST exam, 299–301
right hemidiaphragm, 255–257
right kidney
ascites, 261–262
competencies, 258–259
complications, 259
hepatorenal recess, 258
inferior vena cava and aorta, 260–261
liver and biliary tree, 263
precautions, 259
technical aspects, 257–258
Right ventricular outflow tract (RVOT)
measurement, 126–127
PLAX view, 156
PSAX view, 157
tricuspid valve and, 136–138
Right ventricular system
clinical scenarios, 139–141
competencies, 141–143
complications, 143
diastolic collapse, 164–165
dimensions and wall thickness, 126–129
fractional area change, 131–132
Frank-Starling curve, 124
image acquisition/interpretation, 125
infarction, 139
interventricular septum, 130
IVC and RAP, 135
patient considerations, 124–125

precautions, 143
pressure overload, 140
pulmonary embolism, 140–141
right atrium, 134–135
systolic function, 131–133
TAPSE, 133–134
technical considerations, 124–125
tricuspid annulus, 132–133
TV and RVOT Doppler, 136–138
volume overload, 139–140
Ring-down artifacts, 15
RVOT. *See* Right ventricular outflow tract (RVOT)
RWMA. *See* Regional wall motion abnormalities (RWMA)

S
SC view. *See* Subcostal (SC) view
Sepsis, 139
Shadowing artifacts, 11–12
Shock, 65
evidence-based review, 68–69
types, 67
undifferentiated, 66–68
Simpson's method, 107
Simulation-based medical education, 24–25
Sound waves, 5–8
SPAP. *See* Systolic pulmonary artery pressure (SPAP)
Spleen, 268
liver and, 187, 210, 374
smaller size, 302
Split image artifact, 16–17
Sterile techniques, 38, 39
Stroke volume (SV)
CSA measurement, 110–111
definitions, 84, 109
measurement, 72
velocity-time integral measurement, 111–112
Subarachnoid hemorrhage (SAH)
cardiomyopathy, 349–350
cardiopulmonary evaluation, 349–352
hemodynamic augmentation, 350–352
pulmonary edema, 350
Subclavian vein, 57, 59
anatomy, 47
diaphragm dome, 241
infra-clavicular and axillary approaches, 51–52
supraclavicular approach to, 48–51
Subcostal (SC) view
IVC plethora, 165–166
left ventricular/valvular dysfunction, 93–94
pericardial effusion, 159–160, 162
transducer, 93
Subxiphoid image, 304–306
SV. *See* Stroke volume (SV)
Systolic function
left ventricular/valvular dysfunction, 95–98, 104–105
visual assessment, 95, 96
Systolic pulmonary artery pressure (SPAP), 135, 141

T
Tamponade
cardiac tamponade (*see* Cardiac tamponade)
physiology, 150–153
TAPSE. *See* Tricuspid annular plane systolic excursion (TAPSE)
TEE. *See* Transesophageal echocardiography (TEE)
Thoracentesis, 23, 211, 217
Thoracic ultrasound
pneumothorax, 219, 229
pulmonary edema, 350
Timed gain control (TGC), 10
Tissue transmission, ultrasound waves, 5–8
Tongue, ultrasound view, 177–179
Trachea
air space, 181
cartilage rings, 180, 182
ETT, 183, 184
and larynx, 176
and paratracheal soft tissues, 188
transverse view, 180
Transcranial color-coded sonography (TCCS)
competencies, 338
complication, 339–340
equipment, 324, 325
evidence-based review, 338–339
image acquisition
anatomical distribution, 327, 329
B-mode image, 327, 328
CT axial image, 327, 328
duplex image, of Willis, 328–330
extracranial internal carotid artery, 334–335
probe position, 326, 327, 330
sample volume, 331–333
spectral Doppler waveform, 331, 333–334
transtemporal window, 326

Transcranial color-coded sonography (TCCS) (*cont.*)
image interpretation
acute ischemic stroke, 336, 338
brain death, 336, 337
cerebral blood flow velocities, 336
cerebral vasospasm, 335–336
COGIF scale, 338
patient factors, 324, 326
precautions, 339–340
vs. transcranial Doppler, 324
Transcranial Doppler (TCD), 324
Transducers
abdominal examination, 250
apical four-chamber view, 90, 158
holding technique, 87
inferior vena cava, 70
linear, 3–4, 46
ONSD, 345
parasternal long axis view, 87–88, 155
parasternal short axis view, 89–90, 156, 157
phased array/microconvex, 79
piezoelectric crystals, 78
subcostal view, 93
TCCS, 325
terminologies related to, 85
ZAP, 238
Transesophageal echocardiography (TEE), 29
cardiac tamponade, 169
competencies, 142–143
Transmission, sound waves, 7–8
Transthoracic echocardiography (TTE), 29
Trauma
competencies
blunt abdominal trauma, 309, 310
chest x-ray, 312
diaphragmatic rupture, 315
hemodynamically stable patient, 309–310
motion mode, 312–315
normal sliding pleura, 312, 313
pneumothorax, 311
pregnant trauma patient, 315
thoracic cavity evaluation, 311
unstable patient, 310
complications, 318–319
evidence-based review, 316–317
hemothorax, 317
image acquisition/interpretation, 298–299
left upper quadrant, 301–303
patient considerations, 296–297
pelvic view, 306–309
pericardial image, 304–306
precautions, 318–319
probe selection, 296
right upper quadrant, 299–301
splenorenal space, 301–303
technical considerations, 296–297
uses, 317
Tricuspid annular plane systolic excursion (TAPSE), 133–134
Tricuspid annulus, 132–133
Tricuspid valve (TV), 81
Doppler flow velocities, 168
mitral valve and, 168
and RVOT Doppler, 136–138

U

Ultrasound
beams, 2–3
energy loss mechanisms, 8
gallbladder, 1
types, 3–4
generation, 2–3
physics, 1–2
principles, 78–80
probes, 3–4
tissue transmission, 5–8
Ultrasound-guided vascular access (UGVA), 36
Ultrasound-guided venous access
femoral vein cannulation, 57
image acquisition/interpretation, 40–44
internal jugular vein cannulation, 56
optimization, 61
peripherally inserted central lines, 57–58
peripheral vascular access, 57
subclavian vein cannulation, 57
Umbilical venous catheter (UVC)
competencies, 370
complication, 372
evidence-based review, 370
image acquisition/interpretation, 369–371
patient considerations, 368
technical considerations, 369
Undifferentiated shock
abdominal exam, 67
algorithm, 67
aorta, 67–68
goal-directed echocardiography, 66
IVC ultrasound, 67
venous thrombosis assessment, 68
Upper airway examination
anatomy, 176–177
anesthesia, 189
complications, 189

endotracheal intubation, 185–187
extubation failure, 187
hyomental distance, 185
image acquisition/interpretation, 179–182
laryngeal mask airway, 188
percutaneous dilational tracheostomy, 187–188
precautions, 189
preintubation assessment, 185–186
technique, 177–178
ultrasound examination, 176
Upper respiratory system, 177
US Agency for Healthcare Research and Quality (AHRQ), 58

V
Valvular function, assessment, 29
Vascular access
challenges, 58
competencies, 44–45, 54–55
complications, 59–61
evidence-based review, 58–59
femoral vein cannulation
anatomy, 52–53
procedure, 53–54
internal jugular vein cannulation
anatomy, 45
procedure, 46–47
precautions, 59–61
subclavian vein cannulation
anatomy, 47
procedure, 48–52
technical and patient considerations
image acquisition/interpretation, 40–44
pre-procedural preparations, 38–39
procedure checklist and bundle, 40
vein selection, 37
training requirements, 61
ultrasound-guided arterial cannulation, 55–56
ultrasound-guided venous access
femoral vein cannulation, 57
internal jugular vein cannulation, 56
optimization, 61
peripherally inserted central lines, 57–58
peripheral vascular access, 57
subclavian vein cannulation, 57
Veins
vs. arteries, 39–40
femoral vein, 57, 59
anatomy, 52–53
procedure, 53–54
thrombosis, 42
internal jugular vein, 56, 59
anatomy, 45
freehand access, 45
longitudinal/transverse view, 46
procedure, 46–47
selection, 37
subclavian vein, 57, 59
anatomy, 47
diaphragm dome, 241
infra-clavicular and axillary approaches, 51–52
supraclavicular approach to, 48–51
ultrasound images, 9–10
Velocity-time integral (VTI)
calculation, 111
definitions, 111, 167
LVOT and, 72, 111–113, 168
measurement, 111–112
Venous thromboembolism (VTE)
color Doppler, 275
competencies
lung evaluation, 287
right ventricle, 287
upper extremity venous system, 286
complication, 290
evidence-based review
accuracy and speed, 287–288
right ventricular evaluation, 288–289
high-resolution linear array transducer, 275
limitations, 274
lower extremity
augmentation, 282
common femoral vein and artery, 279, 280
greater saphenous vein, 279, 280
position, 278, 279
proximal deep venous system, 277
superficial femoral vein, 279, 281
symptomatic patients, 276–277
patient considerations, 275–276
precautions, 290
right ventricular evaluation, 284–286
technical considerations, 275–276
upper extremity, 282–283
Venous thrombosis
assessment, 68
ultrasound signs, 43
Visual assessment, 95–98
Vocal cords, 180, 181, 187, 188
Volume overload, right ventricle, 139–140

Volume status, 69
competencies, 71–74
complications, 74
image acquisition/interpretation, 70–71
patient considerations, 69–70
precautions, 74
technical considerations, 69–70
VTI. *See* Velocity-time integral (VTI)

W
Wall motion score index (WMSI), 114–115
Weaning, 245
Web-based curriculum, 24

Z
Zone of apposition (ZAP), diaphragm
B-and M-mode, 239, 240
coronal plane, 238
end-expiration, 238, 240
end-inspiration, 239, 240